

Distribution Agreement

In presenting this thesis or dissertation as a partial fulfillment of the requirements for an advanced degree from Emory University, I hereby grant to Emory University and its agents the non-exclusive license to archive, make accessible, and display my thesis or dissertation in whole or in part in all forms of media, now or hereafter known, including display on the world wide web. I understand that I may select some access restrictions as part of the online submission of this thesis or dissertation. I retain all ownership rights to the copyright of the thesis or dissertation. I also retain the right to use in future works (such as articles or books) all or part of this thesis or dissertation.

Signature:

Wenbin Liu

Date

**THE SYNTHESIS AND APPLICATION OF A SERIES OF C₄-SYMMETRIC
DIRHODIUM CATALYSTS DERIVED FROM 1-(2-CHLOROPHENYL)-2,2-
DIPHENYLCYCLOPROPANECARBOXYLATE LIGANDS**

By

Wenbin Liu
Doctor of Philosophy

Chemistry

Huw M. L. Davies, Ph.D.
Advisor

Nathan T. Jui, Ph.D.
Committee Member

Frank E. McDonald, Ph.D.
Committee Member

Accepted:

Lisa A. Tedesco, Ph.D.
Dean of the James T. Laney School of Graduate Studies

Date

**THE SYNTHESIS AND APPLICATION OF A SERIES OF C₄-SYMMETRIC
DIRHODIUM CATALYSTS DERIVED FROM 1-(2-CHLOROPHENYL)-2,2-
DIPHENYLCYCLOPROPANECARBOXYLATE LIGANDS**

By

Wenbin Liu

B.Sc., The Hong Kong Polytechnic University, 2014

Advisor: Huw M. L. Davies, Ph.D.

An abstract of
A dissertation submitted to the Faculty of the
James T. Laney School of Graduate Studies of Emory University
in partial fulfillment of the requirements for the degree of
Doctor of Philosophy
in Chemistry
2019

Abstract

THE SYNTHESIS AND APPLICATION OF A SERIES OF C₄-SYMMETRIC DIRHODIUM CATALYSTS DERIVED FROM 1-(2-CHLOROPHENYL)-2,2-DIPHENYLCYCLOPROPANECARBOXYLATE LIGANDS

By Wenbin Liu

Rhodium-bound donor/acceptor carbenes have been developed as an influential tool for selective C–H functionalization, in which the donor moiety attenuates the reactivity. Additionally, the selectivity can be further altered by using different dirhodium catalysts with specially designed ligands and therefore, catalyst-controlled site-selective C–H functionalization can be achieved. The first chapter gives an overview about the rhodium carbene chemistry, dirhodium tetracarboxylate catalysts, and site-selective C–H functionalization.

The second chapter describes the development of Rh₂(*S*-2-Cl-5-BrTPCP)₄, which is a sterically encumbered catalyst that induces high site-selectivity for functionalization at terminal unactivated methylene C–H bonds, even in the presence of electronically activated benzylic C–H bonds that are typically favored by previously established dirhodium catalysts. Rh₂(*S*-2-Cl-5-BrTPCP)₄ and its derivatives, which contain different substituents on the 2-chlorophenyl groups in the (*S*)-1-(2-chlorophenyl)-2,2-diphenylcyclopropanecarboxylate ligand scaffold, have similar selectivity profiles and all adopt a C₄-symmetry geometry with an additional *M*-axial chirality between the 2-chlorophenyl and cyclopropane moieties. Computational studies on Rh₂(*S*-2-Cl-5-BrTPCP)₄ suggest the same conformation is favored in dichloromethane and it is rigid without alteration when the carbene binds.

The third chapter demonstrates the ability of the rhodium donor/acceptor carbene chemistry in the synthesis of positional analogs for methylphenidate. Using the right dirhodium catalysts and protecting groups, 2- and 4-substituted analogs are accessed as single regioisomer with high stereoselectivity via C–H insertion on piperidines. The 3-substituted analogs can be prepared indirectly by cyclopropanation followed by reductive ring-opening.

The fourth chapter describes the immobilization of dirhodium triarylcyclopropanecarboxylate catalysts for site- and stereoselective C–H insertion reactions in flow. Systematic studies on the effect of anchor sites suggest the aryl ring *trans* to the carboxylate group, which points to the periphery of the catalyst, is the optimal site for linking to the solid support covalently. Moreover, Rh₂(*S*-2-Cl-5-BrTPCP)₄ is derivatized to Rh₂(*S*-2-Cl-5-CF₃TPCP)₄ for catalyst immobilization.

The fifth chapter introduces a new method for accessing diazo compounds via copper-catalyzed dehydrogenation of hydrazones using oxygen as the terminal oxidant, which is effective for the preparation of diazoesters, diazoketones and diazoamides in high yields.

**The Synthesis and Application of a Series of C₄-Symmetric Dirhodium Catalysts Derived
from 1-(2-Chlorophenyl)-2,2-Diphenylcyclopropanecarboxylate Ligands**

By

Wenbin Liu

B.Sc., The Hong Kong Polytechnic University, 2014

Advisor: Huw M. L. Davies, Ph.D.

A dissertation submitted to the Faculty of the
James T. Laney School of Graduate Studies of Emory University
in partial fulfillment of the requirements for the degree of
Doctor of Philosophy
in Chemistry
2019

Acknowledgments

The past five years has been one of the most important stages in my life that I've grown significantly – both in professional and personal aspects. At the end of my journey in doctoral studies, I would like to thank all the people I encountered during the time. In this section, I want to express my acknowledgments to the people who contributed to this dissertation.

First of all, I would like to give sincere thanks to my advisor, professor Huw M. L. Davies. I remember how exciting I was when he gave me the offer for graduate studies at Emory University and later the opportunity to join his group. I cannot thank him enough for his incredible support and mentorship throughout my graduate career. The opportunities and guidance he provided have not only helped me be more confident, but also opened doors to me for various potential futures and helped me to pursue my career in industry. All the knowledge about C–H functionalization, stereoselectivity, and heterocycle chemistry that he taught me laid the foundation for my graduate studies and equipped me as a better scientist. All the achievements I accomplished these years would not be possible without his support.

I would like to thank my other two committee members, Prof. Nathan T. Jui and Prof. Frank E. McDonald, for being wonderful mentors to me throughout my graduate studies. Their feedbacks on my annual reports and original research proposal were extremely helpful. The synthesis courses they taught are very useful and are beneficial to the development of my projects. I really appreciate Prof. Jui for having me as a rotation student in his group to learn photochemistry, and his strong support when I was looking for jobs. His energetic attitude also has great influence on me. I remember the time he taught me how to conduct reactions in the lab and we analyzed the NMR spectrum in the elevator. I also truly appreciate Prof. McDonald for his advice on proposal

development and how to be a better scientist in chemistry. His encouragement for me throughout the years has been an important support for me.

I also want to thank several faculty members at Emory, Prof. Lanny S. Liebeskind and Prof. Dennis C. Liotta, who taught me courses that are valuable to the development of my technical skills in chemistry. I want to acknowledge Prof. William M. Wuest for his support on the new project and support on my job hunting. I am also thankful to Prof. Cora MacBeth for career advice.

Many thanks should also go to all the professors and students/postdocs in the CCHF center for all the great discuss and support, especially those collaborated with me during my doctoral studies. I want to thank Prof. Christopher W. Jones for his support when I was looking for jobs. The collaboration with Prof. Jones and Dr. Chun-jae Yoo in his group has been an exceptional experience for me, as well as Taylor Hatridge. They taught me some of the basic in chemical engineering that really changed my mind-set as an organic chemistry student. I also want to thank Dr. Djamaladdin G. Musaev for his expertise on computational studies and helped in my catalyst design projects, as well as Dr. Zhi Ren for the discussion on theoretical chemistry. I am thankful to Prof. Matthew S. Sigman and Dr. Tobias Gensch for teaching me the concept of data science and how to utilize it in organic chemistry that will be really beneficial for my future career. I also appreciate Prof. Oliver Reiser and Tobias Babl for their effort and discussion in our collaboration on piperidine manipulations. Also, I would like to thank Dr. Jaume Balsell at Merck for his suggestion that has great impact on the success of my projects.

My enjoyable experience in my graduate studies is also because of the wonderful staff team at Emory. I would like to acknowledge Ann Dasher for her efforts that make my start in the graduate school smooth and her strong support for me to continue my doctoral career. I also want to say thanks to Kira Walsh for arranging all the fun activities and advise on some of my application

materials. I'm thankful to Todd Polley for his support for all the students in the department. I really appreciate the support from Jan McSherry for managing the facilities in the building, Dr. Shaoxiong Wu and Dr. Bing Wang for all the NMR related studies, Dr. John Bacsa for X-ray crystallography, Dr. Fred Strobel for numerous HRMS. Without them, the completion of my doctoral work would not have been possible.

As the Davies group has been my second home for more than five years, I would like to give my special thanks to all the past and present Davies group members for the times we spent together. I really appreciate the support and adviser from Dr. Daniel Morton, who saved me in the dark days and helped me survive in the graduate career. I also admire his style of being extremely organized and utilizing various technologies for effective communications, especially presentation. Next, I must thank my mentor when I joined the Davies group, Dr. Cecilia Tortoreto, whose desk was next to mine. She gave me a lot of great advice in conducting research and introduced me to her international friends that really decorated my enjoyable start in the PhD program. I deeply appreciate for the friendship with Dr. Daniel Rackl. I am impressed by his strong problem-solving skill and being energetic in chemistry. I also want to thank him for introducing me to the collaboration with Chun-jea Yoo on the flow project. I am also thankful to several friends who completed post-doctoral fellowships in the Davies group, including Dr. Zachary Garlets, Dr. Solymar Negretti, Dr. Sidney Wilkerson-Hill, Dr. Jeffrey Mighion and Dr. Sandeep Raikar, for their advice on my projects and discussion on future careers. I would like to thank former group members, Matthew Chuba, Dr. Liangbing Fu, Dr. Hyun-Min Park and Dr. Kuangbiao Liao for all their help in the lab and being great friends throughout the years. I also want to express my deeply thanks to my friends in the same office, Jiantao Fu, Sam Mckinnon and Aaron Bosse, for brightening my days and I wish them all the best in their future. Aaron Bosse deserves additional

thanks for proofreading my thesis. I also want to thank all of the Davies group members including Benjamin Wertz, Bowen Zhang, Bo Wei, Yannick Boni, Jack Sharland, Maizie Lee, Dr. Zhi Ren and Dr. Xun Yang for their help and support that I won't list here.

Support and friendship in the Department of Chemistry are also very important to me. The encouraging and caring support from Jiahui Zhang, Jia Song and Dan Liu is really valuable and deserve special thanks, as well as Tianyuan Zhang, Ziwei Guo, Hanquan Su, Qi Yu, Peipei Ma, Elaine Liu, Allyson Boyington, Cameron Pratt, Ingrid Wilt. I am grateful for having them for discussions on chemistry and life.

My loving family is the ultimate support for me that I can freely pursue what I like. My mom and dad have supported me throughout my entire life, which has brought me to where I am today. Their support, understanding, patience and insight have been very important to me and make me grow into someone like them or better. I hope I have made them proud of me and I will continue to grow that I can be their support in the future. I also want to thank my boyfriend, even though we are separated by long distance, we are always together in spirit. His support and respect throughout the years has been unmeasurable and I look forward to our future.

For my parents

Table of Contents

<i>Chapter 1. Introduction to Selective C–H Functionalization via Rhodium Carbenes.....</i>	<i>1</i>
1.1. Site-selective C–H Functionalization.....	1
1.2. Rhodium Carbene Chemistry	2
1.3. Dirhodium Tetracarboxylate Catalysts	4
<i>Chapter 2. Synthesis and Development of the Sterically Demanding C₄-Symmetric Catalysts, the Rh₂(<i>o</i>-CITPCP)₄ Series, for Overcoming Electronic Preference</i>	<i>11</i>
2.1. Introduction.....	11
2.1.1 Symmetry of Dirhodium (II) Carboxylate Catalysts	11
2.1.2. Site- and Stereoselective Functionalization of Electronically Activated and Unactivated Methylene C–H Bonds	16
2.2. Results and Discussion.....	19
2.2.1. Synthesis and Initial Examination of Rh₂(<i>S</i>-<i>o</i>-CITPCP)₄ Catalyst	19
2.2.2. C–H Insertion of 4,5-Substituted 1,3-Dioxolane	26
2.2.3. Development of Rh₂(2-Cl-4-BrTPCP)₄ and Rh₂(2-Cl-5-BrTPCP)₄.....	29
2.2.5. Catalyst-Controlled Selective Functionalization of Unactivated C–H Bonds in the Presence of Electronically Activated C–H Bonds.....	43
2.2.6. Extension in Rh₂(<i>S</i>-<i>o</i>-CITPCP)₄ Catalysts Family	57
2.2.7. Computational Studies for Structural Understanding of the Complex and Carbene	60
2.3. Conclusion	63

<i>Chapter 3. Catalyst-controlled Site-selective Functionalization of Piperidines for Methylphenidate Analogs</i>	64
3.1. Introduction	64
3.2. Results and Discussion	68
3.2.1. C–H Functionalization of Piperidines at C2 Sites	68
3.2.2. C–H Functionalization of Piperidines at C4 Sites	75
3.2.3. C3 Analog Generation	78
3.3. Conclusion	81
<i>Chapter 4. Efforts Towards Immobilization of Rh₂(TPCP)₄ for Asymmetric C–H Insertion in Flow</i>	82
4.1 Introduction	82
4.1.1 Continuous Flow Chemistry	82
4.1.2 Immobilization of Dirhodium (II) Catalysts and Application in Flow	83
4.2 Results and Discussion	94
4.2.1 Immobilization of Rh₂(S-<i>p</i>-BrTPCP)₄	94
4.2.2 Exploration of Influence of Anchor Site on Rh₂(S-<i>o</i>-ClTPCP)₄	97
4.2.3 Development of immobilized Rh₂(S-2-Cl-5-CF₃TPCP)₄ for Flow Reaction in Cartridge	105
4.3 Conclusion	113
<i>Chapter 5. Oxidation of Hydrazones for Diazo Synthesis with Oxygen as Terminal Oxidant</i> 114	
5.1 Introduction	114
5.1.1 Overview of Diazo Synthesis	114

5.1.2 Hydrazone Oxidation for Diazo Synthesis.....	115
5.2 Results and Discussion.....	118
5.3 Conclusion	125
<i>Experimental Part</i>	<i>127</i>
6.1 General Considerations and Reagents	127
6.2 Experimental Part for Chapter 2	131
6.3 Experimental Part for Chapter 3	227
6.4 Experimental Part for Chapter 4	262
6.5 Experimental Part for Chapter 5	292
<i>References</i>	<i>303</i>
<i>Appendix: X-Ray Crystallographic Data</i>	<i>311</i>

Table of Schemes

Scheme 1.1 Metal carbene generation from diazo compound decomposition	2
Scheme 1.2 Classes of rhodium carbenes.....	3
Scheme 1.3 Synthetic application of rhodium donor/acceptor carbene in C–H functionalization	4
Scheme 1.4 Reactivity profile and surrogate reactions using Rh ₂ (S-DOSP) ₄	6
Scheme 1.5 Structure and reaction example of Rh ₂ (S-PTAD) ₄	8
Scheme 1.6 Structure of the Rh ₂ (TPCP) ₄ catalysts and site-selectivity	9
Scheme 2.1 Dirhodium carbene reaction mechanism and benzylic C–H insertion	16
Scheme 2.3 Synthetic route for Rh ₂ (S-o-CITPCP) ₄ and Rh ₂ (S-o-BrTPCP) ₄	21
Scheme 2.4 Synthesis of Rh ₂ (S-2-Cl-4-BrTPCP) ₄ and Rh ₂ (S-2-Cl-5-BrTPCP) ₄	31
Scheme 2.5 Scope of diazoacetates in C–H insertion of 4-bromoethylbenzene	41
Scheme 2.6 Expanded benzylic substrates for diastereoselectivity examination.....	42
Scheme 2.7 Evaluation of benzene ring protection	44
Scheme 2.8 Influence of electronic and steric factors on the substrates	52
Scheme 2.9 Scope of substrates and diazo compounds.....	54
Scheme 2.10 Demonstration of utility in synthesis of cylindrocyclophane core	55
Scheme 3.1 C–H functionalization on piperidine at C2	65
Scheme 3.2 C–H functionalization on piperidine at C3 and C4.....	66
Scheme 3.3 C–H functionalization at C2 using donor/acceptor carbene	67
Scheme 3.4 Substrate scope of C2 functionalization	74
Scheme 3.5 Substrate scope of C4 functionalization	77
Scheme 3.6 Reductive ring-opening discovered by the Reiser group.....	78
Scheme 3.7 Proposed rationalization for chirality retention	80

Scheme 3.8 Summary for generation C2, C3 and C4 analogs of methylphenidate	81
Scheme 4.1 Synthesis and examination of Rh ₂ (PE-CO ₂) ₄	86
Scheme 4.2 Mono-ligand exchange for immobilized Rh ₂ (S-MEPY) ₄	86
Scheme 4.3 Synthesis of Immobilized Rh polymer-supported pyridine	88
Scheme 4.4 Synthesis of polymer-supported Rh ₂ (S-PTTL) ₄	91
Scheme 4.5 Synthesis and examination of Rh ₂ (S-DOSP) ₃ -(S-silicaSP)	93
Scheme 4.6 Synthesis of Rh ₂ (S-p-BrTPCP) ₃ (S-p-(4-ethynyl)PhTPCP) and immobilization.....	95
Scheme 4.7 Initial tests of immobilized Rh ₂ (S-p-BrTPCP) ₄	96
Scheme 4.8 Synthesis for Rh ₂ (S-o-CITPCP) ₄ derivative with ethynyl on ring A	100
Scheme 4.9 Synthesis of Rh ₂ (S-2-Cl-5-CF ₃ TPCP) ₄	107
Scheme 4.10 Sonogashira coupling and hydrolysis from 244	109
Scheme 4.11 Synthesis of S-2-Cl-5-CF ₃ TPCP-ligand with TIPS-ethynyl at B	110
Scheme 4.12 Synthesis of Rh ₂ (S-2-Cl-5-CF ₃ TPCP) ₃ (ethynyl@B) and immobilization	112
Scheme 5.1 Common approaches for α-diazocarbonyl compounds synthesis	114
Scheme 5.2 Metal oxide as oxidant for hydrazone oxidation in flow	116
Scheme 5.3 Oxidation of hydrazones using TsNIK.....	117
Scheme 5.4 Oxygen as terminal oxidant for hydrazone decomposition	118
Scheme 5.5 Substrates scope for Cu(OAc) ₂ -catalyzed hydrazone oxidation.....	126

Table of Figures

Figure 1.1 Three types of dirhodium (II) catalysts in paddlewheel structures	5
Figure 2.1 Paddlewheel structure and potential geometries	12
Figure 2.2 X-ray crystal structures (top-view) of $\text{Rh}_2(R\text{-}p\text{-BrTPCP})_4$, $\text{Rh}_2(S\text{-}p\text{-PhTPCP})_4$ and $\text{Rh}_2[S\text{-}3,5\text{-di}(p\text{-}^t\text{BuC}_6\text{H}_4)\text{TPCP}]_4$	14
Figure 2.3 X-ray crystal structures (top-view) of $\text{Rh}_2(R\text{-TCPTAD})_4$ and $\text{Rh}_2(S\text{-TPPTTL})_4$	15
Figure 2.4 X-ray crystal structure of $\text{Rh}_2(S\text{-}o\text{-CITPCP})_4$	21
Figure 2.5 ^1H NMR spectra of $\text{Rh}_2(S\text{-}o\text{-BrTPCP})_4$ (top) and $\text{Rh}_2(S\text{-}o\text{-CITPCP})_4$ (bottom)	22
Figure 2.6 Variable-temperature ^1H -NMR of $\text{Rh}_2(S\text{-}o\text{-BrTPCP})_4$ in toluene- d_8	23
Figure 2.7 Crystal structures of $\text{Rh}_2(S\text{-}2\text{-Cl-}4\text{-BrTPCP})_4$ and $\text{Rh}_2(S\text{-}2\text{-Cl-}5\text{-BrTPCP})_4$	33
Figure 2.8 Demonstration for the axial chirality.....	36
Figure 2.9 Variable-temperature NMR studies at 600 MHz in CDCl_3	37
Figure 2.10 Eyring plots for rate constants of rotation in ligands 24 , 56a and 56b	38
Figure 2.11 Newman-projection for intermediate at transition state	43
Figure 2.12 DFT studies on rotational barrier of 56b	61
Figure 2.13 Calculated conformers of $\text{Rh}_2(S\text{-}2\text{-Cl-}5\text{-BrTPCP})_4$ with Gibbs free energies.....	62
Figure 2.14 Calculated structures of rhodium carbenes.....	62
Figure 3.1 Examples of piperidine-containing pharmaceuticals.....	64
Figure 4.1 General schematic description of a continuous flow reactor.....	82
Figure 4.2 Catalyst immobilization methods and construction of covalent binds	84
Figure 4.3 Intermolecular cycloaddition with polymer-supported $\text{Rh}_2(S\text{-TCPTTL})_4$ in flow	92
Figure 4.4 Three anchor sites for immobilizing $\text{Rh}_2(S\text{-}o\text{-CITPCP})_4$	98
Figure 4.5 Structure of $S\text{-}2\text{-Cl-}5\text{-BrTPCP}$ ester derivative 237	106

Figure 5.1 React-IR studies on diazo generation from hydrazone oxidation..... 122

Table of Tables

Table 2.1 Cyclopropanation of methyl 2-(2-chlorophenyl)-2-diazoacetate.....	19
Table 2.2 Initial examination of Rh ₂ (<i>S</i> - <i>o</i> -CITPCP) ₄ on cyclopropanation of styrene	23
Table 2.3 Initial examination of Rh ₂ (<i>R</i> - <i>o</i> -CITPCP) ₄ on C–H insertion of <i>p</i> -cymene	24
Table 2.4 Initial examination of Rh ₂ (<i>R</i> - <i>o</i> -CITPCP) ₄ on C–H insertion of 4-ethyltoluene.....	25
Table 2.5 Initial examination of Rh ₂ (<i>S</i> - <i>o</i> -CITPCP) ₄ on C–H insertion of cyclohexane	26
Table 2.6 Examination of Rh ₂ (<i>S</i> - <i>o</i> -CITPCP) ₄ on C–H insertion of 1,3-dioxolane	27
Table 2.7 Examination of C–H insertion on 4,5-diester-1,3-dioxolane	29
Table 2.8 Examination of C–H insertion on 4-bromoethylbenzene.....	30
Table 2.9 C–H Insertion of 4-bromoethylbenzene using Rh ₂ (<i>S</i> - <i>o</i> -CITPCP) ₄ derivatives.....	34
Table 2.10 Comparison between “pure” and “mixture” batches of Rh ₂ (<i>S</i> -2-Cl-5-BrTPCP) ₄	35
Table 2.11 Calculation of rate constants	38
Table 2.11 Calculation of rotational barriers (ΔG^\ddagger)	38
Table 2.12 Catalyst optimization for C–H functionalization on 1-bromo-4-pentylbenzene.....	46
Table 2.13 Solvent and additive effects on the C–H functionalization of 48	48
Table 2.13 Screening for alkyl chain lengths and diazoacetates.....	51
Table 2.14 Competition reaction.....	56
Table 2.15 Condition optimization for 4-fold Suzuki coupling on Rh ₂ (<i>S</i> -2-Cl-4-BrTPCP) ₄	58
Table 2.16 Synthesis and testing of more Rh ₂ (<i>S</i> - <i>o</i> -CITPCP) ₄ derivatives.....	59
Table 3.1 Catalysts screening using methyl diazoacetate on <i>N</i> -Boc-piperidine	69
Table 3.2 Catalysts screening using trichloroethyl diazoacetate on <i>N</i> -Boc-piperidine.....	71
Table 3.3 C2–H functionalization on <i>N</i> -tosyl-piperidine.....	71
Table 3.4 C2–H functionalization on <i>N</i> - <i>p</i> -bromophenylsulfonyl-piperidine.....	73

Table 3.5 Protecting group optimization for C–H insertion at C4.....	76
Table 3.6 Scope for the C3-substituted analogs.....	79
Table 4.1 Cyclopropanation using immobilized Rh ₂ (<i>S</i> -TBSP) ₄ and recyclability.....	88
Table 4.2 C–H insertion using immobilized Rh ₂ (<i>S</i> -DOSP) ₄ and recyclability	89
Table 4.3 Performance of different dirhodium catalysts with resin-supported pyridine	90
Table 4.4 Catalyst screening on cyclopropanation of asymmetric 1,1-diarylethylene	101
Table 4.5 Synthesis for Rh ₂ (<i>S</i> - <i>o</i> -CITPCP) ₄ derivatives with ethynyl on ring B and C	103
Table 4.6 Testing reaction for Rh ₂ (<i>S</i> - <i>o</i> -CITPCP) ₄ derivatives with linker at site A , B and C ...	104
Table 4.7 Comparison of electronic and steric features among potential functional groups	107
Table 4.8 Testing of Rh ₂ (<i>S</i> -2-Cl-5-CF ₃ TPCP) ₄ in C–H insertion on 4-bromopentylbenzene ...	108
Table 4.9 Catalyst screening on asymmetric cyclopropanation using 2-Cl-5-CF ₃ -diazoacetate	109
Table 4.10 Testing of immobilized catalyst in C–H insertion on 4-bromopentylbenzene	112
Table 5.1 Copper source screening for hydrazone oxidation.....	119
Table 5.2 Further optimization for Cu(OAc) ₂ -catalyzed hydrazone oxidation.....	121
Table 5.3 Continuous modification on loading and usage of air	124

List of Abbreviations

Ac	acetyl
APCI	atmospheric pressure chemical ionization
Ar	aryl
Bn	benzyl
Boc	<i>tert</i> -butyloxycarbonyl
Bu	butyl
Bs	<i>para</i> -bromophenylsulfonyl
DBU	1,8-diazabicycloundec-7-ene
1,2-DCE	1,2-dichloroethane
DCM	dichloromethane
DIBAL-H	diisobutylaluminum hydride
DMAP	<i>N,N</i> -4-(dimethylamino)pyridine
DMB	2,2-dimethylbutane
DMF	2,2-dimethylbutane
dppf	1,1'-bis(diphenylphosphino)ferrocene
dr	diastereomeric ratio
EDG	electron-donating group
ee	enantiomeric excess
Et	ethyl
equiv	equivalents
ESI	electrospray ionization
EWG	electron-withdrawing group
HPLC	high performance liquid chromatography
HRMS	high-resolution mass spectrometry
<i>hν</i>	light
IR	infrared spectroscopy
L	ligand

LDA	lithium diisopropylamide
Me	methyl
mmol	millimoles
Ms	mesyl
NMR	nuclear magnetic resonance
N.R.	no reaction
NSI	nanospray ionization
OMe	methoxy
<i>p</i>-ABSA	<i>para</i> -acetamidobenzenesulfonyl azide
PG	protecting group
Ph	phenyl
Phth	phthalimide
Piv	pivaloyl
Pr	propyl
TBAF	tetrabutylammonium fluoride
TBME	<i>tert</i> -butyl methyl ether
TBS	<i>tert</i> -butyldimethylsilyl
TEA	triethylamine
temp	temperature
Tf	trifluoromethanesulfonyl
THF	tetrahydrofuran
TIPS	triisopropylsilyl
TLC	thin layer chromatography
TMEDA	<i>N,N,N'N'</i> -tetramethylethylenediamine
TMS	trimethylsilyl
TS	transition state
Ts	tosyl

Chapter 1. Introduction to Selective C–H Functionalization via Rhodium Carbenes

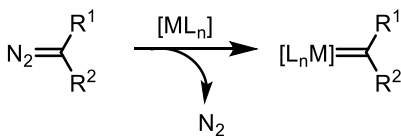
1.1. Site-selective C–H Functionalization

Through a significant amount of efforts from chemists and even chemical engineers, C–H functionalization has moved from an organometallic novelty to become a practical technology as a modern strategic approach to construct complex molecules.¹⁻⁷ A defining challenge for broadening its general utility is the differentiation between several similar C–H bonds in a site-selective and stereoselective manner. Early site-selectivity between C–H bonds was achieved mainly in intramolecular reactions following the Baldwin's rules.^{8,9} Radical reactions, generated by traditional methods or photoredox protocols, are typically controlled by the inherent reactivity profile of the substrates. However, site-selectivity of these reaction can be achieved by means of intramolecular hydrogen transfer such as the Hofmann-Löffler-Freytag reaction.¹⁰⁻¹⁵ Similar to the discovery that the site-selectivity could be controlled intramolecularly in these radical intermediates, extensive works has been done to utilize the directing groups on substrates to dictate the site-selectivity by chelation with a metal catalyst. Recently, transient directing groups and removal/utilization of directing groups in the following steps have also been well studied as a way to limit functional group manipulations.¹⁶⁻²⁰ In contrast to utilizing the inherent property of the substrates, in some cases, the site-selectivity in the radical reactions are influenced by the sterically encumbered hydrogen abstraction reagents.^{21, 22} There is a challenging but potentially more flexible strategy that relies on the metal catalyst itself to control the site- and stereoselectivity, which is independent of the inherent reactivity features of the substrates.²³⁻²⁷ Similarly, enzymes, which are known to be selective for specific classes of substrates and reactions, have been engineered to be applied in desired site-selective C–H activations beyond the scope of the natural enzymes.²⁸⁻³⁰ In addition to the modification on enzymes, highly reactive transition metals

together with various specially designed ligands would also be effective for a general platform for catalyst-controlled selective C–H functionalization. The ultimate outcome of this catalyst-controlled C–H functionalization strategy would be the generation of a toolbox with a series of catalysts, each with a defined characteristic to tune the selectivity at will.

One of the most impressive and currently active approaches for catalyst-controlled C–H functionalization and C–C bond construction is the usage of metal carbenes. These metal carbenes are commonly generated from the decomposition of diazo compounds by various metal catalysts, such as copper and rhodium, and stabilized by the electronic interaction between the metal and the carbene carbon (Scheme 1.1).³¹

Scheme 1.1 Metal carbene generation from diazo compound decomposition

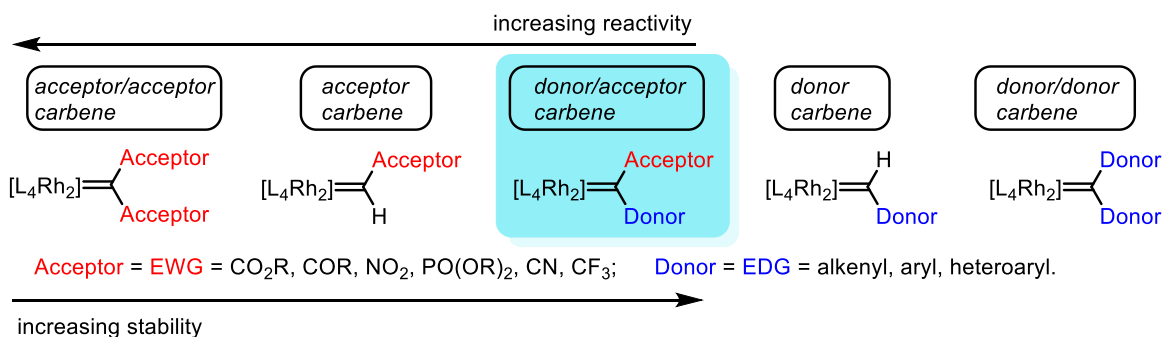


1.2. Rhodium Carbene Chemistry

Dirhodium (II) complexes are the most efficient catalysts for metal carbene transformations.³²
³³ The choice of the metal catalysts can affect the efficiency of diazo decomposition and reactivity of the generated metal carbenes, and therefore is critical for reaction design. Computational studies indicate that rhodium carbenes are very electrophilic,^{34, 35} and their spectroscopic data are comparable to group VI Fischer carbene complexes found in the literatures.³⁶ That is, the rhodium carbene carbon is electron-deficient with σ -donor feature to the rhodium and weak acceptor feature for π back-bonding from rhodium. The reactivity and stability of the rhodium carbenes are directly related to the electronic property of the substituents on the carbene carbon, and they are

consequently classified into five groups (Scheme 1.2).^{31, 37-40} The ‘acceptor’ refers to electron-withdrawing groups which enhance the electrophilicity of the carbon center and therefore increases the reactivity, whereas the ‘donor’ refers to electron-donating groups that stabilize the metal carbenes and therefore lowers the reactivity for increasing selectivity.³⁷ The initial exploration of rhodium carbenes, which used acceptor and acceptor/acceptor carbenes, were mainly focused on the intramolecular reactions due to limited control of site-selectivity in intermolecular reactions with such high reactivity.^{31, 41} Hence, in order to achieve the desired site-selectivity while maintaining appropriate reactivity for intermolecular reactions, the Davies group developed a less reactive class of carbenes with great balance between reactivity and selectivity, the donor/acceptor carbenes in the 1980’s and they have contributed to exploration of this system since then.^{42, 43}

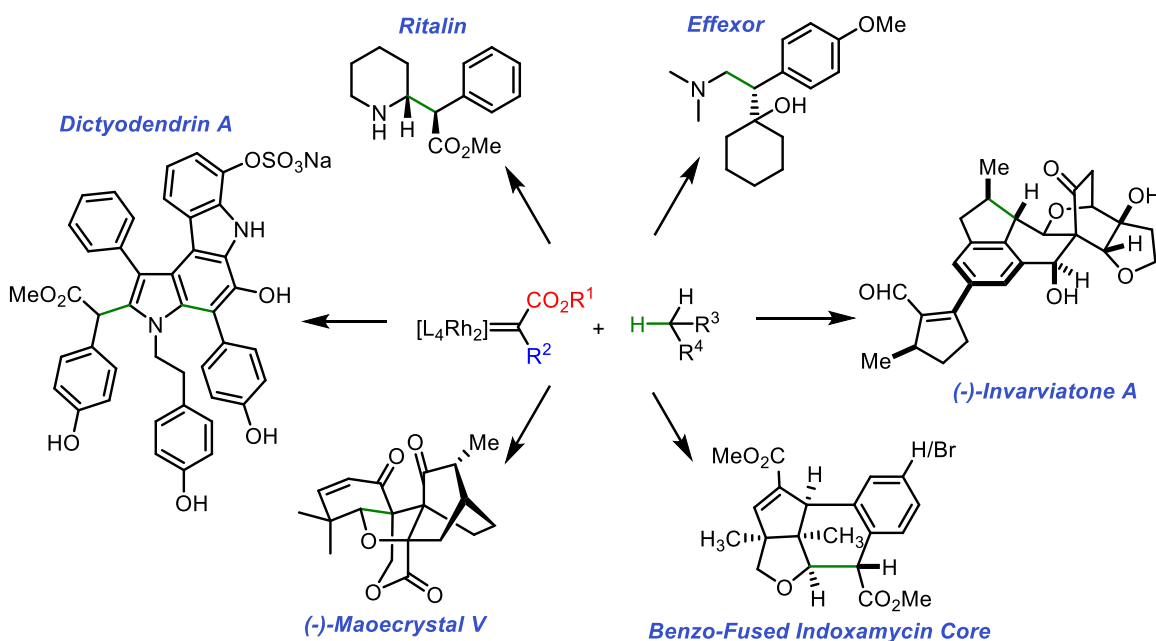
Scheme 1.2 Classes of rhodium carbenes



Since the conception of donor/acceptor carbenes, several dirhodium catalysts have been developed for site- and stereoselective C–H functionalization. This rhodium carbene chemistry has been further applied in the synthesis of different pharmaceuticals and natural products (Scheme 1.3 with the bond generated via rhodium carbene C–H functionalization in green). The simplest example is the synthesis of Ritalin via C2–H insertion of piperidine,⁴⁴ followed by Effexor via primary C–H bond insertion of methylamine.⁴⁵ Collaborations between the Davies group and others lead to the accomplishment of some more complex total synthesis, including the

dictyodendrin A with the Itami group,⁴⁶ (-)-meoecrystal V with the Zakarian group,⁴⁷ and benzo-fused indoxamycin core with the Sorensen and Yu groups.⁴⁸ An intramolecular C–H insertion was also utilized in the construction of (-)-invarvatonone by the Lei group.⁴⁹

Scheme 1.3 Synthetic application of rhodium donor/acceptor carbene in C–H functionalization



1.3. Dirhodium Tetracarboxylate Catalysts

In addition to the substituents on the carbenes, the reactivity and selectivity are also controlled by the dirhodium catalysts, or the ligand framework surrounding the metal center more specifically, which further advance the possibilities of the rhodium carbene chemistry. These dirhodium complexes are mostly stable to heat and moisture under ambient conditions but they are exceptional catalysts for diazo decomposition and formation of the transient rhodium carbenes. All these advantages contribute to the broad application of these dirhodium catalysts. The core of these complexes is binuclear that constructed through a rhodium-rhodium single bond, and octahedral geometry is adopted by each rhodium to give a paddlewheel structure surrounded by

four equatorial μ_2 -ligands and two axial ligands.^{50, 51} The parent complex, $\text{Rh}_2(\text{OAc})_4$, contains four acetate ligands at equatorial positions and two labile axial ligands (normally solvent molecules and omitted for clarity). The axial ligands can be easily replaced by the diazo compounds to form the carbenes as was originally discovered for ethyl diazoacetate decomposition by the Teyszié group in the 1970's.⁵² With the same dirhodium core, the performance of different catalysts can be altered by the appropriate ligands. Further exploration on $\text{Rh}_2(\text{OAc})_4$ with ligand exchanges generated three main types of dirhodium complexes: dirhodium (II) carboxylates, dirhodium (II) phosphonates and dirhodium (II) carboxamides (Figure 1.1).

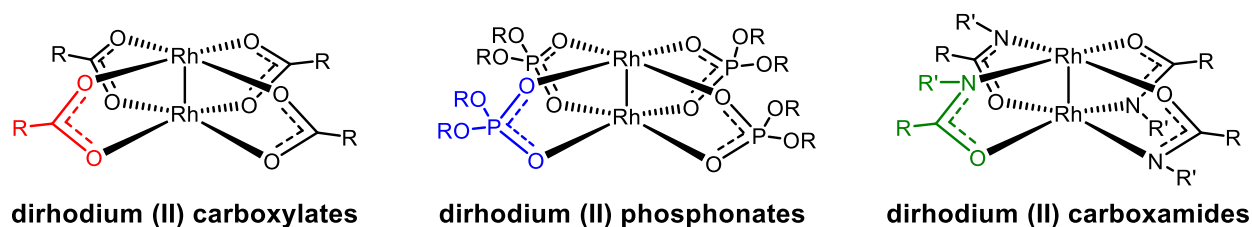
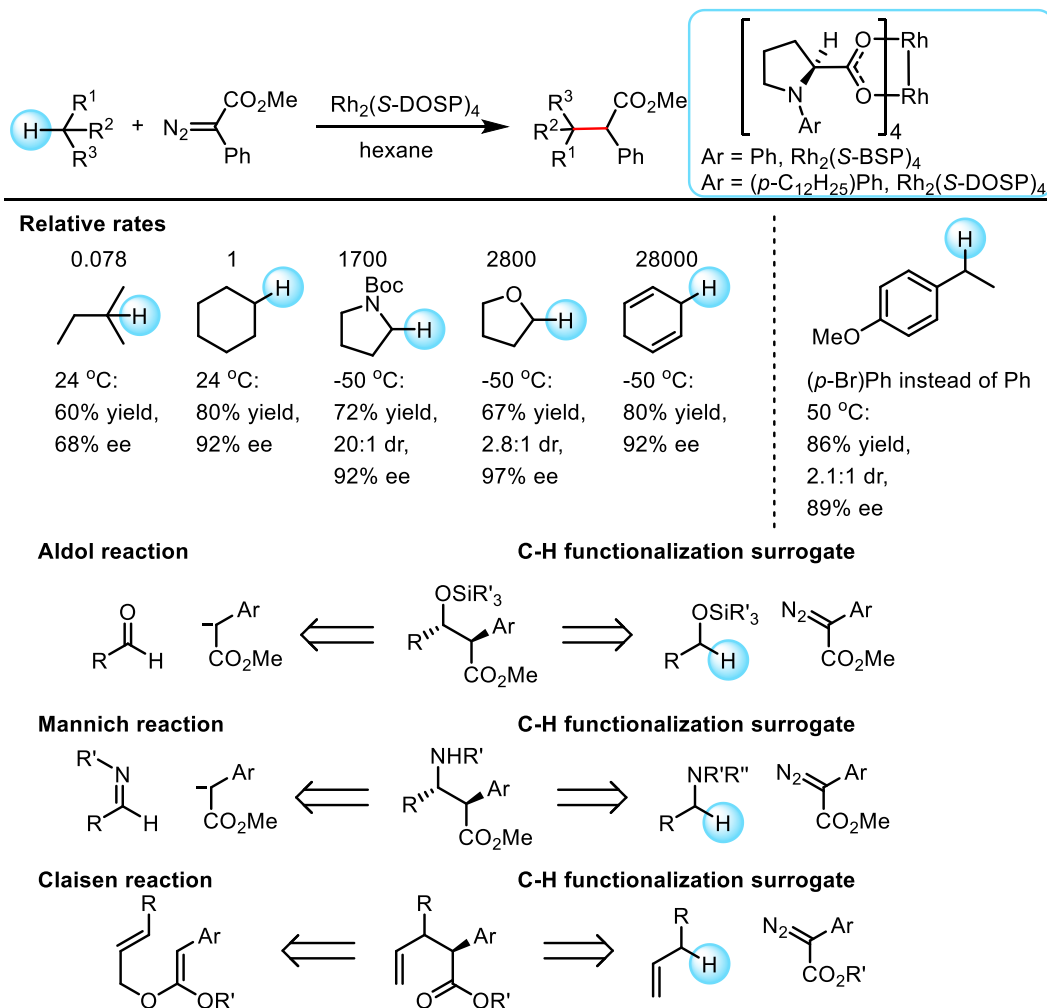


Figure 1.1 Three types of dirhodium (II) catalysts in paddlewheel structures

Despite the clear advantage of $\text{Rh}_2(\text{OAc})_4$ in rhodium carbene transformations, chiral ligands are needed for asymmetric induction. The first evaluation of some early chiral dirhodium complexes by Brunner in 1989 produced very low enantioselectivity ($\leq 12\%$ ee) in cyclopropanation of styrene with ethyl diazoacetate.⁵³ This caused the early hypothesis that asymmetric transformation with this class of catalysts would be ineffective since the chiral ligands are at the equatorial position and points to the periphery of the catalyst and would have insufficient interaction with the axially bound carbene.⁵⁴ The enantioselectivity of the chiral dirhodium complexes were explored further by the McKervy group, and an unprecedented 82% ee was able to be obtained in intramolecular C–H insertions using $\text{Rh}_2(S\text{-BSP})_4$.⁵⁵⁻⁵⁷ This proline-based dirhodium catalyst was later optimized by the Davies group to a currently more widely-used catalyst, $\text{Rh}_2(S\text{-DOSP})_4$, that produced high enantioselectivity (up to 94% ee) in intermolecular

cyclopropanation.^{58, 59} With extensive exploration on the cyclopropanation and/or combined rearrangements using dirhodium donor/acceptor carbene chemistry, its employment in the C–H functionalization (or C–H insertion) was not explored until late 1990s. Since then, multiple projects have been developed for C–H functionalization on hydrocarbons and various substrates containing heteroatoms and functional groups, mostly for fundamental understanding of the reactivity profile^{43, 60, 61} and as surrogates⁶²⁻⁶⁵ to some of the classic organic transformations (Scheme 1.4). Notably, $\text{Rh}_2(\text{S-DOSP})_4$ is capable of functionalizing a wide range of C–H bonds with moderate to high enantioselectivity and generally preferring electronically activated C–H bonds, including benzylic, allylic and C–H bonds adjacent to oxygen or nitrogen atoms.

Scheme 1.4 Reactivity profile and surrogate reactions using $\text{Rh}_2(\text{S-DOSP})_4$

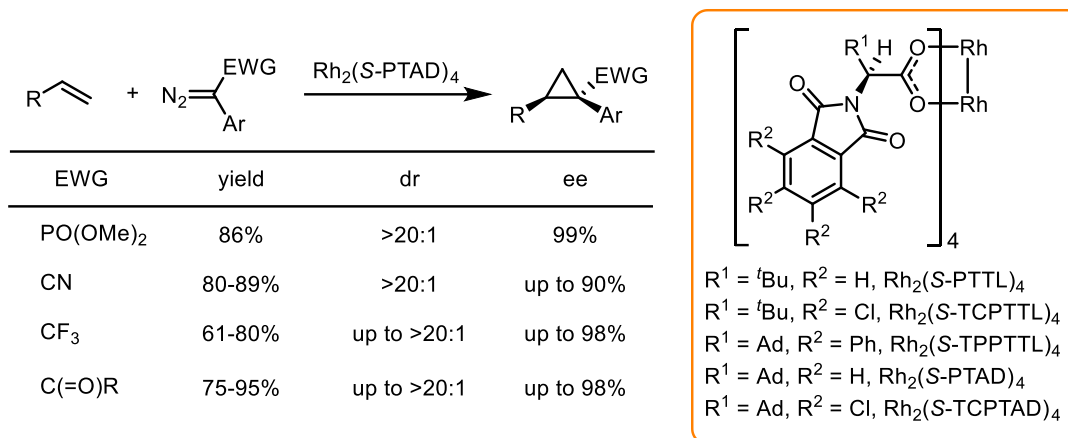


Other proline-based dirhodium catalysts, such as $\text{Rh}_2(\text{S-biDOSP})_4$, with additional linker (phenyl group) between C4 positions on the proline rings of the two ligands rigidifying the catalyst conformations, were also synthesized for further improvement on the stereoselectivity and to overcome the solvent limitation on requiring the use of nonpolar solvents. However, even though $\text{Rh}_2(\text{S-biDOSP})_4$ displays interesting properties, it has not been fully explored because of the complex synthesis route and the use of *tert*-butyllithium.^{66, 67}

Phthalimido-based catalysts were later developed as an important class of chiral dirhodium catalysts. It was initially developed by the Hashimoto group with $\text{Rh}_2(\text{S-PTTL})_4$ and its tetrachloro-derivative, $\text{Rh}_2(\text{S-TCPTTL})_4$, as the most significant representatives.⁶⁸⁻⁷⁰ Inspired by the promising performance of these phthalimido-based dirhodium catalysts in carbene transformation reactions, along with the ability of $\text{Rh}_2(\text{S-DOSP})_4$ to catalyze enantioselective tertiary C–H insertion of adamantane, $\text{Rh}_2(\text{S-PTAD})_4$ was developed as well as $\text{Rh}_2(\text{S-TCPTAD})_4$.^{71, 72} The adamantyl group in $\text{Rh}_2(\text{S-PTAD})_4$ is believed to be able to enhance the asymmetric induction due to its bulkiness compared to the *tert*-butyl group in $\text{Rh}_2(\text{S-PTTL})_4$. Since the development of these phthalimido-based dirhodium catalysts, they not only serve as an alternative tool that is complementary to $\text{Rh}_2(\text{S-DOSP})_4$ in the asymmetric induction, but also expand the scope of donor/acceptor carbenes with acceptor groups beyond alkyl esters, incorporating phosphonates⁷¹, nitrile⁷³, trifluoromethyl⁷⁴ and ketones⁷⁵, with high stereo-control (Scheme 1.5). The tetrachloro-derivative, $\text{Rh}_2(\text{S-TCPTAD})_4$, was recently utilized in the asymmetric site-selective functionalization of terminal unactivated tertiary C–H bonds (Scheme 1.6).⁷⁶ More recently, a newer catalyst, $\text{Rh}_2(\text{S-TPPTTL})_4$, was developed with an additional propeller-like chirality introduced by the 16 phenyl substituents at the same face, and was found

to be superior in desymmetrizing the alkylcyclohexanes at the C3 equatorial C–H bond in a site- and stereoselective manner.⁷⁷

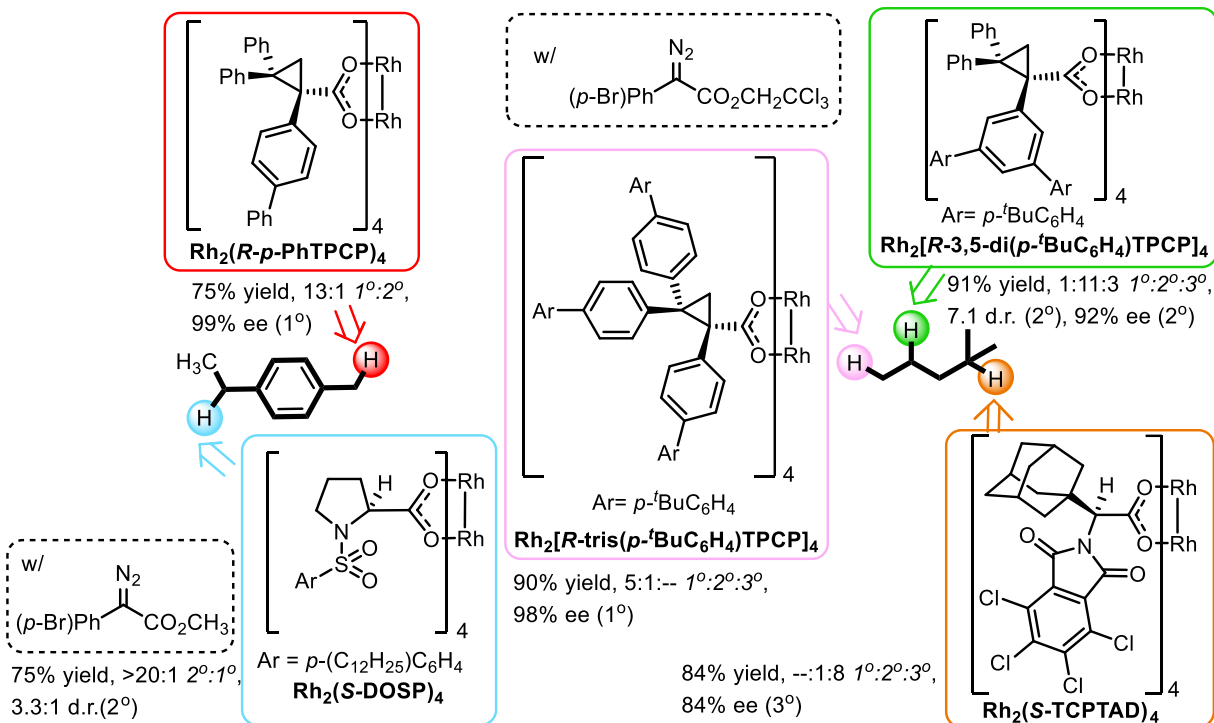
Scheme 1.5 Structure and reaction example of $\text{Rh}_2(\text{S-PTAD})_4$



Taking advantage of the two classes of the chiral dirhodium carboxylate catalysts that can generate a variety of cyclopropanes with high enantioselectivity as single diastereomer, the third class of dirhodium catalysts, $\text{Rh}_2(\text{TPCP})_4$, were developed by the Davies group. These catalysts have triarylcyclopropane carboxylates as the chiral ligands. One of the initial examples, $\text{Rh}_2(\text{R-}p\text{-BrTPCP})_4$ was found to be capable of conducting cyclopropanation reactions with high enantioselectivity, comparable to the first and second generation catalysts.⁷⁸ It was further modified into $\text{Rh}_2(\text{R-}p\text{-PhTPCP})_4$, in which the bromide substituent on the C1-aryl ring was changed to phenyl group, and it was the first time that the site-selectivity for C–H functionalization was switched by only changing the catalyst (Scheme 1.6).⁷⁹ Moreover, the site-selectivity was further improved when a trihaloethyl ester group was used as the acceptor part in the carbene precursor instead of the previously used methyl ester, and this ester switch also gave cleaner reactions.⁸⁰ Recently, two even bulkier catalysts in the $\text{Rh}_2(\text{TPCP})_4$ class were synthesized, $\text{Rh}_2[\text{R-}3,5\text{-di}(p\text{-}^t\text{BuC}_6\text{H}_4)\text{TPCP}]_4$ and $\text{Rh}_2[\text{R-tri}(p\text{-}^t\text{BuC}_6\text{H}_4)\text{TPCP}]_4$ with additional aryl rings at the *meta*-

or *para*-position of the C1-aryl rings. They allowed the functionalization of the unactivated secondary and primary C–H bonds, respectively at sterically the most accessible sites.^{81, 82}

Scheme 1.6 Structure of the Rh₂(TPCP)₄ catalysts and site-selectivity



Besides of the dirhodium (II) carboxylate, the other two types of the chiral dirhodium catalysts have different reactivity and selectivity profile, so they are not explored in this dissertation. The dirhodium (II) phosphonates, firstly introduced by the McKervy group,⁵⁶ are typically more electron-deficient than the carboxylate type because the phosphonate ligands are less basic.³¹ On the other hand, the dirhodium (II) carboxamides, initially developed by Doyle,⁸³ are more electron-rich with highly basic carboxamide ligands that make the corresponding carbene less active but more selective.³¹

With four C₁-ligands coordinated to the Rh-Rh metal center, these dirhodium catalysts are adopting conformations with higher symmetries than the original ligands. Catalysts with high symmetry are desirable in catalyst design, because they can be more predictable in transition states

by limiting the number of possible pathways for how the substrate can approach. Unlike most of other metal catalysts that require high symmetry ligands, such as C_2 and D_2 -symmetry, for high symmetry catalysts, higher symmetry dirhodium complexes can be generated using low symmetry ligands, which could be even C_1 -symmetry, due to their uniquely symmetric dirhodium core.⁸⁴ Catalyst symmetry will be discussed further in chapter 2.

The focus of the projects described in the dissertation is the synthesis and application of a series of C_4 -symmetric dirhodium (II) catalysts derived from 1-(2-chlorophenyl)-2,2-diphenylcyclopropanecarboxylate ligands. The dissertation will cover the synthesis and initial examination of these catalysts for their ability in enhancing diastereoselectivity (Chapter 2), application in C–H functionalization at terminal unactivated methylene site overcoming the electronical preference (benzylic site) (Chapter 2), application in controlled site-selective functionalization of piperidines for methylphenidate analogs (Chapter 3) and immobilization for reactions in flow (Chapter 4). In addition, alternative method for diazo compounds generation that may potentially be beneficial for reactions in flow was also explored (Chapter 5).

Chapter 2. Synthesis and Development of the Sterically Demanding C₄-Symmetric Catalysts, the Rh₂(*o*-CITPCP)₄ Series, for Overcoming Electronic Preference

2.1. Introduction

2.1.1 Symmetry of Dirhodium (II) Carboxylate Catalysts

A variety of dirhodium (II) carboxylate catalysts have been developed for asymmetric reactions using donor/acceptor carbenes. These dirhodium catalysts are structurally unique adopting a paddlewheel structure, where the core with the rhodium-rhodium single bond is surrounded by four carboxylate ligands at the equatorial position and two axial positions are usually occupied by solvent molecules. This paddlewheel structure can be simplified to a disk, which represents the O-Rh-O plane with Rh at the center of the disk (Figure 2.1).⁸⁴ The axial ligands on most of the dirhodium complexes are labile, which could be replaced by carbenes for desired active catalytic transformations, while the paddlewheel structure with the coordination between the dirhodium core and equatorial ligands is stable and would not be alternated during the carbene transformations. Thus, the rhodium carbene reactions occur on the axial positions on these dirhodium paddlewheel-like complexes. In order to generate chiral products from these rhodium carbene intermediates, the equatorial ligands need to induce a chiral environment at the axial active site. One strategy is the utilization of “blocking groups” from the equatorial ligands that orient towards either α (top) or β (bottom) face (axial positions) of the disk. If only two orientations (α or β) is considered for each ligand, coordinating to four C₁-symmetric ligands which are most commonly used in dirhodium (II) carboxylate complex, four types of geometries could be potentially obtained: the “blocking groups” pointing to all-up ($\alpha, \alpha, \alpha, \alpha$ in C₄), 3-up-1-down ($\alpha, \alpha, \alpha, \beta$ in C₁) and 2-up-2-down ($\alpha, \alpha, \beta, \beta$ in C₂ and $\alpha, \beta, \alpha, \beta$ in D₂) (Figure 2.1). The proposed model was motivated by one of the earliest catalysts, proline-based Rh₂(*S*-DOSP)₄, that was

believed to adopt a D_2 -symmetry geometry with two equivalent axial faces for carbene generation, and it predicted most of the stereoselectivity of the asymmetry inductions of this catalyst.^{59, 85} Interestingly, none of these proposed orientations fit with a newly-generated crystal structure of a proline-based rhodium-bismuth complex, which was proposed to be D_2 geometry as its dirhodium analog, but instead the *N*-arylsulfonyl groups in the ligands was found to be flexible enough to orient at the periphery of the complex.⁸⁶ Additionally, computation studies on $Rh_2(S-DOSP)_4$, in collaboration between the Davies and Musaev groups, also found the favored conformation contradicted to the previously proposed model (unpublished results). However, this model with “blocking groups” is found to be widely applicable and predictive for most of the recent classes of dirhodium carboxylate catalysts, such as the phthalimido- and triarylcyclopropane-based complexes, which have been confirmed by their crystal structures experimentally and calculated carbene intermediates. This chapter will mainly focus on the development of a series of new catalysts in the triarylcyclopropane family, so this model will be applicable in this dissertation.

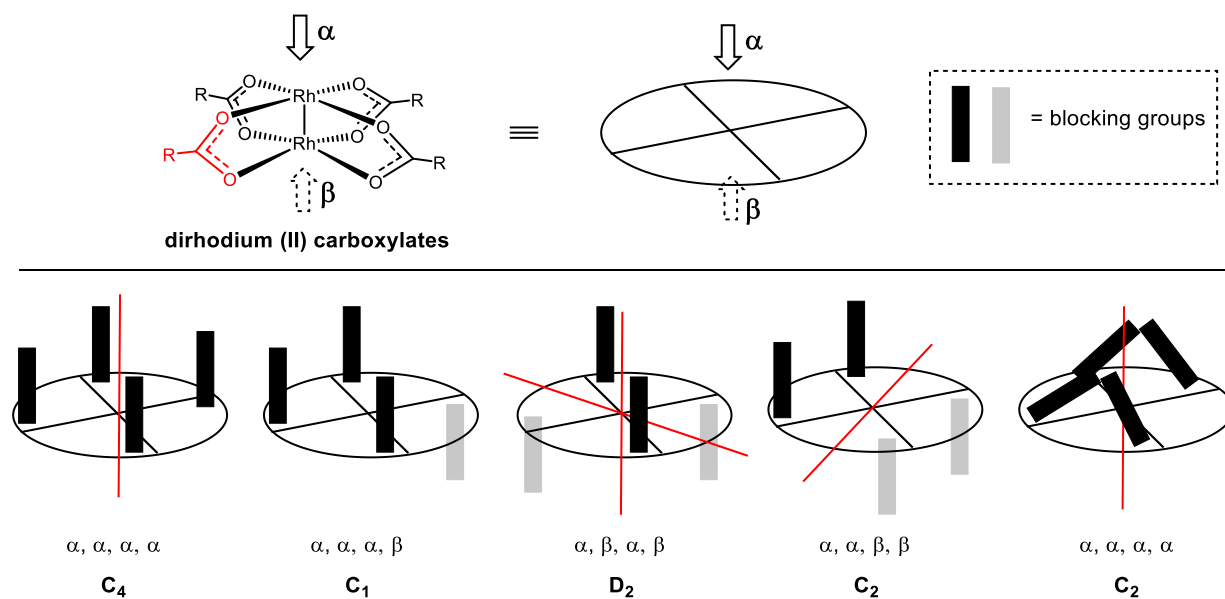


Figure 2.1 Paddlewheel structure and potential geometries

The dirhodium (II) triarylcyclopropanecarboxylates, $\text{Rh}_2(\text{TPCP})_4$, adopt various symmetry orientations (mainly D_2 and C_2) assigned based on their crystal structures and can be described using this proposed “blocking groups” model. This class of catalysts are called the third generation of dirhodium carboxylate catalysts in the Davies group, because the TPCP ligand scaffold is generated from the stereoselective cyclopropanation using the earlier dirhodium catalysts, $\text{Rh}_2(\text{DOSP})_4$ and $\text{Rh}_2(\text{PTAD})_4$. The first published $\text{Rh}_2(\text{TPCP})_4$ catalyst was developed by Dr. Jørn Hansen and Dr. Changming Qin. $\text{Rh}_2(p\text{-BrTPCP})_4$, which contains *p*-Br substituents on the C1-aryl rings, adopts a D_2 symmetric conformation and both Rh faces are equivalent for asymmetric induction (Figure 2.2).⁷⁸ A later modified catalyst, $\text{Rh}_2(p\text{-PhTPCP})_4$, with *p*-Ph instead of *p*-Br substituents, was found to be more sterically demanding and switches the site-selectivity of C–H insertions to electronically activated primary C–H bonds, while the electronically activated methylene sites are preferred by $\text{Rh}_2(S\text{-DOSP})_4$.⁷⁹ A crystal structure of $\text{Rh}_2(p\text{-PhTPCP})_4$ was recently obtained, which showed the catalyst adopting a C_2 -symmetry (Figure 2.2).⁸⁷ However, rather than the C_2 symmetric orientation with 2-up-2-down, $\text{Rh}_2(p\text{-PhTPCP})_4$ has all *p*-Ph aryl groups pointing to the same face due to the π - π stacking effect between the two adjacent biphenyl groups. More recently, $\text{Rh}_2[3,5\text{-di}(p\text{-}^t\text{BuC}_6\text{H}_4)\text{TPCP}]_4$, which contains two *tert*-butylphenyl groups at the *meta*-positions on each C1-aryl ring, was discovered to be D_2 -symmetric in the crystal structure, since the 3,5-di(*p*-^tBuC₆H₄)-aryl groups would be too bulky for two adjacent ones to be on the same face of the rhodium disk.⁸¹

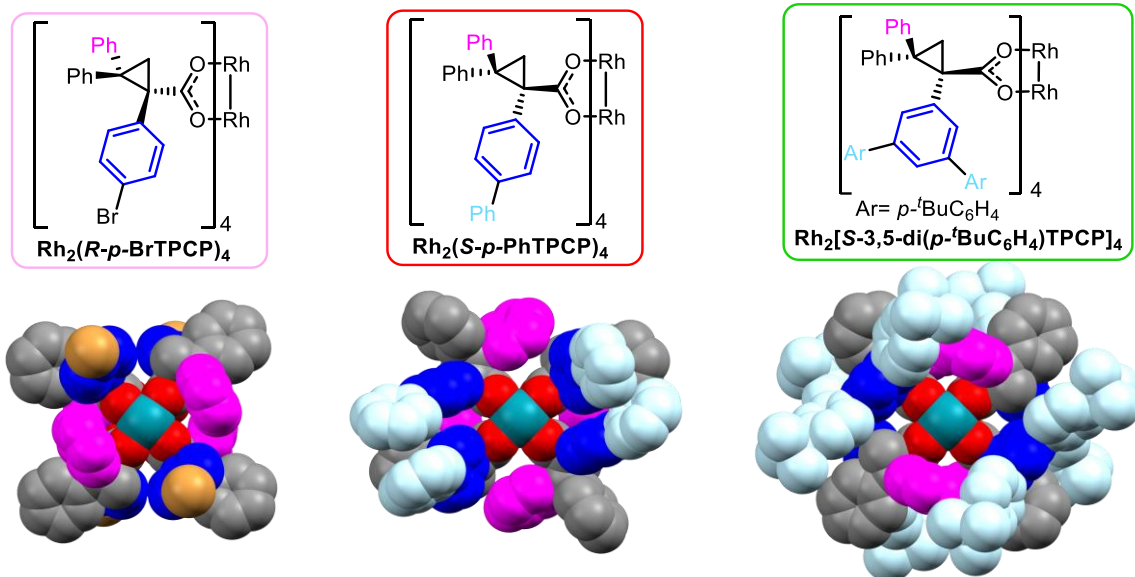


Figure 2.2 X-ray crystal structures (top-view) of $\text{Rh}_2(\text{R-}p\text{-BrTPCP})_4$, $\text{Rh}_2(\text{S-}p\text{-PhTPCP})_4$ and $\text{Rh}_2[\text{S-3,5-di}(p\text{-}^t\text{BuC}_6\text{H}_4)\text{TPCP}]_4$

Initially the complexes with C_1 - or C_4 -symmetry were considered to be impractical originally with the models in Figure 2.1, because the carbene could bind to either face of the catalyst and could result in at least two reaction pathways.⁸⁴ However, the crystal structures of most of the phthalimido-based dirhodium (II) carboxylate catalysts are found to be adopting an approximately C_4 symmetric orientation. A C_4 symmetric “chiral crown” conformation was reported by the Fox group in 2009 for the X-ray crystal structure of $\text{Rh}_2(\text{S-PTTL})_4$,⁸⁸ and a more rigid C_4 symmetric conformation is also found for its tetrachloro-derivative, $\text{Rh}_2(\text{S-TCPTTL})_4$.⁸⁹ This conformation of their dirhodium complexes in the solid state is retained in the rhodium carbene intermediates, whose X-ray crystal structures are obtained by the Fürstner’s group in 2016.³⁹ In these C_4 symmetric structure that $\text{Rh}_2(\text{S-PTTL})_4$ and $\text{Rh}_2(\text{S-TCPTTL})_4$ adopted, the phthalimido groups are oriented to the same face (α) for asymmetric reactions, while the β face is inaccessible due to the bulky *tert*-butyl groups. Replacing the *tert*-butyl groups with bulkier adamantyl groups, $\text{Rh}_2(\text{S-PTAD})_4$ and $\text{Rh}_2(\text{S-TCPTAD})_4$ also adopt the C_4 symmetric conformation (Figure 2.3).⁷⁶

Furthermore, when the phthalimido groups are fully substituted with four phenyl groups, which gives $\text{Rh}_2(\text{S-TPPTTL})_4$, C_4 symmetric conformation is maintained with additional propeller like chirality with the 16 phenyl rings tilting in one way (Figure 2.3).

This dissertation will cover the synthesis of a new series of C_4 -symmetric catalysts in the $\text{Rh}_2(\text{TPCP})_4$ class. A discussion of the unusual structure of these catalysts will be presented as well as their initial exploration on reactivity profile which led to the discovery of their incomparable site-selectivity.

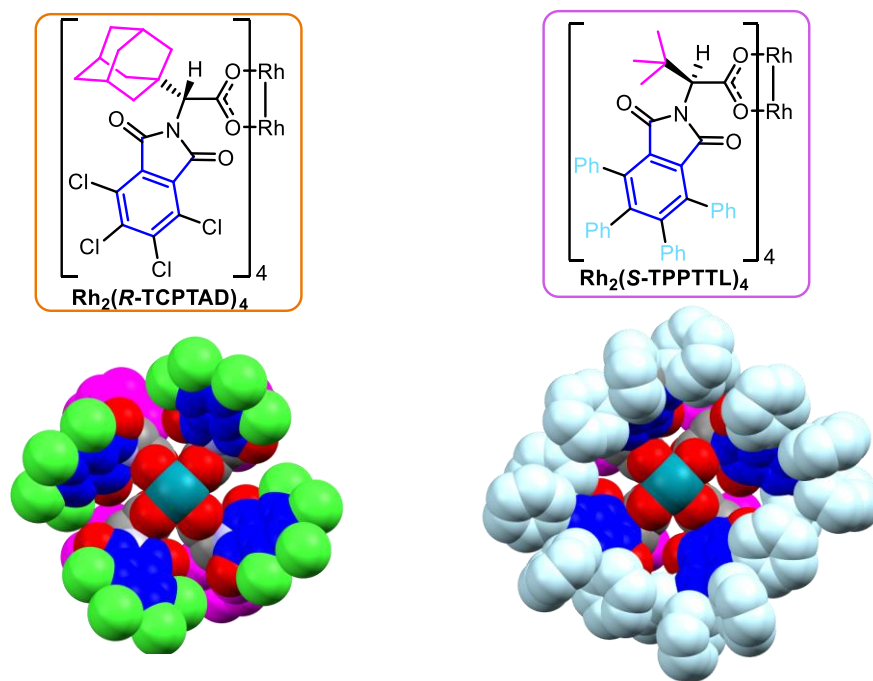
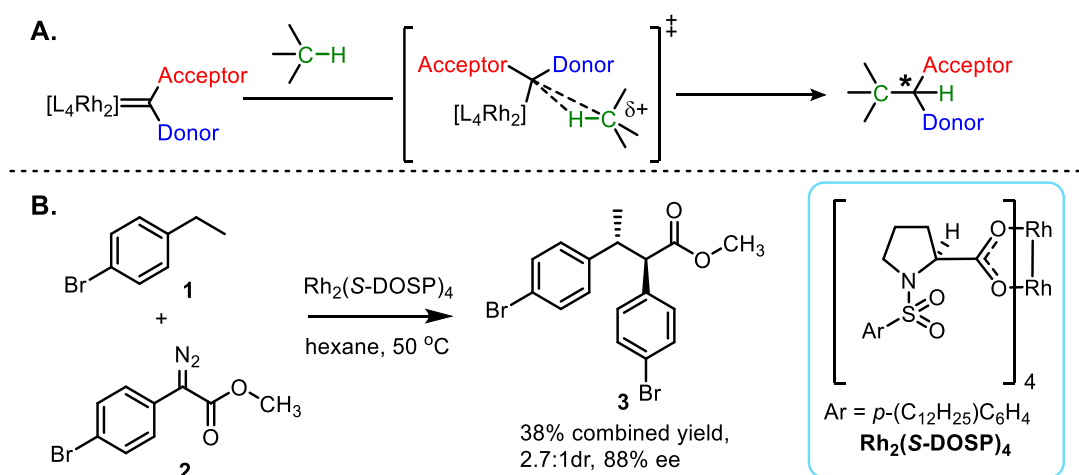


Figure 2.3 X-ray crystal structures (top-view) of $\text{Rh}_2(\text{R-TCPTAD})_4$ and $\text{Rh}_2(\text{S-TPPTTL})_4$

2.1.2. Site- and Stereoselective Functionalization of Electronically Activated and Unactivated Methylene C–H Bonds

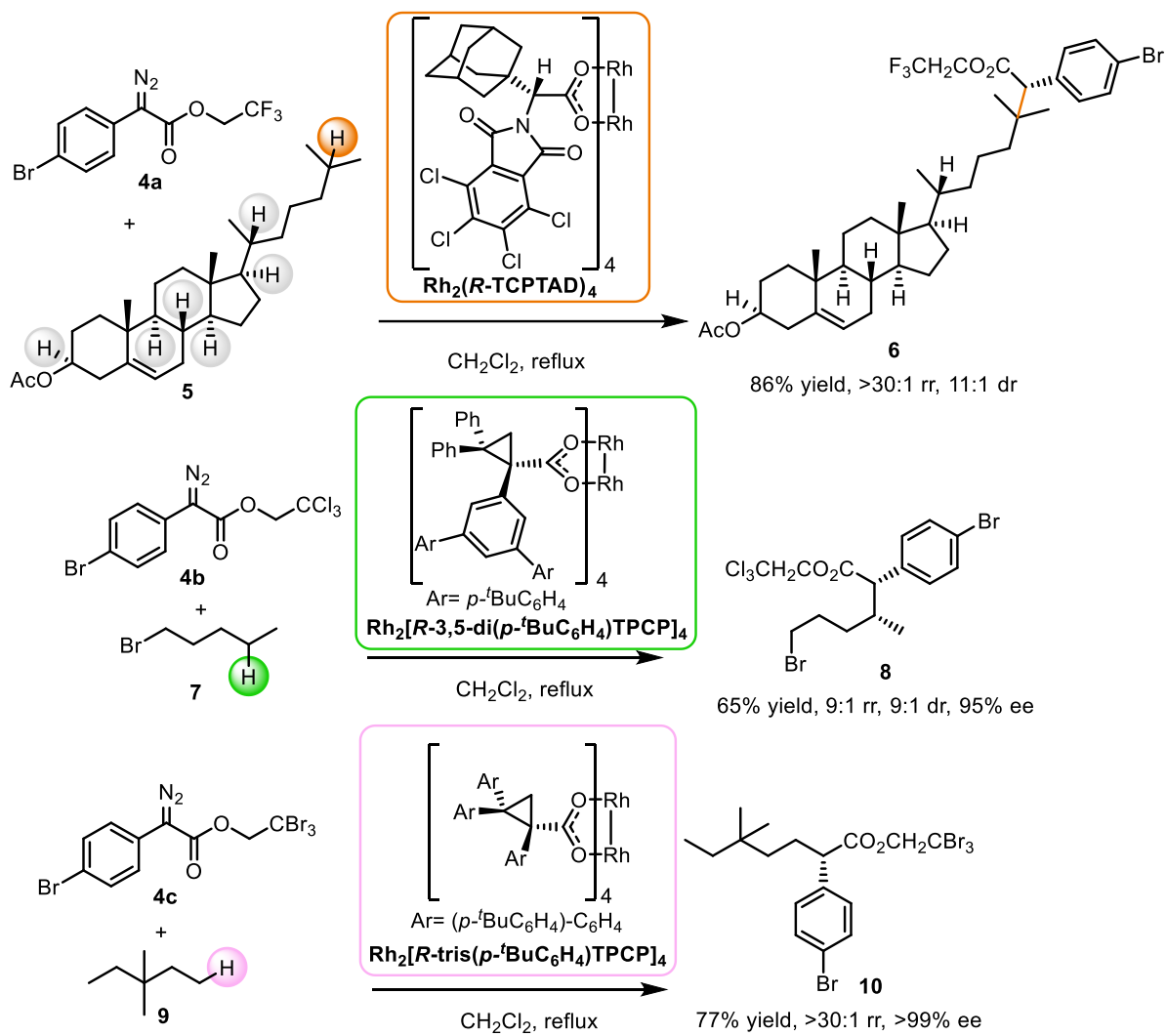
Benzylic C–H bonds can be functionalized selectively using different conditions, including using artificial enzymes⁹⁰, radicals generated by photocatalysts⁹¹ and traditional metal catalysts.⁹² ⁹³ The benzylic, allylic C–H bonds and those adjacent to oxygen or nitrogen atoms have slightly lower bond dissociation energies (89-95 kcal/mol) compared to the regular C–H bonds (97-101 kcal/mol), thus making them generally preferred in site-selective C–H functionalization.⁹⁴ Utilizing the rhodium donor/acceptor carbene chemistry, these C–H bonds are also preferred and considered to be electronically activated due to their ability to stabilize the partial positive charge built-up during the rhodium carbene intermediate (Scheme 2.1A). Most of the earlier studies on functionalization of these electronically activated C–H bonds were carried out using $\text{Rh}_2(\text{S-DOSP})_4$. However, some of the examples give poor diastereo-control, which is worth improving by using some newer dirhodium (II) carboxylate catalysts developed recently. For example, the $\text{Rh}_2(\text{S-DOSP})_4$ -catalyzed carbene insertion to the benzylic C–H bond in 1-bromo-4-ethylbenzene (**1**) using aryldiazoacetate (**2**) resulted in a mixture of diastereomers (**3**) (2.7:1 dr, Scheme 2.1B).⁶¹

Scheme 2.1 Dirhodium carbene reaction mechanism and benzylic C–H insertion



On the other hand, without electronic bias, most of the C–H functionalization approaches cannot distinguish the chemically similar unactivated C–H bonds and result in mixture of regioisomers.^{60, 95, 96} As discussed in chapter 1, the common strategies for controlling site-selectivity utilize Hofmann-Löffler type radical intermediate with 1,5-hydrogen atom transfer (HAT), directing groups, or artificial enzymes. The recent progress on dirhodium (II) catalysts refinement in the Davies group achieved high site-selectivity controlled in functionalization of terminal unactivated C–H bonds by using appropriate steric demanding catalyst. The most sterically accessible tertiary C–H bonds can be selectively targeted by $\text{Rh}_2(R\text{-TCPTAD})_4$,⁷⁶ while unactivated secondary or primary C–H bonds require steric bulky catalysts from the $\text{Rh}_2(\text{TPCP})_4$ family. With **7** tertiary C–H bonds presents in cholesteryl acetate (**5**), the least steric hindered tertiary C–H bond (orange in Scheme 2.2) was converted to C–C bond for product **6** using $\text{Rh}_2(R\text{-TCPTAD})_4$ with high site-selectivity control (>98:2 rr) in 86% yield.⁷⁶ The D_2 -symmetric catalyst, $\text{Rh}_2[S\text{-}3,5\text{-di}(p\text{-}^t\text{BuC}_6\text{H}_4)\text{TPCP}]_4$, favors the terminal methylene site compared to other unactivated C–H bonds, where the terminal methylene C–H bond (green in Scheme 2.2) in 1-bromopentane (**7**) was selectively functionalized in 65% yield (9:1 rr).⁸¹ A much bulkier catalyst with substituents on both C1- and C2-aryl rings, $\text{Rh}_2[R\text{-tris}(p\text{-}^t\text{BuC}_6\text{H}_4)\text{TPCP}]_4$, prefers the most accessible primary C–H bonds and selectively functionalized the 3,3-dimethylpentane (**9**) at the methyl site adjacent to methylene group for **10** as single regioisomer (>30:1 rr).⁸²

Scheme 2.2 Site-selective C–H functionalization using rhodium carbenes

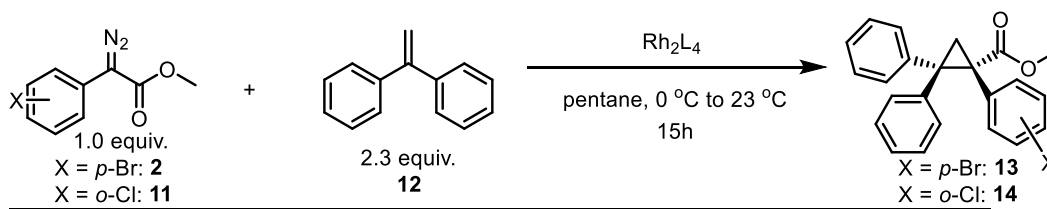


2.2. Results and Discussion

2.2.1. Synthesis and Initial Examination of $\text{Rh}_2(\text{S-}o\text{-CITPCP})_4$ Catalyst

With substituents at both *para*- and *meta*-positions on the C1-aryl rings in the $\text{Rh}_2(\text{TPCP})_4$ family explored, my project was to explore dirhodium (II) triarylcyclopropanecarboxylate complexes with substituents at *ortho*-positions. Firstly, different halogens were used as the *ortho*-substituent, in comparison to the *para*-bromide in $\text{Rh}_2(\text{R-}p\text{-BrTPCP})_4$. The synthetic routes for these complexes were also adapted from the synthesis of $\text{Rh}_2(\text{R-}p\text{-BrTPCP})_4$ ⁷⁸ with slight modification. In the dirhodium-catalyzed cyclopropanation between methyl aryldiazoacetates (**2** or **11**) and 1,1-diphenylethylene (**12**), $\text{Rh}_2(\text{S-DOSP})_4$ was used to make (*S*)-1-(4-bromophenyl)-2,2-diphenylcyclopropane-1-carboxylate (**13**). When *o*-Cl derivative (**11**) of the diazo compound was used instead of *p*-Br (**2**), the enantioselectivity for making **14** dropped significantly from 98% ee to 75% ee and the enantioselectivity was too low for enantio-enrichment via recrystallization (Table 2.1). Inspired by the studies done of Dr. Kathryn Chepiga and co-workers on the guide to enantioselective cyclopropanation, which shows $\text{Rh}_2(\text{S-PTAD})_4$ performs better for diazo compounds with *ortho*-substituted aryl ring,⁹⁷ $\text{Rh}_2(\text{S-PTAD})_4$ was applied to the synthesis of **14** and the product was formed in 84% yield and 98% ee.

Table 2.1 Cyclopropanation of methyl 2-(2-chlorophenyl)-2-diazoacetate



Entry	2 or 11	Rh_2L_4	13 or 14 , yield	dr	ee
1 ^a	2	$\text{Rh}_2(\text{R-DOSP})_4$	13 , 88%	>20:1	98%
2	11	$\text{Rh}_2(\text{S-DOSP})_4$	14 , 62%	>20:1	-75% ^b
3	11	$\text{Rh}_2(\text{S-PTAD})_4$	14 , 84%	>20:1	98%

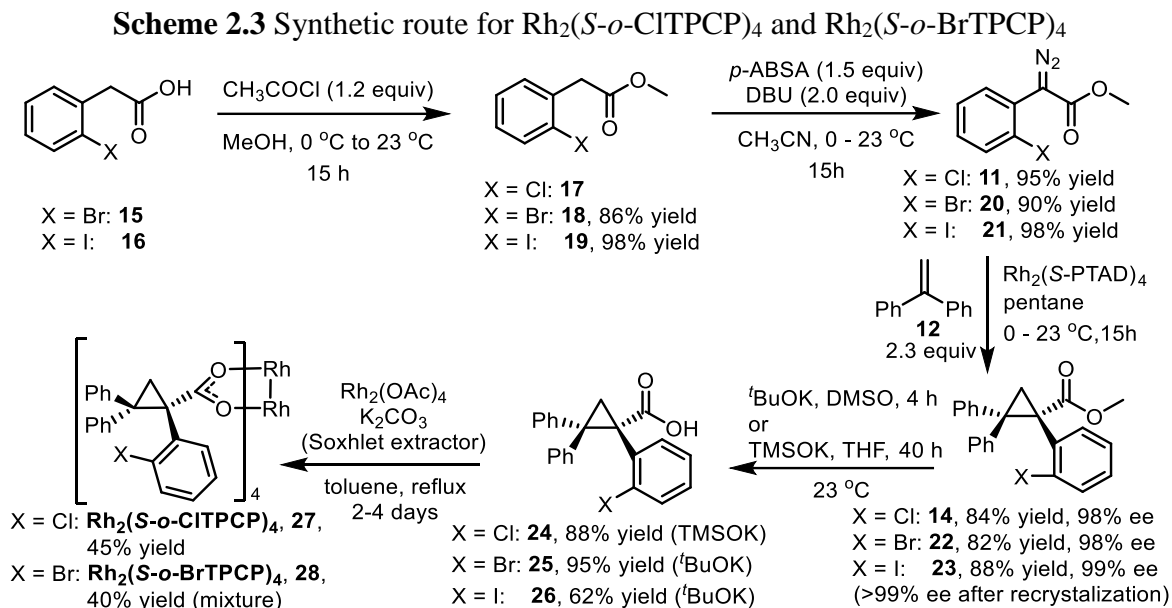
^a Reaction results in literature (*J. Am. Chem. Soc.* **2011**, 133, 19198).

^b Opposite enantiomer of the drawn one was obtained.

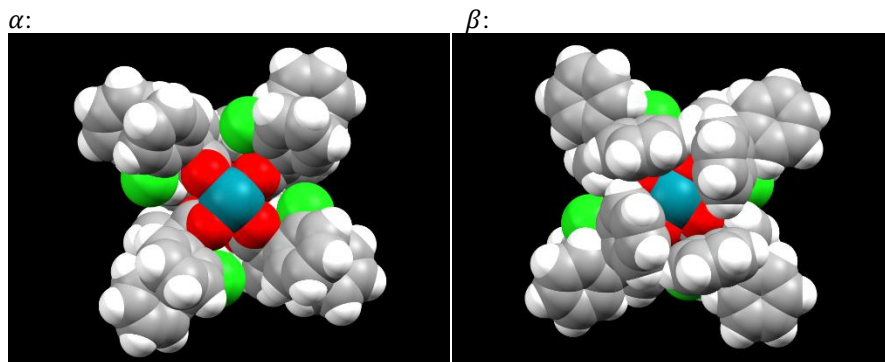
Other modifications of the reported routes included the hydrolysis and ligand exchange steps. The hydrolysis of **14** using the established procedure with t BuOK was not reproducible. The reaction was achieved with an old bottle of t BuOK (as shown for the formation of **25** and **26**), but TLC analysis revealed a mixture of decomposed products on the baseline when a new bottle of the t BuOK reagent was used. We believe some moisture in the old bottle was necessary for the hydrolysis reaction. The hydrolysis conditions were modified by Dr. Daniel Rackl when he developed the procedure for $\text{Rh}_2(R\text{-}p\text{-BrTPCP})_4$ synthesis on multi-grams scale using TMSOK in THF, which was developed by the Rolland group.⁹⁸ The hydrolysis using these conditions was confirmed to be reproducible by different group members and different batches of the reagents. In the ligand exchange for $\text{Rh}_2(S\text{-}o\text{-ClTPCP})_4$, conditions with $[\text{Na}_4\text{Rh}_2(\text{CO}_3)_4]\cdot 2.5\text{H}_2\text{O}$ in refluxing water gave no desired product but mixture of rhodium complexes with lower molecular weight in mass spectroscopy, presumably due to the ligands with *ortho*-substituents being more hindered. Inspired by Michael and co-workers,⁹⁹ $\text{Rh}_2(\text{OAc})_4$ in refluxing toluene was used for ligand exchange and the desired $\text{Rh}_2(S\text{-}o\text{-ClTPCP})_4$ complex was generated in 45% yield after 4 days, as well as its analog $\text{Rh}_2(S\text{-}o\text{-BrTPCP})_4$ (Scheme 2.3), while its *o*-I derivative failed in ligand exchange presumably because the *o*-I substituents are too sterically hindered. The yield for $\text{Rh}_2(S\text{-}o\text{-ClTPCP})_4$ was later improved to 62% on large scale.

A single crystal of $\text{Rh}_2(S\text{-}o\text{-ClTPCP})_4$ was carefully obtained by slow evaporation of its solution in ethyl ether. The crystal structure of isomer-free $\text{Rh}_2(S\text{-}o\text{-ClTPCP})_4$, determined by X-ray crystallography, gives a C_4 symmetric conformation with all four *o*-Cl-aryl groups points to the same face (α) of the O-Rh-O disk (Figure 2.4). The chloride atoms are spaced between the adjacent *o*-Cl-aryl groups and forced these aryl groups to tilt away from the rhodium center, which resulted

in the four phenyl groups on β face tilt towards each other and therefore blocking the accessibility of the axial site of the rhodium on this β face (filled by molecules as small as H₂O).



Without axial molecules:



With axial molecules:

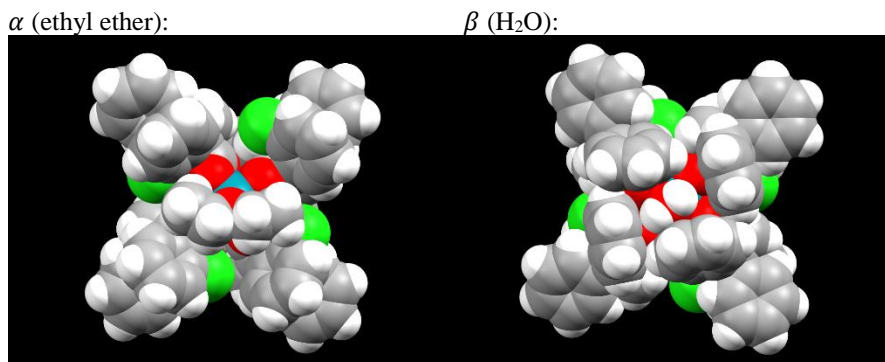


Figure 2.4 X-ray crystal structure of Rh₂(*S*-*o*-CITPCP)₄

On the other hand, $\text{Rh}_2(\text{S-}o\text{-BrTPCP})_4$ was obtained with isomers, as shown in the ^1H NMR spectrum with another set of doublet peaks for the two protons on the cyclopropane ring, whereas there is only one set of two doublet peaks in the ^1H NMR spectrum of $\text{Rh}_2(\text{S-}o\text{-ClTPCP})_4$ (2.30-2.80 ppm in Figure 2.5). Referring to the crystal structure of $\text{Rh}_2(\text{S-}o\text{-ClTPCP})_4$, it can be explained that bromide atoms (or other groups) at this *ortho* positions are not suitable and too big to fit in the space between adjacent aryl rings (the larger atoms require the phenyl groups on β face to tilt further towards each other). That is, bromide may be orientated either behind or in front of the adjacent aryl groups and may generate rotational isomers (rotamers), explaining the isomers seen in the ^1H NMR spectrum.

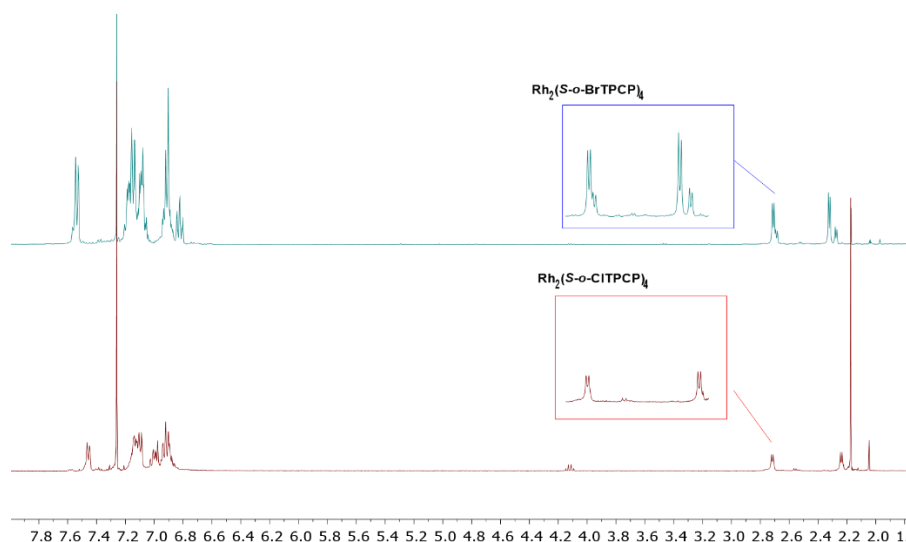


Figure 2.5 ^1H NMR spectra of $\text{Rh}_2(\text{S-}o\text{-BrTPCP})_4$ (top) and $\text{Rh}_2(\text{S-}o\text{-ClTPCP})_4$ (bottom)

Variable-temperature ^1H -NMR of $\text{Rh}_2(\text{S-}o\text{-BrTPCP})_4$ in toluene- d_8 at the range of 23-90 $^\circ\text{C}$ was conducted to see if the rotamers can be interconverted under higher temperature (Figure 2.6). However, there is no sign of merging for the two sets of cyclopropane proton peaks (2.2-2.5 ppm), which indicates the rigidity and high rotation energy barrier of these $\text{Rh}_2(\text{TPCP})_4$ complex.

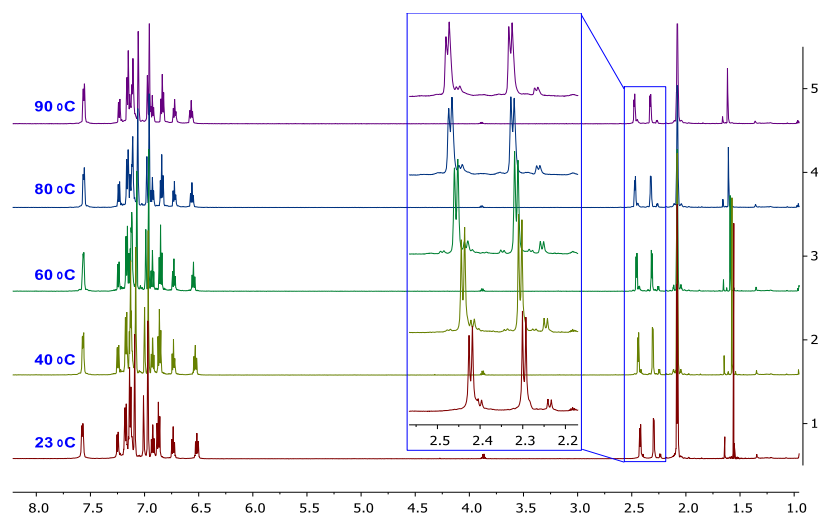


Figure 2.6 Variable-temperature $^1\text{H-NMR}$ of $\text{Rh}_2(\text{S-}o\text{-BrTPCP})_4$ in toluene- d_8

The $\text{Rh}_2(\text{S-}o\text{-ClTPCP})_4$ complex, which has no rotamer issue observed in $^1\text{H-NMR}$ like $\text{Rh}_2(\text{S-}o\text{-BrTPCP})_4$, was then examined in the cyclopropanation reactions (Table 2.2). Styrene **29** was used as the substrate for cyclopropanation together with the methyl phenyldiazoacetate **30**, which is one of the example reactions that showed the high stereo-control with $\text{Rh}_2(\text{R-}p\text{-BrTPCP})_4$.⁷⁸ The performance of $\text{Rh}_2(\text{S-}o\text{-ClTPCP})_4$ in this reaction was similar to $\text{Rh}_2(\text{R-}p\text{-BrTPCP})_4$ in terms of yield and diastereoselectivity, while the enantioselectivity with $\text{Rh}_2(\text{S-}o\text{-CTPCP})_4$ was much lower (24% ee). The low enantioselectivity may raise from its C_4 -symmetric conformation with limited differentiation of the substrate approaching pathways.

Table 2.2 Initial examination of $\text{Rh}_2(\text{S-}o\text{-ClTPCP})_4$ on cyclopropanation of styrene

$\text{Rh}_2(\text{R-}p\text{-BrTPCP})_4$

29 + **30** $\xrightarrow[\text{CH}_2\text{Cl}_2, 23\text{ }^\circ\text{C}]{\text{Rh}_2\text{L}_4 (1\text{ mol}\%)}$ **31**

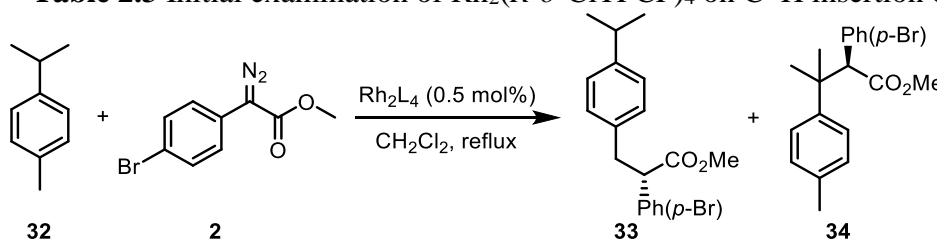
$\text{Rh}_2(\text{S-}o\text{-ClTPCP})_4$

Entry	Rh_2L_4	yield	dr	ee
1	$\text{Rh}_2(\text{R-}p\text{-BrTPCP})_4$	53%	>20:1	86%
2	$\text{Rh}_2(\text{S-}o\text{-ClTPCP})_4$	57%	>20:1	24%

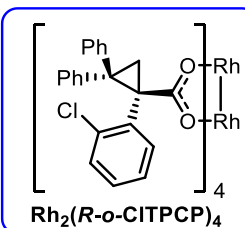
Not deterred by the poor cyclopropanation results, next, the performance of $\text{Rh}_2(S\text{-}o\text{-CITPCP})_4$ in rhodium carbene chemistry was examined in C–H functionalization reactions, including activated benzylic C–H bonds and unactivated methylene C–H bonds in cyclohexane, in order to better understand its reactivity profile. For comparison, $\text{Rh}_2(R\text{-}p\text{-PhTPCP})_4$, which also adopts an all-up conformation but is *pseudo*- C_2 symmetry, was used together with the classic catalyst, $\text{Rh}_2(R\text{-DOSP})_4$.

The $\text{Rh}_2(R\text{-DOSP})_4$ catalyzed C–H insertion of *p*-cymene **32** was reported to give a mixture of primary (**33**) / tertiary (**34**) C–H functionalized products in 1:4 ratio.⁷⁹ On the other hand, primary insertion product **33** was favored when the reactions was catalyzed by $\text{Rh}_2(R\text{-}p\text{-PhPCP})_4$ (>20:1 rr in 75% yield and 96% ee) and $\text{Rh}_2(R\text{-}o\text{-CITPCP})_4$ (16:1 rr in 72% yield and -50% ee) (Table 2.3). This result led to the hypothesis that the steric factors may predominate over the electronic factors when the reactions are catalyzed by dirhodium carboxylates with all-up conformation, such as $\text{Rh}_2(R\text{-}p\text{-PhPCP})_4$ and $\text{Rh}_2(R\text{-}o\text{-CITPCP})_4$.

Table 2.3 Initial examination of $\text{Rh}_2(R\text{-}o\text{-CITPCP})_4$ on C–H insertion of *p*-cymene



Entry	Rh_2L_4	yield	rr (33 : 34)	ee (33)
1 ^a	$\text{Rh}_2(R\text{-DOSP})_4$	72%	1:4	73%
2	$\text{Rh}_2(R\text{-}p\text{-PhTPCP})_4$	75%	>20:1	96%
3	$\text{Rh}_2(R\text{-}o\text{-CITPCP})_4$	72%	16:1	-50% ^b



$\text{Rh}_2(R\text{-}o\text{-CITPCP})_4$

^a Reaction results in literature (*J. Am. Chem. Soc.* **2014**, 136, 9792).
^b Opposite enantiomer of the drawn one was obtained.

In the C–H insertion of 4-ethyltoluene, $\text{Rh}_2(R\text{-DOSP})_4$ was selective for the secondary benzylic C–H and generated **36** as single insertion product (>20:1 rr in 75% yield and 3.3:1 dr for **36**)⁷⁹,

while $\text{Rh}_2(R\text{-}p\text{-PhPCP})_4$ (1:5 rr in 70% yield preferring **36** with 95% ee) and $\text{Rh}_2(R\text{-}o\text{-CITPCP})_4$ (8:1 rr in 75% yield preferring **36** with 12:1 dr) gave a mixture of primary / secondary insertion products (Table 2.4). Compared to $\text{Rh}_2(R\text{-DOSP})_4$, $\text{Rh}_2(R\text{-}o\text{-CITPCP})_4$ is less selective for secondary C–H bonds, but it can afford **36** with higher diastereoselectivity. On the other hand, compared to $\text{Rh}_2(R\text{-}p\text{-PhPCP})_4$, $\text{Rh}_2(R\text{-}o\text{-CITPCP})_4$ was not selective for primary C–H bonds. As for the enantioselectivity, $\text{Rh}_2(R\text{-}o\text{-CITPCP})_4$ gave only moderated ee for secondary C–H bonds and even lower for primary C–H bonds, presumably because the ligand pocket has less limitation for the accessing substrate compared to $\text{Rh}_2(R\text{-}p\text{-PhPCP})_4$ with bulky *p*-substituents on aryl rings. It can also be concluded that the site-selectivity among activated C–H bonds for $\text{Rh}_2(o\text{-CITPCP})_4$ is $2^\circ > 1^\circ > 3^\circ$. Basing on the results above, dirhodium catalysts with additional substituents on $\text{Rh}_2(o\text{-CITPCP})_4$ scaffold were synthesized and examined for later studies (Section 2.2.3).

Table 2.4 Initial examination of $\text{Rh}_2(R\text{-}o\text{-CITPCP})_4$ on C–H insertion of 4-ethyltoluene

Entry	Rh_2L_4	yield	rr (36:37)	dr (36)	ee (36)	ee (37)
1 ^a	$\text{Rh}_2(R\text{-DOSP})_4$	75%	>20:1	3.3:1	--	--
2	$\text{Rh}_2(R\text{-}p\text{-PhPCP})_4$	70%	1:5	2.7:1	--	95%
3	$\text{Rh}_2(R\text{-}o\text{-CITPCP})_4$	75%	8:1	12:1	-75% ^b	-57% ^b

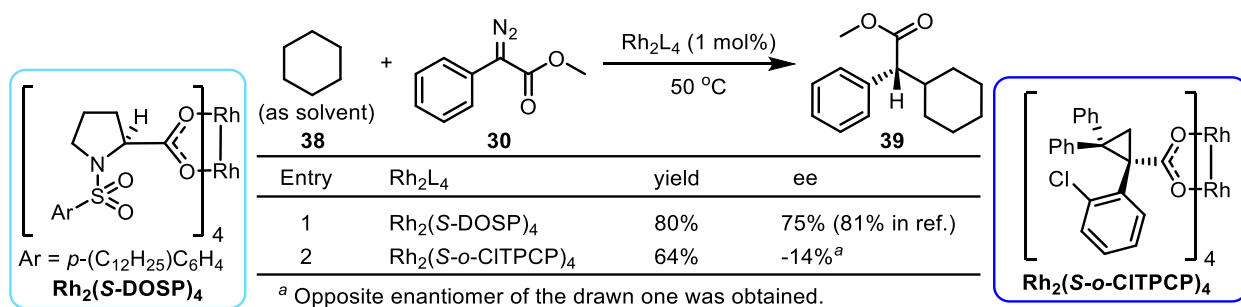
$\text{Rh}_2(R\text{-}o\text{-CITPCP})_4$

^a Reaction results in literature (*J. Am. Chem. Soc.* **2014**, *136*, 9792).
^b Opposite enantiomer of the drawn one was obtained.

Next, the performance of $\text{Rh}_2(S\text{-}o\text{-CITPCP})_4$ in C–H insertion of unactivated C–H bonds was also examined using cyclohexane **38** as substrate, which contains only secondary C–H bonds and its C–C–C angles are similar to those in linear chain. According to Davies and Hansen,⁴³ the $\text{Rh}_2(S\text{-DOSP})_4$ catalyzed the C–H insertion of cyclohexane using diazo compound **30** giving the C–H

insertion product in 84% yield and 87% ee. The same reaction was repeated and tested using $\text{Rh}_2(S\text{-}o\text{-CITPCP})_4$ (Table 2.5). The yield for the reaction catalyzed by $\text{Rh}_2(S\text{-}o\text{-CITPCP})_4$ was moderate, while the enantioselectivity is much lower than previous reactions, possibly due to the solvent effect as $\text{Rh}_2(S\text{-}o\text{-CITPCP})_4$ prefers polar solvents such as dichloromethane.

Table 2.5 Initial examination of $\text{Rh}_2(S\text{-}o\text{-CITPCP})_4$ on C–H insertion of cyclohexane

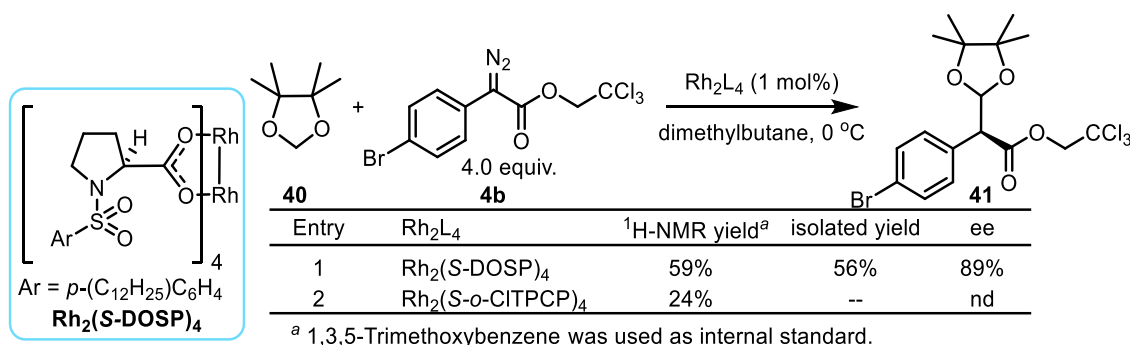


2.2.2. C–H Insertion of 4,5-Substituted 1,3-Dioxolane

The initial examination of $\text{Rh}_2(S\text{-}o\text{-CITPCP})_4$ indicated the electronically activated secondary C–H bonds would be a good target for this dirhodium catalyst, which led to the next interesting substrate, 1,3-dioxolane. Initially, the C–H insertion reaction of the 1,3-dioxolane catalyzed by $\text{Rh}_2(S\text{-DOSP})_4$ has been reported to proceed in low yield (10%) by Fraile and coworkers.¹⁰⁰ Yuxing Wang, during his exploration of this chemistry as a surrogate for the Claisen condensation, reasoned the low yield was caused by the competing ylide formation of the unsubstituted 1,3-dioxolane and proposed modified substrate, 4,4,5,5-tetramethyl-1,3-dioxalene **40**, but it gave slightly improved yields (31%) using $\text{Rh}_2(S\text{-DOSP})_4$ as catalyst.¹⁰¹ Herein, the $\text{Rh}_2(S\text{-}o\text{-CITPCP})_4$ was tested in the C–H insertion reaction of **40**, compared to the same reaction catalyzed $\text{Rh}_2(S\text{-DOSP})_4$ (Table 2.6). Moreover, trihaloethyl ester was previously shown to be an improvement compared to the methyl ester and resulted in cleaner reaction with less dimer byproducts and better

site- and stereoselectivity due to its steric bulkiness and attenuation of the carbene through subtle electronic bias on the acceptor group,⁸⁰ so trichloroethyl diazoacetate **4b** was used in this examination. The reaction catalyzed by $\text{Rh}_2(\text{S-DOSP})_4$ afforded the insertion product in 56% yield and 89% ee (chiral center determined by analogy to other $\text{Rh}_2(\text{S-DOSP})_4$ -catalyzed reactions), while the performance of $\text{Rh}_2(\text{S-}o\text{-CITPCP})_4$ was unsatisfactory with a low NMR yield (24%).

Table 2.6 Examination of $\text{Rh}_2(\text{S-}o\text{-CITPCP})_4$ on C–H insertion of 1,3-dioxolane



Interestingly, when the substrate changed to 1,3-dioxolane-4,5-dicarboxylate esters **42-45**, in which the 4,5-substituents are bulkier and polar, the performance of $\text{Rh}_2(\text{S-}o\text{-CITPCP})_4$ was drastically better than previous dirhodium carboxylate catalysts (Table 2.7). In this reaction, the solvent is also changed to dichloromethane to dissolve **42-45**. As shown in Table 2.7, while all the commonly used catalysts performed poorly in this reaction (13% NMR yield at best with $\text{Rh}_2(\text{S-PTAD})_4$), the $\text{Rh}_2(\text{S-}o\text{-CITPCP})_4$ can catalyze this reaction in a much higher NMR yield (entry 6, 39%). Notably, NMR yield was obtained for faster comparison, and the isolated yield is very close to the NMR yield when 1,3,5-trimethoxybenzene was used as a reliable internal standard (for entry 7, 55% isolated yield vs. 56% NMR yield), and only the diastereoselectivity was determined from crude $^1\text{H-NMR}$ as the starting materials are chiral. Moreover, the $\text{Rh}_2(\text{S-DOSP})_4$, which is the best catalyst for **40**, cannot catalyze the reaction of **42**. It may be because that the ester substrate **42** was not soluble in the nonpolar solvents like dimethylbutane, which is generally a better solvent for

$\text{Rh}_2(\text{S-DOSP})_4$, and cannot react with the metal carbenes, while $\text{Rh}_2(\text{S-DOSP})_4$ is inhibited by the polar solvents like dichloromethane, making their use incompatible. The 2:1 ratio of reactants was found to give better yield by Davies in 2005 in the C–H insertion of 2-phenyl-1,3-dioxolane.¹⁰² Thus reactions with 2:1 ratio were also tested for comparison and it was found that the reaction catalyzed by $\text{Rh}_2(\text{S-}o\text{-CITPCP})_4$ with excess substrate gave an improved NMR yield (56%). When the R' group on the ester in the 1,3-dioxolane was changed to the larger *i*-propyl group (**43**), the diastereoselectivity dropped to 10:1 ratio (entry 9), whereas the methyl ester (**42**) gave 48:1 dr (entry 7). In the reactions catalyzed by $\text{Rh}_2(\text{S-}o\text{-CITPCP})_4$, the diastereoselectivity decreased when the chiral center at 4- and 5-positions (C*) were changed from *Rectus* to *Sinister*-configuration, and it can be rationalized by the effect of match and mismatch between the chiral catalyst and the chiral center on the substrate. Therefore, high diastereoselectivity (48:1) can be achieved for $\text{Rh}_2(\text{S-}o\text{-CITPCP})_4$ -catalyzed reaction, such as the C–H insertion at 2-position in dimethyl (*4R,5R*)-1,3-dioxolane-4,5-dicarboxylate (**42**), and this may be because of the steric restriction of the reaction pocket in $\text{Rh}_2(\text{S-}o\text{-CITPCP})_4$ with all 4 *o*-Cl-aryl rings at the same face.

Table 2.7 Examination of C–H insertion on 4,5-diester-1,3-dioxolane

Entry	<i>R/S</i> at C*	R'	Rh ₂ L ₄	(42-45): 4b	¹ H-NMR yield ^a	dr
1	<i>R</i>	Me (42)	Rh ₂ (<i>S</i> -DOSP) ₄	1:4	0% ^b	--
2	<i>R</i>	Me (42)	Rh ₂ (<i>S</i> -PTTL) ₄	1:4	9%	3:1
3	<i>R</i>	Me (42)	Rh ₂ (<i>R-p</i> -BrTPCP) ₄	1:4	0% ^b	--
4	<i>R</i>	Me (42)	Rh ₂ (<i>R</i> -PTAD) ₄	1:4	6%	--
5	<i>R</i>	Me (42)	Rh ₂ (<i>S</i> -PTAD) ₄	1:4	13%	9:1
6	<i>R</i>	Me (42)	Rh ₂ (<i>S-o</i> -CITPCP) ₄	1:4	39%	56:1
7	<i>R</i>	Me (42)	Rh ₂ (<i>S-o</i> -CITPCP) ₄	2:1	56%	48:1
8	<i>R</i>	<i>i</i> -Pr (43)	Rh ₂ (<i>S-o</i> -CITPCP) ₄	1:4	36%	11:1
9	<i>R</i>	<i>i</i> -Pr (43)	Rh ₂ (<i>S-o</i> -CITPCP) ₄	2:1	54%	10:1
10	<i>S</i>	Me (44)	Rh ₂ (<i>S-o</i> -CITPCP) ₄	1:4	41%	1:2.5
11	<i>S</i>	<i>i</i> -Pr (45)	Rh ₂ (<i>S-o</i> -CITPCP) ₄	1:4	50%	1:3.4
12	<i>S</i>	<i>i</i> -Pr (45)	Rh ₂ (<i>S-o</i> -CITPCP) ₄	2:1	37%	1:2.7

R'' = ^tBu: Rh₂(*S*-PTTL)₄
R'' = Ad: Rh₂(*S*-PTAD)₄

R''' = *p*-Br: Rh₂(*R-p*-BrTPCP)₄
R''' = *o*-Cl: Rh₂(*S-o*-CITPCP)₄

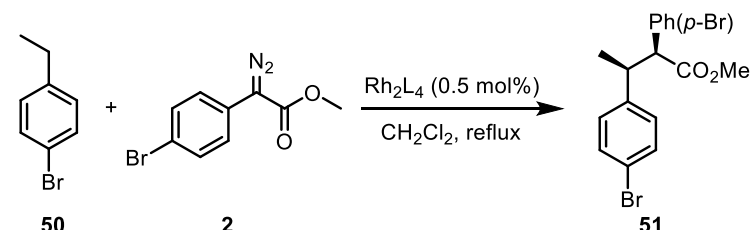
^a 1,3,5-Trimethylbenzene was used as internal standard.
^b Only dimer byproducts and **42** observed.

2.2.3. Development of Rh₂(2-Cl-4-BrTPCP)₄ and Rh₂(2-Cl-5-BrTPCP)₄

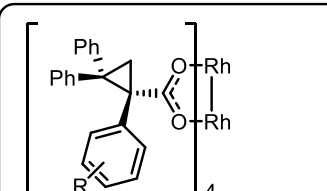
In the initial examination of Rh₂(*S-o*-CITPCP)₄, it was found that this catalyst prefers insertion at secondary C–H bonds and improved diastereoselectivity was observed in both 4-ethyltoluene (**35**) and dimethyl 1,3-dioxolane-4,5-dicarboxylate (**42-45**) systems. Previously, in the studies of Rh₂(DOSP)₄ using methyl aryldiazoacetates, benzene rings with substituents at both 1- and 4-positions were found to be sterically protected from cyclopropanation.^{63, 103} Therefore, the ability of Rh₂(*S-o*-CITPCP)₄ in enhancing diastereoselectivity was further explored in 4-bromoethylbenzene (**50**) in comparison to previous dirhodium carboxylate catalysts (Table 2.8).

Among the previously established dirhodium carboxylate catalysts (entries 1-4), $\text{Rh}_2(\text{R-DOSP})_4$ was the best catalyst for stereoselectivity with 4.3:1 dr and 77% ee. The literature value for this reaction using $\text{Rh}_2(\text{S-DOSP})_4$ in nonpolar solvent (2,2-dimethylbutane) shows higher enantioselectivity (2.7:1 dr and 88% ee).⁶¹ In the $\text{Rh}_2(\text{TPCP})_4$ class of catalysts, $\text{Rh}_2(\text{R-}p\text{-BrTPCP})_4$ and $\text{Rh}_2[\text{R-}3,5\text{-di}(p\text{-}^t\text{BuC}_6\text{H}_4)\text{TPCP}]_4$ with *para*- and *meta*- substituents on the C1-aryl rings, both adopting D_2 symmetry, also gave moderate diastereoselectivity and low enantioselectivity. Notably, significant improvement in diastereoselectivity was observed in the $\text{Rh}_2(\text{S-}o\text{-CITPCP})_4$ -catalyzed reactions (entry 5, 13.3:1 dr). However, only moderate enantioinduction was generated using $\text{Rh}_2(\text{S-}o\text{-CITPCP})_4$, which is undesired. Therefore, further modifications on the $\text{Rh}_2(o\text{-CITPCP})_4$ catalyst scaffold were conducted.

Table 2.8 Examination of C–H insertion on 4-bromoethylbenzene



Entry	Rh_2L_4	yield	dr	ee
1	$\text{Rh}_2(\text{R-DOSP})_4$	63%	4.3:1	77%
2	$\text{Rh}_2(\text{R-PTAD})_4$	29%	2.8:1	-17% ^a
3	$\text{Rh}_2(\text{R-}p\text{-BrTPCP})_4$	9%	2.4:1	35%
4	$\text{Rh}_2[\text{R-}3,5\text{-di}(p\text{-}^t\text{BuC}_6\text{H}_4)\text{TPCP}]_4$	64%	4.3:1	21%
5	$\text{Rh}_2(\text{S-}o\text{-CITPCP})_4$	77%	13.3:1	69%



R = *p*-Br:
 $\text{Rh}_2(\text{R-}p\text{-BrTPCP})_4$

R = 3,5-di(*p*-^tBuC₆H₄):
 $\text{Rh}_2[\text{R-}3,5\text{-di}(p\text{-}^t\text{BuC}_6\text{H}_4)\text{TPCP}]_4$

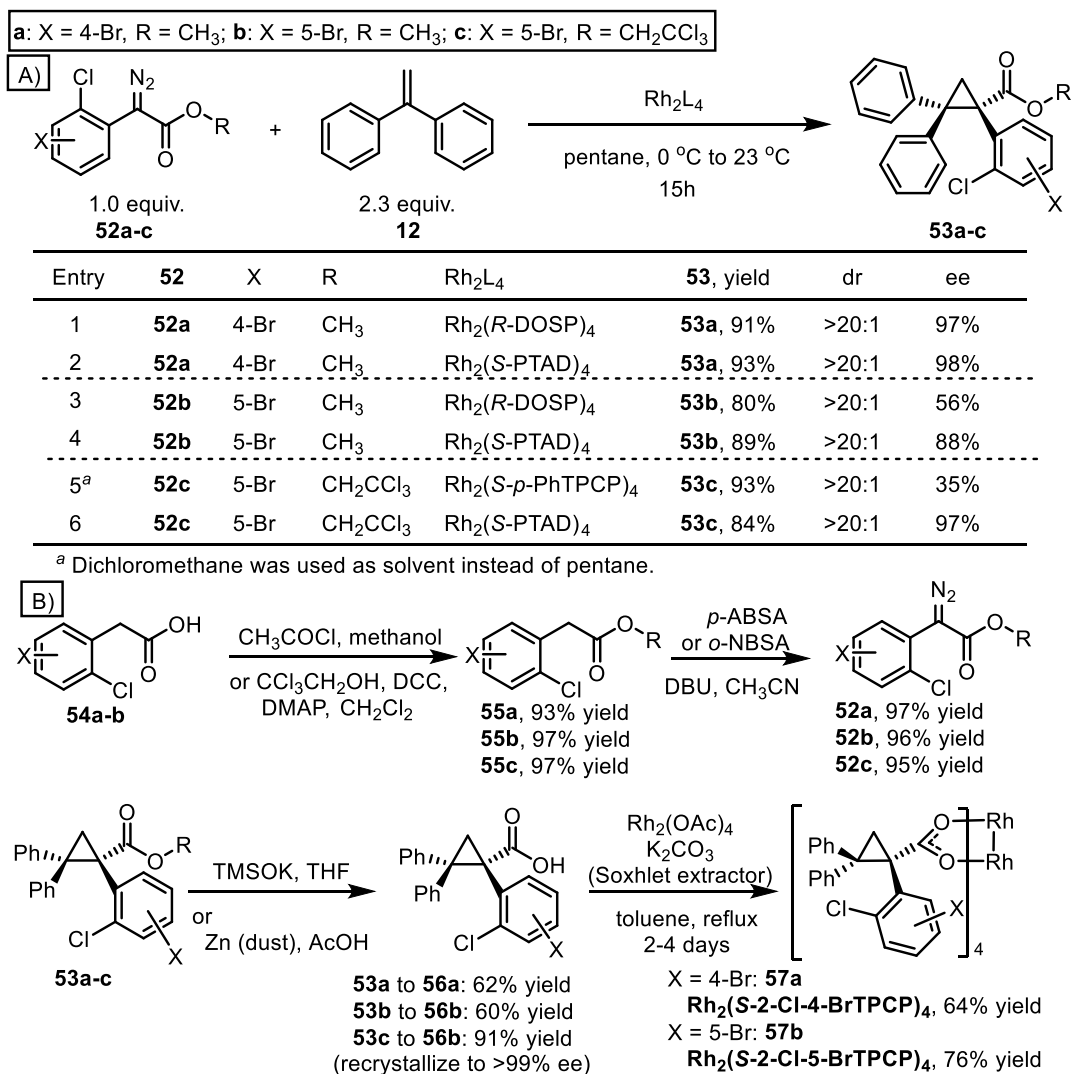
R = *o*-Cl:
 $\text{Rh}_2(\text{S-}o\text{-CITPCP})_4$

^a Opposite enantiomer of the drawn one was obtained.

Initially, in order to limit the size of the reaction pocket with four *o*-Cl-aryl rings, additional *para*-substituent were proposed to be added to the $\text{Rh}_2(o\text{-CITPCP})_4$ catalyst scaffold. Also, at the same time, Kuangbiao Liao explored the reaction conditions that can achieve 4- or 8-fold Suzuki-coupling on the dirhodium tetracarboxylate scaffold directly, leading to the incorporation of

bromide as a useful substituent for potential further derivatizations. $\text{Rh}_2(\text{S-2-Cl-4-BrTPCP})_4$ was synthesized using a similar synthetic route for the $\text{Rh}_2(\text{S-}o\text{-CITPCP})_4$, in which the $\text{Rh}_2(\text{R-DOSP})_4$ was used for cyclopropanation with similar enantioinduction to $\text{Rh}_2(\text{S-PTAD})_4$ but better availability in the lab (Scheme 2.4). Its initial examination was conducted on the C–H insertion reaction of 4-bromoethylbenzene **50** and it gave the same diastereoselectivity (13.3:1 dr) as $\text{Rh}_2(\text{S-}o\text{-CITPCP})_4$ but slightly lower enantioselectivity (63% ee), which was unexpected (Table 2.9).

Scheme 2.4 Synthesis of $\text{Rh}_2(\text{S-2-Cl-4-BrTPCP})_4$ and $\text{Rh}_2(\text{S-2-Cl-5-BrTPCP})_4$



Fortunately, the $\text{Rh}_2(\text{S-2-Cl-4-BrTPCP})_4$ was crystalline and relatively easier to grow single crystals compared to most of the other dirhodium complexes. In the X-ray crystal structure of $\text{Rh}_2(\text{S-2-Cl-4-BrTPCP})_4$ (Figure 2.7), it was found to be adopting the same C_4 symmetry as the parent catalyst, $\text{Rh}_2(\text{S-}o\text{-ClTPCP})_4$. In previous computational studies on the dirhodium donor/acceptor carbenes, the donor part in the carbene has the aryl ring being perpendicular to the O–Rh–O disk, while the acceptor part is oriented in a way that the O=C–OR plane is horizontal and blocks the access for the carbene center, forcing the substrates to approach the carbene center from the donor side at either *Re* face or *Si* face, which is further controlled by the ligands.^{78, 104} In the case of $\text{Rh}_2(\text{S-2-Cl-4-BrTPCP})_4$, the differentiation between the two pathways from *Re* and *Si* faces (arrow A vs arrow B in Figure 2.7) is very small, in which the approach of arrow B has a chloride atom instead of hydrogen but the chloride atom is likely to be lower than the carbene center. In order to induce additional difference with blocking element in one of the pathways, and to further breaking the local symmetry of the *o*-Cl-aryl ring, the bromide substituent is skewed to one side away from the chloride atom to further break-down the local symmetry of the *o*-Cl-aryl ring, leading to the development of $\text{Rh}_2(\text{S-2-Cl-5-BrTPCP})_4$, in which the pathway with arrow A would be blocked by the bromide atom. In the synthesis of $\text{Rh}_2(\text{S-2-Cl-5-BrTPCP})_4$ (Scheme 2.4), $\text{Rh}_2(\text{S-PTAD})_4$ was selected for the cyclopropanation with methyl diazoacetate, **52b**, since an enantioselectivity of 88% ee was obtained, much higher than the 55% ee catalyzed by $\text{Rh}_2(\text{R-DOSP})_4$ (Scheme 2.4A). However, neither the cyclopropane **53b** nor its hydrolysis product (carboxylic acid) **56b** can be enantioenriched through recrystallization after several trials, whereas recrystallization of the trichloroethyl derivative **53c** from hot hexane gave the enantiopure compound. $\text{Rh}_2(\text{S-}p\text{-PhTPCP})_4$ was found to be the best catalyst for cyclopropanation of trichloroethyl diazoacetates,¹⁰⁵ therefore it was examined in the cyclopropanation of diazoacetate

52c in comparison with $\text{Rh}_2(\text{S-PTAD})_4$, which was found to be the best catalyst again for these aryl diazoacetates with *ortho*-chloride on the aryl ring (Scheme 2.4A, entry 5-6, 96% ee vs 35% ee). That is, combination of trichloroethyl diazoacetate and $\text{Rh}_2(\text{S-PTAD})_4$ was the best system for the cyclopropanation in the synthesis of $\text{Rh}_2(\text{S-2-Cl-5-BrTPCP})_4$. $\text{Rh}_2(\text{S-2-Cl-5-BrTPCP})_4$ was then examined in the C–H insertion reaction of 4-bromoethylbenzene **50** and a notable improvement of the enantioselectivity was achieved (Table 2.9, 77% ee), which was comparable to $\text{Rh}_2(\text{R-DOSP})_4$, with only a slight drop in diastereoselectivity (11.5:1 dr).

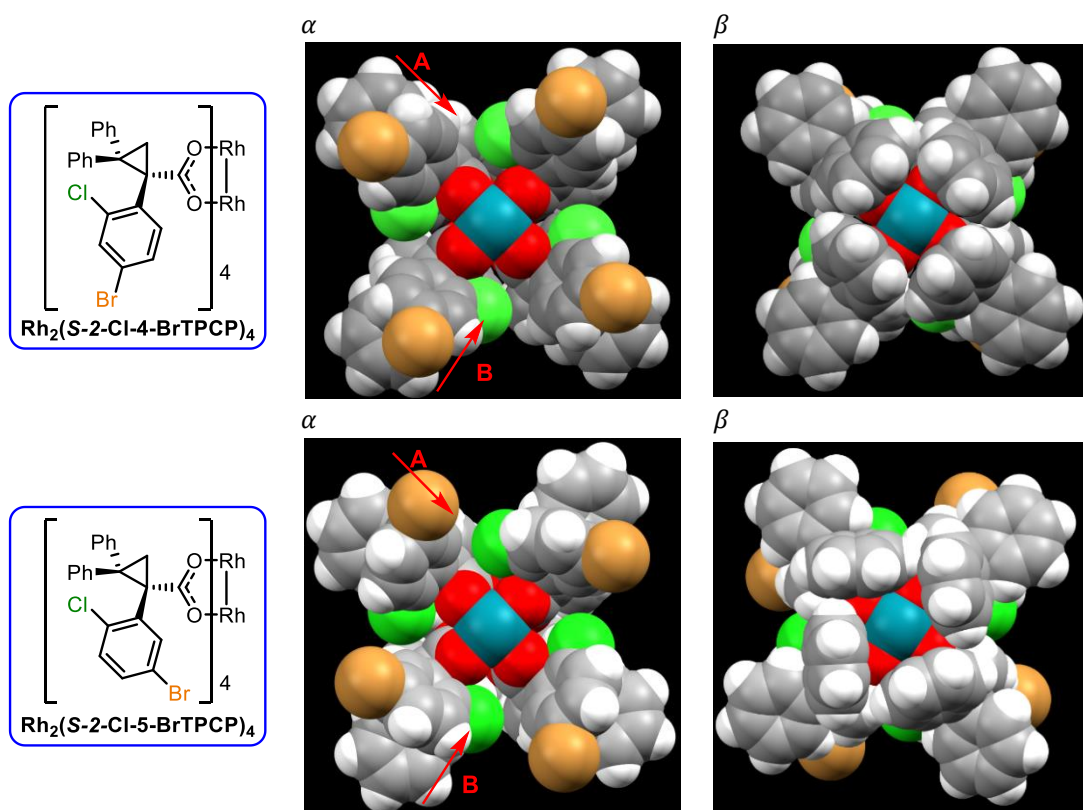
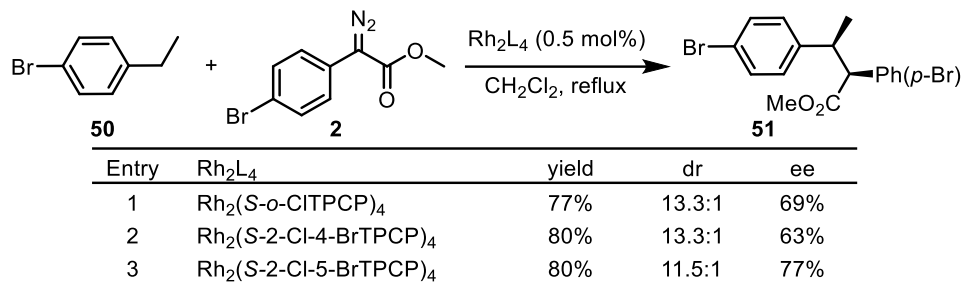
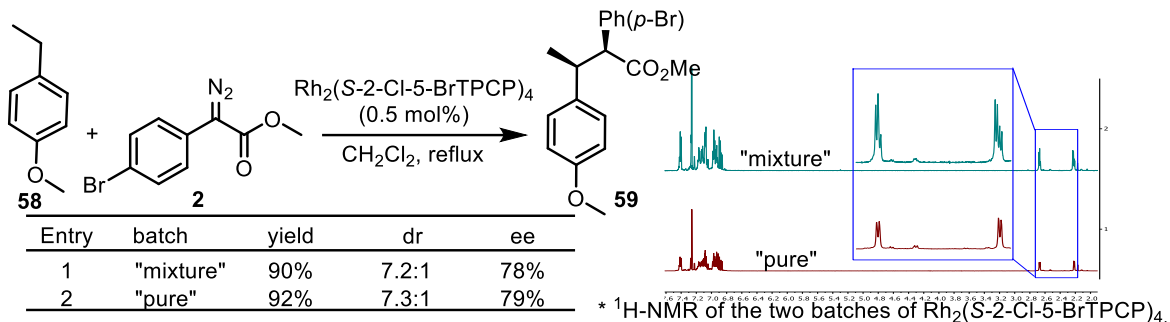


Figure 2.7 Crystal structures of $\text{Rh}_2(\text{S-2-Cl-4-BrTPCP})_4$ and $\text{Rh}_2(\text{S-2-Cl-5-BrTPCP})_4$

Table 2.9 C–H Insertion of 4-bromoethylbenzene using $\text{Rh}_2(\text{S-}o\text{-CITPCP})_4$ derivatives

With the C_4 symmetry conformation, in the $^1\text{H-NMR}$ spectra for $\text{Rh}_2(\text{S-}2\text{-Cl-4-BrTPCP})_4$ and $\text{Rh}_2(\text{S-}2\text{-Cl-5-BrTPCP})_4$, only one set of doublets peaks for the methylene protons on the cyclopropane rings should be observed. However, two sets of methylene peaks were observed, and these signals appeared to be due to the presence of two the presence of rotamers. Fractions with the single isomer versus the mixture were obtained separately when ethyl acetate and hexane were used as eluting solvents for flash column chromatography. They were separated into two batches and the batch with the single isomer was used in all the reactions in this dissertation unless otherwise noted. However, the examination of the batch with isomeric mixture on 1-ethyl-4-methoxybenzene **58** showed same performance in terms of yield and stereoselectivity compared to the “pure” batch, and $\text{Rh}_2(\text{S-}2\text{-Cl-5-BrTPCP})_4$ was chosen here for demonstration (Table 2.10). Therefore, theoretically, it’s not necessary to separate the two batches for C–H functionalization. Moreover, only one set of doublet peaks was observed in all the fractions when $\text{Rh}_2(\text{S-}2\text{-Cl-5-BrTPCP})_4$ is chromatographed using dichloromethane and hexane as eluting solvents.

Table 2.10 Comparison between “pure” and “mixture” batches of $\text{Rh}_2(\text{S-2-Cl-5-BrTPCP})_4$ 

Efforts were then attempted to understand more about the rotamers. Noticeably, in all three crystal structures of these $\text{Rh}_2(\text{TPCP})_4$ complexes with *ortho*-chloride substituent, the polarity vectors on the *o*-Cl-aryl ring are all oriented in an anti-clockwise arrangement when viewed down from the α face (Figure 2.8A). One possible configuration of the rotational isomer would be the one having opposite arrangement with the polarity vectors orienting in a clockwise manner. That is, the rotamer may arise from the rotation of the C–C bond between the cyclopropane and *o*-Cl-aryl rings, which leads to two possible conformers with an additional axial chirality around that C–C bond. High temperature NMR was found to be ineffective to study this as in the examination of $\text{Rh}_2(\text{S-}o\text{-BrTPCP})_4$ in previous section, so studies were conducted on the ligands (free carboxylic acids). In addition, the ^1H NMR spectra of these three ligands (**24**, **56a**, **56b**) are different from all previous TPCP ligands, specifically the peaks corresponding to the methylene protons in cyclopropane ring are considerably broadened at room temperature. This also indicates that these compounds have hindered rotations, presumably caused by the *o*-Cl substituent and the rotation of the C1–C4 bond. Taking *S*-2-Cl-5-BrTPCP ligand **56b** as an example, the two conformers could be **56b'** and **56b''** with *M* and *P* axial chirality at C-4 respectively (Figure 2.8B). The *M* conformer is the one adopted in the dirhodium complexes as shown in the X-ray crystal structures. X-ray crystal structure of *S*-2-Cl-5-BrTPCP ligand was also obtained and both *M* and

P conformers are observed. Hence, the ^1H NMR spectra for these three ligands would show resolution of two rotational isomers at lower temperature, and variable-temperature NMR studies were conducted at -40 - 22 $^\circ\text{C}$.

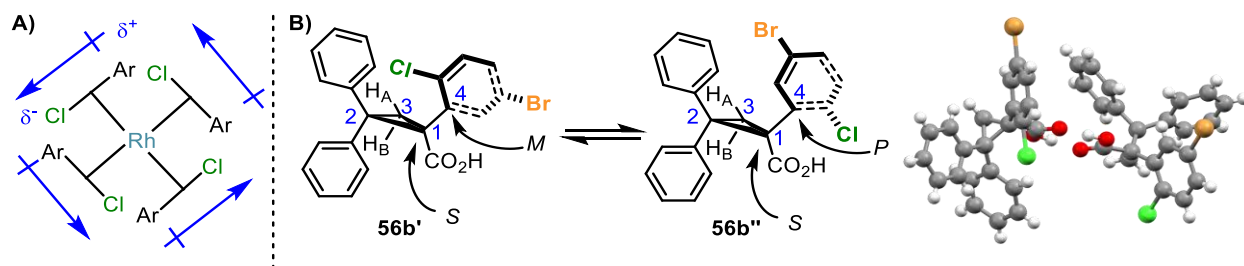


Figure 2.8 Demonstration for the axial chirality

It was estimated by variable-temperature NMR studies that the barriers of rotations for the three ligands are 12.9, 13.0 and 13.2 kcal mol^{-1} at room temperature for $\text{Rh}_2(S\text{-}o\text{-CITPCP})_4$, $\text{Rh}_2(S\text{-}2\text{-Cl-}4\text{-BrTPCP})_4$ and $\text{Rh}_2(S\text{-}2\text{-Cl-}5\text{-BrTPCP})_4$ respectively. Details on the calculation is discussed below. Firstly, significant broadening of all the peaks, especially those corresponding to the methylene protons in the cyclopropane ring, was observed slowly when the temperature was dropped to -15 $^\circ\text{C}$ with 5 $^\circ\text{C}$ intervals. When the temperature was decreased to -40 $^\circ\text{C}$, all three ligands (**24**, **56a**, **56b**) showed resolution that the methylene peaks split into two sets, which indicates two rotamers (Figure 2.9). One rotamer, which has smaller difference in the chemical shifts for the two methylene protons (H_A' and H_B'), is slightly preferred over the other (with methylene peaks as H_A'' and H_B'') for all three cases with ratios of 1.5:1 [$\text{Rh}_2(S\text{-}o\text{-CITPCP})_4$], 1.2:1 [$\text{Rh}_2(S\text{-}2\text{-Cl-}4\text{-BrTPCP})_4$] and 1.8:1 [$\text{Rh}_2(S\text{-}2\text{-Cl-}5\text{-BrTPCP})_4$]. The less preferred rotamer is likely to be the *P* conformer, because the two methylene protons are very different in chemical shifts, which may be caused by shielding effect of the Cl atom on the H_A atom when they are closer to each other in the *P* conformer, whereas the Cl atom is far away from both H_A and H_B atoms.

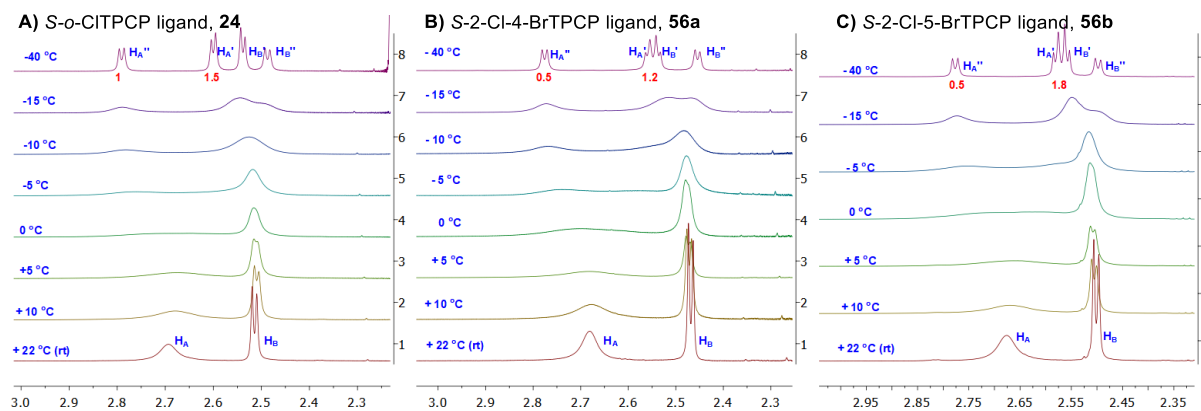
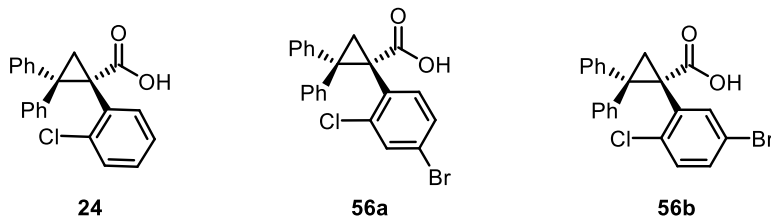


Figure 2.9 Variable-temperature NMR studies at 600 MHz in CDCl_3

Calculations of the rotational barriers was conducted using Eyring plots and the approximate equation of the rate constant for rational equilibrium. The methylene protons H_A and H_B are in an AB coupling system, so the crude estimations of rate constants, k , at coalescence were obtained using an approximate equation (Equation 2.1)^{106, 107} and the rate constants for three ligands are calculated using the parameters obtained from the ^1H NMR spectra (Table 2.11). The rotational barriers, or the change of Gibbs free energy (ΔG^\ddagger) for the interconversion between M and P conformers, are correlated to the changes in entropy (ΔS^\ddagger) and enthalpy (ΔH^\ddagger), or can be correlated to the rate constant, which can also be modified into the Eyring Equation (Equation 2.2). Therefore, Eyring plot, $\ln(k/T)$ vs $1/T$, was plotted using two data points (H_A and H_B at coalescence) for each ligand to deduce ΔG^\ddagger from the slopes and intercepts (Figure 2.10 and Table 2.12).

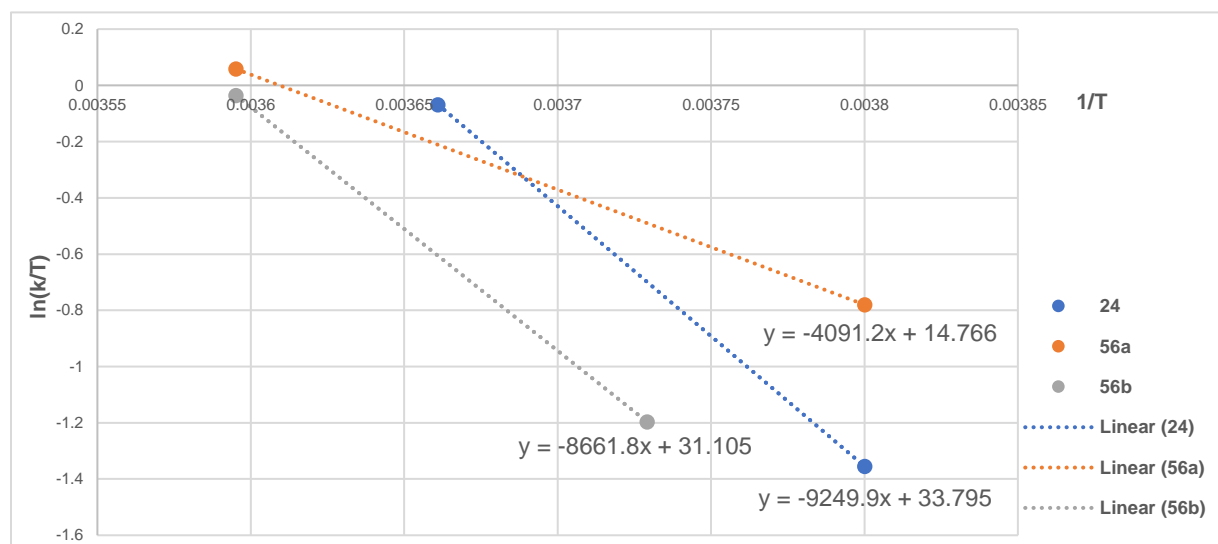
$$k = \frac{\pi \sqrt{\Delta\nu^2 + 6J^2}}{\sqrt{2}} \quad (\text{Equation 2.1})$$

$$\Delta G^\ddagger = \Delta H^\ddagger - T\Delta S^\ddagger \rightarrow \ln\left(\frac{k}{T}\right) = -\frac{\Delta H^\ddagger}{R} \cdot \frac{1}{T} + \frac{\Delta S^\ddagger}{R} + \ln\left(\frac{k_B}{h}\right) \quad (\text{Equation 2.2})$$

**Table 2.11** Calculation of rate constants

Ligands	$\Delta\nu(H_A)$, Hz	$\bar{J}(H_A)$, Hz	$T_c(H_A)$, K	$k(H_A)$, s^{-1}	$\Delta\nu(H_B)$, Hz	$\bar{J}(H_B)$, Hz	$T_c(H_B)$, K	$k(H_B)$, s^{-1}
24	113.91	5.85	273.15	255.05	29.98	5.85	263.15	67.85
56a	131.90	5.90	278.15	294.76	53.96	5.90	263.15	120.58
56b	119.91	6.00	278.15	268.37	35.97	5.95	268.15	81.00

($\Delta\nu(H_A)$) is the chemical shift different between H_A' and H_A'' at $-40\text{ }^\circ\text{C}$; \bar{J} is the average coupling constant of H_A' and H_A'' ; T_c is the coalescence temperature; R is gas constant; k_B is Boltzmann's constant; h is Planck's constant) (same for H_B)

**Figure 2.10** Eyring plots for rate constants of rotation in ligands **24**, **56a** and **56b****Table 2.11** Calculation of rotational barriers (ΔG^\ddagger)

Ligand	ΔH^\ddagger , kcal/mol	ΔS^\ddagger , kcal/mol·K	ΔG^\ddagger (at 273.15K), kcal/mol
24	18.38	0.02	12.94
56a	8.13	-0.02	13.01
56b	17.21	0.01	13.23

2.2.4. Rh₂(*o*-CITPCP)₄ Series Catalysts for Enhancing Diastereoselectivity

Compared to most of the dirhodium carboxylate catalysts developed before Rh₂(*o*-CITPCP)₄, significant improvement in the diastereoselectivity in C–H insertion at the benzylic methylene site was observed for the Rh₂(*o*-CITPCP)₄ series of catalysts (Table 2.8 and 2.9) This effect was considered to be worth further exploration with a broader range of substrates.

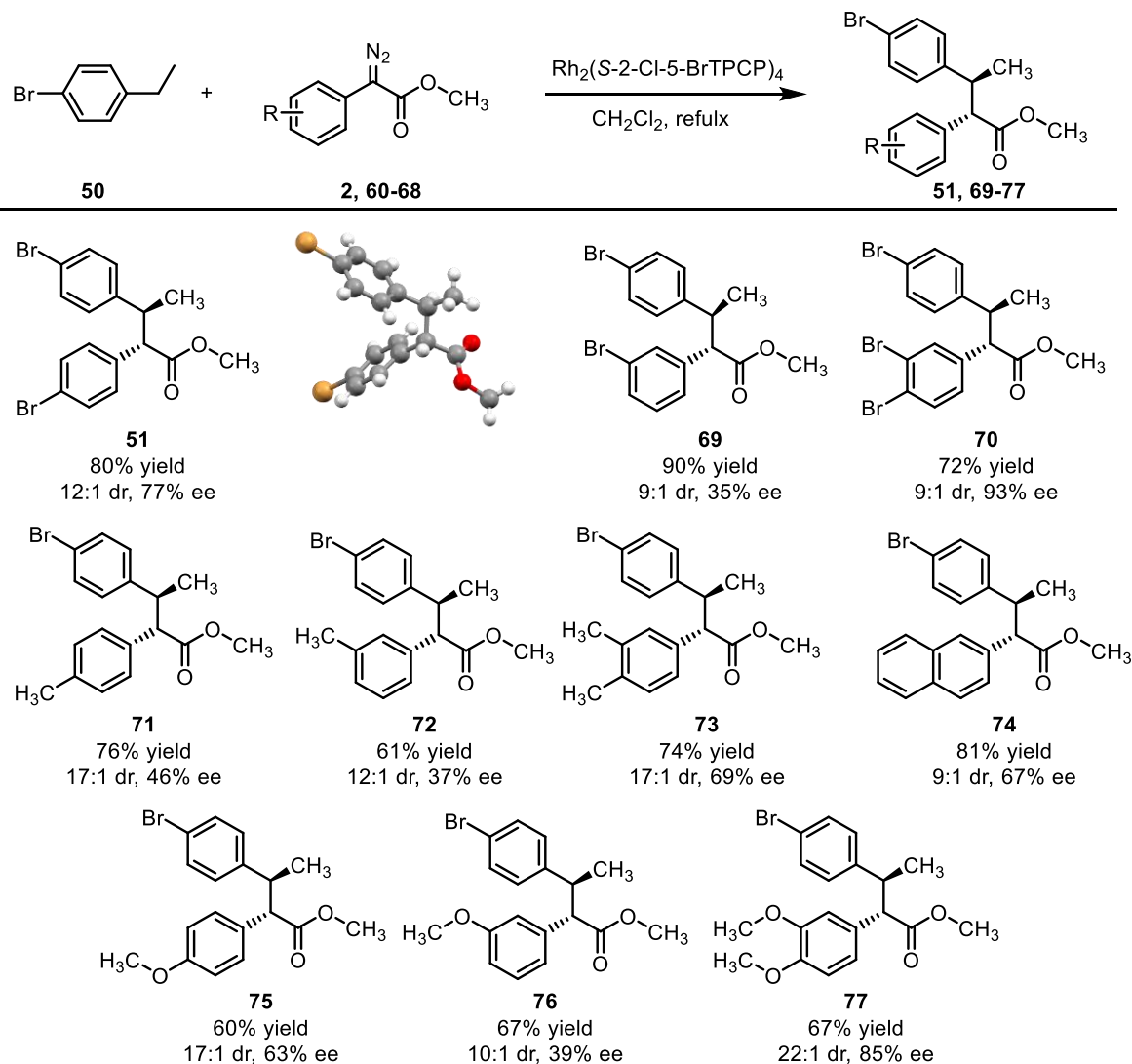
In the initial examination, 4-bromoethylbenzene **50** and methyl 2-(4-bromophenyl)-2-diazoacetate **2**, Rh₂(*S*-2-Cl-5-BrTPCP)₄ is the optimal catalyst and it generate the C–H insertion product **51** in 80% yield, 11.5:1 dr and 77% ee. It was found previously that the substituent on the donor group could alter the electronic and steric properties of the diazo compound and further induce subtle influence on the stereoselectivity of the C–H insertion reactions in addition to the catalyst-control.¹⁰⁸ Variations on the effect of substituents in the methyl diazoacetates was conducted and they showed consistent correlations with the stereoselectivity (Scheme 2.5). A slight or moderate drop in enantioselectivity was observed when the substituent increased in the electron-donating property of the donor part in the carbene (63% ee in **75** with methoxy group vs. 77% ee in **51** with bromide). At the same time, both methyl and methoxy groups are sterically bulkier than the bromide atom, which resulted in noticeable improvement in the diastereoselectivity (17:1 dr for **71** and **75** vs. 11:1 dr for **51**). The influence of steric factors is further demonstrated by other entries. Generally, regardless of the electronic property of these substituents on the aryl ring, for both a weak electron-withdrawing group (bromide) and electron-donating groups (methyl and methoxy), when the substituent is moved from the *para*- to the *meta*-position, considerable decrease in stereoselectivity was observed (**69**, **72**, **76**), presumably caused by the drop in steric control when losing the substituent at the *para*-position. Similar influence was found when the aryl ring had substituents at both the *para*- and the *meta*-positions, resulting in

increased stereinduction, especially enantioselectivity, (**70**, **73**, **77**) compared to the mono-substituted aryldiazoacetates. Interestingly, decrease in diastereoselectivity was observed when the donor moiety was altered from 3,4-dimethylbenzene (17:1 dr in **73**) to a naphthalene group (9:1 dr in **74**), which have similar electronic and steric properties. In summary, the steric factor can considerably influence the diastereoselectivity of the $\text{Rh}_2(\text{S-2-Cl-5-BrTPCP})_4$ -catalyzed C–H functionalization of benzylic methylene sites.

Inspired by the impressive enhancement in diastereoselectivity achieved by the $\text{Rh}_2(o\text{-CITPCP})_4$ series of catalysts, the substrate scope was expanded to other benzylic sp^3 C–H bonds, specifically those that have historically furnished carbene C–H insertion products with poor stereinduction using previous generations of dirhodium catalysts.^{60, 61} In comparison with the broadly-studied $\text{Rh}_2(R\text{-DOSP})_4$, both $\text{Rh}_2(o\text{-CITPCP})_4$ and $\text{Rh}_2(\text{S-2-Cl-5-BrTPCP})_4$ consistently result in enhancement in the diastereoselectivity, and $\text{Rh}_2(\text{S-2-Cl-5-BrTPCP})_4$ -catalyzed reactions were proceed with ~10% higher ee than $\text{Rh}_2(o\text{-CITPCP})_4$ (Scheme 2.6). The relative stereochemistry of the major diastereomer of the products was confirmed from the crystal structures of **51** and **83** obtained from reaction with $\text{Rh}_2(\text{S-2-Cl-5-BrTPCP})_4$. With R^1 representing the sterically larger aryl group, the small group R^2 ranged from methyl, cyclic methylene and oxygen atom, showing improvement in diastereoselectivity in all four examples. The best diastereoselectivity (24->30:1) was observed for **83** with oxygen atom as R^2 , which is much smaller compared to the R^1 aryl group. Noticeably, $\text{Rh}_2(\text{S-2-Cl-5-BrTPCP})_4$ -catalyzed reaction on **81** gave slightly higher diastereoselectivity than the one on **82**, which has an additional electron-donating (methoxy) group on the aryl ring in the substrate **79**, presumably because **79** is more reactive with the electron-donating group that further stabilized the partial positive charge build-

up in the transition state. A Similar effect was also found when compared the dr for **59** and **51**, with methoxy and bromide as *para*-substituents, respectively.

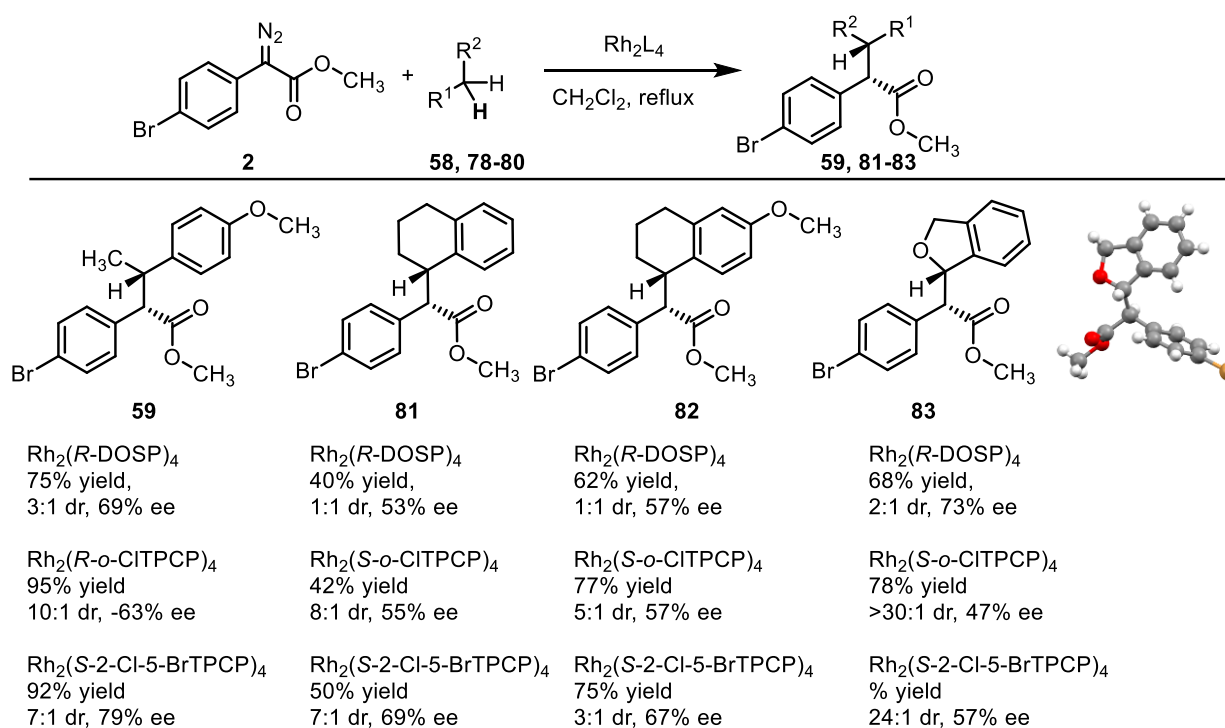
Scheme 2.5 Scope of diazoacetates in C–H insertion of 4-bromoethylbenzene



Previous work has established that the conformational symmetry of the ligands around the paddlewheel complex plays a pivotal role in the selectivity imparting nature of the catalyst.¹⁰⁴ Cooperating with previous computational studies on the transition state of Rh-carbene C–H insertion, the chiral-crown character of these $\text{Rh}_2(o\text{-ClTPCP})_4$ series catalysts, along with the effects of the steric difference between R^1 and R^2 units in the substrates give a clear prediction of

the catalyst's diastereoselectivity (Figure 2.11). In the Newman-projection model, the lowest energy transition state conformation has the smallest substituent on the substrate, a hydrogen atom [S(H)] in these benzylic methylene C–H insertions, “gauche” to both the Rh–O disk and the ester parallel plane. On the other hand, the aryl group of the metal bound carbene, which is perpendicular to the Rh–O disk, has less steric impact, so the Rh–O disk and the bulky components in the ligand are controlling the arrangement of the large [$R^1(\text{Ar})$] and medium (R^2) groups. That is, R^2 would fit between (“gauche” to) the Rh–O disk and carbene aryl ring, because it is smaller than the $R^1(\text{Ar})$ group, which would point away from the Rh–O disk. With additional steric limitation from the ligand, which is weaker in D_2 symmetric $\text{Rh}_2(\text{TPCP})_4$,⁷⁸ the diastereoselectivity was enhanced.

Scheme 2.6 Expanded benzylic substrates for diastereoselectivity examination



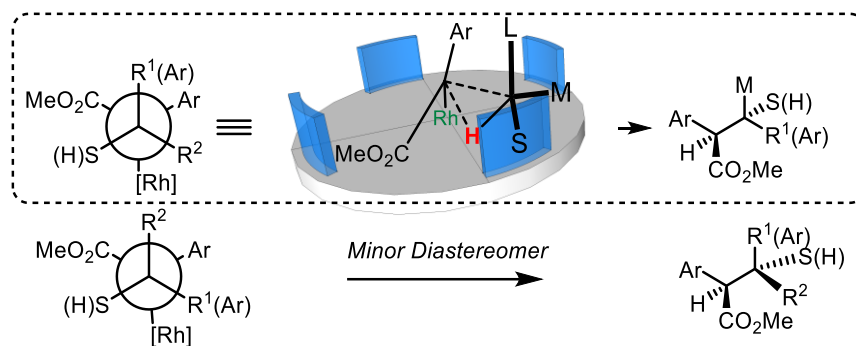


Figure 2.11 Newman-projection for intermediate at transition state

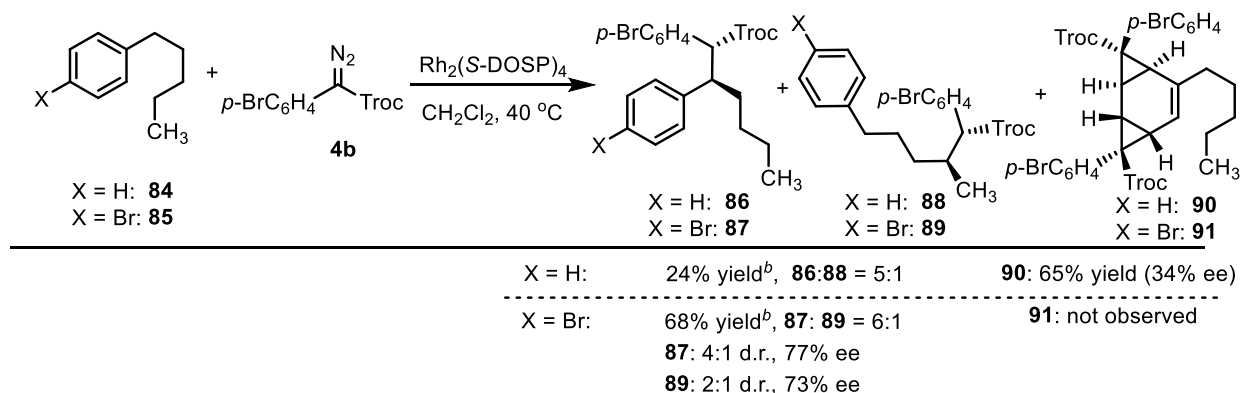
2.2.5. Catalyst-Controlled Selective Functionalization of Unactivated C–H Bonds in the Presence of Electronically Activated C–H Bonds

Inspired by the explorations above, a hypothesis was developed that the C_4 symmetry or chiral-crown structure of the $Rh_2(S\text{-}o\text{-CITPCP})_4$ series catalysts induce more steric limitation at the reactive pocket. Therefore, these catalysts would be more sensitive to steric bias on substrates over electronic factors in the selective C–H functionalization. As described in the introduction (section 2.1.2), benzylic C–H bonds are electronically preferred in rhodium carbene chemistry due to their ability to stabilize the partial positive charge built-up in the transition state. Thus, it would be interesting to utilize the steric feature of the $Rh_2(S\text{-}o\text{-CITPCP})_4$ series of catalysts to challenge this electronic-dominated system, by functionalization of unactivated C–H bonds in the presence of more reactive sites, such as benzylic sites.

Before testing this hypothesis, the benzene rings in the substrates could be suitably protected to prevent cyclopropanation on the benzene rings, which occurs more readily than C–H insertion reactions unless sterically blocked.³⁷ Together with the development of dirhodium carboxylate catalysts, the advancement of using trihaloethyl esters in the donor/acceptor carbene precursors

made the functionalization on unactivated C–H bonds cleaner and more selective, which may be caused by the increased the electrophilicity of the carbenes and increased steric bulk in suppressing the undesired dimerization with these moieties.⁸⁰ These trihaloethyl aryldiazoacetates are also applied to this challenging unactivated substrates described here. Thus, the trend that substituents at both 1- and 4-positions can sterically protect the benzene rings, which was discovered in systems using methyl esters, is re-evaluated here using trihaloethyl aryldiazoacetates (Scheme 2.7). Using 2,2,2-trichloroethyl 2-(4-bromophenyl)-2-diazoacetate **4b** as carbene precursor and Rh₂(S-DOSP)₄ as catalyst, reaction on unprotected pentylbenzene **84** generated a 2.7:1 mixture of double-cyclopropanation product **90** and C–H insertion products (**86** and **88**), in which the ratio of C–H insertions at benzylic site **86** and terminal methylene site **88** is 5:1. In contrast, when the substrate was protected by *para*-bromide substituent in **85**, no cyclopropanation was observed and C–H insertion products were obtained as a 6:1 mixture in 68% yield.

Scheme 2.7 Evaluation of benzene ring protection



With these results, 1-bromo-4-pentylbenzene **85** was chosen as a reference substrate for examination of the proposed challenge by evaluating various dirhodium carboxylate catalysts with trihaloethyl 4-bromophenyldiazoacetates (**4a-c**) in this reaction system (Table 2.12). It was

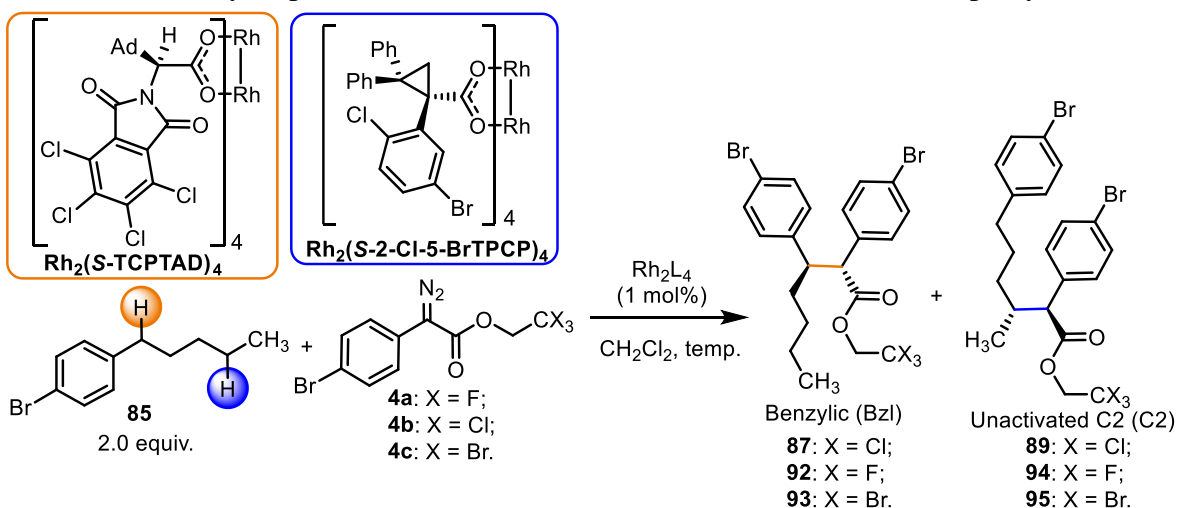
anticipated that only the benzylic and the terminal methylene sites would be the competing sites, because other internal C–H bonds are neither electronically activated nor sterically accessible.

As expected, the proline-based catalyst, $\text{Rh}_2(\text{S-DOSP})_4$, preferred the electronically activated benzylic C–H bonds, affording product **87** (5:1 rr). The phthalimido-derived catalyst, $\text{Rh}_2(\text{S-PTAD})_4$, was less selective for the benzylic C–H insertion product **87** with 2:1 site-selectivity and low enantioselectivity (16% ee). A modified phthalimido-derived catalyst with tetrachloride substituents on each ligand, $\text{Rh}_2(\text{S-TCPTAD})_4$, gave the highest site- and stereoselectivity for benzylic product **87** (9:1 rr, 13:1 dr, 93% ee) with 78% yield. Further optimization was conducted using lower temperatures and different halogens in the trihaloethyl ester of the carbene precursors. The stereoselectivity in a reaction conducted at a lower temperature, 0 °C, was improved slightly over the one using tribromoethyl derivative **93** as carbene precursor at refluxing CH_2Cl_2 (11:1 rr, 16:1 dr), but the yield for the reaction conducted at 0 °C was 10% lower. In contrast, the trifluoroethyl aryldiazoacetates **92** gave considerably lower site- and diastereoselectivity (7:1 rr, 5:1 dr). That is, $\text{Rh}_2(\text{S-TCPTAD})_4$ combined with the tribromoethyl aryldiazoacetates **4c** was found to be the optimal system for benzylic C–H functionalization.

Unlike the proline- and phthalimido-based dirhodium catalysts, the TPCP-derived dirhodium catalysts have been found to favor less sterically hindered sites,^{79, 81, 82} and they switched the site-selectivity preferring the most accessible unactivated C–H bonds (Table 2.12). Both *para*- and *meta*-substituted derivatives, $\text{Rh}_2(\text{S-}p\text{-BrTPCP})_4$, $\text{Rh}_2(\text{S-}p\text{-PhTPCP})_4$ and $\text{Rh}_2[\text{R-3,5-di}(p\text{-}^t\text{BuC}_6\text{H}_4)\text{TPCP}]_4$, preferred C2 insertion product **89** in low site-selectivity (2-3:1 rr). The $\text{Rh}_2(\text{S-}o\text{-ClTPCP})_4$, which was found to be more steric demanding earlier in this chapter, gave significant enhancement in the site-selectivity for **89** (12:1 rr). Similar to the trend observed in the optimization on the $\text{Rh}_2(\text{S-}o\text{-ClTPCP})_4$ series catalysts, $\text{Rh}_2(\text{S-2-Cl-5-BrTPCP})_4$ improved the

stereoselectivity to 20:1 dr and 89% ee. Although lower temperature, 0 °C, improved the site- and stereoselectivity, alternation on the trihaloethyl groups in the carbene precursors resulted in comparable effect, in which the trifluoroethyl derivative **84** gave 23:1 r.r., 28:1 d.r. and 91% ee without loss in yield (86%).

Table 2.12 Catalyst optimization for C–H functionalization on 1-bromo-4-pentylbenzene



Entry	L	44 (X)	temp. (°C)	yield ^a (%)	rr (Bzl:C2)	87,92,94		89,94,95	
						dr	ee (%)	dr	ee (%)
						87,92,94 as major			
1	S-DOSP	4b (Cl)	40	68	6:1	4:1	77	2:1	-73
2	S-PTAD	4b (Cl)	40	62	2:1	6:1	16	1:2	58
3	S-TCPTAD	4b (Cl)	40	78	9:1	13:1	93	2:1	-86
4	S-TCPTAD	4b (Cl)	0	65	13:1	21:1	94	4:1	--
5	S-TCPTAD	4c (Br)	40	75	11:1	16:1	90	3:1	--
6	S-TCPTAD	4a (F)	40	80	7:1	5:1	85	3:1	--
						89,94,95 as major			
7	S- <i>p</i> -BrTPCP	4b (Cl)	40	48	1:2	2:1	--	4:1	-83
8	S- <i>p</i> -PhTPCP	4b (Cl)	40	45	1:2	2:1	--	10:1	-88
9	<i>R</i> -3,5-di(<i>p</i> - ^t Bu) C ₆ H ₄)TPCP	4b (Cl)	40	69	1:3	3:1	--	7:1	89
10	S- <i>o</i> -CITPCP	4b (Cl)	40	90	1:12	5:1	--	17:1	78
11	S-2-Cl-4-BrTPCP	4b (Cl)	40	92	1:11	5:1	--	19:1	74
12	S-2-Cl-5-BrTPCP	4b (Cl)	40	87	1:20	6:1	--	20:1	89
13	S-2-Cl-5-BrTPCP	4b (Cl)	0	80	1:27	8:1	--	>30:1	88
14	S-2-Cl-5-BrTPCP	4c (Br)	40	84	1:13	5:1	--	13:1	84
15	S-2-Cl-5-BrTPCP	4a (F)	40	86	1:24	4:1	--	28:1	91

^a Combined yield of **50** and **51** after flash column chromatography.

Interestingly, the influence of different solvents and hexafluoro-2-propanol (HFIP) as additive was also explored (Table 2.13). Among different polar chlorinated solvents, dichloromethane is the best solvent, while the others inhibited the reactions and gave little or no yield for the C–H insertion products. No improvement was observed even at increased temperature. Fluorinated alcohols are found to have some positive effects on the metal catalyzed reactions.¹⁰⁹⁻¹¹¹ Herein, several fluorinated alcohols with different pKas were tested as additives (2.0 equiv.). Noticeably, when substrate **85** was used directly from commercial bottles, enhancement in stereoselectivity was observed when HFIP (pKa = 9.3) was added (87% ee in entry 6 with ~7% increase from entry 5), and similar trends were shown with perfluoro-*tert*-butanol (pKa = 5.4) and 1,1,1,3,3,3-hexafluoro-2-methylpropan-2-ol (pKa = 9.8). However, fluorinated additive with higher pKa (~12) give lower or no yield of the C–H insertion product (entry 9-11). Most interestingly, when the substrate **85** was dried via lyophilization (entry 12), comparable high stereoselectivity was obtained (20:1 dr and 89% ee), as well as improved site-selectivity (20:1 rr). HFIP was considered to behave as “drying agent” in this case which may interact with the water moieties in the system to keep it away from the rhodium carbenes. All the following reactions in this system was conducted using dried substrates, including the ones in the condition optimization Table 2.12.

Table 2.13 Solvent and additive effects on the C–H functionalization of **48**

Entry	L	solvent	additive	temp. (°C)	yield (%)	rr	dr	ee (%)
1	S- <i>o</i> -CITPCP	CH ₂ Cl ₂	none	40	90	12:1	17:1	77
2	S- <i>o</i> -CITPCP	CH ₂ ClCH ₂ Cl	none	40	9	7:1	12:1	67
3	S- <i>o</i> -CITPCP	CH ₂ ClCH ₂ Cl	none	60	0	--	--	--
4	S- <i>o</i> -CITPCP	CHCl ₃	none	40	0	--	--	--
5	S-2-Cl-5-BrTPCP	CH ₂ Cl ₂	none	40	86	16:1	18:1	80
6	S-2-Cl-5-BrTPCP	CH ₂ Cl ₂	(CF ₃) ₂ CHOH	40	83	22:1	19:1	87
7	S-2-Cl-5-BrTPCP	CH ₂ Cl ₂	(CF ₃) ₃ COH	40	84	19:1	18:1	91
8	S-2-Cl-5-BrTPCP	CH ₂ Cl ₂	(CF ₃) ₂ CH ₃ COH	40	73	19:1	18:1	89
9	S-2-Cl-5-BrTPCP	CH ₂ Cl ₂	CF ₃ (CH ₃) ₂ COH	40	32	17:1	18:1	88
10	S-2-Cl-5-BrTPCP	CH ₂ Cl ₂	CF ₃ CH ₂ OH	40	0	--	--	--
11	S-2-Cl-5-BrTPCP	CH ₂ Cl ₂	CF ₃ COOH	40	0	--	--	--
12 ^a	S-2-Cl-5-BrTPCP	CH ₂ Cl ₂	none	40	87	20:1	20:1	89

^a **85** was lyophilized before use. Otherwise, **85** was used directly from the commercial bottle.

At this stage, with the optimal catalyst, Rh₂(S-2-Cl-5-BrTPCP)₄, five different representative diazoacetates (**2**, **96**, **4a-c**) were examined on 4-bromoalkylbenzenes with different alkyl chain lengths to gather a rough picture of the site-selectivity (Table 2.14). The C–H insertion products at benzylic and terminal methylene sites give unique and well separated peaks in ¹H-NMR that can be used to determine their ratios in the resulting reaction mixture, as seen in the examples of 1-bromo-4-pentylbenzene **85** with trihaloethyl diazoacetates **4a-c**, so ¹H-NMR of the crude reaction mixtures are used for site-selectivity determination without further purification. Despite the diazoacetate used, when the chain lengths got longer, which makes the terminal methylene sites

further away from the aryl ring and therefore more sterically accessible, the site-selectivity for C2 functionalization increased (from left to right at each row in the table, or blue-orange-gray-yellow in the chart). The site-selectivity improvement was biggest when *n* change from 0 to 1, in which the percentages of C2–H insertion product on 4-bromobutylbenzene were generally 5 times more than those on the propyl derivative. Moreover, the trihaloethyl diazoacetates gave better site-selectivity as expected in the catalyst screening stage, and the trifluoroethyl diazoacetate generally performed best with different alkyl chain length in the substrates. These results were used in a collaboration with Dr. Tobias Gensch in the Sigman group to probe and potentially build a model for the site-selectivity in rhodium carbene chemistry.

Next, the influence of electronic and steric factors on the substrate was examined in both $\text{Rh}_2(\text{S-TCPTAD})_4$ - and $\text{Rh}_2(\text{S-2-Cl-5-BrTPCP})_4$ -catalyzed C–H insertion reactions, using substrates with different substituents at the *para*-position of the aryl rings or shorter distances between benzylic and terminal methylene sites (Scheme 2.8). Shortening the distance between the terminal and benzylic methylene sites increase the steric hinderance of the terminal methylene site, and therefore, has considerable effect on the site-selectivity. More specifically, for 1-bromo-4-butylbenzene **97**, the $\text{Rh}_2(\text{S-TCPTAD})_4$ -catalyzed reaction gave enhanced site-selectivity for benzylic product **101c** (25:1 rr), while the terminal C2–H insertion product **105a** was less preferred by $\text{Rh}_2(\text{S-2-Cl-5-BrTPCP})_4$ (5:1 rr), and the stereoselectivity for both cases were maintained at high level as in the reference reaction on **85**. Changing the electronic character of the aryl ring in the substrate also have significant influence on the site-selectivity, because it alters the ability to stabilize the partial positive charge build-up on the benzylic sites. The site-selectivity for reactions, which are catalyzed by $\text{Rh}_2(\text{S-TCPTAD})_4$ combined with tribromoethyl diazoacetate **4c**, increased when the *para*-substituent on the aryl ring changed from electron-withdrawing to electron-

donating. As shown for **102a** with methyl ester as strong electron-withdrawing group, the benzylic site was significantly weakened and therefore showed low site-selectivity (3:1 rr) and poor yield (42%). When the *para*-substituent was changed to an acetoxy group as weak electron-donating group, site-selectivity for Rh₂(*S*-TCPTAD)₄-catalyzed reaction enhanced to 17:1 rr for **103c** in 83% yield. As expected, in the case of strong electron-donating methoxy group, the benzylic product **104c** was generated as single regioisomer by Rh₂(*S*-TCPTAD)₄ in 91% yield and high stereoselection (13:1 dr, 87% ee). In contrast, the preference for terminal C2–H insertion product in reactions using Rh₂(*S*-2-Cl-5-BrTPCP)₄ was weakened by electron-donating groups on the *para*-position of the aryl rings. The Rh₂(*S*-2-Cl-5-BrTPCP)₄-catalyzed reaction on methyl ester derivative **98** gave the highest site-selectivity, in which the terminal C2 product **106a** was generated as single regioisomer with high stereoselectivity (20:1 dr, 92% ee). Notably, terminal C2 product **109a** was still highly favored with a weak electron-donating group, the acetoxy group, substituted on the aryl ring, when Rh₂(*S*-2-Cl-5-BrTPCP)₄ was used as catalyst (18:1 rr). The margin for functionalizing C2–H bonds using Rh₂(*S*-2-Cl-5-BrTPCP)₄ as catalyst is the methoxy substituent, which gave around 1:1 mixture of both regioisomers with maintained high stereoselection (28:1 dr, 93% ee). The site-selectivity is influenced by both the steric environment of the terminal methylene site and the electronic property of the benzylic C–H bonds.

Table 2.13 Screening for alkyl chain lengths and diazoacetates

Peaks used for ratio determination in crude ¹H-NMR (see SI for specific spectra)

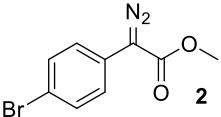
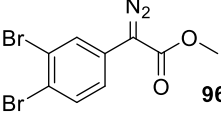
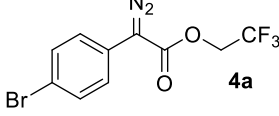
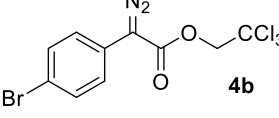
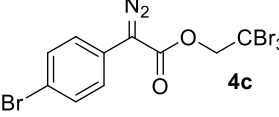
Diastereomer ratio (pink circle) Regioisomer ratio (blue circle)

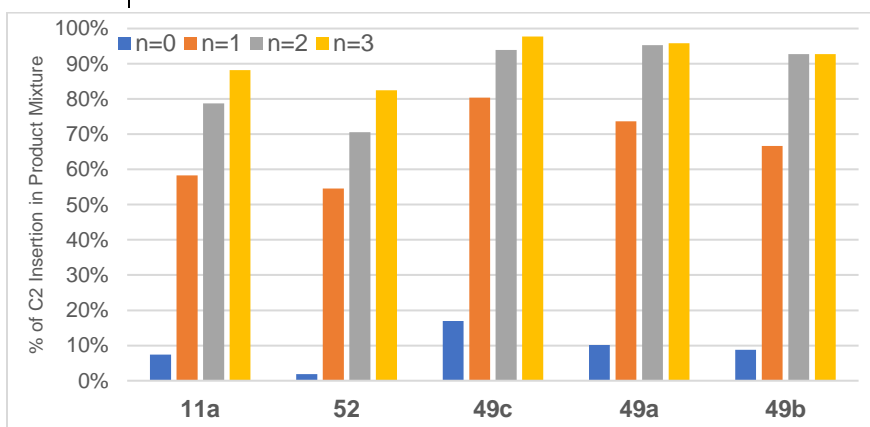
d = doublet
t = triplet

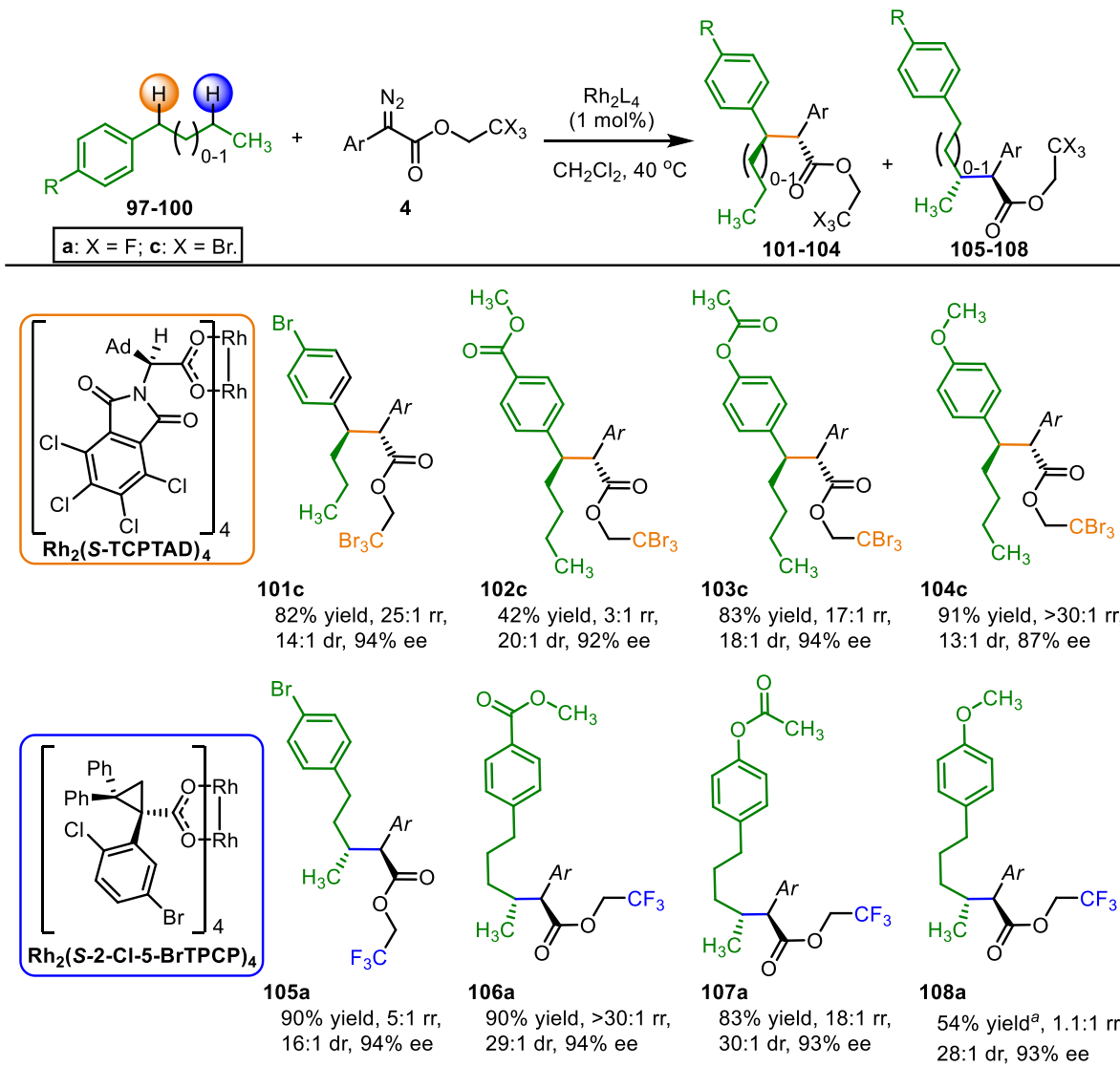
Benzylic Insertion Unactivated C2-H Insertion

Reaction scheme: BrC1=CC=C(C=C1)CC(C)C + ArC(=O)C(=[N+]=[N-])OR >> [Rh2(S-2-Cl-5-BrTPCP)4, CH2Cl2, reflux] ArC(=O)C(C)C(C)C1=CC=C(Br)C=C1 + ArC(=O)C(C)C(C)C1=CC=C(Br)C=C1

Unactivated C2 Benzylic (Bzl)

r.r. = C2: Benzylic	n = 0	n = 1	n = 2	n = 3
 2	1: 12.4 <i>r.r.</i> 5.4: 1 <i>d.r.</i> (C2) 7.2: 1 <i>d.r.</i> (Bzl)	1.4: 1 <i>r.r.</i> 10.5: 1 <i>d.r.</i> (C2) 4.5: 1 <i>d.r.</i> (Bzl)	3.7: 1 <i>r.r.</i> 16.4: 1 <i>d.r.</i> (C2) 4.7: 1 <i>d.r.</i> (Bzl)	7.5: 1 <i>r.r.</i> 12.9: 1 <i>d.r.</i> (C2) 4.2: 1 <i>d.r.</i> (Bzl)
 96	1: 53.1 <i>r.r.</i> 1.7: 1 <i>d.r.</i> (C2) 7.1: 1 <i>d.r.</i> (Bzl)	1.2: 1 <i>r.r.</i> 1.3: 1 <i>d.r.</i> (C2) 3.6: 1 <i>d.r.</i> (Bzl)	2.4: 1 <i>r.r.</i> 8.3: 1 <i>d.r.</i> (C2) 2.7: 1 <i>d.r.</i> (Bzl)	4.7: 1 <i>r.r.</i> 10.0: 1 <i>d.r.</i> (C2) 3.2: 1 <i>d.r.</i> (Bzl)
 4a	1: 4.9 <i>r.r.</i> 6.0: 1 <i>d.r.</i> (C2) 9.6: 1 <i>d.r.</i> (Bzl)	4.1: 1 <i>r.r.</i> 18.3: 1 <i>d.r.</i> (C2) 4.1: 1 <i>d.r.</i> (Bzl)	23.9: 1 <i>r.r.</i> 27.7: 1 <i>d.r.</i> (C2) 3.3: 1 <i>d.r.</i> (Bzl)	42.5: 1 <i>r.r.</i> 27.1: 1 <i>d.r.</i> (C2) 3.3: 1 <i>d.r.</i> (Bzl)
 4b	1: 8.9 <i>r.r.</i> 2.2: 1 <i>d.r.</i> (C2) 10.0: 1 <i>d.r.</i> (Bzl)	2.8: 1 <i>r.r.</i> 13.3: 1 <i>d.r.</i> (C2) 6.7: 1 <i>d.r.</i> (Bzl)	20.2: 1 <i>r.r.</i> 20.0: 1 <i>d.r.</i> (C2) 5.0: 1 <i>d.r.</i> (Bzl)	22.8: 1 <i>r.r.</i> 18.8: 1 <i>d.r.</i> (C2) 7.0: 1 <i>d.r.</i> (Bzl)
 4c	1: 10.4 <i>r.r.</i> 1.4: 1 <i>d.r.</i> (C2) 10.5: 1 <i>d.r.</i> (Bzl)	2.0: 1 <i>r.r.</i> 8.5: 1 <i>d.r.</i> (C2) 8.8: 1 <i>d.r.</i> (Bzl)	12.7: 1 <i>r.r.</i> 12.8: 1 <i>d.r.</i> (C2) 4.4: 1 <i>d.r.</i> (Bzl)	12.8: 1 <i>r.r.</i> 15.3: 1 <i>d.r.</i> (C2) 4.9: 1 <i>d.r.</i> (Bzl)



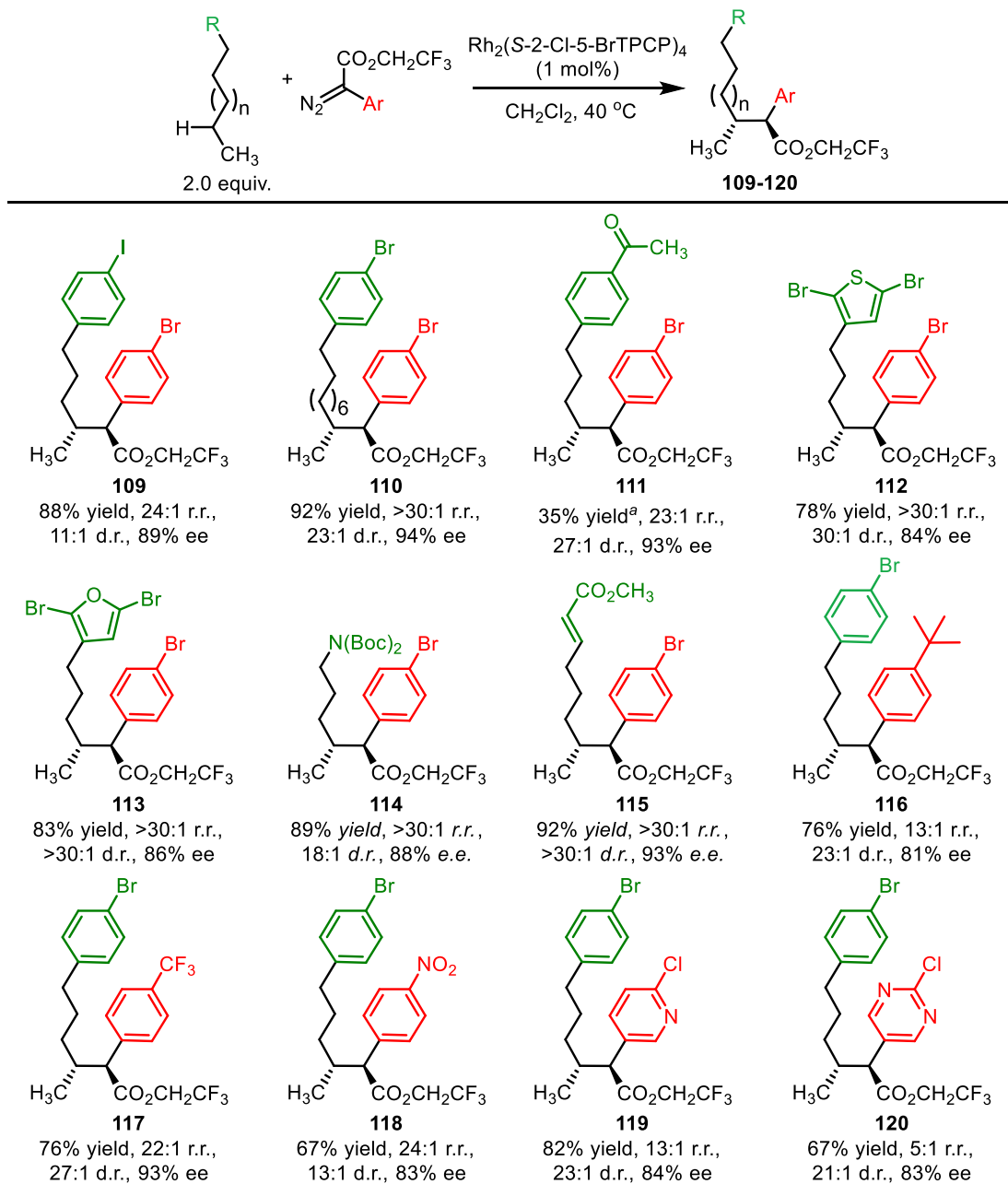
Scheme 2.8 Influence of electronic and steric factors on the substrates

^a 36% yield of primary C-H insertion product at methoxy group (84% ee).

Using Rh₂(S-2-Cl-5-BrTPCP)₄ as optimal catalyst, studies were then conducted on variation of the aryl rings in the diazoacetates and R groups adjacent to the electronically activated sites (Scheme 2.9). These electronically activated sites are not limited to benzylic, but also includes C-H bonds adjacent to heterocycles (**112**, **113**), nitrogen atom (**114**) and allylic sites (**115**). All the reactions demonstrated high levels of stereoselectivity (13:1–30:1 d.r., 83–93% ee), with good site

selectivity (5:1–30:1 r.r.) for the terminal unactivated secondary C–H bonds. An iodide substituent on the aryl ring has similar influence as the bromide substituent in reference reaction and was compatible in forming **109** in 88% yield. Extended alkyl chain with increased amount of internal C–H bonds led to terminal C2 product **110** in high yield (92%) and very high site selectivity (>30:1 r.r.), which indicated the lack of a directing group effect of the aryl ring imparts and emphasizes the pronounced site-selectivity for terminal methylene C–H bonds regardless of the number of internal methylene groups in the substrate. Epoxidation of an aryl ketone readily happens in carbene chemistry,¹¹² and consequently, **111** was obtained in only 35% yield. Heterocyclic rings are compatible in this system, as illustrated in the formation of the derivatives containing thiophene (**112**) and furan (**113**) with >30:1 rr in both cases, as well as the pyridine (**119**) and pyrimidine (**120**) but lower site-selectivity (13:1 rr for **119** and 5:1 rr for **120**). Similarly, these heterocycles need to be substituted to prevent undesired cyclopropanation reactions. Noticeably, preference for electronically activated C–H bonds adjacent to nitrogen and allylic C–H bonds can also be surmounted when they are substituted with electron-withdrawing groups with >30:1 rr and high stereoinduction, as illustrated in the formation of **114** and **115**. The reaction could be extended to a range of aryldiazoacetates, including those with electron-donating substituents (*tert*-butyl in **116**) and electron-withdrawing groups (trifluoromethyl in **117** and nitro in **128**) with good site- and stereoinduction. The absolute configurations were tentatively assigned by analogy to the Rh₂[R-3,5-di(*p*-*t*BuC₆H₄)TPCP]₄-catalyzed C–H functionalization of terminal functionalized n-alkanes and its selectivity in reference reaction of **85**.⁸¹

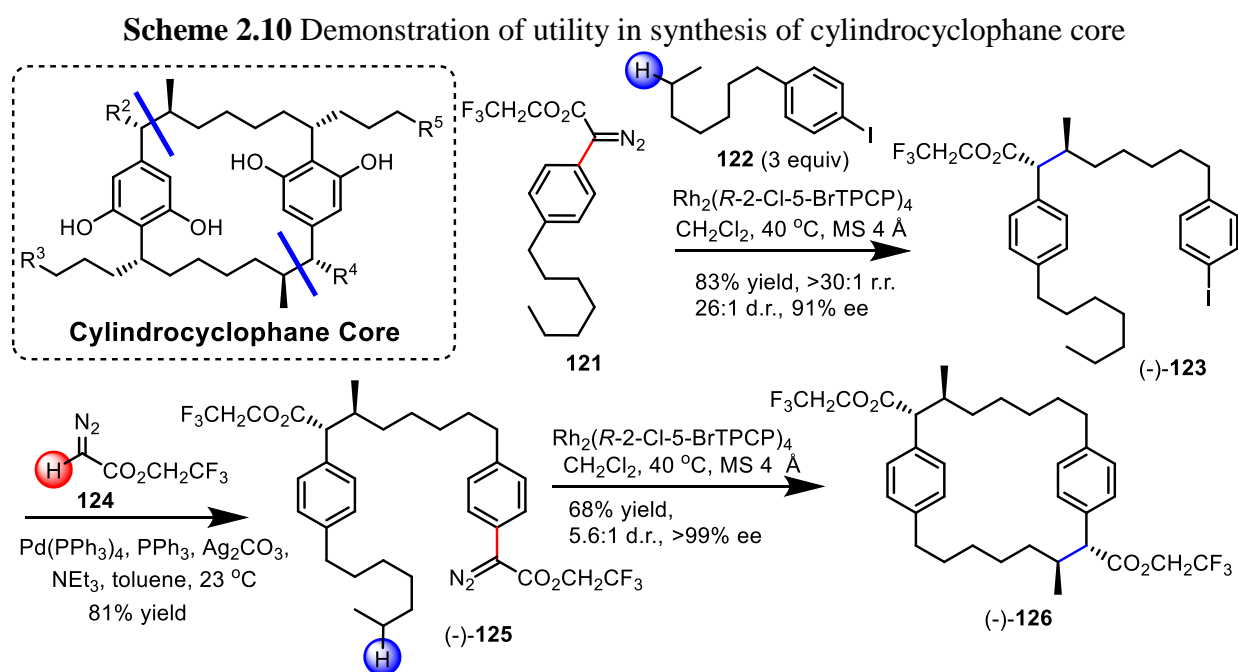
Scheme 2.9 Scope of substrates and diazo compounds



^a 56% epoxide generated as byproduct.

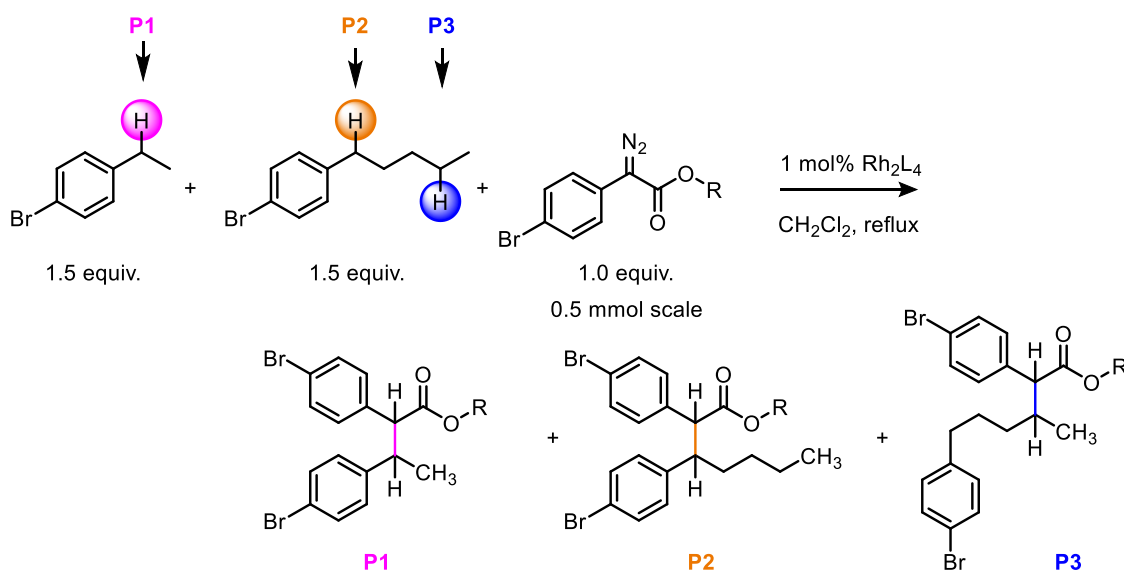
The utility of this system, which selectively functionalize the terminal secondary C–H bonds in the presence of the electronically activated benzylic C–H bond, was further demonstrated in the application for complex molecule synthesis, as demonstrated in the construction of the scaffold for

cylindrocyclophane natural products (Scheme 2.10). This is a collaboration project between Davies group and Stoltz group, and was initially led by Dr. Kuangbiao Liao and later led by a new graduate student, Aaron Bosse. In the initial catalyst examination, Aaron found that the $\text{Rh}_2(S\text{-}2\text{-Cl-}5\text{-BrTPCP})_4$ was a better catalyst than $\text{Rh}_2[R\text{-}3,5\text{-di}(p\text{-}^t\text{BuC}_6\text{H}_4)\text{TPCP}]_4$ for the first intermolecular transformation giving (+)-**123** as single regioisomer. The macrocyclic core was then constructed through a palladium-catalyzed cross-coupling installing the diazo moiety, followed by an intramolecular version of the C–H insertion chemistry. The initial attempt led to (+)-**126** utilizing $\text{Rh}_2(S\text{-}2\text{-Cl-}5\text{-BrTPCP})_4$, whose absolute stereochemistry was confirmed by X-ray crystallography and is consistent with the assignment in the reference reactions above, but the natural product possesses the opposite stereochemistry. Therefore, the optimized result showed in scheme 2.10 was obtained using $\text{Rh}_2(R\text{-}2\text{-Cl-}5\text{-BrTPCP})_4$.¹¹³



In order to gain more insight about the preference between electronically activated benzylic sites and terminal methylene sites, competition reactions were conducted using $\text{Rh}_2(\text{S-2-Cl-5-BrTPCP})_4$, $\text{Rh}_2(\text{S-TCPTAD})_4$ and $\text{Rh}_2(\text{OAc})_4$ (Table 2.14). It is shown that for all three catalysts, the benzylic site for **P1** is the most preferred than all other products, and the selectivity between **P2** and **P3** is similar to observed in the reference reaction. Moreover, $\text{Rh}_2(\text{S-2-Cl-5-BrTPCP})_4$ showed higher preference for **P1** than the other two dirhodium catalysts. These results could potentially provide some insight for computational understanding of the site-selectivity of $\text{Rh}_2(\text{S-2-Cl-5-BrTPCP})_4$.

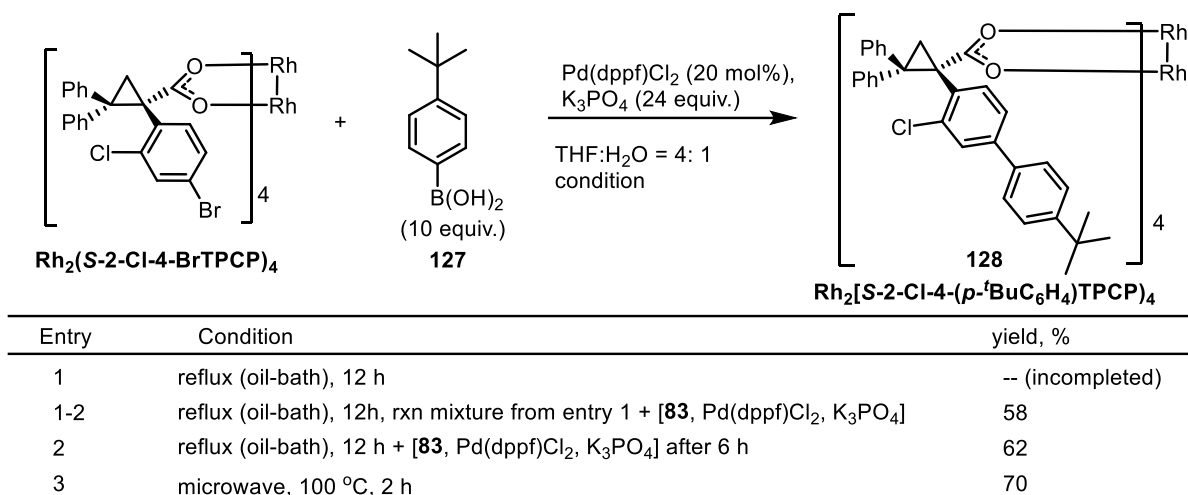
Table 2.14 Competition reaction



R	Rh_2L_4	P1:P2:P3
CH ₃	$\text{Rh}_2(\text{OAc})_4$	21.4:12.3:1
	$\text{Rh}_2(\text{S-TCPTAD})_4$	31.1:7.4:1
	$\text{Rh}_2(\text{S-2-Cl-5-BrTPCP})_4$	30.7:0.3:1
CH ₂ CCl ₃	$\text{Rh}_2(\text{OAc})_4$	18.6:11.7:1
	$\text{Rh}_2(\text{S-TCPHTAD})_4$	23.9:6.7:1
	$\text{Rh}_2(\text{S-2-Cl-5-BrTPCP})_4$	4.9:0.1:1

2.2.6. Extension in Rh₂(*S*-*o*-ClTPCP)₄ Catalysts Family

As discussed earlier in this chapter, adding the additional bromide on the *o*-chlorophenyl ring has the potential for more efficient extension for more Rh₂(*S*-*o*-ClTPCP)₄ derivatives via cross-coupling reactions. Conducting Suzuki coupling reaction directly on the dirhodium (II) tetracarboxylate complexes was initially achieved and optimized by Dr. Kuangbiao Liao in the Davies group in the development of Rh₂[*S*-3,5-di(*p*-^tBuC₆H₄)TPCP]₄, which obtained from 8-fold Suzuki coupling of Rh₂(*S*-3,5-diBrTPCP)₄.⁸¹ The coupling reaction condition was adapted and optimized first for the synthesis of Rh₂[*S*-2-Cl-4-(*p*-^tBuC₆H₄)TPCP]₄ **130** from Rh₂(*S*-2-Cl-4-BrTPCP)₄ (Table 2.15). The initial attempt using the same conditions for Rh₂[*S*-3,5-di(*p*-^tBuC₆H₄)TPCP]₄ with conventional oil-bath heating and same reagent loadings were found to be insufficient, giving mixtures of products with different degrees of coupling as shown in high resolution mass spectroscopy (HRMS). The incomplete reaction mixture was re-subjected to the same reaction condition and desired product with 4-fold couplings was obtained in 58% yield and confirmed with HRMS of the crude reaction solution, so a second trial by adding all other reagents (base, boronic acid and palladium catalyst) again after 6 h was also found to work with 62% yield. An optimal condition was achieved with higher yield (70%) when conducting the reaction using microwave reactor at 100 °C for 2 h. Notably, a new/good batch of the Pd(dppf)Cl₂ was required for efficient coupling.

Table 2.15 Condition optimization for 4-fold Suzuki coupling on $\text{Rh}_2(\text{S-2-Cl-4-BrTPCP})_4$ 

The optimal coupling condition between the dirhodium complexes with arylbromide groups and corresponding boronic acids were applied to the synthesis of more $\text{Rh}_2(\text{S-}o\text{-ClTPCP})_4$ derivatives, and the obtained new catalysts were tested in the reference reaction between 4-bromopentylbenzene **85** and trichloroethyl diazoacetate **4b** (Table 2.16). Generally, all the direct coupling reaction on the $\text{Rh}_2(\text{S-2-Cl-4-BrTPCP})_4$ and $\text{Rh}_2(\text{S-2-Cl-5-BrTPCP})_4$ could be achieved in moderate yield (50-68%), and the reaction with electron-rich aryl groups gave slightly lower yield. In the testing reaction, the resulting $\text{Rh}_2(\text{S-}o\text{-ClTPCP})_4$ derivatives are all preferring the terminal methylene site with various site-selectivity. Both electron-rich (methoxy in **129** and amine in **130**) and electron-poor (trifluoromethyl in **131**) aryl rings gave lower site-selectivity (2.9-4.9:1 rr) than the parental bromide derivative (11:1 rr with $\text{Rh}_2(\text{S-2-Cl-4-BrTPCP})_4$), as well as decrease in stereoselectivity. That is, the electronic property of the *o*-chloroaryl ring needs to be within a suitable range. In contrast, derivatives with no substituent (**132**) or alkyl group (**133**, **135** and **136**) substituted on the coupled aryl rings were relatively better than other derivatives. Interestingly, the derivative **136** with mesityl group coupled furnished the terminal methylene C–H insertion product in a much higher site-selectivity (30.9:1 rr) than the previous optimal catalyst, $\text{Rh}_2(\text{S-2-Cl-5-}$

BrTPCP)₄), and slight loss in stereoselectivity was observed. This implies the unique site-selectivity of this Rh₂(*S*-*o*-CITPCP)₄ catalyst family may arise from a dispersion effect or limited reaction pocket, which is even smaller in **136** with two methyl groups at the *ortho*-positions of each additional aryl rings.

Table 2.16 Synthesis and testing of more Rh₂(*S*-*o*-CITPCP)₄ derivatives

Ar at 4-position	 129 54% yield	 130 50% yield	 131 68% yield		
coupling reaction					
Ar at 5-position	 132 65% yield	 133 66% yield	 134 66% yield	 135 67% yield	 136 62% yield
coupling reaction					

2.2.7. Computational Studies for Structural Understanding of the Complex and Carbene

In order to have a better understanding of the $\text{Rh}_2(\text{S-2-Cl-5-BrTPCP})_4$ complex, computational studies were also conducted by Dr. Zhi Ren, a postdoc in the Davies group, in collaboration with the Musaev group. Most of the results were published¹¹³ and will be briefly summarized here together with an unpublished carbene bound $\text{Rh}_2(\text{S-2-Cl-5-BrTPCP})_4$ structure. All the calculation here were conducted using Gaussian-2009 at the B3LYP-D3BJ level of theory in conjunction with the [Lan12dz (for rhodium) + (6-31G(d)) (for other atoms)] basis sets, with CHCl_3 or CH_2Cl_2 at PCM level of theory as solvent.

In the free *S-2-Cl-5-BrTPCP* ligand, rotational equilibrium between **56b'** and **56b''** (Figure 2.8) is caused by the rotation of the C1–C4 single bond that connects the cyclopropane ring and 2-Cl-5-Br-aryl group, and the CHCl_3 was chosen for the calculation for this rotational barrier as its similar condition to the variable-temperature NMR studies (Figure 2.12). There are two potential rotation directions: one has the aryl ring rotates clockwise from **56b'** to **56b''** with chloride atom orients above the carboxyl group in the transition state (**TS_I**) and the barrier, ΔG_1^\ddagger , is calculated to be $13.9 \text{ kcal mol}^{-1}$; the other direction is anti-clockwise, where the chloride atom passes the C2-*cis*-aryl ring in the transition state (**TS_II**) and gives a barrier, ΔG_2^\ddagger , as $21.1 \text{ kcal mol}^{-1}$. That is, the calculated rotational barrier should be ΔG_1^\ddagger with $13.9 \text{ kcal mol}^{-1}$ in value and is close to the estimation by variable-temperature NMR study ($13.2 \text{ kcal mol}^{-1}$) within margin of error. Moreover, the steric interaction between the chloride atom and the carbonyl carbon atom in **TS_I** is considered to be the cause of the barrier, since their distance was calculated to be 2.94 \AA and is smaller than the sum of their van der Waals radius [$1.70 \text{ (C)} + 1.75 \text{ (Cl)} = 3.45 \text{ \AA}$].

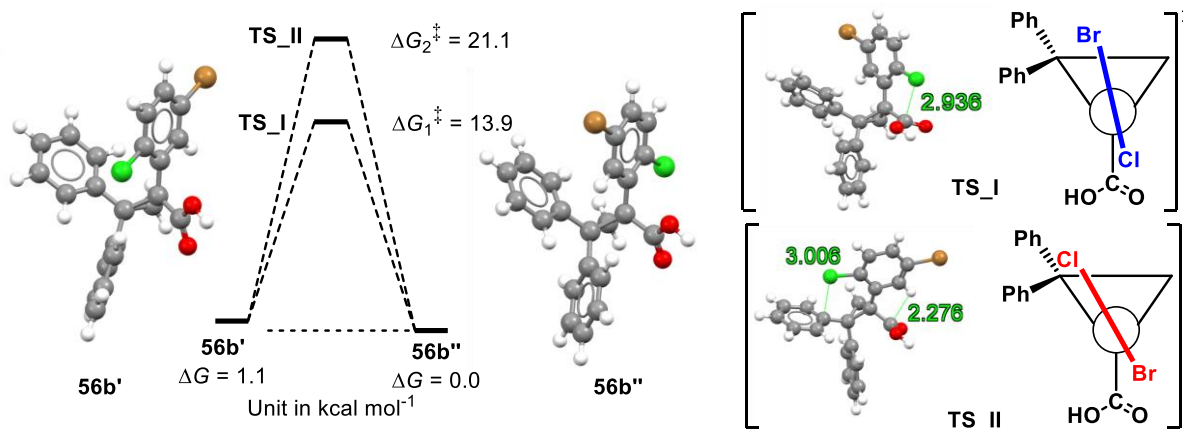


Figure 2.12 DFT studies on rotational barrier of **56b**

In the complex stage when four ligands are coordinated to the dirhodium core, four possible conformers were calculated using CH_2Cl_2 as solvent, which is the common medium for reactions catalyzed by $\text{Rh}_2(\text{S-2-Cl-5-BrTPCP})_4$, to figure out the most stable conformer in the solution state (Figure 2.13). The X-ray crystal structure was optimized in this calculation environment to generated conformer **A** as the reference, in which the ligands are oriented in C_4 arrangement with *M* axial chirality. When the ligands adopt *P* axial chirality with C_4 arrangement, conformer **B** was obtained and found to be $3.3 \text{ kcal mol}^{-1}$ less stable. Imitating the D_2 symmetry in $\text{Rh}_2(\text{R-}p\text{-BrTPCP})_4$, conformer **C** with $\alpha, \beta, \alpha, \beta$ arrangement was calculated with $10.8 \text{ kcal mol}^{-1}$ higher in energy than **A**, which may be induced by the two steric interactions between chloride atoms on adjacent ligands. Removing one of the steric interactions led to conformer **D** with $\alpha, \alpha, \alpha, \beta$ arrangement, which was more stable than **C** as expected with $4.2 \text{ kcal mol}^{-1}$ energy difference compared to reference **A**. In summary, the X-ray crystal structure with C_4 symmetry and *M* axial chirality (conformer **A**) is the most stable conformer in dichloromethane solution.

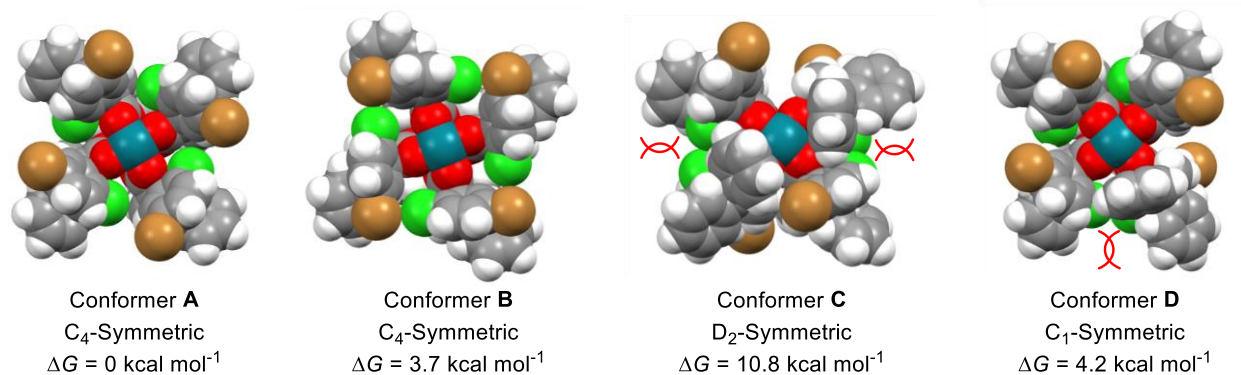


Figure 2.13 Calculated conformers of Rh₂(*S*-2-Cl-5-BrTPCP)₄ with Gibbs free energies

In addition, after extensive optimization of the carbene structure of these Rh₂(*S*-*o*-CITPCP)₄ series catalysts, it is found that these catalysts are very rigid with nearly no change in orientations between the free complex and carbene stages. The carbene structures for both Rh₂(*S*-2-Cl-4-BrTPCP)₄ and Rh₂(*S*-2-Cl-5-BrTPCP)₄ were calculated assuming methyl 2-(4-bromophenyl)-2-diazoacetate **11a** as carbene precursor (Figure 2.14). The rigidity of these Rh₂(*S*-*o*-CITPCP)₄ series catalysts with preference for C₄ symmetry and *M* axial chirality, which is even unchanged when carbene bound, is expected to be a versatile structural element for the unique site-selectivity and stereoselectivity. However, a computational rationalization of the unprecedented site-selectivity, which overcomes the electronically activated sites, is not solved yet and worth further investigation.

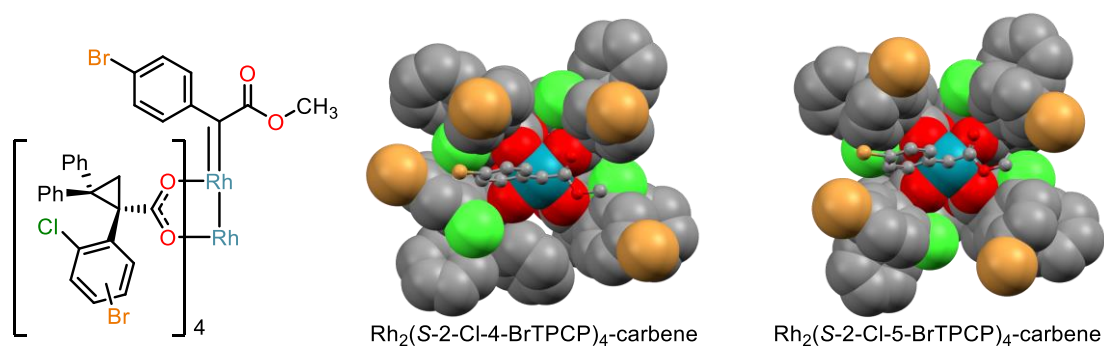


Figure 2.14 Calculated structures of rhodium carbenes

2.3. Conclusion

A new series of $\text{Rh}_2(\text{TPCP})_4$ catalysts with *ortho*-chloride substituent on the C1-aryl ring, $\text{Rh}_2(o\text{-ClTPCP})_4$, was developed and modified to $\text{Rh}_2(S\text{-}2\text{-Cl-}5\text{-BrTPCP})_4$ with improved stereoselection. This family of $\text{Rh}_2(o\text{-ClTPCP})_4$ catalysts was found to be all adopting an $(\alpha, \alpha, \alpha, \alpha)$ orientation and the M axial chirality in both X-ray crystallography and DFT calculation. The structural conformations of these catalysts are even retained in the rhodium carbene stage and implies their structural rigidity. Experimental explorations on various substrates with enhanced diastereoselection revealed that these $\text{Rh}_2(o\text{-ClTPCP})_4$ catalysts are sterically constrained, which would explain in general terms why they are capable of unusual site-selectivity for sterically accessible C–H bonds overriding the electronic-control.

Chapter 3. Catalyst-controlled Site-selective Functionalization of Piperidines for Methylphenidate Analogs

3.1. Introduction

The piperidine ring is one of the most common moieties in various small molecule pharmaceuticals.¹¹⁴⁻¹¹⁶ Examples include *Fexofenadine* with substituent at C4, *Ibrutinib* with chiral substituent at C3 and *Ritalin* (methylphenidate) with substituent at C2 (Figure 3.1). The substituted piperidine rings in the pharmaceuticals are usually synthesized thru ring construction or functional groups manipulation of piperidines that already contain substituents.¹¹⁷⁻¹²⁰ However, the latter strategy is limited by the commercial availability of chiral piperidines. To overcome this limitation, an ideal strategy is to use site- and stereoselective C–H functionalization on the simple unsubstituted piperidine to diversify at all desired positions.

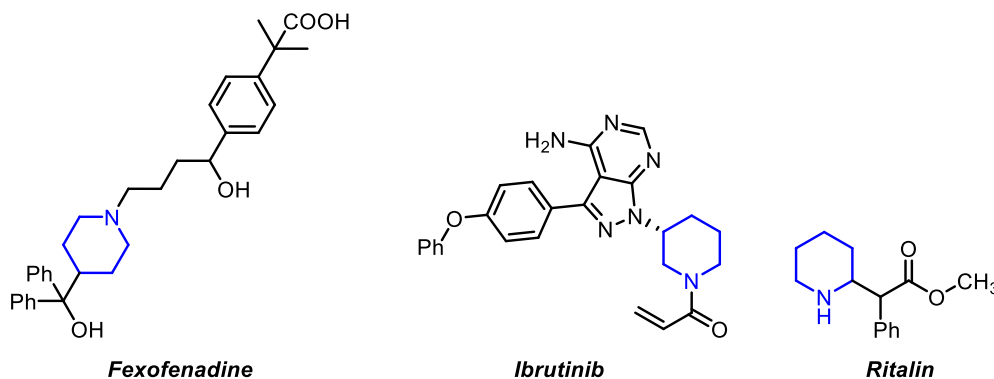
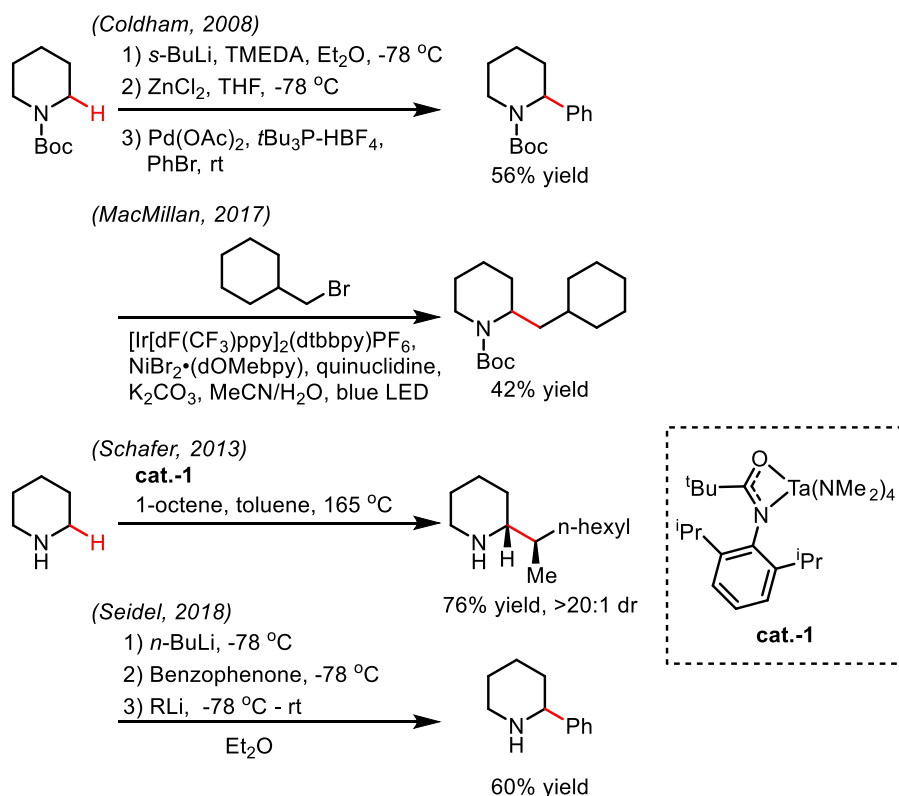


Figure 3.1 Examples of piperidine-containing pharmaceuticals

Numerous studies have demonstrated the functionalization on aliphatic cyclic amines by breaking the C–H bonds to install other substituents, especially the C–H functionalization at the C2 position on these piperidine derivatives (Scheme 3.1).^{121, 122} The C2–H bonds are generally preferred with the polarity-match and electronic effect of the adjacent nitrogen atom, as well as the directing feature of the protecting groups on the nitrogen atom. Most of the approaches are

conducted on *N*-Boc-protected piperidines, and the C2–H bond was broken by a strong base,¹²³ directed transition-metals^{124, 125} or in a radical manner via photoredox catalysts.^{126, 127} Progress in C–H functionalization at the C2 sites has progressed significantly and now some methodologies work on secondary amines, where an unprotected free N–H bond is presented, including the hydroamino-alkylation using a tantalum catalyst under harsh condition (165 °C)¹²⁸ or the arylation utilizing the imine intermediate generated through hydride transfer.^{129, 130}

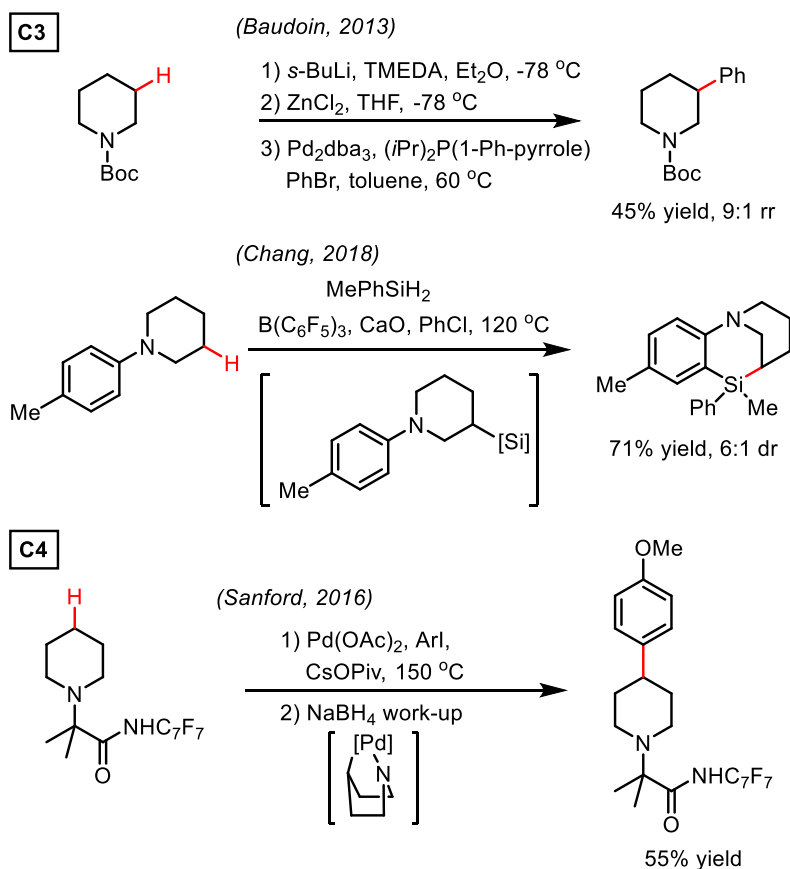
Scheme 3.1 C–H functionalization on piperidine at C2



When it comes to the functionalization of the C–H bonds at relatively remote C3 and C4 positions on the piperidine ring, limited methods can be applied with good site-selectivity. One example of using catalyst/ligand-controlled switch of site-selectivity from C2 to C3 was achieved by the Baudoin group, in which a pyrrole-containing phosphine ligand was utilized, but lower site-selectivity was observed for coupling with other aryl groups (e.g. 2:1 rr with naphthalene) resulting

in narrow substrate scope.¹³¹ Another example, investigated by the Chang group, involves the β -selective hydrosilylation of the enamine intermediate generated from piperidine dehydrogenation,¹³² which was adapted from the previous development of dearomative hydrosilylation on pyridines.^{133, 134} Even less examples are found for the C4–H insertion. It wasn't until 2016 when the Sanford group developed the coordinating group with an amide derived from *p*-CF₃C₆F₄ aniline, which chelates to the palladium catalyst and directs it to the C4–H in a low-populated boat conformer, generating the C4-arylation product in 55% yield.¹³⁵ However, due to the requirement of the boat conformer in the transition state, this approach is mainly used for bicyclic systems or conformationally biased substrates.

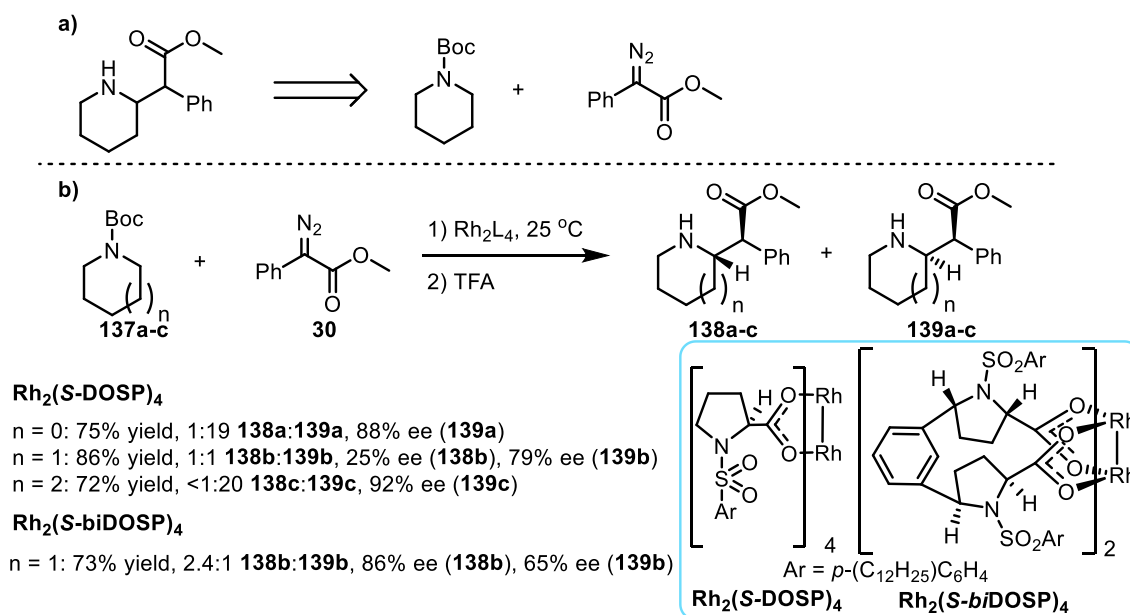
Scheme 3.2 C–H functionalization on piperidine at C3 and C4



Among numerous drug molecules, *Ritalin*, a therapeutic agent for attention deficit hyperactivity disorder (ADHS), is the most attractive using the donor/acceptor carbene chemistry developed in

the Davies group, since it contains the typical donor/acceptor moiety without alternation and can be assembled through this chemistry in one-step (Scheme 3.3a). The C–H insertion on aliphatic cyclic amines at C2 sites using donor/acceptor rhodium carbene chemistry has been established using the proline-base dirhodium catalyst, $\text{Rh}_2(\text{S-DOSP})_4$. It works well in the 5- and 7- member rings system with high stereoselection preferring **139a** and **139c**, while nearly completely lost in diastereoselectivity was observed in the substrate of 6-member ring ($n=1$, piperidine ring) (Scheme 3.3b).⁶⁴ Using a modified catalyst, $\text{Rh}_2(\text{S-biDOSP})_4$, the diastereoselectivity of C–H insertion on piperidine via metal-carbene was optimized to 2.4:1 dr preferring the *threo*-isomer **138b**, which is the active enantiomer ingredient for *Ritalin*.¹³⁶

Scheme 3.3 C–H functionalization at C2 using donor/acceptor carbene



With the recent development of phthalimido- and TPCP-based dirhodium catalysts, exploration on further improvement in diastereoselectivity was conducted, as well as the potential for functionalization of the remote C–H bonds.

3.2. Results and Discussion

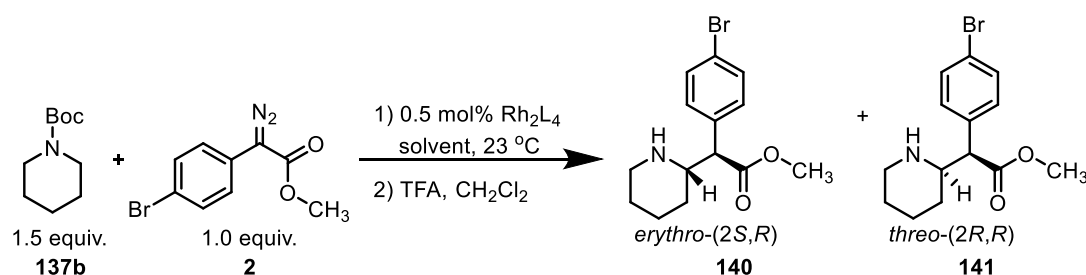
3.2.1. C–H Functionalization of Piperidines at C2 Sites

As discussed in the introduction, the C–H bonds adjacent to nitrogen atoms are electronically activated and ready to be functionalized by rhodium carbene chemistry. However, poor to moderate stereoselection was found in the C–H insertion on *N*-Boc protected piperidines at C2 sites using the proline-based dirhodium catalysts for donor/acceptor carbene generation.¹³⁶ The optimal result was found using the bridged bidentate catalyst, Rh₂(*S*-biDOSP)₄, which formed **138b** in 2.4:1 dr and 86% ee as shown in scheme 3.3, which notably is not the preferred diastereomer for rhodium carbene C–H insertion in other saturated cyclic heterocycles. Additionally, the bridged ligand for Rh₂(*S*-biDOSP)₄ is synthesized using 1,3-dilithiobenzene,^{59, 67} which is not practical for large scale synthesis of the catalyst. Moreover, more dirhodium carboxylate catalysts have been developed since then, especially the Rh₂(*S*-*o*-ClTPCP)₄ series catalysts that have been observed to enhance diastereoselectivity, promoting the re-study of C2 functionalization on piperidine.

The study began with a screening of several representative dirhodium carboxylate catalysts under conditions similar to the original system, in which the methyl 2-(4-bromophenyl)-2-diazoacetate **2** was used to react with *N*-Boc-piperidine **137b** (Table 3.1). Firstly, the standard catalyst, Rh₂(*S*-DOSP)₄ was tested in the nonpolar solvent, pentane, and resulted in a 1.5:1 mixture of diastereomers with 69% ee for the (2*R,S*) isomer. Changing the solvent to dichloromethane, which is commonly used for the newer generations of the dirhodium catalysts, resulted in decreased stereoselectivity for Rh₂(*S*-DOSP)₄ as expected. Then, various phthalimido- and TPCP-based dirhodium catalyst were examined parallelly, however, most of them showed similar or worse stereoselection for functionalization at C2 position with diastereomeric ratio (dr) ranging

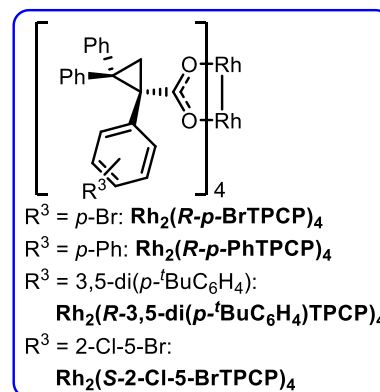
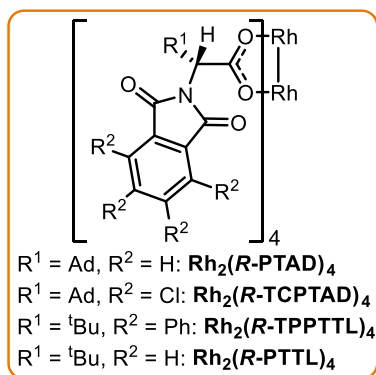
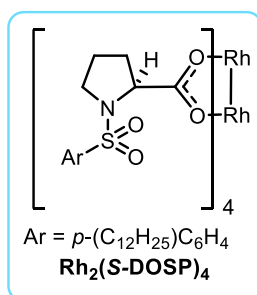
from 1:1 to 2:1 and low to moderate enantioselectivity (27-66% ee). As expected, the exceptional catalyst was $\text{Rh}_2(\text{S-2-Cl-5-BrTPCP})_4$, which surpassed the limit of all other catalysts and furnished C2–H insertion product **140** with 5.3:1 dr and 83% ee. The absolute stereochemistry of the insertion product was induced basing on previous literature from the shielding effect shown in ^1H NMR,¹³⁶ and the major diastereomer obtained here is the *erythro*-isomer that matches with the preference for cyclic amines of other ring sizes.

Table 3.1 Catalysts screening using methyl diazoacetate on *N*-Boc-piperidine



entry	L	solvent	yield (%)	dr	ee (%) ^a (140)	ee (%) ^a (141)
1	S-DOSP	pentane	69	1.5:1	-69%	-44%
2	S-DOSP	CH_2Cl_2	53	1.1:1	-41%	-29%
3	<i>R</i> -PTAD	CH_2Cl_2	62	2.2:1	-70%	-14%
4	<i>R</i> -TCPTAD	CH_2Cl_2	69	1.4:1	66%	72%
5	<i>R</i> -TPPTL	CH_2Cl_2	69	1.5:1	54%	-32%
6	<i>R</i> -PTTL	CH_2Cl_2	69	2.3:1	-69%	-10%
7	<i>R-p</i> -BrTPCP	CH_2Cl_2	41	1.2:1	27%	-30%
8	<i>R-p</i> -PhTPCP	CH_2Cl_2	40	1.5:1	33%	-45%
9	<i>R</i> -3,5-di(<i>p</i> - ^t BuC ₆ H ₄)TPCP	CH_2Cl_2	55	2.0:1	44%	20%
10	S-2-Cl-5-BrTPCP	CH_2Cl_2	83	5.3:1	83%	85%

^a negative value indicates opposite enantiomer was obtained.



Because of the recent advancement in improved selectivity using trichloroethyl diazoacetates,⁸⁰ the optimization was then extended to the use of 2,2,2-trichloroethyl 2-(4-bromophenyl)-2-diazoacetate **4b** (Table 3.2). Unexpectedly, the level of stereoselectivity in the reaction of **137b** catalyzed by $\text{Rh}_2(\text{S-2-Cl-5-BrTPCP})_4$, which was the optimal catalyst for methyl diazoacetate **2**, dropped considerably with the bulkier and more active carbene, generated from the trichloroethyl precursor (3.6:1 dr and 65% ee for **142**). The reason for the drop in diastereoselectivity is unclear at this stage but presumably is due to the steric bulkiness of the trichloroethyl group and rigid reaction pocket of the catalyst. In contrast, the catalyst with the flexible ligand structure, $\text{Rh}_2(\text{R-DOSP})_4$ furnished **142** with slightly improved diastereoselectivity comparing to the methyl derivative (3.4:1 dr vs 1.1:1 dr). Interestingly, the phthalimido-based catalysts gave significant improvement in the stereoselectivity. The $\text{Rh}_2(\text{R-PTAD})_4$ -catalyzed transformation furnished **142** with 16:1 dr and 80% ee in 58% yield, while higher yield (83%) and enantioselectivity (93% ee) were obtained using its tetrachloride derivative, $\text{Rh}_2(\text{R-TCPTAD})_4$, with small sacrifice in diastereoselectivity (11:1 dr). Moreover, further enhancement in diastereoselectivity was achieved (27:1 d.r.) when $\text{Rh}_2(\text{R-TPPTTL})_4$ was used as catalyst, but the enantioselectivity dropped to 69% ee. Notably, the ligand configuration of this catalyst has been found to be adjustable and adapt to the carbene and substrates, similar to how an enzyme's active site changes when a substrate is bound.⁷⁷ That is, $\text{Rh}_2(\text{R-TPPTTL})_4$ is less rigid than $\text{Rh}_2(\text{S-2-Cl-5-BrTPCP})_4$ but also less flexible than $\text{Rh}_2(\text{R-DOSP})_4$, giving a rationale for the improved selectivity in this transformation. Similar results with slightly higher enantioinduction was obtained using $\text{Rh}_2(\text{R-PTTL})_4$ developed by the Hashimoto group.⁶⁹

With the catalyst now optimized for the transformation, effort was then taken to modify the protecting group on the nitrogen in the piperidine ring, to a sulfonyl protecting group, to see if the

change of electronic factors could increase the overall selectivity and yield (Table 3.3). With the change of protecting group, all typical dirhodium catalysts were re-examined. When the piperidine was protected by tosyl group (**143**), the standard catalyst, $\text{Rh}_2(\text{R-DOSP})_4$, resulted in improved diastereoselectivity comparing to the result obtained with Boc as protecting group, but its yield and enantioselectivity were largely declined. The $\text{Rh}_2(\text{R-TPPTTL})_4$ furnished **144** with slightly higher enantioselectivity but decreased diastereocontrol. In addition, other C–H insertion byproducts were observed in the reaction using $\text{Rh}_2(\text{S-2-Cl-5-BrTPCP})_4$, such as primary benzylic C–H insertion product on the tosyl protecting group, thus *p*-bromophenylsulfonyl (Bs) group was applied for further examination.

Table 3.2 Catalysts screening using trichloroethyl diazoacetate on *N*-Boc-piperidine

entry	L	yield (%)	dr	ee (%) ^a (142)
1	S-2-Cl-5-BrTPCP	73	3.6:1	65%
2	R-DOSP	52	3.4:1	14%
3	R-PTAD	58	16.4:1	-80%
4	R-TCPTAD	83	10.5:1	93%
5	R-TPPTTL	80	27.0:1	69%
6	R-PTTL	78	23.7:1	-84%

^a negative value indicates opposite enantiomer was obtained.

Table 3.3 C2–H functionalization on *N*-tosyl-piperidine

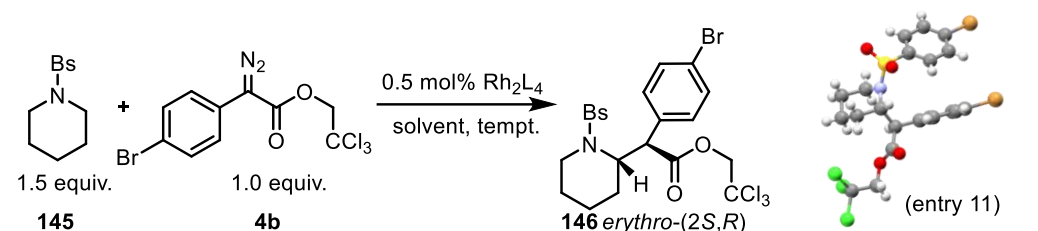
entry	L	yield (%)	dr	ee (%)
1	R-DOSP	38	8.2:1	57%
2	S-2-Cl-5-BrTPCP	13 ^a	7.3:1	84%
3	R-TPPTTL	65	10.2:1	76%

^a other C–H insertion products: @ C4 on piperidine and benzylic CH₃ on Ts (tosyl).

Again, with the change in protecting group, most of the dirhodium carboxylate catalysts were re-examined on the *N-p*-bromo-phenylsulfonyl protected piperidine **145** using trichloroethyl diazoacetate **4b** (Table 3.4). The first change noticed is the performance of the standard catalyst, $\text{Rh}_2(R\text{-DOSP})_4$, which showed significant improvement in the diastereoselectivity (17.7:1 dr) with *p*-bromophenyl-sulfonyl as protecting group instead of Boc. Hence, the nonpolar solvent, pentane, was tested and showed further improvement on both the diastereo- and enantioselectivity as expected, but a 7:1 mixture of C–H insertions into the solvent pentane and substrate **145** was observed (trifluorotoluene or TFT was used to improve the solubility of the substrate). When only TFT was used as solvent, no C–H insertion product was detected and fully recovered **145** was isolated in the $\text{Rh}_2(R\text{-DOSP})_4$ -catalyzed reaction. The results from entries 2 and 3 implied that the C–H bonds in *N-p*-bromophenylsulfonyl-piperidine **145** might be less active. Noticeably, most of the TPCP-based dirhodium catalysts led to only trace amount of C–H functionalization product under these reaction conditions. Uniquely, $\text{Rh}_2(S\text{-2-Cl-5-BrTPCP})_4$ -catalyzed reaction generated **146** as single diastereomer with 66% ee, additionally the C–H functionalization product at the C4 position of the piperidine was also detected as an exciting byproduct. It led to the further studies for functionalization at C4 position of the piperidines using $\text{Rh}_2(S\text{-2-Cl-5-BrTPCP})_4$ in section 3.2.2. $\text{Rh}_2(R\text{-PTAD})_4$ -catalyzed reaction furnished C2–H insertion product **146** with moderated stereoselectivity, while $\text{Rh}_2(R\text{-TCPTAD})_4$ gave low diastereoselectivity (3.2:1 dr) but high enantioselectivity (97% ee). Interestingly, $\text{Rh}_2(R\text{-TPPTTL})_4$, which gave the highest diastereoselectivity in the previous examination, furnished **146** as a single diastereomer here with slightly improved enantioselectivity (77% ee), and the X-ray crystal structure of the product obtained here confirmed the absolute stereochemistry tentatively assigned. The effect of the reaction temperature was then studied. The yield for $\text{Rh}_2(R\text{-TPPTTL})_4$ -catalyzed reaction could be

improved at refluxing dichloromethane with only a small decrease in diastereoselectivity (21.5:1 dr), while the lower temperature (0 °C) resulted in significant drop in yield and decreased enantioselectivity. Therefore, $\text{Rh}_2(\text{R-TPPTTL})_4$ was chosen as the optimal catalyst when piperidines were protected by the *N-p*-bromophenylsulfonyl group.

Table 3.4 C2–H functionalization on *N-p*-bromophenylsulfonyl-piperidine



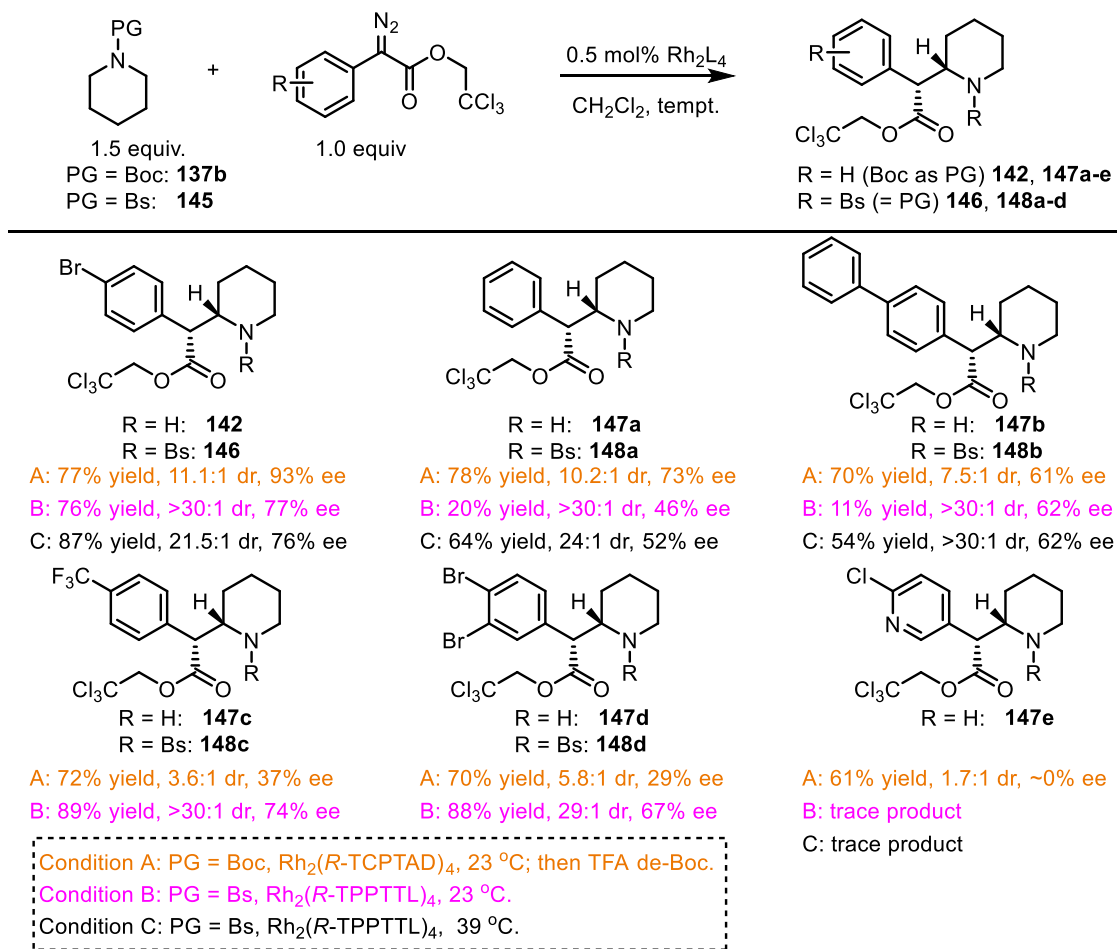
entry	L	solvent	tempt.	yield (%)	dr	ee (%)
1	<i>R</i> -DOSP	CH ₂ Cl ₂	23	61	17.7:1	67%
2	<i>R</i> -DOSP	pentane/TFT	23	13 ^a	>30:1	76%
3	<i>R</i> -DOSP	TFT	23	no C-H insertion product		
4	<i>R-p</i> -BrTPCP	CH ₂ Cl ₂	23	trace C-H insertion product in crude ¹ H-NMR		
5	<i>R-p</i> -PhTPCP	CH ₂ Cl ₂	23	trace C-H insertion product in crude ¹ H-NMR		
6	<i>R</i> -3,5-di(<i>p</i> - ^t BuC ₆ H ₄)TPCP	CH ₂ Cl ₂	23	trace C-H insertion product in crude ¹ H-NMR		
7	<i>S</i> -2-Cl-5-BrTPCP	CH ₂ Cl ₂	23	16 ^b	>30:1	66%
8	<i>R</i> -PTAD	CH ₂ Cl ₂	23	67	13.5:1	-72%
9	<i>R</i> -TCPTAD	CH ₂ Cl ₂	23	75	3.2:1	97%
10	<i>R</i> -PTTL	CH ₂ Cl ₂	23	65	7.1:1	-74%
11	<i>R</i>-TPPTTL	CH₂Cl₂	23	76	>30:1	77%
12	<i>R</i>-TPPTTL	CH₂Cl₂	39	87	21.5:1	76%
13	<i>R</i> -TPPTTL	CH ₂ Cl ₂	0	42	26.4:1	72%

other C-H insertion products: ^a @ C2 on pentane; ^b @ C4 on piperidine

The aryldiazoacetates scope of the C2–H functionalization of piperidine was explored using the two most optimized conditions, *N*-Boc as the protecting group on piperidine catalyzed by $\text{Rh}_2(\text{R-TCPTAD})_4$ and *N-p*-bromophenylsulfonyl as the protecting group catalyzed by $\text{Rh}_2(\text{R-TPPTTL})_4$ (Scheme 3.4). Moderated yields and diastereoselectivity were obtained under $\text{Rh}_2(\text{R-TCPTAD})_4$ -catalyzed condition, but the enantioselectivity decreased to 37% ee with electron deficient

aryldiazoacetates, which contained *p*-trifluoromethyl on the donor aryl ring. In contrast, the $\text{Rh}_2(\text{R-TPPTTL})_4$ -catalyzed reactions were highly diastereoselective for all the substrates (21->30:1 dr) and the enantioselectivity was maintained relatively constant at a moderate level (52-73% ee). However, in this condition, carbene precursors with *p*-phenyl or no substituent on the aryl ring led to significant low yield, so reaction temperature was raised to refluxing conditions (C) to generate **148a** and **148b**.

Scheme 3.4 Substrate scope of C2 functionalization



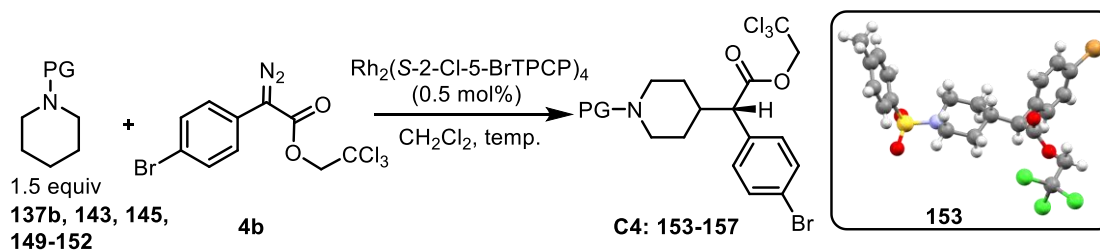
3.2.2. C–H Functionalization of Piperidines at C4 Sites

Initially, direct C–H insertion of protected piperidines at the C4 site was not expected using current rhodium donor/acceptor carbene chemistry. Before the discovery of C4–H insertion found during the optimization in Table 3.4, initial attempts were conducted by Tobias Babl, a visiting scholar from the Reiser group in Germany, on *N*-Boc-dihydropyridine with C4 site dually activated by two adjacent alkenes. However, this substrate was prone to decomposition to form pyridine and neat conditions were required for effective C–H insertion.¹³⁷ Additionally, C–H insertion at C4 site of saturated piperidine rings would be more innovative and worth exploration. Therefore, I explored the transformation and the results are summarized as below.

As discovered in the optimization for functionalization at C2 site using sulfonyl groups as protecting groups, the C4–H insertion product was detected only in the $\text{Rh}_2(\text{S-2-Cl-5-BrTPCP})_4$ -catalyzed reactions. At this stage, taking $\text{Rh}_2(\text{S-2-Cl-5-BrTPCP})_4$ as the optimal catalyst, further optimization of the protecting group was conducted (Table 3.5). When Boc was used as protecting group, C–H insertion of **137b** gave only C2–H insertion product as shown in Table 3.1. When the tosyl group was used for amine protection (**143**), C–H insertion at C4 was detected in a 4:1 mixture of C–H insertion products at both the C4 and the C2 sites, and the C4–H insertion product **153** was obtained with very high asymmetric induction (96% ee). The absolute configuration and stereochemistry was confirmed by X-ray crystallography. Next, different substituents instead of the methyl group on the benzenesulfonyl protecting group were also examined. Changing from the electron-donating methyl group to the electron-withdrawing bromide and trifluoromethyl groups, slightly improved the site-selectivity for C4 position. However, the even stronger electron-withdrawing group, the nitro group, resulted in no C–H insertion reaction, presumably because it strongly deactivates the reactivity of the C–H bonds on the piperidine ring. Interestingly, the

sterically smaller protecting group, the mesyl group, which was expected to be preferring the C2 product because of less steric hindrance, led to the highest site-selectivity for the C4 product (5.6:1 rr) among all of the sulfonyl protecting groups. That is, electronic effect is dominating regardless of the steric bulk of the protecting group. A strong electron-withdrawing group with two adjacent carbonyls, the aryloxoacetyl group, was tested in substrate **152**, and the $\text{Rh}_2(\text{S-2-Cl-5-BrTPCP})_4$ -catalyzed reaction gave C4 product **157** as a single regioisomer with 97% ee, but only 50% yield. Adjusting the temperature and substrate ratio enhanced the yield to 61% at 39 °C and 1:1.5 of **152:4b** without influence on the site- and enantioselectivity.

Table 3.5 Protecting group optimization for C–H insertion at C4



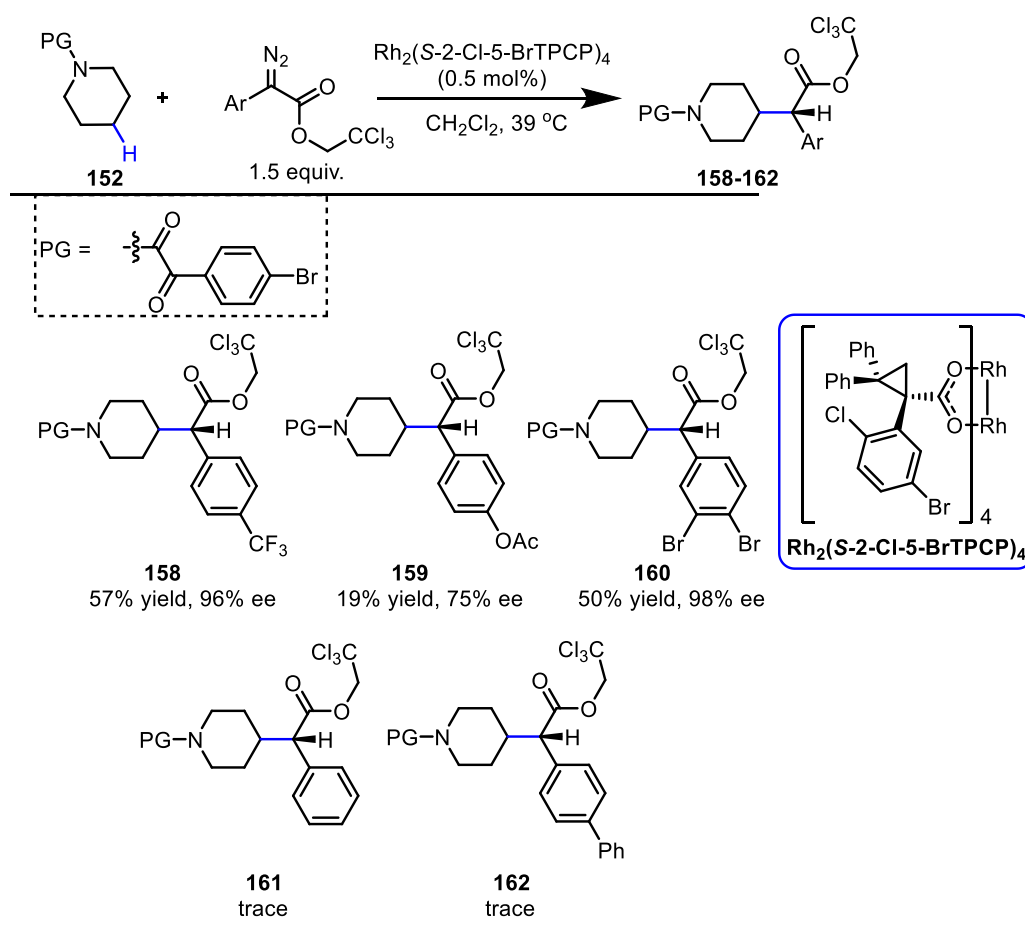
entry	x	PG	temp. (°C)	r.r. (C4:C2)	yield (%)	ee (%)
1	137b		23	<1:30	--	--
2	143		23	4.0:1	30 ^a (153)	96
3	145		23	4.2:1	67 (154)	90
4	149		23	4.7:1	65 (155)	96
5	150		23	-- (no C-H insertion product detected)		
6	151		23	5.6:1	78 (156)	97
7	152		23	>30:1	50 (157)	97
8	152		39	>30:1	57 (157)	97
g^b	152		39	>30:1	61 (157)	97

^a other C-H insertion products: @ benzylic CH_3 on Ts (tosyl).

^b 1.5 equiv of **152** and 1.0 equiv of **4b** were used.

The efficiency of $\text{Rh}_2(\text{S-2-Cl-5-BrTPCP})_4$ in functionalization of **152** at the C4 position was explored using the optimized conditions (Scheme 3.5). When the substituents on the aryl ring in the diazoacetates were electron-withdrawing groups, trifluoromethyl in **158** and 3,4-dibromide in **160**, high enantiocontrol was obtained (96-98% ee) with moderate yields (50-57%). When the electron-rich aryl ring, *p*-acetoxyphenyl, in the diazoacetate was used, both the yield and enantioselectivity decrease (19% yield, 75% ee for **159**). The low yields are presumably caused by the low reactivity of the C–H bonds on the *N*-aryloxyacetyl protected piperidine, and only trace amounts of the desired products (**161** and **162**) were observed in the crude ^1H NMR when other aryl rings were used as the carbene precursors.

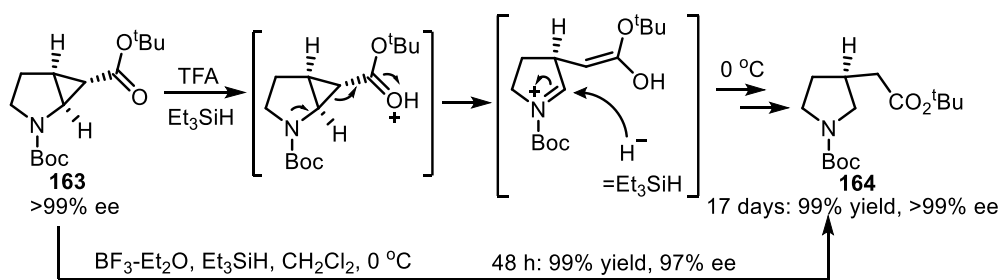
Scheme 3.5 Substrate scope of C4 functionalization



3.2.3. C3 Analog Generation

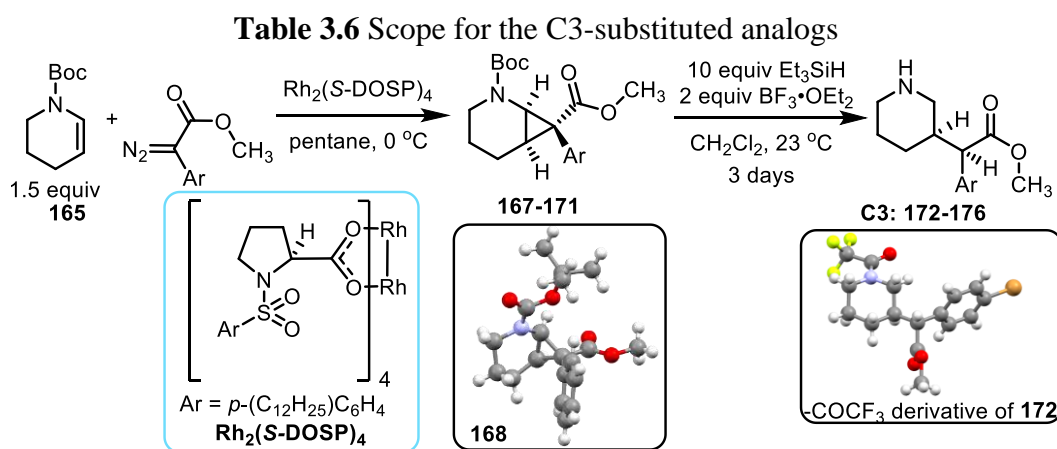
Having established the C–H functionalization of piperidine at both the C2 and the C4 sites, the possibility of introducing the arylacetate group at the C3 site was then explored. The direct C–H insertion on piperidine rings was not considered to be a viable option, because the C3 site would be deactivated towards carbene C–H insertions caused by the inductively electron-withdrawing effect of the nitrogen atom and has no steric advantage over the C4 site. Therefore, an indirect approach was utilized via asymmetric cyclopropanation of a tetrahydropyridine followed by a reductive ring-opening of the cyclopropane intermediate. It was discovered by the Reiser group in 2017 that the cyclopropane ring in **163** under Et_3SiH and $\text{BF}_3 \cdot \text{Et}_2\text{O}$ treatment could lead to the reductive ring-opening product **164** in nearly quantitative yield, notably with maintained stereo-control at the chiral carbon center on the pyrrolidine ring (Scheme 3.6).¹³⁸ It was promising to examine here and test if the chiral center adjacent to the ester group generated by donor/acceptor carbenes could be maintained under similar condition, therefore, a collaboration with the Reiser group was proposed and this exploration was conducted by Tobias Babl from the Reiser group.

Scheme 3.6 Reductive ring-opening discovered by the Reiser group



Exploration was conducted by Tobias Babl to figure out optimal reaction conditions for enantioselective cyclopropanation and efficient reductive ring-opening without losing stereo-control of the chiral centers. The details of this study were discussed in his master thesis and only the final scope of the reaction is summarized here (Table 3.6). The classic dirhodium catalyst,

$\text{Rh}_2(\text{R-DOSP})_4$, was found to be the optimal catalyst for cyclopropanation on *N*-Boc-tetrahydropyridine **165** using methyl diazoacetates in nonpolar solvent. This result was expected since $\text{Rh}_2(\text{R-DOSP})_4$ is well established for cyclopropanation using methyl ester of aryldiazoacetates.⁹⁷ Reductive ring-opening of the cyclopropane **167-171** using 2 equiv of Et_3SiH and 10 equiv of $\text{BF}_3 \cdot \text{Et}_2\text{O}$ resulted in concomitant removal of the *N*-Boc protecting group and the generation of the desired C3-substituted analogs **172-176** in 67-92% yield as single diastereomers with retention of the asymmetric induction obtained in the cyclopropanation.



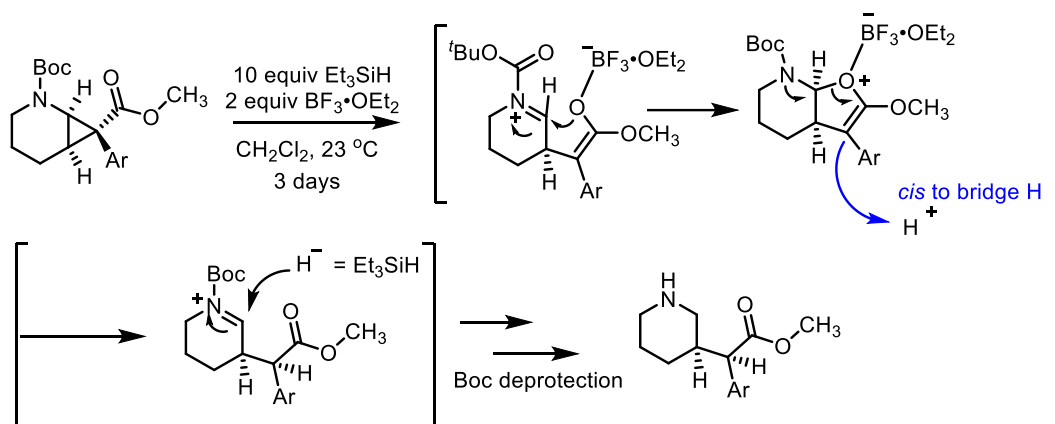
entry	Ar	167-171		172-176		
		yield (%)	ee (%)	yield (%)	d.r.	ee (%)
1		93 (167)	92	67 (172)	>30:1	93
2		87 (168)	95	70 (173)	>30:1	91
3 ^a		86 (169)	90	92 (174)	>30:1	90
4 ^a		85 (170)	86	77 (175)	>30:1	87
5 ^a		90 (171)	81	90 (176)	>30:1	80

^a Minimal amount of trifluorotoluene was added to dissolve the aryldiazoacetate.

The absolute stereochemistry of both the cyclopropanation and ring-opened product was confirmed by X-ray crystal structures as shown in Table 3.6. Basing on the proposed mechanism

for the reductive ring-opening of **163**, the chiral center adjacent to the ester would be racemized with the formation of enolate intermediate, however, C3-substituted analogs **172-176** were all obtained as single diastereomer with high enantiomeric ratio. It is proposed that the diastereoselectivity is caused by the formation of a bicyclic intermediate from the ring-opened enolate, in which the bottom face *cis* to the bridging hydrogens is more accessible (Scheme 3.7).

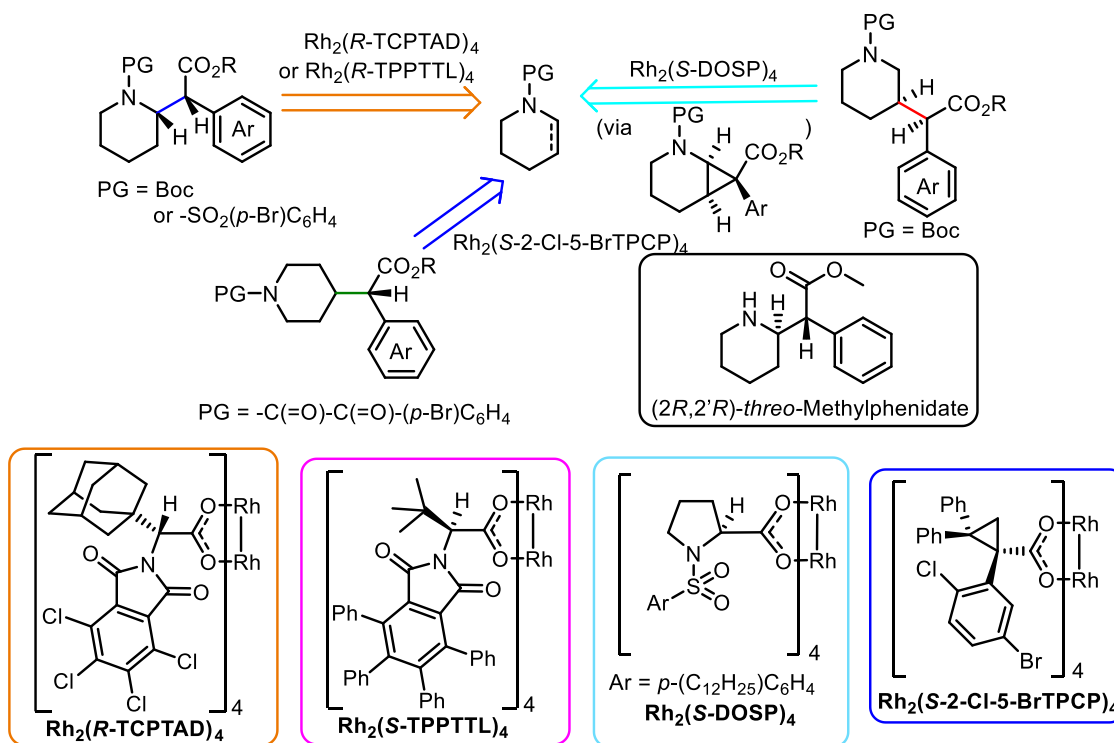
Scheme 3.7 Proposed rationalization for chirality retention



3.3. Conclusion

In this chapter, rhodium-catalyzed C–H insertions and cyclopropanations of donor/acceptor carbenes have been used for the synthesis of positional analogs of methylphenidate. The site-selectivity is controlled by the catalyst and the amine protecting group. C–H functionalization of *N*-Boc-piperidine using $\text{Rh}_2(R\text{-TCPTAD})_4$, or *N*-*p*-bromophenylsulfonyl using $\text{Rh}_2(R\text{-TPPTTL})_4$ generated C2-substituted analogs. In contrast, when *N*-aryloxoacetyl-piperidines were used in combination with $\text{Rh}_2(S\text{-2-Cl-5-BrTPCP})_4$, the C–H functionalization produced C4-substituted analogs. Finally, the C3-substituted analogs were prepared indirectly by cyclopropanation of *N*-Boc-tetrahydropyridine followed by reductive regio- and stereoselective ring-opening of the cyclopropanes (Scheme 3.8).

Scheme 3.8 Summary for generation C2, C3 and C4 analogs of methylphenidate



Chapter 4. Efforts Towards Immobilization of $\text{Rh}_2(\text{TPCP})_4$ for Asymmetric C–H Insertion in Flow

4.1 Introduction

4.1.1 Continuous Flow Chemistry

Continuous flow chemistry focuses on conducting organic reactions in a narrow tube or passing through a cartridge, where the mobile phase is moved along the channels continuously. Ideally, in the continuous flow system setup, after the starting materials are mixed at the junction and pumped down the tube/cartridge reactor, the product can be collected at the exit (Figure 4.1). The Jamison group developed a protocol for the flow reactor setup for simple batch reaction translation and further manipulation utilizing parts that could be found in general organic laboratories.¹³⁹ In the past two decades or less, the research in organic synthesis using continuous flow system has evolved rapidly, resulting in multiple achievements demonstrated by the synthesis of active pharmaceutical ingredients (API) or effective functional-group transformations.^{140, 141} Compared to the classic batch reaction in a round-bottom flask, performing reactions in continuous flow can provide better control of the reaction parameters, and be utilized as a safer technic for handling dangerous (toxic and explosive) materials by avoiding accumulation of intermediates.¹⁴²⁻¹⁴⁷

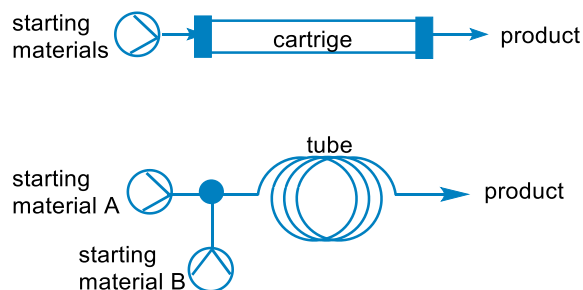


Figure 4.1 General schematic description of a continuous flow reactor

One particular advantage of the continuous flow system in catalytic organic chemistry is the ability to immobilize the catalyst, which enables the catalyst to be recycled. In addition to the benefit of being environmental-friendly, this approach is also cost efficient when expensive catalysts are required, such as the rhodium catalysts developed in the Davies group. High turnover numbers (TON), which indicate the effectiveness of a catalyst in terms of the amount of the desired product generated, requires extremely low catalyst loading in large volume of homogeneous batch reactions, and effective mixing could be a common challenge. In contrast, the ability of continuous flow system in recycling immobilized catalysts, while at the same time improving micromixing¹⁴⁸ and catalyst to substrate ratio¹⁴⁹ in the small reaction volume at each point of the flow reactor, could provide an alternative way for higher TON.

4.1.2 Immobilization of Dirhodium (II) Catalysts and Application in Flow

The benefit of having catalysts immobilized for recycling has attracted extensive research, especially for the asymmetric transformations using chiral catalysts. The performance of the immobilized catalysts, such as TON, reaction rates, stereoselectivity and recyclability can be influenced by the choice of immobilization method, support and anchor site.¹⁴⁹ Optimization of these variables and balance among their influence is important but challenging for matching the effectiveness of homogenous catalysis.

Various methods for metal catalyst immobilization have been developed (Figure 4.2a).¹⁴⁹⁻¹⁵¹ Some of the examples trap the catalysts inside cage-like pores of porous materials, but it is limited by the ineffective diffusion of the reactants and products in and out the pores. Some other more common methods utilize adsorption effects, either physisorption or chemisorption like ion-pairs,

to connect the catalysts to the support materials, which requires little or no modification of the original catalysts. However, the adsorption interactions are relatively weak, and the catalysts are prone to be leached, so practical solvents and temperature range are limited. The most frequently used method utilizes covalent bindings between the ligands on the catalysts and solid supports, which has higher tolerance to different reaction conditions and less potential leaching problem, though extra steps are required for the construction of the linker for covalent bind.

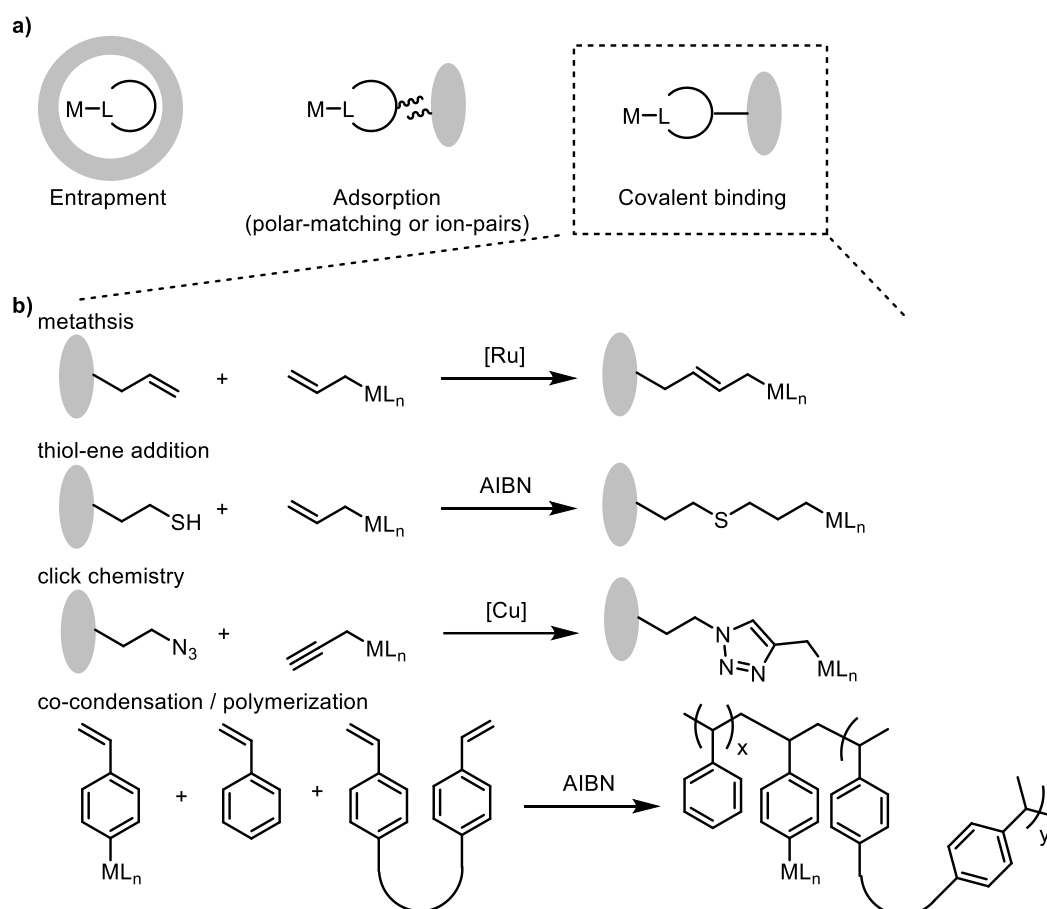


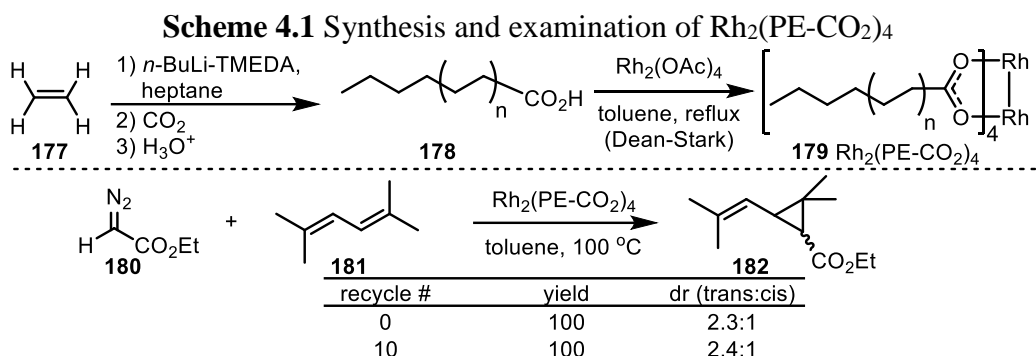
Figure 4.2 Catalyst immobilization methods and construction of covalent binds

The covalent bindings can be incorporated by either post-grafting or co-condensation approaches (Figure 4.2b).¹⁴⁹ For efficient grafting of the functionalized catalysts onto the desired support, reactions with high yields under relative mild conditions are preferred for incorporation

of the covalent bindings. Examples of post-grafting methods including the well-studied copper-catalyzed click chemistry ([3+2] alkyne–azide cycloadditions)^{152, 153} and ruthenium-catalyzed metathesis, as well as the recently developed thiol-ene addition for coupling between thiols and alkenes¹⁵⁴. In addition, the efficient metathesis by metal catalyst or radical initiator was also developed into the co-condensation or polymerization methods for catalyst immobilization, in which small monomers are polymerized to form polymer support while incorporating the desired catalysts.¹⁵⁵

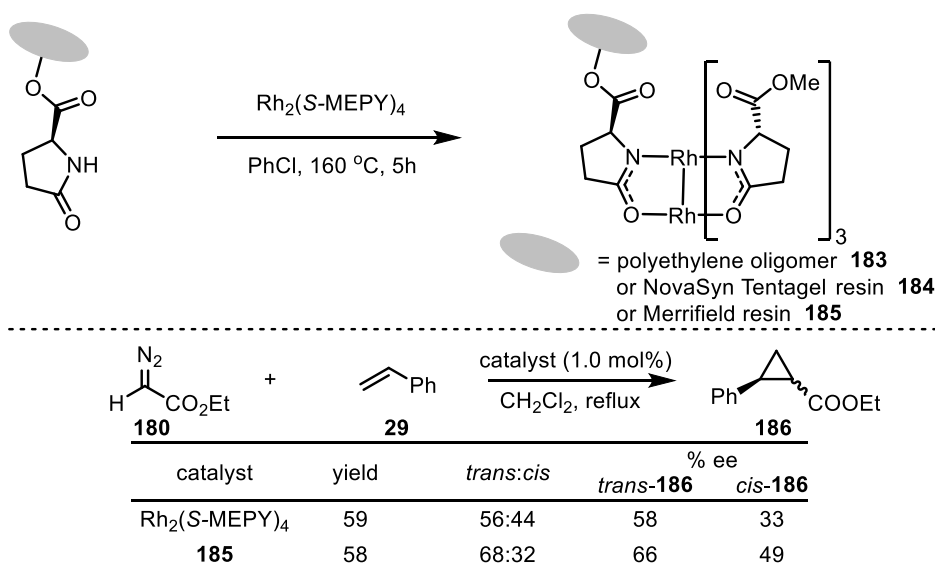
The scaffold of dirhodium catalysts with chiral ligands has been extensively used for asymmetric transformations,¹⁵⁶⁻¹⁵⁸ however, rhodium is a precious metal and the dirhodium catalysts are expensive on the market, with the parent catalyst, $\text{Rh}_2(\text{OAc})_4$, as much as \$200-300/g from the standard commercial suppliers. Several studies have been conducted to immobilize different chiral dirhodium (II) catalysts to make them more practical by increasing their recyclability and overall efficiency.

The first attempt to immobilize the original dirhodium catalyst, $\text{Rh}_2(\text{OAc})_4$, was accomplished by the Bergbreiter group (Scheme 4.1).¹⁵⁹ In this study, all four acetate ligands on the $\text{Rh}_2(\text{OAc})_4$ was replaced with polyethylene carboxylate **178** (PE-CO₂), which was prepared from oligomerization ($M_n \sim 1500-2000$) of ethylene **177** followed by carboxylation at the chain terminal. The resulted polyethylene-bound rhodium catalyst, $\text{Rh}_2(\text{PE-CO}_2)_4$, was tested in cyclopropanation of 7 different substrates with ethyl 2-diazoacetate **180** and sometimes higher diastereoselectivity (*trans/cis*) was obtained comparing to the homogeneous $\text{Rh}_2(\text{OAc})_4$. More importantly, on alkene **181**, a quantitative yield and high diastereoselectivity were retained after reusing $\text{Rh}_2(\text{PE-CO}_2)_4$ for 10 times, while the homogeneous $\text{Rh}_2(\text{OAc})_4$ gave a significant drop in yield after 3 runs.



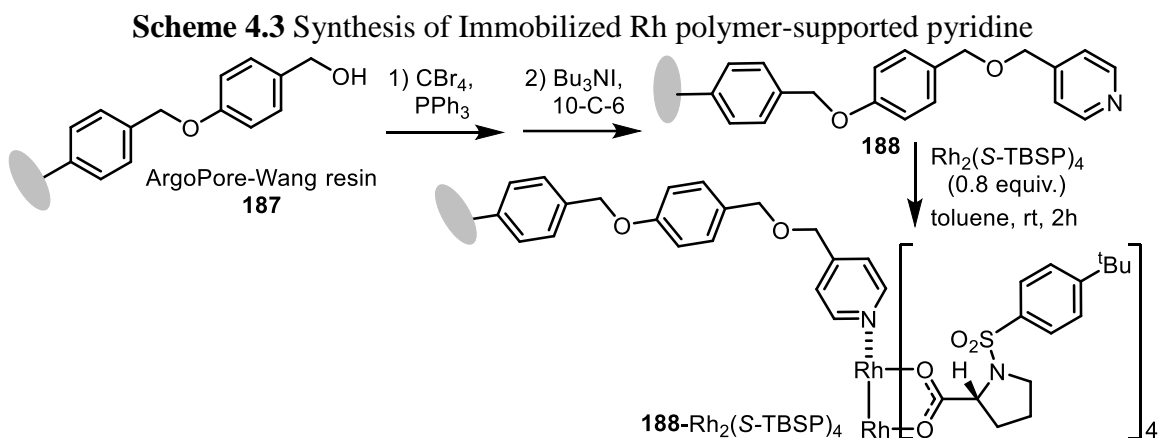
Followed by that study, collaboration between the Bergbreiter and Doyle groups achieved the first immobilized chiral dirhodium catalyst, $\text{PE-Rh}_2(\text{S-PYCA})_4$ **183**, in which one of the 5-methyl carboxylate pyrrolidone ligands was bound to polyethylene oligomer replacing the methyl ester (Scheme 4.2).¹⁶⁰ However, the polyethylene-bound chiral dirhodium catalyst was found to be less reactive and stereoselective than its homogeneous analog, $\text{Rh}_2(\text{S-MEPY})_4$, in intramolecular C–H insertion reactions. Further modifications to the supporting materials were conducted to improve the performance. It was found that changing the polyethylene oligomer to NovaSyn Tentagel resin or Merrifield resin resulted in better enantioselectivity than the homogeneous $\text{Rh}_2(\text{S-MEPY})_4$.¹⁶¹

Scheme 4.2 Mono-ligand exchange for immobilized $\text{Rh}_2(\text{S-MEPY})_4$



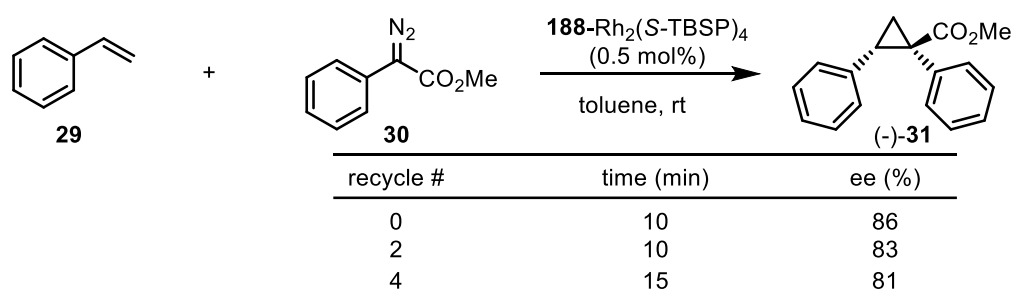
Exploration of immobilization of these dirhodium (II) tetracarboxamidate catalysts, which are obtained from mono-ligand exchange using supported ligands, was continued, and the Doyle group concluded that the exchanged supported ligands could modify both electronic and steric properties of the target dirhodium (II) tetracarboxamidate catalysts.¹⁶² This result is expected as the dirhodium (II) tetracarboxamidate catalysts with different ligands showed different reactivity profiles.

During the same period, the Davies group also explored methods to immobilize the dirhodium (II) tetracarboxylate catalysts on solid support in a general and practical manner. Initial studies were focused on the proline-based catalyst, $\text{Rh}_2(\text{S-TBSP})_4$. Unlike the mono-ligand exchange strategy that could potentially alter the chiral influence of the catalysts, polymer-supported pyridine **188** was used, which can coordinate to the axial position of the dirhodium carboxylate complexes without changing the chiral ligand frameworks and leave the other rhodium face available for carbene reactions (Scheme 4.3).¹⁶³ The desired supported pyridine **188** was generated from the commercial available ArgoPore-Wang resin **187** using the route shown in Scheme 3.3 and it was chosen because of its highly cross-linked microporous structure and its compatibility to a wide range of solvents. The reaction conditions for catalyst immobilization were optimized using toluene as solvent in a later systematic study and 86% catalyst immobilization was reached with 0.16 mmol/g loading (ICP).¹⁶⁴



The immobilized $\text{Rh}_2(\text{S-TBSP})_4$ by ArgoPore-Wang resin-supported pyridine was examined in cyclopropanation reactions using donor/acceptor carbenes. The homogeneous $\text{Rh}_2(\text{S-TBSP})_4$ furnished cyclopropane (-)-**31** in 87-90% ee with the standard transformation between styrene **29** and methyl 2-diazo-2-phenylacetate **30**.¹⁶⁴ Using the **188-Rh}_2(\text{S-TBSP})_4 made through the optimized conditions, similar enantioselectivity was obtained (86% ee) and with only a slight drop after 5 times of recycling (81% ee) (Table 4.1).¹⁶⁴**

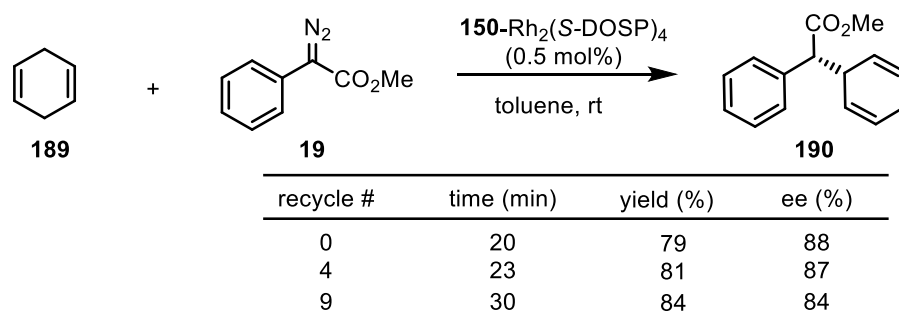
Table 4.1 Cyclopropanation using immobilized $\text{Rh}_2(\text{S-TBSP})_4$ and recyclability



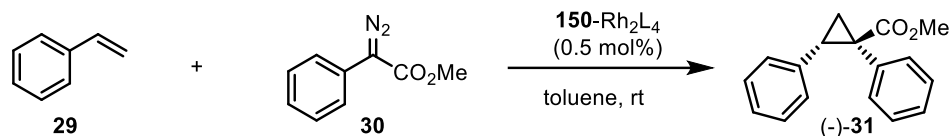
At the same time, the efficiency of this immobilization strategy in C–H insertion reactions via rhodium carbene chemistry was investigated. Davies *et al.* applied the ArgoPore-Wang resin-supported pyridine in the immobilization of $\text{Rh}_2(\text{S-DOSP})_4$, which was the most effective catalyst in intermolecular C–H insertion reactions at that period,¹⁶⁵ and examined it in the C–H insertion of cyclohexa-1,4-diene **189** (Table 4.2). The results are as promising as the ones obtained using

188-Rh₂(*S*-TBSP)₄ in cyclopropanation. The **188**-Rh₂(*S*-DOSP)₄ was recycled 9 times without any loss in overall yields (79-84% yield), but slightly longer reaction times were needed when the recycle number increased. More importantly for immobilization of a chiral catalyst, only minimal drop in enantioselectivity (88% to 84% ee) was observed at the 10th time of using the same batch of catalyst.

Table 4.2 C–H insertion using immobilized Rh₂(*S*-DOSP)₄ and recyclability

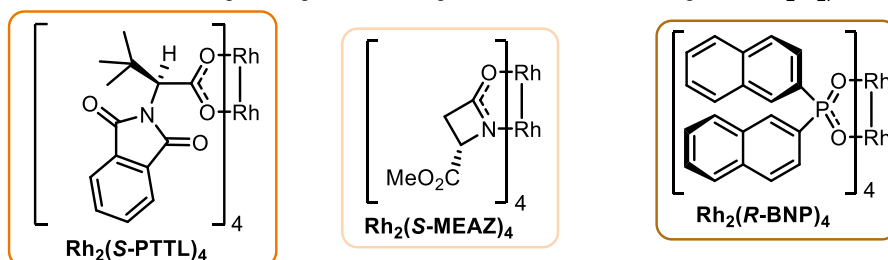


These encouraging results promoted the application of this ArgoPore-Wang resin-supported pyridine as a “universal strategy for immobilization”, leading to the testing of chiral dirhodium catalysts with very different ligands: phthalimido-based carboxylate like Rh₂(*S*-PTTL)₄, carboxamidate like Rh₂(*S*-MEPY)₄ and phosphonates like Rh₂(*R*-BNP)₄.¹⁶⁶ After efficient immobilization of all three catalysts, examination using standard cyclopropanation showed equivalent level of enantioselectivity comparing to their homogenous counterparts (Table 4.3).

Table 4.3 Performance of different dirhodium catalysts with resin-supported pyridine

188-Rh₂L₄	time (min)	yield (%)	ee (%)	ee (%) ^a
188-Rh₂(S-PTTL)₄	12	82	10	13
188-Rh₂(S-MEAZ)₄ ^b	>180	76	68	69
188-Rh₂(R-BNP)₄	15	85	40	42

^a Using homogenous analogs. ^b Solvent was changed to CH₂Cl₂.



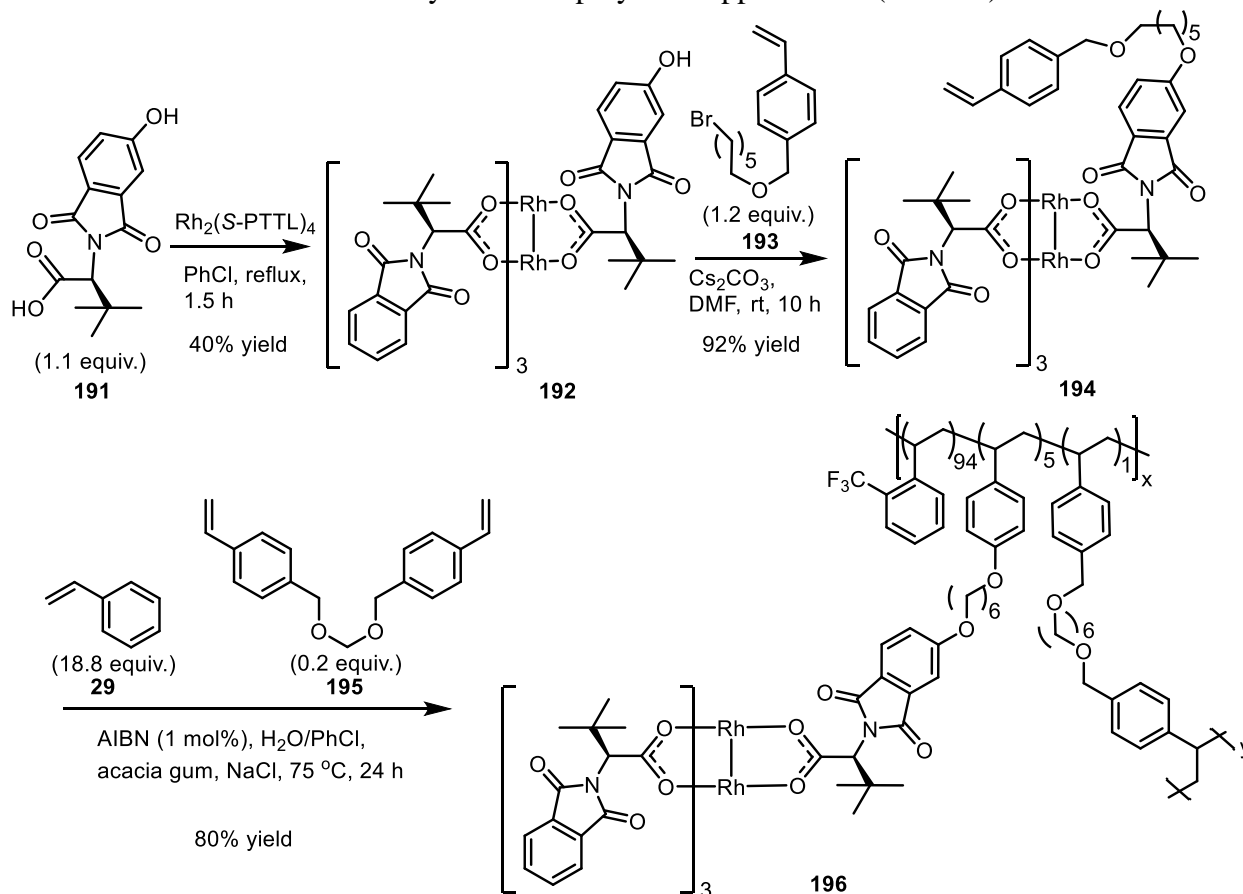
The resin-supported pyridine strategy was shown to be impressive with the easy immobilization conditions and high recyclability without loss in reactivity and selectivity compared to the original homogenous dirhodium catalysts. However, catalyst leaching was detected after each use of these immobilization catalysts, with a 3% loss in rhodium charge was detected for **188-Rh₂(S-TBSP)₄** after first time usage by analyzing the reaction mixture after removal of solid supported catalyst using inductively coupled plasma emission spectroscopy (ICP-AES). The leaching could be a serious problem after multiple usage, therefore, immobilization with covalent bindings is still necessary.

There wasn't much promising progress on immobilization of chiral dirhodium catalysts with covalent binding until 2010. The Hashimoto group reported an effective immobilized Rh₂(S-PTTL)₄, in which one of the ligands was covalently linked to a polymer chain.¹⁵⁵ The immobilization was completed in three steps: a mono-ligand exchange of Rh₂(S-PTTL)₄ with a hydroxy-functionalized ligand derivative **191**, followed by an O-alkylation with styrene derivative **193** as a spacer, and finished up with copolymerization of the rhodium complex **156** with styrene

29 and cross-linker **195** (5:94:1 ratio) to give the polymer-supported $\text{Rh}_2(\text{S-PTTL})_4$ **196** in ~29% overall yield (Scheme 4.4).¹⁵⁵ The catalyst **196** was unprecedentedly robust giving the same levels of reactivity and enantioselectivity (91% to 92% ee) in intramolecular C–H insertion for methyl (*S*)-2-hydroxy-1-methyl-1-phenyl-1*H*-indene-3-carboxylate after 100 sequential usages.¹⁵⁵

This immobilization method with copolymerization was similarly applied to $\text{Rh}_2(\text{S-TCPTTL})_4$ and was used for enantioselective carbonyl ylide cycloaddition reaction to generate **197** in continuous flow system. The column contained a mixture of sea sand and the polymer supported $\text{Rh}_2(\text{S-TCPTTL})_4$.¹⁶⁷ The leaching was negligible with only 2.1 ppm after 60 h continuous flow of reactants.

Scheme 4.4 Synthesis of polymer-supported $\text{Rh}_2(\text{S-PTTL})_4$



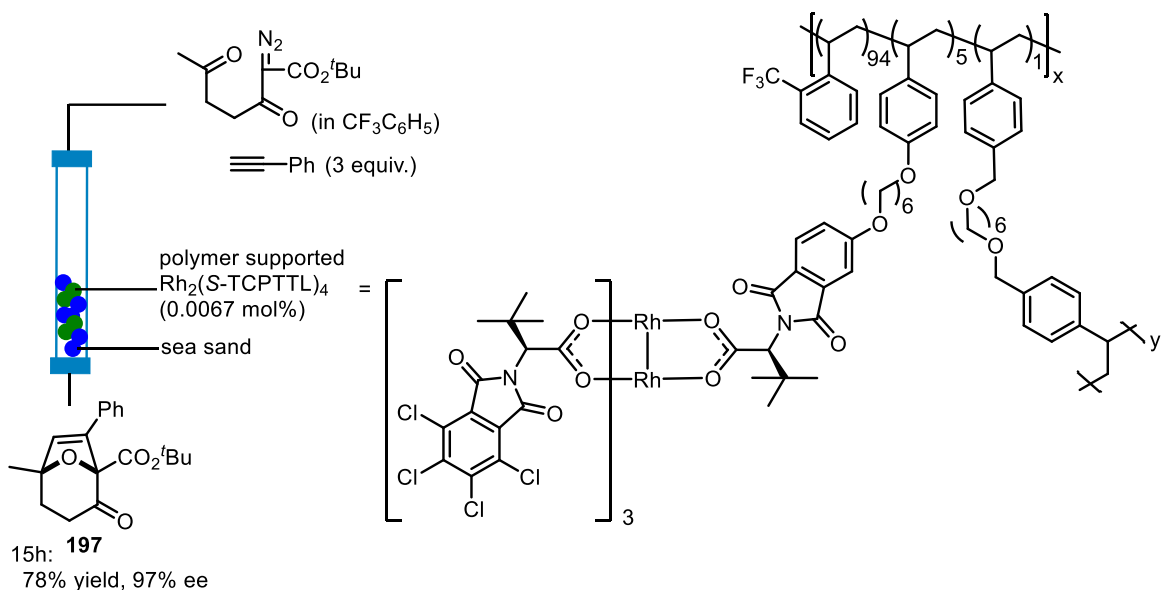
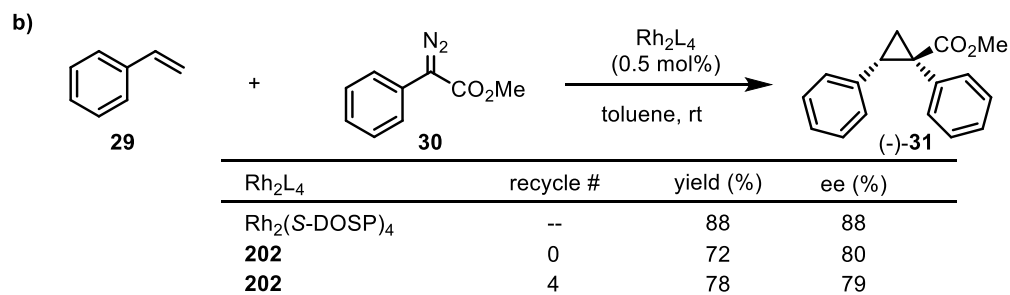
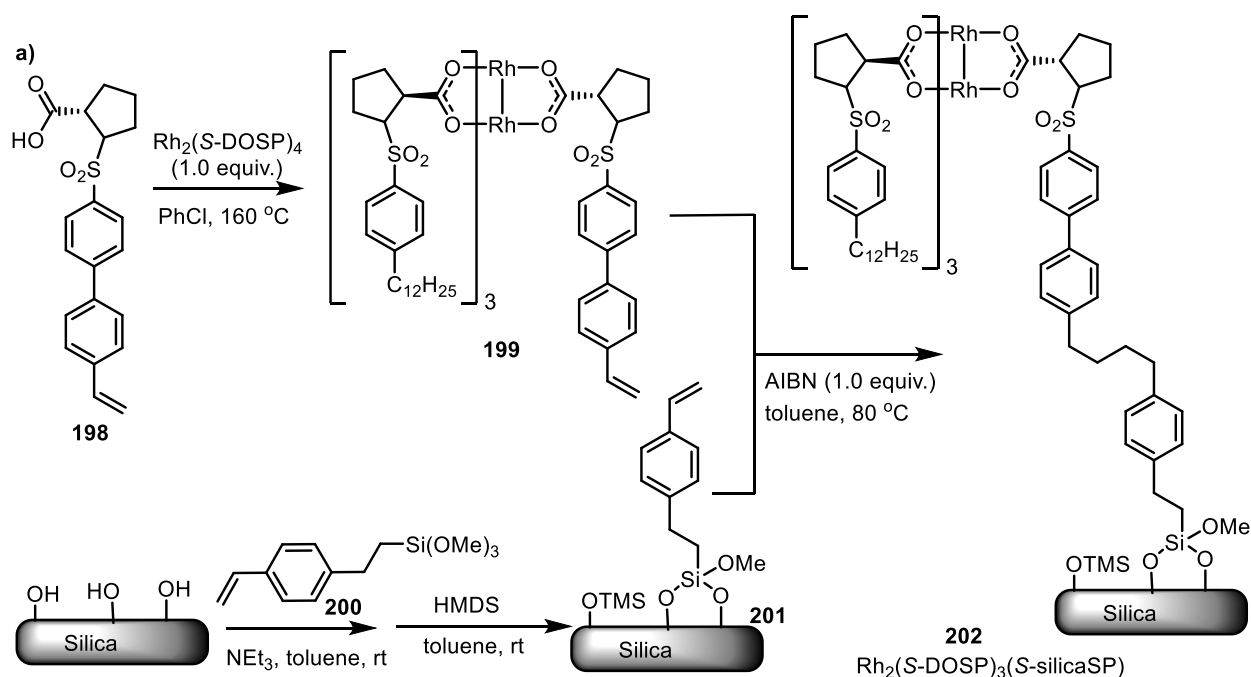


Figure 4.3 Intermolecular cycloaddition with polymer-supported $\text{Rh}_2(\text{S-TCPTTL})_4$ in flow

Following the impressive results on the covalently immobilized chiral dirhodium catalyst and the application in a flow reactor by Takeda *et al.*,¹⁶⁷ a collaboration between the Jones group and Davies group was conducted to immobilize $\text{Rh}_2(\text{S-DOSP})_4$ by covalently connect one *S*-DOSP-ligand to a silica support (Scheme 4.5).¹⁶⁸ This silica-immobilized $\text{Rh}_2(\text{S-DOSP})_4$ was synthesized by mono-ligand exchange with a *N*-(arylsulfonyl)prolinate **198**, which has a terminal alkenyl group, followed by AIBN-initiated radical coupling to graft the catalyst with a modified silica powder and generate $\text{Rh}_2(\text{S-DOSP})_3(\text{S-silicaSP})$ **202**.¹⁶⁸ Notably, the silica support was modified with all hydroxy groups capped by trimethylsilyl groups, and a trimethoxy(4-vinylphenethyl)silane moiety **200** was pre-installed on the silica surface. Examination of this immobilized chiral dirhodium catalyst, $\text{Rh}_2(\text{S-DOSP})_3(\text{S-silicaSP})$ **202**, showed that it performed comparably to the homogenous catalyst $\text{Rh}_2(\text{S-DOSP})_4$ in cyclopropanation and even intermolecular C–H insertion reactions on various substrates. Notably, retention of activity and stereoselectivity was achieved through 5 cycles.¹⁶⁸

The silica-supported $\text{Rh}_2(\text{S-DOSP})_4$ was then used in a flow reactor, where these silica particles with dirhodium catalysts bound was embedded in the porous polymer matrix at the wall of a hollow-fiber reactor.¹⁶⁹ Similar results were obtained between the batch and flow reaction using silica-supported $\text{Rh}_2(\text{S-DOSP})_4$, and the level of enantioselectivity was maintained through 1000 TON (88% to 84% ee).¹⁶⁹

Scheme 4.5 Synthesis and examination of $\text{Rh}_2(\text{S-DOSP})_3(\text{S-silicaSP})$



4.2 Results and Discussion

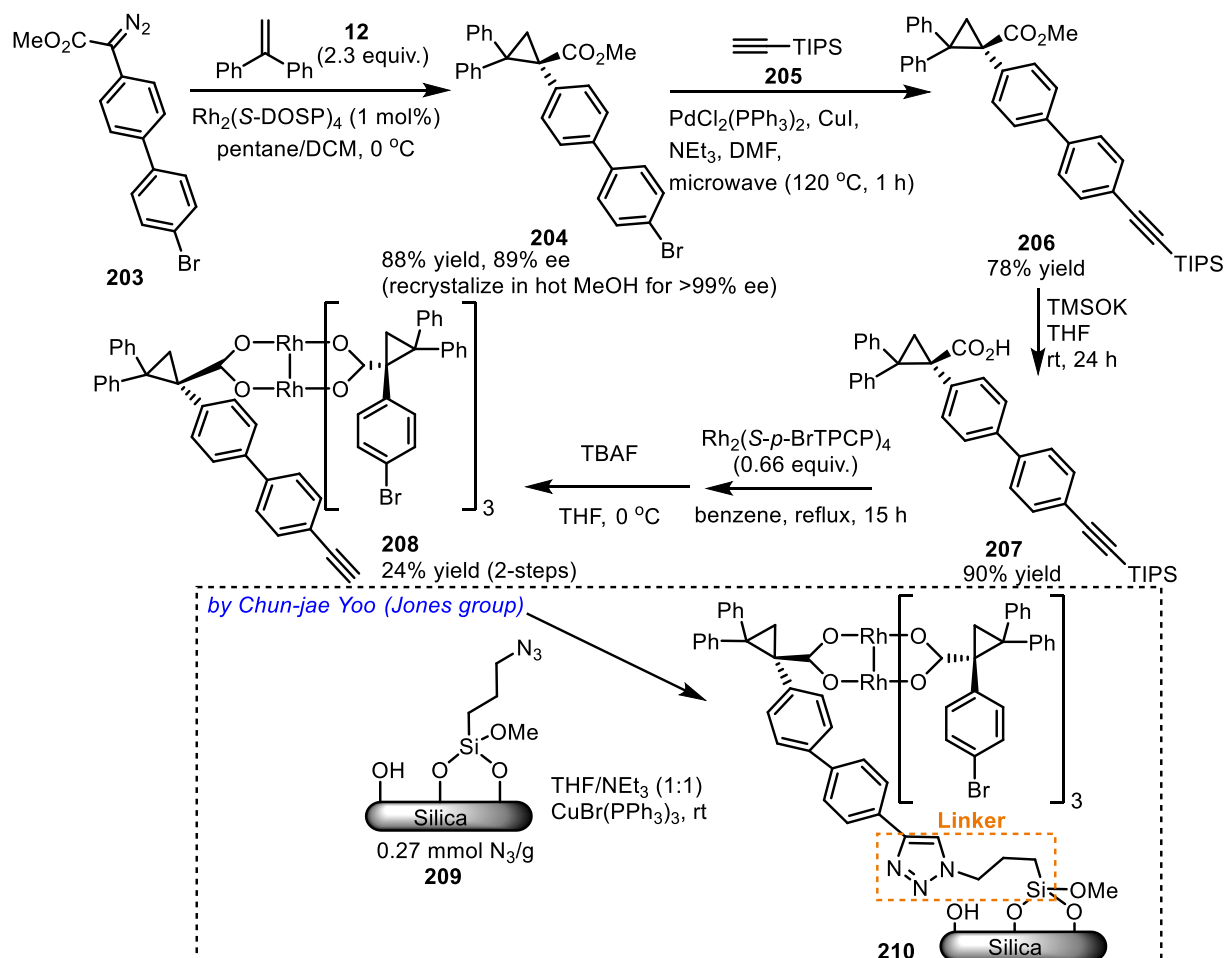
4.2.1 Immobilization of $\text{Rh}_2(\text{S-}p\text{-BrTPCP})_4$

The immobilization of $\text{Rh}_2(\text{S-}p\text{-BrTPCP})_4$ project began before my involvement, and I joined when it was close to completion with my role being to synthesize more $\text{Rh}_2(\text{S-}p\text{-BrTPCP})_3(\text{S-}p\text{-}(4\text{-ethynyl})\text{PhTPCP})$, which was then grafted onto the fiber reactor for reactions in flow. The synthesis route was optimized by a post-doctoral fellow in the Davies group, Dr. Daniel Rackl, and he also optimized the flow reaction condition together with Dr. Chun-jae Yoo, a chemical engineering graduate student in the Jones group at Georgia Tech who is an expert in flow reactor construction. After Dr. Rackl moved back to Germany, I helped with the catalyst synthesis and passed the materials to Dr. Yoo for grafting and then conducting the reactions in flow. The optimized synthesis route I used for $\text{Rh}_2(\text{S-}p\text{-BrTPCP})_3(\text{S-}p\text{-}(4\text{-ethynyl})\text{PhTPCP})$ is summarized here, together with part of the results for conducting reactions in flow. The full details of the study is available in the publication of this work.¹⁷⁰

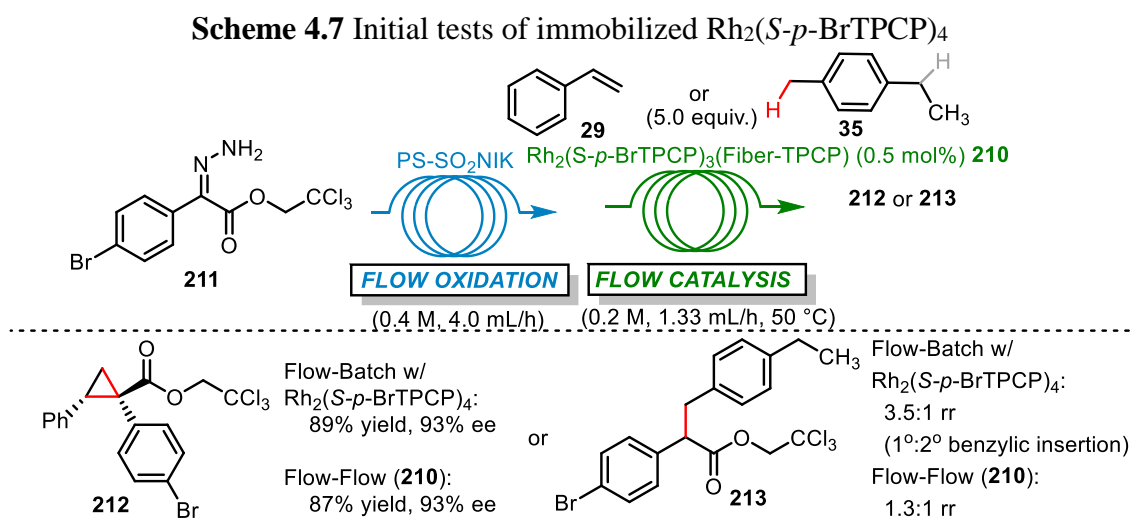
The synthesis of $\text{Rh}_2(\text{S-}p\text{-BrTPCP})_3(\text{S-}p\text{-}(4\text{-ethynyl})\text{PhTPCP})$ **208** involves the synthesis of the desired *S-p*-BrTPCP-ligand derivative **207**, followed by mono-ligand-exchange and deprotection to reveal the terminal ethynyl group (Scheme 4.6). An additional phenyl ring between the phenyl ring on the *S-p*-BrTPCP-ligand and linker was added as a spacer. Initial attempts by Dr. Rackl ruled out the possibilities of installing the ethynyl group via Suzuki coupling on the ligand synthesis stage or post functionalization on the $\text{Rh}_2(\text{S-}p\text{-BrTPCP})_4$ complex, resulting in the optimized route shown here. The cyclopropane scaffold of the methyl ester of *S-p*-BrTPCP-ligand derivative **204** was generated from the asymmetric cyclopropanation via rhodium carbene chemistry using $\text{Rh}_2(\text{S-DOSP})_4$. Then, the bromide substituent on the phenyl ring in **204** was replaced by a triisopropylsilyl (TIPS)-protected ethynyl group for **206** via Sonogashira coupling

using palladium (II) catalyst and copper (I) salt under microwave conditions, followed by hydrolysis using the bulky base, potassium trimethylsilanolate (TMSOK), which attacks the methyl group without epimerizing the chiral center adjacent to the carbonyl group. Next, the mono-ligand exchange was conducted before the deprotection of TIPS since the free ethynyl group could decompose under the heating reaction conditions for ligand exchange. Noticeably, the stoichiometric ratio between the ligand and dirhodium complex was optimized to 1.1:1 to minimize the formation of over-ligand exchange products (i.e. more than one *S-p*-BrTPCP-ligand replaced by **207**), as well as the reaction temperature. Finally, the TIPS protecting group was removed for **208**, which was then grafted onto the silica-support via click chemistry by Dr. Yoo.

Scheme 4.6 Synthesis of $\text{Rh}_2(\textit{S-p}\text{-BrTPCP})_3(\textit{S-p}\text{-}(4\text{-ethynyl})\text{PhTPCP})$ and immobilization



The obtained immobilized $\text{Rh}_2(\text{S-}p\text{-BrTPCP})_4$, covalently bound in the wall of a hollow fiber reactor, was then examined in the regular rhodium carbene reactions by Dr. Rackl and Dr. Yoo. The carbene precursors, such as 2,2,2-trichloroethyl 2-(4-bromophenyl)-2-diazoacetate, used here were also generated in flow under the reaction conditions they developed, where the hydrazone compounds were oxidized when it passed through a cartridge with polystyrene-supported *N*-iodo-*p*-toluenesulfonamide potassium salt (PS-SO₂NIK).¹⁷¹ The first examination was conducted on cyclopropanation with styrene, and similar performances with a slight drop in reactivity (91% to 87% yield) and enantioselectivity (95% to 93% ee) were detected when the flow-to-flow reaction was compared to the homogenous $\text{Rh}_2(\text{S-}p\text{-BrTPCP})_4$ reaction in batch.¹⁷⁰ However, unmatched results were observed when it was examined on the C–H insertion reactions. In the C–H insertion of 4-ethyltoluene **35** using the diazoacetate obtained in flow after oxidation of **211**, the reaction using homogenous $\text{Rh}_2(\text{S-}p\text{-BrTPCP})_4$ furnished the primary benzylic insertion product with 3.5:1 site-selectivity, while the selectivity dropped to 1.3:1 for the fiber-supported $\text{Rh}_2(\text{S-}p\text{-BrTPCP})_4$ **210**.¹⁷² Good results were reported for substrates with only electronically activated primary sites but the immobilized catalyst was less selective than the homogenous catalysts with substrates that have competing secondary C–H bonds.¹⁷⁰



Though promising results were obtained using this flow-to-flow system with fiber-supported $\text{Rh}_2(S\text{-}p\text{-BrTPCP})_4$, the results from the C–H insertion reactions in flow imply the influence of the anchor site on the catalyst ligand framework could attenuate the selectivity profile. As discussed in chapter 2, it was known in the literature that the $\text{Rh}_2(\text{TPCP})_4$ complexes are adopting different configuration with high symmetry when different functional groups are substituted on the C1-aryl ring, and they give different selectivity profiles in C–H insertion reactions. For example, $\text{Rh}_2(S\text{-}p\text{-BrTPCP})_4$ and $\text{Rh}_2(S\text{-}p\text{-PhTPCP})_4$ adopt D_2 , and *pseudo*- C_2 symmetric conformations respectively, and have different levels of preference for primary benzylic C–H bonds. In the original synthetic route developed by Dr. Rackl for fiber-supported $\text{Rh}_2(S\text{-}p\text{-BrTPCP})_4$, the anchor site is derived from the aryldiazoacetate but that aryl group is considered to be a critical component of the chiral pocket of the $\text{Rh}_2(\text{TPCP})_4$ class of catalysts. Therefore, we became interested in developing linker strategies that would allow immobilization at any of the three aryl groups in the TPCP catalysts

4.2.2 Exploration of Influence of Anchor Site on $\text{Rh}_2(S\text{-}o\text{-CITPCP})_4$

In this project, my role was to design and synthesize derivatives of $\text{Rh}_2(S\text{-}o\text{-CITPCP})_4$, in which one of the ligands has an additional terminal ethynyl group (for linker installation) at each of the three different aryl rings in the ligands and to evaluate these modified catalysts in batch. The immobilization was then carried out by Dr. Yoo in the Jones laboratory. The resulted silica-supported catalysts were sent back to me to evaluate their catalytic activity and selectivity. Through this, the influence of anchor site for immobilizing the class of $\text{Rh}_2(\text{TPCP})_4$ catalysts could be determined.

In the class of $\text{Rh}_2(\text{TPCP})_4$ catalysts with the triaryl cyclopropane scaffold, the linker could be potentially be installed on any of the three aryl rings, with a similar linker connection strategy used for $\text{Rh}_2(S\text{-}p\text{-BrTPCP})_3(S\text{-}p\text{-}(4\text{-ethynyl})\text{PhTPCP})$ **208**. The linker location could influence how well the immobilized catalysts perform compared to the original homogenous counterparts. The $\text{Rh}_2(S\text{-}o\text{-ClTPCP})_4$ catalyst was chosen as the model catalyst for this project due to its unique C_4 symmetric configuration, in which three different aryl rings on the same cyclopropane ring are pointed in three different directions (Figure 4.4). The C1-aryl ring **A** points to the active face where the carbene binds to the rhodium in the reaction; the C2-phenyl ring **B**, which is *cis* to the *o*-Cl-aryl group, points to the equatorial side of the Rh–O disk and is furthest away from the Rh center; while the other C2-phenyl ring **C**, which is *trans* to the *o*-Cl-aryl group, is at the “closed” rhodium face, where four phenyl rings tilt toward each other and block the access of the carbene.

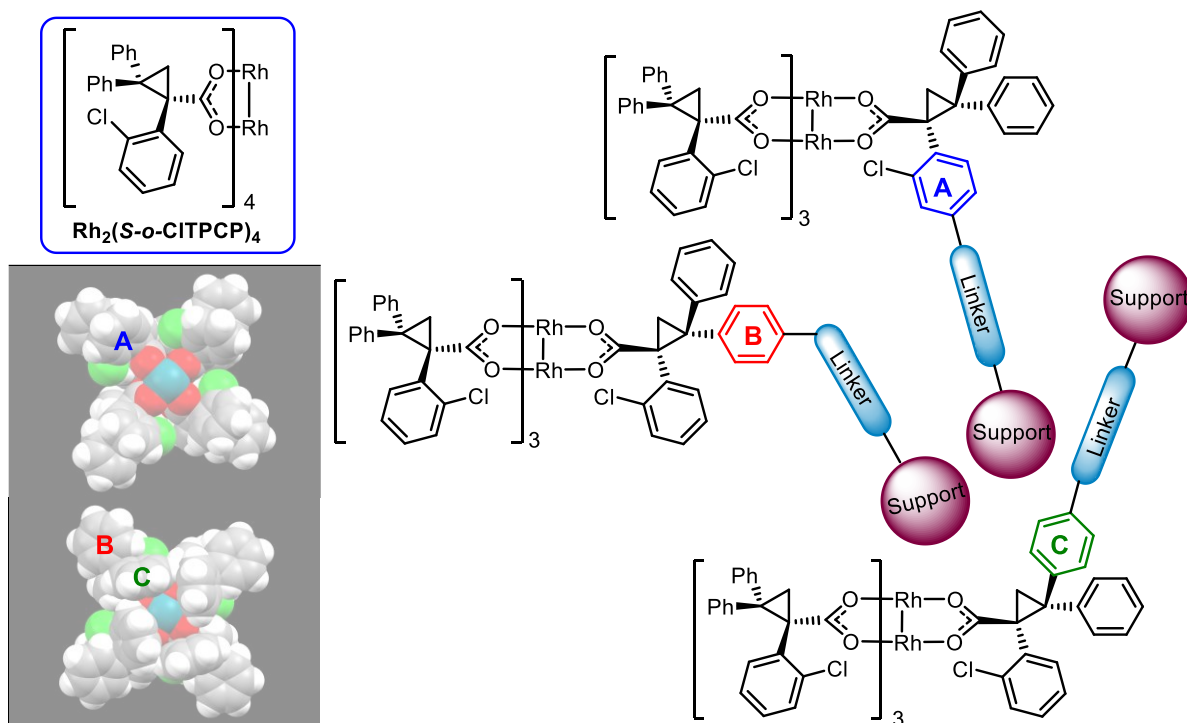


Figure 4.4 Three anchor sites for immobilizing $\text{Rh}_2(S\text{-}o\text{-ClTPCP})_4$

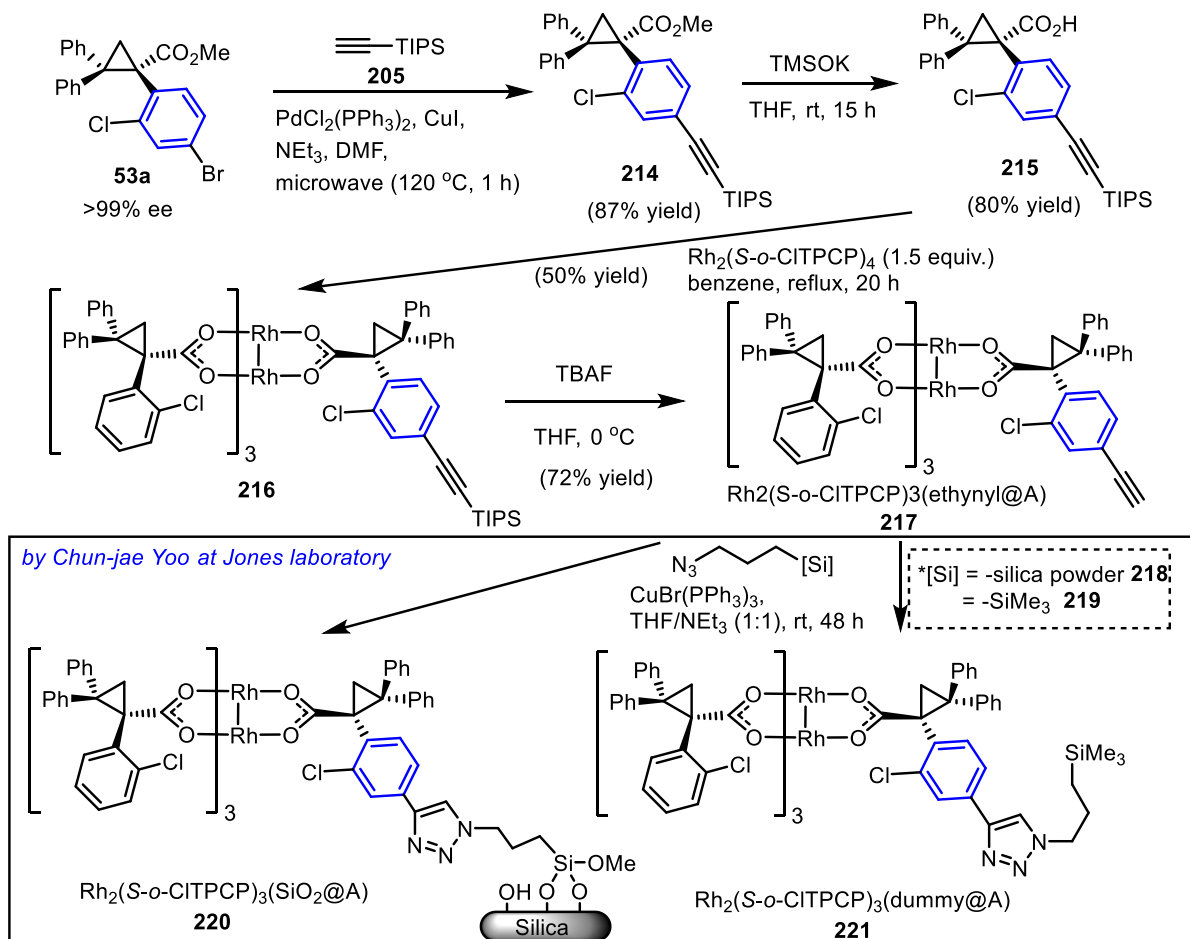
In my hypothesis, it would be the best for $\text{Rh}_2(S\text{-}o\text{-ClTPCP})_4$ immobilization having the linker at ring **B**. With the linker on ring **A**, it could potentially interact with the rhodium carbene binding

site, which influences the performance of the catalyst similar to the effect of different substituents on ring **A**. Additionally, the linker on ring **A** may also affect the geometry of the catalyst. When the linker is on ring **C**, it is far away from the carbene binding site and it is reasonable to expect that it may perform similar to the original catalyst. However, the packing of the four phenyl rings on the “closed” face of the catalyst may be changed with an additional linker on one of phenyl rings, which may change the tilted angle of this ligand and therefore alter the orientation of the *o*-Cl-aryl ring in this ligand on the opposite face of the catalyst. Moreover, for Rh₂(TPCP)₄ catalysts with D₂ symmetry, ring **C** is on the same face with ring **A** at the reaction pocket, thus the effect of having the linker on **C** would be the same as having it on **A** in the cases of these catalysts. Therefore, the linker on ring **B** would be expected to have the least influence on the catalysts’ geometries and reaction profiles, because ring **B** is always at the equatorial side pointing to the periphery of the catalysts in all the crystal structures of Rh₂(TPCP)₄ obtained so far.

The synthesis of these Rh₂(*S*-*o*-ClTPCP)₄ derivatives follows a similar disconnection strategy for Rh₂(*S*-*p*-BrTPCP)₃(*S*-*p*-(4-ethynyl)PhTPCP) **208**. The synthesis of derivative **217** with ethynyl group on ring **A** was relatively straight forward starting from the enantiopure methyl ester of the *S*-2-Cl-4-BrTPCP-ligand **53a**, which was obtained from the synthesis of Rh₂(*S*-2-Cl-4-BrTPCP)₄ (Scheme 4.8). The TIPS-protected ethynyl group was installed via the same Sonogashira coupling conditions irradiated by microwave in 87% yield, followed by TMSOK S_N2-type hydrolysis to generate *S*-2-Cl-4-ethynylTPCP ligand **215** in 80% yield without influencing the chiral centers. The Rh₂(*S*-*o*-ClTPCP)₃(TIPS-ethynyl@A) **216** was obtained after carefully controlled mono-ligand exchange in reactant ratio, temperature and time. Without changing the reaction temperature (refluxing benzene) and time (overnight), initial trial with 0.66 equiv of Rh₂(*S*-*o*-ClTPCP)₄ (limiting reagent), as in the case of Rh₂(*S*-*p*-BrTPCP)₄, showed additional green spots by TLC,

suggesting over-ligand exchange products in addition to the desired mono-ligand exchange product. Consequently, the stoichiometry of the reactions was changed and an excess of $\text{Rh}_2(\text{S-}o\text{-CITPCP})_4$ (1.5 equiv) was used. Under these conditions, the desired mono-ligand exchange product **178** was obtained in 50% yield, and its purity was confirmed by TLC and high-resolution mass spectroscopy (HRMS). Finally, the desired complex $\text{Rh}_2(\text{S-}o\text{-CITPCP})_3(\text{ethynyl@A})$ **179** was revealed after TIPS deprotection by tetra-*n*-butylammonium fluoride (TBAF) solution in tetrahydrofuran. This compound was given to Dr. Yoo for the synthesis of silica-supported $\text{Rh}_2(\text{S-}o\text{-CITPCP})_3(\text{SiO}_2\text{@A})$ **220** using silica-supported azide **218** and homogenous $\text{Rh}_2(\text{S-}o\text{-CITPCP})_3(\text{dummy@A})$ **221** using azide **219** as described in the published procedures¹⁷⁰.

Scheme 4.8 Synthesis for $\text{Rh}_2(\text{S-}o\text{-CITPCP})_4$ derivative with ethynyl on ring A



The synthesis for $\text{Rh}_2(S\text{-}o\text{-CITPCP})_3(\text{ethynyl@B})$ and $\text{Rh}_2(S\text{-}o\text{-CITPCP})_3(\text{ethynyl@C})$ have additional complexity with more steps before the Sonogashira coupling, since they would require bromide substituent on the C2-aryl rings. A key step would be the cyclopropanation of an asymmetric 1,1-diarylethylene **222**. Although cyclopropanation of styrene with asymmetric alkene using rhodium carbene are generally found to be highly diastereoselective,⁹⁷ the cyclopropanation of 1,1-diarylethylenes with different aryl groups tends to give close 1:1 mixture of diastereomers unless there is an electron-donating group on one of the aryl rings.¹⁷³ Therefore, a catalyst screening on cyclopropanation of 1-bromo-4-(1-phenylvinyl)benzene **222** was conducted in order to determine if the catalysts can influence the diastereoselectivity of the cyclopropanation (Table 4.4). Methyl diazoacetate **11** was used to avoid further modification to the already optimized synthetic sequence for the formation of $\text{Rh}_2(S\text{-}o\text{-CITPCP})_3(\text{ethynyl@A})$. The enantiopure samples of the separated diastereomers could be obtained via recrystallization, so it was not necessary to use the more sophisticated trichloroethyl diazoacetates. Screening of the common catalysts for effective cyclopropanation showed small changes in the diastereoselectivity, with $\text{Rh}_2(\text{PTAD})_4$ gave highest ratio between **223** and **224** (2.3:1) preferring the hypothetically desired diastereomer with bromide on ring **B**, as well as highest enantiocontrol for both diastereomers. Therefore, $\text{Rh}_2(S\text{-PTAD})_4$ was used as the catalyst for the synthetic route to both of the desired diastereomers.

Table 4.4 Catalyst screening on cyclopropanation of asymmetric 1,1-diarylethylene

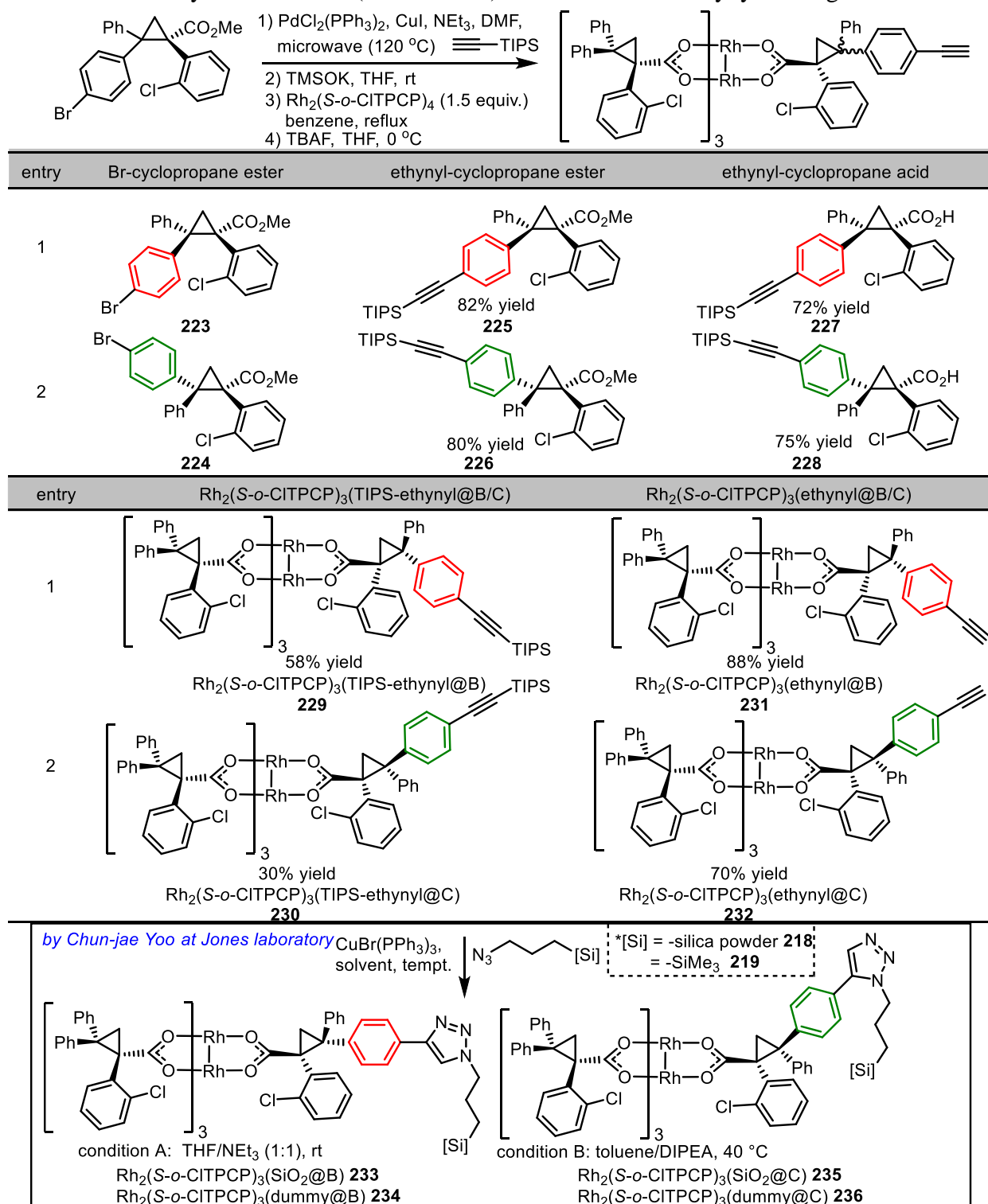
Entry	Rh_2L_4	solvent	yield, %	dr (223 : 224)	ee, % (223)	ee, % (224)
1	$\text{Rh}_2(\text{OAc})_4$	CH_2Cl_2	85	1:1.2	--	--
2	$\text{Rh}_2(S\text{-DOSP})_4$	pentane	88	1.3:1	-97	-94
3	$\text{Rh}_2(R\text{-PTAD})_4$	pentane	90	2.3:1	-99	-97
4	$\text{Rh}_2(S\text{-}p\text{-BrTPCP})_4$	CH_2Cl_2	78	1.2:1	-35	-69

Note: The minor enantiomers (as drawn) are the desired one for later synthesis, so negative value are shown.

The completion of the synthesis for $\text{Rh}_2(S\text{-}o\text{-CITPCP})_3(\text{ethynyl@B})$ and $\text{Rh}_2(S\text{-}o\text{-CITPCP})_3(\text{ethynyl@C})$ followed the approach used for the synthesis of the derivative with ethynyl on ring **A** using enantiopure methyl esters (Table 4.5). After several trials for enantio-enrichment, the enantiopure cyclopropane methyl esters **223** and **224** were obtained by recrystallization of hot solutions of the pure diastereomers in hexane and 1% diethyl ether/hexane, respectively. The Sonogashira coupling reactions for both derivatives proceeded smoothly to afford the installation of TIPS-protected ethynyl group for ethynyl-cyclopropane esters **225** and **226** in 80-82% yield, which required anhydrous dimethylformamide (DMF) solvent for full conversion of the starting *p*-bromoaryls. Careful monitoring by TLC was also needed during hydrolysis of the methyl ester using TMSOK because undesired TIPS-deprotecting was also observed if the reaction went too long. Under the optimal conditions, the cyclopropanecarboxylic acid **227** and **228** were formed in 72-75% yield. As mentioned before, the mono-ligand exchange was the key step to afford the pure $\text{Rh}_2(S\text{-}o\text{-CITPCP})_3(\text{TIPS-ethynyl@B/C})$ in higher yield. The confirmation of having 3:1 ratio of ligands in the complex and purity was determined by HRMS and single spot on TLC. The ^1H NMR of the catalyst is not informative enough, since the complexes with different ratio of the mixed ligands all have same types of protons without a definitive pattern. The $\text{Rh}_2(S\text{-}o\text{-CITPCP})_3(\text{TIPS-ethynyl@B})$ **229** was obtained in 58% yield with relatively shorter reaction time (16 h), while the $\text{Rh}_2(S\text{-}o\text{-CITPCP})_3(\text{TIPS-ethynyl@C})$ **230** was more difficult and needed longer reaction time (24 h) and the yield was lower (30%). The free ethynyl group was revealed by treatment with TBAF at 0 °C to form **231** and **232** in good yields (70-88%). The $\text{Rh}_2(S\text{-}o\text{-CITPCP})_3(\text{ethynyl@B/C})$ complexes with terminal ethynyl groups are less stable for long-term storage, so Dr. Yoo carried out the click reactions on them with both silica powder **218** and dummy link **219** in the same week of the deprotection for compounds **233-236**. Notably, higher temperature and different amine base

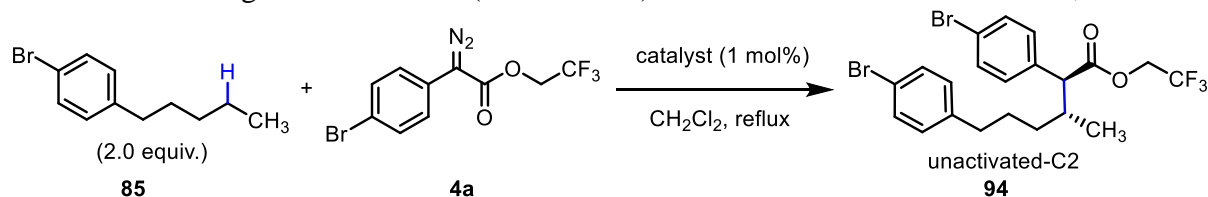
(DIPEA instead of NEt_3) were used for the click reaction with **232**, since the ethynyl group at ring C is less accessible.

Table 4.5 Synthesis for $\text{Rh}_2(\text{S-}o\text{-CITPCP})_4$ derivatives with ethynyl on ring B and C



The silica-supported $\text{Rh}_2(\text{S-}o\text{-CITPCP})_4$ derivatives, together with the homogenous dummy-linked $\text{Rh}_2(\text{S-}o\text{-CITPCP})_4$ derivatives, were examined in the reference reaction between 4-bromopentylbenzene **85** and trifluoroethyl diazoacetate **4a** (Table 4.6). The results showed that the reactivity and selectivity of homogenous dummy-linked and heterogenous silica-supported $\text{Rh}_2(\text{S-}o\text{-CITPCP})_4$ derivatives with linkers at the same sites performed similar to each other. Interestingly, the performance of these catalysts with one ligand modified were comparable to the parent homogenous catalyst $\text{Rh}_2(\text{S-}o\text{-CITPCP})_4$, which implies the TPCP scaffold is rigid and the linker has little impact on its reactivity and selectivity. However, among the derivatives with linkers at the three different sites, differences could be detected. In both cases of the dummy linker and silica powder immobilized, the derivatives with linker at ring **A** (**221** and **220** respectively), which is the *o*-chloroaryl ring at the reaction pocket, catalyzed the reactions with relatively lower yield, site- (6.8-8.4:1 rr vs 11.5:1 rr for $\text{Rh}_2(\text{S-}o\text{-CITPCP})_4$) and stereoselectivity (65-72% ee vs 78% ee) compared to the other derivatives. The derivatives with linker at ring **B** (**234** and **233**) and **C** (**236** and **235**) performed similarly (77-78% ee vs 78% ee for $\text{Rh}_2(\text{S-}o\text{-CITPCP})_4$), and especially, silica-supported derivatives **235** gave slightly better results than its analog **233**.

Table 4.6 Testing reaction for $\text{Rh}_2(\text{S-}o\text{-CITPCP})_4$ derivatives with linker at site **A**, **B** and **C**



catalyst	yield	rr (C2:Benzylic)	dr (C2)	ee, % (C2,major diastomer)
$\text{Rh}_2(\text{S-}o\text{-CITPCP})_4$	87	11.5:1	22.6:1	77
221 $\text{Rh}_2(\text{S-}o\text{-CITPCP})_3(\text{dummy@A})$	72	8.4:1	18.4:1	72
234 $\text{Rh}_2(\text{S-}o\text{-CITPCP})_3(\text{dummy@B})$	83	14.6:1	17.6:1	77
236 $\text{Rh}_2(\text{S-}o\text{-CITPCP})_3(\text{dummy@C})$	80	11.0:1	19.3:1	77
220 $\text{Rh}_2(\text{S-}o\text{-CITPCP})_3(\text{SiO}_2\text{@A})$	69	6.8:1	15.9:1	65
233 $\text{Rh}_2(\text{S-}o\text{-CITPCP})_3(\text{SiO}_2\text{@B})$	83	9.9:1	19.8:1	76
235 $\text{Rh}_2(\text{S-}o\text{-CITPCP})_3(\text{SiO}_2\text{@C})$	78	12.0:1	21.1:1	79

Nonetheless, immobilization of the family of Rh_2TPCP_4 catalysts with linker at ring **B**, which is *cis* to the C1-aryl ring and points to the equatorial position in the catalysts' geometry, is considered to be the optimal anchor site for all TPCP-based dirhodium catalysts. Though in the case of $\text{Rh}_2(S\text{-}o\text{-ClTPCP})_4$, having linker at ring **B** and **C** are comparable with poorer performance for those with linker at **A**, for most of other Rh_2TPCP_4 catalysts, having linker at ring **C** could encounter the same problem as those at **A**, when the geometry of other Rh_2TPCP_4 catalysts is considered. For example, the $\text{Rh}_2(R\text{-}p\text{-BrTPCP})_4$ adopts D_2 symmetry with the *trans*-phenyl ring (**C**) and *p*-bromophenyl ring (**A**) oriented in the same reaction pocket. Therefore, immobilizing the $\text{Rh}_2(S\text{-}o\text{-ClTPCP})_4$ series catalysts at site **B** was chosen to continue the project for translating the reaction from batch to flow.

4.2.3 Development of immobilized $\text{Rh}_2(S\text{-}2\text{-Cl-5-CF}_3\text{TPCP})_4$ for Flow Reaction in Cartridge

To develop the most effective flow reaction, the optimal catalyst in $\text{Rh}_2(S\text{-}o\text{-ClTPCP})_4$ series was used. Therefore, $\text{Rh}_2(S\text{-}2\text{-Cl-5-BrTPCP})_4$ was expected to be immobilized with the anchor site on ring **B** for later studies. However, the installation of linker precursor, ethynyl group, requires the Sonogashira coupling transformation on aryl bromides, and there are two aryl bromides in the *S*-2-Cl-5-BrTPCP ester derivative **237** (Figure 4.5). There are mainly two choices: one required exploration an alternative leaving group for selective Sonogashira coupling in the presence of the aryl bromide and was very time consuming with no literature precedent, while the other would change the target catalyst to another analog with similar or better performance. In addition, more derivatives of $\text{Rh}_2(S\text{-}o\text{-ClTPCP})_4$ family were obtained and examined at this stage. Therefore, effort was focused on the attempt for replacement of $\text{Rh}_2(S\text{-}2\text{-Cl-5-BrTPCP})_4$.

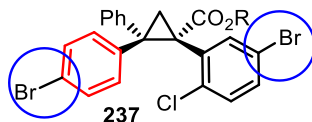


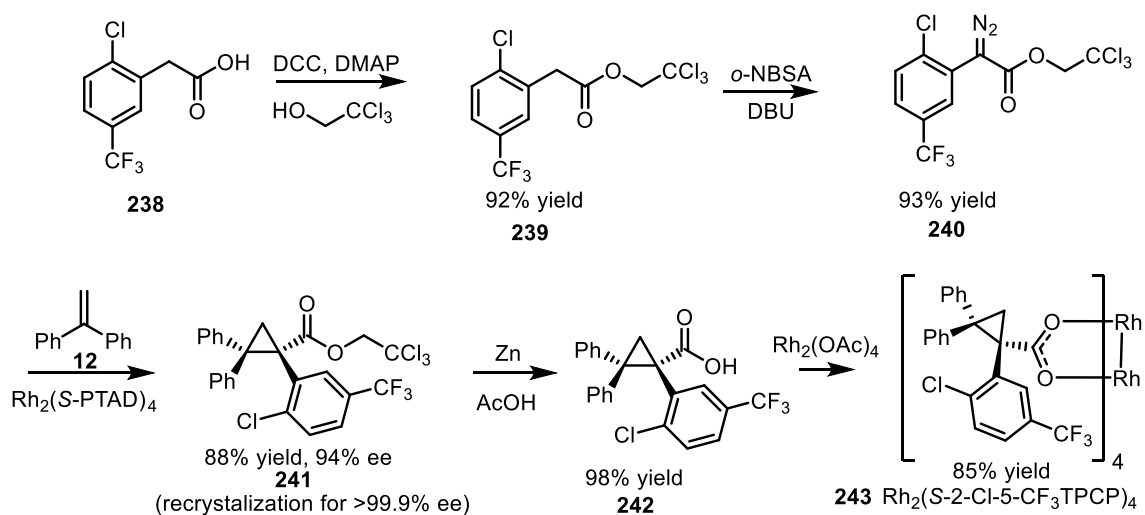
Figure 4.5 Structure of *S*-2-Cl-5-BrTPCP ester derivative **237**

Based on the results discussed the session 2.2.6, among various $\text{Rh}_2(\text{S-2-Cl-5-BrTPCP})_4$ analogs, worse results were observed when changing the bromide to either more electron-withdrawing group (CF_3 substituted aryl) or strong electron-donating groups (methoxyl or amine substituted aryl). (Note: mesityl group was not examined at this point.) That is, a substituent would be needed, which has comparable electronic (and ideally steric) properties as bromide but no lability to Sonogashira coupling conditions. In order to do so, the tables of Hammett constant¹⁷⁴ was referred for hints at the electronic properties of different functional groups and A-values,¹⁷⁵ which are derived from the energy difference between two conformers of mono-substituted cyclohexanes and relates to the substituent's steric bulk, as well as the Van der Waals radius for potential hints (Table 4.7). In terms of the electronic features, trifluoromethyl group has the closest Hammett constants (both σ_m and σ_p) compared to the bromide group among other hydrocarbon functional groups. When taking A-values into account, the value for trifluoromethyl group is 2.1, much larger than the value for bromide, but is similar to the methyl group that is already the smallest among all hydrocarbon functional groups. Hence, the sizes of bromide and trifluoromethyl group were compared. The van der Waals radius for bromide and fluoride are 182 pm and 119 pm respectively, and the C–F bond length in some of the crystal structures I obtained is around 134 pm, so the size of trifluoromethyl group would be slightly bigger but close to bromide. According to these analyses, the trifluoromethyl group was chosen as a replacement for bromide, and the synthesis and the performance of the proposed $\text{Rh}_2(\text{S-2-Cl-5-CF}_3\text{TPCP})_4$ was examined.

Table 4.7 Comparison of electronic and steric features among potential functional groups

R	σ_m	σ_p	A-value	
R = Br	0.39	0.23	0.38	r (Br) = 182 pm
R = CF ₃	0.43	0.54	2.1	r (F) = 119 pm
R = CH ₃	-0.07	-0.17	1.7	d (C-F) = 134 pm
R = Ph	0.06	-0.01	3	

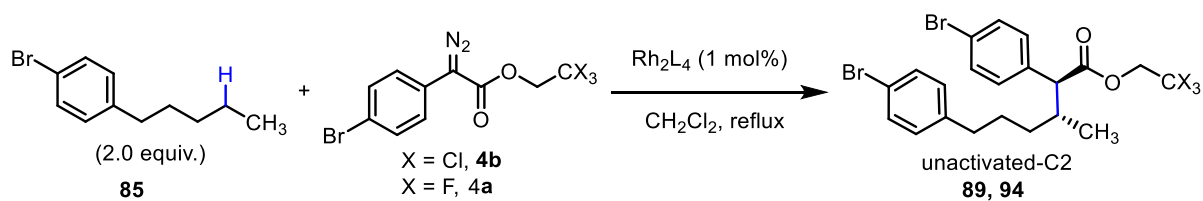
The Rh₂(*S*-2-Cl-5-CF₃TPCP)₄ was obtained using the same route for Rh₂(*S*-2-Cl-5-BrTPCP)₄ (Scheme 4.9). After the corresponding trichloroethyl diazoacetate **240** was generated in 93% yield through a diazo transfer reaction, the cyclopropanation was conducted using Rh₂(*S*-PTAD)₄ as catalyst, which gave **241** in 94% ee, significantly better than Rh₂(*S*-DOSP)₄ (9% ee). The cyclopropane ester was recrystallized in hot hexane to form enantiomerically pure sample of **203**, followed by hydrolysis using zinc dust to furnish the *S*-2-Cl-5-CF₃TPCP-ligand **242** in 98% yield. The ligand exchange reaction for this ligand was found to be more efficient than other Rh₂(*S*-*o*-CITPCP)₄ series catalysts, and finished the desired Rh₂(*S*-2-Cl-5-CF₃TPCP)₄ in 85% yield.

Scheme 4.9 Synthesis of Rh₂(*S*-2-Cl-5-CF₃TPCP)₄

With the Rh₂(*S*-2-Cl-5-CF₃TPCP)₄ in hand, examination on the reference reaction with 4-bromopentylbenzene was conducted in comparison with Rh₂(*S*-2-Cl-5-BrTPCP)₄ (Table 4.8). As

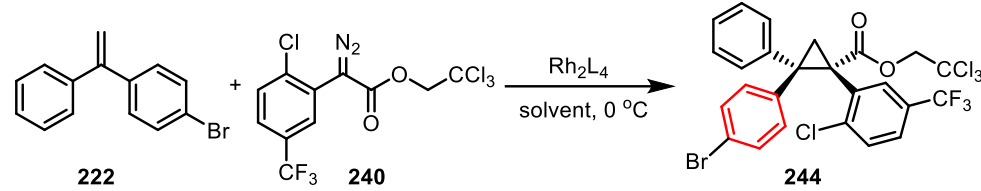
expected, the reactivity and selectivity of these two catalysts are very similar to each other. $\text{Rh}_2(\text{S-2-Cl-5-CF}_3\text{TPCP})_4$ gave a better site-selectivity (21:1 vs 20:1 rr with X = Cl, and 28:1 vs 24:1 rr with X = F) and similar enantiocontrol (87% vs 87% ee with X = Cl, and 93% vs 91% ee with X = F), while yield and diastereoselectivity were still high with acceptable decrease. Therefore, the $\text{Rh}_2(\text{S-2-Cl-5-CF}_3\text{TPCP})_4$ was found to be comparable to its bromide analog and is an optimal catalyst for continuing the project of conducting reactions in continuous flow.

Table 4.8 Testing of $\text{Rh}_2(\text{S-2-Cl-5-CF}_3\text{TPCP})_4$ in C–H insertion on 4-bromopentylbenzene



Rh_2L_4	X	yield	rr (C2:Benzylic)	dr (C2)	ee, % (C2)
$\text{Rh}_2(\text{S-2-Cl-5-BrTPCP})_4$	Cl	87	20:1	20:1	89
$\text{Rh}_2(\text{S-2-Cl-5-CF}_3\text{TPCP})_4$	Cl	85	21:1	13:1	87
$\text{Rh}_2(\text{S-2-Cl-5-BrTPCP})_4$	F	86	24:1	28:1	91
$\text{Rh}_2(\text{S-2-Cl-5-CF}_3\text{TPCP})_4$	F	82	28:1	20:1	93

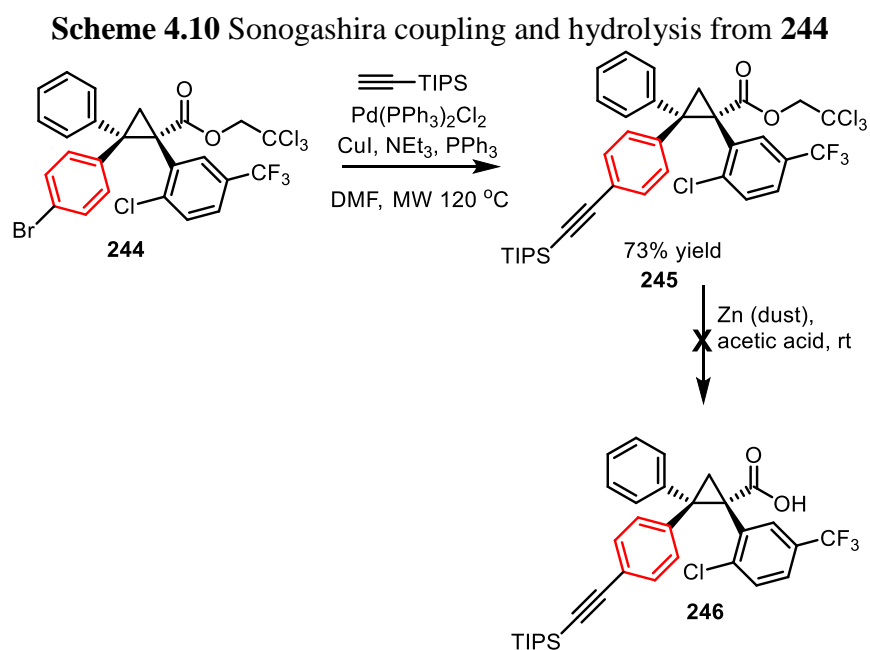
Similar to the immobilization of $\text{Rh}_2(\text{S-}o\text{-ClTPCP})_4$, the first step for the synthesis of these Rh_2TPCP_4 with linker at site **B** was the catalyst screening for cyclopropanation using unsymmetrical 1,1-diarylethylene **222** (Table 4.9). Unfortunately, all the catalysts screened gave nearly a 1:1 mixture of both diastereomers, although the $\text{Rh}_2(\text{S-PTAD})_4$ furnished the desired diastereomer with bromide on ring **B** with the highest level of enantioinduction (94% ee). Considering the performance of immobilized $\text{Rh}_2(\text{S-}o\text{-ClTPCP})_4$ with linker at site **B** and **C** were similar, no further optimization in terms of diastereoselectivity of this cyclopropanation reaction was conducted.

Table 4.9 Catalyst screening on asymmetric cyclopropanation using 2-chloro-5-(trifluoromethyl)diazoacetate


Entry	Rh ₂ L ₄	solvent	yield, %	dr (Br@B:C)	ee, % (244)
1	Rh ₂ (<i>R</i> -DOSP) ₄	pentane	95	1:1.6	-17
2	Rh₂(<i>S</i>-PTAD)₄	pentane	96	1:1.0	94
3	Rh ₂ (<i>S</i> -PTTL) ₄	CH ₂ Cl ₂	95	1:1.3	85
4	Rh ₂ (<i>S</i> -TCPTAD) ₄	CH ₂ Cl ₂	92	1:1.2	92
5	Rh ₂ (<i>R</i> -TPPTTL) ₄	CH ₂ Cl ₂	90	1:1.2	-11

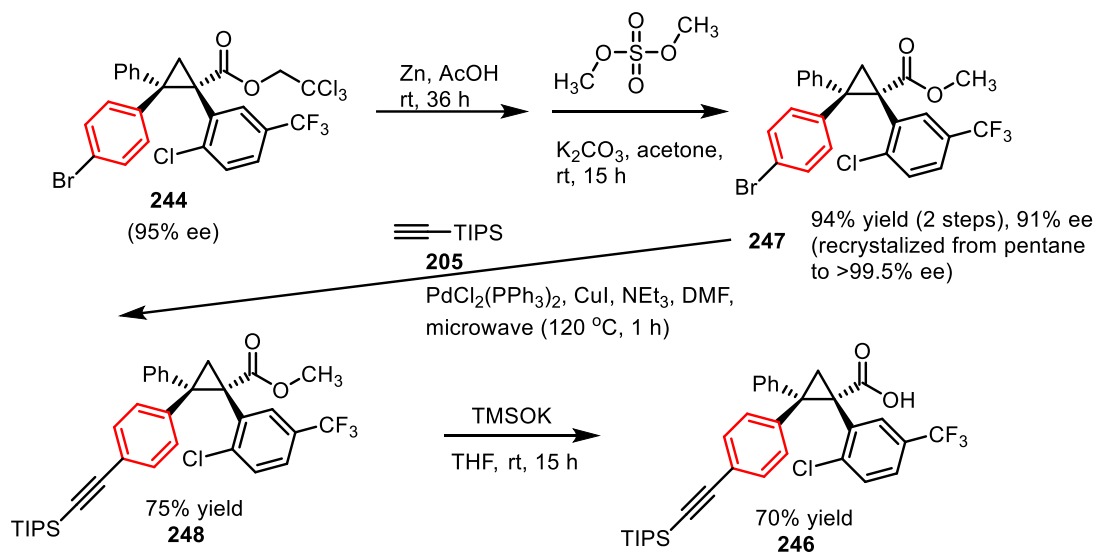
Note: negative value in ee indicates the major enantiomer was opposite to the one drawn.

Taking the Rh₂(*S*-PTAD)₄-catalyzed asymmetric cyclopropanation forward, the desired product **244** was purified by column chromatography and recrystallized to >99.5% ee from solution in pentane for further synthesis (Scheme 4.10). As expected, the Sonogashira coupling for TIPS-ethynyl group installation went smoothly in 73% yield. However, the zinc facilitated hydrolysis of the 2,2,2-trichloroethoxycarbonyl group in compound **245** failed and only starting material was recovered, and alternative route was needed to be explored.



Since the immobilization route worked for methyl esters, the cyclopropane-methyl ester was then desired. Firstly, the cyclopropanation was re-explored using methyl ester version of 2-Cl-5-CF₃ diazoacetate, but both Rh₂(*S*-PTAD)₄ and Rh₂(*R*-DOSP)₄ gave 1:1 mixture of diastereomers and poor enantiocontrol (35-75% ee). With the condition for the synthesis of cyclopropane-trichloroethyl ester **244** with high enantioselectivity optimized, it could be converted to the methyl ester analog **247**. Similar transformation was reported,¹⁰⁵ and the desired methyl ester analog **247** could be obtained without significant losing in enantiomeric ratio from a 2-step-1-pot reaction: the regular hydrolysis of trichloroethoxycarbonyl group in **206**, followed by esterification using dimethylsulfate and potassium carbonate after (Scheme 4.11). The methyl ester analog **247** was obtained in 94 % yield and 91% ee from **244** with 95% ee (directly after cyclopropanation), then recrystallization in pentane gave the enantiopure compound **247**. The rest of the synthesis for the desired *S*-2-Cl-5-CF₃TPCP-ligand **246** with TIPS-ethynyl at site **B** was straight forward with the same Sonogashira coupling and hydrolysis conditions used for its Rh₂(*S*-*o*-CITPCP)₄ analog.

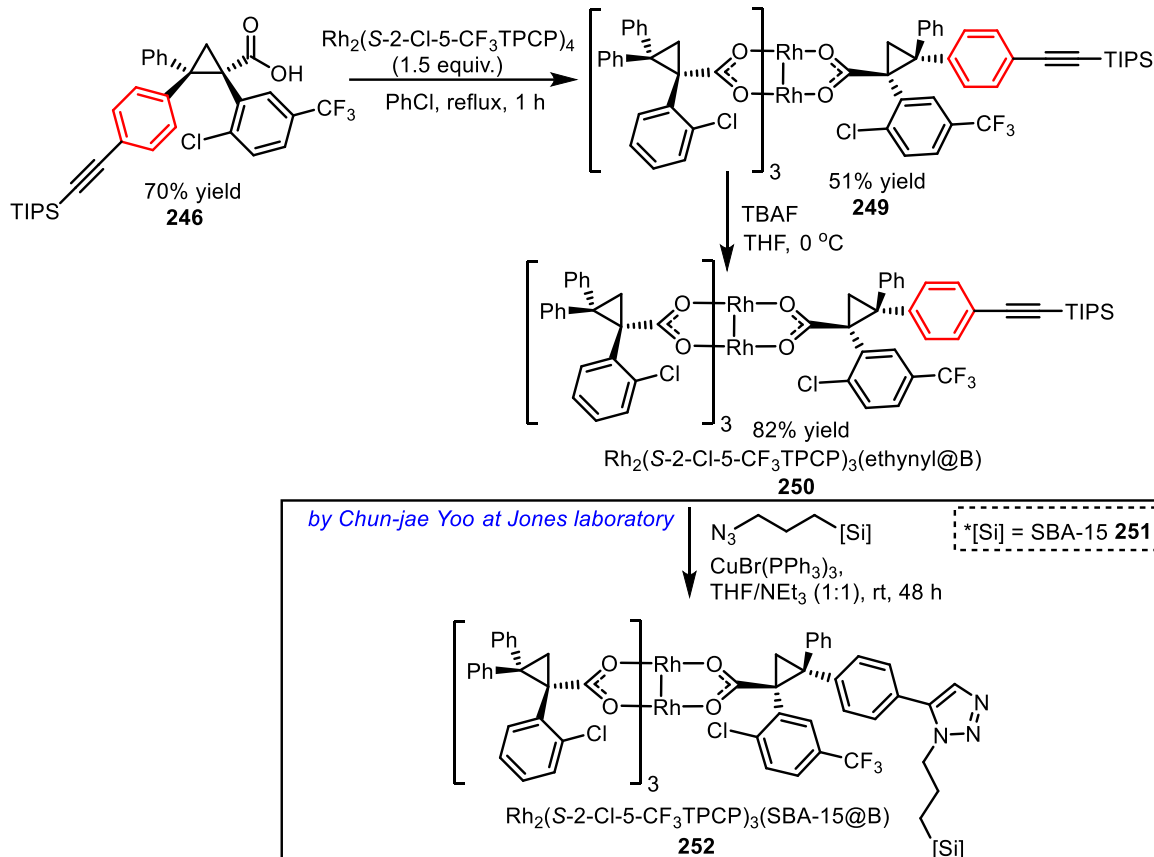
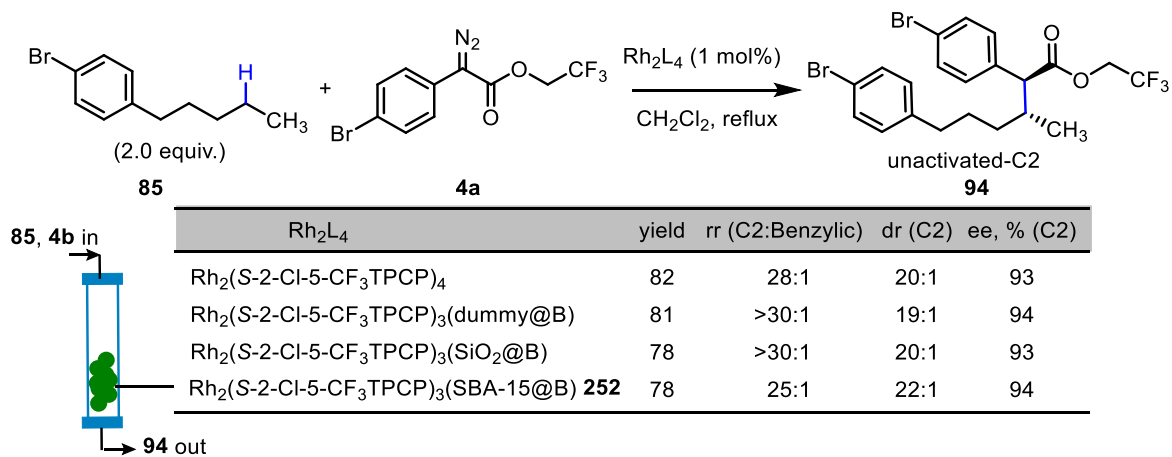
Scheme 4.11 Synthesis of *S*-2-Cl-5-CF₃TPCP-ligand with TIPS-ethynyl at **B**



With the desired ligand **246** in hand, the mono-ligand exchange reaction was conducted with slight modification and the $\text{Rh}_2(\text{S-2-Cl-5-CF}_3\text{TPCP})_3(\text{ethynyl@B})$ was generated after TIPS cleavage (Scheme 4.12). The reaction conditions for ligand exchange here were changed to 1 hour under refluxing chlorobenzene, since the previous condition in benzene resulted in no reaction, possibly due to the potentially more rigid ligand framework with fluoride-induced interaction. After TIPS deprotection to reveal the free ethynyl group, $\text{Rh}_2(\text{S-2-Cl-5-CF}_3\text{TPCP})_3(\text{ethynyl@B})$ **250** was obtained in 42% overall yield from the ligand **246** (2 steps). During the time I worked on these synthesis, Dr. Yoo tested the effect of three different silica supports (conventional silica powder, SBA-15 with longer and shorter pore length) with $\text{Rh}_2(\text{S-}o\text{-Cl-TPCP})_3(\text{ethynyl@B})$ **192** and decided to go with the platelet SBA-15 (shorter length) due to more efficient catalyst-substrate interaction. Therefore, Dr. Yoo conducted the click reaction between the $\text{Rh}_2(\text{S-2-Cl-5-CF}_3\text{TPCP})_3(\text{ethynyl@B})$ **250** and platelet SBA-15-supported azide for immobilized catalyst, $\text{Rh}_2(\text{S-2-Cl-5-CF}_3\text{TPCP})_3(\text{SBA-15@B})$ **252**.

The resulting $\text{Rh}_2(\text{S-2-Cl-5-CF}_3\text{TPCP})_3(\text{dummy@B})$ and $\text{Rh}_2(\text{S-2-Cl-5-CF}_3\text{TPCP})_3(\text{SiO}_2\text{@B})$ were tested on the reference reaction by me, and the silica-supported $\text{Rh}_2(\text{S-2-Cl-5-CF}_3\text{TPCP})_4$ **252** was tested in flow by Dr. Yoo after packing it in a small cartridge (Table 4.10). The performance of these immobilized $\text{Rh}_2(\text{S-2-Cl-5-CF}_3\text{TPCP})_4$ in flow reactor was comparable to its original homogenous catalyst with site-, diastereoselectivity and enantioselectivity remained at the same level.

Further examination with broader substrate scope and recyclability of the immobilized catalysts is still on-going by Taylor Hatridge, a new graduate student in the Jones group.

Scheme 4.12 Synthesis of $\text{Rh}_2(\text{S-2-Cl-5-CF}_3\text{TPCP})_3(\text{ethynyl@B})$ and immobilization**Table 4.10** Testing of immobilized catalyst in C–H insertion on 4-bromopentylbenzene

4.3 Conclusion

These studies provided a new pathway for the design and synthesis of the immobilized $\text{Rh}_2(\text{TPCP})_4$ catalysts, including the exploration on the effect of anchor site for the linker connection. The silica-supported $\text{Rh}_2(\text{S-}p\text{-BrTPCP})_4$ was synthesized and embedded in the polymer matrix wall of the hollow fiber reaction, which produced comparable performance with the original homogenous catalyst with good recyclability. In the system of $\text{Rh}_2(\text{S-}o\text{-ClTPCP})_4$ immobilization, influence of having the linker on either ring **A**, **B** and **C** were examined, and found the reactivity and selectivity dropped slightly only when the linker was at the active pocket (**A**). With the need of using the optimal catalyst in $\text{Rh}_2(\text{S-}o\text{-ClTPCP})_4$ series, $\text{Rh}_2(\text{S-}2\text{-Cl-5-CF}_3\text{TPCP})_4$ was developed and its immobilization was achieved with promising result in the initial examination in flow.

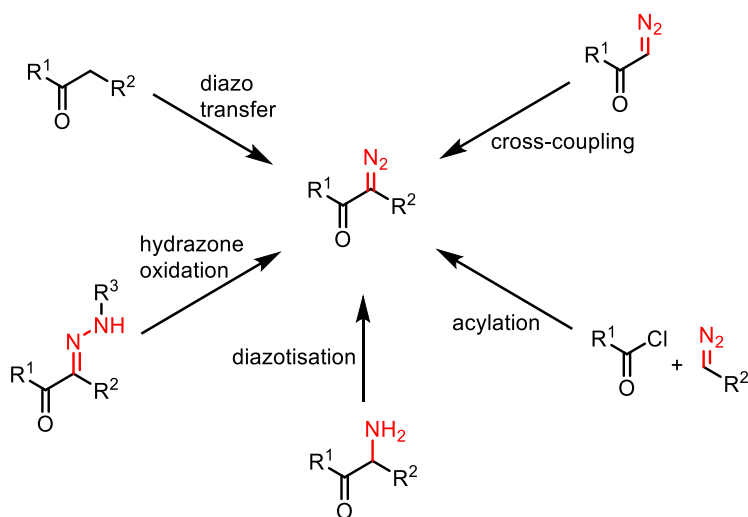
Chapter 5. Oxidation of Hydrazones for Diazo Synthesis with Oxygen as Terminal Oxidant

5.1 Introduction

5.1.1 Overview of Diazo Synthesis

Diazo compounds are not only key reagents in the rhodium carbene chemistry discussed in previous chapters, but also widely used in various other transformations. Some of the commonly used methods for the synthesis of these α -diazocarbonyl compounds include diazo transfer, hydrazone oxidation, diazotization, acylation and cross-coupling (Scheme 5.1).¹⁷⁶ These methods have different advantages and limitations that they are sometimes complementary to each other under specific circumstances.

Scheme 5.1 Common approaches for α -diazocarbonyl compounds synthesis



The most widely used approach for diazo synthesis is the diazo transfer, or known as *Regitz* diazo transfer, using sulfonyl azides and suitable bases. This transformation is initiated by the deprotonation of protons adjacent to a carbonyl group with a base and the resulting enolate anion reacts with the nitrogen at the end of a sulfonyl azide. These sulfonyl azides, including tosyl azide (TsN_3), mesyl azide (MsN_3), 4-acetamidobenzenesulfonyl azide (*p*-ABSA) and *o*-

nitrobenzenesulfonyl azide (*o*-NBSA), are also called diazo transfer reagents. α -Diazocarbonyl compounds are also commonly generated from oxidation of hydrazones, which are obtained via condensation of corresponding aldehyde/ketone with hydrazines. This method was first developed by Bamford and Stevens¹⁷⁷ and later modified by several other chemists, which will be discussed in the next section. Aliphatic amines can be converted to diazo compounds via diazotization using nitrosating reagents, such as sodium nitrite/hydrogen chloride, but the scope is limited to electron-deficient amines.³¹ Acylation and cross-coupling conditions have also been applied in the diazo synthesis by further modifying a diazo compound with additional substituents, including the *Arndt-Eistert* reaction and palladium-catalyzed C–C coupling.^{178, 179}

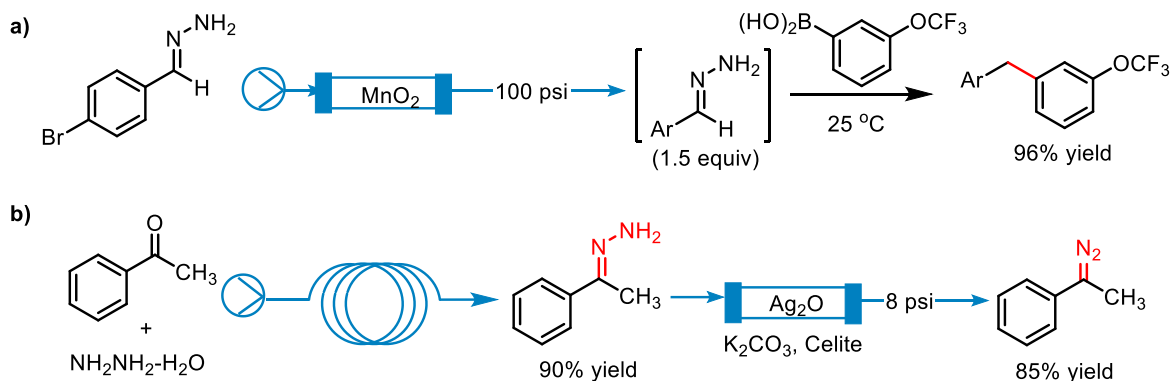
5.1.2 Hydrazone Oxidation for Diazo Synthesis

Due to the stability of the tosylhydrazones and simple hydrazones, thermal decomposition or dehydrogenation (*Bamford-Stevens* reaction) of these compounds are considered as a safe alternative method for diazo synthesis. Oxidation of simple hydrazones would be more attractive in terms of atom economy, with only two hydrogen atoms needing to be removed for the diazo compounds to be formed.

In the oxidation of hydrazones, metal oxides are usually used as oxidant, especially with electron-rich substrates with alkyl or aryl groups as substituents adjacent to the nitrogen-bound carbon. One of the earliest examples is the use of yellow mercuric oxide (HgO) for preparation of 2-diazopropane by Staudinger and Gaule in 1916.¹⁸⁰ This transformation was later improved by Whiting *et. al.* with additional catalytic amount of base, such as potassium hydroxide, for better reproducibility.¹⁸¹ Other metal oxides, such as Ag₂O¹⁸², MnO₂^{74, 183, 184} and Ni₂O₃,¹⁸⁵ were also

explored, resulting in more efficient and transformations. Some of the transformations were converted to the flow system with packed solid metal oxides in the cartridge. Their efficiency was further enhanced with continuous removal of the generated diazo compounds, which are unstable thus were reacted directly afterwards with coupling partners. The Ley group showed this advantage by using MnO_2 as an oxidant for generating unstable mono-substituted diazo intermediates in flow, followed by sp^2 - sp^3 cross-coupling reactions at room temperature, and up to 96% yield in two steps were obtained demonstrating the effectiveness of this approach (Scheme 5.2a).¹⁸⁶ Similarly, the Charette group developed a safe and facile flow system for the preparation of numerous diazoalkanes using a Ag_2O column (Scheme 5.2b).¹⁸⁷ In addition, $\text{Pb}(\text{OAc})_4$ was also applied as an oxidant with advantage for the preparation and separation of those sensitive diazo compounds.¹⁸⁸

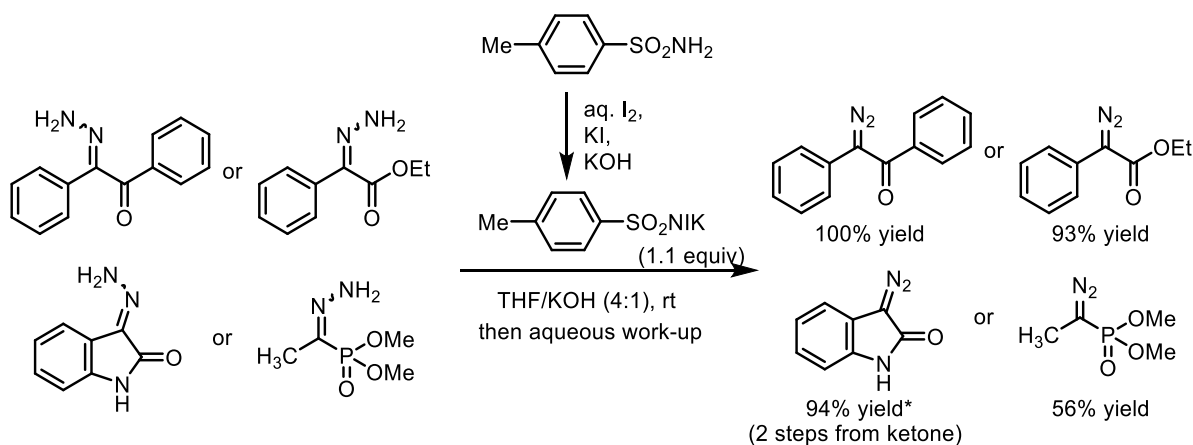
Scheme 5.2 Metal oxide as oxidant for hydrazone oxidation in flow



Non-metal oxidants were also explored for hydrazone oxidation, in which hazardous metal waste could be avoided. Iodine-based oxidants were one of the common alternatives used here. Generation of diazoketones were observed when the benzil hydrazones were treated under electrolytic oxidation condition in the presence of KI, but they were decomposed quickly following the Wolff rearrangement.¹⁸⁹ Similarly, *o*-iodoxybenzoic acid (IBX) was also used in the oxidation

of hydrazones by Nicolaou *et. al.* and resulted in the corresponding diazoketones or azines.¹⁹⁰ More recently, the Moody group developed an efficient system with easy purification method for the preparation of diazo compounds using *N*-iodo-*p*-toluenesulfonamide (TsNIK) and potassium hydroxide as base (Scheme 5.3).¹⁹¹ A wide range of diazo compounds were generated with high yields, including α -diazooesters, α -diazouamides, α -diazoketones and α -diazophosphonates. The active TsNIK was immobilized on polystyrene-resin support (PS-TsNIK) for effective diazo compounds generation in flow, followed by heteroatom alkylation¹⁹² or dirhodium carbene insertion.¹⁷¹ The TsNIK oxidant could be regenerated by molecular iodine. Moreover, similar to the Swern oxidation condition, chlorodimethylsulfonium chloride generated from DMSO activation was also applied in oxidation for diazoalkanes.¹⁹³

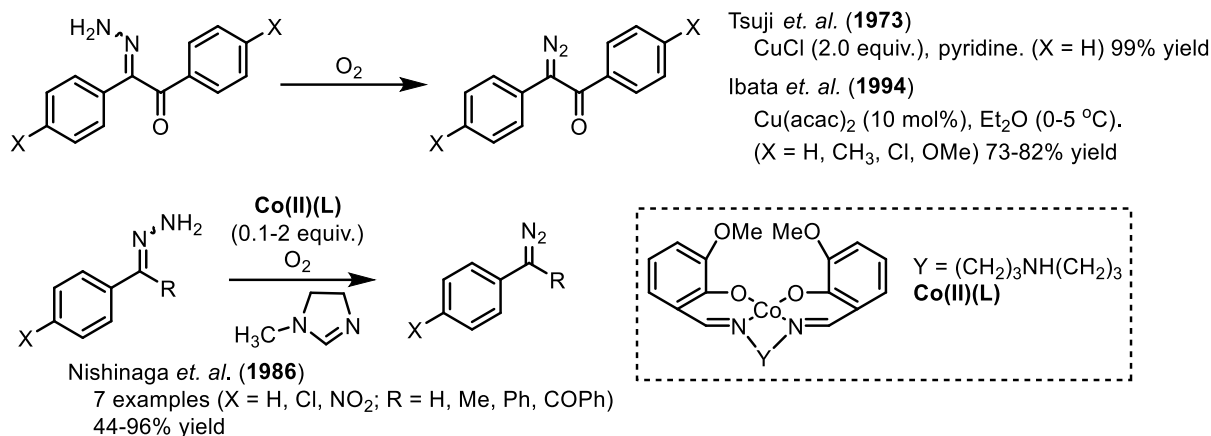
Scheme 5.3 Oxidation of hydrazones using TsNIK



Molecular oxygen or air would be a much more environmental-friendly and sustainable oxidant, but only limited examples have showed its possibility in hydrazone oxidation (Scheme 5.4). In 1973, Tsuji and co-workers observed the generation of benzil diazo compound by treating the corresponding hydrazone with 2 equiv of CuCl under oxygen atmosphere.¹⁹⁴ Later, catalytic amount (10 mol%) of the metal complexes, such as Cu(acac)₂¹⁹⁵ and Co(II)(L)¹⁹⁶ were successfully

applied in the donor-donor diazo compounds synthesis from hydrazones. However, limited substrate scopes were shown in these examples.

Scheme 5.4 Oxygen as terminal oxidant for hydrazone decomposition



5.2 Results and Discussion

Although the generation of diazo compounds has been achieved in flow using the cartridge with Ag₂O,¹⁸⁷ MnO₂¹⁸⁶ or PS-TSNIK.^{171, 192} The possibility of utilizing oxygen as the terminal oxidant with solid-supported catalyst in cartridge for hydrazone oxidation is still worth exploration as the next evolution for flow oxidation of hydrazones. In such proposed system, environmental-friendly H₂O would be the main byproduct generated and the cartridge could be reused ideally as long as the catalyst is active. Inspired by the previous work where copper salts were used together with molecular oxygen as the oxidant for hydrazone oxidation, cheap copper salts are proposed to be used here as catalysts. Moreover, since most of the copper salts have limited mobility in solvent-wet regular silica, silica powder was proposed as solid phase for trapping copper catalysts in the cartridge and was included in the investigation.

The initial screening for copper salts was conducted using the hydrazone **211**, which should lead to the standard 2,2,2-trichloroethyl 2-(4-bromophenyl)-2-diazoacetate **4b** after oxidation, as reference substrate (Table 5.1). Copper (0) powder gave no conversion and full recovery of the hydrazone starting material was obtained. The same observation was found with copper (I) iodide, copper (I) bromide, copper (II) bromide and copper (I) oxide. Interestingly, the triflate salts of both copper (I) and (II) resulted in hydrazone decomposition with the copper (I) triflate having the least starting material left. However, triflate salts are also active for the decomposition of the generated diazo compound **4b** and only over-reacted byproducts were observed in the crude ¹H-NMR. The ketone byproduct **253** could be generated from carbene reacting with oxygen or H₂O followed by oxidation, while the azine dimer **254** and N–H insertion product **255** were generated by reacting the carbene with another equivalent of diazo compound or hydrazone molecule. We then decided to examine copper (II) acetate, which would be expected to be less efficient in diazo decomposition because the copper would be less electron deficient. Indeed, under these conditions the desired donor/acceptor diazo compound **4b** was formed in 26% yield with 44% recovery of the hydrazone **211**. Hence, Cu(OAc)₂ was considered as the best catalyst for further optimization in this system.

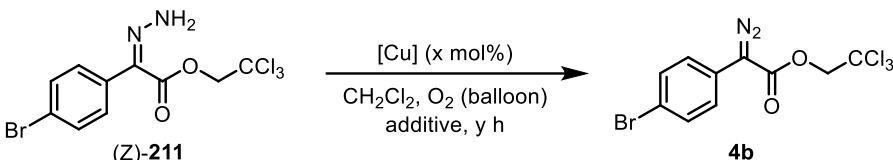
Table 5.1 Copper source screening for hydrazone oxidation

Entry	[Cu]	211 recovered, %	4b : 253 : 254 : 255	isolated 4b yield, %
1	Cu ⁰ powder	100	--	0
2	Cu ^I	100	--	0
3	Cu ^I ₂ O	100	--	0
4	Cu ^I Br	100	--	0
5	Cu ^I (CF ₃ SO ₃)	4	--:1:--:1.4	0
6	Cu ^{II} Br	100	--	0
7	Cu ^{II} (CF ₃ SO ₃) ₂	88	--:1.4:1:--	0
8	Cu^{II}(OAc)₂	44	5.2:1:1.6:3.4	26

* For a scale of 0.5 mmol hydrazone with 5 mL CH₂Cl₂, 100 mg silica was used.

Notably, dichloromethane was used as solvent without modification since it is the optimal solvent for most of rhodium carbene reactions recently developed in the Davies group. Additionally, since the hydrazone oxidation would be coupled to rhodium carbene reactions, the solvents would ideally be the same for one continuous process run in flow.

Further optimization on the reaction conditions in terms of the catalyst loading and additives were then explored (Table 5.2). Diazo compound **4b** was generated in slightly higher yield with shorter reaction time (32% in 1 h vs. 26% in 3 h), so 1-hour reaction times were used for further optimization. Moreover, similar yields were observed between reactions having the hydrazone solution added in 1-pot versus dropwise, and the dropwise addition resulted in higher recovery of the starting material, which implied less consumption for byproducts. As expected, additional H₂O inhibited the transformation (entry 4) and enhanced conversion was detected with higher catalyst loading (entry 5). Using cheaper copper (II) acetate with monohydrate was found to give slightly lower yield with greater amount of starting material recovery, presumably because it is less reactive in both hydrazone oxidation and carbene generation, which could be advantageous here. Noticeably, removal of the silica in the system resulted in similar performance, implying that silica was not influencing the hydrazone oxidation but may be tricky for acid sensitive diazo compounds with its inherent acidity. With this reason and the inspiration of the *Bamford-Stevens* reaction, in which base was used to promote the reaction, weak base such as triethyl amine was added as additive to this system. Impressively, full conversion of the hydrazone was observed with 80% isolated yield of the desired diazo compound **4b**. Further modification using pyridine instead of triethylamine led to the highest yield of **4b** (92% in entry 9).

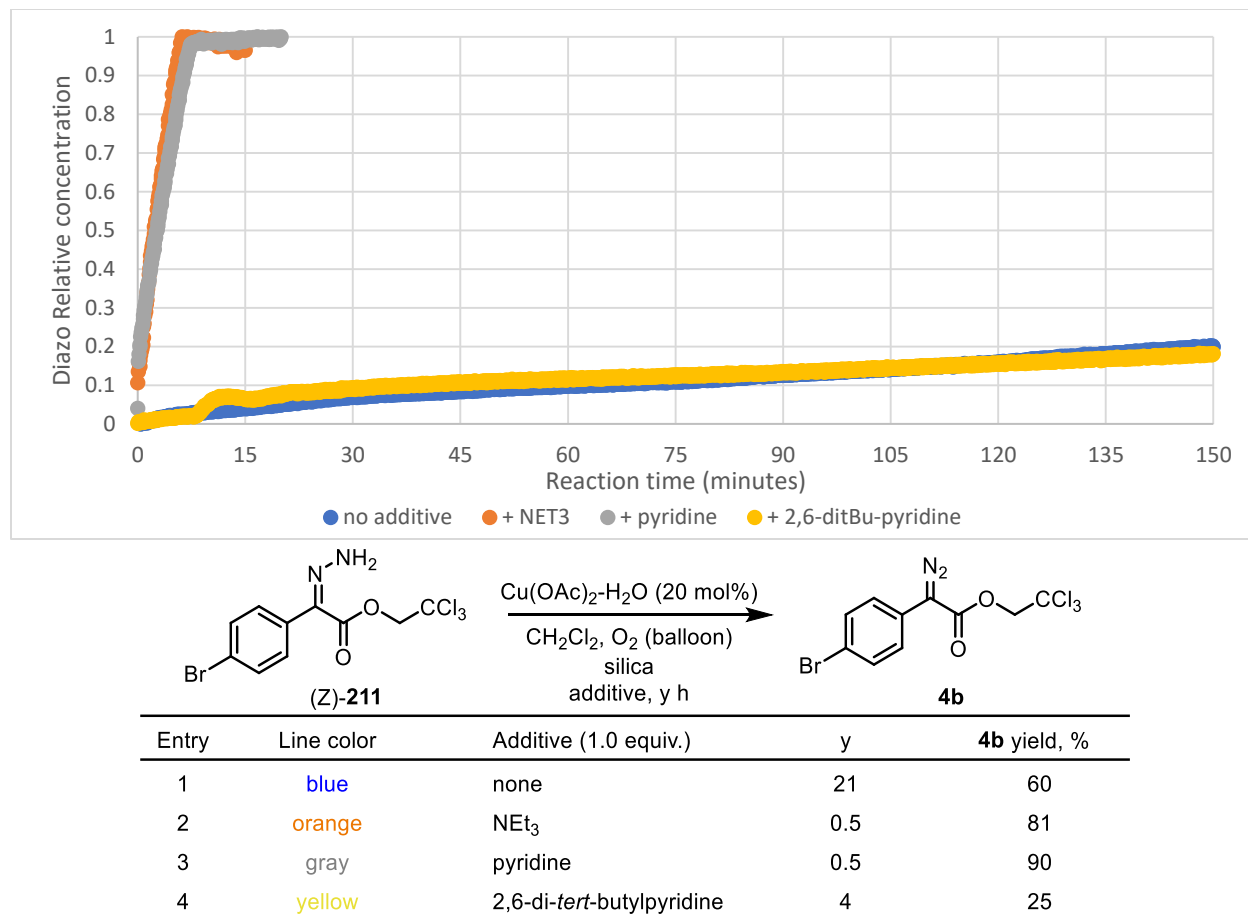
Table 5.2 Further optimization for Cu(OAc)₂-catalyzed hydrazone oxidation


Entry	[Cu]	x	y	Additive	211 recovered, %	4b yield, %
1	Cu(OAc) ₂	20	3	silica	44	26
2	Cu(OAc) ₂	20	1	silica	38	32
3 ^b	Cu(OAc) ₂	20	1	silica	49	30
4	Cu(OAc) ₂	20	1	silica, 0.1 mL H ₂ O	98	trace
5	Cu(OAc) ₂	100	1	silica	16	43
6	Cu(OAc) ₂ -H ₂ O	20	1	silica	63	26
7	Cu(OAc) ₂ -H ₂ O	20	1	none	78	21
8	Cu(OAc) ₂ -H ₂ O	20	1	silica, 1.0 eq. NEt ₃	--	80
9	Cu(OAc)₂-H₂O	20	1	silica, 1.0 eq. pyridine	3	92

^a For a scale of 0.5 mmol hydrazone with 5 mL CH₂Cl₂, 100 mg silica was used.

^b Hydrazone was added dropwise instead of 1-pot addition.

In order to have a better understanding of the reaction time with base additive, React-IR was applied to monitor the generation of diazo compound **4b** basing on the N≡N absorption band at ~2100 cm⁻¹ (Figure 5.1). Assuming the concentration of diazo compound when the hydrazone is fully consumed as relative concentration 1, the reactions with triethylamine and pyridine as additives were finished within 10 min. Interestingly, without additive, the generation of diazo **4b** was steady with a nearly constant rate, and 60% yield was obtained after removal of the copper salt via short silica plug. On the other hand, the bulky base, 2,6-di-*tert*-butylpyridine, showed the same performance as no additive with no accelerating effect on the reaction. 2,6-Di-*tert*-butylpyridine was basic as proton acceptor, but the two *tert*-butyl substituents limited the coordinating ability of the nitrogen atom of the pyridine ring with other large metal atoms.



* For a scale of 1.5 mmol hydrazone with 15 mL CH₂Cl₂, 300 mg silica was used.

Figure 5.1 React-IR studies on diazo generation from hydrazone oxidation

At this stage it is unclear why the pyridine and triethylamine bases have such a positive influence on the reaction. Possibly the nitrogen containing bases are coordinating to the copper (II) metal center to form better catalysts for more efficient hydrazone oxidation. Alternatively, it may be the bases induce a radical process that may enhance the rate of the reaction. The acceleration in the rate of the reaction was also possibly caused by the homogenous feature of the copper (II) catalyst after addition of triethylamine or pyridine. Cu(OAc)₂ is heterogenous (insoluble) in the reaction system (dichloromethane as solvent) without additive. After mixing the Cu(OAc)₂·H₂O with pyridine in dichloromethane for 1 h, the filtrate was obtained from a simple filtration with cotton, which was found to be able to convert hydrazone **211** into **4b** in 82% yield in 30 min. This

observation indicates the homogenous feature of the catalytic transformation. Further studies will be needed to determine a definitive answer for the remarkable rate enhancement caused by the amine bases.

Further modification of the reaction conditions were examined with emphasis on lowering the catalyst and additive loading, as well as exploring the use of air instead to pure oxygen in balloon as the terminal oxidant (Table 5.3). Entry 1 is the same reaction as entry 9 in Table 5.2 with 20 mol% loading of the copper catalyst and 1.0 equiv of the pyridine additive. Lowering the catalyst loading to 10 mol% showed no influence on the yield of **4b**. Considering the reasonable price of the copper acetate monohydrate and unknown TON, no further testing was conducted with even lower catalyst loading. Next, decreased loading of the pyridine additive was explored with 0.5% pyridine in dichloromethane as solvent, which could be also taken as 0.6 equiv loading, and slight improvement in the yield was detected even after repeating it twice (entry 3, 95% on average). The reaction conditions used for entry 3 (Table 5.3) are considered as the optimal conditions with oxygen balloon for further examination on reaction scope. Replacing the oxygen balloon with an air balloon resulted in lower efficiency with significant decrease in yield (28% with air vs. 92% with oxygen), presumably due to the low concentration of the oxygen in air. Interestingly, high yield was restored when the reaction was conducted open to air with 0.5% pyridine in dichloromethane as solvent (94% on average), and is was marked as the optimal conditions for reaction using air as the oxidant. Moreover, in both cases of oxygen and air, reactions without silica gave lower yields (entry 4 and 8) and may be caused by the balance between acidic silica and basic pyridine that relates to the stability of the diazo compounds. Therefore, the optimal reaction condition for the desire hydrazone oxidation is 10 mol% of $\text{Cu}(\text{OAc})_2\cdot\text{H}_2\text{O}$ with 200 mg/mmol silica in 0.5% pyridine in dichloromethane under oxygen atmosphere or open to air.

Table 5.3 Continuous modification on loading and usage of air

Entry	O ₂ source	x	z loading	4b yield, %
1	O ₂ balloon	20	1.0 equiv.	92
2	O ₂ balloon	10	1.0 equiv.	92
3	O₂ balloon	10	0.6 equiv. (0.5% in solvent)	95^b
4 ^c	O ₂ balloon	10	0.6 equiv. (0.5% in solvent)	84
5	air balloon	10	1.0 equiv.	28 ^d
6	open air	10	1.0 equiv.	89
7	open air	10	0.6 equiv. (0.5% in solvent)	94^b
8 ^c	open air	10	0.6 equiv. (0.5% in solvent)	79

^a For a scale of 0.5 mmol hydrazone with 5 mL CH₂Cl₂, 100 mg silica was used.

^b Average of three runs. ^c No silica added. ^d 60% recovery of **211**.

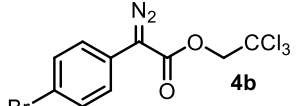
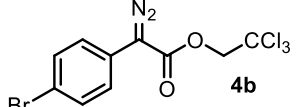
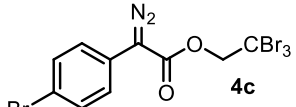
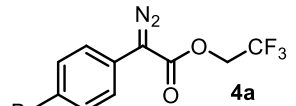
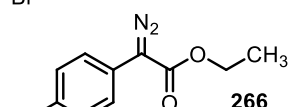
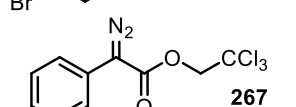
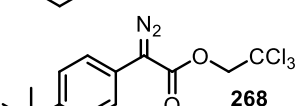
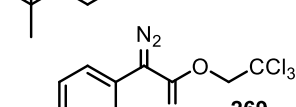
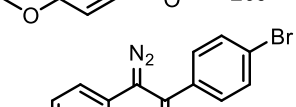
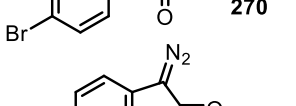
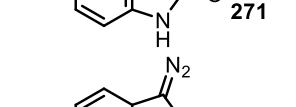
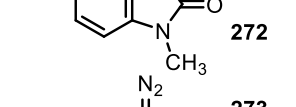
With the optimal conditions for oxidizing the hydrazone **211** in hand, a broader range of substrates was explored (Scheme 5.5). Firstly, although the *Z* conformer of hydrazone **211** was generated as the dominant isomer, the *E* conformer was isolated and examined in the optimal conditions and 96% isolated yields were obtained for reactions using oxygen balloon and open air, which are comparable to the results with *Z* conformer. Hence, the examination of other substrates was conducted on mixture of *E* and *Z* conformers without separation. Efficient hydrazone oxidation was maintained with variation on the ester moiety, and only slightly lowered yield was observed for tribromoethyl derivative **4c**. When the aryl moiety was substituted with electron-donating groups or no substituent, which showed efficient transformation with PS-TsNIK as oxidant,¹⁷¹ 94-97% yield was achieved in this Cu(OAc)₂-catalyzed reaction with oxygen as terminal oxidant. Less satisfactory yield (88%) was obtained with the methoxy substituted derivative **261** when the reaction was conducted open to the air, presumably due to the side reactions between the generated diazo compound **269** and components in air. Diazoketones could also be generated effectively using this method, and small modification on the reaction condition

(reaction in dark with higher loading of basic pyridine additive) was applied to minimize the decomposition of the unstable diazoketone **270** via Wolff rearrangement. Furthermore, isatin hydrazones were converted to the corresponding diazoamides **271** and **272** quantitatively with the insoluble hydrazones added in 1-pot as a solid. However, electron-rich derivatives, such as the (diphenylmethylene)hydrazone, failed to be oxidized to the corresponding donor/donor diazo compounds and instead, gave full recovery of the hydrazone starting material. In most cases, the diazo compounds were obtained in high purity after simple silica plug work-up, though column chromatography was still conducted for isolated yields.

5.3 Conclusion

A new method for dehydrogenation of hydrazones to the corresponding donor/acceptor diazo compounds was developed using oxygen as the terminal oxidant and low-cost copper acetate monohydrate as catalyst. React-IR studies showed significant acceleration of the reaction when pyridine was used as an additive. This method is effective for the preparation of relative stable diazo compounds such as diazoesters, diazoketones and diazoamides in high yields. Further expansion of the scope and attempt for flow reaction set-up are under investigation.

Scheme 5.5 Substrates scope for Cu(OAc)₂-catalyzed hydrazone oxidation

$\begin{array}{c} \text{N} \\ \parallel \\ \text{R}^1\text{C}=\text{C}\text{R}^2 \\ \text{NH}_2 \end{array}$ 211, 256-265		$\xrightarrow[\text{O}_2 \text{ source, silica}^a, 1 \text{ h}]{\text{Cu(OAc)}_2\text{-H}_2\text{O (x mol\%)} \\ \text{0.5\% pyridine in CH}_2\text{Cl}_2}$	$\begin{array}{c} \text{N}_2 \\ \parallel \\ \text{R}^1\text{C}=\text{C}\text{R}^2 \end{array}$ 4a-c, 266-273	
product	Z:E (hydrazone)	yield, % (w/ O ₂ balloon)	yield, % (open air)	
 4b	all Z	95	94	
 4b	all E	96	96	
 4c	all Z	91	89	
 4a	all Z	98	97	
 266	1:1	95	93	
 267	all Z	95	95	
 268	all Z	97	96	
 269	all Z	94	88	
 270	all Z	92 ^b	--	
 271	2:1	99	98	
 272	17:1	98	98	
 273	N/A	trace ^c	--	

^a For a scale of 0.5 mmol hydrazone with 5 mL CH₂Cl₂, 100 mg silica was used. ^b 2% pyridine in CH₂Cl₂ was used and the reaction was conducted in dark. ^c 96% starting material recovered.

Experimental Part

6.1 General Considerations and Reagents

All solvents used in the reactions were purified and dried by a *Glass Contour Solvent System* unless otherwise stated. The dichloromethane used for the C–H Functionalization was dried over activated 4 Å molecular sieves for more than 24 h after degassed at reflux for 1 h under argon, then stored with activated 4 Å molecular sieves under argon atmosphere and was used directly. Technical grade solvents were used for work-up and flash column chromatography.

^1H and ^{13}C NMR spectra were recorded at 600 MHz (^{13}C at 150 MHz) on Bruker-600 spectrometer or INOVA-600 spectrometer, or 500 MHz (^{13}C at 126 MHz) on INOVA-500 spectrometer. ^{19}F NMR spectra were recorded at 283 MHz on Mercury-300 or 377 MHz on Inova-400. NMR spectra were run in solutions of CDCl_3 , $(\text{CD}_3)_2\text{CO}$ or C_6D_6 with residual protonated solvent as internal standard (7.26 ppm for ^1H and 77.16 ppm for ^{13}C in CDCl_3 , 7.16 ppm for ^1H in C_6D_6 , 2.05 ppm for ^1H in $(\text{CD}_3)_2\text{CO}$), and were reported in parts per million (ppm). Abbreviations for signal multiplicity are as follow: s = singlet, d = doublet, t = triplet, q = quartet, m = multiplet, dd = doublet of doublet, etc. Coupling constants (J) in Hz were calculated directly from the spectra.

Thin layer chromatographic (TLC) analysis was performed on Merck silica gel 60 F254 aluminum-sheet TLC plates, visualizing with UV light and/or staining with aqueous KMnO_4 stain. IR spectra were collected on a Nicolet iS10 FT-IR spectrometer. Optical rotations were measured on Jasco P-2000 polarimeters. Melting points (mp) were measured in open capillary tubes with a Mel-Temp Electrothermal melting points apparatus and are uncorrected. Mass spectra were taken on a Thermo Finnigan LTQ-FTMS spectrometer with APCI, ESI or NSI by the Department of Chemistry at Emory University.

Analytical enantioselective chromatographs were measured on either Varian Prostar instrument or Agilent-1100 series instrument, and isopropanol/hexane were used as gradient. Chiral HPLC conditions were determined by obtaining separation of the racemic products generated using $\text{Rh}_2(R/S\text{-DOSP})_4$ or 1:1 (*R:S*) mixture optimal catalysts.

In situ IR monitoring experiments were carried out with a Mettler Toledo ReactIR 45m instrument equipped with a 9.5 mm x 12'' AgX 1.5 m SiComp probe.

The following compounds were commercially available and used directly (unless otherwise stated):

1,1-diphenylethylene, methyl 2-(2-chlorophenyl)acetate, 1,8-diazabicyclo[5.4.0]undec-7-ene (DBU), 2-(2-bromophenyl)acetic acid, 2-(2-iodophenyl)acetic acid, acetyl chloride, potassium trimethylsilanolate (heated under vacuum before use for anhydrous powder), potassium *tert*-butoxide, potassium carbonate, $\text{Rh}_2(\text{OAc})_4$, styrene (pushed through a silica-filled pipette prior to use), *p*-cymene, 1-ethyl-4-methylbenzene, cyclohexane, 1-bromo-4-ethylbenzene, 2-(4-bromo-2-chlorophenyl)acetic acid, 2-(5-bromo-2-chlorophenyl)acetic acid, 2,2,2-trichloroethan-1-ol, zinc dust, 1-ethyl-4-methoxybenzene, methyl 2-(3,4-dimethylphenyl)acetate, 1,2,3,4-tetrahydronaphthalene, 6-methoxy-1,2,3,4-tetrahydronaphthalene, 1,3-dihydroisobenzofuran, pentylbenzene, 1-bromo-4-pentylbenzene, hexafluoro-2-propanol, perfluoro-*tert*-butanol, 1,1,1-trifluoro-2-methylpropan-2-ol, 1,1,1,3,3,3-hexafluoro-2-methylpropan-2-ol, 2,2,2-trifluoroethan-1-ol, 2,2,2-trifluoroacetic acid, 1-bromo-4-decylbenzene, 1-bromo-4-hexylbenzene, 1-bromo-4-butylbenzene, 1-bromo-4-propylbenzene, $\text{Ni}(\text{dppp})\text{Cl}_2$, *N*-bromosuccinimide, 4-pentylbenzoic acid, 4-*n*-pentylphenol, 2-bromopentane, 4-methoxyphenylmagnesium bromide (0.5 M in THF),

CoCl₂, tetramethylethylenediamine (TMEDA) pentylmagnesium bromide solution (2.0 M in diethyl ether), 3-bromothiophene; di-*tert*-butylpyrocarbonate, hexanal, di-*iso*-butylaluminum hydride (DIBAL-H), methyl (triphenylphosphoranylidene)acetate, 4-*tert*-butyliodobenzene, 1-iodo-4-nitrobenzene, triphenylphosphine, 1-iodo-4-pentylbenzene, silver carbonate, 4-dimethylaminopyridine (DMAP), 3-bromofuran, *N,N'*-dicyclohexylcarbodiimide, Pd(PPh₃)₄, Ni(dppf)Cl₂, Pd(PPh₃)₂Cl₂, 4-pentylacetophenone, potassium phosphate tribasic, triethylamine, pentan-1-amine, di-*tert*-butyl dicarbonate, methyl trans-2-octenoate, tetrabutylammonium fluoride solution (TBAF, 1.0 M in THF), *N*-bromosuccinimide (NBS), (4-(*tert*-butyl)phenyl)boronic acid, (4-methoxy-3,5-dimethylphenyl)boronic acid, (4-(dimethylamino)phenyl)boronic acid, (3,5-dimethylphenyl)boronic acid, (3,5-bis(trifluoromethyl)phenyl)boronic acid, phenylboronic acid, mesitylboronic acid, *tert*-butyl 3,4-dihydropyridine-1(2*H*)-carboxylate, ethynyltriisopropylsilane, copper(I) iodide, copper(0) powder, copper(I) bromide, copper(II) bromide, copper(I) oxide, copper(I) triflate, copper(II) triflate, copper(II) acetate, copper(II) acetate monohydrate, (4-bromophenyl)(phenyl)methanone, 2-(2-chloro-5-(trifluoromethyl)phenyl)acetic acid, dimethyl sulfate, pyridine (anhydrous), 2,6-di-*tert*-butylpyridine, (diphenylmethylene)hydrazine.

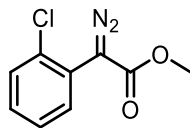
The following compounds were prepared by procedures adapted from literatures and confirmed with ¹H NMR:

p-Acetamidobenzenesulfonyl azide (*p*-ABSA),¹⁹⁷ *o*-nitrobenzenesulfonyl azide (*o*-NBSA),¹⁹⁸ Rh₂(PTAD)₄,⁷¹ Rh₂(TCPTAD)₄,⁷² Rh₂(PTTL)₄,¹⁹⁹ Rh₂(TPPTTL)₄,⁷⁷ Rh₂(*p*-BrTPCP)₄,⁷⁸ Rh₂(*p*-PhTPCP)₄,⁷⁹ Rh₂[3,5-di(*p*-¹BuC₆H₄)TPCP]₄,⁸¹ methyl 2-diazo-2-phenylacetate,⁶⁰ methyl 2-(4-bromophenyl)-2-diazoacetate,⁸⁰ methyl 2-(3-bromophenyl)-2-diazoacetate,⁶⁰ methyl 2-(3,4-dibromophenyl)-2-diazoacetate,²⁰⁰ methyl 2-(4-methylphenyl)-2-diazoacetate,⁶⁰ methyl 2-(3-

methylphenyl)-2-diazoacetate,²⁰¹ methyl 2-(4-methoxyphenyl)-2-diazoacetate,⁶⁰ methyl 2-(4-methoxyphenyl)-2-diazoacetate,²⁰¹ methyl 2-(3,4-dimethoxyphenyl)-2-diazoacetate,²⁰² methyl 2-diazo-2-(naphthalen-2-yl)acetate,²⁰³ methyl 2-diazo-2-(4-(trifluoromethyl)phenyl)acetate,⁶⁰ methyl 2-([1,1'-biphenyl]-4-yl)-2-diazoacetate,²⁰¹ 2,2,2-trichloroethyl 2-(4-bromophenyl)-2-diazoacetate,⁸⁰ 2,2,2-trifluoroethyl 2-(4-bromophenyl)-2-diazoacetate,²⁰⁴ 2,2,2-tribromoethyl 2-(4-bromophenyl)-2-diazoacetate,²⁰⁴ 2,2,2-trichloroethyl 2-diazoacetate,¹⁷⁹ 2,2,2-trichloroethyl 2-diazoacetate,²⁰⁵ 2,2,2-trifluoroethyl 2-(6-chloropyridin-3-yl)-2-diazoacetate,⁷⁶ 2,2,2-trifluoroethyl 2-(2-chloropyrimidin-5-yl)-2-diazoacetate,⁷⁶ 2,2,2-trifluoroethyl-2-diazo-2-(4-(trifluoromethyl)phenyl)acetate,⁷⁶ 2,2,2-trichloroethyl 2-diazo-2-phenylacetate,¹⁷⁹ 2,2,2-trichloroethyl 2-diazo-2-(4-(trifluoromethyl)phenyl)acetate,¹⁷⁹ 2,2,2-trichloroethyl 2-(6-chloropyridin-3-yl)-2-diazoacetate,¹⁷⁹ 2,2,2-trichloroethyl 2-(4-acetoxyphenyl)-2-diazoacetate,¹⁷⁹ 4,4,5,5-tetramethyl-1,3-dioxolane,²⁰⁶ methyl (*E*)-oct-2-enoate,²⁰⁷ *tert*-butyl piperidine-1-carboxylate,²⁰⁸ 1-tosylpiperidine,²⁰⁸ 1-(4-Bromophenyl)-2-(piperidin-1-yl)ethane-1,2-dione,²⁰⁹ 2-(3,4-dibromophenyl)acetic acid,²¹⁰ 2,2,2-trichloroethyl (*Z*)-2-(4-bromophenyl)-2-hydrazonoacetate,¹⁷¹ 2,2,2-trichloroethyl (*E*)-2-(4-bromophenyl)-2-hydrazonoacetate,¹⁷¹ 2,2,2-trichloroethyl (*Z*)-2-hydrazono-2-phenylacetate,¹⁷¹ 2,2,2-trichloroethyl (*Z*)-2-(4-(*tert*-butyl)phenyl)-2-hydrazonoacetate,¹⁷¹ 2,2,2-trichloroethyl (*Z*)-2-hydrazono-2-(4-methoxyphenyl)acetate,¹⁷¹ (*E*) and (*Z*)-ethyl 2-(4-bromophenyl)-2-hydrazonoacetate,¹⁹¹ (*E*) and (*Z*)-3-hydrazonoindolin-2-one,¹⁹¹ (*E*) and (*Z*)-3-Hydrazono-1-methylindolin-2-one,¹⁹¹ (*Z*)-1,2-bis(4-bromophenyl)-2-hydrazineylideneethan-1-one,²¹¹ 2-(4-bromophenyl)-2-oxoacetic acid.²¹²

6.2 Experimental Part for Chapter 2

Catalysts Synthesis



Methyl 2-(2-chlorophenyl)-2-diazoacetate (11)

A dry 250 mL round-bottom flash was charged with methyl 2-(2-chlorophenyl)acetate (4.62 g, 25 mmol, 1.0 equiv) and *p*-ABSA (9.01 g, 37.5 mmol, 1.5 equiv). After the flask was flushed with argon gas (3 times), 40 mL of acetonitrile was added via syringes. Then, the reaction mixture was cooled to 0 °C via ice bath. DBU (7.5 mL, 50 mmol, 2.0 equiv) was then added into the solution dropwise, and it was stirred for 15 min under 0 °C before warmed up to room temperature (23 °C). The reaction mixture was then stirred for another 4 h monitored by TLC. The reaction mixture was then quenched with saturated aqueous NH₄Cl solution and extracted three times with diethyl ether. The combined organic layer was washed with deionized water to remove any residual salts and dried over Na₂SO₄. The crude mixture was concentrated under reduced pressure and purified by flash column chromatography (pentane/ether = 20/1) to provide yellow solid in 95% yield.

mp: 34-35 °C;

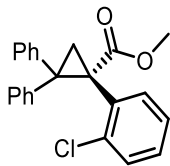
R_f = 0.45 (hexane/ethyl acetate = 9/1);

¹H NMR (400 MHz, CDCl₃) δ 7.54 (dd, *J* = 7.7, 1.9 Hz, 1H), 7.43 (dd, *J* = 7.9, 1.5 Hz, 1H), 7.33 (tdd, *J* = 7.7, 1.6, 0.5 Hz, 1H), 7.29 (ddd, *J* = 7.7, 1.8, 0.6 Hz, 1H), 3.85 (s, 3H);

¹³C NMR (100 MHz, CDCl₃) δ 165.9, 133.7, 132.3, 130.0, 129.6, 127.1, 123.8, 52.3 (The peak of the diazo carbon was not observed);

IR (neat) 2951, 2094, 1698, 1434 cm⁻¹;

FTMS (+p NSI) calcd for C₉H₈N₂O₂Cl (M+H)⁺ 211.0269 found 211.0268.



Methyl (S)-1-(2-chlorophenyl)-2,2-diphenylcyclopropane-1-carboxylate (14)

An oven-dried 50 mL round-bottom flask was charged with $\text{Rh}_2(\text{S-PTAD})_4$ (27.6 mg, 0.018 mmol, 0.5 mol%) and 1,1-diphenylethylene (3.10 mL, 17.5 mmol, 5.0 equiv). After the flask was flushed with argon gas (3 times), 8 mL of dry degassed pentane was added via syringe. Then, the reaction mixture was cooled to 0 °C via ice bath. Methyl 2-(2-chlorophenyl)-2-diazoacetate (737.2 mg, 3.5 mmol, 1.0 equiv) was weighted in a 20 mL scintillation vial and flushed with argon (3 times). The aryldiazo in the vial was dissolved in 9 mL of the dry degassed pentane and transferred into the flask with syringe pump over 2 h under 0 °C. Then, the reaction mixture was allowed to stir overnight. After monitored by TLC, the reaction mixture was concentrated under vacuum. The residue was purified by flash column chromatography (hexane/ethyl acetate = 100/1 to 50/1) to provide product as white solid in 84% yield.

mp: 112-114 °C; **R_f** = 0.51 (hexane/ethyl acetate = 9/1); **[α]²⁰_D:** -84.4° (c = 1.61, CHCl_3);

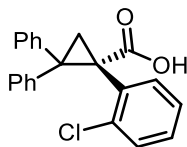
¹H NMR (400 MHz, CDCl_3) δ 7.54 (d, *J* = 7.3 Hz, 2H), 7.38 (t, *J* = 7.4 Hz, 2H), 7.33 – 7.23 (m, 2H), 7.14 – 7.07 (m, 2H), 7.04 – 6.95 (m, 4H), 6.86 – 6.81 (m, 2H), 3.39 (s, 3H), 2.79 (d, *J* = 5.8 Hz, 1H), 2.49 (d, *J* = 5.8 Hz, 1H);

¹³C NMR (100 MHz, CDCl_3) δ 170.8, 141.4, 139.2, 134.1, 130.4, 129.6, 128.5, 128.3, 128.3, 127.3, 127.0, 126.1, 125.9, 52.3, 45.0, 42.0, 26.2;

IR (neat) 3058, 3025, 2948, 1723, 1449 cm^{-1} ;

FTMS (+p NSI) calcd for $\text{C}_{23}\text{H}_{20}\text{O}_2\text{Cl}$ (M+H)⁺ 363.1146 found 363.1145;

HPLC (S,S-Whelk column, 1% i-propanol in hexane, 1 mL min⁻¹, 1 mg mL⁻¹, 30 min, UV 254 nm) retention times of 6.11 min (major) and 20.08 min (minor) 98% ee (The major enantiomer was determined basing on similar reactions in literature⁹⁷).



(S)-1-(2-Chlorophenyl)-2,2-diphenylcyclopropane-1-carboxylic acid (24)

A 100 mL round-bottom flask was charged with ester from previous step (1.09 g, 3 mmol, 1.0 equiv) and dissolved in 40 mL of dry dimethyl sulfoxide. After the flask was flushed with argon gas (3 times), potassium trimethylsilanolate (3.85g, 30 mmol, 10 equiv) was added in one portion. Then, the reaction mixture was stirred under room temperature and monitored by TLC until the starting material was consumed completely (30 h). The reacted mixture was quenched with 40 mL of 0.4 M aqueous citric acid by stirring for 1 h. Then, the solution was extracted by ethyl acetate (3 times), washed by brine and dries over Na₂SO₄. The crude product was concentrated under reduced pressure and purified by flash column chromatography (hexane/ethyl acetate = 6/1) to afford white solid in 88% yield, and recrystallization for enantiopure product using hot hexane/ethyl acetate (50/1) as solvent.

mp: 168-170 °C; **Rf** = 0.43 (hexane/ethyl acetate = 3/2); **[α]²⁰_D:** -100.4° (c = 1.09, CHCl₃);

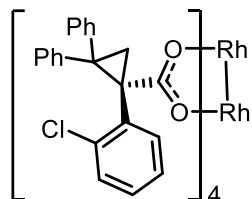
¹H NMR (400 MHz, CDCl₃) δ 7.52 (d, *J* = 6.6 Hz, 2H), 7.37 (t, *J* = 7.2 Hz, 2H), 7.31 (t, *J* = 7.2 Hz, 1H), 7.25 – 7.18 (m, 1H), 7.08 (td, *J* = 7.9, 1.7 Hz, 2H), 6.99 (dt, *J* = 5.7, 3.0 Hz, 4H), 6.85 – 6.79 (m, 2H), 2.78 – 2.61 (m, 1H), 2.51 (d, *J* = 5.8 Hz, 1H);

¹³C NMR (100 MHz, CDCl₃) δ 176.0, 140.9, 138.9, 136.8, 133.7, 130.3, 129.6, 128.7, 128.3, 127.3, 127.1, 126.3, 125.8, 46.0, 41.6, 26.6;

IR (neat) 3059, 3024, 1690, 1449 cm⁻¹;

FTMS (+p NSI) calcd for C₂₂H₁₈O₂Cl (M+H)⁺ 349.0990 found 349.0990;

HPLC (ADH column, 4% *i*-propanol in hexane, 1 mL min⁻¹, 1 mg mL⁻¹. 30 min, UV 230 nm) retention times of 18.61 min (major) and 26.83 min (minor) 98% ee (>99% ee after recrystallization).



Dirhodium tetrakis[(*S*)-1-(2-chlorophenyl)-2,2-diphenylcyclopropane-1-carboxylic acid]

(27)

A 100 mL round-bottom flask was charged with carboxylic acid from previous step (1.05 g, 3 mmol, 8.0 equiv) and Rh₂(OAc)₄ (165.8 mg, 0.38 mmol, 1.0 equiv). Then, approximately 75 mL toluene was added into the flask. A Soxhlet extractor with suitable amount of K₂CO₃ in it was added on the top of that flask, as well as a condenser (with slow flow of water). The solution was heated to reflux for days and monitored by the color of the solution & TLC. The reacted mixture was concentrated under reduced pressure, and the residue was purified by flash column chromatography (hexane/ethyl acetate = 12/1 to 4/1) to afford green solid in 45% yield.

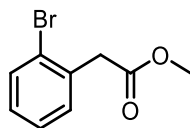
mp: >200 °C (decomp.); **Rf** = 0.33 (hexane/ethyl acetate = 4/1);

¹H NMR (400 MHz, Chloroform-*d*) δ 7.49 – 7.43 (m, 2H), 7.20 – 7.06 (m, 6H), 7.05 – 6.97 (m, 2H), 6.96 – 6.88 (m, 4H), 2.72 (d, *J* = 4.8 Hz, 1H), 2.24 (d, *J* = 4.7 Hz, 1H);

¹³C NMR (100 MHz, Chloroform-*d*) δ 187.9, 142.7, 139.5, 136.7, 135.6, 131.3, 130.8, 130.4, 129.0, 128.4, 127.8, 127.2, 127.0, 125.9, 125.5, 45.5, 41.9, 25.6;

IR (neat) 3053, 1580, 1494, 1446, 1382, 1277, 1045, 986, 906, 749 cm⁻¹;

FTMS (+p ESI) calcd for C₃₈H₆₈Cl₄O₈NRh₂ [M+NH₄]⁺ 1614.1804 found 1614.1790.



Methyl 2-(2-bromophenyl)acetate (18)

A dry 50 mL round-bottom flask was charged with 2-(2-bromophenyl)acetic acid (4.52 g, 21 mmol, 1.0 equiv). After the flask was flushed with argon gas (3 times), 30 mL of anhydrous methanol was added via syringes slowly. Then, the reaction mixture was cooled to 0 °C via ice bath. The acetyl chloride (1.80 mL, 25.2 mmol, 1.2 equiv) was then added into the solution dropwise at 0 °C. The reaction mixture was warmed to room temperature (23 °C) and stirred overnight. The reacted solution was poured into a separation funnel containing ethyl ether and saturated NH₄Cl. The NH₄Cl layer was then extracted twice with ether. The combined organic layer was concentrated under reduced pressure and purified by flash column chromatography (pentane/ether = 20/1) to afford the colorless oil in 86% yield after concentration and drying under vacuum.

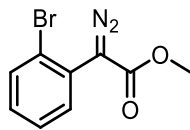
R_f = 0.39 (pentane/ether = 6/1);

¹H NMR (400 MHz, CDCl₃) δ 7.57 (dt, *J* = 7.8, 0.8 Hz, 1H), 7.31 – 7.27 (m, 2H), 7.15 (ddd, *J* = 8.0, 5.3, 3.9 Hz, 1H), 3.80 (s, 2H), 3.72 (s, 3H);

¹³C NMR (100 MHz, CDCl₃) δ 171.0, 134.1, 132.8, 131.5, 128.9, 127.6, 125.0, 52.2, 41.5;

IR (neat) 2951, 1735, 1435 cm⁻¹;

FTMS (+p NSI) calcd for C₉H₁₀O₂Br (M+H)⁺ 228.9859 found 228.9856.



Methyl 2-(2-bromophenyl)-2-diazoacetate (20)

A dry 250 mL round-bottom flask was charged with methyl 2-(2-bromophenyl)acetate (5.73 g, 25 mmol, 1.0 equiv) and *p*-ABSA (9.01 g, 37.5 mmol, 1.5 equiv). After the flask was flushed with argon gas (3 times), 40 mL of acetonitrile was added via syringes. Then, the reaction mixture was cooled to 0 °C via ice bath. The DBU (7.5 mL, 50 mmol, 2.0 equiv) was then added into the solution dropwise, and it was stirred for 15 min under 0 °C before warmed up to room temperature (23 °C). The reaction mixture was then stirred for another 4 h. After monitored by TLC, the reaction mixture was then quenched with saturated NH₄Cl solution and extracted three times with ethyl ether. The combined organic layer was washed with deionized water to remove any residual salts and dried over MgSO₄. Then, it was concentrated under reduced pressure and purified by flash column chromatography (pentane/ether = 20/1) to afford yellow solid in 90% yield.

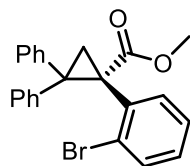
mp: 30-31 °C; **R_f** = 0.49 (pentane/ethyl ether = 6/1);

¹H NMR (400 MHz, CDCl₃) δ 7.62 (dd, *J* = 8.1, 1.2 Hz, 1H), 7.52 (dd, *J* = 7.9, 1.7 Hz, 1H), 7.38 (td, *J* = 7.6, 1.3 Hz, 1H), 7.22 (ddd, *J* = 8.1, 7.3, 1.7 Hz, 1H), 3.84 (s, 3H);

¹³C NMR (100 MHz, CDCl₃) δ 165.9, 133.3, 132.9, 130.1, 127.7, 125.7, 124.4, 52.3 (The resonance resulting from the diazo carbon was not observed);

IR (neat) 2952, 2093, 1698, 1434 cm⁻¹;

FTMS (+p NSI) calcd for C₉H₈N₂O₂Br (M+H)⁺ 254.9764 found 254.9763.



Methyl (*S*)-1-(2-bromophenyl)-2,2-diphenylcyclopropane-1-carboxylate (22)

An oven-dried 50 mL round-bottom flask was charged with $\text{Rh}_2(\text{S-PTAD})_4$ (27.6 mg, 0.018 mmol, 0.5 mol%) and 1,1-diphenylethylene (3.10 mL, 17.5 mmol, 5.0 equiv). After the flask was flushed with argon gas (3 times), and 8 mL of dry, degassed pentane were added via syringe. Then, the reaction mixture was cooled to 0 °C via ice bath. The methyl 2-(2-iodophenyl)-2-diazoacetate (892.7 mg, 3.5 mmol, 1.0 equiv) was weighted in a 20 mL scintillation vial and flushed with argon (3 times). The diazo compound was dissolved in 9 mL of pentane and transferred to the flask with syringe pump over 2 h under 0 °C. Then, the reaction mixture was stirred overnight. After check by TLC, the reaction mixture was concentrated. The residue was purified by flash column chromatography (hexane/ethyl acetate = 100/1 to 50/1) to afford product as white solid in 82% yield. The enantiopure product was obtained from recrystallization from hot hexane solution.

mp: 129-131 °C; **R_f** = 0.55 (hexane/ethyl acetate = 9/1); **[α]²⁰_D**: -78.3° (c = 1.33, CHCl_3);

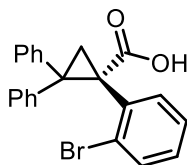
¹H NMR (400 MHz, CDCl_3) δ 7.48 (dd, *J* = 17.3, 7.5 Hz, 3H), 7.36 (tt, *J* = 6.8, 0.8 Hz, 2H), 7.31 – 7.26 (m, 1H), 7.07 – 6.91 (m, 6H), 6.78 (dd, *J* = 6.3, 2.9 Hz, 2H), 3.36 (s, 3H), 2.83 (d, *J* = 6.0 Hz, 1H), 2.45 (d, *J* = 6.0 Hz, 1H);

¹³C NMR (100 MHz, CDCl_3) δ 170.6, 141.4, 139.3, 135.7, 135.2, 132.9, 130.5, 128.6, 128.4, 128.3, 127.3, 127.0, 126.2, 126.1, 52.3, 45.4, 44.1, 27.0;

IR (neat) 3058, 3025, 2948, 1727, 1449 cm^{-1} ;

FTMS (+p NSI) calcd for $\text{C}_{23}\text{H}_{20}\text{O}_2\text{Br}$ ($\text{M}+\text{H}$)⁺ 407.0641 found 407.0639;

HPLC (*S,S*-Whelk column, 1% *i*-propanol in hexane, 1 mL min⁻¹, 1 mg mL⁻¹, 30 min, UV 254 nm) retention times of 8.59 min (major) and 21.74 min (minor) 98% ee.



(*S*)-1-(2-Bromophenyl)-2,2-diphenylcyclopropane-1-carboxylic acid (25)

A dry 100 mL round-bottom flask was charged with methyl (*S*)-1-(2-bromophenyl)-2,2-diphenylcyclopropane-1-carboxylate (1.22 g, 3 mmol, 1.0 equiv) in 25 mL of dry DMSO. After the flask was flushed with argon gas (3 times), potassium *tert*-butoxide (740.6 mg, 6.6 mmol, 2.2 equiv) was added in 3 portions over 30 min under argon. Then, the reaction mixture was stirred under room temperature and monitored by TLC until the starting material was consumed completely (4 h). The reacted mixture was cooled via ice bath and acidified by saturated NH₄Cl aqueous solution (~30 mL), followed by a slow addition of 1M HCl solution with vigorous stirring until the pH value reached 1-2. Then, the solution was extracted by dichloromethane (or ethyl acetate), washed by brine and dries over MgSO₄. After it was concentrated under reduced pressure, the crude product was purified by flash column chromatography (hexane/ethyl acetate = 6/1) to afford white solid in 95% yield.

mp: 172-174 °C; **R_f** = 0.31 (hexane/ethyl acetate = 4/1); **[α]²⁰_D:** -132.5° (c = 0.30, CHCl₃);

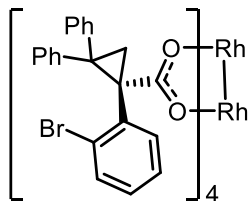
¹H NMR (400 MHz, CDCl₃) δ 7.50 (s, 2H), 7.38 (t, *J* = 7.4 Hz, 2H), 7.35 – 7.29 (m, 1H), 7.27 (m, 1H), 7.01 (s, 5H), 6.80 (d, *J* = 6.6 Hz, 3H), 2.52 (d, *J* = 6.0 Hz, 1H), 2.05 (dd, *J* = 3.8, 0.7 Hz, 1H);

¹³C NMR (100 MHz, CDCl₃) δ 175.3, 140.9, 139.0, 135.3, 132.9, 130.4, 128.7, 128.5, 128.4, 127.4, 127.1, 126.3, 46.4, 43.6, 27.4;

IR (neat) 3059, 3024, 1690, 1450 cm⁻¹;

FTMS (+p NSI) calcd for $C_{22}H_{18}O_2Br$ (M+H)⁺ 393.0485 found 349.0990;

HPLC (ADH column, 4% *i*-propanol in hexane, 1 mL min⁻¹, 1 mg mL⁻¹. 30 min, UV 230 nm) retention times of 20.97 min (major) and 23.90 min (minor) >99% ee (The enantiomeric excess was consistent with the ester used after hydrolysis).



Dirhodium tetrakis((*S*)-1-(2-bromophenyl)-2,2-diphenylcyclopropanecarboxylate) (28)

A 100 mL round-bottom flask was charged with carboxylic acid from previous step (1.12 g, 2.84 mmol, 8.0 equiv) and $Rh_2(OAc)_4$ (156.9 mg, 0.36 mmol, 1.0 equiv). Then, approximately 75 mL toluene was added into the flask. A Soxhlet extractor with suitable amount of K_2CO_3 in it was added on the top of that flask, as well as a condenser (with slow flow of water). The solution was heated to reflux for days and monitored by the color of the solution & TLC. The reacted mixture was concentrated under reduced pressure, and the residue was purified by flash column chromatography (hexane/ethyl acetate = 12/1 to 4/1) to afford green solid in 40% yield.

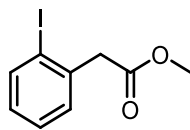
mp: >200 °C (decomp.); **R_f** = 0.34 (hexane/ethyl acetate = 4/1);

¹H NMR (400 MHz, Chloroform-*d*) (rotamers *A*:*B* = 2.8:1) δ 7.58 – 7.51 (m, 2H), 7.22 – 7.03 (m, 9H), 6.96 – 6.85 (m, 4H), 6.82 (tt, *J* = 7.4, 1.6 Hz, 1H), [2.71 (*rotamer A*, d, *J* = 4.8 Hz), 2.69 (*B*, d, *J* = 4.7 Hz), 1H], [2.32 (*rotamer A*, d, *J* = 4.7 Hz), 2.28 (*B*, d, *J* = 4.7 Hz), 1H];

¹³C NMR (101 MHz, Chloroform-*d*) (both rotamers) δ 187.5, 187.0, 143.3, 142.8, 139.1, 139.0, 136.8, 132.5, 131.6, 131.5, 131.4, 128.6, 128.6, 128.0, 127.9, 127.1, 126.8, 126.8, 126.4, 125.9, 125.4, 125.2, 45.5, 45.3, 43.7, 43.6, 26.1, 25.9;

IR (neat) 3057, 3023, 1586, 1386, 1027, 752, 696 cm⁻¹;

FTMS (+p ESI) calcd for $C_{88}H_{68}Br_4O_8NRh_2$ $[M+H]^+$ 1773.9404 found 1773.9415.



Methyl 2-(2-iodophenyl)acetate (19)

A dry 50 mL round-bottom flask was charged with 2-(2-iodophenyl)acetic acid (3.93 g, 15 mmol, 1.0 equiv). After the flask was flushed with argon gas (3 times), 16 mL of anhydrous methanol was added via syringes slowly. Then, the reaction mixture was cooled to 0 °C via ice bath. The acetyl chloride (1.28 mL, 18 mmol, 1.2 equiv) was then added into the solution dropwise at 0 °C. The reaction mixture was warmed to room temperature (23 °C) and stirred overnight. The reacted solution was poured into a separation funnel containing ethyl ether and saturated NH_4Cl . The NH_4Cl layer was then extracted twice with ether. The combined organic layer was concentrated under reduced pressure and purified by flash column chromatography (pentane/ether = 20/1) to afford the colorless oil in 98% yield after concentration and drying under vacuum.

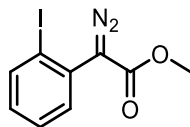
R_f = 0.34 (hexane/ethyl acetate = 9/1);

¹H NMR (600 MHz, CDCl₃) δ 7.85 (dd, *J* = 8.0, 1.2 Hz, 1H), 7.35 – 7.27 (m, 2H), 6.97 (td, *J* = 7.6, 1.9 Hz, 1H), 3.81 (s, 2H), 3.72 (s, 3H);

¹³C NMR (151 MHz, CDCl₃) δ 170.9, 139.5, 137.7, 130.6, 128.9, 128.4, 101.0, 52.2, 46.1;

IR (neat) 3053, 2949, 1734, 1466, 1435, 1339, 1217, 1161, 1013, 758, 731 cm^{-1} ;

FTMS (+p NSI) calcd for $C_9H_{10}O_2I$ $(M+H)^+$ 276.9720 found 276.9718.



Methyl 2-(2-iodophenyl)-2-diazoacetate (21)

A dry 100 mL round-bottom flask was charged with methyl 2-(2-iodophenyl)acetate (4.09 g, 14.8 mmol, 1.0 equiv) and *p*-ABSA (5.33 g, 22.2 mmol, 1.5 equiv). After the flask was flushed with argon gas (3 times), 20 mL of acetonitrile was added via syringes. Then, the reaction mixture was cooled to 0 °C via ice bath. The DBU (4.43 mL, 29.6 mmol, 2.0 equiv) was then added into the solution dropwise, and it was stirred for 15 min under 0 °C before warmed up to room temperature (23 °C). The reaction mixture was then stirred for another 4 h. After monitored by TLC, the reaction mixture was then quenched with saturated NH₄Cl solution and extracted three times with ethyl ether. The combined organic layer was washed with deionized water to remove any residual salts and dried over MgSO₄. Then, it was concentrated under reduced pressure and purified by flash column chromatography (pentane/ether = 20/1) to afford yellow oil in 98% yield.

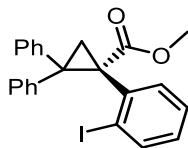
R_f = 0.16 (pentane/ethyl ether = 19/1);

¹H NMR (600 MHz, CDCl₃) δ 7.92 (dd, *J* = 8.0, 1.3 Hz, 1H), 7.47 (dd, *J* = 7.8, 1.7 Hz, 1H), 7.42 (ddd, *J* = 7.8, 7.3, 1.3 Hz, 1H), 7.06 (ddd, *J* = 8.0, 7.3, 1.7 Hz, 1H), 3.83 (s, 3H);

¹³C NMR (151 MHz, CDCl₃) δ 165.9, 139.8, 133.0, 130.5, 129.7, 128.6, 101.0, 52.3 (The resonance resulting from the diazo carbon was not observed);

IR (neat) 2951, 2094, 1698, 1470, 1434, 1283, 1245, 1193, 1158, 1064, 756 cm⁻¹;

FTMS (+p NSI) calcd for C₉H₇N₂O₂INa (M+Na)⁺ 324.9444 found 324.9443.



Methyl (*S*)-1-(2-iodophenyl)-2,2-diphenylcyclopropane-1-carboxylate (23)

An oven-dried 50 mL round-bottom flask was charged with $\text{Rh}_2(\text{S-PTAD})_4$ (27.6 mg, 0.018 mmol, 0.5 mol%) and 1,1-diphenylethylene (3.10 mL, 17.5 mmol, 5.0 equiv). After the flask was flushed with argon gas (3 times), and 8 mL of dry, degassed pentane were added via syringe. Then, the reaction mixture was cooled to 0 °C via ice bath. The methyl 2-(2-iodophenyl)-2-diazoacetate (1.06 g, 3.5 mmol, 1.0 equiv) was weighted in a 20 mL scintillation vial and flushed with argon (3 times). The diazo compound was dissolved in 9 mL of pentane and transferred to the flask with syringe pump over 2 h under 0 °C. Then, the reaction mixture was stirred overnight. After check by TLC, the reaction mixture was concentrated. The residue was purified by flash column chromatography (hexane/ethyl acetate = 100/1 to 50/1) to afford product as white solid in 88% yield. The enantiopure product was obtained from recrystallization from hot hexane solution.

mp: 106-108 °C; **R_f** = 0.42 (hexane/ethyl acetate = 9/1); **[α]²⁰_D:** -364.1° (c = 1.00, CHCl_3 , 99% ee);

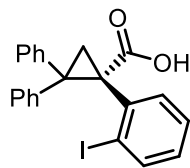
¹H NMR (400 MHz, CDCl_3) δ 7.81 (d, *J* = 7.9 Hz, 1H), 7.48 (s, 2H), 7.38 (t, *J* = 7.7 Hz, 2H), 7.33 – 7.29 (m, 1H), 7.02 (td, *J* = 5.7, 5.1, 2.5 Hz, 3H), 6.96 (s, 1H), 6.84 (td, *J* = 7.4, 1.8 Hz, 1H), 6.79 – 6.71 (m, 2H), 3.37 (s, 3H), 2.96 (s, 1H), 2.43 (d, *J* = 6.1 Hz, 1H);

¹³C NMR (100 MHz, CDCl_3) δ 170.5, 141.4, 139.5, 139.3, 138.8, 136.0, 130.5, 128.6, 128.5, 128.3, 127.4, 127.1, 126.8, 126.2, 101.8, 52.4, 47.9, 46.3, 28.3;

IR (neat) 3058, 3024, 2947, 1729, 1497, 1449, 1432, 1298, 1216, 1141, 1018, 749, 704 cm^{-1} ;

FTMS (+p NSI) calcd for $\text{C}_{23}\text{H}_{20}\text{O}_2\text{I}$ ($\text{M}+\text{H}$)⁺ 455.0502 found 455.0499;

HPLC (S,S-Whelk column, 1% *i*-propanol in hexane, 1 mL min^{-1} , 1 mg mL^{-1} , 30 min, UV 254 nm) retention times of 8.18 min (major) and 22.13 min (minor) 99% ee.



(S)-1-(2-Iodophenyl)-2,2-diphenylcyclopropane-1-carboxylic acid (26)

A dry 50 mL round-bottom flask was charged with methyl (S)-1-(2-iodophenyl)-2,2-diphenylcyclopropane-1-carboxylate (1.40 g, 3.1 mmol, 1.0 equiv) in 20 mL of dry DMSO. After the flask was flushed with argon gas (3 times), potassium *tert*-butoxide (760.3 mg, 6.8 mmol, 2.2 equiv) was added in 3 portions over 30 min under argon. Then, the reaction mixture was stirred under room temperature and monitored by TLC until the starting material was consumed completely (4 h). The reacted mixture was cooled via ice bath and acidified by saturated NH₄Cl aqueous solution (~30 mL), followed by a slow addition of 1M HCl solution with vigorous stirring until the pH value reached 1-2. Then, the solution was extracted by dichloromethane (or ethyl acetate), washed by brine and dries over MgSO₄. After it was concentrated under reduced pressure, the crude product was purified by flash column chromatography (hexane/ethyl acetate = 6/1) to afford white solid in 62% yield. The enantiomeric excess was consistent with the ester used after hydrolysis.

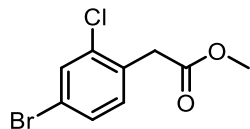
mp: 175-177 °C; **R_f** = 0.29 (hexane/ethyl acetate = 4/1); **[α]²⁰_D**: -363.4° (c = 1.00, CHCl₃, 99% ee);

¹H NMR (400 MHz, CDCl₃) δ 7.82 (br, s, 1H), 7.50 – 7.29 (m, 5H), 7.02 (br, s, 3H), 6.93 – 6.67 (m, 5H), 2.88 (br, s, 1H), 2.46 (d, *J* = 6.2 Hz, 1H);

¹³C NMR (100 MHz, CDCl₃) δ 175.7, 140.9, 139.5, 139.1, 138.2, 136.0, 130.3, 128.7, 128.5, 127.5, 127.2, 126.7, 126.3, 101.7, 47.6, 47.4, 28.7;

IR (neat) 3059, 3024, 2627, 1691, 1497, 1450, 1300, 1259 1233, 1014, 749, 703 cm⁻¹;

FTMS (+p NSI) calcd for C₂₂H₁₈O₂I (M+H)⁺ 441.0346 found 441.0343;



2-(4-Bromo-2-chlorophenyl)acetic acid (55a)

A dry 50 mL round-bottom flask was charged with 2-(4-bromo-2-chlorophenyl)acetic acid (5.24 g, 21 mmol, 1.0 equiv). After the flask was flushed with argon gas (3 times), 30 mL of anhydrous methanol was added via syringes slowly. Then, the reaction mixture was cooled to 0 °C via ice bath. The acetyl chloride (1.80 mL, 25.2 mmol, 1.2 equiv) was then added into the solution dropwise at 0 °C. The reaction mixture was warmed to room temperature (23 °C) and stirred overnight. The reacted solution was poured into a separation funnel containing ethyl ether and saturated NH₄Cl. The NH₄Cl layer was then extracted twice with diethyl ether. The combined organic layer was concentrated under reduced pressure and purified by flash column chromatography (pentane/ether = 20/1) to afford the colorless oil in 93% yield.

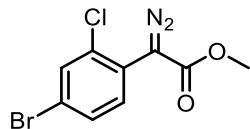
Rf = 0.53 (hexane/ethyl acetate = 9/1);

¹H NMR (400 MHz, CDCl₃) δ 7.56 (d, *J* = 2.0 Hz, 1H), 7.37 (dd, *J* = 8.2, 2.0 Hz, 1H), 7.16 (d, *J* = 8.2 Hz, 1H), 3.73 (s, 2H), 3.71 (s, 3H);

¹³C NMR (101 MHz, CDCl₃) δ 170.5, 135.5, 132.5, 132.1, 131.4, 130.1, 121.5, 52.3, 38.4;

IR (neat) 2952, 1736, 1473, 1339, 1251, 1217, 1193, 1165, 1053, 814 cm⁻¹;

FTMS (+p NSI) calcd for C₉H₉O₂BrCl (M+H)⁺ 262.9469 found 262.9474.



Methyl 2-(4-bromo-2-chlorophenyl)-2-diazoacetate (52a)

A dry 250 mL round-bottom flask was charged with methyl 2-(4-bromo-2-chlorophenyl)acetate (5.59 g, 25 mmol, 1.0 equiv) and *p*-ABSA (9.01 g, 37.5 mmol, 1.5 equiv). After the flask was flushed with argon gas (3 times), 40 mL of acetonitrile was added via syringes. Then, the reaction mixture was cooled to 0 °C via ice bath. DBU (7.5 mL, 50 mmol, 2.0 equiv) was then added into the solution dropwise, and it was stirred for 15 min under 0 °C. After the allowed time passed, the reaction mixture was warmed to room temperature (23 °C) and stirred for another 4 h monitored by TLC. The reaction mixture was then quenched with saturated aqueous NH₄Cl solution and extracted three times with diethyl ether. The combined organic layer was washed with deionized water to remove any residual salts and dried over Na₂SO₄. The crude mixture was concentrated under reduced pressure and purified by flash column chromatography (pentane/ether = 20/1) to provide yellow solid in 97% yield.

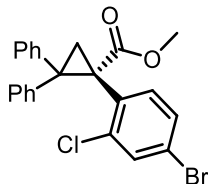
mp: 89-91 °C; **Rf** = 0.63 (hexane/diethyl ether = 6/1);

¹H NMR (400 MHz, CDCl₃) δ 7.59 (d, *J* = 1.9 Hz, 1H), 7.45 (dd, *J* = 8.5, 1.9 Hz, 1H), 7.42 (d, *J* = 8.5 Hz, 1H), 3.84 (s, 3H);

¹³C NMR (101 MHz, CDCl₃) δ 165.5, 134.2, 133.0, 132.6, 130.5, 123.0, 122.5, 52.4 (The peak of the diazo carbon was not observed);

IR (neat) 3094, 2954, 2099, 1703, 1471, 1431, 1282, 1241, 1158, 1071, 1024, 817, 737 cm⁻¹;

FTMS (+p NSI) calcd for C₉H₇N₂O₂BrCl (M+H)⁺ 288.9374 found 288.9373.



Methyl (S)-1-(4-bromo-2-chlorophenyl)-2,2-diphenylcyclopropane-1-carboxylate (53a)

An oven-dried 100 mL round-bottom flask was charged with $\text{Rh}_2(\text{R-DOSP})_4$ (38 mg, 0.02 mmol, 1 mol%) and 1,1-diphenylethylene (2.05 mL, 11.5 mmol, 2.3 equiv). After the flask was flushed with argon gas (3 times), 15 mL of dry degassed pentane was added via syringe. Then, the reaction mixture was cooled to 0 °C via ice bath. Methyl 2-(4-bromo-2-chlorophenyl)-2-diazoacetate (1.45 g, 5 mmol, 1.0 equiv) was weighted in two 20 mL scintillation vials and flushed with argon (3 times), then it was dissolved in 16 mL of the dry degassed pentane respectively and transferred into the flask with syringe pump over 1 h under 0 °C. Then, the reaction mixture was stirred overnight. After monitored by TLC, the reaction mixture was concentrated under vacuum. The residue was purified by flash column chromatography (hexane/ethyl acetate = 100/1 to 12/1) to provide product as white solid in 91% yield.

mp: 119-120 °C; **Rf** = 0.34 (hexane/ethyl acetate = 9/1); **$[\alpha]^{20}_{\text{D}}$** : -282.4° (c = 1.22, CHCl_3);

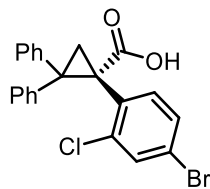
$^1\text{H NMR}$ (400 MHz, CDCl_3) δ 7.51 (d, J = 7.1 Hz, 2H), 7.44 (d, J = 2.0 Hz, 1H), 7.38 (t, J = 7.3 Hz, 2H), 7.34 – 7.28 (m, 1H), 7.16 – 7.10 (m, 1H), 7.04 (dd, J = 5.0, 1.9 Hz, 3H), 6.97 (d, J = 8.2 Hz, 1H), 6.89 – 6.82 (m, 2H), 3.39 (s, 3H), 2.80 (d, J = 5.9 Hz, 1H), 2.46 (d, J = 5.9 Hz, 1H);

$^{13}\text{C NMR}$ (101 MHz, CDCl_3) δ 170.3, 141.2, 138.8, 137.7, 135.4, 133.5, 132.2, 130.3, 129.1, 128.4, 128.3, 127.5, 127.1, 126.4, 121.5, 52.4, 45.0, 41.6, 26.0;

IR (neat) 3059, 3025, 2950, 1725, 1451, 1290, 1255, 912, 785, 733 cm^{-1} ;

FTMS (+p NSI) calcd for $\text{C}_{23}\text{H}_{19}\text{O}_2\text{BrCl}$ ($\text{M}+\text{H}$)⁺ 441.0251 found 441.0255;

HPLC (S,S-Whelk column, 3% *i*-propanol in hexane, 1 mL min^{-1} , 1 mg mL^{-1} . 30 min, UV 254 nm) retention times of 6.63 min (major) and 18.79 min (minor) 97% ee.



(S)-1-(4-Bromo-2-chlorophenyl)-2,2-diphenylcyclopropane-1-carboxylic acid (56a)

A 100 mL round-bottom flask was charged with ester from previous step (1.81g, 4.1 mmol, 1.0 equiv) and dissolved in 40 mL of dry DMSO. After the flask was flushed with argon gas (3 times), TMSOK (4.21 g, 32.8 mmol, 8 equiv) was added in one portion. Then, the reaction mixture was stirred under room temperature and monitored by TLC until the starting material was consumed completely (30 h). The reacted mixture was quenched with 40 mL of 0.4 M aqueous citric acid by stirring for 1 h. Then, the solution was extracted by ethyl acetate (3 times), washed by brine and dries over Na₂SO₄. The crude product was concentrated under reduced pressure and purified by flash column chromatography (hexane/ethyl acetate = 6/1) to afford white solid in 67% yield. The enantiopure was obtained after recrystallization from hot hexane solution.

mp: 103-104 °C; **R_f** = 0.21 (hexane/ethyl acetate = 3/2); **[α]²⁰_D**: -337.4° (c = 1.24, CHCl₃);

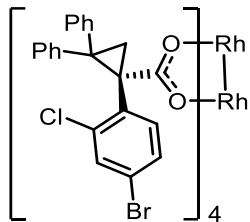
¹H NMR (600 MHz, CDCl₃) δ 7.54 – 7.44 (m, 2H), 7.41 (s, 1H), 7.36 (t, *J* = 7.6 Hz, 2H), 7.31 (t, *J* = 7.3 Hz, 1H), 7.10 (s, 1H), 7.03 (t, *J* = 5.5 Hz, 3H), 6.97 – 6.77 (m, 3H), 2.70 (s, 1H), 2.48 (d, *J* = 5.9 Hz, 1H);

¹³C NMR (101 MHz, CDCl₃) δ 175.6, 140.7, 138.4, 137.7, 133.0, 132.2, 130.2, 129.1, 128.4, 128.3, 127.5, 127.2, 126.6, 121.7, 46.1, 41.1, 26.4;

IR (neat) 3060, 3025, 1692, 1474, 1299, 1253, 1233, 908, 782, 730, 703 cm⁻¹;

FTMS (-p NSI) calcd for C₂₂H₁₅O₂BrCl (M-H)⁻ 424.9949 found 424.9954;

HPLC (ADH column, 5% *i*-propanol in hexane, 1 mL min⁻¹, 1 mg mL⁻¹. 30 min, UV 230 nm) retention times of 14.67 min (minor) and 18.20 min (major) 98% ee.



Dirhodium tetrakis((*S*)-1-(4-bromo-2-chlorophenyl)-2,2-diphenylcyclopropanecarboxylate)

(57a)

A 100 mL round-bottom flask was charged with carboxylic acid from previous step (1.28 g, 3 mmol, 8.0 equiv) and $\text{Rh}_2(\text{OAc})_4$ (165.8 mg, 0.38 mmol, 1.0 equiv). Then, approximately 70 mL toluene was added into the flask. A Soxhlet extractor with suitable amount of K_2CO_3 in it was added on the top of that flask, as well as a condenser (with slow flow of water). The solution was heated to reflux for 3 days and monitored by the color of the solution and TLC. The reacted mixture was concentrated under reduced pressure, and the residue was purified by flash column chromatography (hexane/ethyl acetate = 15/1) to afford the product as green solid in 64% yield.

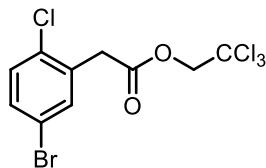
mp: >200 °C (decomp.); **Rf** = 0.53 (hexane/ethyl acetate = 4/1);

^1H NMR (600 MHz, CDCl_3) δ 7.39 (d, J = 7.1 Hz, 2H), 7.19 – 7.14 (m, 3H), 7.10 (dd, J = 22.3, 7.1 Hz, 4H), 6.95 (td, J = 9.2, 8.7, 6.4 Hz, 4H), 2.69 (d, J = 4.9 Hz, 1H), 2.23 (d, J = 4.8 Hz, 1H);

^{13}C NMR (101 MHz, CDCl_3) δ 187.5, 142.4, 138.9, 137.4, 134.8, 131.7, 131.7, 131.1, 129.3, 128.3, 127.3, 126.3, 125.5, 120.6, 45.8, 41.3, 25.4;

IR (neat) 3059, 1579, 1473, 1391, 1373, 795, 734, 709, 692 cm^{-1} ;

FTMS (+p NSI) calcd for $\text{C}_{88}\text{H}_{61}\text{O}_8\text{Br}_4\text{Cl}_4\text{Rh}_2$ ($\text{M}+\text{H}$) $^+$ 1906.7959 found 1906.8014.



2,2,2-Trichloroethyl 2-(5-bromo-2-chlorophenyl)acetate (55c)

A dry 50 mL round-bottom flask was charged with 2-(5-bromo-2-chlorophenyl)acetic acid (2.50 g, 10 mmol, 1.0 equiv), 4-dimethylaminopyridine (122.2 mg, 1 mmol, 0.1 equiv) and 2,2,2-trichloroethanol (1.79 g, 12 mmol, 1.2 equiv). After the flask was flushed with argon gas (3 times), 22 mL of degassed dry dichloromethane was added via syringes slowly. Then, the reaction mixture was cooled to 0 °C via ice bath. A solution of DCC (2.30 g, 11 mmol, 1.1 equiv) in degassed dry dichloromethane (12 mL) was then added into the solution dropwise at 0 °C. The reaction mixture was warmed to room temperature (23 °C) and stirred overnight. Suction filtration was applied to remove the solid byproducts and the filtrate was concentrated under reduced pressure. The residue mixture was purified by flash column chromatography (hexane/ethyl acetate = 20/1) to afford the colorless oil in 97% yield.

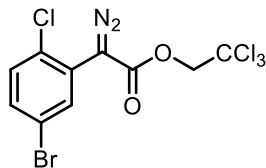
R_f = 0.57 (hexane/ethyl acetate = 9/1);

¹H NMR (600 MHz, CDCl₃) δ 7.49 (d, *J* = 2.0 Hz, 1H), 7.38 (dd, *J* = 8.5, 2.1 Hz, 1H), 7.27 (d, *J* = 8.5 Hz, 1H), 4.78 (s, 2H), 3.89 (s, 2H);

¹³C NMR (126 MHz, CDCl₃) δ 168.4, 134.4, 133.6, 133.3, 132.1, 130.9, 120.5, 94.6, 74.4, 38.4.;

IR (neat) 2954, 1755, 1467, 1206, 1135, 1086, 1049, 810, 749, 718 cm⁻¹;

FTMS (+p NSI) calcd for C₁₀H₆O₂BrCl₄ (M-H)⁻ 376.8311 found 376.8315.



2,2,2-Trichloroethyl 2-(5-bromo-2-chlorophenyl)-2-diazoacetate (52c)

A dry 50 mL round-bottom flask was charged with 2,2,2-trichloroethyl 2-(5-bromo-2-chlorophenyl)acetate (1.90 g, 5 mmol, 1.0 equiv) and *o*-NBSA (1.72 g, 7.5 mmol, 1.5 equiv). After the flask was flushed with argon gas (3 times), 15 mL of anhydrous acetonitrile was added via syringes. Then, the reaction mixture was cooled to 0 °C via ice bath. DBU (1.60 mL, 11 mmol, 2.2 equiv) was then added into the solution dropwise, and it was stirred for 1 h under 0 °C. After the allowed time passed, the reaction mixture was warmed to room temperature (23 °C) and quenched with saturated aqueous NH₄Cl solution and extracted 3 times with diethyl ether. The combined organic layer was washed with brine and dried over Na₂SO₄. The crude mixture was concentrated under reduced pressure and purified by flash column chromatography (pentane/diethyl ether = 9/1) to provide yellow solid in 95% yield.

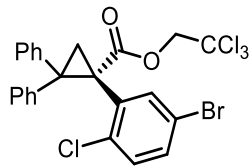
mp: 81-82 °C; **R_f** = 0.70 (hexane/diethyl ether = 4/1);

¹H NMR (400 MHz, CDCl₃) δ 7.76 (d, *J* = 2.3 Hz, 1H), 7.42 (dd, *J* = 8.6, 2.3 Hz, 1H), 7.31 (d, *J* = 8.6 Hz, 1H), 4.90 (s, 2H);

¹³C NMR (126 MHz, CDCl₃) δ 163.4, 134.9, 132.8, 132.4, 131.4, 124.9, 120.8, 94.9, 74.2 (The peak of the diazo carbon was not observed);

IR (neat) 2935, 2104, 1705, 1471, 1275, 1234, 1145, 1094, 1059, 792, 732, 714 cm⁻¹;

FTMS (+p ESI) calcd for C₁₀H₆N₂O₂BrCl₄ (M+H)⁺ 404.8361 found 404.8355.



2,2,2-Trichloroethyl (S)-1-(5-bromo-2-chlorophenyl)-2,2-diphenylcyclopropane-1-carboxylate (53c)

An oven-dried 100 mL round-bottom flask was charged with $\text{Rh}_2(\text{R-DOSP})_4$ (38 mg, 0.02 mmol, 1 mol%) and 1,1-diphenylethylene (2.05 mL, 11.5 mmol, 2.3 equiv). After the flask was flushed with argon gas (3 times), 15 mL of dry degassed pentane was added via syringe. Then, the reaction mixture was cooled to 0 °C via ice bath. 2,2,2-Trichloroethyl 2-(5-bromo-2-chlorophenyl)-2-diazoacetate (2.03 g, 5 mmol, 1.0 equiv) was weighted in two 20 mL scintillation vials and flushed with argon (3 times), then it was dissolved in 16 mL of the dry degassed pentane respectively and transferred into the flask with syringe pump over 1 h under 0 °C. Then, the reaction mixture was stirred overnight. After monitored by TLC, the reaction mixture was concentrated under vacuum. The residue was purified by flash column chromatography (hexane/ethyl acetate = 100/1 to 12/1) to provide product as white solid in 84% yield. The enantiopure product was obtained after recrystallization from hot hexane solution.

mp: 58-59°C; **Rf** = 0.64 (hexane/diethyl ether = 6/1); $[\alpha]^{20}_{\text{D}}$: -239.5° (c = 1.26, CHCl_3);

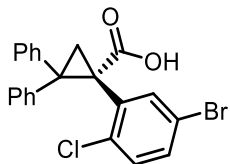
$^1\text{H NMR}$ (600 MHz, CDCl_3) δ 7.56 (d, J = 5.9 Hz, 2H), 7.38 (t, J = 7.6 Hz, 2H), 7.31 (tt, J = 6.7, 1.2 Hz, 1H), 7.26 – 7.25 (m, 1H), 7.23 (dd, J = 8.4, 2.3 Hz, 1H), 7.09 (d, J = 24.8 Hz, 4H), 6.92 – 6.84 (m, 2H), 4.57 (d, J = 12.0 Hz, 1H), 4.23 (d, J = 11.9 Hz, 1H), 2.86 (s, 1H), 2.58 (d, J = 6.1 Hz, 1H);

$^{13}\text{C NMR}$ (101 MHz, CDCl_3) δ 168.3, 140.5, 138.1, 131.8, 130.9, 130.4, 128.5, 128.3, 127.6, 127.5, 126.8, 119.3, 105.3, 94.2, 75.0, 46.1, 41.4, 26.3;

IR (neat) 3060, 3025, 2950, 1740, 1455, 1450, 1199, 1143, 1104, 1047, 815, 786, 720, 704 cm^{-1} ;

FTMS (+p NSI) calcd for C₂₄H₁₈O₂BrCl₄ (M+H)⁺ 556.9239 found 556.9253;

HPLC (S,S-Whelk column, 0% *i*-propanol in hexane, 1 mL min⁻¹, 1 mg mL⁻¹, 30 min, UV 230 nm) retention times of 11.34 min (major) and 14.27 min (minor) 97% ee.



(S)-1-(5-Bromo-2-chlorophenyl)-2,2-diphenylcyclopropane-1-carboxylic acid (56b)

In a 100 mL round-bottom flask, ester from previous step (1.58 g, 2.8 mmol, 1.0 equiv) was dissolved in 25 mL of glacial acetic acid. Then, zinc dust (927 mg, 14.0 mmol, 5.0 equiv) was added and the reaction mixture was stirred under room temperature (23 °C) for 36 h. After allowed time passed, the remaining zinc dust was removed via filtration. The filtrate was diluted with DI H₂O (100 mL) and extracted with ethyl acetate (3 times), washed with brine. The crude product was concentrated and purified by flash column chromatography (hexane/ethyl acetate = 9/1) to afford white solid in 91% yield.

mp: 85-86 °C; **R_f** = 0.64 (hexane/diethyl ether = 6/1); **[α]²⁰_D:** -297.1° (c = 1.28, CHCl₃);

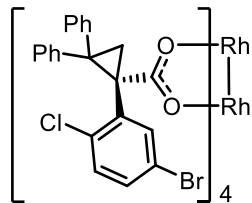
¹H NMR (600 MHz, CDCl₃) δ 7.51 (d, *J* = 7.4 Hz, 2H), 7.37 (t, *J* = 7.5 Hz, 2H), 7.32 (t, *J* = 7.3 Hz, 1H), 7.20 (dd, *J* = 8.5, 2.2 Hz, 1H), 7.04 (s, 4H), 6.89 – 6.83 (m, 2H), 2.69 (s, 1H), 2.51 (d, *J* = 5.9 Hz, 1H);

¹³C NMR (126 MHz, CDCl₃) δ 175.7, 140.6, 138.3, 135.9, 131.7, 130.9, 130.3, 128.5, 128.3, 127.5, 127.3, 126.8, 119.4, 119.4, 46.4, 41.2, 26.3;

IR (neat) 3025 (br), 1691, 1465, 1450, 1296, 1253, 1229, 1042, 905, 812, 726, 702, 694 cm⁻¹;

FTMS (-p NSI) calcd for C₂₂H₁₇O₂BrCl (M+H)⁺ 427.0095 found 427.0104;

HPLC (ADH column, 5% *i*-propanol in hexane, 1 mL min⁻¹, 1 mg mL⁻¹, 30 min, UV 230 nm) retention times of 10.71 min (major) and 13.01 min (minor) >99% ee.



**Dirhodium tetrakis((*S*)-1-(5-bromo-2-chlorophenyl)-2,2-diphenylcyclopropanecarboxylate)
(57b)**

A 100 mL round-bottom flask was charged with carboxylic acid from previous step (1.28 g, 3 mmol, 8.0 equiv) and $\text{Rh}_2(\text{OAc})_4$ (165.8 mg, 0.38 mmol, 1.0 equiv). Then, approximately 70 mL toluene was added into the flask. A Soxhlet extractor with suitable amount of K_2CO_3 in it was added on the top of that flask, as well as a condenser (with slow flow of water). The solution was heated to reflux for 3 days and monitored by the color of the solution and TLC. The reacted mixture was concentrated under reduced pressure, and the residue was purified by flash column chromatography (dry loading, hexane/dichloromethane = 3/1) to afford green solid in 76% yield.

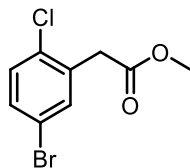
mp: >200 °C (decomp.); **Rf** = 0.50 (hexane/ethyl acetate = 4/1);

^1H NMR (400 MHz, CDCl_3) δ 7.43 – 7.38 (m, 2H), 7.28 – 7.26 (m, 1H), 7.19 – 7.15 (m, 2H), 7.12 (d, J = 7.5 Hz, 2H), 7.10 – 7.06 (m, 3H), 6.99 – 6.93 (m, 3H), 6.88 (dd, J = 12.3, 8.4 Hz, 1H), 2.68 (d, J = 5.0 Hz, 1H), 2.23 (d, J = 5.0 Hz, 1H);

^{13}C NMR (101 MHz, CDCl_3) δ 187.4, 142.2, 138.6, 137.9, 135.7, 133.7, 131.2, 130.9, 130.6, 128.3, 127.3, 127.2, 126.2, 125.7, 119.4, 45.6, 41.8, 25.5;

IR (neat) 3057, 2923, 1587, 1495, 1466, 1448, 1377, 1047, 811, 733, 703 cm^{-1} ;

FTMS (+p ESI) calcd for $\text{C}_{88}\text{H}_{61}\text{O}_8\text{Br}_4\text{Cl}_4\text{Rh}_2$ ($\text{M}+\text{H}$)⁺ 1906.7959 found 1906.7871.



Methyl 2-(5-bromo-2-chlorophenyl)acetate (55b)

A dry 50 mL round-bottom flask was charged with 2-(5-bromo-2-chlorophenyl)acetic acid (2.50 g, 10 mmol, 1.0 equiv). After the flask was flushed with argon gas (3 times), 15 mL of methanol was added via syringes slowly. Then, the reaction mixture was cooled to 0 °C via ice bath. The acetyl chloride (0.85 mL, 12 mmol, 1.2 equiv) was then added into the solution dropwise at 0 °C. The reaction mixture was warmed to room temperature (23 °C) and stirred overnight. The reacted solution was poured into a separation funnel containing ethyl ether and saturated NH₄Cl. The NH₄Cl layer was then extracted twice with diethyl ether. The combined organic layer was concentrated under reduced pressure and purified by flash column chromatography (pentane/ether = 20/1) to afford the colorless oil in 97% yield.

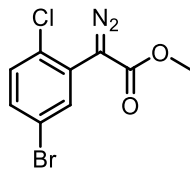
R_f = 0.49 (hexane/ethyl acetate = 9/1);

¹H NMR (600 MHz, CDCl₃) δ 7.43 (d, *J* = 2.4 Hz, 1H), 7.35 (dd, *J* = 8.5, 2.4 Hz, 1H), 7.25 (d, *J* = 8.4 Hz, 1H), 3.73 (s, 2H), 3.72 (s, 3H);

¹³C NMR (126 MHz, CDCl₃) δ 170.3, 134.3, 134.3, 133.6, 131.7, 130.9, 120.4, 52.3, 38.7;

IR (neat) 2952, 1736, 1466, 1435, 1336, 1211, 1164, 1086, 1049, 1011, 811 cm⁻¹;

FTMS (+p NSI) calcd for C₉H₉O₂BrCl (M+H)⁺ 262.9469 found 262.9468.



Methyl 2-(5-bromo-2-chlorophenyl)-2-diazoacetate (52c)

A dry 250 mL round-bottom flask was charged with methyl 2-(5-bromo-2-chlorophenyl)acetate (790.6 mg, 3 mmol, 1.0 equiv) and *p*-ABSA (1.08 g, 4.5 mmol, 1.5 equiv). After the flask was flushed with argon gas (3 times), 10 mL of acetonitrile was added via syringes. Then, the reaction mixture was cooled to 0 °C via ice bath. DBU (0.9 mL, 50 mmol, 2.0 equiv) was then added into the solution dropwise, and it was stirred for 15 min under 0 °C. After the allowed time passed, the reaction mixture was warmed to room temperature (23 °C) and stirred for another 4 h monitored by TLC. The reaction mixture was then quenched with saturated aqueous NH₄Cl solution and extracted three times with diethyl ether. The combined organic layer was washed with deionized water to remove any residual salts and dried over Na₂SO₄. The crude mixture was concentrated under reduced pressure and purified by flash column chromatography (pentane/ether = 20/1) to provide yellow solid in 96% yield.

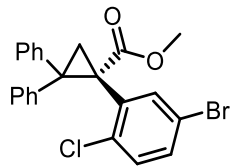
mp: 75-76 °C; **R_f** = 0.56 (hexane/ethyl acetate = 9/1);

¹H NMR (600 MHz, CDCl₃) δ 7.69 (d, *J* = 2.4 Hz, 1H), 7.36 (dd, *J* = 8.6, 2.4 Hz, 1H), 7.24 (d, *J* = 6.4 Hz, 1H), 3.83 (s, 3H);

¹³C NMR (126 MHz, CDCl₃) δ 165.4, 134.6, 132.4, 132.3, 131.3, 125.8, 120.7, 52.4 (The peak of the diazo carbon was not observed);

IR (neat) 2953, 2100, 1708, 1471, 1436, 1394, 1330, 1280, 1241, 1193, 1161, 1090, 1029, 807, 739 cm⁻¹;

FTMS (+p NSI) calcd for C₉H₆N₂O₂BrClNa (M+Na)⁺ 310.9193 found 310.9194.



Methyl (S)-1-(5-bromo-2-chlorophenyl)-2,2-diphenylcyclopropane-1-carboxylate (53b)

An oven-dried 250 mL round-bottom flask was charged with $\text{Rh}_2(\text{S-PTAD})_4$ (31 mg, 0.02 mmol, 0.5 mol%) and 1,1-diphenylethylene (3.3 mL, 20 mmol, 5 equiv). After the flask was flushed with argon gas (3 times), 30 mL of dry degassed pentane was added via syringe. Then, the reaction mixture was cooled to 0 °C via ice bath. Methyl 2-(5-bromo-2-chlorophenyl)-2-diazoacetate (1.12 g, 4 mmol, 1.0 equiv) was weighted in a dry 100 mL round-bottom flask and flushed with argon (3 times), then it was dissolved in 70 mL of the dry degassed pentane, which transferred into the flask with syringe pump over 1 h under 0 °C. Then, the reaction mixture was stirred overnight. After monitored by TLC, the reaction mixture was concentrated under vacuum. The residue was purified by flash column chromatography (hexane/ethyl acetate = 100/1 to 12/1) to provide product as white solid in 89% yield.

mp: 56-58 °C; **Rf** = 0.49 (15% diethyl ether in hexane); **$[\alpha]^{20}_{\text{D}}$** : -249.6° (*c* = 1.00, CHCl_3 , 88% ee);

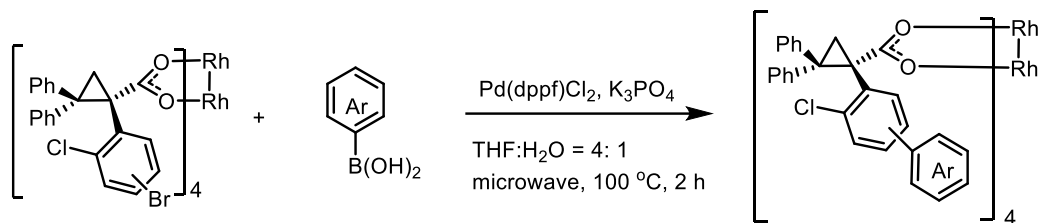
$^1\text{H NMR}$ (600 MHz, CDCl_3) δ 7.52 (d, *J* = 7.5 Hz, 2H), 7.40 – 7.35 (m, 2H), 7.33 – 7.28 (m, 1H), 7.25 – 7.19 (m, 2H), 7.10 (d, *J* = 8.5 Hz, 1H), 7.07 – 7.03 (m, 3H), 6.90 – 6.85 (m, 2H), 3.40 (s, 3H), 2.77 (d, *J* = 6.0 Hz, 1H), 2.47 (d, *J* = 5.9 Hz, 1H);

$^{13}\text{C NMR}$ (126 MHz, CDCl_3) δ 170.2, 141.1, 138.6, 137.1, 136.4, 135.9, 131.5, 130.9, 130.3, 128.4, 128.3, 127.5, 127.2, 126.5, 119.3, 52.4, 45.3, 41.7, 25.9;

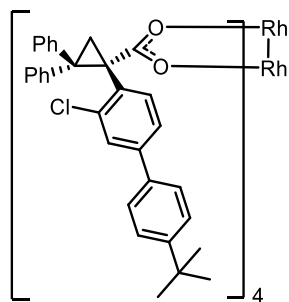
IR (neat) 3059, 3025, 2949, 1724, 1496, 1450, 1297, 1247, 1214, 1143, 908, 729, 703 cm^{-1} ;

FTMS (+p NSI) calcd for $\text{C}_{23}\text{H}_{19}\text{O}_2\text{BrCl}$ ($\text{M}+\text{H}$)⁺ 441.0251 found 441.0248;

HPLC (S,S-Whelk column, 2% *i*-propanol in hexane, 1 mL min^{-1} , 1 mg mL^{-1} . 30 min, UV 254 nm) retention times of 6.67 min (major) and 7.95 min (minor) 88% ee.



An oven-dried microwave reaction tube (G30) was charged with the $\text{Rh}_2(\text{S-2-Cl-4-BrTPCP})_4$ [or $\text{Rh}_2(\text{S-2-Cl-5-BrTPCP})_4$] (95.6 mg, 0.05 mmol, 1.0 equiv), corresponding boronic acid (0.5 mmol, 10 equiv) and K_3PO_4 (255 mg, 1.2 mmol, 24 equiv), followed by 6 mL of THF and 1.5 mL of DI H_2O . After the reaction vessel was purged with argon (bubbling argon gas until addition 1 ml THF evaporated), $\text{Pd}(\text{dppf})\text{Cl}_2$ (7.4 mg, 0.01 mmol, 20 mol%) was added and the septum was replaced with a new one. The reaction mixture was irradiated in a Biotage microwave to 100 °C for 2 h. The resulted green solution was concentrated and extracted with DCM (3 times). The organic layer was concentrated and purified by flash column chromatography (hexane/dichloromethane = 4/1 to 1/1, or hexane/ethyl acetate 19/1 to 5/1) to give the desire product as green solid.



Dirhodium tetrakis((*S*)- 1-(4'-(*tert*-butyl)-3-chloro-[1,1'-biphenyl]-4-yl)-2,2-diphenylcyclopropane-1-carboxylate) (128)

It was obtained in 70% yield following the general procedure above using $\text{Rh}_2(\text{S-2-Cl-4-BrTPCP})_4$ and (4-(*tert*-butyl)phenyl)boronic acid (89 mg).

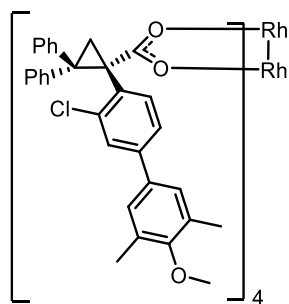
R_f = 0.71 (hexane/ethyl acetate = 4/1);

^1H NMR (600 MHz, CDCl_3) δ 7.51 (dd, $J = 6.6, 2.8$ Hz, 2H), 7.40 – 7.33 (m, 4H), 7.20 – 7.10 (m, 7H), 6.98 – 6.83 (m, 4H), 2.75 (d, $J = 4.6$ Hz, 1H), 2.29 (d, $J = 4.8$ Hz, 1H), 1.31 (d, $J = 5.5$ Hz, 9H);

^{13}C NMR (151 MHz, CDCl_3) δ 187.4, 150.4, 143.4, 140.4, 139.7, 137.0, 136.7, 134.3, 131.4, 130.8, 128.4, 127.6, 127.3, 127.1, 126.6, 125.9, 125.5, 125.2, 124.3, 45.5, 41.5, 34.5, 31.3, 25.4;

IR (neat) 3028, 2960, 2867, 1726, 1574, 1494, 1386, 1271, 907, 731, 711, 694, 552 cm^{-1} ;

FTMS (+p ESI) calcd for $\text{C}_{128}\text{H}_{112}\text{O}_8\text{Cl}_4\text{Rh}_2$ (M) $^+$ 2122.5221 found 2122.5172.



Dirhodium tetrakis((*S*)-1-(3-chloro-4'-methoxy-3',5'-dimethyl-[1,1'-biphenyl]-4-yl)-2,2-diphenylcyclopropane-1-carboxylate) (129)

It was obtained in 54% yield following the general procedure above using $\text{Rh}_2(\text{S-2-Cl-4-BrTPCP})_4$ and (4-methoxy-3,5-dimethylphenyl)boronic acid (90 mg).

R_f = 0.59 (hexane/dichloromethane = 2/3);

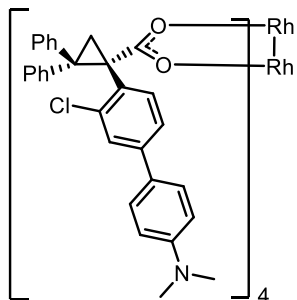
^1H NMR (600 MHz, CDCl_3) δ 7.48 (dt, $J = 21.8, 3.6$ Hz, 2H), 7.22 – 7.07 (m, 9H), 6.99 (s, 1H), 6.93 – 6.83 (m, 3H), 3.65 (d, $J = 30.5$ Hz, 3H), 2.73 (d, $J = 4.2$ Hz, 1H), 2.28 (d, $J = 4.5$ Hz, 1H), 2.25 (s, 3H), 2.18 (s, 3H);

^{13}C NMR (151 MHz, CDCl_3) δ 187.3, 156.7, 143.5, 142.9, 140.5, 140.3, 139.8, 137.9, 137.1, 137.0, 135.3, 135.2, 134.5, 134.3, 131.4, 131.3, 131.2, 131.0, 130.9, 130.7, 129.0, 128.5, 128.4,

128.2, 127.5, 127.3, 127.3, 127.2, 127.1, 127.0, 125.9, 125.9, 125.3, 125.1, 124.3, 124.1, 77.2, 59.8, 45.5, 41.5, 25.4, 21.5, 16.1;

IR (neat) 3613, 3056, 2926, 2246, 1585, 1476, 1386, 1237, 1016, 909, 732, 694 cm^{-1} ;

FTMS (+p ESI) calcd for $\text{C}_{124}\text{H}_{104}\text{O}_{12}\text{Cl}_4\text{Rh}_2$ (M)⁺ 2130.4392 found 2130.4327.



Dirhodium tetrakis((*S*)-1-(3-chloro-4'-(dimethylamino)-[1,1'-biphenyl]-4-yl)-2,2-diphenylcyclopropane-1-carboxylate) (130)

It was obtained in 50% yield following the general procedure above using $\text{Rh}_2(\text{S-2-Cl-4-BrTPCP})_4$ and (4-(dimethylamino)phenyl)boronic acid (82.5 mg).

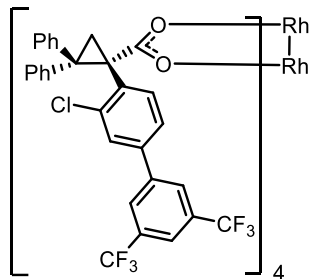
R_f = 0.57 (hexane/dichloromethane = 2/3);

¹H NMR (400 MHz, CDCl₃) δ 7.42 – 7.32 (m, 4H), 7.19 – 7.05 (m, 10H), 6.97 – 6.89 (m, 3H), 3.05 – 2.62 (m, 3H), 2.59 (d, *J* = 6.3 Hz, 1H), 2.22 (d, *J* = 6.1 Hz, 1H), 2.19 – 2.14 (m, 1H), 1.99 – 1.91 (m, 2H);

¹³C NMR (100 MHz, CDCl₃) δ 187.4, 154.2, 143.0, 142.4, 142.2, 139.9, 139.3, 137.7, 136.5, 131.4, 131.1, 127.3, 127.2, 126.2, 125.8, 125.3, 120.1, 119.5, 46.0, 45.3, 41.4, 41.2, 25.0;

IR (neat) 3024, 2921, 2850, 1739, 1587, 1491, 1376, 1150, 1045, 812, 734, 692, 509 cm^{-1} ;

FTMS (+p ESI) calcd for $\text{C}_{120}\text{H}_{100}\text{O}_8\text{N}_4\text{Cl}_4\text{Rh}_2$ (M)⁺ 2070.4405 found 2070.4368.



Dirhodium tetrakis((*S*)-1-(3-chloro-3',5'-bis(trifluoromethyl)-[1,1'-biphenyl]-4-yl)-2,2-diphenylcyclopropane-1-carboxylate) (131)

It was obtained in 68% yield following the general procedure above using $\text{Rh}_2(\text{S-2-Cl-4-BrTPCP})_4$ and (3,5-bis(trifluoromethyl)phenyl)boronic acid (129 mg).

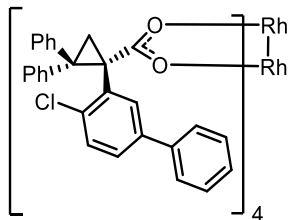
Rf = 0.54 (hexane/dichloromethane = 2/3);

^1H NMR (600 MHz, CDCl_3) δ 7.85 – 7.77 (m, 3H), 7.54 – 7.45 (m, 2H), 7.32 – 7.27 (m, 2H), 7.25 (d, J = 1.8 Hz, 1H), 7.23 – 7.14 (m, 5H), 6.98 (dd, J = 8.5, 6.9 Hz, 2H), 6.95 – 6.89 (m, 1H), 2.84 (d, J = 4.9 Hz, 1H), 2.38 (d, J = 4.8 Hz, 1H);

^{13}C NMR (151 MHz, CDCl_3) δ 187.8, 143.1, 142.5, 141.4, 139.2, 137.7, 136.7, 132.1 (q, J = 33.4 Hz), 131.5, 131.2, 128.4, 127.7, 127.4, 127.3, 126.9, 126.3, 125.9, 124.7, 123.2 (d, J = 272.7 Hz), 121.2, 46.1, 41.6, 25.6;

IR (neat) 3618, 3058, 1738, 1585, 1496, 1383, 1279, 1185, 1136, 701 cm^{-1} ;

FTMS (+p ESI) calcd for $\text{C}_{120}\text{H}_{72}\text{O}_8\text{F}_{24}\text{Cl}_4\text{Rh}_2$ (M) $^+$ 2442.1708 found 2442.1624.



Dirhodium tetrakis((*S*)-1-(4-chloro-[1,1'-biphenyl]-3-yl)-2,2-diphenylcyclopropane-1-carboxylate) (132)

It was obtained in 65% yield following the general procedure above using $\text{Rh}_2(\text{S-2-Cl-5-BrTPCP})_4$ and phenylboronic acid (61 mg).

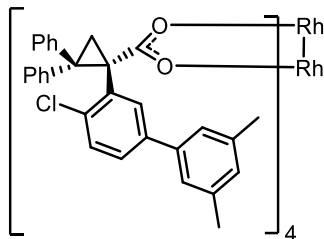
Rf = 0.40 (hexane/ethyl acetate = 4/1);

^1H NMR (600 MHz, CDCl_3) δ 7.55 – 7.51 (m, 2H), 7.50 – 7.41 (m, 5H), 7.38 – 7.32 (m, 1H), 7.22 – 7.13 (m, 4H), 7.10 – 7.05 (m, 2H), 6.98 (d, J = 8.2 Hz, 1H), 6.96 – 6.90 (m, 3H), 2.75 (d, J = 4.9 Hz, 1H), 2.35 (d, J = 4.8 Hz, 1H);

^{13}C NMR (151 MHz, CDCl_3) δ 188.0, 142.5, 140.3, 139.2, 138.9, 136.3, 135.9, 131.5, 130.1, 129.1, 128.7, 128.5, 127.3, 127.3, 127.0, 127.0, 126.4, 125.9, 125.6, 45.3, 42.4, 25.8;

IR (neat) 3609, 3086, 3057, 3028, 1740, 1585, 1470, 1400, 1380, 1042, 909, 760, 695 cm^{-1} ;

FTMS (+p ESI) calcd for $\text{C}_{112}\text{H}_{80}\text{O}_8\text{Cl}_4\text{Rh}_2$ (M)⁺ 1898.2717 found 1898.2694.



Dirhodium tetrakis((*S*)-1-(4-chloro-3',5'-dimethyl-[1,1'-biphenyl]-3-yl)-2,2-diphenylcyclopropane-1-carboxylate) (133)

It was obtained in 66% yield following the general procedure above using $\text{Rh}_2(\text{S-2-Cl-5-BrTPCP})_4$ and (3,5-dimethylphenyl)boronic acid (75 mg).

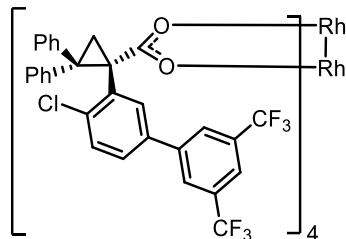
R_f = 0.54 (hexane/ethyl acetate = 4/1);

¹H NMR (600 MHz, CDCl₃) δ 7.51 – 7.47 (m, 2H), 7.40 (d, J = 2.2 Hz, 1H), 7.21 – 7.08 (m, 9H), 7.00 (dq, J = 1.7, 0.9 Hz, 1H), 6.95 – 6.89 (m, 3H), 2.79 (d, J = 4.9 Hz, 1H), 2.40 (s, 6H), 2.34 (d, J = 4.8 Hz, 1H);

¹³C NMR (151 MHz, CDCl₃) δ 187.9, 142.7, 140.4, 139.4, 139.0, 138.2, 136.0, 135.8, 131.4, 129.8, 129.1, 128.9, 128.5, 127.3, 127.0, 126.5, 125.9, 125.5, 124.9, 77.2, 45.5, 42.3, 25.7, 21.5;

IR (neat) 3619, 3055, 3024, 2929, 1735, 1588, 1376, 819, 732, 703 cm^{-1} ;

FTMS (+p ESI) calcd for $\text{C}_{120}\text{H}_{96}\text{O}_8\text{Cl}_4\text{Rh}_2$ (M)⁺ 2010.3969 found 2010.4002.



Dirhodium tetrakis((*S*)-1-(4-chloro-3',5'-bis(trifluoromethyl)-[1,1'-biphenyl]-3-yl)-2,2-diphenylcyclopropane-1-carboxylate) (134)

It was obtained in 66% yield following the general procedure above using $\text{Rh}_2(\text{S-2-Cl-5-BrTPCP})_4$ and (3,5-bis(trifluoromethyl)phenyl)boronic acid (129 mg).

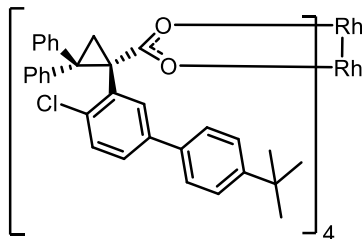
Rf = 0.5 (hexane/dichloromethane = 1/1);

^1H NMR (600 MHz, CDCl_3) δ 7.92 (d, J = 1.8 Hz, 2H), 7.54 – 7.48 (m, 2H), 7.37 – 7.29 (m, 2H), 7.22 – 7.10 (m, 7H), 6.95 (dddt, J = 12.6, 8.4, 7.2, 2.7 Hz, 3H), 2.86 (d, J = 4.9 Hz, 1H), 2.41 (d, J = 4.9 Hz, 1H);

^{13}C NMR (151 MHz, CDCl_3) δ 187.7, 142.4, 141.9, 137.8, 136.8, 135.9, 132.1 (q, J = 33.1 Hz), 131.2, 130.2, 130.0, 128.3, 128.0, 127.4, 127.0, 126.8, 126.4, 125.7, 124.3, 122.5, 121.0, 120.7, 119.2, 46.2, 41.9, 35.3;

IR (neat) 3620, 3058, 2931, 1735, 1580, 1375, 1279, 1183, 1135, 704 cm^{-1} ;

FTMS (+p ESI) calcd for $\text{C}_{120}\text{H}_{72}\text{O}_8\text{F}_{24}\text{Cl}_4\text{Rh}_2$ (M)⁺ 2442.1708 found 2442.1735.



Dirhodium tetrakis((*S*)-1-(4'-(*tert*-butyl)-4-chloro-[1,1'-biphenyl]-3-yl)-2,2-diphenylcyclopropane-1-carboxylate) (135)

It was obtained in 67% yield following the general procedure above using $\text{Rh}_2(\text{S-2-Cl-4-BrTPCP})_4$ and (4-(*tert*-butyl)phenyl)boronic acid (89 mg).

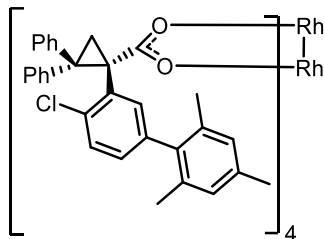
R_f = 0.48 (hexane/dichloromethane = 3/2);

¹H NMR (600 MHz, CDCl₃) δ 7.48 (td, J = 10.0, 8.6, 5.2 Hz, 7H), 7.23 – 7.13 (m, 4H), 7.11 – 7.06 (m, 2H), 7.02 (d, J = 8.3 Hz, 1H), 6.96 – 6.88 (m, 3H), 2.75 (d, J = 4.8 Hz, 1H), 2.34 (d, J = 4.8 Hz, 1H), 1.38 (s, 9H);

¹³C NMR (151 MHz, CDCl₃) δ 188.0, 150.4, 142.6, 139.3, 138.6, 137.4, 136.1, 135.7, 131.5, 129.8, 129.2, 128.6, 128.3, 127.3, 127.0, 126.6, 126.2, 125.9, 125.6, 45.4, 42.4, 34.6, 31.4;

IR (neat) 3619, 3537, 3056, 2960, 2868, 1728, 1585, 1472, 1379, 1112, 909, 840, 731, 703 cm^{-1} ;

FTMS (+p ESI) calcd for $\text{C}_{128}\text{H}_{112}\text{O}_8\text{Cl}_4\text{Rh}_2$ (M)⁺ 2122.5221 found 2122.5153.



Dirhodium tetrakis((*S*)-1-(4-chloro-2',4',6'-trimethyl-[1,1'-biphenyl]-3-yl)-2,2-diphenylcyclopropane-1-carboxylate) (136)

It was obtained in 67% yield following the general procedure above using $\text{Rh}_2(\text{S-2-Cl-4-BrTPCP})_4$ and mesitylboronic acid (82 mg).

Rf = 0.44 (hexane/dichloromethane = 1/1);

$^1\text{H NMR}$ (600 MHz, CDCl_3) δ 7.50 – 7.42 (m, 2H), 7.20 – 7.08 (m, 5H), 6.95 – 6.84 (m, 7H), 6.70 (dd, $J = 8.0, 2.1$ Hz, 1H), 2.68 (d, $J = 4.9$ Hz, 1H), 2.33 (s, 3H), 2.26 (d, $J = 4.8$ Hz, 1H), 1.98 (s, 3H), 1.70 (s, 3H);

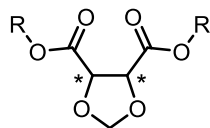
$^{13}\text{C NMR}$ (151 MHz, CDCl_3) δ 187.6, 142.7, 139.7, 138.7, 138.1, 136.8, 136.4, 136.0, 135.2, 131.7, 131.2, 130.2, 128.9, 128.5, 128.3, 127.9, 127.8, 127.2, 127.1, 125.9, 125.5, 45.7, 41.9, 35.3, 21.1, 20.9, 20.3;

IR (neat) 3618, 3056, 2921, 1734, 1586, 1468, 1400, 1380, 1044, 825, 703 cm^{-1} ;

FTMS (+p ESI) calcd for $\text{C}_{124}\text{H}_{104}\text{O}_8\text{Cl}_4\text{Rh}_2$ (M) $^+$ 2066.4595 found 2066.4632.

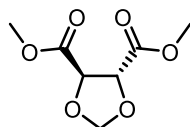
Starting Materials

Synthesis for 1,3-Dioxolane-4,5-dicarboxylate



These products were prepared according to a literature protocol.²¹³

A 250 mL round-bottom flask with condenser was charged with corresponding tartrate (50 mmol, 1.0 equiv). 100 mL Ethyl acetate was added for dissolving, and then dimethoxymethane (60 mmol, 1.2 equiv) and $\text{BF}_3\text{-Et}_2\text{O}$ (125 mmol, 2.5 equiv) were added to the solution. The resulting mixture was refluxed for 7 h. The reaction was then cooled to room temperature and carefully quenched with saturated sodium bicarbonate solution. The organic layer was washed with H_2O , brine and dried over MgSO_4 . The organic liquid was concentrated and purified by flash column chromatography (hexane/ethyl acetate = 9/1) to afford products in white solid.



Dimethyl (4*R*,5*R*)-1,3-dioxolane-4,5-dicarboxylate (**42**)

Prepared according to the general procedure above for 1,3-dioxolane-4,5-dicarboxylate using (+)-dimethyl L-tartrate.

Colorless oil: **R_f** = 0.23 (hexane/ethyl acetate = 4/1); **[α]²⁰_D**: -18.4° (c = 1.55, CHCl_3);

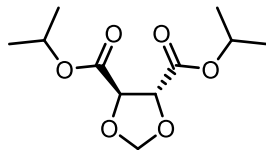
¹H NMR (400 MHz, CDCl_3) δ 5.26 (s, 2H), 4.78 (s, 2H), 3.83 (s, 6H);

¹³C NMR (100 MHz, CDCl_3) δ 169.5, 97.3, 76.5, 52.7;

IR (neat) 2959, 2902, 1740, 1228 cm^{-1} ;

FTMS (+p NSI) calcd for $\text{C}_7\text{H}_{11}\text{O}_6$ (M+H)⁺ 191.05501 found 191.0548.

Its (4*S*,5*S*) enantiomer **44** was prepared using (-)-di-methyl D-tartrate: White solid (**[α]²⁰_D**: +23.1° (c = 1.02, CHCl_3); **mp** 28-30 °C).



Di-*iso*-propyl (4*R*,5*R*)-1,3-dioxolane-4,5-dicarboxylate (43)

Prepared according to the general procedure for 1,3-dioxolane-4,5-dicarboxylate using (+)-di-*iso*-propyl L-tartrate.

mp: 38-39 °C; **R_f** = 0.43 (hexane/ethyl acetate = 4/1); **[α]²⁰_D:** -14.8° (c = 1.17, CHCl₃);

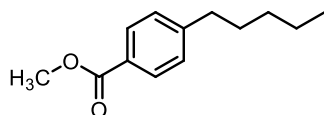
¹H NMR (400 MHz, CDCl₃) δ 5.24 (s, 2H), 5.12 (p, *J* = 6.3 Hz, 2H), 4.63 (s, 2H), 1.29 (d, *J* = 6.3, 12H);

¹³C NMR (100 MHz, CDCl₃) δ 168.8, 97.4, 76.9, 69.8, 21.7;

IR (neat) 2982, 2945, 1738, 1233 cm⁻¹;

FTMS (+p NSI) calcd for C₁₁H₁₉O₆ (M+H)⁺ 247.1176 found 247.1175.

Its (4*S*,5*S*) enantiomer **45** was prepared using (-)-di-*iso*-propyl D-tartrate: White solid (**[α]²⁰_D:** +16.7° (c = 1.36, CHCl₃); **mp** 43-44 °C).



Methyl 4-pentylbenzoate (100)

A dry 50-mL round-bottom flask was charged with 4-*n*-pentylbenzoic acid (961.3 mg, 5 mmol, 1.0 equiv). After the flask was flushed with argon gas (3 times), 10 mL of anhydrous methanol was added via syringes slowly. Then, the reaction mixture was cooled to 0 °C via ice bath. The acetyl chloride (0.43 mL, 6 mmol, 1.2 equiv) was then added into the solution dropwise at 0 °C. The reaction mixture was warmed to room temperature (23 °C) and stirred overnight. The reacted solution was poured into a separation funnel containing ethyl ether and saturated NH₄Cl. The

NH₄Cl layer was then extracted twice with diethyl ether. The combined organic layer was concentrated under reduced pressure and purified by flash column chromatography (pentane/diethyl ether = 20/1) to afford the colorless oil in 92% yield.

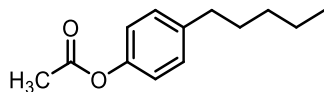
R_f = 0.63 (pentane/diethyl ether = 19/1);

¹H NMR (600 MHz, CDCl₃) δ 7.95 (d, *J* = 8.2 Hz, 2H), 7.24 (d, *J* = 8.0 Hz, 2H), 3.90 (s, 3H), 2.70 – 2.62 (m, 2H), 1.63 (p, *J* = 7.6 Hz, 2H), 1.39 – 1.27 (m, 4H), 0.89 (t, *J* = 7.0 Hz, 3H);

¹³C NMR (151 MHz, CDCl₃) δ 167.4, 148.7, 129.8, 128.6, 127.7, 52.1, 36.1, 31.6, 31.0, 22.7, 14.2;

IR (neat) 2930, 2858, 1720, 1273, 1107, 762, 703 cm⁻¹;

HRMS (+p APCI) calcd for C₁₃H₁₉O₂ (M+H)⁺ 207.1380 found 207.1379.



4-Pentylphenyl acetate (101)

The synthesis is adapted from literature:²¹⁴ A dry 10-mL round-bottom flask was charged with 4-*n*-pentylphenol (1.64 g, 10 mmol, 1.0 equiv). After the flask was flushed with argon gas (3 times), acetic anhydride (1.42 ml, 15 mmol, 1.5 equiv) and pyridine (0.5 ml, 6 mmol, 0.6 equiv) were added. Then, the reaction mixture was stirred at room temperature (23 °C) until the full consumption of 4-*n*-pentylphenol (35 mins by TLC monitoring). The resulting solution was poured into an Erlenmeyer flask with 80 mL of DI H₂O and stirred vigorously for 30 mins. The mixture was then extracted with ethyl acetate (50 mL X 3) and the combined organic layer was washed sequentially with aqueous HCl (1 M), saturated aqueous NaHCO₃, DI H₂O and brine. The collected solution was dried over Na₂SO₄ and concentrated under reduced pressure to afford the pure product as colorless oil in 94% yield.

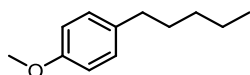
R_f = 0.64 (pentane/diethyl ether = 4/1);

¹H NMR (600 MHz, CDCl₃) δ 7.17 (d, *J* = 8.7 Hz, 2H), 6.98 (d, *J* = 8.5 Hz, 2H), 2.63 – 2.54 (m, 2H), 2.28 (s, 3H), 1.65 – 1.56 (m, 2H), 1.39 – 1.25 (m, 4H), 0.89 (t, *J* = 7.0 Hz, 3H);

¹³C NMR (151 MHz, CDCl₃) δ 169.8, 148.7, 140.6, 129.4, 121.3, 35.5, 31.6, 31.3, 22.7, 21.3, 14.2;

IR (neat) 2956, 2929, 2858, 1761, 1507, 1368, 1213, 1191, 1165, 910 cm⁻¹;

HRMS (+p NSI) calcd for C₁₃H₁₉O₂ (M+H)⁺ 207.1380 found 207.1380.



1-Methoxy-4-pentylbenzene (102)

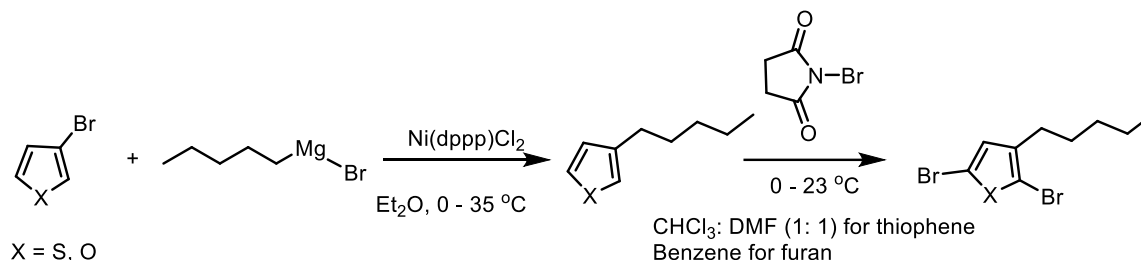
The synthesis is adapted from literature:²¹⁵ A dry 10-mL round-bottom flask was charged with 2-bromopentane (2.49 mL, 20 mmol, 1.0 equiv), CoCl₂ (130 mg, 1 mmol, 5 mol%) and TMEDA (0.14 mL, 1 mmol, 5 mol%). After the flask was flushed with argon gas (3 times), 10 mL of anhydrous THF was added and the solution was cooled to 0 °C via ice bath. 4-Methoxyphenylmagnesium bromide (0.5 M in THF, 44 ml, 22 mmol, 1.1 equiv) was added to the reaction mixture slowly over 50 mins. Then, the reaction mixture was stirred at 0 °C for another 30 mins. The resulting solution was quenched with 20 mL of aqueous HCl (1 M) and extracted with diethyl ether (50 mL X 3). The combined organic layer was dried over Na₂SO₄ and concentrated under reduced pressure. The product was purified by distillation under reduced pressure (Kugelrogr, 92 °C at 0.7 mbar) to afford the pure product as colorless oil in 90% yield.

¹H NMR (600 MHz, CDCl₃) δ 7.09 (d, *J* = 8.9 Hz, 2H), 6.82 (d, *J* = 8.6 Hz, 2H), 3.78 (s, 3H), 2.58 – 2.48 (m, 2H), 1.62 – 1.54 (m, 2H), 1.38 – 1.26 (m, 4H), 0.89 (t, *J* = 7.1 Hz, 3H);

¹³C NMR (151 MHz, CDCl₃) δ 157.6, 135.1, 129.2, 113.6, 55.2, 35.0, 31.5, 31.4, 22.6, 14.0;

IR (neat) 2955, 2927, 2855, 1612, 1510, 1464, 1243, 1175, 1038, 828, 807 cm^{-1} ;

HRMS (+p NSI) calcd for $\text{C}_{12}\text{H}_{19}\text{O}$ ($\text{M}+\text{H}$)⁺ 179.1430 found 179.1431.

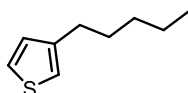


The synthesis for 2,5-dibromo-3-n-pentylthiophene and 2,5-dibromo-3-n-pentylfuran is adapted from literature:^{216, 217} (reactions were done in dark and products were used immediately)

A 250-mL flame-dried round-bottom flask was charged with $\text{Ni}(\text{dppp})\text{Cl}_2$ (81 mg, 0.15 mmol, 0.5 mol%) and 3-bromothiophene (or 3-bromofuran, 30 mmol, 1.0 equiv). After the flask was flushed with argon, 30 mL of distilled diethyl ether was added to dissolve the mixture. Then, the mixture was cooled to 0 °C via ice bath, followed by the addition of n-pentylmagnesium bromide solution (2.0 M in diethyl ether, 60 mL, 4.0 equiv) slowly by syringe pump. After the addition, the mixture was heated to reflux (35 °C) for overnight. The resulted solution was quenched by adding DI H_2O dropwise at 0 °C until no bubble generate and extracted by hexane (3x100 mL). After dried over Na_2SO_4 , the crude product was concentrated under reduced pressure and purified by flash column chromatography (hexane) to provide colorless oil of 3-n-pentylthiophene in 63% yield (or 3-n-pentylfuran in 58% yield).

The product from last step was dissolved in 60 mL of corresponding anhydrous solvents in a 100 mL flame-dried 3-neck round-bottom flask under argon. Then, N-bromosuccinimide (2.2 equiv) was added slowly at 0 °C and the resulted mixture was stirred overnight at room temperature (23 °C). The reacted solution was quenched by DI H_2O and $\text{Na}_2\text{S}_2\text{O}_3$, followed by the extraction by

hexane (3x50 mL). After dried over Na₂SO₄, the crude product was concentrated under reduced pressure and purified by flash column chromatography (hexane) to provide colorless oil of 2,5-dibromo-3-n-pentylthiophene in 75% yield (or 2,5-dibromo-3-n-pentylfuran in 60% yield).



3-*n*-Pentylthiophene

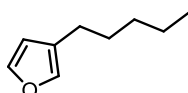
R_f = 0.72 (hexane);

¹H NMR (600 MHz, CDCl₃) δ 7.23 (dd, *J* = 4.9, 2.9 Hz, 1H), 6.94 (dd, *J* = 4.9, 1.3 Hz, 1H), 6.92 (dq, *J* = 3.1, 1.0 Hz, 1H), 2.65 – 2.59 (m, 2H), 1.62 (p, *J* = 7.6 Hz, 2H), 1.38 – 1.28 (m, 4H), 0.90 (t, *J* = 7.0 Hz, 3H);

¹³C NMR (151 MHz, CDCl₃) δ 143.4, 128.4, 125.2, 119.9, 31.7, 30.4, 22.7, 14.2;

IR (neat) 2956, 2926, 2857, 1458, 860, 834, 771, 681 cm⁻¹;

HRMS (+p APCI) calcd for C₉H₁₅S (M+H)⁺ 155.0889 found 155.0889.



3-*n*-Pentylfuran

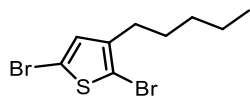
R_f = 0.67 (hexane);

¹H NMR (600 MHz, CDCl₃) δ 7.34 (s, 1H), 7.20 (s, 1H), 6.26 (s, 1H), 2.40 (t, *J* = 7.7 Hz, 2H), 1.56 (q, *J* = 7.0 Hz, 2H), 1.37 – 1.28 (m, 4H), 0.90 (t, *J* = 6.5 Hz, 3H);

¹³C NMR (151 MHz, CDCl₃) δ 142.7, 138.9, 125.5, 111.2, 31.7, 29.9, 24.9, 22.6, 14.2;

IR (neat) 2957, 2928, 2859, 1759, 1465, 1341, 1065, 945 cm⁻¹;

HRMS (+p APCI) calcd for C₉H₁₅O (M+H)⁺ 139.1117 found 139.1118.



2,5-Dibromo-3-*n*-pentylthiophene

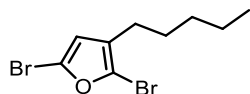
R_f = 0.85 (hexane);

¹H NMR (600 MHz, CDCl₃) δ 6.78 (s, 1H), 2.53 – 2.48 (m, 2H), 1.58 – 1.51 (m, 2H), 1.37 – 1.26 (m, 4H), 0.90 (t, *J* = 7.1 Hz, 3H);

¹³C NMR (151 MHz, CDCl₃) δ 143.2, 131.1, 110.4, 108.1, 31.4, 29.6, 29.4, 22.6, 14.1;

IR (neat) 2955, 2926, 2857, 1541, 1465, 1418, 1004, 824 cm⁻¹;

HRMS (-p NSI) calcd for C₉H₁₁Br₂S (M-H)⁻ 308.8954 found 308.8939.



2,5-Dibromo-3-*n*-pentylfuran:

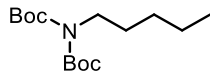
R_f = 0.71 (hexane);

¹H NMR (600 MHz, CDCl₃) δ 6.23 (s, 1H), 2.34 – 2.27 (m, 2H), 1.50 (p, *J* = 7.5 Hz, 2H), 1.37 – 1.25 (m, 4H), 0.89 (t, *J* = 7.1 Hz, 3H);

¹³C NMR (151 MHz, CDCl₃) δ 127.5, 121.3, 119.7, 114.9, 31.3, 29.0, 25.3, 22.5, 14.1;

IR (neat) 2956, 2929, 2858, 1592, 1493, 1466, 1135, 1105, 1077, 930, 804 cm⁻¹;

HRMS (+p NSI) calcd for C₉H₁₂Br₂O (M)⁺ 293.9249 found 293.9244.



***N,N*-di-Boc-pentylamine**

In a dry 100 mL round-bottom flask, amylamine (3.5 mL, 30 mmol, 1.0 equiv) and 4-dimethylaminopyridine (366.5 mg, 3 mmol, 0.1 equiv) was dissolved in 17 mL of acetonitrile under argon. After the slow addition of di-*tert*-butylpyrocarbonate (Boc₂O, 6.5 g, 30 mmol, 1.0 equiv) in 5 mL acetonitrile, the mixture was stirred at room temperature overnight. Then, the reaction mixture was diluted with 6 mL of toluene and concentrated at 60 °C under reduced pressure. The residue was dissolved in 13 mL of acetonitrile, the second portion of 4-dimethylaminopyridine (366.5 mg, 3 mmol, 0.1 equiv) was added, followed by another slow addition of di-*tert*-butylpyrocarbonate (Boc₂O, 6.5 g, 30 mmol, 1.0 equiv) in 5 mL acetonitrile. The resulted mixture was heated to 60 °C and stirred for 16 h. The residue obtained from concentration was re-dissolved in dichloromethane (50 mL) and NaHCO₃ (diluted aqueous solution, 20 mL). The combined solution in dichloromethane, which is generated from the extraction of the aqueous layer, was washed with brine and dried over Na₂SO₄. The crude mixture was concentrated under reduced pressure and purified on a RediSepRf 80 g SiO₂ Isolera column with 0-5% ethyl acetate in hexanes of 30 column volumes to provide colorless oil in 62% yield.

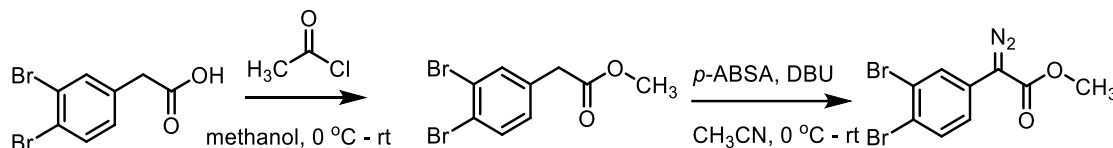
Rf = 0.50 (hexane/ethyl acetate = 9/1);

¹H NMR (600 MHz, CDCl₃) δ 3.58 – 3.51 (m, 2H), 1.58 – 1.54 (m, 2H), 1.50 (s, 18H), 1.36 – 1.29 (m, 2H), 1.29 – 1.23 (m, 2H), 0.89 (t, *J* = 7.2 Hz, 3H);

¹³C NMR (151 MHz, CDCl₃) δ 152.7, 82.0, 46.5, 29.0, 28.7, 28.1, 22.4, 14.1;

IR (neat) 2960, 2933, 2159, 2029, 1976, 1719, 1698, 1367, 1126, 912, 736 cm⁻¹;

FTMS (+p NSI) calcd for C₁₅H₃₀NO₄ (M+H)⁺ 288.21693 found 288.2170.



Methyl 2-diazo-2-(3,4-dibromophenyl)acetate (96)

In a 250 mL round-bottom flask with argon atmosphere inside, 2-(3,4-dibromophenyl)acetic acid (4.6 g, 15.6 mmol, 1.0 equiv) was dissolved in 100 mL of methanol and cooled to 0 °C via ice bath. Acetyl chloride (2 mL, 18.8 mmol, 1.2 equiv) was added via a syringe. The reaction mixture was stirred for 15 hours, at which point it was warmed up to room temperature (23 °C). The reacted mixture was diluted with 100 mL of ethyl acetate and washed with NaHCO₃. The organic layer was concentrated under reduced pressure and purified by flash column chromatography (10% ethyl acetate in hexane) to afford the orange solid in 93% yield (4.5 g). It was used immediately in the next step.

Methyl 2-(3,4-dibromophenyl)acetate (3.0 g, 9.7 mmol) was added in a flame-dried round-bottom flask, together with *p*-ABSA (3.03 g, 12.6 mmol, 1.3 equiv). After the flask was flushed with argon gas (3 times), 50 mL of dry acetonitrile was added to the mixture for dissolving. Then, the reaction mixture was cooled to 0 °C via ice bath. DBU (2.0 mL, 12.6 mmol, 1.3 equiv) was added dropwise at 0 °C. The mixture was allowed to stir at 0 °C for an additional 15 min, followed by 24 hours at room temperature (23 °C) after removing the ice bath. The resulting orange solution was quenched with 60 mL of saturated aqueous NH₄Cl. The aqueous layer was extracted with diethyl ether (50 mL X 3) and the combined organic layer was washed with brine. Then, it was concentrated under reduced pressure and purified by flash column chromatography (5-8% diethyl ether in hexane) to provide orange solid in 95% yield (3.1 g).

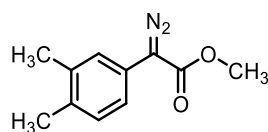
R_f = 0.20 (5% diethyl ether in hexane);

¹H NMR (500 MHz, CDCl₃) δ 7.77 (d, *J* = 2.3 Hz, 1H), 7.57 (d, *J* = 8.5 Hz, 1H), 7.25 (dd, *J* = 8.6, 2.3 Hz, 1H), 3.87 (s, 3H);

¹³C NMR (126 MHz, CDCl₃) δ 164.8, 133.9, 128.3, 126.9, 125.6, 123.5, 121.4, 52.4 (The resonance resulting from the diazo carbon was not observed);

IR (neat) 3091, 3005, 2952, 2092, 1702, 1470, 1358, 1238, 1196, 1160, 1049, 806, 737 cm⁻¹;

HRMS (+p ESI) calcd for C₉H₇Br₂N₂O₂ (M+H)⁺ 332.8869 found 332.8872.



Methyl 2-(3,4-methylphenyl)-2-diazoacetate (64)

Methyl 2-(3,4-dimethylphenyl)acetate (891.2 mg, 5 mmol, 1.0 equiv) was added in a flame-dried round-bottom flask, together with *p*-ABSA (1.80 g, 7.5 mmol, 1.5 equiv). After the flask was flushed with argon gas (3 times), 20 mL of acetonitrile was added via syringes. Then, the reaction mixture was cooled to 0 °C via ice bath. DBU (0.18 mL, 10 mmol, 2.0 equiv) was then added into the solution dropwise, and it was stirred for 15 min under 0 °C. After the allowed time passed, the reaction mixture was warmed to room temperature (23 °C) and stirred for another 4 h monitored by TLC. The reaction mixture was then quenched with saturated aqueous NH₄Cl solution and extracted three times with diethyl ether. The combined organic layer was washed with deionized water to remove any residual salts and dried over Na₂SO₄. The crude mixture was concentrated under reduced pressure and purified by flash column chromatography (pentane/ether = 20/1) to provide yellow solid in 54% yield.

R_f = 0.38 (5% diethyl ether in hexane);

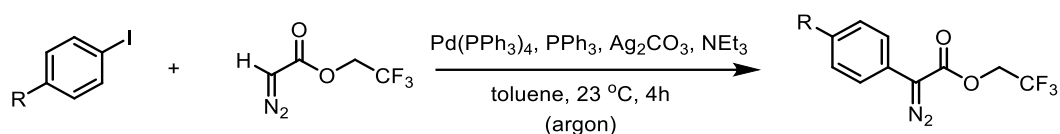
¹H NMR (600 MHz, CDCl₃) δ 7.25 (d, *J* = 2.0 Hz, 1H), 7.21 (dd, *J* = 7.9, 2.1 Hz, 1H), 7.16 (d, *J* = 8.0 Hz, 1H), 3.86 (s, 3H), 2.28 (s, 3H), 2.26 (s, 4H);

¹³C NMR (151 MHz, CDCl₃) δ 165.9, 137.3, 134.5, 130.2, 125.4, 122.4, 121.8, 51.9, 19.9, 19.3

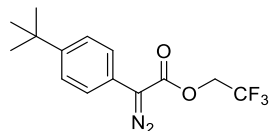
(The resonance resulting from the diazo carbon was not observed);

IR (neat) 2951, 2094, 1698, 1470, 1434, 1283, 1245, 1193, 1158, 1064, 756 cm⁻¹;

HRMS (+p ESI) calcd for C₁₁H₁₂N₂O₂Na (M+Na)⁺ 227.0791 found 227.0789.



The synthesis is adapted from literatures:¹⁷⁹ A 50-mL round-bottom flask was charged with aryl iodide (10 mmol, 1.0 equiv), Pd(PPh₃)₄ (577.8 mg, 0.5 mmol, 5 mol%), PPh₃ (262.3 mg, 1 mmol, 10 mol%) and Ag₂CO₃ (1.38 g, 5 mmol, 0.5 equiv). After the flask was flushed with argon, 40 mL of toluene was added, followed by the addition of NEt₃ (1.8 mL, 13 mmol, 1.3 equiv) and 2,2,2-trifluoroethyl 2-diazoacetate (2.18 g, 13 mmol, 1.3 equiv). The resulted mixture was stirred at room temperature (23 °C) for 4 h and then, filtered through a short silica plug (3.5 cm *diameter*, 5 cm *height*), eluting with ethyl acetate (20 mL). The crude product was concentrated and purified by column chromatography (pentane/diethyl ether = 9/1) to afford 2,2,2-trifluoroethyl 2-(4-(*tert*-butyl)phenyl)-2-diazoacetate as yellow oil in 62% yield (or 2,2,2-trifluoroethyl 2-diazo-2-(4-nitrophenyl)acetate as yellow solid in 65% yield).



2,2,2-Trifluoroethyl 2-(4-(*tert*-butyl)phenyl)-2-diazoacetate

R_f = 0.71 (pentane/diethyl ether = 9/1);

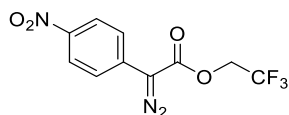
¹H NMR (600 MHz, CDCl₃) δ 7.44 (d, *J* = 8.8 Hz, 2H), 7.38 (d, *J* = 8.6 Hz, 2H), 4.65 (q, *J* = 8.4 Hz, 2H), 1.32 (s, 9H);

¹³C NMR (151 MHz, CDCl₃) δ 163.6, 149.9, 126.3, 124.3, 123.1 (q, *J* = 277.5 Hz); 121.3, 60.4 (q, *J* = 36.9 Hz), 34.7, 31.4 (The resonance resulting from the diazo carbon was not observed);

¹⁹F NMR (282 MHz, CDCl₃) δ -73.9 (t, *J* = 8.3 Hz);

IR (neat) 2966, 2091, 1716, 1410, 1352, 1280, 1244, 1167, 1145, 1111, 1073, 975, 835 cm⁻¹;

HRMS (+p NSI) calcd for C₁₄H₁₅F₃N₂O₂ (M)⁺ 300.1080 found 300.1085.



2,2,2-Trifluoroethyl 2-diazo-2-(4-nitrophenyl)acetate

mp: 83-85 °C; **R_f** = 0.18 (pentane/diethyl ether = 9/1);

¹H NMR (600 MHz, CDCl₃) δ 8.26 (d, *J* = 9.2 Hz, 2H), 7.65 (d, *J* = 9.2 Hz, 2H), 4.69 (q, *J* = 8.2 Hz, 2H);

¹³C NMR (151 MHz, CDCl₃) δ 162.0, 145.7, 132.8, 124.6, 123.5, 122.8 (q, *J* = 277.5 Hz), 60.8 (q, *J* = 37.2 Hz) (The resonance resulting from the diazo carbon was not observed);

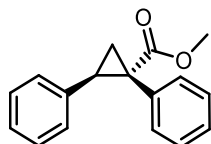
¹⁹F NMR (282 MHz, CDCl₃) δ -73.9 (t, *J* = 8.3 Hz);

IR (neat) 3116, 2100, 1716, 1593, 1514, 1335, 1279, 1236, 1140, 1068, 973, 850, 750 cm⁻¹;

HRMS (+p NSI) calcd for C₁₀H₇F₃N₃O₄ (M+H)⁺ 290.0383 found 290.0388.

Rhodium Carbene Reactions

Cyclopropanation of Styrene



Methyl (1*S*,2*R*)-1,2-diphenylcyclopropane-1-carboxylate (31)

To an oven dried 25 mL round-bottom flask, kept under a dry atmosphere of argon, added styrene (208.3 mg, 2.0 mmol, 5.0 equiv) and $\text{Rh}_2(\text{S-}o\text{-CITPCP})_4$ (6.4 mg, 0.004 mmol, 1 mol%), followed by 1.0 mL of dry and degassed CH_2Cl_2 . The methyl 2-diazo-2-phenylacetate (70.5 mg, 0.4 mmol, 1.0 equiv), which was dissolved in 2.0 mL of dry and degassed CH_2Cl_2 , was then transferred to the reaction flask dropwise over 1 h at room temperature (23 °C). The mixture was stirred overnight after addition. The reaction mixture was concentrated *in vacuo* and ^1H NMR was taken for the crude products for diastereomeric ratio determination. The crude product was purified by flash column chromatography (hexane/ethyl acetate = 100/1) to afford white solid in 57% yield. The NMR spectra are consistent with previously reported data.²¹⁸

^1H NMR (400 MHz, CDCl_3) δ 7.16 – 7.08 (m, 3H), 7.07 – 6.97 (m, 5H), 6.81 – 6.68 (m, 2H), 3.65 (s, 3H), 3.09 (dd, $J = 9.4, 7.3$ Hz, 1H), 2.12 (dd, $J = 9.3, 4.9$ Hz, 1H), 1.86 (dd, $J = 7.3, 4.9$ Hz, 1H);

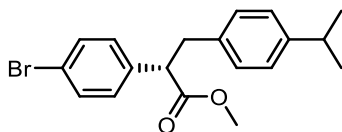
^{13}C NMR (100 MHz, CDCl_3) δ 174.3, 136.3, 134.7, 131.9, 128.0, 127.6, 127.0, 126.3, 52.6, 37.4, 33.1, 20.5;

HPLC (S,S-Whelk column, 1.5% *i*-propanol in hexane, 0.7 mL min^{-1} , 1 mg mL^{-1} . 30 min, UV 230 nm) retention times of 13.00 min (major) and 15.57 min (minor) 24% ee.

*C–H Insertion of *p*-Cymene and 4-Ethyltoluene*

An oven-dried 10 mL round-bottom flask with condenser was charged with Rh₂L₄ catalyst (0.0025 mmol, 0.5 mol%) and corresponding substrate (0.6 mmol, 1.2 equiv). After the flask was flushed with argon gas (3 times), and 1 mL of dry, degassed dichloromethane were added via syringe. Then, the reaction mixture was heated to reflux. Methyl 2-(4-bromophenyl)-2-diazoacetate (0.5 mmol, 1.0 equiv) was weighted in a 20 mL scintillation vial and flushed with argon (3 times). The diazo compound in the vial was dissolved in 1.5 mL of the dry, degassed dichloromethane and transferred to the flask with syringe pump over 1.5 h. The diazo residue was rinsed with 0.5 mL dichloromethane and was transferred into the reaction over 0.5 h. Then, the reaction mixture was refluxed for additional 2.5 h. The reacted solution was cooled down to room temperature and concentrated under vacuum. The crude residue was analyzed by ¹H NMR and purified by flash column chromatography (hexane/ethyl acetate = 50/1) to provide product(s) as colorless oil.

The NMR spectra are consistent with the reported data in a literature.⁷⁹



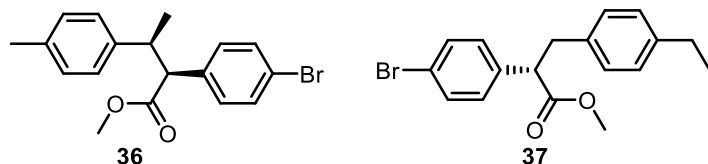
Methyl (*S*)-2-(4-bromophenyl)-3-(4-isopropylphenyl)propanoate (33)

Following the general procedure above using Rh₂(*S*-*o*-CITPCP)₄ as catalyst, it was obtained as major product after flash column chromatography in 72% yield.

¹H NMR (400 MHz, CDCl₃) δ 7.44 (d, *J* = 8.2 Hz, 2H), 7.20 (d, *J* = 8.1 Hz, 2H), 7.12 (d, *J* = 7.2 Hz, 2H), 7.04 (d, *J* = 7.1 Hz, 2H), 3.83 (t, *J* = 7.8 Hz, 1H), 3.62 (s, 3H), 3.38 (dd, *J* = 13.8, 8.5 Hz, 1H), 2.98 (dd, *J* = 13.8, 6.9 Hz, 1H), 2.87 (p, *J* = 6.9 Hz, 1H), 1.24 (d, *J* = 7.2 Hz, 6H);

¹³C NMR (100 MHz, CDCl₃) δ 173.5, 147.0, 137.7, 135.8, 131.7, 129.7, 128.8, 126.5, 121.3, 53.0, 52.1, 39.2, 33.7, 24.0;

HPLC (S,S-Whelk column, 0% *i*-propanol in hexane, 0.5 mL min⁻¹, 1 mg mL⁻¹, 40 min, UV 230 nm) retention times of 24.04 min (minor) and 31.35 min (major) 50% ee.

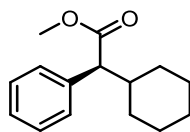


Following the general procedure above using Rh₂(*S*-*o*-CITPCP)₄ as catalyst, **25** and **26** were obtained as 8:1 mixture after flash column chromatography (inseparable) in 75% yield.

HPLC for **36** (S,S-Whelk column, 0.5% *i*-propanol in hexane, 0.25 mL min⁻¹, 1 mg mL⁻¹, 70 min, UV 230 nm) retention times of 49.85 min (minor) and 61.46 min (major) 57% ee.

HPLC for **37** (S,S-Whelk column, 0.3% *i*-propanol in hexane, 0.3 mL min⁻¹, 1 mg mL⁻¹, 100 min, UV 230 nm) retention times of 31.98 min (minor) and 69.51 min (major) 75% ee.

C-H Insertion of Cyclohexane



Methyl (*S*)-2-cyclohexyl-2-phenylacetate (39)

An oven-dried 25 mL round-bottom flask with condenser was charged with Rh₂(*S*-*o*-CITPCP)₄ (6.4 mg, 0.004 mmol, 1 mol%) and degassed by vacuum/argon cycle (3 times). Then, 3 mL of degassed, anhydrous cyclohexane was added for dissolving and the solution was heated to 50 °C. The methyl 2-diazo-2-phenylacetate (70.5 mg, 0.4 mmol, 1.0 equiv) was weighted in a 20 mL vials and dissolved in 8 mL of anhydrous cyclohexane after flushed with argon. The diazo solution was transferred to the reaction flask dropwise over 1.5 h via syringe pump. After the addition, the

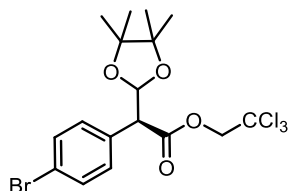
reaction was stirred for overnight at 50 °C. The reacted mixture was then concentrated and purified by flash column chromatography (hexane/ethyl acetate = 50/1) to provide product as colorless oil in 64% yield. The NMR spectra are consistent with the reported data in literature.⁴³

¹H NMR (400 MHz, CDCl₃) δ 7.45 – 7.07 (m, 5H), 3.63 (s, 3H), 3.22 (d, *J* = 10.6 Hz, 1H), 2.01 (m, 1H), 1.84 – 1.52 (m, 4H), 1.30 (m, 2H), 1.20 – 0.97 (m, 3H), 0.80 – 0.65 (m, 1H);

¹³C NMR (100 MHz, CDCl₃) δ 174.4, 137.8, 128.5, 128.4, 127.2, 58.8, 51.7, 41.1, 32.0, 30.4, 26.3, 26.0, 25.9;

HPLC (ODH column, 0.5% *i*-propanol/hexane, 0.5 ml/min, 1 mg mL⁻¹, 30 min, UV 230nm) retention times of 10.32 min (minor) and 11.83 min (major) 14% ee.

C–H Insertion of 1,3-Dioxolane



2,2,2-Trichloroethyl (S)-2-(4-bromophenyl)-2-(4,4,5,5-tetramethyl-1,3-dioxolan-2-yl)acetate (41)

The Rh₂L₄ catalyst (0.004 mmol, 1 mol%) and CaCl₂ (4 mmol, 443.9 mg, 10 equiv) were weighed and purged with argon in an oven-dried 25 mL flask. 4,4,5,5-tetramethyl-1,3-dioxolane (208.3 mg, 1.6 mmol, 4.0 equiv) was weighed, dissolved in 2 mL of dimethylbutane (DMB) and transferred into the reaction flask. The 2,2,2-trichloroethyl 2-(4-bromophenyl)-2-diazoacetate (102.0 mg, 0.4 mmol, 1.0 equiv) was weighed in a separation vial, flushed with argon and dissolved in 10 mL of DMB. After the reaction flask was cooled to 0 °C, the diazo solution was transferred into the reaction flask over 2 h under 0 °C. Then, it was stirred overnight, at which point it was warmed up

to room temperature. After the gravity filtration using cotton (washed with ethyl ether), the solution was concentration and crude ^1H NMR was taken for the crude products using 1,3,5-trimethylbenzene as internal standard. The product was purified by flash column chromatography (pentane/ether = 20/1) to afford colorless oil. (TLC was stained by PMA).

Rf = 0.5 (hexane/ethyl acetate = 9/1);

^1H NMR (400 MHz, CDCl_3) δ 7.47 (d, J = 8.5 Hz, 2H), 7.31 (d, J = 8.3 Hz, 2H), 5.55 (d, J = 7.9 Hz, 1H), 4.79 (d, J = 12.0 Hz, 1H), 4.75 (d, J = 12.0 Hz, 1H), 3.78 (d, J = 7.4 Hz, 1H), 1.18 (s, 12H);

^{13}C NMR (100 MHz, CDCl_3) δ 169.0, 132.5, 131.7, 130.7, 122.2, 100.8, 94.6, 83.0, 82.7, 74.1, 57.8, 23.9, 22.1, 22.0;

IR (neat) 2980, 1754, 1509, 1369, 1147, 1119, 1096, 1057, 1017, 717 cm^{-1} ;

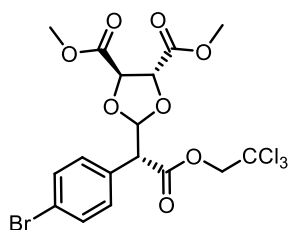
FTMS (+p ESI) calcd for $\text{C}_{17}\text{H}_{21}\text{O}_4\text{BrCl}_3$ $[\text{M}+\text{H}]^+$ 472.9683 found 472.9696;

HPLC (ADH column, 0.7% *i*-propanol/hexane, 1.0 ml/min, 1 mg mL^{-1} , 30 min UV 230nm) retention times of 5.41 min (minor) and 6.15 min (major) 89% ee with $\text{Rh}_2(\text{S-DOSP})_4$.

General Procedure A

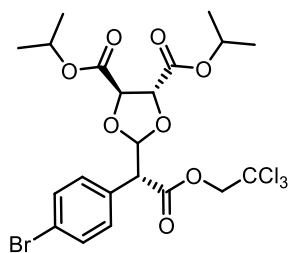
The Rh_2L_4 catalyst (0.005 mmol, 1 mol%) and corresponding 1,3-dioxolane-4,5-dicarboxylate (380.3 mg, 2.0 mmol, 4.0 equiv) were weighed and purged with argon in an oven-dried 25 mL flask, then the mixture was dissolved in 4 mL of DCM. The 2,2,2-trichloroethyl 2-(4-bromophenyl)-2-diazoacetate (0.5 mmol, 186.2 mg, 1.0 equiv) was weighed in a separation vial, flushed with argon and dissolved in 10 mL of DCM. After the reaction flask was cooled to 0 $^\circ\text{C}$, the diazo was transferred into the reaction flask over 2 h under 0 $^\circ\text{C}$. Then, it was stirred overnight, at which point it was warmed up to room temperature. ^1H NMR was taken for the crude products

using 1,3,5-trimethylbenzene as internal standard. The products were inseparable from the starting materials by flash column chromatography and fractions with mixture of 1,3-dioxolane-4,5-dicarboxylate and product were obtained. ^1H NMR spectra were determined by comparison between mixture and starting materials.



Dimethyl (4*R*,5*R*)-2-((*R*)-1-(4-bromophenyl)-2-oxo-2-(2,2,2-trichloroethoxy)ethyl)-1,3-dioxolane-4,5-dicarboxylate (46)

^1H NMR (400 MHz, Chloroform-*d*) δ 7.50 (d, $J = 8.5$ Hz, 2H), 7.44 – 7.33 (d, $J = 8.5$ Hz 2H), 5.91 (d, $J = 7.6$ Hz, 1H), 4.88 (d, $J = 2.9$ Hz, 1H), 4.83 (d, $J = 11.9$ Hz, 1H), 4.72 (d, $J = 11.9$ Hz, 1H), 4.72 (d, $J = 2.9$ Hz, 1H), 4.12 (d, $J = 7.6$ Hz, 1H), 3.82 (d, $J = 1.6$ Hz, 6H).



Di-*iso*-propyl (4*R*,5*R*)-2-((*R*)-1-(4-bromophenyl)-2-oxo-2-(2,2,2-trichloroethoxy)ethyl)-1,3-dioxolane-4,5-dicarboxylate (47)

^1H NMR (400 MHz, Chloroform-*d*) δ 7.48 (d, $J = 8.6$ Hz, 2H), 7.29 (d, $J = 8.6$ Hz 2H), 5.96 (d, $J = 7.7$ Hz, 1H), 5.12 (q, $J = 6.3$ Hz, 2H), 4.79 (d, $J = 11.9$ Hz, 1H), 4.76 (d, $J = 11.9$ Hz, 1H), 4.70 (d, $J = 3.6$ Hz, 1H), 4.69 (d, $J = 3.6$ Hz, 1H), 4.11 (d, $J = 7.7$ Hz, 1H), 1.27 (d, $J = 6.3$ Hz, 12H).

C–H Insertion at Secondary Benzylic Sites with Enhanced Diastereoselectivity

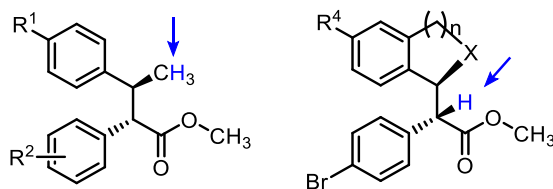
General Procedure B

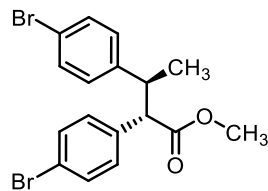
A 5 mL round-bottom flask equipped with reflux condenser was charged with corresponding substrate (0.75 mmol, 1.5 equiv) and Rh₂L₄ (0.0025 mmol, 0.5 mol%). After the vessel was flushed with argon gas (3 cycles), 1 mL of dry degassed CH₂Cl₂ was added and heated to reflux under argon atmosphere for 5 min. A 20 mL scintillation vial was charged with corresponding diazo compound (0.5 mmol, 1.0 equiv), flushed with argon gas (3 cycles), and dry degassed CH₂Cl₂ was added. The diazo solution was transferred into a syringe to make up a 2.0 mL solution in syringe with CH₂Cl₂ from washing the diazo vial. The solution in syringe was added to reaction mixture via syringe pump over 100 min (1.20 mL/h), under reflux condition and argon atmosphere. After addition, the reaction mixture was stirred for another 30 min, then concentrated under vacuum for crude ¹H NMR. The residue was purified by flash column chromatography (hexane/ ethyl acetate = 100/1 to 20/1) to afford desired product.

Diastereomer Ratios Determination

The crude ¹H NMR in general procedure was employed for diastereomer ratios determination, and it was obtained using the following settings: Instrument: INOVA-600 MHz spectrometer with an ID probe; Number of scans: 32; Relaxation time: 5 seconds.

The crude ¹H NMR spectra data was analyzed using MestReNova 11.0.2 (Mestrelab Research S.L.). Before integration, spectra were processed through an auto-phase correction. The ratios were measured by integration of the peaks corresponding to the hydrogens indicated below.





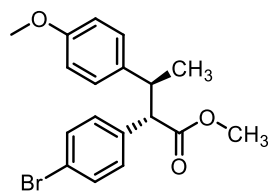
Methyl (2*S*,3*S*)-2,3-bis(4-bromophenyl)butanoate (51)

It was obtained as colorless oil from reaction between 1-bromo-4-ethylbenzene and methyl 2-(4-bromophenyl)-2-diazoacetate using *G.P. B* with $\text{Rh}_2(\text{S-2-Cl-5-BrTPCP})_4$ as catalyst. The NMR spectra are consistent with the reported data in literature.⁶¹

¹H NMR (600 MHz, CDCl₃) δ 7.26 (dd, $J = 10.7, 8.3$ Hz, 4H), 7.00 (d, $J = 8.4$ Hz, 2H), 6.84 (d, $J = 8.4$ Hz, 2H), 3.70 (s, 3H), 3.62 (d, $J = 11.1$ Hz, 1H), 3.39 (dq, $J = 11.0, 6.8$ Hz, 1H), 1.35 (d, $J = 6.8$ Hz, 3H);

¹³C NMR (151 MHz, CDCl₃) δ 173.3, 142.2, 136.1, 131.4, 131.4, 130.1, 129.2, 121.3, 120.1, 58.4, 52.2, 43.3, 20.9;

HPLC (ASH column, 0% *i*-propanol/hexane, 0.5 ml/min, 1 mg mL⁻¹, 30 min, UV 230nm) retention times of 16.53 min (minor) and 18.22 min (major) 77% ee.



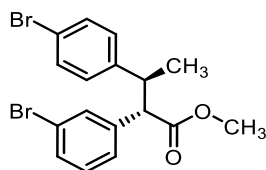
Methyl (2*S*,3*S*)-2-(4-bromophenyl)-3-(4-methoxyphenyl)butanoate (59)

It was obtained as colorless oil from reaction between 1-ethyl-4-methoxybenzene and methyl 2-(4-bromophenyl)-2-diazoacetate using *G.P. B* with $\text{Rh}_2(\text{S-2-Cl-5-BrTPCP})_4$ as catalyst. The NMR spectra are consistent with the reported data in literature.⁶¹

^1H NMR (400 MHz, CDCl_3) δ 7.25 (d, $J = 8.5$ Hz, 2H), 7.01 (d, $J = 8.4$ Hz, 2H), 6.87 (d, $J = 8.6$ Hz, 2H), 6.66 (d, $J = 8.7$ Hz, 2H), 3.71 (s, 3H), 3.70 (s, 3H), 3.62 (d, $J = 11.1$ Hz, 1H), 3.36 (dq, $J = 11.1, 6.8$ Hz, 1H), 1.34 (d, $J = 6.8$ Hz, 3H);

^{13}C NMR (100 MHz, CDCl_3) δ 173.7, 157.9, 136.6, 135.2, 131.2, 130.2, 128.4, 121.0, 113.6, 58.8, 55.1, 52.1, 43.0, 21.1;

HPLC (S,S-Whelk column, 0.3% *i*-propanol/hexane, 0.8 ml/min, 1 mg mL^{-1} , 80 min, UV 230nm) retention times of 30.95 min (major) and 52.48 min (minor) 79% ee.



Methyl (2S,3S)-2-(3-bromophenyl)-3-(4-bromophenyl)butanoate (69)

It was obtained as colorless oil from reaction between 1-bromo-4-ethylbenzene and methyl 2-(3-bromophenyl)-2-diazoacetate using *G.P. B* with $\text{Rh}_2(\text{S-2-Cl-5-BrTPCP})_4$ as catalyst.

R_f = 0.58 (pentane/diethyl ether = 6/1); **$[\alpha]^{20}_{\text{D}}$** : +35.0° ($c = 1.19$, CHCl_3);

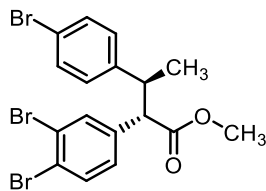
^1H NMR (600 MHz, CDCl_3) δ 7.34 (s, 1H), 7.27 – 7.23 (m, 3H), 7.02 – 6.97 (m, 2H), 6.85 (d, $J = 8.4$ Hz, 2H), 3.71 (s, 3H), 3.62 (d, $J = 11.1$ Hz, 1H), 3.41 (dq, $J = 11.2, 6.8$ Hz, 1H), 1.35 (d, $J = 6.8$ Hz, 3H);

^{13}C NMR (126 MHz, CDCl_3) δ 173.2, 142.1, 139.3, 131.4, 131.3, 130.4, 129.8, 129.2, 127.3, 122.3, 120.2, 58.6, 52.3, 43.3, 20.8;

IR (neat) cm^{-1} 2950, 1732, 1592, 1568, 1489, 1428, 1262, 1159, 1074, 1009, 821, 730 cm^{-1} ;

FTMS (+p NSI) calcd for $\text{C}_{17}\text{H}_{17}\text{O}_2\text{Br}_2$ ($\text{M}+\text{H}$)⁺ 410.9590 found 410.9684;

HPLC (S,S-Whelk column, 0.5% *i*-propanol in hexane, 0.5 mL min^{-1} , 1 mg mL^{-1} . 60 min, UV 230 nm) retention times of 28.49 min (major) and 33.11 min (minor) 35% ee.



Methyl (2*S*,3*S*)-3-(4-bromophenyl)-2-(3,4-dibromophenyl)butanoate (70)

It was obtained as white solid from reaction between 1-bromo-4-ethylbenzene and methyl 2-diazo-2-(3,4-dibromophenyl)acetate using *G.P. B* with $\text{Rh}_2(\text{S-2-Cl-5-BrTPCP})_4$ as catalyst.

mp: 115-116 °C; **Rf** = 0.58 (pentane/diethyl ether = 6/1); **[α]²⁰_D:** +120.8° (c = 1.02, CHCl_3);

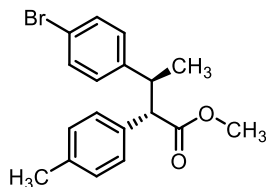
¹H NMR (600 MHz, CDCl_3) δ 7.43 (d, *J* = 2.1 Hz, 1H), 7.37 (d, *J* = 8.3 Hz, 1H), 7.28 (d, *J* = 8.4 Hz, 2H), 6.89 (dd, *J* = 8.3, 2.1 Hz, 1H), 6.85 (d, *J* = 8.4 Hz, 2H), 3.72 (s, 3H), 3.60 (d, *J* = 11.1 Hz, 1H), 3.38 (dq, *J* = 11.1, 6.8 Hz, 1H), 1.34 (d, *J* = 6.8 Hz, 3H);

¹³C NMR (126 MHz, CDCl_3) δ 172.9, 141.8, 138.1, 133.5, 133.4, 131.5, 129.2, 128.7, 124.7, 123.6, 120.4, 58.0, 52.4, 43.2, 20.9;

IR (neat) cm^{-1} 2950, 1732, 1462, 1260, 1161, 1010, 908, 822, 722 cm^{-1} ;

FTMS (+p NSI) calcd for $\text{C}_{17}\text{H}_{16}\text{O}_2\text{Br}_3$ (M+H)⁺ 488.8695 found 488.8693;

HPLC (S,S-Whelk column, 0.5% *i*-propanol in hexane, 0.5 mL min⁻¹, 1 mg mL⁻¹. 80 min, UV 230 nm) retention times of 39.65 min (major) and 59.91 min (minor) 94% ee.



Methyl (2*S*,3*S*)-3-(4-bromophenyl)-2-(*p*-tolyl)butanoate (71)

It was obtained as colorless oil from reaction between 1-bromo-4-ethylbenzene and methyl 2-diazo-2-(4-methylphenyl)acetate using *G.P. B* with $\text{Rh}_2(\text{S-2-Cl-5-BrTPCP})_4$ as catalyst.

R_f = 0.56 (pentane/diethyl ether = 6/1); [α]²⁰_D: +71.0° (c = 1.65, CHCl₃);

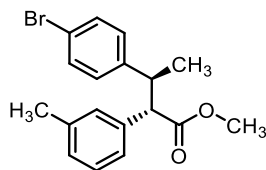
¹H NMR (600 MHz, CDCl₃) δ 7.23 (d, *J* = 8.4 Hz, 2H), 7.01 (d, *J* = 8.1 Hz, 2H), 6.94 (d, *J* = 8.3 Hz, 2H), 6.86 (d, *J* = 8.4 Hz, 2H), 3.69 (s, 3H), 3.63 (d, *J* = 11.1 Hz, 1H), 3.43 (dq, *J* = 11.1, 6.8 Hz, 1H), 2.22 (s, 3H), 1.34 (d, *J* = 6.9 Hz, 3H);

¹³C NMR (126 MHz, CDCl₃) δ 174.0, 142.8, 136.8, 134.0, 131.2, 129.3, 129.0, 128.3, 119.8, 58.5, 52.0, 43.1, 21.0, 21.0;

IR (neat) cm⁻¹ 2950, 1732, 1488, 1428, 1156, 1073, 1009, 821, 747 cm⁻¹;

FTMS (+p NSI) calcd for C₁₈H₁₉O₂BrNa (M+Na)⁺ 369.0461 found 369.0465;

HPLC (S,S-Whelk column, 0.5% *i*-propanol in hexane, 0.5 mL min⁻¹, 1 mg mL⁻¹. 60 min, UV 230 nm) retention times of 28.41 min (major) and 36.74 min (minor) 46% ee.



Methyl (2*S*,3*S*)-3-(4-bromophenyl)-2-(*m*-tolyl)butanoate (72)

It was obtained as colorless oil from reaction between 1-bromo-4-ethylbenzene and methyl 2-diazo-2-(3-methylphenyl)acetate using *G.P. B* with Rh₂(*S*-2-Cl-5-BrTPCP)₄ as catalyst.

R_f = 0.65 (pentane/diethyl ether = 6/1); [α]²⁰_D: +52.2° (c = 0.98, CHCl₃);

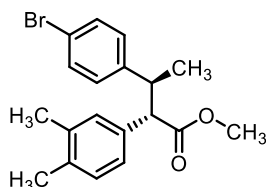
¹H NMR (600 MHz, CDCl₃) δ 7.23 (d, *J* = 8.4 Hz, 2H), 7.02 (t, *J* = 7.5 Hz, 1H), 6.95 – 6.89 (m, 3H), 6.86 (d, *J* = 8.4 Hz, 2H), 3.70 (s, 3H), 3.62 (d, *J* = 11.1 Hz, 1H), 3.44 (dq, *J* = 11.0, 6.8 Hz, 1H), 2.22 (s, 3H), 1.35 (d, *J* = 6.7 Hz, 3H);

¹³C NMR (126 MHz, CDCl₃) δ 173.9, 142.7, 137.8, 137.0, 131.1, 129.3, 129.1, 128.1, 128.0, 125.5, 119.8, 58.9, 52.1, 43.1, 21.4, 20.9;

IR (neat) cm⁻¹ 2950, 1732, 1489, 1162, 1009, 822, 738, 697 cm⁻¹;

FTMS (+p NSI) calcd for $C_{18}H_{20}O_2Br$ (M+H)⁺ 347.0641 found 361.0646;

HPLC (S,S-Whelk column, 0.5% *i*-propanol in hexane, 0.5 mL min⁻¹, 1 mg mL⁻¹. 60 min, UV 230 nm) retention times of 29.49 min (major) and 33.59 min (minor) 37% ee.



Methyl (2S,3S)-3-(4-bromophenyl)-2-(3,4-dimethylphenyl)butanoate (73)

It was obtained as colorless oil from reaction between 1-bromo-4-ethylbenzene and methyl 2-diazo-2-(3,4-dimethylphenyl)acetate using *G.P. B* with $Rh_2(S-2-Cl-5-BrTPCP)_4$ as catalyst.

Rf = 0.61 (pentane/diethyl ether = 6/1); $[\alpha]^{20}_D$: +95.0° (c = 1.16, CHCl₃);

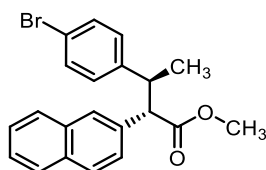
¹H NMR (600 MHz, CDCl₃) δ 7.24 (d, *J* = 8.4 Hz, 2H), 6.91 – 6.83 (m, 5H), 3.69 (s, 3H), 3.62 (d, *J* = 11.1 Hz, 1H), 3.44 (dq, *J* = 11.0, 6.8 Hz, 1H), 2.13 (s, 6H), 1.34 (dd, *J* = 6.8, 0.7 Hz, 3H);

¹³C NMR (126 MHz, CDCl₃) δ 174.0, 142.9, 136.4, 135.5, 134.4, 131.1, 129.6, 129.4, 125.8, 119.8, 58.4, 52.0, 42.9, 21.1, 19.7, 19.4;

IR (neat) cm⁻¹ 2949, 1732, 1490, 1434, 1263, 1155, 1009, 822, 750, 740 cm⁻¹;

FTMS (+p NSI) calcd for $C_{19}H_{22}O_2Br$ (M+H)⁺ 361.0798 found 361.0895;

HPLC (OJH column, 0.5% *i*-propanol in hexane, 1 mL min⁻¹, 1 mg mL⁻¹. 30 min, UV 230 nm) retention times of 6.61 min (minor) and 9.77 min (major) 69% ee.



Methyl (2*S*,3*S*)-3-(4-bromophenyl)-2-(naphthalen-2-yl)butanoate (74)

It was obtained as white solid from reaction between 1-bromo-4-ethylbenzene and methyl 2-diazo-2-(naphthalen-2-yl)acetate using *G.P. B* with $\text{Rh}_2(\text{S-2-Cl-5-BrTPCP})_4$ as catalyst.

mp: 116-117 °C; **Rf** = 0.50 (pentane/diethyl ether = 6/1); **$[\alpha]^{20}_{\text{D}}$** : +126.1° (c = 1.04, CHCl_3);

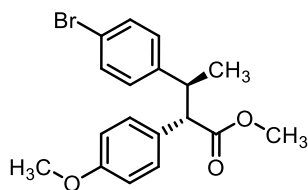
$^1\text{H NMR}$ (600 MHz, CDCl_3) δ 7.76 – 7.71 (m, 2H), 7.66 (d, J = 8.5 Hz, 1H), 7.63 (s, 1H), 7.42 (pt, J = 4.9, 2.5 Hz, 2H), 7.32 (d, J = 8.5 Hz, 2H), 7.20 (d, J = 8.4 Hz, 2H), 6.91 (d, J = 8.3 Hz, 2H), 3.88 (d, J = 11.1 Hz, 1H), 3.72 (s, 3H), 3.62 (dddd, J = 13.5, 11.1, 6.7, 1.5 Hz, 1H), 1.43 (d, J = 6.8 Hz, 3H);

$^{13}\text{C NMR}$ (126 MHz, CDCl_3) δ 173.8, 142.6, 134.6, 133.2, 132.5, 131.3, 129.3, 128.0, 127.8, 127.6, 127.6, 126.3, 126.0, 125.9, 112.0, 59.0, 52.2, 43.2, 21.2;

IR (neat) cm^{-1} 2952, 1730, 1489, 1161, 1010, 905, 822, 726 cm^{-1} ;

FTMS (+p NSI) calcd for $\text{C}_{21}\text{H}_{20}\text{O}_2\text{Br}$ ($\text{M}+\text{H}$)⁺ 383.0641 found 383.0648;

HPLC (ODH column, 0.5% *i*-propanol in hexane, 0.5 mL min^{-1} , 1 mg mL^{-1} . 40 min, UV 230 nm) retention times of 23.76 min (minor) and 32.67 min (major) 67% ee.

**Methyl (2*S*,3*S*)-3-(4-bromophenyl)-2-(4-methoxyphenyl)butanoate (75)**

It was obtained as white solid from reaction between 1-bromo-4-ethylbenzene and methyl 2-diazo-2-(4-methoxyphenyl)acetate using *G.P. B* with $\text{Rh}_2(\text{S-2-Cl-5-BrTPCP})_4$ as catalyst.

mp: 87-88 °C; **Rf** = 0.43 (pentane/diethyl ether = 6/1); **$[\alpha]^{20}_{\text{D}}$:** +39.6° (c = 0.87, CHCl_3);

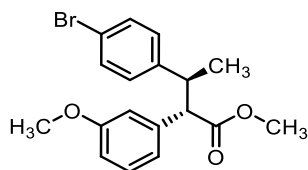
$^1\text{H NMR}$ (600 MHz, CDCl_3) δ 7.23 (d, J = 8.4 Hz, 2H), 7.03 (d, J = 8.7 Hz, 2H), 6.85 (d, J = 8.4 Hz, 2H), 6.67 (d, J = 8.8 Hz, 2H), 3.71 (s, 3H), 3.70 (s, 3H), 3.60 (d, J = 11.1 Hz, 1H), 3.40 (dq, J = 11.8, 6.8 Hz, 1H), 1.34 (d, J = 6.7 Hz, 3H);

$^{13}\text{C NMR}$ (101 MHz, CDCl_3) δ 174.1, 158.6, 142.8, 131.2, 129.4, 129.3, 129.2, 119.8, 113.7, 58.1, 55.1, 52.0, 43.3, 20.9;

IR (neat) cm^{-1} 2952, 2836, 1731, 1610, 1510, 1249, 1158, 1034, 1009, 908, 824, 752 cm^{-1} ;

FTMS (+p NSI) calcd for $\text{C}_{18}\text{H}_{19}\text{O}_2\text{BrNa}$ ($\text{M}+\text{Na}$)⁺ 385.0410 found 385.0500;

HPLC (ADH column, 0.5% *i*-propanol in hexane, 0.5 mL min^{-1} , 1 mg mL^{-1} . 80 min, UV 230 nm) retention times of 40.51 min (major) and 52.71 min (minor) 63% ee.



Methyl (2*S*,3*S*)-3-(4-bromophenyl)-2-(3-methoxyphenyl)butanoate (76)

It was obtained as colorless oil from reaction between 1-bromo-4-ethylbenzene and methyl 2-diazo-2-(3-methoxyphenyl)acetate using *G.P. B* with $\text{Rh}_2(\text{S-2-Cl-5-BrTPCP})_4$ as catalyst.

Rf = 0.49 (pentane/diethyl ether = 6/1); **$[\alpha]^{20}_{\text{D}}$:** +60.8° (c = 1.04, CHCl_3);

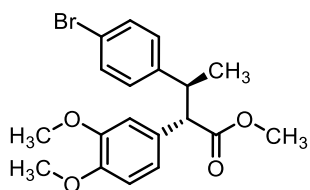
$^1\text{H NMR}$ (600 MHz, CDCl_3) δ 7.23 (d, J = 8.3 Hz, 2H), 7.05 (t, J = 7.9 Hz, 1H), 6.87 (d, J = 8.4 Hz, 2H), 6.71 – 6.67 (m, 2H), 6.67 – 6.63 (m, 1H), 3.70 (s, 3H), 3.69 (s, 3H), 3.63 (d, J = 11.1 Hz, 1H), 3.43 (dq, J = 10.9, 6.7 Hz, 1H), 1.35 (d, J = 6.8 Hz, 3H);

^{13}C NMR (126 MHz, CDCl_3) δ 173.7, 159.4, 142.6, 138.6, 131.2, 129.3, 129.2, 120.9, 119.9, 114.2, 112.6, 58.9, 55.1, 52.1, 43.2, 20.9;

IR (neat) cm^{-1} 2951, 2835, 1732, 1599, 1585, 1489, 1428, 1259, 1160, 1009, 822, 742, 694 cm^{-1} ;

FTMS (+p NSI) calcd for $\text{C}_{18}\text{H}_{20}\text{O}_3\text{Br}$ ($\text{M}+\text{H}$) $^+$ 363.0590 found 363.0691;

HPLC (ASH column, 0.5% *i*-propanol in hexane, 1 mL min^{-1} , 1 mg mL^{-1} . 30 min, UV 230 nm) retention times of 7.11 min (minor) and 11.40 min (major) 39% ee.



Methyl (2*S*,3*S*)-3-(4-bromophenyl)-2-(3,4-dimethoxyphenyl)butanoate (77)

It was obtained as colorless oil from reaction between 1-bromo-4-ethylbenzene and methyl 2-diazo-2-(3,4-dimethoxyphenyl)acetate using *G.P. B* with $\text{Rh}_2(\text{S-2-Cl-5-BrTPCP})_4$ as catalyst.

Rf = 0.36 (pentane/diethyl ether = 6/1); $[\alpha]^{20}_{\text{D}}$: +124.0 $^\circ$ (c = 1.10, CHCl_3);

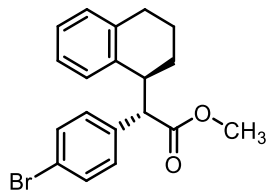
^1H NMR (600 MHz, CDCl_3) δ 7.24 (d, J = 8.4 Hz, 2H), 6.84 (d, J = 8.4 Hz, 2H), 6.63 (m, 2H), 6.60 (d, J = 1.2 Hz, 1H), 3.79 (s, 3H), 3.75 (s, 3H), 3.71 (s, 3H), 3.57 (d, J = 11.1 Hz, 1H), 3.42 – 3.35 (m, 1H), 1.35 (d, J = 6.8 Hz, 3H);

^{13}C NMR (126 MHz, CDCl_3) δ 174.0, 148.5, 148.0, 142.7, 131.2, 129.6, 129.3, 120.7, 119.9, 111.4, 110.7, 58.5, 55.8, 55.7, 52.1, 43.5, 20.7;

IR (neat) cm^{-1} 2952, 2835, 1732, 1515, 1261, 1155, 1028, 1009, 824, 744 cm^{-1} ;

FTMS (+p NSI) calcd for $\text{C}_{19}\text{H}_{22}\text{O}_4\text{Br}_3$ ($\text{M}+\text{H}$) $^+$ 393.0690 found 393.0731;

HPLC (ADH column, 2% *i*-propanol in hexane, 1 mL min^{-1} , 1 mg mL^{-1} . 30 min, UV 230 nm) retention times of 14.19 min (major) and 18.71 min (minor) 85% ee.



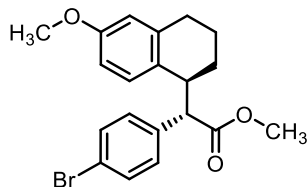
Methyl (S)-2-(4-bromophenyl)-2-((S)-1,2,3,4-tetrahydronaphthalen-1-yl)acetate (81)

It was obtained as white solid from reaction between 1,2,3,4-tetrahydronaphthalene and methyl 2-(4-bromophenyl)-2-diazoacetate using *G.P. B* with $\text{Rh}_2(\text{S-2-Cl-5-BrTPCP})_4$ as catalyst. The NMR spectra are consistent with the reported data in literature.⁶¹

¹H NMR (600 MHz, CDCl₃) δ 7.37 (d, $J = 8.5$ Hz, 2H), 7.08 – 7.00 (m, 4H), 6.76 – 6.69 (m, 1H), 6.18 (d, $J = 7.7$ Hz, 1H), 3.78 (d, $J = 10.6$ Hz, 1H), 3.70 (s, 3H), 3.42 – 3.37 (m, 1H), 2.88 (ddd, $J = 17.1, 6.8, 4.0$ Hz, 1H), 2.79 (ddd, $J = 16.7, 9.5, 6.9$ Hz, 1H), 2.03 – 1.90 (m, 2H), 1.90 – 1.84 (m, 1H), 1.84 – 1.76 (m, 1H);

¹³C NMR (151 MHz, CDCl₃) δ 173.5, 136.9, 136.7, 136.6, 131.4, 130.8, 129.8, 129.1, 126.3, 124.5, 121.4, 56.3, 52.0, 42.3, 28.6, 26.7, 18.6;

HPLC (OD column, 0.3% *i*-propanol/hexane, 0.5 ml/min, 1 mg mL⁻¹, 40 min, UV 230nm) retention times of 18.13 min (major) and 22.91 min (minor) 69% ee.



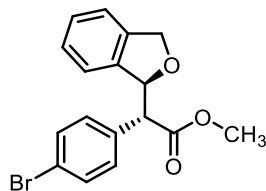
Methyl (S)-2-(4-bromophenyl)-2-((S)-6-methoxy-1,2,3,4-tetrahydronaphthalen-1-yl)acetate (82)

It was obtained as white solid from reaction between 6-methoxy-1,2,3,4-tetrahydronaphthalene and methyl 2-(4-bromophenyl)-2-diazoacetate using *G.P. B* with $\text{Rh}_2(\text{S-2-Cl-5-BrTPCP})_4$ as catalyst. The NMR spectra are consistent with the reported data in literature.⁶¹

¹H NMR (600 MHz, CDCl₃) δ 7.47 (d, $J = 8.5$ Hz, 2H), 7.31 (d, $J = 8.4$ Hz, 2H), 7.07 (dd, $J = 9.6, 8.5$ Hz, 1H), 6.68 – 6.62 (m, 2H), 3.78 (s, 3H), 3.70 (d, $J = 8.8$ Hz, 1H), 3.53 (s, 3H), 3.52 – 3.48 (m, 1H), 2.83 (ddd, $J = 17.2, 6.8, 3.1$ Hz, 1H), 2.74 (ddd, $J = 17.3, 10.5, 7.1$ Hz, 1H), 1.76 – 1.66 (m, 1H), 1.64 – 1.58 (m, 1H), 1.57 – 1.52 (m, 1H), 1.49 – 1.40 (m, 1H);

¹³C NMR (151 MHz, CDCl₃) δ 174.2, 158.2, 138.0, 136.7, 131.7, 130.4, 130.3, 129.9, 121.4, 114.0, 111.5, 56.8, 55.1, 51.9, 40.2, 28.7, 24.8, 17.6;

HPLC (R,R-Whelk column, 1% *i*-propanol/hexane, 1 ml/min, 1 mg mL⁻¹, 40 min, UV 230nm) retention times of 17.07 min (minor) and 28.43 min (major) 67% ee.



Methyl (*R*)-2-(4-bromophenyl)-2-((*S*)-1,3-dihydroisobenzofuran-1-yl)acetate (83)

It was obtained as white solid from reaction between 1,3-dihydroisobenzofuran and methyl 2-(4-bromophenyl)-2-diazoacetate using *G.P. B* with $\text{Rh}_2(\text{S-2-Cl-5-BrTPCP})_4$ as catalyst.

mp: 120-121°C; **R_f** = 0.59 (pentane/diethyl ether = 4/1); **[α]²⁰_D:** +57.4° (c = 1.065, CHCl₃);

¹H NMR (600 MHz, CDCl₃) δ 7.48 (d, $J = 8.4$ Hz, 2H), 7.21 (m, 4H), 7.02 (t, $J = 7.4$ Hz, 1H), 6.19 (d, $J = 7.7$ Hz, 1H), 5.81 (d, $J = 11.0$ Hz, 1H), 5.13 (dd, $J = 12.3, 2.4$ Hz, 1H), 5.07 (d, $J = 12.3$ Hz, 1H), 3.74 (m, 4H).;

^{13}C NMR (101 MHz, CDCl_3) δ 172.1, 139.5, 138.6, 133.3, 131.8, 130.9, 128.1, 126.8, 122., 122.2, 121.0, 84.8, 72.7, 57.5, 52.4;

IR (neat) cm^{-1} 2950, 2858, 1734, 1488, 1194, 1157, 1040, 1011, 908, 820, 749, 729;

FTMS (+p NSI) calcd for $\text{C}_{17}\text{H}_{16}\text{O}_3\text{Br}$ ($\text{M}+\text{H}$)⁺ 347.0277 found 347. 0282;

HPLC (OD column, 1% *i*-propanol in hexane, 1 mL min⁻¹, 1 mg mL⁻¹. 30 min, UV 230 nm) retention times of 12.57 min (major) and 15.34 min (minor) 57% ee.

C–H Insertion at Terminal Methylene Sites in the Presence of Activated Benzylic Methylene

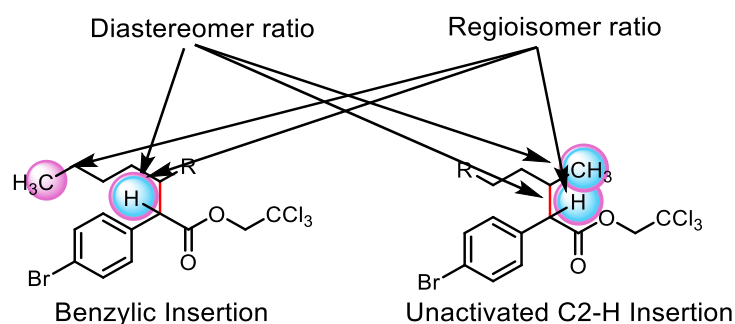
General Procedure C

A 16 mL reaction vial (21x70mm) with screw cap (open top with PTFE faced silicone septum) was charged with Rh_2L_4 (0.003 mmol, 1 mol%) and corresponding substrate (0.6 mmol, 2.0 equiv). The reaction vessel was then evacuated and back filled with argon (3 times), followed by the addition of dry degassed CH_2Cl_2 (3 mL) and the solution was heated to 39 °C (refluxing CH_2Cl_2) for 10 min. Desired donor/acceptor diazo compounds (0.3 mmol, 1.0 equiv) was weighed in a 20 mL scintillation vial and dissolved in 6 mL of dry degassed CH_2Cl_2 under argon atmosphere. Then, under reflux condition and argon atmosphere, the diazo solution was added to the reaction vessel dropwise via syringe pump over 3 h. The reaction mixture was stirred at 39 °C for another 30 min, and then concentrated under vacuum for crude ^1H NMR. Finally, the crude product was purified by flash column chromatography (pentane/diethyl ether = 100/0 to 11/1) to afford the product (mixture of regioisomers and diastereomers) as colorless oil.

Regioisomer and Diastereomer Ratios Determination

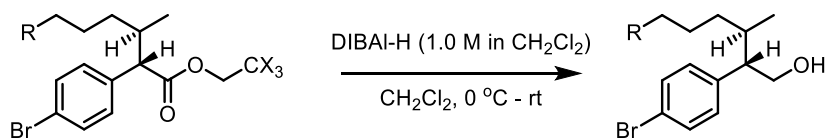
The crude ^1H NMR in general procedure was utilized for regioisomer and diastereomer ratios determination, and it was obtained using Bruker-600 MHz spectrometer with an ID probe, and the acquisition was done with 16 times of scans and 1 seconds of relaxation time.

The crude ^1H NMR spectra data was analyzed with MestReNova 11.0 (MestRelab Research S.L.). Before integration, spectra were processed through a Segments Smoother baseline correction manually. The ratios were measured by integration of the peaks corresponding to the hydrogens indicated below.

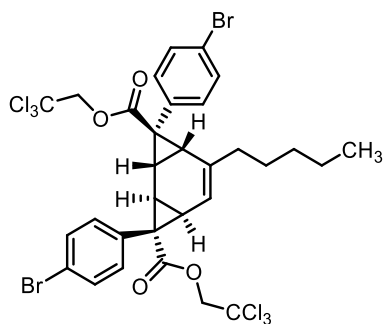


Enantiomer Ratio Determination

Most of the enantiomer ratios of these C–H insertion products were obtained by separation on our available chiral HPLC columns directly. However, for some C–H functionalization reactions, their regioisomers and diastereomers are inseparable by flash column chromatography, which cause additional difficulty for enantiomers separation on our available chiral HPLC columns. Hence, for better separation, some of them were reduced to alcohols, without influence on the chiral centers, and used for enantiomeric excess (ee) determination of corresponding C–H functionalization products.



A flask with solution of corresponding ester (0.2 mmol, 1.0 equiv) in CH₂Cl₂ (1 mL) was flushed with argon and cooled to 0 °C via ice bath. Under argon atmosphere, a solution of 1 M diisobutylaluminum hydride (DIBAL-H) in CH₂Cl₂ (0.4 mL, 0.4 mmol, 2.0 equiv) was added dropwise into the flask at 0 °C, and the mixture was stirred for 4 h at room temperature. The reaction was quenched by adding 2 mL of 2 M aqueous HCl solution dropwise. The resulted solution was extracted by diethyl ether (3x3 mL) and dried over Na₂SO₄. The crude product was concentrated and confirmed by ¹H NMR, then the crude alcohol product was used for HPLC directly.



Bis(2,2,2-trichloroethyl) (1R,2S,3R,7R,8S)-3,8-bis(4-bromophenyl)-5-pentyltricyclooct-5-ene-3,8-dicarboxylate (90)

This compound was obtained according to *G.P. C* between *n*-pentylbenzene (89.0 mg, 0.6 mmol, 2.0 equiv) and 2,2,2-trichloroethyl 2-(4-bromophenyl)-2-diazoacetate (111.7 mg, 0.3 mmol, 1.0 equiv), catalyzed by Rh₂(*S*-DOSP)₄ (5.7 mg, 0.003 mmol, 1.0 mol%). The product was purified by flash column chromatography on silica gel (gradient elution: 0 – 2% diethyl ether in pentane) to afford white solid in 65% yield.

mp: 48-49 °C; **R_f** = 0.58 (pentane/diethyl ether = 4/1); **[α]_D²⁰:** -44.8° (c = 1.03, CHCl₃, 34% ee); **¹H NMR (600 MHz, CDCl₃) δ** 7.44 (dd, *J* = 8.6, 2.8 Hz, 4H), 7.09 (d, *J* = 7.9 Hz, 2H), 7.06 (d, *J* = 8.3 Hz, 2H), 5.16 (d, *J* = 4.9 Hz, 1H), 4.66 – 4.62 (m, 3H), 4.59 (d, *J* = 11.9 Hz, 1H), 2.69 (dd,

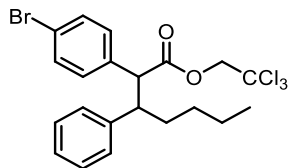
$J = 9.4, 1.2$ Hz, 1H), 2.63 (dd, $J = 9.4, 1.2$ Hz, 1H), 1.99 – 1.92 (m, 1H), 1.86 – 1.79 (m, 1H), 1.73 (dd, $J = 9.4, 4.9$ Hz, 1H), 1.67 (d, $J = 9.3$ Hz, 1H), 1.27 – 1.20 (m, 2H), 1.09 (m, 1H), 1.03 (p, $J = 7.0$ Hz, 2H), 1.00 – 0.94 (m, 1H), 0.86 (t, $J = 7.4$ Hz, 3H);

^{13}C NMR (151 MHz, CDCl_3) δ 170.9, 167.9, 135.9, 134.8, 133.8, 132.0, 131.5, 131.2, 131.1, 129.2, 121.8, 121.6, 117.6, 94.8, 74.4, 74.3, 39.0, 38.8, 37.0, 31.5, 30.8, 28.3, 27.8, 27.4, 26.6, 22.5, 13.9;

IR (neat) 2928, 2856, 1731, 1489, 1208, 1151, 1072, 1011, 827, 770. 716 cm^{-1} ;

HRMS (+p APCI) calcd for $\text{C}_{31}\text{H}_{28}\text{O}_4\text{Br}_2\text{Cl}_6$ (M) $^+$ 831.8480 found 831.8481;

HPLC (ADH column, 1% *i*-propanol in hexane, 1 mL min^{-1} , 1 mg mL^{-1} , 30 min, UV 230 nm) retention times of 10.43 min (major) and 21.53 min (minor) 34% ee with $\text{Rh}_2(\text{S-DOSP})_4$.



2,2,2-Trichloroethyl 2-(4-bromophenyl)-3-phenylheptanoate (86)

This compound was obtained according to *G.P. C* between *n*-pentylbenzene (89.0 mg, 0.6 mmol, 2.0 equiv) and 2,2,2-trichloroethyl 2-(4-bromophenyl)-2-diazoacetate (111.7 mg, 0.3 mmol, 1.0 equiv), catalyzed by $\text{Rh}_2(\text{S-DOSP})_4$ (5.7 mg, 0.003 mmol, 1.0 mol%). The product was purified by flash column chromatography on silica gel (gradient elution: 0 – 2% diethyl ether in pentane) to afford colorless oil in 24% yield.

Rf = 0.72 (pentane/diethyl ether = 4/1);

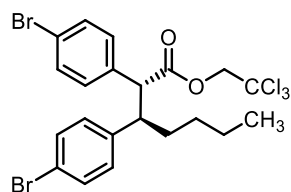
^1H NMR (600 MHz, CDCl_3) δ 7.23 (d, $J = 8.5$ Hz, 2H), 7.13 (t, $J = 7.4$ Hz, 2H), 7.08 – 7.05 (m, 1H), 7.04 (d, $J = 8.5$ Hz, 2H), 6.96 (d, $J = 7.0$ Hz, 2H), 4.82 (d, $J = 11.9$ Hz, 1H), 4.70 (d, $J = 12.0$ Hz, 1H), 3.86 (d, $J = 11.4$ Hz, 1H), 3.32 (td, $J = 11.2, 3.4$ Hz, 1H), 1.85 – 1.77 (m, 1H), 1.76 –

1.69 (m, 1H), 1.31 – 1.26 (m, 1H), 1.23 – 1.16 (m, 1H), 1.16 – 1.09 (m, 1H), 1.09 – 1.00 (m, 1H), 0.79 (t, $J = 7.3$ Hz, 3H);

^{13}C NMR (151 MHz, CDCl_3) δ 171.8, 140.8, 135.7, 131.4, 130.5, 128.4, 128.4, 126.6, 121.4, 94.9, 74.5, 58.1, 49.3, 34.8, 29.6, 22.7, 14.0;

IR (neat) 3028, 2955, 2930, 2858, 1750, 1488, 1135, 1074, 1035, 764, 723, 700 cm^{-1} ;

HRMS (+p APCI) calcd for $\text{C}_{21}\text{H}_{23}\text{O}_2^{81}\text{BrCl}_3$ ($\text{M}+\text{H}$) $^+$ 492.9921 found 492.9909.



2,2,2-Trichloroethyl (2R,3R)-2,3-bis(4-bromophenyl)heptanoate (87)

This compound was obtained according to *G.P. C* between 1-bromo-4-pentylbenzene (136.3 mg, 0.6 mmol, 2.0 equiv) and 2,2,2-trichloroethyl 2-(4-bromophenyl)-2-diazoacetate (111.7 mg, 0.3 mmol, 1.0 equiv), catalyzed by $\text{Rh}_2(\text{S-TCPTAD})_4$ (6.4 mg, 0.003 mmol, 1.0 mol%). The product was purified by flash column chromatography on silica gel (gradient elution: 0 – 2% diethyl ether in pentane) to afford colorless oil in 78% yield.

Rf = 0.63 (pentane/diethyl ether = 19/1); $[\alpha]^{20}_{\text{D}}$: -55.3° ($c = 1.08$, CHCl_3 , 93% ee);

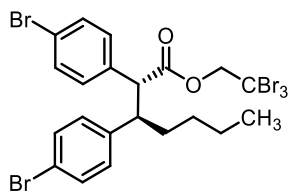
^1H NMR (600 MHz, $(\text{CD}_3)_2\text{CO}$) δ 7.33 (t, $J = 8.7$ Hz, 4H), 7.23 (d, $J = 8.5$ Hz, 2H), 7.16 (d, $J = 8.4$ Hz, 2H), 4.96 (d, $J = 12.2$ Hz, 1H), 4.90 (d, $J = 12.3$ Hz, 1H), 4.11 (d, $J = 11.5$ Hz, 1H), 3.46 (td, $J = 11.3, 3.3$ Hz, 1H), 1.92 – 1.85 (m, 1H), 1.81 – 1.72 (m, 1H), 1.35 – 1.30 (m, 1H), 1.26 – 1.17 (m, 1H), 1.17 – 1.09 (m, 1H), 1.08 – 1.00 (m, 1H), 0.79 (t, $J = 7.3$ Hz, 3H);

^{13}C NMR (151 MHz, $(\text{CD}_3)_2\text{CO}$) δ 172.2, 141.7, 137.3, 132.3, 132.1, 131.9, 131.7, 121.8, 120.6, 96.2, 74.9, 57.9, 49.3, 35.5, 30.5, 23.2, 14.3;

IR (neat) 2955, 2930, 2859, 1750, 1488, 1136, 1074, 1101, 825, 760, 731 cm^{-1} ;

HRMS (+p APCI) calcd for $\text{C}_{21}\text{H}_{22}\text{O}_2\text{Br}_2\text{Cl}_3$ ($\text{M}+\text{H}$)⁺ 568.9047 found 568.9048;

HPLC (the ester product was reduced to 2,3-bis(4-bromophenyl)heptan-1-ol for better separation) (ODH column, 5% *i*-propanol in hexane, 0.5 mL min^{-1} , 1 mg mL^{-1} , 60 min, UV 230 nm) retention times of 19.57 min (minor) and 24.69 min (major) 93% ee with $\text{Rh}_2(\text{S-TCPTAD})_4$.



2,2,2-Tribromoethyl (2*R*,3*R*)-2,3-bis(4-bromophenyl)heptanoate (93)

This compound was obtained according to *G.P. C* between 1-bromo-4-pentylbenzene (136.3 mg, 0.6 mmol, 2.0 equiv) and 2,2,2-tribromoethyl 2-(4-bromophenyl)-2-diazoacetate (151.7 mg, 0.3 mmol, 1.0 equiv), catalyzed by $\text{Rh}_2(\text{S-TCPTAD})_4$ (6.4 mg, 0.003 mmol, 1.0 mol%). The product was purified by flash column chromatography on silica gel (gradient elution: 0 – 2% diethyl ether in pentane) to afford colorless oil in 75% yield.

R_f = 0.63 (pentane/diethyl ether = 19/1); [α]_D²⁰: -42.1° (*c* = 1.00, CHCl_3 , 90% ee);

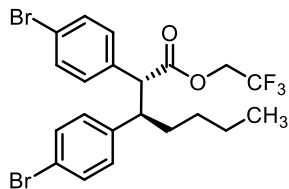
¹H NMR (600 MHz, CDCl_3) δ 7.27 (s, 2H), 7.26 (s, 2H), 7.06 (d, *J* = 8.5 Hz, 2H), 6.86 (d, *J* = 8.4 Hz, 2H), 4.97 (d, *J* = 12.3 Hz, 1H), 4.90 (d, *J* = 12.3 Hz, 1H), 3.83 (d, *J* = 11.4 Hz, 1H), 3.34 (td, *J* = 11.3, 3.3 Hz, 1H), 1.89 – 1.82 (m, 1H), 1.73 – 1.65 (m, 1H), 1.30 – 1.24 (m, 1H), 1.23 – 1.16 (m, 1H), 1.15 – 1.07 (m, 1H), 1.06 – 0.99 (m, 1H), 0.80 (t, *J* = 7.3 Hz, 3H);

¹³C NMR (151 MHz, CDCl_3) δ 171.2, 140.0, 135.4, 131.6, 131.6, 130.5, 130.1, 121.7, 120.4, 58.0, 48.7, 35.1, 34.8, 29.5, 22.6, 14.1;

IR (neat) 2930, 2857, 1746, 1488, 1134, 1074, 1011, 822, 736 cm^{-1} ;

HRMS (+p APCI) calcd for $C_{21}H_{22}O_2^{79}Br_4^{81}Br$ (M+H)⁺ 702.7511 found 702.7513;

HPLC (the ester product was reduced to 2,3-bis(4-bromophenyl)heptan-1-ol for better separation) (ODH column, 5% *i*-propanol in hexane, 0.5 mL min⁻¹, 1 mg mL⁻¹, 60 min, UV 230 nm) retention times of 19.16 min (minor) and 24.14 min (major) 90% ee with Rh₂(*S*-TCPTAD)₄.



2,2,2-Trifluoroethyl (2*R*,3*R*)-2,3-bis(4-bromophenyl)heptanoate (92)

This compound was obtained according to *G.P. C* between 1-bromo-4-pentylbenzene (136.3 mg, 0.6 mmol, 2.0 equiv) and 2,2,2-trifluoroethyl 2-(4-bromophenyl)-2-diazoacetate (96.9 mg, 0.3 mmol, 1.0 equiv), catalyzed by Rh₂(*S*-TCPTAD)₄ (6.4 mg, 0.003 mmol, 1.0 mol%). The product was purified by flash column chromatography on silica gel (gradient elution: 0 – 2% diethyl ether in pentane) to afford colorless oil in 80% yield.

R_f = 0.63 (pentane/diethyl ether = 19/1); [**α**]²⁰_D: -59.4° (c = 1.02, CHCl₃, 85% ee);

¹H NMR (600 MHz, (CD₃)₂CO) δ 7.28 – 7.24 (m, 4H), 6.98 (d, *J* = 8.5 Hz, 2H), 6.82 (d, *J* = 8.4 Hz, 2H), 4.61 (dq, *J* = 12.7, 8.4 Hz, 1H), 4.38 (dq, *J* = 12.7, 8.4 Hz, 1H), 3.76 (d, *J* = 11.3 Hz, 1H), 3.25 (td, *J* = 11.1, 3.6 Hz, 1H), 1.77 – 1.59 (m, 2H), 1.30 – 1.24 (m, 1H), 1.23 – 1.16 (m, 1H), 1.11 – 1.05 (m, 1H), 1.05 – 1.01 (m, 1H), 0.80 (t, *J* = 7.3 Hz, 3H);

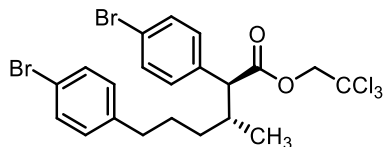
¹³C NMR (151 MHz, CDCl₃) δ 171.7, 139.8, 135.2, 131.7, 131.6, 130.3, 130.0, 122.9 (q, *J* = 277.4 Hz), 121.8, 120.5, 60.70 (q, *J* = 36.6 Hz), 57.5, 49.0, 34.4, 29.4, 22.5, 13.9;

¹⁹F NMR (282 MHz, CDCl₃) δ -73.6 (t, *J* = 8.4 Hz).

IR (neat) 2958, 2932, 2860, 1754, 1488, 1407, 1280, 1169, 1138, 1074, 1101, 738 cm⁻¹;

HRMS (+p APCI) calcd for C₂₁H₂₂O₂Br₂F₃ (M+H)⁺ 520.9933 found 520.9934;

HPLC (the ester product was reduced to 2,3-bis(4-bromophenyl)heptan-1-ol for better separation) (ODH column, 5% *i*-propanol in hexane, 0.5 mL min⁻¹, 1 mg mL⁻¹, 60 min, UV 230 nm) retention times of 19.34 min (minor) and 24.28 min (major) 85% ee with Rh₂(*S*-TCPTAD)₄.



2,2,2-Trichloroethyl (2*S*,3*R*)-2,6-bis(4-bromophenyl)-3-methylhexanoate (89)

This compound was obtained according to *G.P. C* between 1-bromo-4-pentylbenzene (136.3 mg, 0.6 mmol, 2.0 equiv) and 2,2,2-trichloroethyl 2-(4-bromophenyl)-2-diazoacetate (111.7 mg, 0.3 mmol, 1.0 equiv), catalyzed by Rh₂(*S*-2-Cl-5-BrTPCP)₄ (5.7 mg, 0.003 mmol, 1.0 mol%). The product was purified by flash column chromatography on silica gel (gradient elution: 0 – 2% diethyl ether in pentane) to afford colorless oil in 87% yield. The pure major diastereomer of C2 insertion product was obtained from prep HPLC (Ascentis® C18 column, 90–95% acetonitrile in H₂O with 0.1% trifluoroacetic acid).

R_f = 0.60 (pentane/diethyl ether = 19/1); [**α**]_D²⁰: +19.8° (c = 0.95, CHCl₃, 89% ee);

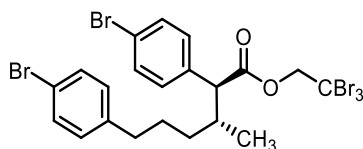
¹H NMR (600 MHz, (CD₃)₂CO) δ 7.52 (d, *J* = 8.4 Hz, 2H), 7.38 (d, *J* = 8.4 Hz, 2H), 7.35 (d, *J* = 8.5 Hz, 2H), 7.06 (d, *J* = 8.3 Hz, 2H), 4.90 (d, *J* = 12.3 Hz, 1H), 4.81 (d, *J* = 12.2 Hz, 1H), 3.53 (d, *J* = 10.5 Hz, 1H), 2.54 – 2.47 (m, 1H), 2.44 – 2.37 (m, 1H), 2.33 – 2.23 (m, 1H), 1.71 – 1.61 (m, 1H), 1.56 – 1.47 (m, 1H), 1.27 – 1.20 (m, 1H), 1.07 (d, *J* = 6.5 Hz, 3H), 1.05 – 0.98 (m, 1H);

¹³C NMR (151 MHz, (CD₃)₂CO) δ 172.3, 142.6, 137.8, 132.6, 132.1, 131.8, 131.5, 122.0, 119.9, 96.2, 74.7, 58.4, 36.9, 35.6, 33.4, 28.6, 18.2.;

IR (neat) 2933, 2858, 1749, 1488, 1130, 1073, 1011, 827, 761, 719 cm⁻¹;

HRMS (+p NSI) calcd for $C_{21}H_{22}O_2Br_2Cl_3$ (M+H)⁺ 568.9047 found 568.9048;

HPLC (the ester product was reduced to 2,6-bis(4-bromophenyl)-3-methylhexan-1-ol for better separation) (OJH column, 5% *i*-propanol in hexane, 0.5 mL min⁻¹, 1 mg mL⁻¹, 180 min, UV 230 nm) retention times of 99.82 min (minor) and 146.59 min (major) (89% ee with Rh₂(*S*-2-Cl-5-BrTPCP)₄).



2,2,2-Tribromoethyl (2*S*,3*R*)-2,6-bis(4-bromophenyl)-3-methylhexanoate (95)

This compound was obtained according to *G.P. C* between 1-bromo-4-pentylbenzene (136.3 mg, 0.6 mmol, 2.0 equiv) and 2,2,2-tribromoethyl 2-(4-bromophenyl)-2-diazoacetate (151.7 mg, 0.3 mmol, 1.0 equiv), catalyzed by Rh₂(*S*-2-Cl-5-BrTPCP)₄ (5.7 mg, 0.003 mmol, 1.0 mol%). The product was purified by flash column chromatography on silica gel (gradient elution: 0 – 2% diethyl ether in pentane) to afford colorless oil in 84% yield.

R_f = 0.39 (pentane/diethyl ether = 19/1); [**α**]²⁰_D: +2.9° (c = 0.83, CHCl₃, 84% ee);

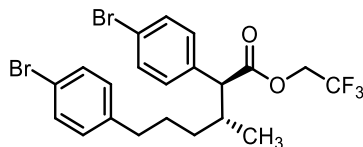
¹H NMR (600 MHz, CDCl₃) δ 7.44 (d, *J* = 8.4 Hz, 2H), 7.35 (d, *J* = 8.3 Hz, 2H), 7.23 (d, *J* = 8.4 Hz, 2H), 6.92 (d, *J* = 8.3 Hz, 2H), 4.91 (d, *J* = 12.3 Hz, 1H), 4.83 (d, *J* = 12.3 Hz, 1H), 3.38 (d, *J* = 10.7 Hz, 1H), 2.50 – 2.43 (m, 1H), 2.38 – 2.31 (m, 1H), 2.31 – 2.24 (m, 1H), 1.64 – 1.56 (m, 1H), 1.51 – 1.40 (m, 1H), 1.24 – 1.17 (m, 1H), 1.08 (d, *J* = 6.5 Hz, 3H), 1.01 – 0.91 (m, 1H);

¹³C NMR (151 MHz, CDCl₃) δ 171.5, 141.2, 136.2, 131.9, 131.4, 130.6, 130.2, 121.8, 119.6, 58.2, 36.0, 35.3, 35.2, 32.8, 28.0, 18.1;

IR (neat) 2936, 2858, 1746, 1488, 1128, 1073, 1011, 825, 737 cm⁻¹;

HRMS (+p NSI) calcd for $C_{21}H_{22}O_2Br_5$ (M+H)⁺ 700.7531 found 700.7541;

HPLC (the ester product was reduced to 2,6-bis(4-bromophenyl)-3-methylhexan-1-ol for better separation) (OJH column, 5% *i*-propanol in hexane, 0.5 mL min⁻¹, 1 mg mL⁻¹, 180 min, UV 230 nm) retention times of 109.22 min (minor) and 160.76 min (major) 84% ee with Rh₂(*S*-2-Cl-5-BrTPCP)₄.



2,2,2-Trifluoroethyl (2*S*,3*R*)-2,6-bis(4-bromophenyl)-3-methylhexanoate (94)

This compound was obtained according to *G.P. C* between 1-bromo-4-pentylbenzene (136.3 mg, 0.6 mmol, 2.0 equiv) and 2,2,2-trifluoroethyl 2-(4-bromophenyl)-2-diazoacetate (96.9 mg, 0.3 mmol, 1.0 equiv), catalyzed by Rh₂(*S*-2-Cl-5-BrTPCP)₄ (5.7 mg, 0.003 mmol, 1.0 mol%). The product was purified by flash column chromatography on silica gel (gradient elution: 0 – 2% diethyl ether in pentane) to afford colorless oil in 86% yield.

R_f = 0.55 (pentane/diethyl ether = 19/1); [**α**]_D²⁰: +29.6° (c = 1.00, CHCl₃, 91% ee);

¹H NMR (600 MHz, CDCl₃) δ 7.44 (d, *J* = 8.4 Hz, 2H), 7.34 (d, *J* = 8.3 Hz, 2H), 7.16 (d, *J* = 8.4 Hz, 2H), 6.92 (d, *J* = 8.3 Hz, 2H), 4.54 (dq, *J* = 12.7, 8.4 Hz, 1H), 4.32 (dq, *J* = 12.7, 8.4 Hz, 1H), 3.32 (d, *J* = 10.6 Hz, 1H), 2.49 – 2.42 (m, 1H), 2.37 – 2.30 (m, 1H), 2.25 – 2.15 (m, 1H), 1.62 – 1.55 (m, 1H), 1.48 – 1.39 (m, 1H), 1.20 – 1.13 (m, 1H), 1.01 (d, *J* = 6.5 Hz, 3H), 0.97 – 0.90 (m, 1H);

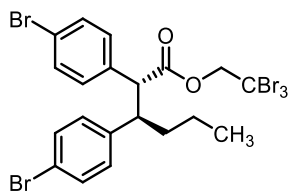
¹³C NMR (151 MHz, CDCl₃) δ 172.0, 141.2, 136.0, 132.0, 131.4, 130.3, 130.2, 123.0 (q, *J* = 277.3 Hz), 121.9, 119.6, 60.5 (q, *J* = 36.6 Hz), 57.6, 36.4, 35.2, 32.7, 28.0, 17.7;

IR (neat) 2937, 2860, 1754, 1488, 1281, 1168, 1134, 1074, 1011, 819 cm⁻¹;

¹⁹F NMR (282 MHz, CDCl₃) δ -73.7 (t, *J* = 8.3 Hz);

HRMS (+p NSI) calcd for $C_{21}H_{22}O_2Br_2F_3$ ($M+H$)⁺ 520.9933 found 520.9929;

HPLC (the ester product was reduced to 2,6-bis(4-bromophenyl)-3-methylhexan-1-ol for better separation) (OJH column, 5% *i*-propanol in hexane, 0.5 mL min⁻¹, 1 mg mL⁻¹, 180 min, UV 230 nm) retention times of 96.81 min (minor) and 140.95 min (major) 91% ee with Rh₂(*S*-2-Cl-5-BrTPCP)₄.



2,2,2-Tribromoethyl (2*R*,3*R*)-2,3-bis(4-bromophenyl)hexanoate (101c)

This compound was obtained according to *G.P. C* between 1-bromo-4-butylbenzene (127.9 mg, 0.6 mmol, 2.0 equiv) and 2,2,2-tribromoethyl 2-(4-bromophenyl)-2-diazoacetate (151.7 mg, 0.3 mmol, 1.0 equiv), catalyzed by Rh₂(*S*-TCPTAD)₄ (6.4 mg, 0.003 mmol, 1.0 mol%). The product was purified by flash column chromatography on silica gel (gradient elution: 0 – 2% diethyl ether in pentane) to afford colorless oil in 82% yield.

R_f = 0.49 (pentane/diethyl ether = 19/1); [**α**]_D²⁰: -44.2° (c = 1.06, CHCl₃, 94% ee);

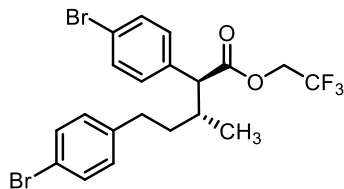
¹H NMR (600 MHz, CDCl₃) δ 7.27 (d, *J* = 2.5 Hz, 2H), 7.26 (d, *J* = 2.6 Hz, 2H), 7.07 (d, *J* = 8.5 Hz, 2H), 6.87 (d, *J* = 8.4 Hz, 2H), 4.96 (d, *J* = 12.3 Hz, 1H), 4.92 (d, *J* = 12.2 Hz, 1H), 3.84 (d, *J* = 11.4 Hz, 1H), 3.37 (td, *J* = 11.3, 3.4 Hz, 1H), 1.86 – 1.79 (m, 1H), 1.73 – 1.66 (m, 1H), 1.17 – 1.06 (m, 2H), 0.83 (t, *J* = 7.3 Hz, 3H);

¹³C NMR (151 MHz, CDCl₃) δ 171.2, 139.9, 135.3, 131.6, 131.5, 130.5, 130.1, 121.7, 120.4, 77.4, 58.0, 48.5, 37.2, 35.1, 20.6, 14.0;

IR (neat) 2956, 2870, 1744, 1487, 1133, 1073, 1010, 820, 731 cm⁻¹;

HRMS (+p APCI) calcd for $C_{20}H_{20}O_2^{79}Br_4^{81}Br$ (M+H)⁺ 688.7354 found 688.7352;

HPLC (the ester product was reduced to 2,5-bis(4-bromophenyl)-3-methylpentan-1-ol for better separation) (ODH column, 6% *i*-propanol in hexane, 0.25 mL min⁻¹, 1 mg mL⁻¹, 70 min, UV 230 nm) retention times of 31.63 min (minor) and 39.48 min (major) 94% ee with Rh₂(*S*-TCPTAD)₄.



2,2,2-Trifluoroethyl (2*S*,3*R*)-2,5-bis(4-bromophenyl)-3-methylpentanoate (105a)

This compound was obtained according to *G.P. C* between 1-bromo-4-butylbenzene (127.9 mg, 0.6 mmol, 2.0 equiv) and 2,2,2-trifluoroethyl 2-(4-bromophenyl)-2-diazoacetate (96.9 mg, 0.3 mmol, 1.0 equiv), catalyzed by Rh₂(*S*-2-Cl-5-BrTPCP)₄ (5.7 mg, 0.003 mmol, 1.0 mol%). The product was purified by flash column chromatography on silica gel (gradient elution: 0 – 2% diethyl ether in pentane) to afford colorless oil in 90% yield.

R_f = 0.44 (pentane/diethyl ether = 19/1); [**α**]_D²⁰: +16.8° (c = 1.09, CHCl₃, 92% ee);

¹H NMR (600 MHz, CDCl₃) δ 7.36 (d, *J* = 7.9 Hz, 2H), 7.26 (d, *J* = 7.4 Hz, 2H), 7.06 (d, *J* = 8.2 Hz, 2H), 6.79 (d, *J* = 7.9 Hz, 2H), 4.47 (dq, *J* = 12.3, 8.4 Hz, 1H), 4.24 (dq, *J* = 12.0, 8.3 Hz, 1H), 3.30 (d, *J* = 10.5 Hz, 1H), 2.56 – 2.49 (m, 1H), 2.35 – 2.27 (m, 1H), 2.17 – 2.08 (m, 1H), 1.42 – 1.35 (m, 1H), 1.17 – 1.10 (m, 1H), 1.01 (d, *J* = 6.5 Hz, 3H).;

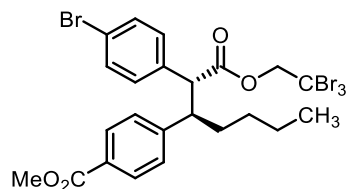
¹³C NMR (125 MHz, CDCl₃) δ 171.8, 140.7, 135.8, 132.0, 131.5, 130.3, 130.2, 122.9 (q, *J* = 277.3 Hz), 122.0, 119.7, 60.5 (q, *J* = 36.6 Hz), 57.6, 35.8, 35.0, 32.2, 17.7;

¹⁹F NMR (282 MHz, CDCl₃) δ -73.7 (t, *J* = 8.5 Hz);

IR (neat) 2932, 1749, 1488, 1130, 1072, 1011, 826, 801, 760, 717 cm⁻¹;

HRMS (+p NSI) calcd for $C_{20}H_{20}O_2Br_2F_3$ (M+H)⁺ 506.9777 found 506.9790;

HPLC (the ester product was reduced to 2,5-bis(4-bromophenyl)-3-methylpentan-1-ol for better separation) (ODH column, 6% *i*-propanol in hexane, 0.25 mL min⁻¹, 1 mg mL⁻¹, 70 min, UV 230 nm) retention times of 43.05 min (major) and 50.56 min (minor) 92% ee with Rh₂(*S*-2-Cl-5-BrTPCP)₄.



Methyl 4-((2*R*,3*R*)-2-(4-bromophenyl)-1-oxo-1-(2,2,2-tribromoethoxy)heptan-3-yl)benzoate (102c)

This compound was obtained according to *G.P. C* between methyl 4-pentylbenzoate (123.8 mg, 0.6 mmol, 2.0 equiv) and 2,2,2-tribromoethyl 2-(4-bromophenyl)-2-diazoacetate (151.7 mg, 0.3 mmol, 1.0 equiv), catalyzed by Rh₂(*S*-TCPTAD)₄ (6.4 mg, 0.003 mmol, 1.0 mol%). The product was purified by flash column chromatography on silica gel (gradient elution: 0 – 2% diethyl ether in pentane) to afford colorless oil in 42% yield.

R_f = 0.56 (pentane/diethyl ether = 19/1); [**α**]^{20_D}: -46.0° (c = 0.27, CHCl₃, 92% ee);

¹H NMR (600 MHz, CDCl₃) δ 7.81 (d, *J* = 8.4 Hz, 2H), 7.23 (d, *J* = 8.5 Hz, 2H), 7.06 (dd, *J* = 8.4, 4.5 Hz, 4H), 4.98 (d, *J* = 12.2 Hz, 1H), 4.91 (d, *J* = 12.2 Hz, 1H), 3.89 (d, *J* = 11.5 Hz, 1H),

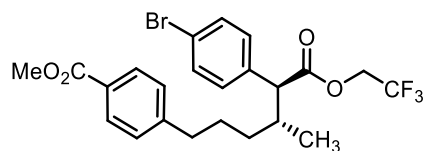
3.86 (s, 3H), 3.44 (td, $J = 11.2, 3.3$ Hz, 1H), 1.93 – 1.87 (m, 1H), 1.78 – 1.71 (m, 1H), 1.32 – 1.26 (m, 1H), 1.23 – 1.17 (m, 1H), 1.16 – 1.06 (m, 1H), 1.05 – 0.95 (m, 1H), 0.79 (t, $J = 7.3$ Hz, 3H);

^{13}C NMR (151 MHz, CDCl_3) δ 171.2, 167.0, 146.6, 135.3, 131.6, 130.5, 129.8, 128.7, 128.5, 121.7, 57.9, 52.2, 49.3, 35.1, 34.8, 29.9, 29.6, 22.6, 14.0;

IR (neat) 2953, 2929, 2857, 1747, 1720, 1281, 1137, 1111, 761 cm^{-1} ;

HRMS (+p APCI) calcd for $\text{C}_{23}\text{H}_{25}\text{O}_4\text{Br}_4$ ($\text{M}+\text{H}$) $^+$ 680.8481 found 680.8472;

HPLC (ADH column, 5% *i*-propanol in hexane, 1 mL min^{-1} , 1 mg mL^{-1} , 60 min, UV 230 nm) retention times of 16.69 min (minor) and 39.38 min (major) 92% ee with $\text{Rh}_2(\text{S-TCPTAD})_4$.



Methyl 4-((4R,5S)-5-(4-bromophenyl)-4-methyl-6-oxo-6-(2,2,2-trifluoroethoxy)hexyl)benzoate (106a)

This compound was obtained according to *G.P. C* between methyl 4-pentylbenzoate (123.8 mg, 0.6 mmol, 2.0 equiv) and 2,2,2-trifluoroethyl 2-(4-bromophenyl)-2-diazoacetate (96.9 mg, 0.3 mmol, 1.0 equiv), catalyzed by $\text{Rh}_2(\text{S-2-Cl-5-BrTPCP})_4$ (5.7 mg, 0.003 mmol, 1.0 mol%). The product was purified by flash column chromatography on silica gel (gradient elution: 2 – 6% diethyl ether in pentane) to afford colorless oil in 90% yield.

Rf = 0.18 (pentane/diethyl ether = 19/1); $[\alpha]^{20}_{\text{D}}$: +23.6° ($c = 1.00$, CHCl_3 , 94% ee);

^1H NMR (600 MHz, CDCl_3) δ 7.90 (d, $J = 8.3$ Hz, 2H), 7.43 (d, $J = 8.4$ Hz, 2H), 7.16 (d, $J = 8.4$ Hz, 2H), 7.11 (d, $J = 8.2$ Hz, 2H), 4.54 (dq, $J = 12.7, 8.4$ Hz, 1H), 4.32 (dq, $J = 12.7, 8.4$ Hz, 1H), 3.90 (s, 3H), 3.32 (d, $J = 10.6$ Hz, 1H), 2.59 – 2.52 (m, 1H), 2.47 – 2.40 (m, 1H), 2.26 – 2.15 (m, 1H), 1.66 – 1.58 (m, 1H), 1.53 – 1.42 (m, 1H), 1.22 – 1.15 (m, 1H), 1.01 (d, $J = 6.5$ Hz, 3H), 0.98 – 0.91 (m, 1H);

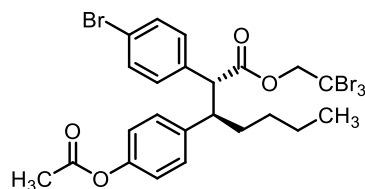
^{13}C NMR (125 MHz, CDCl_3) δ 172.0, 167.2, 147.8, 136.0, 132.0, 130.3, 129.8, 128.4, 127.9, 123.0 (q, $J = 277.3$ Hz), 121.9, 60.5 (q, $J = 36.6$ Hz), 57.6, 52.1, 36.4, 35.8, 32.8, 27.8, 17.7;

^{19}F NMR (282 MHz, CDCl_3) δ -73.7 (t, $J = 8.4$ Hz);

IR (neat) 2937, 1753, 1719, 1489, 1436, 1277, 1167, 1132, 1109, 1011, 978, 762 cm^{-1} ;

HRMS (+p NSI) calcd for $\text{C}_{23}\text{H}_{25}\text{O}_4\text{BrF}_3$ ($\text{M}+\text{H}$) $^+$ 501.0883 found 501.0885;

HPLC (the ester product was reduced to 2,5-bis(4-bromophenyl)-3-methylpentan-1-ol for better separation) (ODH column, 0.5% *i*-propanol in hexane, 1.5 mL min^{-1} , 1 mg mL^{-1} , 60 min, UV 230 nm) retention times of 25.16 min (minor) and 27.00 min (major) 94% ee with $\text{Rh}_2(\text{S-2-Cl-5-BrTPCP})_4$.



2,2,2-Tribromoethyl (2*R*,3*R*)-3-(4-acetoxyphenyl)-2-(4-bromophenyl)heptanoate (103c)

This compound was obtained according to *G.P. C* between 4-pentylphenyl acetate (123.8 mg, 0.6 mmol, 2.0 equiv) and 2,2,2-tribromoethyl 2-(4-bromophenyl)-2-diazoacetate (151.7 mg, 0.3 mmol, 1.0 equiv), catalyzed by $\text{Rh}_2(\text{S-TCPTAD})_4$ (6.4 mg, 0.003 mmol, 1.0 mol%). The product was purified by flash column chromatography on silica gel (gradient elution: 0 – 5% diethyl ether in pentane) to afford colorless oil in 83% yield.

$\text{Rf} = 0.16$ (pentane/diethyl ether = 19/1); $[\alpha]^{20}_{\text{D}}$: -46.1° ($c = 0.96$, CHCl_3 , 94% ee);

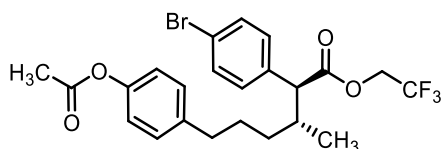
^1H NMR (600 MHz, CDCl_3) δ 7.25 (d, $J = 8.5$ Hz, 2H), 7.05 (d, $J = 8.5$ Hz, 2H), 6.97 (d, $J = 8.5$ Hz, 2H), 6.88 (d, $J = 8.6$ Hz, 2H), 4.97 (d, $J = 12.2$ Hz, 1H), 4.90 (d, $J = 12.2$ Hz, 1H), 3.84 (d, $J = 11.3$ Hz, 1H), 3.36 (td, $J = 11.2, 3.3$ Hz, 1H), 2.24 (s, 3H), 1.90 – 1.81 (m, 1H), 1.77 – 1.67 (m, 1H), 1.32 – 1.24 (m, 1H), 1.24 – 1.18 (m, 1H), 1.16 – 1.02 (m, 2H), 0.80 (t, $J = 7.3$ Hz, 3H);

^{13}C NMR (151 MHz, CDCl_3) δ 171.2, 169.2, 149.1, 138.2, 135.4, 131.4, 130.4, 129.1, 121.4, 121.2, 58.1, 48.6, 35.0, 34.7, 29.4, 22.5, 21.2, 13.9;

IR (neat) 2930, 2858, 1747, 1506, 1488, 1368, 1202, 1134, 1011, 911, 733, 632 cm^{-1} ;

HRMS (-p APCI) calcd for $\text{C}_{23}\text{H}_{23}\text{O}_4\text{Br}_4$ (M-H) $^-$ 678.8335 found 678.8341;

HPLC (ADH column, 1% *i*-propanol in hexane, 0.5 mL min^{-1} , 1 mg mL^{-1} , 90 min, UV 230 nm) retention times of 45.26 min (minor) and 62.57 min (major) 94% ee with $\text{Rh}_2(\text{S-TCPTAD})_4$.



2,2,2-Trifluoroethyl (2*S*,3*R*)-6-(4-acetoxyphenyl)-2-(4-bromophenyl)-3-methylhexanoate (107a)

This compound was obtained according to *G.P. C* between 4-pentylphenyl acetate (123.8 mg, 0.6 mmol, 2.0 equiv) and 2,2,2-trifluoroethyl 2-(4-bromophenyl)-2-diazoacetate (96.9 mg, 0.3 mmol, 1.0 equiv), catalyzed by $\text{Rh}_2(\text{S-2-Cl-5-BrTPCP})_4$ (5.7 mg, 0.003 mmol, 1.0 mol%). The product was purified by flash column chromatography on silica gel (gradient elution: 0 – 5% diethyl ether in pentane) to afford colorless oil in 90% yield.

Rf = 0.16 (pentane/diethyl ether = 19/1); $[\alpha]^{20}_{\text{D}}$: +19.4° ($c = 1.01$, CHCl_3 , 94% ee);

^1H NMR (600 MHz, CDCl_3) δ 7.45 (d, $J = 8.5$ Hz, 2H), 7.17 (d, $J = 8.4$ Hz, 2H), 7.04 (d, $J = 8.6$ Hz, 2H), 6.94 (d, $J = 8.5$ Hz, 2H), 4.54 (dq, $J = 12.7, 8.5$ Hz, 1H), 4.32 (dq, $J = 12.7, 8.4$ Hz, 1H), 3.33 (d, $J = 10.5$ Hz, 1H), 2.48 (ddd, $J = 14.7, 9.3, 5.9$ Hz, 1H), 2.37 (ddd, $J = 13.9, 9.3, 6.5$ Hz, 1H), 2.28 (s, 3H), 2.25 – 2.14 (m, 1H), 1.65 – 1.56 (m, 1H), 1.49 – 1.39 (m, 1H), 1.23 – 1.15 (m, 1H), 1.01 (d, $J = 6.5$ Hz, 3H), 0.99 – 0.90 (m, 1H).;

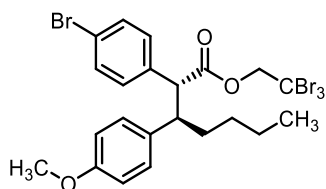
^{13}C NMR (151 MHz, CDCl_3) δ 171.8, 169.6, 148.7, 139.7, 135.9, 131.8, 130.2, 129.1, 122.8 (q, $J = 277.4$ Hz), 121.7, 121.2, 60.3 (q, $J = 36.7$ Hz), 57.5, 36.3, 35.1, 32.7, 28.0, 21.1, 17.6;

^{19}F NMR (282 MHz, CDCl_3) δ -73.7 (t, $J = 8.4$ Hz);

IR (neat) 2937, 2861, 1755, 1507, 1489, 1217, 1195, 1166, 1134, 1011, 979 cm^{-1} ;

HRMS (-p APCI) calcd for $\text{C}_{23}\text{H}_{23}\text{O}_4\text{BrF}_3$ (M-H) $^-$ 499.0737 found 499.0742;

HPLC (ADH column, 1% *i*-propanol in hexane, 0.5 mL min^{-1} , 1 mg mL^{-1} , 60 min, UV 230 nm) retention times of 34.22 min (minor) and 36.44 min (major) 94% ee with $\text{Rh}_2(\text{S-2-Cl-5-BrTPCP})_4$.



2,2,2-Tribromoethyl (2*R*,3*R*)-2-(4-bromophenyl)-3-(4-methoxyphenyl)heptanoate (104c)

This compound was obtained according to *G.P. C* between 1-methoxy-4-pentylbenzene (107.0 mg, 0.6 mmol, 2.0 equiv) and 2,2,2-tribromoethyl 2-(4-bromophenyl)-2-diazoacetate (151.7 mg, 0.3 mmol, 1.0 equiv), catalyzed by $\text{Rh}_2(\text{S-TCPTAD})_4$ (6.4 mg, 0.003 mmol, 1.0 mol%). The product was purified by flash column chromatography on silica gel (gradient elution: 0 – 3% diethyl ether in pentane) to afford colorless oil in 91% yield.

$\text{Rf} = 0.51$ (pentane/diethyl ether = 19/1); $[\alpha]^{20}_{\text{D}}$: -47.9° ($c = 0.93$, CHCl_3 , 87% ee);

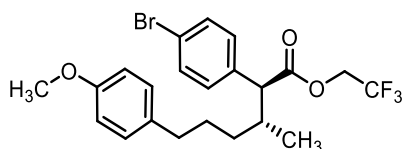
^1H NMR (600 MHz, CDCl_3) δ 7.24 (d, $J = 8.5$ Hz, 2H), 7.07 (d, $J = 8.5$ Hz, 2H), 6.88 (d, $J = 8.7$ Hz, 2H), 6.67 (d, $J = 8.7$ Hz, 2H), 4.97 (d, $J = 12.2$ Hz, 1H), 4.90 (d, $J = 12.3$ Hz, 1H), 3.83 (d, $J = 11.3$ Hz, 1H), 3.72 (s, 3H), 3.30 (td, $J = 11.2, 3.4$ Hz, 1H), 1.87 – 1.78 (m, 1H), 1.74 – 1.65 (m, 1H), 1.31 – 1.23 (m, 1H), 1.24 – 1.16 (m, 1H), 1.16 – 1.03 (m, 2H), 0.79 (t, $J = 7.3$ Hz, 3H);

^{13}C NMR (151 MHz, CDCl_3) δ 171.5, 157.9, 135.7, 132.7, 131.3, 130.5, 129.1, 121.2, 113.6, 58.3, 55.1, 48.3, 35.1, 34.8, 29.5, 22.5, 13.9;

IR (neat) 2954, 2930, 2857, 1745, 1611, 1512, 1488, 1247, 1133, 1114, 1074, 1037, 828, 732, 717, 632 cm^{-1} ;

HRMS (+p NSI) calcd for $\text{C}_{22}\text{H}_{25}\text{O}_3\text{Br}_3$ ^{81}Br (M+H) $^+$ 654.8511 found 654.8523;

HPLC (ADH column, 1% *i*-propanol in hexane, 0.5 mL min^{-1} , 1 mg mL^{-1} , 60 min, UV 230 nm) retention times of 18.41 min (minor) and 32.61 min (major) 87% ee with $\text{Rh}_2(\text{S-TCPTAD})_4$.



2,2,2-Trifluoroethyl (2*S*,3*R*)-2-(4-bromophenyl)-6-(4-methoxyphenyl)-3-methylhexanoate (108a)

This compound was obtained according to *G.P. C* between 1-methoxy-4-pentylbenzene (107.0 mg, 0.6 mmol, 2.0 equiv) and 2,2,2-trifluoroethyl 2-(4-bromophenyl)-2-diazoacetate (96.9 mg, 0.3 mmol, 1.0 equiv), catalyzed by $\text{Rh}_2(\text{S-2-Cl-5-BrTPCP})_4$ (5.7 mg, 0.003 mmol, 1.0 mol%). The product was purified by flash column chromatography on silica gel (gradient elution: 0 – 3% diethyl ether in pentane) to afford colorless oil in 39% yield (mixture of minor diastereomer of benzylic and C2 insertion product) and 15% yield of major diastereomer of benzylic insertion product. The pure major diastereomer of C2 insertion product was obtained from prep HPLC (Ascentis® C18 column, 85% acetonitrile in H_2O with 0.1% trifluoroacetic acid).

Rf = 0.29 (pentane/diethyl ether = 19/1); $[\alpha]^{20}_{\text{D}}$: +26.0° (*c* = 1.02, CHCl_3 , 93% ee);

^1H NMR (600 MHz, CDCl_3) δ 7.44 (d, *J* = 8.4 Hz, 2H), 7.17 (d, *J* = 8.4 Hz, 2H), 6.96 (d, *J* = 8.8 Hz, 2H), 6.77 (d, *J* = 8.6 Hz, 2H), 4.53 (dq, *J* = 12.7, 8.4 Hz, 1H), 4.32 (dq, *J* = 12.7, 8.4 Hz, 1H),

3.78 (s, 3H), 3.32 (d, $J = 10.5$ Hz, 1H), 2.45 (ddd, $J = 14.5, 9.1, 5.9$ Hz, 1H), 2.32 (ddd, $J = 13.8, 9.1, 6.7$ Hz, 1H), 2.27 – 2.16 (m, 1H), 1.61 – 1.52 (m, 2H), 1.48 – 1.38 (m, 1H), 1.22 – 1.14 (m, 1H), 1.01 (d, $J = 6.5$ Hz, 3H), 0.98 – 0.90 (m, 1H);

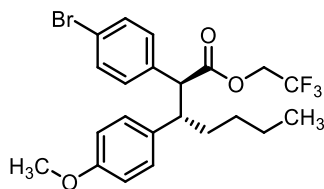
^{13}C NMR (151 MHz, CDCl_3) δ 171.9, 157.7, 136.0, 134.2, 131.8, 130.2, 129.1, 122.8 (q, $J = 277.5$ Hz), 121.6, 113.7, 60.3 (q, $J = 36.6$ Hz), 57.5, 55.3, 36.3, 34.7, 32.6, 28.2, 17.6;

^{19}F NMR (282 MHz, CDCl_3) δ -73.7 (t, $J = 8.4$ Hz);

IR (neat) 2936, 2858, 1754, 1513, 1281, 1246, 1173, 1134, 1038, 1012, 979, 821 cm^{-1} ;

HRMS (+p APCI) calcd for $\text{C}_{22}\text{H}_{25}\text{O}_4\text{BrF}_3$ ($\text{M}+\text{H}$) $^+$ 473.0934 found 473.0943;

HPLC (R,R-Whelk column, 0.5% *i*-propanol in hexane, 0.5 mL min^{-1} , 1 mg mL^{-1} , 60 min, UV 230 nm) retention times of 41.67 min (minor) and 49.72 min (major) 93% ee with $\text{Rh}_2(\text{S-2-Cl-5-BrTPCP})_4$.



2,2,2-Trifluoroethyl (2S,3S)-2-(4-bromophenyl)-3-(4-methoxyphenyl)heptanoate (104a)

This compound was obtained according to *G.P. C* between 1-methoxy-4-pentylbenzene (107.0 mg, 0.6 mmol, 2.0 equiv) and 2,2,2-trifluoroethyl 2-(4-bromophenyl)-2-diazoacetate (96.9 mg, 0.3 mmol, 1.0 equiv), catalyzed by $\text{Rh}_2(\text{S-2-Cl-5-BrTPCP})_4$ (5.7 mg, 0.003 mmol, 1.0 mol%). The product was purified by flash column chromatography on silica gel (gradient elution: 0 – 3% diethyl ether in pentane) to afford 15% yield of major diastereomer of benzylic insertion product.

Rf = 0.51 (pentane/diethyl ether = 19/1); $[\alpha]^{20}_{\text{D}}$: +69.8° ($c = 0.79$, CHCl_3 , 82% ee);

^1H NMR (600 MHz, CDCl_3) δ 7.25 (d, $J = 8.5$ Hz, 2H), 6.99 (d, $J = 8.5$ Hz, 2H), 6.84 (d, $J = 8.6$ Hz, 2H), 6.66 (d, $J = 8.7$ Hz, 2H), 4.60 (dq, $J = 12.7, 8.4$ Hz, 1H), 4.38 (dq, $J = 12.7, 8.4$ Hz, 1H), 3.76 (d, $J = 11.2$ Hz, 1H), 3.71 (s, 3H), 3.21 (td, $J = 10.7, 4.4$ Hz, 1H), 1.72 – 1.60 (m, 2H), 1.32 – 1.27 (m, 1H), 1.23 – 1.16 (m, 1H), 1.13 – 0.99 (m, 2H), 0.80 (t, $J = 7.3$ Hz, 3H);

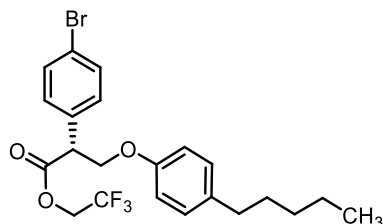
^{13}C NMR (151 MHz, CDCl_3) δ 171.9, 158.0, 135.5, 132.5, 131.4, 130.2, 129.1, 122.9 (q, $J = 277.1$ Hz), 121.3, 113.6, 60.5 (q, $J = 36.6$ Hz), 57.8, 55.1, 48.6, 34.4, 29.4, 22.4, 13.8;

^{19}F NMR (282 MHz, CDCl_3) δ -73.6 (t, $J = 8.4$ Hz);

IR (neat) 2957, 2932, 2859, 1753, 1512, 1489, 1281, 1174, 1137, 1037, 1012, 828 cm^{-1} ;

HRMS (-p APCI) calcd for $\text{C}_{22}\text{H}_{23}\text{O}_4\text{BrF}_3$ (M-H) $^-$ 471.0788 found 471.0792;

HPLC (R,R-Whelk column, 0.5% *i*-propanol in hexane, 1 mL min^{-1} , 1 mg mL^{-1} , 40 min, UV 230 nm) retention times of 18.64 min (major) and 20.20 min (minor) 82% ee with $\text{Rh}_2(\text{S-2-Cl-5-BrTPCP})_4$.



2,2,2-Trifluoroethyl (R)-2-(4-bromophenyl)-3-(4-pentylphenoxy)propanoate

This compound was obtained according to *G.P. C* between 1-methoxy-4-pentylbenzene (107.0 mg, 0.6 mmol, 2.0 equiv) and 2,2,2-trifluoroethyl 2-(4-bromophenyl)-2-diazoacetate (96.9 mg, 0.3 mmol, 1.0 equiv), catalyzed by $\text{Rh}_2(\text{S-2-Cl-5-BrTPCP})_4$ (5.7 mg, 0.003 mmol, 1.0 mol%). The product was purified by flash column chromatography on silica gel (gradient elution: 0 – 3% diethyl ether in pentane) to afford colorless oil in 36% yield.

R_f = 0.59 (pentane/diethyl ether = 19/1); [α] $^{20}_{\text{D}}$: +21.3° (c = 0.98, CHCl_3 , 84% ee);

^1H NMR (600 MHz, CDCl_3) δ 7.50 (d, $J = 8.5$ Hz, 2H), 7.25 (d, $J = 8.4$ Hz, 3H), 7.07 (d, $J = 8.7$ Hz, 2H), 6.78 (d, $J = 8.6$ Hz, 2H), 4.60 – 4.53 (m, 1H), 4.52 – 4.45 (m, 2H), 4.20 – 4.09 (m, 2H), 2.56 – 2.49 (m, 2H), 1.60 – 1.54 (m, 2H), 1.34 – 1.26 (m, 4H), 0.88 (t, $J = 7.1$ Hz, 3H);

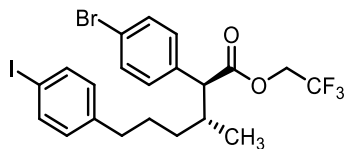
^{13}C NMR (151 MHz, CDCl_3) δ 170.1, 156.1, 136.0, 133.2, 132.1, 129.9, 129.3, 122.7 (q, $J = 277.4$ Hz), 122.4, 114.6, 69.0, 60.7 (q, $J = 36.9$ Hz), 50.7, 35.0, 31.4, 31.4, 22.5, 14.0;

^{19}F NMR (282 MHz, CDCl_3) δ -73.7 (t, $J = 8.4$ Hz);

IR (neat) 2967, 2929, 1760, 1511, 1490, 1282, 1242, 1169, 1149, 1012, 824 cm^{-1} ;

HRMS (-p APCI) calcd for $\text{C}_{22}\text{H}_{23}\text{O}_4\text{BrF}_3$ (M-H) $^-$ 471.0788 found 471.0792;

HPLC (OD column, 0.5% *i*-propanol in hexane, 1 mL min^{-1} , 1 mg mL^{-1} , 45 min, UV 230 nm) retention times of 20.13 min (major) and 24.92 min (minor) 84% ee with $\text{Rh}_2(\text{S-2-Cl-5-BrTPCP})_4$.



2,2,2-Trifluoroethyl (2S,3R)-2-(4-bromophenyl)-6-(4-iodophenyl)-3-methylhexanoate (109)

This compound was obtained according to *G.P. C* between 1-iodo-4-pentylbenzene (164.5 mg, 0.6 mmol, 2.0 equiv) and 2,2,2-trifluoroethyl 2-(4-bromophenyl)-2-diazoacetate (96.9 mg, 0.3 mmol, 1.0 equiv), catalyzed by $\text{Rh}_2(\text{S-2-Cl-5-BrTPCP})_4$ (5.7 mg, 0.003 mmol, 1.0 mol%). The product was purified by flash column chromatography on silica gel (gradient elution: 0 – 2% diethyl ether in pentane) to afford colorless oil in 88% yield.

Rf = 0.35 (pentane/diethyl ether = 19/1); **$[\alpha]^{20}_{\text{D}}$** : +23.2° ($c = 1.05$, CHCl_3 , 89% ee);

^1H NMR (600 MHz, CDCl_3) δ 7.54 (d, $J = 8.2$ Hz, 2H), 7.44 (d, $J = 8.4$ Hz, 2H), 7.16 (d, $J = 8.4$ Hz, 2H), 6.80 (d, $J = 8.3$ Hz, 2H), 4.54 (dq, $J = 12.6, 8.4$ Hz, 1H), 4.32 (dq, $J = 12.7, 8.4$ Hz, 1H), 3.32 (d, $J = 10.6$ Hz, 1H), 2.48 – 2.41 (m, 1H), 2.36 – 2.28 (m, 1H), 2.25 – 2.15 (m, 1H), 1.48 –

1.38 (m, 1H), 1.48 – 1.38 (m, 1H), 1.20 – 1.13 (m, 1H), 1.01 (d, $J = 6.5$ Hz, 3H), 0.97 – 0.89 (m, 1H);

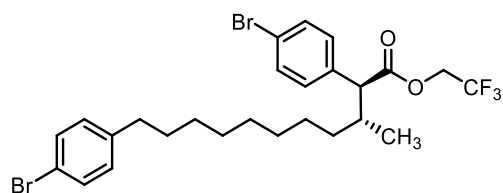
^{13}C NMR (151 MHz, CDCl_3) δ 172.0, 141.9, 137.4, 136.0, 132.0, 130.5, 130.3, 123.0 (q, $J = 277.3$ Hz), 121.9, 90.9, 60.5 (q, $J = 36.6$ Hz), 57.6, 36.4, 35.3, 32.7, 28.0, 17.7;

^{19}F NMR (282 MHz, CDCl_3) δ -73.7 (t, $J = 8.4$ Hz);

IR (neat) 2937, 2860, 1754, 1487, 1280, 1168, 1134, 1008, 879, 820, 734 cm^{-1} ;

HRMS (+p NSI) calcd for $\text{C}_{21}\text{H}_{22}\text{O}_2\text{Br}_2\text{F}_3\text{I}$ (M+H) $^+$ 568.9794 found 568.9792;

HPLC (ADH column, 0.5% *i*-propanol in hexane, 0.5 mL min^{-1} , 1 mg mL^{-1} , 60 min, UV 230 nm) retention times of 21.39 min (minor) and 22.93 min (major) 89% ee with $\text{Rh}_2(\text{S-2-Cl-5-BrTPCP})_4$.



2,2,2-Trifluoroethyl (2S,3R)-2,11-bis(4-bromophenyl)-3-methylundecanoate (110)

This compound was obtained according to *G.P. C* between 1-bromo-4-decylbenzene (178.4 mg, 0.6 mmol, 2.0 equiv) and 2,2,2-trifluoroethyl 2-(4-bromophenyl)-2-diazoacetate (96.9 mg, 0.3 mmol, 1.0 equiv), catalyzed by $\text{Rh}_2(\text{S-2-Cl-5-BrTPCP})_4$ (5.7 mg, 0.003 mmol, 1.0 mol%). The product was purified by flash column chromatography on silica gel (gradient elution: 0 – 1% diethyl ether in pentane) to afford colorless oil in 92% yield.

$\text{Rf} = 0.63$ (pentane/diethyl ether = 19/1); $[\alpha]^{20}_{\text{D}}$: +17.9° ($c = 1.00$, CHCl_3 , 94% ee);

^1H NMR (600 MHz, CDCl_3) δ 7.45 (d, $J = 8.5$ Hz, 2H), 7.38 (d, $J = 8.3$ Hz, 2H), 7.20 (d, $J = 8.5$ Hz, 2H), 7.03 (d, $J = 8.4$ Hz, 2H), 4.54 (dq, $J = 12.7, 8.4$ Hz, 1H), 4.33 (dq, $J = 12.7, 8.4$ Hz, 1H), 3.33 (d, $J = 10.5$ Hz, 1H), 2.53 (t, $J = 7.7$ Hz, 2H), 2.22 – 2.12 (m, 1H), 1.58 – 1.50 (m, 2H), 1.32

– 1.18 (m, 5H), 1.19 – 1.08 (m, 5H), 1.07 – 1.02 (m, 1H), 1.00 (d, $J = 6.5$ Hz, 3H), 0.93 – 0.83 (m, 1H);

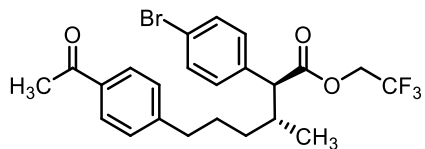
^{13}C NMR (151 MHz, CDCl_3) δ 172.1, 141.9, 136.3, 131.9, 131.4, 130.4, 130.3, 123.0 (q, $J = 277.3$ Hz), 121.8, 119.4, 60.5 (q, $J = 36.6$ Hz), 57.8, 36.5, 35.5, 33.3, 31.4, 29.6, 29.5, 29.5, 29.3, 26.3, 17.7;

^{19}F NMR (282 MHz, CDCl_3) δ -73.7 (t, $J = 8.5$ Hz);

IR (neat) 2929, 2855, 1755, 1488, 1281, 1169, 1132, 1074, 1102, 979, 912, 761, 737 cm^{-1} ;

HRMS (-p NSI) calcd for $\text{C}_{26}\text{H}_{31}\text{O}_2\text{Br}_2\text{F}_3\text{Cl}$ ($\text{M}+\text{Cl}$) $^-$ 625.0337 found 625.0361;

HPLC (ADH column, 0.3% *i*-propanol in hexane, 0.5 mL min^{-1} , 1 mg mL^{-1} , 60 min, UV 230 nm) retention times of 33.36 min (minor) and 46.06 min (major) 94% ee with $\text{Rh}_2(\text{S-2-Cl-5-BrTPCP})_4$.



2,2,2-Trifluoroethyl (2S,3R)-6-(4-acetylphenyl)-2-(4-bromophenyl)-3-methylhexanoate (111)

This compound was obtained according to *G.P. C* between 1-(4-pentylphenyl)ethan-1-one (114.2 mg, 0.6 mmol, 2.0 equiv) and 2,2,2-trifluoroethyl 2-(4-bromophenyl)-2-diazoacetate (96.9 mg, 0.3 mmol, 1.0 equiv), catalyzed by $\text{Rh}_2(\text{S-2-Cl-5-BrTPCP})_4$ (5.7 mg, 0.003 mmol, 1.0 mol%). The product was purified by flash column chromatography on silica gel (gradient elution: 2 – 10% diethyl ether in pentane) to afford colorless oil in 35% yield.

$\text{Rf} = 0.04$ (pentane/diethyl ether = 19/1); $[\alpha]^{20}_{\text{D}}$: -5.9° ($c = 1.23$, CHCl_3 , 93% ee);

^1H NMR (600 MHz, CDCl_3) δ 7.83 (d, $J = 8.2$ Hz, 2H), 7.43 (d, $J = 8.5$ Hz, 2H), 7.17 (d, $J = 8.4$ Hz, 2H), 7.13 (d, $J = 8.2$ Hz, 2H), 4.54 (dq, $J = 12.7, 8.4$ Hz, 1H), 4.32 (dq, $J = 12.7, 8.4$ Hz, 1H), 3.32 (d, $J = 10.6$ Hz, 1H), 2.62 – 2.53 (m, 4H), 2.48 – 2.41 (m, 1H), 2.25 – 2.18 (m, 1H), 1.66 –

1.58 (m, 1H), 1.53 – 1.44 (m, 1H), 1.22 – 1.15 (m, 1H), 1.02 (d, $J = 6.5$ Hz, 3H), 0.99 – 0.92 (m, 1H);

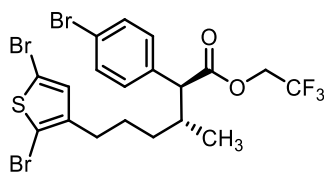
^{13}C NMR (151 MHz, CDCl_3) δ 198.0, 172.0, 148.0, 136.0, 135.2, 132.0, 130.3, 128.6, 128.6, 123.0 (q, $J = 277.4$ Hz), 121.9, 60.5 (q, $J = 36.6$ Hz), 57.6, 36.4, 35.8, 32.8, 27.8, 26.7, 17.8;

^{19}F NMR (282 MHz, CDCl_3) δ -73.7 (t, $J = 8.4$ Hz);

IR (neat) 2935, 2860, 1752, 1681, 1268, 1165, 1132, 1074, 1011, 978, 818 cm^{-1} ;

HRMS (+p NSI) calcd for $\text{C}_{23}\text{H}_{25}\text{O}_3\text{BrF}_3$ ($\text{M}+\text{H}$) $^+$ 485.0934 found 485.0946;

HPLC (ADH column, 1% *i*-propanol in hexane, 1 mL min^{-1} , 1 mg mL^{-1} , 60 min, UV 210 nm) retention times of 33.13 min (major) and 37.95 min (minor) 93% ee with $\text{Rh}_2(\text{S-2-Cl-5-BrTPCP})_4$.



2,2,2-Trifluoroethyl (2S,3R)-2-(4-bromophenyl)-6-(2,5-dibromothiophen-3-yl)-3-methylhexanoate (112)

This compound was obtained according to *G.P. C* between 2,5-dibromo-3-pentylthiophene (187.2 mg, 0.6 mmol, 2.0 equiv) and 2,2,2-trifluoroethyl 2-(4-bromophenyl)-2-diazoacetate (96.9 mg, 0.3 mmol, 1.0 equiv), catalyzed by $\text{Rh}_2(\text{S-2-Cl-5-BrTPCP})_4$ (5.7 mg, 0.003 mmol, 1.0 mol%). The product was purified by flash column chromatography on silica gel (gradient elution: 0 – 2% diethyl ether in pentane) to afford colorless oil in 78% yield.

R_f = 0.38 (pentane/diethyl ether = 19/1); [α] $^{20}_{\text{D}}$: +21.6° (c = 1.08, CHCl_3 , 84% ee);

^1H NMR (600 MHz, CDCl_3) δ 7.45 (d, $J = 8.4$ Hz, 2H), 7.18 (d, $J = 8.4$ Hz, 2H), 6.62 (s, 1H), 4.55 (dq, $J = 12.7, 8.4$ Hz, 1H), 4.33 (dq, $J = 12.7, 8.4$ Hz, 1H), 3.33 (d, $J = 10.6$ Hz, 1H), 2.42 –

2.36 (m, 1H), 2.35 – 2.29 (m, 1H), 2.25 – 2.17 (m, 1H), 1.57 – 1.52 (m, 1H), 1.44 – 1.34 (m, 1H), 1.19 – 1.12 (m, 1H), 1.02 (d, $J = 6.6$ Hz, 3H), 0.97 – 0.90 (m, 1H);

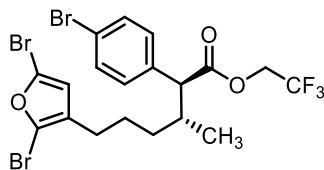
^{13}C NMR (151 MHz, CDCl_3) δ 171.9, 142.3, 135.9, 132.0, 130.8, 130.3, 122.95 (q, $J = 277.3$ Hz), 122.0, 110.7, 108.3, 60.5 (q, $J = 36.6$ Hz), 57.6, 36.3, 32.5, 29.3, 26.2, 17.7;

^{19}F NMR (282 MHz, CDCl_3) δ -73.7 (t, $J = 8.4$ Hz);

IR (neat) 2938, 2862, 1754, 1489, 1281, 1168, 1133, 1011, 979, 820 cm^{-1} ;

HRMS (+p NSI) calcd for $\text{C}_{19}\text{H}_{19}\text{SO}_2\text{Br}_3\text{F}_3$ ($\text{M}+\text{H}$) $^+$ 604.8602 found 604.8613;

HPLC (R,R-Whelk column, 0.1% *i*-propanol in hexane, 0.6 mL min^{-1} , 1 mg mL^{-1} , 90 min, UV 230 nm) retention times of 54.10 min (minor) and 68.83 min (major) 84% ee with $\text{Rh}_2(\text{S-2-Cl-5-BrTPCP})_4$.



2,2,2-Trichloroethyl (2*S*,3*R*)-2-(4-bromophenyl)-6-(2,5-dibromofuran-3-yl)-3-methylhexanoate (113)

This compound was obtained according to *G.P. C* between 2,5-dibromo-3-pentylfuran (161.4 mg, 0.6 mmol, 2.0 equiv) and 2,2,2-trifluoroethyl 2-(4-bromophenyl)-2-diazoacetate (96.9 mg, 0.3 mmol, 1.0 equiv), catalyzed by $\text{Rh}_2(\text{S-2-Cl-5-BrTPCP})_4$ (5.7 mg, 0.003 mmol, 1.0 mol%). The product was purified by flash column chromatography on silica gel (gradient elution: 0 – 2% diethyl ether in pentane) to afford colorless oil in 83% yield.

R_f = 0.38 (pentane/diethyl ether = 19/1); [α] $^{20}_{\text{D}}$: +16.0° (c = 1.00, CHCl_3 , 86% ee);

^1H NMR (600 MHz, CDCl_3) δ 7.46 (d, $J = 8.5$ Hz, 2H), 7.18 (d, $J = 8.4$ Hz, 2H), 6.06 (s, 1H), 4.55 (dq, $J = 12.7, 8.4$ Hz, 1H), 4.32 (dq, $J = 12.7, 8.4$ Hz, 1H), 3.32 (d, $J = 10.6$ Hz, 1H), 2.24 –

2.16 (m, 2H), 2.15 – 2.09 (m, 1H), 1.53 – 1.45 (m, 1H), 1.41 – 1.31 (m, 1H), 1.18 – 1.11 (m, 1H), 1.01 (d, $J = 6.6$ Hz, 3H), 0.96 – 0.88 (m, 1H);

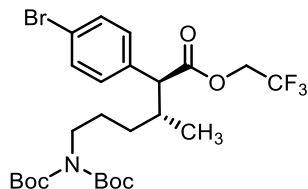
^{13}C NMR (151 MHz, CDCl_3) δ 171.9, 135.9, 132.0, 130.3, 126.8, 123.0 (q, $J = 277.3$ Hz), 122.0, 121.6, 119.8, 114.6, 60.5 (q, $J = 36.7$ Hz), 57.6, 36.2, 32.5, 25.8, 25.1, 17.7;

^{19}F NMR (282 MHz, CDCl_3) δ -73.7 (t, $J = 8.4$ Hz);

IR (neat) 2937, 2859, 1735, 1489, 1280, 1166, 1130, 1075, 1011, 979, 929, 818 cm^{-1} ;

HRMS (+p NSI) calcd for $\text{C}_{19}\text{H}_{19}\text{O}_3\text{Br}_3\text{F}_3$ ($\text{M}+\text{H}$) $^+$ 588.8831 found 588.8846;

HPLC (R,R-Whelk column, 0.3% *i*-propanol in hexane, 0.5 mL min^{-1} , 1 mg mL^{-1} , 90 min, UV 230 nm) retention times of 37.50 min (minor) and 45.33 min (major) 86% ee with $\text{Rh}_2(\text{S-2-Cl-5-BrTPCP})_4$.



2,2,2-Trifluoroethyl (2S,3R)-2-(4-bromophenyl)-6-(N,N-di-boc-amine)-3-methylhexanoate (114)

This compound was obtained according to *G.P. C* between *N,N*-di-Boc-pentylamine (172.4 mg, 0.6 mmol, 2.0 equiv) and 2,2,2-trifluoroethyl 2-(4-bromophenyl)-2-diazoacetate (96.9 mg, 0.3 mmol, 1.0 equiv), catalyzed by $\text{Rh}_2(\text{S-2-Cl-5-BrTPCP})_4$ (5.7 mg, 0.003 mmol, 1.0 mol%). The product was purified by flash column chromatography on silica gel (gradient elution: 0 – 2% diethyl ether in pentane) to afford colorless oil in 89% yield.

Rf = 0.11 (pentane/diethyl ether = 19/1); **$[\alpha]_D^{20}$** : +18.1° ($c = 1.27$, CHCl_3);

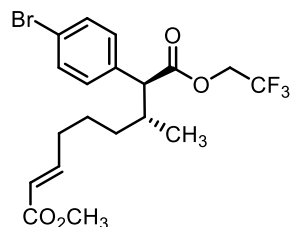
¹H NMR (600 MHz, CDCl₃) δ 7.44 (d, *J* = 8.4 Hz, 2H), 7.19 (d, *J* = 8.5 Hz, 2H), 4.53 (dq, *J* = 12.7, 8.4 Hz, 1H), 4.33 (dq, *J* = 12.7, 8.4 Hz, 1H), 3.44 – 3.34 (m, 2H), 3.33 (d, *J* = 10.6 Hz, 1H), 2.25 – 2.15 (m, 1H), 1.63 – 1.58 (m, 1H), 1.47-1.36 (m, 19H), 1.18 – 1.10 (m, 1H), 1.02 (d, *J* = 6.5 Hz, 3H), 0.93 – 0.84 (m, 1H);

¹³C NMR (125 MHz, CDCl₃) δ 171.9, 152.7, 135.9, 132.0, 130.3, 121.9, 82.3, 60.5 (q, *J* = 36.6 Hz), 57.8, 46.4, 36.3, 30.4, 28.2, 25.9, 17.7;

IR (neat) 2978, 2935, 1748, 1693, 1367, 1278, 1165, 1122, 1074, 1011, 979, 855, 760, 737 cm⁻¹;

HRMS (+p NSI) calcd for C₂₅H₃₄NO₆BrF₃ (M-H)⁻ 580.1527 found 580.1529;

HPLC (R,R-Whelk column, 3% *i*-propanol in hexane, 0.6 mL min⁻¹, 1 mg mL⁻¹, 60 min, UV 210 nm) retention times of 30.59 min (major) and 27.11 min (minor) 88% ee with Rh₂(*S*-2Cl15Br-TPCP)₄.



1-Methyl 9-(2,2,2-trifluoroethyl) (7*R*,8*S*,*E*)-8-(4-bromophenyl)-7-methylnon-2-enedioate (115)

This compound was obtained according to *G.P. C* between methyl (*E*)-oct-2-enoate (93.8 mg, 0.6 mmol, 2.0 equiv) and 2,2,2-trifluoroethyl 2-(4-bromophenyl)-2-diazoacetate (96.9 mg, 0.3 mmol, 1.0 equiv), catalyzed by Rh₂(*S*-2-Cl-5-BrTPCP)₄ (5.7 mg, 0.003 mmol, 1.0 mol%). The product was purified by flash column chromatography on silica gel (gradient elution: 0 – 2% diethyl ether in pentane) to afford colorless oil in 92% yield.

R_f = 0.09 (pentane/diethyl ether = 19/1); [**α**]_D²⁰: +17.0° (c = 1.00, CHCl₃);

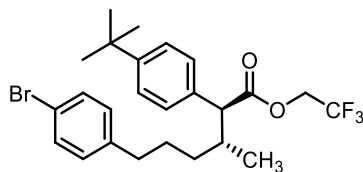
¹H NMR (600 MHz, CDCl₃) δ 7.46 (d, *J* = 8.5 Hz, 2H), 7.19 (d, *J* = 8.4 Hz, 2H), 6.83 (dt, *J* = 15.6, 6.9 Hz, 1H), 5.72 (d, *J* = 15.7 Hz, 1H), 4.55 (dq, *J* = 12.7, 8.4 Hz, 1H), 4.33 (dq, *J* = 12.7, 8.4 Hz, 1H), 3.72 (s, 3H), 3.33 (d, *J* = 10.5 Hz, 1H), 2.25 – 2.15 (m, 1H), 2.14 – 2.05 (m, 1H), 2.05 – 1.95 (m, 1H), 1.51 – 1.41 (m, 1H), 1.36 – 1.27 (m, 1H), 1.19 – 1.12 (m, 1H), 1.01 (d, *J* = 6.5 Hz, 3H), 0.97 – 0.89 (m, 1H);

¹³C NMR (125 MHz, CDCl₃) δ 171.9, 167.1, 149.0, 135.9, 132.0, 130.3, 121.9, 121.3, 60.5 (q, *J* = 36.6 Hz), 57.7, 51.6, 36.3, 32.8, 32.0, 24.8, 17.7;

IR (neat) 2934, 2859, 1749, 1721, 1657, 1488, 1270, 1129, 1073, 1011, 826, 760, 715 cm⁻¹;

HRMS (+p NSI) calcd for C₁₉H₂₃O₄BrF₃ (M+H)⁺ 451.0726 found 451.0732;

HPLC (ADH column, 1% *i*-propanol in hexane, 0.25 mL min⁻¹, 1 mg mL⁻¹, 60 min, UV 230 nm) retention times of 29.51 min (major) and 38.69 min (minor) 93% ee with Rh₂(*S*-2-Cl₅Br-TPCP)₄.



2,2,2-Trifluoroethyl (2*S*,3*R*)-6-(4-bromophenyl)-2-(4-(*tert*-butyl)phenyl)-3-methylhexanoate (116)

This compound was obtained according to *G.P. C* between 1-bromo-4-pentylbenzene (136.3 mg, 0.6 mmol, 2.0 equiv) and 2,2,2-trifluoroethyl 2-(4-(*tert*-butyl)phenyl)-2-diazoacetate (83.9 mg, 0.3 mmol, 1.0 equiv), catalyzed by Rh₂(*S*-2-Cl₅-BrTPCP)₄ (5.7 mg, 0.003 mmol, 1.0 mol%). The product was purified by flash column chromatography on silica gel (gradient elution: 0 – 2% diethyl ether in pentane) to afford colorless oil in 76% yield.

R_f = 0.32 (pentane/diethyl ether = 19/1); [**α**]_D²⁰: +20.4° (c = 1.11, CHCl₃, 81% ee);

^1H NMR (600 MHz, CDCl_3) δ 7.31 (dd, $J = 8.3, 6.3$ Hz, 4H), 7.20 (d, $J = 8.3$ Hz, 2H), 6.91 (d, $J = 8.4$ Hz, 2H), 4.56 (dq, $J = 12.7, 8.5$ Hz, 1H), 4.28 (dq, $J = 12.7, 8.5$ Hz, 1H), 3.33 (d, $J = 10.6$ Hz, 1H), 2.49 – 2.42 (m, 1H), 2.39 – 2.31 (m, 1H), 2.27 – 2.17 (m, 1H), 1.62 – 1.55 (m, 1H), 1.48 – 1.40 (m, 1H), 1.32 (s, 9H), 1.21 – 1.17 (m, 1H), 1.01 (d, $J = 6.5$ Hz, 3H), 0.97 – 0.90 (m, 1H);

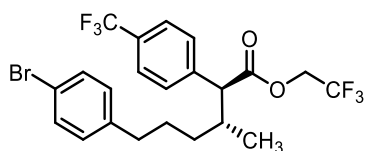
^{13}C NMR (151 MHz, CDCl_3) δ 172.6, 150.7, 141.4, 133.8, 131.4, 130.2, 128.3, 125.7, 123.1 (q, $J = 277.2$ Hz), 119.5, 60.4 (q, $J = 36.5$ Hz), 57.8, 36.2, 35.1, 34.7, 32.8, 31.5, 28.0, 17.8;

^{19}F NMR (282 MHz, CDCl_3) δ -73.7 (t, $J = 8.4$ Hz);

IR (neat) 2965, 2866, 1755, 1488, 1281, 1168, 1132, 979, 912, 738 cm^{-1} ;

HRMS (+p NSI) calcd for $\text{C}_{25}\text{H}_{31}\text{O}_2\text{BrF}_3$ ($\text{M}+\text{H}$) $^+$ 499.1454 found 499.1468;

HPLC (the ester product was reduced to 6-(4-bromophenyl)-2-(4-(tert-butyl)phenyl)-3-methylhexan-1-ol for better separation) (ADH column, 2% *i*-propanol in hexane, 1 mL min^{-1} , 1 mg mL^{-1} , 30 min, UV 230 nm) retention times of 11.08 min (minor) and 11.86 min (major) 81% ee with $\text{Rh}_2(\text{S-2-Cl-5-BrTPCP})_4$.



2,2,2-Trifluoroethyl (2*S*,3*R*)-6-(4-bromophenyl)-3-methyl-2-(4-(trifluoromethyl)phenyl)hexanoate (117)

This compound was obtained according to *G.P. C* between 1-bromo-4-pentylbenzene (136.3 mg, 0.6 mmol, 2.0 equiv) and 2,2,2-trifluoroethyl 2-diazo-2-(4-(trifluoromethyl)phenyl)acetate (93.7 mg, 0.3 mmol, 1.0 equiv), catalyzed by $\text{Rh}_2(\text{S-2-Cl-5-BrTPCP})_4$ (5.7 mg, 0.003 mmol, 1.0 mol%). The product was purified by flash column chromatography on silica gel (gradient elution: 0 – 2% diethyl ether in pentane) to afford colorless oil in 76% yield.

Rf = 0.64 (pentane/diethyl ether = 9/1); **[α]²⁰_D**: +25.3° (c = 1.04, CHCl₃, 93% ee);

¹H NMR (600 MHz, CDCl₃) δ 7.58 (d, *J* = 8.1 Hz, 2H), 7.41 (d, *J* = 8.0 Hz, 2H), 7.33 (d, *J* = 8.3 Hz, 2H), 6.91 (d, *J* = 8.3 Hz, 2H), 4.55 (dq, *J* = 12.7, 8.4 Hz, 1H), 4.33 (dq, *J* = 12.7, 8.4 Hz, 1H), 3.43 (d, *J* = 10.5 Hz, 1H), 2.49 – 2.43 (m, 1H), 2.37 – 2.30 (m, 1H), 2.29 – 2.19 (m, 1H), 1.64 – 1.55 (m, 1H), 1.49 – 1.41 (m, 1H), 1.19 – 1.12 (m, 1H), 1.03 (d, *J* = 6.5 Hz, 3H), 0.99 – 0.91 (m, 1H).;

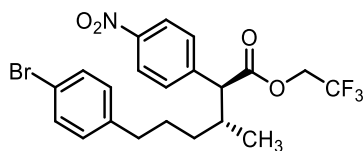
¹³C NMR (151 MHz, CDCl₃) δ 171.7, 141.1, 141.0, 131.4, 130.1, 129.1, 125.8 (q, *J* = 3.7 Hz), 124.1 (q, *J* = 272.0 Hz), 122.9 (q, *J* = 277.4 Hz), 119.6, 60.9, 60.7, 60.4, 60.2, 58.0, 36.5, 35.1, 32.7, 28.0, 17.7;

¹⁹F NMR (282 MHz, CDCl₃) δ -62.6, -73.7 (t, *J* = 8.8 Hz);

IR (neat) 2970, 2937, 2862, 1755, 1325, 1165, 1128, 1069, 1019, 834 cm⁻¹;

HRMS (+p APCI) calcd for C₂₂H₂₂O₂BrF₆ (M+H)⁺ 511.0702 found 511.0700;

HPLC (ODH column, 0.5% *i*-propanol in hexane, 0.5 mL min⁻¹, 1 mg mL⁻¹, 30 min, UV 230 nm) retention times of 14.03 min (major) and 15.63 min (minor) 93% ee with Rh₂(*S*-2-Cl-5-BrTPCP)₄.



2,2,2-Trifluoroethyl (2*S*,3*R*)-6-(4-bromophenyl)-3-methyl-2-(4-nitrophenyl)hexanoate (118)

This compound was obtained according to *G.P. C* between 1-bromo-4-pentylbenzene (136.3 mg, 0.6 mmol, 2.0 equiv) and 2,2,2-trifluoroethyl 2-diazo-2-(4-nitrophenyl)acetate (86.8 mg, 0.3 mmol, 1.0 equiv), catalyzed by Rh₂(*S*-2-Cl-5-BrTPCP)₄ (5.7 mg, 0.003 mmol, 1.0 mol%). The product was purified by flash column chromatography on silica gel (gradient elution: 4 – 6% diethyl ether in pentane) to afford colorless oil in 67% yield.

R_f = 0.53 (pentane/diethyl ether = 6/1); [**α**]²⁰_D: +25.0° (c = 1.02, CHCl₃, 83% ee);

¹H NMR (600 MHz, CDCl₃) δ 8.18 (d, *J* = 8.8 Hz, 2H), 7.47 (d, *J* = 8.7 Hz, 2H), 7.33 (d, *J* = 8.3 Hz, 2H), 6.92 (d, *J* = 8.3 Hz, 2H), 4.55 (dq, *J* = 12.7, 8.4 Hz, 1H), 4.36 (dq, *J* = 12.7, 8.3 Hz, 1H), 3.50 (d, *J* = 10.4 Hz, 1H), 2.49 – 2.42 (m, 1H), 2.38 – 2.32 (m, 1H), 2.31 – 2.22 (m, 1H), 1.65 – 1.56 (m, 1H), 1.51 – 1.42 (m, 1H), 1.18 – 1.09 (m, 1H), 1.04 (d, *J* = 6.5 Hz, 1H), 1.00 – 0.93 (m, 1H);

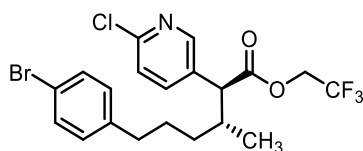
¹³C NMR (151 MHz, CDCl₃) δ 171.2, 147.7, 144.3, 140.9, 131.5, 130.1, 129.6, 124.0, 122.8 (q, *J* = 277.3 Hz), 119.7, 60.7 (q, *J* = 36.9 Hz), 57.9, 36.8, 35.1, 32.8, 28.0, 17.6;

¹⁹F NMR (282 MHz, CDCl₃) δ -73.7 (t, *J* = 8.4 Hz);

IR (neat) 2937, 2860, 1754, 1523, 1347, 1276, 1167, 1136, 979, 840 cm⁻¹;

HRMS (+p APCI) calcd for C₂₁H₂₂O₄NBrF₃ (M+H)⁺ 488.0679 found 488.0678;

HPLC (ADH column, 1% *i*-propanol in hexane, 0.5 mL min⁻¹, 1 mg mL⁻¹, 60 min, UV 230 nm) retention times of 32.57 min (minor) and 36.81 min (major) 83% ee with Rh₂(*S*-2-Cl-5-BrTPCP)₄.



2,2,2-Trifluoroethyl (2*S*,3*R*)-6-(4-bromophenyl)-2-(6-chloropyridin-3-yl)-3-methylhexanoate (119)

This compound was obtained according to *G.P. C* between 1-bromo-4-pentylbenzene (136.3 mg, 0.6 mmol, 2.0 equiv) and 2,2,2-trifluoroethyl 2-(6-chloropyridin-3-yl)-2-diazoacetate (90.1 mg, 0.3 mmol, 1.0 equiv), catalyzed by Rh₂(*S*-2-Cl-5-BrTPCP)₄ (5.7 mg, 0.003 mmol, 1.0 mol%). The product was purified by flash column chromatography on silica gel (gradient elution: 3 – 6% diethyl ether in pentane) to afford colorless oil in 84% yield.

R_f = 0.15 (pentane/diethyl ether = 9/1); [α]²⁰_D: +13.7° (c = 0.94, CHCl₃, 84% ee);

¹H NMR (600 MHz, CDCl₃) δ 8.21 (d, *J* = 2.6 Hz, 1H), 7.57 (dd, *J* = 8.3, 2.5 Hz, 1H), 7.29 (d, *J* = 8.3 Hz, 2H), 7.23 (d, *J* = 8.3 Hz, 1H), 6.86 (d, *J* = 8.3 Hz, 2H), 4.49 (dq, *J* = 12.7, 8.3 Hz, 1H), 4.29 (dq, *J* = 12.7, 8.4 Hz, 1H), 3.33 (d, *J* = 10.2 Hz, 1H), 2.44 – 2.36 (m, 1H), 2.34 – 2.25 (m, 1H), 2.16 – 2.06 (m, 1H), 1.59 – 1.49 (m, 1H), 1.44 – 1.32 (m, 1H), 1.13 – 1.05 (m, 1H), 0.96 (d, *J* = 6.6 Hz, 3H), 0.93 – 0.85 (m, 1H);

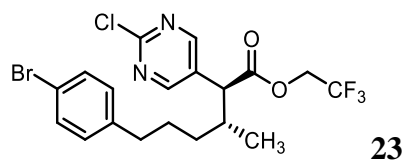
¹³C NMR (151 MHz, CDCl₃) δ 171.4, 151.2, 150.0, 140.9, 138.5, 131.7, 131.5, 130.1, 124.6, 122.8 (q, *J* = 277.3 Hz), 119.7, 60.7 (q, *J* = 36.8 Hz), 54.7, 36.7, 35.1, 32.7, 28.0, 17.6;

¹⁹F NMR (282 MHz, CDCl₃) δ -73.7 (t, *J* = 8.3 Hz);

IR (neat) 2934, 2860, 1754, 1460, 1278, 1168, 1139, 1106, 979, 832, 741 cm⁻¹;

HRMS (+p NSI) calcd for C₂₀H₂₁O₂NBrClF₃ (M+H)⁺ 478.0391 found 478.0407;

HPLC (ADH column, 1% *i*-propanol in hexane, 0.5 mL min⁻¹, 1 mg mL⁻¹, 60 min, UV 230 nm) retention times of 32.57 min (minor) and 36.81 min (major) 84% ee with Rh₂(*S*-2-Cl-5-BrTPCP)₄.



2,2,2-Trifluoroethyl (2*S*,3*R*)-6-(4-bromophenyl)-2-(2-chloropyrimidin-5-yl)-3-methylhexanoate (120)

This compound was obtained according to *G.P. C* between 1-bromo-4-pentylbenzene (136.3 mg, 0.6 mmol, 2.0 equiv) and 2,2,2-trifluoroethyl 2-(2-chloropyrimidin-5-yl)-2-diazoacetate (84.2 mg, 0.3 mmol, 1.0 equiv), catalyzed by Rh₂(*S*-2-Cl-5-BrTPCP)₄ (5.7 mg, 0.003 mmol, 1.0 mol%). The product was purified by flash column chromatography on silica gel (gradient elution: 5 – 8% diethyl ether in pentane) to afford colorless oil in 83% yield.

R_f = 0.38 (pentane/diethyl ether = 3/1); [**α**]²⁰_D: +17.5° (c = 1.00, CHCl₃, 83% ee);

¹H NMR (600 MHz, CDCl₃) δ 8.59 (s, 2H), 7.37 (d, *J* = 8.3 Hz, 2H), 6.95 (d, *J* = 8.3 Hz, 2H), 4.59 (dq, *J* = 12.7, 8.3 Hz, 1H), 4.40 (dq, *J* = 12.7, 8.3 Hz, 1H), 3.44 (d, *J* = 9.5 Hz, 1H), 2.54 – 2.46 (m, 1H), 2.43 – 2.34 (m, 1H), 2.26 – 2.17 (m, 1H), 1.67 – 1.58 (m, 1H), 1.53 – 1.44 (m, 1H), 1.24 – 1.17 (m, 1H), 1.08 – 0.94 (m, 4H);

¹³C NMR (151 MHz, CDCl₃) δ 170.6, 161.1, 159.6, 140.7, 131.6, 130.1, 129.2, 122.7 (q, *J* = 277.3 Hz), 119.9, 61.0 (q, *J* = 36.9 Hz), 52.6, 37.0, 35.2, 32.9, 28.2, 17.4;

¹⁹F NMR (282 MHz, CDCl₃) δ -73.6 (t, *J* = 8.3 Hz);

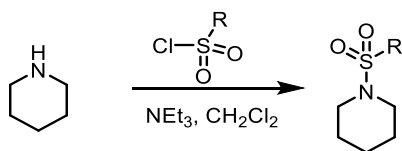
IR (neat) 2934, 2861, 1754, 1547, 1398, 1279, 1159, 1011 cm⁻¹;

HRMS (+p APCI) calcd for C₁₉H₂₀O₂N₂BrClF₃ (M+H)⁺ 479.0343 found 479.0346;

HPLC (ADH column, 2% *i*-propanol in hexane, 1 mL min⁻¹, 1 mg mL⁻¹, 30 min, UV 230 nm) retention times of 14.48 min (minor) and 19.58 min (major) 83% ee with Rh₂(*S*-2-Cl-5-BrTPCP)₄.

6.3 Experimental Part for Chapter 3

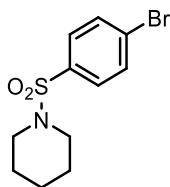
Starting Materials



Sulfonyl protected piperidines were prepared using adapted procedure similar to the one for 1-tosylpiperidine:²⁰⁸

To a solution of corresponding sulfonyl chloride (50 mmol, 1.0 equiv) in 150 mL of CH₂Cl₂, piperidine (5.9 mL, 60 mmol, 1.2 equiv) was added drop-wise with the generation of white fume, followed by the slow addition of triethylamine (10.5 mL, 75 mmol, 1.5 equiv). The mixture was

stirred at room temperature (23 °C) for 15 hours. The consumption of piperidine was monitored by TLC (30% ethyl acetate in hexane). The solvent was removed under reduced pressure and the residue was purified by flash silica gel column chromatography using gradient as indicated.

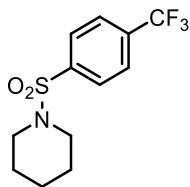


1-((4-Bromophenyl)sulfonyl)piperidine (145)

Purification was carried out with 8-12% ethyl acetate in hexane to give **109** as white solid in 78% yield (39 mmol, 11.9 g). The NMR data are consistent with literature values.²¹⁹

¹H NMR (600 MHz, CDCl₃) δ 7.67 (d, *J* = 8.6 Hz, 2H), 7.62 (d, *J* = 8.6 Hz, 2H), 2.99 (t, *J* = 5.5 Hz, 4H), 1.69 – 1.61 (m, 4H), 1.48 – 1.39 (m, 2H).

¹³C NMR (151 MHz, CDCl₃) δ 135.5, 132.2, 129.1, 127.6, 46.9, 25.1, 23.5.



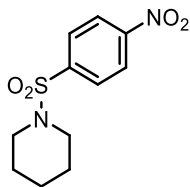
1-((4-(Trifluoromethyl)phenyl)sulfonyl)piperidine (149)

It was done in 30 mmol scale of 4-(trifluoromethyl)benzenesulfonyl chloride. Purification was carried out with 8-15% ethyl acetate in hexane to give **113** as white solid in 93% yield (28 mmol, 8.2 g). The NMR data are consistent with literature values.²¹⁹

¹H NMR (500 MHz, CDCl₃) δ 7.90 (dt, *J* = 8.1, 0.7 Hz, 2H), 7.81 (dt, *J* = 8.3, 0.6 Hz, 2H), 3.03 (t, *J* = 5.5 Hz, 4H), 1.74 – 1.59 (m, 4H), 1.53 – 1.38 (m, 2H).

¹³C NMR (126 MHz, CDCl₃) δ 140.2, 134.3 (q, *J* = 32.9 Hz), 128.2, 128.0, 126.2 (q, *J* = 3.6 Hz), 123.4 (d, *J* = 272.6 Hz), 47.0, 25.2, 23.5.

^{19}F NMR (282 MHz, CDCl_3) δ -63.12.

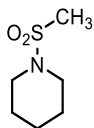


1-((4-Nitrophenyl)sulfonyl)piperidine (114)

It was done in 30 mmol scale of 4-nitrobenzenesulfonyl chloride. Purification was carried out with 8-15% ethyl acetate in hexane to give **114** as white solid in 83% yield (25 mmol, 6.7 g). The NMR data are consistent with literature values.²²⁰

^1H NMR (500 MHz, CDCl_3) δ 8.39 (d, $J = 8.9$ Hz, 2H), 7.96 (d, $J = 8.9$ Hz, 2H), 3.06 (t, $J = 5.5$ Hz, 4H), 1.67 (p, $J = 5.9$ Hz, 4H), 1.47 (tt, $J = 8.3, 4.6$ Hz, 2H).

^{13}C NMR (126 MHz, CDCl_3) δ 150.1, 142.6, 128.8, 124.3, 47.0, 25.2, 23.4.

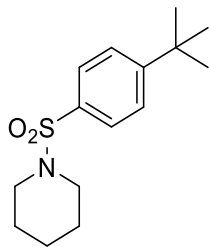


1-(Methylsulfonyl)piperidine (150)

It was done in 30 mmol scale of methanesulfonyl chloride. Purification was carried out with 8-15% ethyl acetate in hexane to give **115** as white solid in 82% yield (24.5 mmol, 4.0 g). The NMR data are consistent with literature values.²²¹

^1H NMR (500 MHz, CDCl_3) δ 3.18 (t, $J = 5.6$ Hz, 4H), 2.77 (s, 3H), 1.72 – 1.64 (m, 4H), 1.61 – 1.53 (m, 2H).

^{13}C NMR (126 MHz, CDCl_3) δ 46.6, 34.1, 25.2, 23.5.

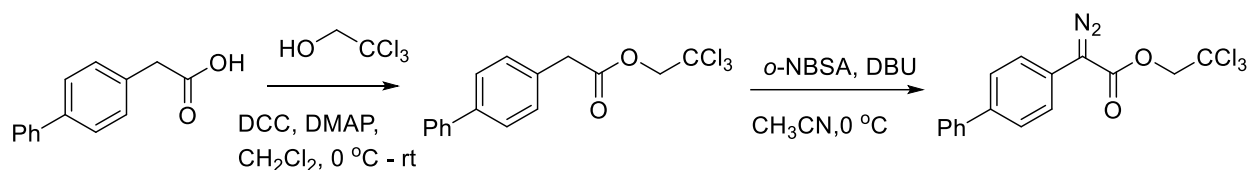


1-((4-(*tert*-Butyl)phenyl)sulfonyl)piperidine

Purification was carried out with 10-12% ethyl acetate in hexane to give the desired product as white solid in 98% yield (49 mmol, 13.8 g). The NMR data are consistent with literature values.²¹⁹

¹H NMR (600 MHz, CDCl₃) δ 7.67 (d, J = 8.2 Hz, 2H), 7.52 (d, J = 8.5 Hz, 2H), 2.99 (t, J = 5.5 Hz, 4H), 1.68 – 1.61 (m, 4H), 1.47 – 1.39 (m, 2H), 1.35 (s, 9H).

¹³C NMR (151 MHz, CDCl₃) δ 156.2, 133.3, 127.6, 125.9, 46.9, 35.1, 31.1, 25.2, 23.5.



2,2,2-Trichloroethyl 2-([1,1'-biphenyl]-4-yl)-2-diazoacetate

A dry 100 mL round-bottom flask was charged with 2-([1,1'-biphenyl]-4-yl)acetic acid (2.12g, 10 mmol, 1.0 equiv), DMAP (122.2 mg, 1 mmol, 0.1 equiv) and 2,2,2-trichloroethanol (1.2 mL, 12 mmol, 1.2 equiv). After the flask was flushed with argon gas (3 times), 20 mL of dry dichloromethane was added to the mixture. Then, the reaction mixture was cooled to 0 °C via ice bath. The solution of DCC (2.27 g, 11 mmol, 1.1 equiv) in 20 mL of dry dichloromethane was then added slowly at 0 °C. The reaction mixture was stirred for 15 hours, at which point it was warmed up to room temperature (23 °C). The reacted mixture was filtered through Celite[®] under reduced pressure and washed with dichloromethane. The filtrate was collected and concentrated under reduced pressure. The crude compound was purified by silica plug (3.8 cm diameter, 6 cm

height, 5% ethyl acetate in hexane) to afford the white solid in 99% yield (9.9 mmol, 3.4 g). The product was used immediately in the next step.

The ester from previous step (3.4 g, 9.9 mmol, 1.0 equiv) was added in a flame-dried round-bottom flask, together with *o*-NBSA (3.39 g, 14.85 mmol, 1.5 equiv). After the flask was flushed with argon gas (3 times), 30 mL of dry acetonitrile was added to the mixture for dissolving. Then, the reaction mixture was cooled to 0 °C via ice bath. DBU (3.3 mL, 21.78 mmol, 2.2 equiv) was added drop-wise at 0 °C. The mixture was stirred for 1 hour at 0 °C, followed by pouring into a separation funnel with 40 mL of saturated aqueous NH₄Cl for quenching. The aqueous layer was extracted with diethyl ether (30 mL X 2) and the combined organic layer was washed with brine. Then, it was concentrated under reduced pressure and purified by flash column chromatography (5-8% dichloromethane in hexane) to provide orange solid in 82% yield.

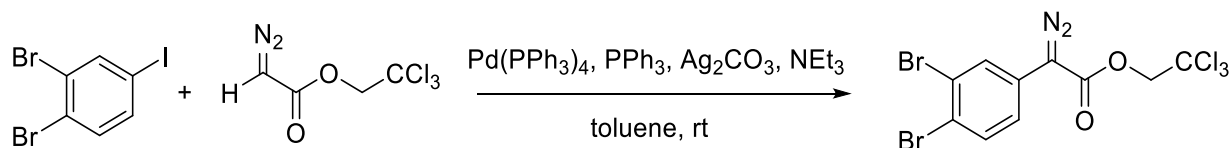
Rf = 0.50 (20% dichloromethane in hexane);

¹H NMR (500 MHz, CDCl₃) δ 7.62 (d, *J* = 8.5 Hz, 2H), 7.57 (d, *J* = 7.9 Hz, 2H), 7.54 (d, *J* = 8.5 Hz, 2H), 7.42 (t, *J* = 7.7 Hz, 2H), 7.33 (t, *J* = 7.4 Hz, 1H), 4.90 (s, 2H);

¹³C NMR (126 MHz, CDCl₃) δ 163.4, 140.2, 139.1, 129.0, 127.8, 127.6, 127.0, 124.4, 123.5, 95.1, 73.9 (The resonance resulting from the diazo carbon was not observed);

IR (neat) 3054, 3037, 2954, 2086, 1699, 1489, 1376, 1342, 1230, 1054, 760, 718, 582 cm⁻¹;

HRMS (+p APCI) calcd for C₁₆H₁₂Cl₃O₂ (M+H-N₂)⁺ 340.9897 found 340.9900.



2,2,2-Trichloroethyl 2-diazo-2-(3,4-dibromophenyl)acetate

A 100-mL round-bottom flask was charged with 1,2-dibromo-4-iodobenzene (3.62 g, 10 mmol, 1.0 equiv), Pd(PPh₃)₄ (577.8 mg, 0.5 mmol, 5 mol%), PPh₃ (262.3 mg, 1 mmol, 10 mol%) and Ag₂CO₃ (1.38 g, 5 mmol, 0.5 equiv). After the flask was flushed with argon, 40 mL of dry toluene was added, followed by the addition of NEt₃ (1.8 mL, 13 mmol, 1.3 equiv) and 2,2,2-trifluoroethyl 2-diazoacetate (2.18 g, 13 mmol, 1.3 equiv). The resulted mixture was stirred at room temperature for 4 h and then, filtered through a short silica plug (3.5 cm *diameter*, 5 cm *height*), eluting with ethyl acetate (20 mL). The crude product was concentrated and purified by column chromatography (6% diethyl ether in pentane) to afford yellow solid in 62% yield.

Rf = 0.69 (10% diethyl ether in pentane);

¹H NMR (500 MHz, CDCl₃) δ 7.80 (d, *J* = 2.3 Hz, 1H), 7.60 (d, *J* = 8.5 Hz, 1H), 7.29 – 7.21 (m, 1H), 4.91 (s, 2H);

¹³C NMR (126 MHz, CDCl₃) δ 162.6, 134.1, 128.5, 126.0, 125.8, 123.6, 122.1, 94.9, 74.1 (The resonance resulting from the diazo carbon was not observed);

IR (neat) 3098, 2954, 2094, 1711, 1469, 1372, 1340, 1273, 1234, 1046, 790, 712, 579 cm⁻¹;

HRMS (+p ESI) calcd for C₁₀H₆Br₂Cl₃N₂O₂ (M+H)⁺ 448.7856 found 448.7862.

Rhodium Carbene Reactions

General Procedure D

A 16-mL reaction vial (21x70mm) with screw cap (open top with PTFE faced silicone septum) was charged with Rh₂L₄ (0.0025 mmol, 0.5 mol%) and corresponding substrate (0.75 mmol, 1.5 equiv). The reaction vessel was then evacuated and back filled with argon (3 times), followed by the addition of dry degassed CH₂Cl₂ (2 mL). Corresponding donor/acceptor diazo compounds (0.5

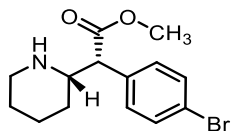
mmol, 1.0 equiv) was weighed in a 20 mL scintillation vial and dissolved in 4 mL of dry degassed CH_2Cl_2 under argon atmosphere. Then, under room temperature (23 °C) and argon atmosphere, the diazo solution was added to the reaction vessel dropwise via syringe pump over 2 h. The reaction mixture was stirred at room temperature (23 °C) for another 4 h, and crude ^1H NMR was obtained after the resulted mixture was concentrated under vacuum. Finally, the desired product was obtained after purification using flash column chromatography with indicated eluting gradient.

General Procedure E

Similar to G.P. D, but an additional step (Boc-deprotection) was added after the completion of the reaction, before the concentration for crude ^1H NMR: After the reaction mixture was stirred at room temperature (23 °C) for another 4 h, 1 mL of TFA (trichloroacetic acid) was added to the reaction mixture slowly and stirred at room temperature (23 °C) for 15 h. The resulted mixture was concentrated under reduce pressure and dissolved in 4 mL of dichloromethane, followed by addition of aqueous saturated NaHCO_3 drop-wise until no more bubble generated (~4 mL). The aqueous layer was extracted by 10 mL dichloromethane (3 times). The combined organic layer was concentrated for crude ^1H NMR and purified using flash column chromatography with indicated eluting gradient.

Regioisomer and Diastereomer Ratios Determination

The crude ^1H NMR spectra in general procedures were utilized for regioisomer and diastereomer ratios determination, and it was obtained using Bruker-600 MHz spectrometer with a Prodigy probe, and the acquisition was done with 16 times of scans and 1 seconds of relaxation time.



Methyl (R)-2-(4-bromophenyl)-2-((S)-piperidin-2-yl)acetate (140, *erythro*)

Following *G.P. E* (*tert*-butyl piperidine-1-carboxylate as substrate, reacting with methyl 2-(4-bromophenyl)-2-diazoacetate), the desired C2-product (mixture of both diastereomers) was purified by flash column chromatography (0-4% methanol in dichloromethane) as yellow oil.

Characterization data for the *erythro*-diastereomer was conducted on sample obtained in Rh₂(*S*-2-Cl-5-BrTPCP)₄-catalyzed reaction (83% ee).

R_f = 0.36 (5% methanol in dichloromethane); [**α**]_D²⁰: +22.2° (c = 0.45, CHCl₃, 83% ee);

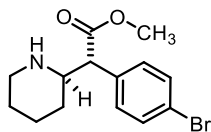
¹H NMR (500 MHz, CDCl₃) δ 7.47 (d, *J* = 8.4 Hz, 2H), 7.29 (d, *J* = 8.4 Hz, 2H), 3.66 (s, 3H), 3.43 (d, *J* = 10.0 Hz, 1H), 3.06 (td, *J* = 10.2, 2.3 Hz, 1H), 2.93 (d, *J* = 11.7 Hz, 1H), 2.50 (td, *J* = 11.5, 2.9 Hz, 1H), 1.88 – 1.70 (m, 2H), 1.61 – 1.54 (m, 1H), 1.46 – 1.33 (m, 2H), 1.30 – 1.17 (m, 1H);

¹³C NMR (126 MHz, CDCl₃) δ 172.8, 135.2, 132.1, 130.5, 122.1, 59.1, 57.9, 52.2, 47.2, 31.2, 25.9, 24.6;

IR (neat) 2934, 2854, 1734, 1488, 1435, 1331, 1161, 1119, 1011, 763 cm⁻¹;

HRMS (+p APCI) calcd for C₁₄H₁₉BrNO₂ (M+H)⁺ 312.0594 found 312.0594;

HPLC (ODH column, 1% *i*-propanol in hexane, 0.5 mL min⁻¹, 1 mg mL⁻¹, 30 min, UV 230 nm) retention times of 11.17 min (major) and 12.59 min (minor) 83% ee with Rh₂(*S*-2-Cl-5-BrTPCP)₄.



Methyl 2-(4-bromophenyl)-2-(piperidin-2-yl)acetate (141, *threo*)

Characterization data for the *threo*-diastereomer was conducted on sample obtained in Rh₂(R-DOSP)₄-catalyzed reaction (ee not determined).

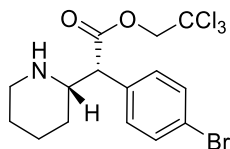
Yellow oil. **R_f** = 0.32 (5% methanol in dichloromethane);

¹H NMR (500 MHz, CDCl₃) δ 7.44 (d, *J* = 8.4 Hz, 2H), 7.17 (d, *J* = 8.4 Hz, 2H), 3.65 (s, 3H), 3.41 (d, *J* = 10.0 Hz, 1H), 3.08 (td, *J* = 10.4, 2.6 Hz, 2H), 2.68 (td, *J* = 11.9, 2.7 Hz, 1H), 2.01 (s, broad, 1H), 1.75 – 1.65 (m, 1H), 1.64 – 1.52 (m, 1H), 1.37 (qt, *J* = 12.4, 3.9 Hz, 1H), 1.29 – 1.19 (m, 2H), 1.01 – 1.87 (m, 1H);

¹³C NMR (126 MHz, CDCl₃) δ 173.4, 135.4, 131.8, 130.2, 121.6, 58.8, 58.1, 52.1, 46.9, 30.0, 26.1, 24.3;

IR (neat) 2931, 2853, 1731, 1489, 1434, 1196, 1163, 1012, 824, 765 cm⁻¹;

HRMS (+p APCI) calcd for C₁₄H₁₉BrNO₂ (M+H)⁺ 312.0594 found 312.0595;



2,2,2-Trichloroethyl (R)-2-(4-bromophenyl)-2-((S)-piperidin-2-yl)acetate (142, erythro)

Following *G.P. E* (*tert*-butyl piperidine-1-carboxylate as substrate, reacting 2,2,2-trichloroethyl 2-(4-bromophenyl)-2-diazoacetate), the desired C2-product (mixture of both diastereomers) was purified by flash column chromatography (0-4% methanol in dichloromethane) as yellow oil.

Characterization data for the *erythro*-diastereomer was conducted on sample obtained in Rh₂(R-TCPTAD)₄-catalyzed reaction (93% ee).

R_f = 0.36 (5% methanol in dichloromethane); [**α**]_D²⁰: -2.8° (c = 1.00, CHCl₃, 93% ee);

¹H NMR (500 MHz, CDCl₃) δ 7.49 (d, *J* = 8.4 Hz, 2H), 7.32 (d, *J* = 8.4 Hz, 2H), 4.76 (d, *J* = 12.0 Hz, 1H), 4.66 (d, *J* = 12.0 Hz, 1H), 3.58 (d, *J* = 10.0 Hz, 1H), 3.15 (td, *J* = 10.1, 2.2 Hz, 1H), 2.96

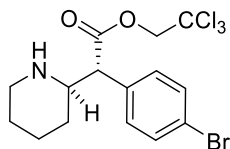
(d, $J = 11.5$ Hz, 1H), 2.53 (td, $J = 11.4, 2.7$ Hz, 1H), 1.90 – 1.74 (m, 2H), 1.63 – 1.54 (m, 1H), 1.47 – 1.34 (m, 2H), 1.33 – 1.25 (m, 1H);

^{13}C NMR (126 MHz, CDCl_3) δ 170.5, 134.3, 132.2, 130.7, 122.5, 94.8, 74.2, 58.7, 57.9, 47.1, 31.1, 25.9, 24.5;

IR (neat) 2935, 2855, 1749, 1488, 1452, 1139, 1116, 1073, 1012, 761, 722 cm^{-1} ;

HRMS (+p APCI) calcd for $\text{C}_{15}\text{H}_{18}\text{BrCl}_3\text{NO}_2$ ($\text{M}+\text{H}$) $^+$ 427.9581 found 427.9589;

HPLC (ODH column, 0.5% *i*-propanol in hexane, 0.35 mL min^{-1} , 1 mg mL^{-1} , 60 min, UV 230 nm) retention times of 26.84 min (major) and 28.93 min (minor) 93% ee with $\text{Rh}_2(\text{R-TCPTAD})_4$.



2,2,2-Trichloroethyl 2-(4-bromophenyl)-2-(piperidin-2-yl)acetate (*threo*)

Characterization data for the *threo*-diastereomer was conducted on sample obtained in $\text{Rh}_2(\text{R-DOSP})_4$ -catalyzed reaction (ee not determined).

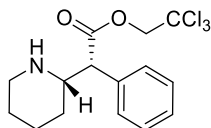
Yellow oil. **Rf** = 0.29 (5% methanol in dichloromethane);

^1H NMR (500 MHz, CDCl_3) δ 7.46 (d, $J = 8.6$ Hz, 2H), 7.22 (d, $J = 8.1$ Hz, 2H), 4.72 (s, 2H), 3.56 (d, $J = 10.1$ Hz, 1H), 3.18 (td, $J = 10.5, 2.6$ Hz, 1H), 3.08 (d, $J = 12.3$ Hz, 1H), 2.69 (td, $J = 11.9, 2.8$ Hz, 1H), 1.80 – 1.66 (m, 1H), 1.59 (d, $J = 12.9$ Hz, 1H), 1.44 – 1.18 (m, 3H), 0.96 (qd, $J = 12.2, 3.6$ Hz, 1H);

^{13}C NMR (126 MHz, CDCl_3) δ 171.4, 134.7, 132.0, 130.6, 122.0, 94.8, 74.3, 58.9, 58.2, 46.9, 30.2, 26.4, 24.4;

IR (neat) 2936, 2922, 2857, 1652, 1568, 1380, 1013, 763, 724, 529 cm^{-1} ;

HRMS (+p APCI) calcd for $\text{C}_{15}\text{H}_{18}\text{BrCl}_3\text{NO}_2$ ($\text{M}+\text{H}$)⁺ 427.9581 found 427.9587;



2,2,2-Trichloroethyl (*R*)-2-phenyl-2-((*S*)-piperidin-2-yl)acetate (147a, *erythro*)

Following *G.P. E* (*tert*-butyl piperidine-1-carboxylate as substrate, reacting 2,2,2-trichloroethyl 2-diazo-2-phenylacetate), the desired C2-product (mixture of both diastereomers) was purified by flash column chromatography (0-4% methanol in dichloromethane) as yellow oil.

Characterization data for the *erythro*-diastereomer was conducted on sample obtained in $\text{Rh}_2(\text{R-TCPTAD})_4$ -catalyzed reaction (73% ee).

R_f = 0.30 (5% methanol in dichloromethane); [α]_D²⁰: +6.4° (c = 1.00, CHCl_3 , 73% ee);

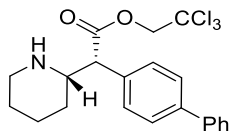
¹H NMR (500 MHz, CDCl_3) δ 7.49 – 7.41 (m, 2H), 7.39 – 7.28 (m, 3H), 4.76 (d, *J* = 12.0 Hz, 1H), 4.65 (d, *J* = 12.0 Hz, 1H), 3.61 (d, *J* = 10.2 Hz, 1H), 3.19 (td, *J* = 10.2, 2.4 Hz, 1H), 2.94 (d, *J* = 11.5 Hz, 1H), 2.53 (td, *J* = 11.5, 2.8 Hz, 1H), 1.88 (d, *J* = 14.2 Hz, 1H), 1.82 (d, *J* = 13.7 Hz, 1H), 1.62 – 1.56 (m, 1H), 1.50 – 1.36 (m, 2H), 1.36 – 1.26 (m, 1H);

¹³C NMR (126 MHz, CDCl_3) δ 170.9, 135.3, 129.1, 129.0, 128.3, 94.9, 74.2, 58.7, 58.5, 47.1, 31.2, 25.9, 24.5;

IR (neat) 2934, 2854, 1748, 1454, 1332, 1289, 1138, 1115, 774, 718, 699 cm^{-1} ;

HRMS (+p APCI) calcd for $\text{C}_{15}\text{H}_{19}\text{Cl}_3\text{NO}_2$ ($\text{M}+\text{H}$)⁺ 350.0476. found 350.0478;

HPLC (ODH column, 1% *i*-propanol in hexane, 1 mL min⁻¹, 1 mg mL⁻¹, 30 min, UV 230 nm) retention times of 5.41 min (minor) and 5.94 min (major) 73% ee with $\text{Rh}_2(\text{R-TCPTAD})_4$.



2,2,2-Trichloroethyl (*R*)-2-([1,1'-biphenyl]-4-yl)-2-((*S*)-piperidin-2-yl)acetate (147b, *erythro*)

Following *G.P. E* (*tert*-butyl piperidine-1-carboxylate as substrate, reacting 2,2,2-trichloroethyl 2-([1,1'-biphenyl]-4-yl)-2-diazoacetate), the desired C2-product (mixture of both diastereomers) was purified by flash column chromatography (0-4% methanol in dichloromethane) as yellow oil.

Characterization data for the *erythro*-diastereomer was conducted on sample obtained in Rh₂(*R*-TCPTAD)₄-catalyzed reaction (61% ee).

R_f = 0.36 (5% methanol in dichloromethane); [**α**]_D²⁰: -4.3° (c = 0.91, CHCl₃, 61% ee);

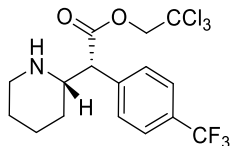
¹H NMR (500 MHz, CDCl₃) δ 7.62 – 7.56 (m, 4H), 7.51 (d, *J* = 8.3 Hz, 2H), 7.44 (t, *J* = 7.6 Hz, 2H), 7.39 – 7.32 (m, 1H), 4.80 (d, *J* = 12.0 Hz, 1H), 4.66 (d, *J* = 12.0 Hz, 1H), 3.65 (d, *J* = 10.1 Hz, 1H), 3.23 (td, *J* = 10.1, 2.4 Hz, 1H), 2.97 (d, *J* = 11.6 Hz, 1H), 2.56 (td, *J* = 11.5, 2.8 Hz, 1H), 1.97 – 1.86 (m, 1H), 1.86 – 1.81 (m, 1H), 1.65 – 1.56 (m, 1H), 1.53 – 1.39 (m, 2H), 1.39 – 1.28 (m, 1H);

¹³C NMR (126 MHz, CDCl₃) δ 170.9, 141.2, 140.6, 134.3, 129.4, 129.0, 127.8, 127.6, 127.2, 94.9, 74.3, 58.8, 58.2, 47.2, 31.3, 26.0, 24.6;

IR (neat) 3030, 2935, 2854, 1749, 1487, 1451, 1331, 1139, 1117, 776, 741, 725, 698 cm⁻¹;

HRMS (+p APCI) calcd for C₂₁H₂₂Cl₃NO₂ (M+H)⁺ 426.0789 found 426.0794;

HPLC (obtained on its 2,2,2-trifluoroacetamide derivative) (ADH column, 3% *i*-propanol in hexane, 1 mL min⁻¹, 1 mg mL⁻¹, 40 min, UV 230 nm) retention times of 23.99 min (major) and 27.95 min (minor) 61% ee with Rh₂(*R*-TCPTAD)₄.



2,2,2-Trichloroethyl (*R*)-2-((*S*)-piperidin-2-yl)-2-(4-(trifluoromethyl)phenyl)acetate

(147c, *erythro*)

Following *G.P. E* (*tert*-butyl piperidine-1-carboxylate as substrate, reacting 2,2,2-trichloroethyl 2-diazo-2-(4-(trifluoromethyl)phenyl)acetate), the desired C2-product (mixture of diastereomers) was purified by flash column chromatography (0-4% methanol in dichloromethane) as yellow oil. Characterization data for the *erythro*-diastereomer was conducted on sample obtained in Rh₂(*R*-TCPTAD)₄-catalyzed reaction (37% ee).

R_f = 0.40 (5% methanol in dichloromethane); [**α**]_D²⁰: +1.7° (c = 0.91, CHCl₃, 37% ee);

¹H NMR (500 MHz, CDCl₃) δ 7.63 (d, *J* = 8.7 Hz, 2H), 7.58 (d, *J* = 8.2 Hz, 2H), 4.77 (d, *J* = 12.0 Hz, 1H), 4.66 (d, *J* = 11.9 Hz, 1H), 3.69 (d, *J* = 9.9 Hz, 1H), 3.22 (td, *J* = 10.0, 2.4 Hz, 1H), 2.96 (d, *J* = 12.8 Hz, 1H), 2.54 (td, *J* = 11.5, 2.9 Hz, 1H), 1.92 – 1.77 (m, 2H), 1.65 – 1.54 (m, 1H), 1.48 – 1.36 (m, 2H), 1.35 – 1.26 (m, 1H);

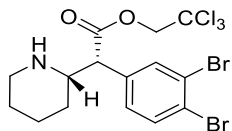
¹³C NMR (126 MHz, CDCl₃) δ 170.3, 139.4, 130.6 (q, *J* = 32.6 Hz), 129.5, 126.0 (q, *J* = 3.8 Hz), 124.1 (q, *J* = 272.2 Hz), 94.7, 74.3, 58.8, 58.3, 47.1, 31.1, 25.9, 24.5;

¹⁹F NMR (282 MHz, CDCl₃) δ -62.67;

IR (neat) 2938, 2957, 1750, 1324, 1164, 1117, 1068, 1019, 846, 758, 718, 601, 571 cm⁻¹;

HRMS (+p APCI) calcd for C₁₆H₁₈Cl₃F₃NO₂ (M+H)⁺ 418.0350 found 418.0351;

HPLC (ODH column, 0.5% *i*-propanol in hexane, 1.5 mL min⁻¹, 1 mg mL⁻¹, 30 min, UV 230 nm) retention times of 3.84 min (major) and 4.58 min (minor) 37% ee with Rh₂(*R*-TCPTAD)₄.



2,2,2-Trichloroethyl (*R*)-2-(3,4-dibromophenyl)-2-((*S*)-piperidin-2-yl)acetate (147d, *erythro*)

Following *G.P. E* (*tert*-butyl piperidine-1-carboxylate as substrate, reacting 2,2,2-trichloroethyl 2-diazo-2-(3,4-dibromophenyl)acetate), the desired C2-product (mixture of both diastereomers) was purified by flash column chromatography (0-4% methanol in dichloromethane) as yellow oil.

Characterization data for the *erythro*-diastereomer was conducted on sample obtained in $\text{Rh}_2(\text{R-TCPTAD})_4$ -catalyzed reaction (29% ee).

R_f = 0.43 (5% methanol in dichloromethane); [α] $^{20}_{\text{D}}$: -4.3° (c = 1.00, CHCl_3 , 29% ee);

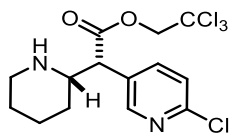
$^1\text{H NMR}$ (500 MHz, CDCl_3) δ 7.73 (d, J = 2.1 Hz, 1H), 7.60 (d, J = 8.2 Hz, 1H), 7.26 (dd, J = 8.4, 2.3 Hz, 1H), 4.79 (d, J = 12.0 Hz, 1H), 4.65 (d, J = 11.9 Hz, 1H), 3.55 (d, J = 9.8 Hz, 1H), 3.13 (td, J = 10.1, 2.3 Hz, 1H), 2.97 (d, J = 11.8 Hz, 1H), 2.55 (td, J = 11.6, 2.9 Hz, 1H), 1.87 – 1.78 (m, 2H), 1.65 – 1.58 (m, 1H), 1.46 – 1.32 (m, 2H), 1.32 – 1.23 (m, 1H);

$^{13}\text{C NMR}$ (126 MHz, CDCl_3) δ 170.0, 136.3, 134.1, 134.1, 129.2, 125.5, 124.8, 94.7, 74.3, 58.7, 57.6, 47.0, 31.1, 25.8, 24.4;

IR (neat) 2936, 2855, 1747, 1461, 1139, 1113, 1014, 907, 727, 571 cm^{-1} ;

HRMS (+p APCI) calcd for $\text{C}_{15}\text{H}_{17}\text{Br}_2\text{Cl}_3\text{NO}_2$ ($\text{M}+\text{H}$) $^+$ 505.8686 found 505.8693;

HPLC (ODH column, 0.5% *i*-propanol in hexane, 1 mL min^{-1} , 1 mg mL^{-1} , 30 min, UV 230 nm) retention times of 7.69 min (major) and 8.32 min (minor) 29% ee with $\text{Rh}_2(\text{R-TCPTAD})_4$.



2,2,2-trichloroethyl (*R*)-2-(6-chloropyridin-3-yl)-2-((*S*)-piperidin-2-yl)acetate

(147e, erythro)

Following *G.P. E* (*tert*-butyl piperidine-1-carboxylate as substrate, reacting 2,2,2-trichloroethyl 2-(6-chloropyridin-3-yl)-2-diazoacetate, the desired C2-product (mixture of both diastereomers) was purified by flash column chromatography (0-4% methanol in dichloromethane) as red oil.

Characterization data for the *erythro*-diastereomer was conducted on sample obtained in Rh₂(*R*-TCPTAD)₄-catalyzed reaction (~0% ee).

Rf = 0.27 (5% methanol in dichloromethane);

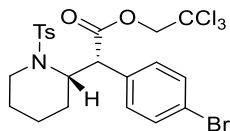
¹H NMR (500 MHz, CDCl₃) *Diastereomer 1* : [*Diastereomer 2*] (3.45: 1) δ 8.41 (d, *J* = 2.5 Hz, 4H), [8.35 (d, *J* = 2.5 Hz, 1H)], 7.82 (dd, *J* = 8.3, 2.5 Hz, 4H), [7.72 (dd, *J* = 8.3, 2.5 Hz, 1H)], 7.33 (dd, *J* = 10.7, 8.3 Hz, 5H) [both diastereomers], 4.80 – 4.75 (m, 5H) [both diastereomers], 4.75 – 4.67 (m, 5H) [both diastereomers], 3.70 – 3.63 (m, 5H) [both diastereomers], 3.19 (td, *J* = 10.6, 9.8, 2.3 Hz, 5H) [both diastereomers], [3.09 (d, *J* = 13.1 Hz, 1H)], 2.98 (d, *J* = 11.2 Hz, 4H), [2.68 (t, *J* = 12.1 Hz, 1H)], 2.55 (td, *J* = 11.5, 2.9 Hz, 4H), 1.89 – 1.66 (m, 11H) [both diastereomers], 1.45 – 1.21 (m, 18H) [both diastereomers], [1.05 – 0.94 (m, 1H)];

¹³C NMR (126 MHz, CDCl₃) δ 169.9, 151.4, 150.2, [150.0], 139.0, [138.7], 130.0, 124.5, [124.4], 94.4, 74.2, [58.7], 58.4, [55.2], 54.9, 46.8, [46.7], 30.9, [29.7], 25.7, 24.2, [24.1];

IR (neat) 3312, 3094, 2924, 2853, 1753, 1724, 1670, 1617, 1586, 1511, 1461, 1370, 1142, 1106, 1023, 720 cm⁻¹;

HRMS (FTMS +p NSI) calcd for C₁₄H₁₇Cl₄N₂O₂ (M+H)⁺ 385.0039 found 385.0019;

HPLC (ODH column, 1% *i*-propanol in hexane, 0.5 mL min⁻¹, 1 mg mL⁻¹, 30 min, UV 230 nm) retention times of 23.86 min and 26.31 min, 0% ee with Rh₂(*R*-TCPTAD)₄.



2,2,2-Trichloroethyl (R)-2-(4-bromophenyl)-2-((S)-1-tosylpiperidin-2-yl)acetate (144)

Following *G.P. D* (1-tosylpiperidine as substrate, reacting 2,2,2-trichloroethyl 2-(4-bromophenyl)-2-diazoacetate), the desired C2-product was obtained using 0-12% ethyl acetate in hexane as eluting gradient in flash column chromatography (a 2nd column with 35-100% dichloromethane in hexane was conducted if the product is not pure enough) as white solid.

Characterization data for the *erythro*-diastereomer was conducted on sample obtained in Rh₂(*R*-TPPTTL)₄-catalyzed reaction (76% ee).

mp: 131-133 °C; **Rf** = 0.45 (20% ethyl acetate/hexane); **[α]²⁰_D**: +24.9° (c = 1.00, CHCl₃, 76% ee);

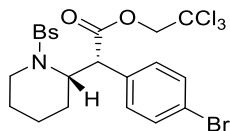
¹H NMR (600 MHz, CDCl₃) δ 7.35 (d, *J* = 8.5 Hz, 2H), 7.23 (d, *J* = 8.5 Hz, 2H), 7.17 (d, *J* = 8.3 Hz, 2H), 7.11 (d, *J* = 8.0 Hz, 2H), 4.88 (dd, *J* = 11.6, 4.5 Hz, 1H), 4.84 (d, *J* = 12.0 Hz, 1H), 4.58 (d, *J* = 12.0 Hz, 1H), 4.22 (d, *J* = 11.7 Hz, 1H), 3.55 (d, *J* = 15.1 Hz, 1H), 2.92 – 2.82 (m, 1H), 2.40 (s, 3H), 1.88 – 1.80 (m, 1H), 1.80 – 1.66 (m, 3H), 1.54 – 1.46 (m, 2H).;

¹³C NMR (151 MHz, CDCl₃) δ 170.2, 143.2, 137.6, 134.0, 131.9, 130.5, 129.5, 127.2, 122.5, 94.6, 74.4, 54.5, 50.8, 41.3, 27.3, 24.2, 21.7, 18.9;

IR (neat) 2945, 2869, 1750, 1489, 1338, 1325, 1294, 1155, 1092, 932, 908, 816, 767, 718, 657, 552 cm⁻¹;

HRMS (+p APCI) calcd for C₂₂H₂₄BrCl₃SNO₄ (M+H)⁺ 581.9670 found 581.9671;

HPLC (ADH column, 5% *i*-propanol in hexane, 0.5 mL min⁻¹, 1 mg mL⁻¹, 80 min, UV 230 nm) retention times of 40.94 min (major) and 55.33 min (minor) 76% ee with Rh₂(*R*-TPPTTL)₄.



2,2,2-Trichloroethyl (*R*)-2-(4-bromophenyl)-2-((*S*)-1-((4-bromophenyl)sulfonyl)piperidin-2-yl)acetate (146)

Following *G.P. D* (1-((4-bromophenyl)sulfonyl)piperidine as substrate, reacting 2,2,2-trichloroethyl 2-(4-bromophenyl)-2-diazoacetate), the desired C2-product was obtained using 0-12% ethyl acetate in hexane as eluting gradient in flash column chromatography (a 2nd column with 35-100% dichloromethane in hexane was conducted if the product is not pure enough) as white solid.

Characterization data for the *erythro*-diastereomer was conducted on sample obtained in Rh₂(*R*-TCPTAD)₄-catalyzed reaction (97% ee).

mp: 159-161 °C; **R_f** = 0.44 (20% ethyl acetate/hexane); **[α]²⁰_D**: +29.4° (c = 1.00, CHCl₃, 97% ee);

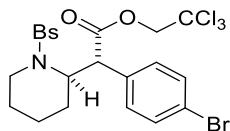
¹H NMR (600 MHz, CDCl₃) δ 7.45 (d, *J* = 8.6 Hz, 2H), 7.38 (d, *J* = 8.5 Hz, 2H), 7.23 (d, *J* = 8.5 Hz, 2H), 7.11 (d, *J* = 8.6 Hz, 2H), 4.90 – 4.80 (m, 2H), 4.59 (d, *J* = 12.0 Hz, 1H), 4.21 (d, *J* = 11.8 Hz, 1H), 3.58 – 3.47 (m, 1H), 2.90 (ddd, *J* = 14.8, 12.5, 3.6 Hz, 1H), 1.89 – 1.80 (m, 1H), 1.81 – 1.67 (m, 3H), 1.60 – 1.50 (m, 2H);

¹³C NMR (151 MHz, CDCl₃) δ 169.9, 139.3, 133.8, 132.1, 131.9, 130.3, 128.6, 127.3, 122.5, 94.4, 74.3, 54.7, 50.5, 41.3, 27.3, 24.1, 18.7;

IR (neat) 2946, 2869, 1751, 1489, 1327, 1158, 1011, 933, 822, 768, 755, 609 cm⁻¹;

HRMS (+p APCI) calcd for C₂₁H₂₁Br₂Cl₃SNO₄ (M+H)⁺ 645.8618 found 645.8622;

HPLC (ADH column, 5% *i*-propanol in hexane, 0.5 mL min⁻¹, 1 mg mL⁻¹, 80 min, UV 230 nm) retention times of 44.54 min (major) and 66.29 min (minor) 97% ee with Rh₂(*R*-TCPTAD)₄.



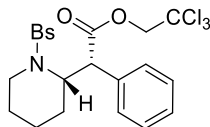
2,2,2-Trichloroethyl 2-(4-bromophenyl)-2-(1-((4-bromophenyl)sulfonyl)piperidin-2-yl)acetate (*threo*)

Characterization data for the *threo*-diastereomer was conducted on sample obtained in Rh₂(R-TCPTAD)₄-catalyzed reaction (ee not determined).

White solid, **R_f** = 0.45 (20% ethyl acetate in hexane);

¹H NMR (600 MHz, CDCl₃) δ 7.73 (d, *J* = 8.8 Hz, 2H), 7.65 (d, *J* = 8.6 Hz, 2H), 7.50 (d, *J* = 8.6 Hz, 2H), 7.37 (d, *J* = 8.5 Hz, 2H), 4.79 (dd, *J* = 11.6, 4.7 Hz, 1H), 4.58 (d, *J* = 11.9 Hz, 1H), 4.45 (d, *J* = 11.9 Hz, 1H), 4.25 (d, *J* = 11.7 Hz, 1H), 3.80 (dd, *J* = 15.0, 4.7 Hz, 1H), 3.36 – 3.23 (m, 1H), 1.60 – 1.41 (m, 3H), 1.38 – 1.27 (m, 2H), 1.24 – 1.18 (m, 1H);

¹³C NMR (151 MHz, CDCl₃) δ 169.7, 140.4, 133.4, 132.3, 132.2, 130.5, 128.8, 127.5, 122.6, 94.4, 74.5, 56.0, 50.8, 41.4, 24.5, 23.7, 18.0.



2,2,2-Trichloroethyl (R)-2-((S)-1-((4-bromophenyl)sulfonyl)piperidin-2-yl)-2-phenylacetate (148a)

Following *G.P. D* (1-((4-bromophenyl)sulfonyl)piperidine) as substrate, reacting 2,2,2-trichloroethyl 2-diazo-2-phenylacetate) with reaction under reflux dichloromethane (39 °C), the desired C2-product was obtained using 0-12% ethyl acetate in hexane as eluting gradient in flash column chromatography (a 2nd column with 35-100% dichloromethane in hexane was conducted if the product is not pure enough) as white solid.

Characterization data for the *erythro*-diastereomer was conducted on sample obtained in Rh₂(*R*-TPPTTL)₄-catalyzed reaction (52% ee).

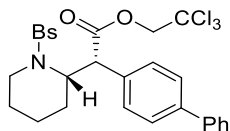
mp: 146-148 °C; **R_f** = 0.48 (20% ethyl acetate/hexane); **[α]²⁰_D:** +9.9° (c = 1.00, CHCl₃, 52% ee); **¹H NMR (600 MHz, CDCl₃) δ** 7.38 (d, *J* = 7.4 Hz, 2H), 7.33 (dd, *J* = 11.9, 7.8 Hz, 3H), 7.29 (d, *J* = 7.7 Hz, 2H), 7.00 (d, *J* = 8.4 Hz, 2H), 4.97 (dd, *J* = 11.9, 4.7 Hz, 1H), 4.86 (d, *J* = 11.9 Hz, 1H), 4.58 (d, *J* = 12.0 Hz, 1H), 4.26 (d, *J* = 11.7 Hz, 1H), 3.40 (d, *J* = 14.5, 1H), 2.96 – 2.87 (m, 1H), 1.92 – 1.70 (m, 4H), 1.61 – 1.53 (m, 2H);

¹³C NMR (151 MHz, CDCl₃) δ 170.4, 139.4, 135.0, 132.1, 129.0, 128.9, 128.3, 127.1, 94.7, 74.3, 54.6, 51.2, 41.3, 27.6, 24.2, 18.8;

IR (neat) 2947, 2868, 1749, 1575, 1470, 1455, 1319, 1287, 1156, 1089, 1067, 1010, 934, 907, 761 cm⁻¹;

HRMS (+p APCI) calcd for C₂₁H₂₂BrCl₃SNO₄ (M+H)⁺ 567.9513 found 567.9518;

HPLC (ODH column, 2% *i*-propanol in hexane, 0.6 mL min⁻¹, 1 mg mL⁻¹, 60 min, UV 230 nm) retention times of 39.84 min (minor) and 44.79 min (major) 52% ee with Rh₂(*R*-TPPTTL)₄.



2,2,2-Trichloroethyl (R)-2-([1,1'-biphenyl]-4-yl)-2-((S)-1-((4-bromophenyl)sulfonyl)-piperidin-2-yl)acetate (148b)

Following *G.P. D* (1-((4-bromophenyl)sulfonyl)piperidine as substrate, reacting 2,2,2-trichloroethyl 2-([1,1'-biphenyl]-4-yl)-2-diazoacetate) with reaction under reflux dichloromethane (39 °C), the desired C2-product was obtained using 0-12% ethyl acetate in hexane as eluting gradient in flash column chromatography (a 2nd column with 35-100% dichloromethane in hexane was conducted if the product is not pure enough) as white solid.

Characterization data for the *erythro*-diastereomer was conducted on sample obtained in Rh₂(*R*-TPPTTL)₄-catalyzed reaction (62% ee).

mp: 52-54 °C; **Rf** = 0.46 (20% ethyl acetate in hexane); **[α]²⁰_D:** +31.3° (c = 1.00, CHCl₃, 62% ee);

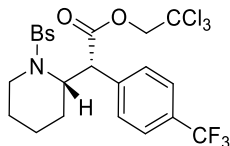
¹H NMR (600 MHz, CDCl₃) δ 7.60 (dd, *J* = 8.3, 1.2 Hz, 2H), 7.51 (d, *J* = 8.4 Hz, 2H), 7.47 (t, *J* = 7.7 Hz, 2H), 7.43 (d, *J* = 8.3 Hz, 2H), 7.38 (tt, *J* = 6.9, 1.2 Hz, 1H), 7.27 (d, *J* = 8.7 Hz, 2H), 7.04 (d, *J* = 8.7 Hz, 2H), 4.99 (dd, *J* = 11.8, 4.8 Hz, 1H), 4.89 (d, *J* = 12.0 Hz, 1H), 4.59 (d, *J* = 12.0 Hz, 1H), 4.31 (d, *J* = 11.8 Hz, 1H), 3.50 – 3.43 (m, 1H), 2.95 (ddd, *J* = 14.7, 12.2, 3.8 Hz, 1H), 1.97 – 1.88 (m, 1H), 1.87 – 1.74 (m, 3H), 1.68 – 1.57 (m, 2H);

¹³C NMR (151 MHz, CDCl₃) δ 170.4, 141.3, 140.2, 139.4, 134.0, 132.0, 129.3, 129.1, 128.9, 127.8, 127.5, 127.1, 127.1, 94.7, 74.4, 54.6, 50.9, 41.4, 27.7, 24.4, 18.9;

IR (neat) 3031, 2947, 2868, 1749, 1575, 1487, 1326, 1156, 1089, 1009, 933, 908, 760, 729 cm⁻¹;

HRMS (+p APCI) calcd for C₂₇H₂₆BrCl₃SNO₄ (M+H)⁺ 643.9826 found 643.9829;

HPLC (R,R-Whelk column, 10% *i*-propanol in hexane, 1 mL min⁻¹, 1 mg mL⁻¹, 60 min, UV 230 nm) retention times of 41.77 min (minor) and 45.52 min (major) 62% ee with Rh₂(*R*-TPPTTL)₄.



2,2,2-Trichloroethyl (R)-2-((S)-1-((4-bromophenyl)sulfonyl)piperidin-2-yl)-2-(4-(trifluoromethyl)phenyl)acetate (148c)

Following *G.P. D* (1-((4-bromophenyl)sulfonyl)piperidine as substrate, reacting 2,2,2-trichloroethyl 2-diazo-2-(4-(trifluoromethyl)phenyl)acetate), the desired C2-product was obtained using 0-12% ethyl acetate in hexane as eluting gradient in flash column chromatography (a 2nd column with 35-100% dichloromethane in hexane was conducted if the product is not pure enough) as white solid.

Characterization data for the *erythro*-diastereomer was conducted on sample obtained in Rh₂(R-TPPTTL)₄-catalyzed reaction (74% ee).

mp: 119-121 °C; **R_f** = 0.43 (20% ethyl acetate/hexane); **[α]²⁰_D**: +11.8° (c = 1.00, CHCl₃, 74% ee);

¹H NMR (600 MHz, CDCl₃) δ 7.55 (d, *J* = 8.3 Hz, 2H), 7.51 (d, *J* = 8.3 Hz, 2H), 7.41 (d, *J* = 8.7 Hz, 2H), 7.11 (d, *J* = 8.6 Hz, 2H), 4.95 (dd, *J* = 11.8, 4.7 Hz, 1H), 4.85 (d, *J* = 12.0 Hz, 1H), 4.60 (d, *J* = 12.0 Hz, 1H), 4.33 (d, *J* = 11.7 Hz, 1H), 3.54 – 3.46 (m, 1H), 2.90 (ddd, *J* = 14.9, 12.8, 3.4 Hz, 1H), 1.89 – 1.81 (m 1H), 1.80 – 1.71 (m, 3H), 1.59 – 1.49 (m, 2H);

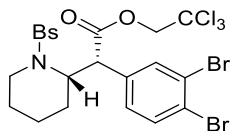
¹³C NMR (151 MHz, CDCl₃) δ 169.6, 139.2, 138.7, 132.1, 130.6 (q, *J* = 32.6 Hz), 129.2, 128.6, 127.4, 125.7 (q, *J* = 3.8 Hz), 123.9 (q, *J* = 272.2 Hz), 94.4, 74.3, 54.5, 51.0, 41.3, 27.1, 23.9, 18.6;

¹⁹F NMR (282 MHz, CDCl₃) δ -62.45;

IR (neat) 2948, 2870, 1750, 1575, 1322, 1291, 1156, 1122, 1068, 907, 829, 752, 730, 609 cm⁻¹;

HRMS (+p APCI) calcd for C₂₂H₂₁BrCl₃F₃SNO₄ (M+H)⁺ 635.9387 found 635.9391;

HPLC (ADH column, 5% *i*-propanol in hexane, 1 mL min⁻¹, 1 mg mL⁻¹, 40 min, UV 230 nm) retention times of 26.67 min (major) and 29.89 min (minor) 74% ee with Rh₂(R-TPPTTL)₄.



2,2,2-Trichloroethyl (*R*)-2-((*S*)-1-((4-bromophenyl)sulfonyl)piperidin-2-yl)-2-(3,4-dibromophenyl)acetate (148d)

Following *G.P. D* (1-((4-bromophenyl)sulfonyl)piperidine as substrate, reacting 2,2,2-trichloroethyl 2-diazo-2-(3,4-dibromophenyl)acetate), the desired C2-product was obtained using 0-12% ethyl acetate in hexane as eluting gradient in flash column chromatography (a 2nd column with 35-100% dichloromethane in hexane was conducted if the product is not pure enough) as white solid. Characterization data for the *erythro*-diastereomer was conducted on sample obtained in Rh₂(*R*-TPPTTL)₄-catalyzed reaction (67% ee).

mp: 134-136 °C; **R_f** = 0.40 (20% ethyl acetate/hexane); **[α]²⁰_D**: +11.4° (c = 1.00, CHCl₃, 67% ee);

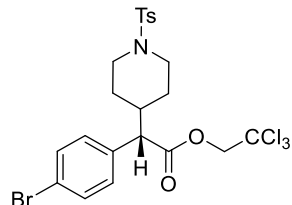
¹H NMR (600 MHz, CDCl₃) δ 7.59 (d, *J* = 2.2 Hz, 1H), 7.50 – 7.42 (m, 3H), 7.22 – 7.17 (m, 3H), 4.88 (d, *J* = 11.9 Hz, 1H), 4.81 (dd, *J* = 11.7, 4.7 Hz, 1H), 4.58 (d, *J* = 12.0 Hz, 1H), 4.18 (d, *J* = 11.7 Hz, 1H), 3.68 – 3.61 (m, 1H), 2.92 (ddd, *J* = 14.7, 13.0, 3.0 Hz, 1H), 1.87 – 1.79 (m, 1H), 1.77 – 1.70 (m, 3H), 1.63 – 1.56 (m, 1H), 1.54 – 1.46 (m, 1H);

¹³C NMR (151 MHz, CDCl₃) δ 169.4, 139.5, 135.5, 133.8, 133.8, 132.1, 128.6, 128.2, 127.4, 125.1, 124.9, 94.3, 74.3, 55.0, 50.2, 41.4, 27.3, 24.2, 18.6;

IR (neat) 2945, 2869, 1749, 1575, 1464, 1326, 1155, 1089, 1068, 1010, 908, 821, 729, 609 cm⁻¹;

HRMS (+p APCI) calcd for C₂₁H₂₀Br₃Cl₃SNO₄ (M+H)⁺ 723.7723 found 723.7728;

HPLC (ADH column, 5% *i*-propanol in hexane, 1 mL min⁻¹, 1 mg mL⁻¹, 60 min, UV 230 nm) retention times of 28.28 min (major) and 37.17 min (minor) 67% ee with Rh₂(*R*-TPPTTL)₄.



2,2,2-Trichloroethyl (S)-2-(4-bromophenyl)-2-(1-tosylpiperidin-4-yl)acetate (153)

Following *G.P. D* (1-tosylpiperidine as substrate, reacting 2,2,2-trichloroethyl 2-(4-bromophenyl)-2-diazoacetate, $\text{Rh}_2(\text{S-2-Cl-5-BrTPCP})_4$ as catalyst), the desired C4-product was purified by flash column chromatography (0-10% ethyl acetate in hexane) as white solid.

Characterization data was conducted on sample obtained in $\text{Rh}_2(\text{S-2-Cl-5-BrTPCP})_4$ -catalyzed reaction (96% ee).

mp: 61-63 °C; **Rf** = 0.38 (20% ethyl acetate/hexane); **$[\alpha]_D^{20}$:** -40.5° (c = 1.00, CHCl_3 , 96% ee);

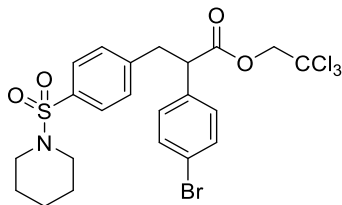
$^1\text{H NMR}$ (600 MHz, CDCl_3) δ 7.61 (d, J = 8.2 Hz, 2H), 7.44 (d, J = 8.5 Hz, 2H), 7.31 (d, J = 7.8 Hz, 2H), 7.16 (d, J = 8.5 Hz, 2H), 4.74 (d, J = 12.0 Hz, 1H), 4.61 (d, J = 12.0 Hz, 1H), 3.85 – 3.78 (m, 1H), 3.75 – 3.67 (m, 1H), 3.34 (d, J = 10.6 Hz, 1H), 2.43 (s, 3H), 2.27 (td, J = 12.0, 2.7 Hz, 1H), 2.13 (td, J = 12.0, 2.7 Hz, 1H), 2.00 – 1.87 (m, 2H), 1.48 (qd, J = 12.2, 4.2 Hz, 1H), 1.34 (dp, J = 13.3, 2.8 Hz, 1H), 1.18 (qd, J = 12.1, 4.3 Hz, 1H);

$^{13}\text{C NMR}$ (151 MHz, CDCl_3) δ 171.0, 143.7, 134.9, 133.0, 132.1, 130.3, 129.8, 127.9, 122.2, 94.7, 74.3, 56.9, 46.2, 38.5, 30.4, 29.0, 21.7;

IR (neat) 2948, 2924, 2848, 1749, 1489, 1355, 1338, 1165, 932, 817, 726, 549 cm^{-1} ;

HRMS (+p APCI) calcd for $\text{C}_{22}\text{H}_{24}\text{BrCl}_3\text{SNO}_4$ ($\text{M}+\text{H}$)⁺ 581.9670 found 581.9675;

HPLC (OD column, 10% *i*-propanol in hexane, 1 mL min^{-1} , 1 mg mL^{-1} , 60 min, UV 230 nm) retention times of 21.61 min (major) and 37.29 min (minor) 96% ee with $\text{Rh}_2(\text{S-2-Cl-5-BrTPCP})_4$.



2,2,2-Trichloroethyl 2-(4-bromophenyl)-3-(4-(piperidin-1-ylsulfonyl)phenyl)propanoate

Following *G.P. D* (1-tosylpiperidine as substrate, reacting 2,2,2-trichloroethyl 2-(4-bromophenyl)-2-diazoacetate, $\text{Rh}_2(\text{S-2-Cl-5-BrTPCP})_4$ as catalyst), the primary benzylic insertion byproduct was obtained using 0-10% ethyl acetate in hexane as eluting gradient in flash column chromatography as white solid.

Characterization data was conducted on sample obtained in $\text{Rh}_2(\text{S-2-Cl-5-BrTPCP})_4$ -catalyzed reaction (ee not determined).

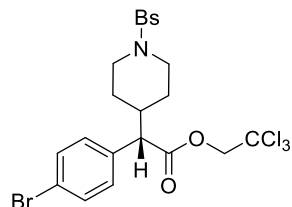
mp: 42-44 °C; **Rf** = 0.33 (20% ethyl acetate/hexane);

^1H NMR (600 MHz, CDCl_3) δ 7.63 (d, J = 8.4 Hz, 2H), 7.45 (d, J = 8.4 Hz, 2H), 7.28 (d, J = 8.3 Hz, 2H), 7.20 (d, J = 8.5 Hz, 2H), 4.72 (d, J = 12.0 Hz, 1H), 4.64 (d, J = 12.0 Hz, 1H), 3.98 (dd, J = 8.6, 7.1 Hz, 1H), 3.52 (dd, J = 13.9, 8.6 Hz, 1H), 3.14 (dd, J = 13.9, 7.1 Hz, 1H), 2.94 (t, J = 5.5 Hz, 4H), 1.63 (p, J = 5.9 Hz, 4H), 1.46 – 1.39 (m, 2H);

^{13}C NMR (151 MHz, CDCl_3) δ 171.0, 143.2, 136.0, 135.0, 132.1, 129.9, 129.7, 128.0, 122.2, 94.7, 74.3, 52.5, 47.1, 39.1, 25.3, 23.7;

IR (neat) 2941, 2854, 1751, 1489, 1340, 1166, 1149, 930, 720, 588, 564 cm^{-1} ;

HRMS (+p APCI) calcd for $\text{C}_{22}\text{H}_{24}\text{BrCl}_3\text{SNO}_4$ ($\text{M}+\text{H}$)⁺ 581.9670 found 581.9671;



2,2,2-Trichloroethyl (S)-2-(4-bromophenyl)-2-(1-((4-bromophenyl)sulfonyl)piperidin-4-yl)acetate (154)

Following *G.P. D* (1-((4-bromophenyl)sulfonyl)piperidine as substrate, reacting 2,2,2-trichloroethyl 2-(4-bromophenyl)-2-diazoacetate, $\text{Rh}_2(\text{S-2-Cl-5-BrTPCP})_4$ as catalyst), the desired C4-product was obtained using 0-10% ethyl acetate in hexane as eluting gradient in flash column chromatography as white solid.

Characterization data was conducted on sample obtained in $\text{Rh}_2(\text{S-2-Cl-5-BrTPCP})_4$ -catalyzed reaction (90% ee).

mp: 154-156 °C; **Rf** = 0.46 (20% ethyl acetate/hexane); **$[\alpha]_D^{20}$:** -29.1° (c = 1.00, CHCl_3 , 90% ee);

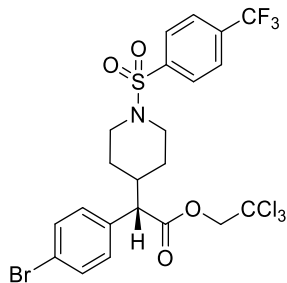
$^1\text{H NMR}$ (600 MHz, CDCl_3) δ 7.67 (d, J = 8.6 Hz, 2H), 7.59 (d, J = 8.6 Hz, 2H), 7.44 (d, J = 8.5 Hz, 2H), 7.16 (d, J = 8.4 Hz, 2H), 4.75 (d, J = 12.0 Hz, 1H), 4.62 (d, J = 12.0 Hz, 1H), 3.83 (ddt, J = 11.7, 4.6, 2.6 Hz, 1H), 3.71 (ddt, J = 11.7, 4.5, 2.5 Hz, 1H), 3.35 (d, J = 10.6 Hz, 1H), 2.30 (td, J = 12.0, 2.7 Hz, 1H), 2.17 (td, J = 12.0, 2.7 Hz, 1H), 2.03 – 1.87 (m, 2H), 1.48 (qd, J = 12.3, 4.3 Hz, 1H), 1.36 (dt, J = 13.4, 2.7 Hz, 1H), 1.19 (qd, J = 12.2, 4.3 Hz, 1H);

$^{13}\text{C NMR}$ (151 MHz, CDCl_3) δ 170.8, 135.1, 134.6, 132.3, 132.0, 130.1, 129.1, 127.9, 122.1, 94.5, 74.1, 56.7, 46.1, 46.0, 38.3, 30.2, 28.8;

IR (neat) 2949, 2849, 1749, 1575, 1489, 1358, 1341, 1166, 1011, 934, 825, 750, 595 cm^{-1} ;

HRMS (+p APCI) calcd for $\text{C}_{21}\text{H}_{21}\text{Br}_2\text{Cl}_3\text{SNO}_4$ ($\text{M}+\text{H}$)⁺ 645.8618 found 645.8621;

HPLC (OD column, 15% *i*-propanol in hexane, 1 mL min^{-1} , 1 mg mL^{-1} , 60 min, UV 230 nm) retention times of 21.66 min (major) and 34.30 min (minor) 90% ee with $\text{Rh}_2(\text{S-2-Cl-5-BrTPCP})_4$.



2,2,2-Trichloroethyl (S)-2-(4-bromophenyl)-2-(1-((4-(trifluoromethyl)phenyl)sulfonyl)-piperidin-4-yl)acetate (155)

Following *G.P. D* (1-((4-(trifluoromethyl)phenyl)sulfonyl)piperidine as substrate, reacting 2,2,2-trichloroethyl 2-(4-bromophenyl)-2-diazoacetate, $\text{Rh}_2(\text{S-2-Cl-5-BrTPCP})_4$ as catalyst), the desired C4-product was obtained using 0-10% ethyl acetate in hexane as eluting gradient in flash column chromatography as white solid.

Characterization data was conducted on sample obtained in $\text{Rh}_2(\text{S-2-Cl-5-BrTPCP})_4$ -catalyzed reaction (96% ee).

mp: 158-160 °C; **Rf** = 0.49 (20% ethyl acetate/hexane); **$[\alpha]^{20}_{\text{D}}$** : -29.1° (c = 1.00, CHCl_3 , 96% ee);

$^1\text{H NMR}$ (600 MHz, CDCl_3) δ 7.86 (d, J = 8.2 Hz, 2H), 7.80 (d, J = 8.2 Hz, 2H), 7.45 (d, J = 8.5 Hz, 2H), 7.16 (d, J = 8.4 Hz, 2H), 4.75 (d, J = 12.0 Hz, 1H), 4.62 (d, J = 12.0 Hz, 1H), 3.88 (ddt, J = 11.7, 4.4, 2.4 Hz, 1H), 3.76 (ddq, J = 11.7, 4.5, 2.5 Hz, 1H), 3.35 (d, J = 10.6 Hz, 1H), 2.34 (td, J = 12.0, 2.7 Hz, 1H), 2.20 (td, J = 12.0, 2.7 Hz, 1H), 2.07 – 1.88 (m, 2H), 1.50 (qd, J = 12.3, 4.3 Hz, 1H), 1.38 (dt, J = 13.4, 3.0 Hz, 1H), 1.20 (qd, J = 12.2, 4.3 Hz, 1H);

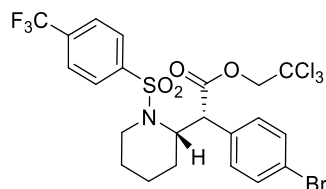
$^{13}\text{C NMR}$ (151 MHz, CDCl_3) δ 170.8, 139.8, 134.6, 134.5 (q, J = 33.0 Hz), 132.1, 130.1, 128.1, 126.2 (q, J = 3.6 Hz), 123.2 (d, J = 272.9 Hz), 122.2, 94.5, 74.1, 56.7, 46.1, 46.0, 38.2, 30.2, 28.8;

$^{19}\text{F NMR}$ (282 MHz, CDCl_3) δ -63.12;

IR (neat) 2951, 1750, 1489, 1404, 1323, 1170, 1134, 1062, 726, 596 cm^{-1} ;

HRMS (+p APCI) calcd for $\text{C}_{22}\text{H}_{21}\text{BrCl}_3\text{F}_3\text{SNO}_4$ (M+H)⁺ 635.9387 found 635.9390;

HPLC (R,R-Whelk column, 20% *i*-propanol in hexane, 1 mL min⁻¹, 1 mg mL⁻¹, 60 min, UV 230 nm) retention times of 31.20 min (major) and 50.10 min (minor) 96% ee with Rh₂(S-2-Cl-5-BrTPCP)₄.



2,2,2-Trichloroethyl (R)-2-(4-bromophenyl)-2-((S)-1-((4-(trifluoromethyl)phenyl)sulfonyl)piperidin-2-yl)acetate

Following *G.P. D* (1-((4-(trifluoromethyl)phenyl)sulfonyl)piperidine as substrate, reacting 2,2,2-trichloroethyl 2-(4-bromophenyl)-2-diazoacetate, Rh₂(S-2-Cl-5-BrTPCP)₄ as catalyst), the desired C2-product was obtained using 0-10% ethyl acetate in hexane as eluting gradient in flash column chromatography as white solid.

Characterization data was conducted on sample obtained in Rh₂(S-2-Cl-5-BrTPCP)₄-catalyzed reaction (81% ee).

mp: 136-138 °C; **Rf** = 0.45 (20% ethyl acetate/hexane); **[α]²⁰_D**: +22.5° (c = 0.66, CHCl₃, 81% ee);

¹H NMR (600 MHz, CDCl₃) δ 7.58 (d, *J* = 8.2 Hz, 2H), 7.37 (dd, *J* = 10.4, 8.4 Hz, 4H), 7.23 (d, *J* = 8.5 Hz, 2H), 4.89 (dd, *J* = 11.6, 4.8 Hz, 1H), 4.85 (d, *J* = 12.0 Hz, 1H), 4.59 (d, *J* = 12.0 Hz, 1H), 4.22 (d, *J* = 11.7 Hz, 1H), 3.56 (dd, *J* = 14.9, 4.4 Hz, 1H), 2.93 (ddd, *J* = 14.7, 12.9, 3.1 Hz, 1H), 1.92 – 1.70 (m, 4H), 1.60 (d, *J* = 13.7 Hz, 1H), 1.58 – 1.48 (m, 2H);

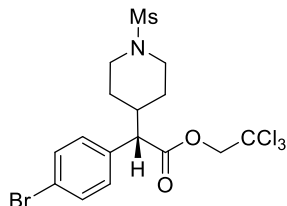
¹³C NMR (151 MHz, CDCl₃) δ 169.8, 143.9, 134.0 (d, *J* = 33.1 Hz), 133.7, 131.9, 130.3, 127.5, 125.9 (q, *J* = 3.8 Hz), 123.2 (q, *J* = 273.0 Hz), 122.5, 94.4, 74.3, 54.9, 50.5, 41.4, 27.4, 24.2, 18.6;

¹⁹F NMR (282 MHz, CDCl₃) δ -62.99;

IR (neat) 2947, 1752, 1489, 1323, 1161, 1136, 1063, 934, 720 cm^{-1} ;

HRMS (+p APCI) calcd for $\text{C}_{22}\text{H}_{21}\text{BrCl}_3\text{F}_3\text{SNO}_4$ ($\text{M}+\text{H}$)⁺ 635.9387 found 635.9389;

HPLC (ADH column, 5% *i*-propanol in hexane, 1 mL min^{-1} , 1 mg mL^{-1} , 60 min, UV 230 nm) retention times of 16.01 min (major) and 31.83 min (minor) 81% ee with $\text{Rh}_2(\text{S-2-Cl-5-BrTPCP})_4$.



2,2,2-Trichloroethyl (S)-2-(4-bromophenyl)-2-(1-(methylsulfonyl)piperidin-4-yl)acetate (156)

Following *G.P. D* (1-(methylsulfonyl)piperidine as substrate, reacting 2,2,2-trichloroethyl 2-(4-bromophenyl)-2-diazoacetate, $\text{Rh}_2(\text{S-2-Cl-5-BrTPCP})_4$ as catalyst), the desired C4-product was obtained using 0-10% ethyl acetate in hexane as eluting gradient in flash column chromatography as white solid.

Characterization data was conducted on sample obtained in $\text{Rh}_2(\text{S-2-Cl-5-BrTPCP})_4$ -catalyzed reaction (97% ee).

mp: 170-172 °C; **Rf** = 0.08 (20% ethyl acetate/hexane); **[α]²⁰_D:** +18.6° (*c* = 1.00, CHCl_3 , 97% ee);

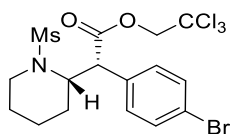
¹H NMR (600 MHz, CDCl_3) δ 7.48 (d, *J* = 8.4 Hz, 2H), 7.22 (d, *J* = 8.5 Hz, 2H), 4.78 (d, *J* = 12.0 Hz, 1H), 4.65 (d, *J* = 11.9 Hz, 1H), 3.88 – 3.80 (m, 1H), 3.77 – 3.70 (m, 1H), 3.40 (d, *J* = 10.7 Hz, 1H), 2.76 (s, 3H), 2.70 (td, *J* = 12.1, 2.7 Hz, 1H), 2.57 (td, *J* = 12.1, 2.7 Hz, 1H), 2.20 – 2.12 (m, 2H), 1.98 (dt, *J* = 13.1, 3.0 Hz, 1H), 1.49 (qd, *J* = 12.1, 4.3 Hz, 1H), 1.42 (dt, *J* = 13.3, 2.2 Hz, 1H), 1.20 (qd, *J* = 12.1, 4.3 Hz, 1H);

¹³C NMR (151 MHz, CDCl_3) δ 170.9, 134.7, 132.1, 130.2, 122.2, 94.6, 74.2, 56.8, 45.9, 45.8, 38.5, 34.8, 30.5, 29.0;

IR (neat) 3023, 2948, 2851, 1748, 1489, 1332, 1255, 1216, 1155, 957, 934, 827, 759, 723, 517, 505 cm^{-1} ;

HRMS (+p APCI) calcd for $\text{C}_{16}\text{H}_{20}\text{BrCl}_3\text{SNO}_4$ ($\text{M}+\text{H}$)⁺ 505.9357 found 505.9362;

HPLC (R,R-Whelk column, 20% *i*-propanol in hexane, 1 mL min^{-1} , 1 mg mL^{-1} , 80 min, UV 230 nm) retention times of 41.56 min (major) and 53.30 min (minor) 97% ee with $\text{Rh}_2(\text{S-2-Cl-5-BrTPCP})_4$.



2,2,2-Trichloroethyl (R)-2-(4-bromophenyl)-2-((S)-1-(methylsulfonyl)piperidin-2-yl)acetate

Following *G.P. D* (1-(methylsulfonyl)piperidine as substrate, reacting 2,2,2-trichloroethyl 2-(4-bromophenyl)-2-diazoacetate, $\text{Rh}_2(\text{S-2-Cl-5-BrTPCP})_4$ as catalyst), the desired C2-product was obtained using 0-10% ethyl acetate in hexane as eluting gradient in flash column chromatography as white solid.

Characterization data was conducted on sample obtained in $\text{Rh}_2(\text{S-2-Cl-5-BrTPCP})_4$ -catalyzed reaction (80% ee).

mp: 84-86 °C; **Rf** = 0.18 (20% ethyl acetate/hexane); **$[\alpha]_D^{20}$:** +11.8° (*c* = 1.00, CHCl_3 , 80% ee);

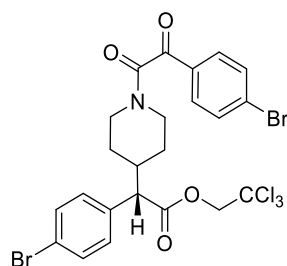
$^1\text{H NMR}$ (600 MHz, CDCl_3) δ 7.51 (d, *J* = 8.5 Hz, 2H), 7.38 (d, *J* = 8.5 Hz, 2H), 4.91 – 4.82 (m, 2H), 4.61 (d, *J* = 12.0 Hz, 1H), 4.24 (d, *J* = 11.8 Hz, 1H), 3.56 (dd, *J* = 14.7, 4.4 Hz, 1H), 2.95 – 2.86 (m, 1H), 2.06 (s, 3H), 1.92 – 1.84 (m, 1H), 1.84 – 1.76 (m, 3H), 1.72 – 1.59 (m, 2H);

$^{13}\text{C NMR}$ (151 MHz, CDCl_3) δ 170.0, 134.6, 132.2, 130.8, 122.7, 94.6, 74.4, 55.1, 50.7, 41.0, 39.9, 28.2, 25.2, 18.9;

IR (neat) 2938, 2856, 1749, 1489, 1320, 1146, 1053, 959, 940, 777, 715, 519 cm^{-1} ;

HRMS (+p APCI) calcd for $C_{16}H_{20}BrCl_3SNO_4$ (M+H)⁺ 505.9357 found 505.9358;

HPLC (ADH column, 5% *i*-propanol in hexane, 1 mL min⁻¹, 1 mg mL⁻¹, 45 min, UV 230 nm) retention times of 28.79 min (major) and 33.36 min (minor) 80% ee with Rh₂(*S*-2-Cl-5-BrTPCP)₄.



2,2,2-Trichloroethyl (*S*)-2-(4-bromophenyl)-2-(1-(2-(4-bromophenyl)-2-oxoacetyl)piperidin-4-yl)acetate (157)

Following *G.P. D* (1-(4-bromophenyl)-2-(piperidin-1-yl)ethane-1,2-dione as substrate, reacting 2,2,2-trichloroethyl 2-(4-bromophenyl)-2-diazoacetate, Rh₂(*S*-2-Cl-5-BrTPCP)₄ as catalyst) with reaction under reflux dichloromethane (39 °C) and 1.5: 1 (diazoacetate: protected-piperidine), the desired C4-product was purified by flash column chromatography (0-10% ethyl acetate in hexane) as white solid.

Characterization data was conducted on sample obtained in Rh₂(*S*-2-Cl-5-BrTPCP)₄-catalyzed reaction (97% ee) as mixture with 1:1 ratio of rotamers.

mp. 58-60 °C; **R_f** = 0.31 (20% ethyl acetate/hexane); **[α]²⁰_D**: +46.1° (c = 1.00, CHCl₃, 97% ee);

¹H NMR (600 MHz, CDCl₃) (*mixture of both rotamers with 1:1 ratio*) δ 7.79 (dd, *J* = 13.0, 8.5 Hz, 2H), 7.65 (dd, *J* = 9.9, 8.5 Hz, 2H), 7.47 (dd, *J* = 23.4, 8.5 Hz, 2H), 7.22 (dd, *J* = 13.7, 8.4 Hz, 2H), 4.81 (d, *J* = 12.0 Hz, 0.5H), 4.75 (d, *J* = 12.0 Hz, 0.5H), 4.73 – 4.67 (m, 0.5H), 4.64 (t, *J* = 11.9 Hz, 1H), 4.61 – 4.54 (m, 0.5H), 3.60 (dt, *J* = 13.7, 2.2 Hz, 0.5H), 3.48 (dt, *J* = 13.7, 2.1 Hz, 0.5H), 3.41 (dd, *J* = 10.6, 3.1 Hz, 1H), 3.17 – 3.07 (m, 0.5H), 3.03 – 2.93 (m, 0.5H), 2.84 (td, *J* =

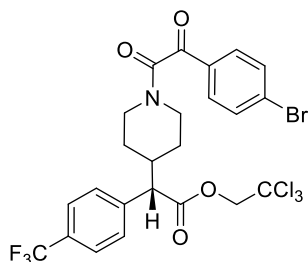
13.1, 2.9 Hz, 0.5H), 2.70 (td, $J = 13.0, 2.9$ Hz, 0.5H), 2.35 (qt, $J = 11.5, 3.7$ Hz, 1H), 2.04 (dt, $J = 13.4, 2.8$ Hz, 0.5H), 1.89 (dt, $J = 13.1, 2.9$ Hz, 0.5H), 1.52 – 1.28 (m, 2H), 1.14 (qd, $J = 12.5, 4.4$ Hz, 0.5H), 1.06 (qd, $J = 12.5, 4.3$ Hz, 0.5H);

^{13}C NMR (151 MHz, CDCl_3) (mixture of both rotamers with 1:1 ratio) δ 190.3, (190.3), 170.8, (170.8), 164.7, (164.7), 134.5, (134.5), 132.4, (132.4), 132.1, (132.1), 131.9, (131.9), 131.0, (130.9), 130.3, (130.3), 130.1, (130.1), 122.2, (122.2), 94.6, (94.5), 74.2, (74.1), 56.8, (56.8), 45.9, (45.8), 41.3, (41.2), 39.1, (39.0), 31.1, (30.5), 29.8, (29.0);

IR (neat) 2949, 2867, 1749, 1681, 1643, 1585, 1488, 1449, 1399, 1267, 1228, 1140, 1071, 762 cm^{-1} ;

HRMS (+p APCI) calcd for $\text{C}_{22}\text{H}_{21}\text{Br}_2\text{Cl}_3\text{NO}_4$ (M) $^+$ 637.8897 found 637.8897;

HPLC (ADH column, 5% *i*-propanol in hexane, 1 mL min^{-1} , 1 mg mL^{-1} , 80 min, UV 230 nm) retention times of 49.67 min (major) and 60.07 min (minor) 97% ee with $\text{Rh}_2(\text{S-2-Cl-5-BrTPCP})_4$.



2,2,2-Trichloroethyl (S)-2-(1-(2-(4-bromophenyl)-2-oxoacetyl)piperidin-4-yl)-2-(4-(trifluoromethyl)phenyl)acetate (158)

Following *G.P. D* (1-(4-bromophenyl)-2-(piperidin-1-yl)ethane-1,2-dione as substrate, reacting 2,2,2-trichloroethyl 2-diazo-2-(4-(trifluoromethyl)phenyl)acetate, $\text{Rh}_2(\text{S-2-Cl-5-BrTPCP})_4$ as catalyst) with reaction under reflux dichloromethane (39 °C) and 1.5: 1 (diazoacetate: protected-

piperidine), the desired C4-product was purified by flash column chromatography (0-10% ethyl acetate in hexane) as white solid.

Characterization data was conducted on sample obtained in $\text{Rh}_2(\text{S-2-Cl-5-BrTPCP})_4$ -catalyzed reaction (96% ee) as mixture with 1:1 ratio of rotamers.

mp: 50-52 °C; **Rf** = 0.37 (20% ethyl acetate/hexane); **$[\alpha]_D^{20}$:** +42.3° (c = 1.00, CHCl_3 , 96% ee);

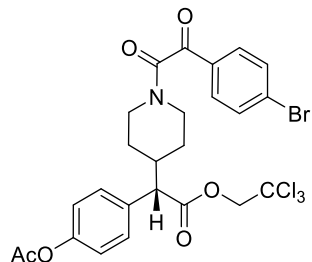
$^1\text{H NMR}$ (600 MHz, CDCl_3) (*mixture of both rotamers with 1:1 ratio*) δ 7.79 (dd, J = 15.6, 8.6 Hz, 2H), 7.68 – 7.62 (m, 3H), 7.62 – 7.58 (m, 1H), 7.48 (dd, J = 12.7, 8.1 Hz, 2H), 4.83 (d, J = 12.0 Hz, 0.5H), 4.77 (d, J = 12.0 Hz, 0.5H), 4.72 (ddt, J = 13.4, 4.6, 2.4 Hz, 0.5H), 4.68 – 4.58 (m, 1.5H), 3.62 (ddt, J = 13.8, 4.4, 2.3 Hz, 0.5H), 3.53 (dd, J = 10.6, 3.4 Hz, 1H), 3.49 (ddt, J = 13.9, 4.6, 2.4 Hz, 0.5H), 3.13 (ddd, J = 13.7, 12.4, 2.9 Hz, 0.5H), 2.99 (ddd, J = 13.8, 12.3, 2.8 Hz, 0.5H), 2.89 – 2.81 (m, 0.5H), 2.71 (ddd, J = 13.4, 12.5, 3.0 Hz, 0.5H), 2.46 – 2.36 (m, 1H), 2.07 (dt, J = 13.5, 2.8 Hz, 0.5H), 1.92 (dt, J = 13.1, 3.0 Hz, 0.5H), 1.51 – 1.35 (m, 1.5H), 1.29 (dt, J = 13.3, 3.0 Hz, 0.5H), 1.17 (dtd, J = 13.6, 12.3, 4.5 Hz, 0.5H), 1.09 (dtd, J = 13.3, 12.2, 4.4 Hz, 0.5H);

$^{13}\text{C NMR}$ (151 MHz, CDCl_3) (*mixture of both rotamers with 1:1 ratio*) δ 190.5, (190.5), 170.7, (170.7), 164.9, (164.9), 139.7, (139.7), 132.6, (132.6), 132.1, (132.0), 131.1, (131.1), 130.7 (d, J = 32.7 Hz), (130.6 (d, J = 32.7 Hz)), 130.5, (130.5), 129.1, 126.1 (q, J = 3.7 Hz), (126.0 (q, J = 3.9 Hz)), 124.0 (d, J = 272.2 Hz), (124.0 (d, J = 272.2 Hz)), 94.6, (94.6), 74.4, (74.3), 57.4, (57.4), 46.0, (46.0), 41.4, (41.3), 39.4, (39.3), 31.3, (30.6), 30.0, (29.2);

IR (*neat*) 2950, 2869, 1751, 1682, 1643, 1586, 1325, 1127, 1068, 760 cm^{-1} ;

HRMS (+p APCI) calcd for $\text{C}_{24}\text{H}_{21}\text{BrCl}_3\text{F}_3\text{NO}_4$ ($\text{M}+\text{H}$)⁺ 627.9666 found 627.9674;

HPLC (ODH column, 10% *i*-propanol in hexane, 1 mL min^{-1} , 1 mg mL^{-1} , 45 min, UV 230 nm) retention times of 18.09 min (minor) and 28.06 min (major) 96% ee with $\text{Rh}_2(\text{S-2-Cl-5-BrTPCP})_4$.



2,2,2-Trichloroethyl (S)-2-(4-acetoxyphenyl)-2-(1-(2-(4-bromophenyl)-2-oxoacetyl)piperidin-4-yl)acetate (159)

Following *G.P. D* (1-(4-bromophenyl)-2-(piperidin-1-yl)ethane-1,2-dione as substrate, reacting 2,2,2-trichloroethyl 2-(4-acetoxyphenyl)-2-diazoacetate, $\text{Rh}_2(\text{S-2-Cl-5-BrTPCP})_4$ as catalyst) with reaction under reflux dichloromethane (39 °C) and 1.5: 1 (diazoacetate: protected-piperidine), the desired C4-product was purified by flash column chromatography (0-10% ethyl acetate in hexane) as white solid.

Characterization data was conducted on sample obtained in $\text{Rh}_2(\text{S-2-Cl-5-BrTPCP})_4$ -catalyzed reaction (75% ee) as mixture with 1:1 ratio of rotamers.

mp: 55-58 °C; **Rf** = 0.18 (20% ethyl acetate/hexane); **$[\alpha]_D^{20}$:** +29.8° (c = 0.45, CHCl_3 , 75% ee);

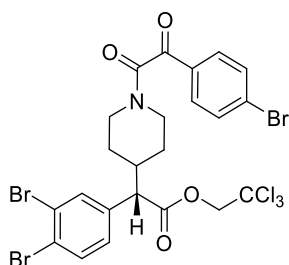
$^1\text{H NMR}$ (600 MHz, CDCl_3) (mixture of both rotamers with 1:1 ratio) δ 7.79 (dd, $J = 13.8, 8.6$ Hz, 2H), 7.66 (dd, $J = 10.2, 8.6$ Hz, 2H), 7.35 (dd, $J = 14.0, 8.6$ Hz, 2H), 7.07 (dd, $J = 25.2, 8.6$ Hz, 2H), 4.85 (d, $J = 12.0$ Hz, 0.5H), 4.79 (d, $J = 12.0$ Hz, 0.5H), 4.71 (ddt, $J = 13.4, 4.5, 2.2$ Hz, 0.5H), 4.64 – 4.57 (m, 1.5H), 3.60 (ddt, $J = 13.7, 4.4, 2.3$ Hz, 0.5H), 3.51 – 3.41 (m, 1.5H), 3.13 (ddd, $J = 13.8, 12.4, 2.9$ Hz, 0.5H), 2.98 (ddd, $J = 13.8, 12.3, 2.8$ Hz, 0.5H), 2.84 (td, $J = 13.1, 3.0$ Hz, 0.5H), 2.71 (td, $J = 13.1, 3.0$ Hz, 0.5H), 2.40 – 2.32 (m, 1H), 2.31 (s, 1.5H), 2.29 (s, 1.5H), 2.05 (dt, $J = 13.4, 3.1$ Hz, 0.5H), 1.90 (dt, $J = 13.0, 2.9$ Hz, 0.5H), 1.51 (dt, $J = 13.0, 2.7$ Hz, 0.5H), 1.48 – 1.31 (m, 1.5H), 1.15 (dtd, $J = 13.7, 12.3, 4.4$ Hz, 0.5H), 1.06 (qd, $J = 12.5, 4.3$ Hz, 0.5H);

^{13}C NMR (151 MHz, CDCl_3) (mixture of both rotamers with 1:1 ratio) δ 190.4, (190.4), 171.1, (171.0), 169.3, (169.3), 164.8, (164.7), 150.5, (150.4), 133.0, (133.0), 132.5, (132.4), 131.9, (131.9), 131.0, (131.0), 130.3, (130.3), 129.5, (129.5), 122.1, (122.0), 94.6, (94.6), 74.2, (74.1), 56.8, 46.0, (45.9), 41.3, (41.2), 39.3, (39.2), 31.1, (30.5), 29.9, (29.1), 21.2, (21.1);

IR (neat) 2950, 1750, 1682, 1641, 1586, 1506, 1370, 1201, 1170, 1139, 911, 728 cm^{-1} ;

HRMS (+p APCI) calcd for $\text{C}_{25}\text{H}_{24}\text{BrCl}_3\text{NO}_6$ ($\text{M}+\text{H}$) $^+$ 617.9847 found 617.9847;

HPLC (ODH column, 15% *i*-propanol in hexane, 1 mL min^{-1} , 1 mg mL^{-1} , 80 min, UV 230 nm) retention times of 23.99 min (minor) and 45.95 min (major) 75% ee with $\text{Rh}_2(\text{S-2-Cl-5-BrTPCP})_4$.



2,2,2-trichloroethyl (S)-2-(1-(2-(4-bromophenyl)-2-oxoacetyl)piperidin-4-yl)-2-(3,4-dibromophenyl)acetate (160)

Following *G.P. D* (1-(4-bromophenyl)-2-(piperidin-1-yl)ethane-1,2-dione as substrate, reacting 2,2,2-trichloroethyl 2-diazo-2-(3,4-dibromophenyl)acetate, $\text{Rh}_2(\text{S-2-Cl-5-BrTPCP})_4$ as catalyst) with reaction under reflux dichloromethane (39 °C) and 1.5: 1 (diazoacetate: protected-piperidine), the desired C4-product was purified by flash column chromatography (0-10% ethyl acetate in hexane) as white solid.

Characterization data was conducted on sample obtained in $\text{Rh}_2(\text{S-2-Cl-5-BrTPCP})_4$ -catalyzed reaction (98% ee) as mixture with 1:1 ratio of rotamers.

mp: 62-64 °C; **R_f** = 0.31 (20% ethyl acetate/hexane); **[α] $^{20}_{\text{D}}$:** +42.6° (*c* = 1.00, CHCl_3 , 98% ee);

¹H NMR (500 MHz, CDCl₃) (*mixture of both rotamers with 1:1 ratio*) δ 7.79 (dd, *J* = 10.9, 8.6 Hz, 2H), 7.68 – 7.55 (m, 4H), 7.15 (ddd, *J* = 9.3, 8.2, 2.1 Hz, 1H), 4.84 (d, *J* = 11.9 Hz, 0.5H), 4.78 (d, *J* = 12.0 Hz, 0.5H), 4.74 – 4.68 (m, 0.5H), 4.68 – 4.58 (m, 1.5H), 3.65 – 3.57 (m, 0.5H), 3.55 – 3.46 (m, 0.5H), 3.39 (dd, *J* = 10.6, 1.9 Hz, 1H), 3.12 (ddd, *J* = 13.8, 12.3, 2.9 Hz, 0.5H), 3.00 (ddd, *J* = 13.8, 12.3, 2.8 Hz, 0.5H), 2.87 – 2.78 (m, 0.5H), 2.77 – 2.67 (m, 0.5H), 2.39 – 2.27 (m, 1H), 2.07 – 1.98 (m, 0.5H), 1.91 – 1.84 (m, 0.5H), 1.53 – 1.47 (m, 0.5H), 1.47 – 1.30 (m, 1.5H), 1.13 (dq, *J* = 42.3, 12.5, 4.4 Hz, 1H);

¹³C NMR (126 MHz, CDCl₃) (*mixture of both rotamers with 1:1 ratio*) δ 190.3, (190.3), 170.3, (170.3), 164.7, (164.7), 136.4, (136.4), 134.1, (134.0), 133.5, (133.5), 132.5, 131.9, (131.9), 131.0, (131.0), 130.4, 128.7, (128.7), 125.5, (125.4), 124.7, (124.6), 94.5, (94.4), 74.3, (74.2), 56.5, 45.9, (45.8), 41.2, (41.1), 39.2, (39.1), 31.1, (30.4), 29.9, (29.0);

IR (neat) 3010, 2949, 2867, 1750, 1682, 1643, 1585, 1486, 1141, 761 cm⁻¹;

HRMS (+p APCI) calcd for C₂₃H₂₀Br₃Cl₃NO₄ (M+H)⁺ 715.8003 found 715.8015;

HPLC (R,R-Whelk column, 20% *i*-propanol in hexane, 1 mL min⁻¹, 1 mg mL⁻¹, 100 min, UV 230 nm) retention times of 66.36 min (major) and 84.85 min (minor) 98% ee with Rh₂(*S*-2-Cl-5-BrTPCP)₄.

6.4 Experimental Part for Chapter 4

Catalyst Synthesis

General Procedure F (Cyclopropanation for triarylcyclopropane carboxylate)

A flame-dried 500 mL round bottom flask with magnetic stir bar was charged with 1,1-diarylethylene (46 mmol, 2.3 equiv) and $\text{Rh}_2(\text{S-PTAD})_4$ (155.9 mg, 0.1 mmol, 0.5 mol%). After the flask was flushed with argon gas (3 times), 30 mL of dry pentane was added, and the reaction mixture was cooled to 0 °C via ice bath. A solution of corresponding diazo compound (20 mmol, 1.0 equiv) in 200 mL of dry pentane was then added into the reaction mixture dropwise via additional funnel (syringe pump for small scale with less solvent) at 0 °C. The reaction mixture was stirred overnight (at which point it was warmed up to room temperature (23 °C)). The mixture was concentrated and purified by flash column chromatography (hexane/ethyl acetate = 50/1) to afford the major diastereomer and the minor diastereomer separately as white solid. The enantiopure product was obtained by recrystallization.

General Procedure G

(Sonogashira Coupling for Converting bromide to (triisopropylsilyl)ethynyl group)

A G10 (10 mL) microwave tube was charged with corresponding 4-bromoarenes (2.50 mmol, 1.0 equiv), copper(I) iodide (23.8 mg, 0.35 mmol, 5.0 mol%), triphenylphosphine (131.1 mg, 0.5 mmol, 0.2 equiv) and triethylamine (2.5 mL, 18.0 mmol, 7.2 equiv). After the reaction vessel was flush with argon, ethynyltriisopropylsilane (0.62 mL, 2.75 mmol, 1.1 equiv), $\text{Pd}(\text{dppf})\text{Cl}_2$ (87.8 mg, 0.125 mmol, 5.0 mol%) and anhydrous dimethylformamide (0.7 mL) was added quickly to give a yellow slurry, and the septum was replaced with a new one for microwave reactor. The reaction mixture was irradiated in a microwave to 120 °C for 1 h with heavy stirring to give a

brown suspension with white crystalline material. The resulted mixtures were filtered through a plug of Celite[®] 545 in a sintered glass funnel and washed with dichloromethane (20 mL). The filtrate was concentrated under reduced pressure and purified by flash column chromatography (hexane/ethyl acetate = 50/1 to 20/1) to afford the desired product as white solid.

General procedure H (Hydrolysis of methyl esters)

*The desired TIPS protecting group could be potentially removed under this hydrolysis condition, so reaction needed to be monitored carefully with shorter reaction time and the methyl ester starting material could be recovered for next cycle.

A flame-dried 250 mL round bottom flask was charged with corresponding methyl ester (1.0 equiv) and flushed with argon (3 cycles). Anhydrous tetrahydrofuran (4 mL/mmol of ester) was added, followed by the addition of TMSOK (6.0 equiv) in one portion. The reaction mixture was stirred at room temperature (23 °C) and monitored by TLC. When a third spot (byproduct with TIPS removal) just started to appear on TLC, the reaction mixture was quenched by addition of 0.4 M citric acid (3 mL/mmol of ester) and stirred for 1 h. The mixture was extracted by ethyl acetate (3 times) and the collected organic layer was washed with brine. The organic solution was concentrated and purified by flash column chromatography (hexane/ethyl acetate = 20/1 to 6/1) to afford the desired product as white solid.

General procedure I (Mono-ligand exchange)

A flame-dried 100 mL 3-neck round-bottom flask was charged with corresponding dirhodium tetracarboxylate catalyst (0.20 mmol, 1.00 equiv) and corresponding ligand with (triisopropylsilyl)ethynyl group (0.22 mmol, 1.10 equiv). The vessel was flushed with argon (3

cycles). 20 mL of Benzene (for $\text{Rh}_2(\text{S-2-CITPCP})_4$) or chlorobenzene (for $\text{Rh}_2(\text{S-2-Cl-5-CF}_3\text{TPCP})_4$) was added to give a green slurry. The reaction mixture was stirred under reflux for 16 h (for $\text{Rh}_2(\text{S-2-CITPCP})_4$) or 1 h (for $\text{Rh}_2(\text{S-2-Cl-5-CF}_3\text{TPCP})_4$). The reaction mixture was cooled down to room temperature and concentrated under reduced pressure, then purified by flash column chromatography (hexane/ethyl acetate = 12/1 to 6/1) to afford the desired mono-exchange product as green solid (mass spectroscopy was used for fractions identification and confirmation).

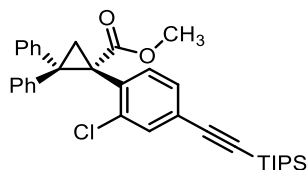
General procedure J (TIPS deprotection)

A flame-dried 50 mL round-bottom flask was charged with corresponding mono-exchange product (0.10 mmol) and flushed with argon (3 cycles). Anhydrous tetrahydrofuran (5 mL) was added to give a green solution and the reaction mixture was cooled to 0 °C via ice/water bath. A solution of TBAF in THF (1.0 M, 0.1 mL, 0.1 mmol, 1.0 equiv) was added dropwise via syringe at 0 °C. The reaction mixture was stirred at 0 °C until full consumption of starting material (monitored by TLC analysis, normally 0.5-1 h). The reaction mixture was quenched by the addition of DI water (10 mL). The reaction mixture was extracted with dichloromethane (3 x 20 mL). The combined organic layer was concentrated and purified by flash column chromatography (hexane/ethyl acetate = 12/1 to 6/1) to afford the desired product as green solid (mass spectroscopy was used for product identification and confirmation).

C–H Functionalization Reactions

G.P. C was followed for all testing reaction on 4-bromopentylbenzene.

Synthesis for Rh₂(S-o-CITPCP)₃(ethynyl@A)



Methyl (S)-1-(2-chloro-4-((triisopropylsilyl)ethynyl)phenyl)-2,2-diphenylcyclopropane-1-carboxylate (214)

It was obtained in 87% yield following *G.P. G* using enantiopure methyl (S)-1-(4-bromo-2-chlorophenyl)-2,2-diphenylcyclopropane-1-carboxylate as starting material.

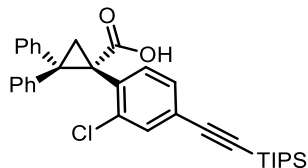
mp: 58-60 °C; **R_f** = 0.51 (10% ethyl acetate/hexane); **[α]²⁰_D**: -309.1° (c = 1.00, CHCl₃, 99.9% ee);

¹H NMR (600 MHz, CDCl₃) δ 7.54 – 7.49 (m, 2H), 7.39 – 7.35 (m, 3H), 7.29 (ddt, *J* = 8.1, 6.8, 1.3 Hz, 1H), 7.12 – 7.07 (m, 1H), 7.06 – 6.99 (m, 4H), 6.90 – 6.84 (m, 2H), 3.39 (s, 3H), 2.79 (d, *J* = 5.8 Hz, 1H), 2.46 (d, *J* = 5.8 Hz, 1H), 1.11 (s, 21H);

¹³C NMR (151 MHz, CDCl₃) δ 170.4, 141.4, 139.0, 136.6, 134.6, 133.9, 132.9, 130.4, 129.4, 128.4, 128.3, 127.5, 127.1, 126.3, 123.9, 105.3, 92.4, 52.4, 45.1, 41.9, 26.2, 18.6, 11.3;

IR (neat) 3025, 2944, 2865, 2160, 1736, 1450, 1381, 1366, 1217, 881, 748, 705 cm⁻¹;

HRMS (+p NSI) calcd for C₃₄H₄₀ClO₂Si (M+H)⁺ 543.2481 found 543.2478.



(S)-1-(2-Chloro-4-((triisopropylsilyl)ethynyl)phenyl)-2,2-diphenylcyclopropane-1-carboxylic acid (215)

It was obtained in 80% yield following *G.P. H* using methyl (S)-1-(2-chloro-4-((triisopropylsilyl)ethynyl)phenyl)-2,2-diphenylcyclopropane-1-carboxylate from previous step as starting material.

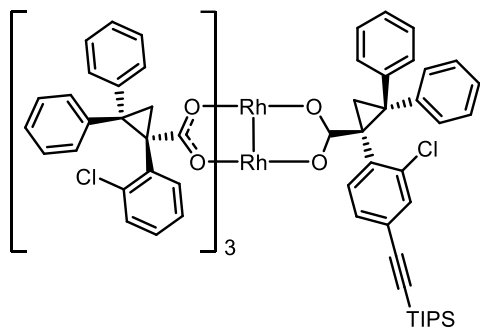
mp: 132-134 °C; **Rf** = 0.25(20% ethyl acetate/hexane); **[α]²⁰_D:** -343.7°(c = 1.00, CHCl₃, 99.9% ee);

¹H NMR (600 MHz, CDCl₃) δ 7.55 – 7.43 (m, 2H), 7.36 (td, *J* = 7.2, 6.4, 1.9 Hz, 3H), 7.33 – 7.28 (m, 1H), 7.13 – 6.92 (m, 5H), 6.88 – 6.80 (m, 2H), 2.70 (s, 1H), 2.49 (d, *J* = 5.9 Hz, 1H), 1.10 (s, 21H);

¹³C NMR (151 MHz, CDCl₃) δ 175.1, 140.9, 138.7, 136.6, 134.1, 132.9, 130.3, 129.4, 128.4, 127.5, 127.2, 126.5, 124.1, 105.2, 92.5, 77.2, 46.1, 41.4, 26.6, 18.6, 11.3;

IR (neat) 3026, 2943, 2865, 2161, 1738, 1697, 1495, 1231, 1217, 881, 748, 703 cm⁻¹;

HRMS (+p NSI) calcd for C₃₃H₃₈ClO₂Si (M+H)⁺ 529.2324 found 529.2320.



Rh₂(S-*o*-CITPCP)₃(TIPS-ethynyl@A) (216)

It was obtained in 50% yield following *G.P. I* using $\text{Rh}_2(S\text{-}o\text{-CITPCP})_4$ (319.4 mg) and (*S*)-1-(2-chloro-4-((triisopropylsilyl)ethynyl)phenyl)-2,2-diphenylcyclopropane-1-carboxylic acid (116.4 mg) as starting materials. The reaction was refluxed at 84 °C for 16 h with benzene as solvent.

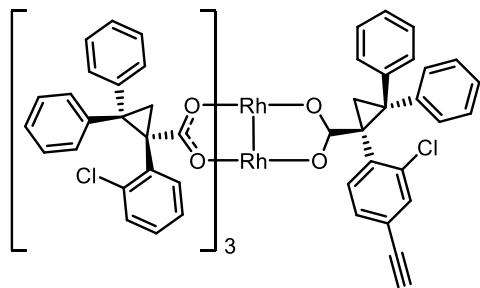
mp: >200 °C (decomp.); **R_f** = 0.69 (30% ethyl acetate/hexane);

¹H NMR (600 MHz, CDCl₃) δ 7.47 – 7.43 (m, 7H), 7.18 – 7.06 (m, 26H), 7.03 – 6.87 (m, 22H), 2.77 – 2.66 (m, 4H), 2.30 – 2.20 (m, 4H), 1.09 (s, 21H);

¹³C NMR (151 MHz, CDCl₃) δ 188.0, 188.0, 187.5, 142.8, 142.7, 142.7, 139.5, 139.5, 139.4, 136.7, 136.4, 136.2, 135.6, 135.6, 132.3, 131.3, 131.1, 130.8, 130.7, 130.5, 129.8, 129.1, 128.5, 128.4, 127.8, 127.8, 127.3, 127.3, 127.2, 127.0, 126.2, 125.9, 125.9, 125.5, 125.5, 123.1, 105.7, 91.5, 45.9, 45.6, 41.9, 41.8, 25.7, 25.6, 18.6, 11.3;

IR (neat) 3606, 3529, 3057, 2924, 2864, 1583, 1388, 730, 703, 694 cm⁻¹;

HRMS (+p ESI) calcd for C₉₉H₈₄Cl₄O₈Rh₂Si (M)⁺ 1774.2800 found 177.2820.



Rh₂(*S*-*o*-CITPCP)₃(ethynyl@A) (217)

It was obtained in 72% yield following *G.P. J* using $\text{Rh}_2(S\text{-}o\text{-CITPCP})_3(\text{TIPS-ethynyl@A})$ from previous step as starting material.

mp: >200 °C (decomp.); **R_f** = 0.55 (30% ethyl acetate/hexane);

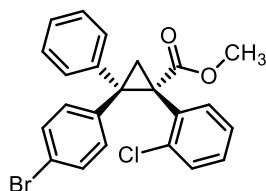
¹H NMR (600 MHz, CDCl₃) δ 7.47 – 7.43 (m, 7H), 7.17 – 7.08 (m, 26H), 7.02 – 6.87 (m, 22H), 2.99 (s, 1H), 2.75 – 2.66 (m, 4H), 2.30 – 2.20 (m, 4H);

^{13}C NMR (151 MHz, CDCl_3) δ 188.0, 188.0, 187.4, 142.7, 142.5, 139.5, 139.2, 137.0, 136.8, 136.7, 136.6, 135.7, 135.7, 132.4, 131.3, 131.2, 131.1, 130.8, 130.7, 130.6, 129.7, 129.1, 128.5, 128.4, 128.1, 127.8, 127.3, 127.2, 127.2, 127.0, 126.2, 125.9, 125.8, 125.6, 125.5, 121.5, 82.4, 68.2, 45.8, 45.5, 41.9, 41.7, 25.5, 25.4;

IR (neat) 3614, 3287, 3057, 2924, 2853, 1585, 1447, 1389, 751, 703 cm^{-1} ;

HRMS (+p ESI) calcd for $\text{C}_{90}\text{H}_{64}\text{Cl}_4\text{O}_8\text{Rh}_2$ (M) $^+$ 1618.1460 found 1618.1512.

Synthesis for $\text{Rh}_2(\text{S-}o\text{-CITPCP})_3(\text{ethynyl@B})$



Methyl (1S,2S)-2-(4-bromophenyl)-1-(2-chlorophenyl)-2-phenylcyclopropane-1-carboxylate (223)

It was obtained as major diastereomer in 62% yield following *G.P. F* using 1-bromo-4-(1-phenylvinyl)benzene (11.9 g) and methyl 2-(2-chlorophenyl)-2-diazoacetate (4.21 g) as starting materials, and $\text{Rh}_2(\text{S-PTAD})_4$ as catalyst. The enantiopure product was obtained from recrystallization from 1% ethyl acetate/hexane solution (after cooled at 4 $^\circ\text{C}$).

mp: 60-62 $^\circ\text{C}$; **Rf** = 0.35 (10% ethyl acetate/hexane); **$[\alpha]^{20}_{\text{D}}$:** -283.7 $^\circ$ (c = 1.00, CHCl_3 , 99.9% ee);

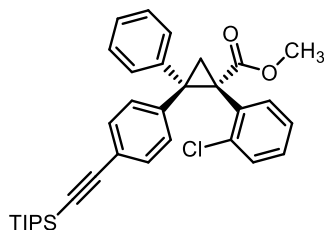
^1H NMR (600 MHz, CDCl_3) δ 7.51 (d, J = 7.4 Hz, 2H), 7.37 (t, J = 7.6 Hz, 2H), 7.32 – 7.28 (m, 1H), 7.27 – 7.23 (m, 1H), 7.13 (td, J = 7.5, 1.5 Hz, 2H), 7.10 – 7.03 (m, 3H), 6.67 (d, J = 8.7 Hz, 2H), 3.38 (s, 3H), 2.78 (d, J = 5.9 Hz, 1H), 2.41 (d, J = 5.9 Hz, 1H);

^{13}C NMR (151 MHz, CDCl_3) δ 170.4, 140.9, 138.6, 136.8, 134.0, 133.8, 130.3, 130.3, 130.0, 129.8, 128.8, 128.4, 127.3, 126.1, 120.3, 52.4, 44.4, 42.1, 26.4;

IR (neat) 3059, 2948, 1724, 1491, 1433, 1299, 1249, 1216, 1142, 1007, 909, 755, 730, 703 cm^{-1} ;

HRMS (+p APCI) calcd for C₂₃H₁₉BrClO₂ (M+H)⁺ 441.0251 found 441.0247;

HPLC (ADH column, 1% *i*-propanol in hexane, 1 mL min⁻¹, 1 mg mL⁻¹, 30 min, UV 230 nm) retention times of 17.65 min (minor) and 24.64 min (major) 95% ee with Rh₂(*S*-PTAD)₄.



Methyl (1*S*,2*S*)-1-(2-chlorophenyl)-2-phenyl-2-(4-((triisopropylsilyl)ethynyl)phenyl)-cyclopropane-1-carboxylate (225)

It was obtained in 82% yield following *G.P. G* using enantiopure methyl (1*S*,2*S*)-2-(4-bromophenyl)-1-(2-chlorophenyl)-2-phenylcyclopropane-1-carboxylate from previous step as starting material.

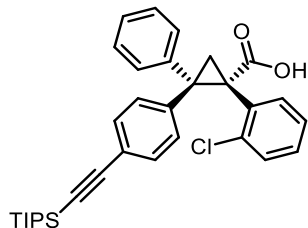
mp: 116-118 °C; **R_f** = 0.64 (10% ethyl acetate/hexane); **[α]²⁰_D:** -232.0° (c = 1.00, CHCl₃, >99% ee);

¹H NMR (600 MHz, CDCl₃) δ 7.50 (d, *J* = 7.3 Hz, 2H), 7.38 – 7.33 (m, 2H), 7.27 (ddd, *J* = 17.2, 7.8, 1.4 Hz, 2H), 7.13 (td, *J* = 7.5, 1.5 Hz, 2H), 7.10 – 7.07 (m, 2H), 7.05 (t, *J* = 7.5 Hz, 1H), 6.75 (d, *J* = 8.7 Hz, 2H), 3.38 (s, 3H), 2.78 (d, *J* = 5.8 Hz, 1H), 2.43 (d, *J* = 5.7 Hz, 1H), 1.07 (s, 21H);

¹³C NMR (151 MHz, CDCl₃) δ 170.5, 141.1, 139.9, 136.8, 134.1, 133.9, 131.0, 130.3, 129.8, 128.8, 128.4, 128.2, 127.2, 126.1, 121.2, 106.9, 90.7, 52.3, 44.8, 42.3, 26.5, 18.6, 11.3;

IR (neat) 3026, 2943, 2864, 2154, 1727, 1508, 1433, 1299, 1216, 1142, 1036, 882, 842, 733, 703, 619 cm⁻¹;

HRMS (+p APCI) calcd for C₃₄H₄₀ClO₂Si (M+H)⁺ 543.2481 found 543.2475.



(1*S*,2*S*)-1-(2-Chlorophenyl)-2-phenyl-2-(4-((triisopropylsilyl)ethynyl)phenyl)cyclopropane-1-carboxylic acid (227)

It was obtained in 72% yield following *G.P. H* using methyl (1*S*,2*S*)-1-(2-chlorophenyl)-2-phenyl-2-(4-((triisopropylsilyl)ethynyl)phenyl)-cyclopropane-1-carboxylate from previous step as starting material.

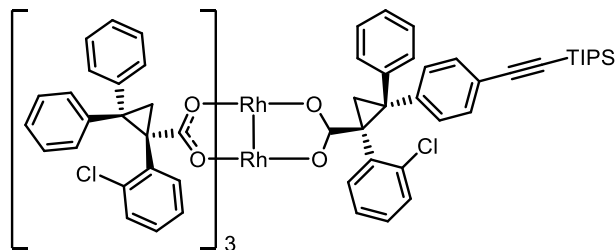
mp: 145-146 °C; **R_f** = 0.43 (10% ethyl acetate/hexane); **[α]²⁰_D**: -283.6° (c = 1.00, CHCl₃, 99.9% ee);

¹H NMR (600 MHz, CDCl₃) δ 7.56 – 7.41 (m, 2H), 7.37 (td, *J* = 7.3, 6.5, 1.2 Hz, 2H), 7.34 – 7.30 (m, 1H), 7.26 – 7.21 (m, 1H), 7.16 – 6.95 (m, 5H), 6.76 (d, *J* = 8.2 Hz, 2H), 2.77 – 2.60 (m, 1H), 2.47 (d, *J* = 5.8 Hz, 1H), 1.09 (s, 21H);

¹³C NMR (151 MHz, CDCl₃) δ 176.0, 140.6, 139.5, 136.7, 133.4, 131.0, 130.3, 130.2, 129.8, 128.9, 128.4, 128.2, 127.2, 126.1, 121.3, 106.8, 90.8, 77.2, 45.8, 41.9, 26.9, 18.6, 11.3.;

IR (neat) 3027, 2943, 2865, 2155, 1738, 1695, 1508, 1231, 883, 846, 752, 703 cm⁻¹;

HRMS (-p NSI) calcd for C₃₃H₃₆ClO₂Si (M-H)⁻ 527.2179 found 527.2179.



Rh₂(*S*-*o*-CITPCP)₃(TIPS-ethynyl@B) (229)

It was obtained in 58% yield following *G.P. I* using Rh₂(*S*-*o*-CITPCP)₄ (319.4 mg) and (1*S*,2*S*)-1-(2-chlorophenyl)-2-phenyl-2-(4-((triisopropylsilyl)ethynyl)phenyl)cyclopropane-1-carboxylic acid (116.4 mg) as starting materials. The reaction was refluxed in benzene at 84 °C for 16 h.

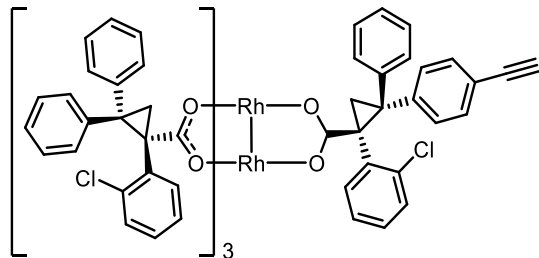
mp: >200 °C (decomp.); **R_f** = 0.64 (30% ethyl acetate/hexane);

¹H NMR (600 MHz, CDCl₃) δ 6.48 – 6.39 (m, 8H), 6.17 – 6.09 (m, 22H), 6.05 – 5.97 (m, 13H), 5.94 – 5.87 (m, 12H), 1.75 – 1.65 (m, 4H), 1.30 – 1.21 (m, 4H), 0.06 (s, 21H);

¹³C NMR (151 MHz, CDCl₃) δ 188.0, 188.0, 187.8, 142.7, 142.4, 140.2, 139.5, 139.5, 136.8, 136.8, 136.7, 135.6, 135.4, 131.3, 131.2, 130.9, 130.8, 130.7, 130.4, 129.3, 129.1, 128.5, 128.4, 128.4, 128.1, 127.8, 127.3, 127.2, 127.0, 126.0, 125.9, 125.9, 125.6, 125.5, 120.9, 107.1, 90.2, 45.6, 45.4, 42.1, 41.9, 25.9, 25.6, 18.6, 11.3;

IR (neat) 3608, 3528, 3057, 2925, 2864, 2157, 1584, 1388, 752, 731, 703, 662 cm⁻¹;

HRMS (+p ESI) calcd for C₉₉H₈₄Cl₄O₈Rh₂Si (M)⁺ 1774.2800 found 1774.2833.



Rh₂(*S*-*o*-CITPCP)₃(ethynyl@B) (231)

It was obtained in 88% yield following *G.P. J* using Rh₂(*S*-*o*-CITPCP)₃(TIPS-ethynyl@B) from previous step as starting material.

mp: >200 °C (decomp.); **R_f** = 0.50 (30% ethyl acetate/hexane);

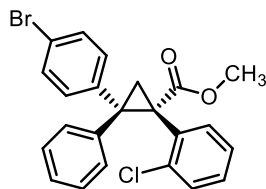
¹H NMR (600 MHz, CDCl₃) δ 7.50 – 7.41 (m, 8H), 7.19 – 7.09 (m, 21H), 7.04 (s, 4H), 7.02 – 6.86 (m, 22H), 2.93 (s, 1H), 2.69 (dd, *J* = 19.6, 4.8 Hz, 4H), 2.28 – 2.16 (m, 4H);

¹³C NMR (151 MHz, CDCl₃) δ 188.0, 187.4, 187.4, 187.0, 143.4, 142.8, 142.7, 140.7, 140.6, 139.6, 139.6, 139.5, 136.7, 136.7, 136.6, 135.7, 135.3, 131.4, 131.3, 130.9, 130.8, 130.8, 130.6, 130.6, 130.6, 130.5, 129.3, 129.1, 129.1, 128.5, 128.4, 128.4, 128.0, 127.8, 127.7, 127.3, 127.2, 127.2, 127.1, 127.0, 127.0, 125.9, 125.9, 125.9, 125.8, 125.8, 125.5, 125.4, 125.2, 119.4, 83.6, 68.1, 45.6, 45.3, 45.3, 45.0, 41.9, 41.8, 25.6, 25.3;

IR (neat) 3648, 3299, 3057, 3057, 2924, 1585, 1447, 1388, 753, 704 cm⁻¹;

HRMS (+p ESI) calcd for C₉₀H₆₅Cl₄O₈Rh₂ (M+H)⁺ 1619.1538 found 1619.1519.

Synthesis for Rh₂(S-o-CITPCP)₃(ethynyl@C)



Methyl (1S,2R)-2-(4-bromophenyl)-1-(2-chlorophenyl)-2-phenylcyclopropane-1-carboxylate (224)

It was obtained as minor diastereomer in 26% yield following *G.P. F* using 1-bromo-4-(1-phenylvinyl)benzene (11.9 g) and methyl 2-(2-chlorophenyl)-2-diazoacetate (4.21 g) as starting materials, and Rh₂(S-PTAD)₄ as catalyst. The enantiopure product was obtained from recrystallization from 1% diethyl ether/pentane solution (after cooled at 4 °C).

mp: 66-68 °C; **R_f** = 0.45 (10% ethyl acetate/hexane); **[α]²⁰_D**: -289.3° (c = 1.00, CHCl₃, 99.9% ee);

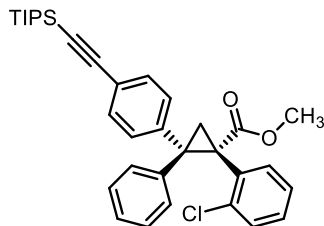
¹H NMR (600 MHz, CDCl₃) δ 7.49 (d, *J* = 8.6 Hz, 2H), 7.42 (d, *J* = 8.5 Hz, 2H), 7.23 (dd, *J* = 8.2, 1.4 Hz, 1H), 7.09 (ddd, *J* = 8.0, 7.2, 1.5 Hz, 2H), 7.03 – 6.95 (m, 4H), 6.81 (dd, *J* = 8.1, 1.7 Hz, 2H), 3.43 (s, 3H), 2.71 (d, *J* = 5.8 Hz, 1H), 2.49 (d, *J* = 5.8 Hz, 1H);

¹³C NMR (151 MHz, CDCl₃) δ 170.7, 140.6, 138.6, 136.8, 133.9, 133.8, 132.1, 131.5, 129.6, 128.7, 128.3, 127.4, 126.4, 126.0, 121.0, 52.5, 44.4, 41.9, 26.2;

IR (neat) 3059, 3024, 2949, 1724, 1497, 1433, 1301, 1251, 1218, 1142, 1010, 753, 729, 699 cm⁻¹;

HRMS (+p APCI) calcd for C₂₃H₁₉BrClO₂ (M+H)⁺ 441.0251 found 441.0246;

HPLC (ADH column, 1% *i*-propanol in hexane, 1 mL min⁻¹, 1 mg mL⁻¹, 30 min, UV 230 nm) retention times of 17.86 min (major) and 26.43 min (minor) 97% ee with Rh₂(S-PTAD)₄.



Methyl (1*S*,2*R*)-1-(2-chlorophenyl)-2-phenyl-2-(4-((triisopropylsilyl)ethynyl)phenyl)-cyclopropane-1-carboxylate (226)

It was obtained in 80% yield following *G.P. G* using enantiopure methyl (1*S*,2*R*)-2-(4-bromophenyl)-1-(2-chlorophenyl)-2-phenylcyclopropane-1-carboxylate from previous step as starting material.

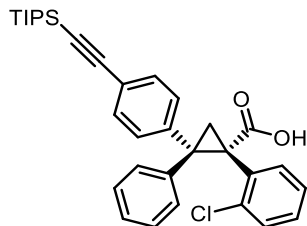
mp: 150-152 °C; **R_f**= 0.70 (10% ethyl acetate/hexane); **[α]²⁰_D**: -285.1° (c = 1.00, CHCl₃, 99.9% ee);

¹H NMR (600 MHz, CDCl₃) δ 7.50 – 7.43 (m, 4H), 7.23 (dd, *J* = 8.1, 1.3 Hz, 1H), 7.11 – 7.05 (m, 2H), 7.02 – 6.94 (m, 4H), 6.82 – 6.78 (m, 2H), 3.43 (s, 3H), 2.74 (d, *J* = 5.8 Hz, 1H), 2.48 (d, *J* = 5.9 Hz, 1H), 1.14 (s, 21H);

¹³C NMR (151 MHz, CDCl₃) δ 170.7, 141.8, 138.8, 136.8, 134.0, 133.9, 132.0, 130.3, 129.6, 128.6, 128.3, 127.3, 126.3, 125.9, 122.2, 107.1, 90.7, 52.5, 44.8, 42.0, 26.3, 18.7, 11.3;

IR (neat) 2943, 2864, 2154, 1724, 1502, 1433, 1298, 1216, 1141, 908, 882, 837, 728, 693 cm⁻¹;

HRMS (+p APCI) calcd for C₃₄H₄₀ClO₂Si (M+H)⁺ 543.2481 found 543.2473.



(1*S*,2*R*)-1-(2-Chlorophenyl)-2-phenyl-2-(4-((triisopropylsilyl)ethynyl)phenyl)cyclopropane-1-carboxylic acid (228)

It was obtained in 75% yield following *G.P. H* using methyl (1*S*,2*R*)-1-(2-chlorophenyl)-2-phenyl-2-(4-((triisopropylsilyl)ethynyl)phenyl)-cyclopropane-1-carboxylate from previous step as starting material.

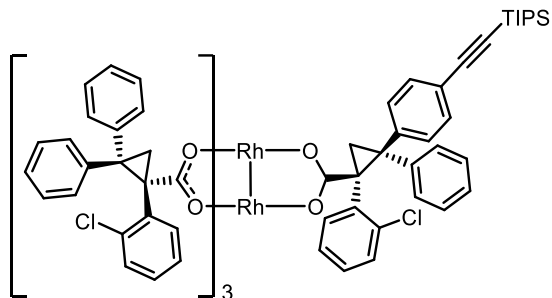
mp: 116-118 °C; **R_f** = 0.12 (10% ethyl acetate/hexane); **[α]²⁰_D**: -331.3° (c = 1.00, CHCl₃, 99.9% ee);

¹H NMR (600 MHz, CDCl₃) δ 7.55 – 7.41 (m, 4H), 7.22 (s, 1H), 7.08 (td, *J* = 7.7, 1.7 Hz, 2H), 7.04 – 6.91 (m, 4H), 6.82 (d, *J* = 7.5 Hz, 2H), 2.68 (s, 1H), 2.52 (d, *J* = 5.9 Hz, 1H), 1.19 (s, 21H);

¹³C NMR (151 MHz, CDCl₃) δ 176.0, 141.4, 138.5, 136.8, 133.5, 132.3, 132.1, 130.2, 129.6, 128.8, 128.4, 127.4, 126.4, 125.9, 122.2, 107.1, 90.7, 45.8, 41.7, 26.6, 18.7, 11.4;

IR (neat) 2942, 2865, 2154, 1738, 1695, 1503, 1463, 1231, 883, 750, 694 cm⁻¹;

HRMS (-p NSI) calcd for C₃₃H₃₆ClO₂Si (M-H)⁻ 527.2179 found 527.2179.



Rh₂(*S*-*o*-CITPCP)₃(TIPS-ethynyl@C) (230)

It was obtained in 58% yield following *G.P. I* using Rh₂(*S*-*o*-CITPCP)₄ (319.4 mg) and (1*S*,2*R*)-1-(2-chlorophenyl)-2-phenyl-2-(4-((triisopropylsilyl)ethynyl)phenyl)cyclopropane-1-carboxylic acid (116.4 mg) as starting materials. The reaction was refluxed in benzene at 84 °C for 16 h.

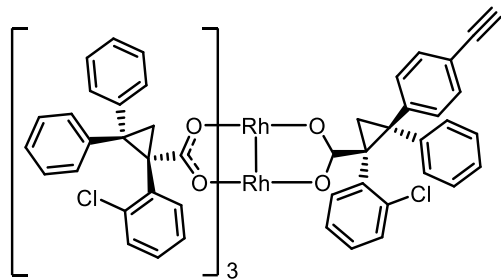
mp: >200 °C (decomp.); **R_f** = 0.49 (30% ethyl acetate/hexane);

¹H NMR (600 MHz, CDCl₃) δ 7.49 – 7.43 (m, 7H), 7.34 (q, *J* = 8.4 Hz, 3H), 7.15 – 7.09 (m, 20H), 7.04 – 6.98 (m, 7H), 6.94 – 6.87 (m, 18H), 2.71 (dd, *J* = 10.5, 4.7 Hz, 4H), 2.25 (dd, *J* = 17.9, 5.2 Hz, 4H), 1.31 (s, 21H);

¹³C NMR (151 MHz, CDCl₃) δ 188.0, 188.0, 187.9, 187.9, 142.8, 142.7, 139.5, 139.5, 136.8, 136.8, 136.5, 135.7, 135.7, 135.7, 135.7, 131.4, 131.3, 131.3, 131.1, 131.1, 130.8, 130.8, 130.8, 129.1, 129.0, 128.9, 128.5, 128.4, 128.4, 127.8, 127.8, 127.7, 127.7, 127.5, 127.2, 127.1, 127.0, 127.0, 127.0, 126.9, 126.0, 125.9, 125.9, 125.9, 125.8, 125.8, 125.5, 125.4, 45.6, 45.5, 45.5, 44.9, 42.0, 41.9, 41.9, 25.8, 25.7, 25.6, 25.2, 22.7, 18.9, 18.9, 11.6;

IR (neat) 3618, 3056, 2924, 2864, 2157, 2584, 2496, 1447, 1388, 1279, 1046, 907, 730, 704 cm⁻¹;

HRMS (+p APCI) calcd for C₉₉H₈₄Cl₄O₈Rh₂Si (M)⁺ 1774.2800 found 1774.2843.



Rh₂(*S*-*o*-CITPCP)₃(ethynyl@C) (232)

It was obtained in 70% yield following *G.P. J* using Rh₂(*S*-*o*-CITPCP)₃(TIPS-ethynyl@C) from previous step as starting material.

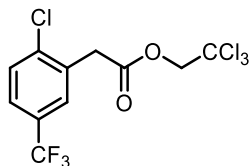
mp: >200 °C (decomp.); **R_f** = 0.53 (30% ethyl acetate/hexane);

¹H NMR (600 MHz, CDCl₃) δ 7.47 (tt, *J* = 7.1, 3.7 Hz, 6H), 7.39 (d, *J* = 8.4 Hz, 2H), 7.31 (d, *J* = 8.3 Hz, 2H), 7.17 – 7.09 (m, 19H), 7.07 – 7.04 (m, 2H), 7.02 – 6.96 (m, 8H), 6.93 – 6.87 (m, 16H), 3.21 (s, 1H), 2.72 (dd, *J* = 9.3, 4.8 Hz, 4H), 2.27 – 2.19 (m, 4H);

¹³C NMR (151 MHz, CDCl₃) δ 188.0, 188.0, 188.0, 187.8, 143.5, 142.8, 142.7, 139.5, 139.5, 139.1, 136.8, 136.7, 135.7, 135.7, 135.7, 135.6, 131.4, 131.3, 131.1, 131.1, 131.1, 130.8, 130.7, 129.1, 129.1, 129.0, 128.6, 128.5, 128.4, 127.8, 127.8, 127.8, 127.5, 127.2, 127.1, 127.0, 127.0, 127.0, 126.1, 125.9, 125.9, 125.9, 125.8, 125.5, 119.4, 84.2, 45.6, 45.5, 45.1, 42.0, 41.9, 31.9, 29.7, 29.7, 26.0, 25.7, 25.6, 25.4;

IR (neat) 3646, 3295, 3057, 3057, 2920, 1585, 1447, 1388, 753, 704 cm⁻¹;

HRMS (+p NSI) calcd for C₉₀H₆₄Cl₄O₈Rh₂ (M)⁺ 1618.1465 found 1618.1508.

Synthesis $Rh_2(S-2-Cl-5-CF_3TPCP)_4$ **2,2,2-Trichloroethyl 2-(2-chloro-5-(trifluoromethyl)phenyl)acetate (239)**

A flame-dried 100 mL round bottom flask with magnetic stir bar was charged with 2-(2-chloro-5-(trifluoromethyl)phenyl)acetic acid (5.3 g, 22.3 mmol, 1.00 equiv), 2,2,2-trichloroethan-1-ol (2.6 mL, 26.8 mmol, 1.20 equiv) and DMAP (272.3 mg, 2.2 mmol, 0.10 equiv). After the flask was flushed with argon gas (3 times), 30 mL of dry dichloromethane was added, and the reaction mixture was cooled to 0 °C via ice bath. A solution of DCC (5.1 g, 24.5 mmol, 1.1 equiv) in dry dichloromethane (30 mL) was then added into the solution slowly via syringe at 0 °C. The ice bath was removed, and the reaction mixture was stirred overnight (at some point it was warmed to room temperature (23 °C)). Suction filtration was applied to remove the solid byproducts and the filtrate was concentrated under reduced pressure (washed with dichloromethane). The residue mixture was purified by flash column chromatography (hexane/ethyl acetate = 20/1) to afford the colorless oil in 92% yield.

Rf = 0.56 (10% ethyl acetate/hexane);

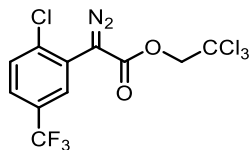
1H NMR (600 MHz, $CDCl_3$) δ 7.62 – 7.61 (m, 1H), 7.57 – 7.49 (m, 2H), 4.79 (s, 2H), 3.99 (s, 2H);

^{13}C NMR (151 MHz, $CDCl_3$) δ 168.1, 138.5, 132.4, 130.2, 129.6 (q, J = 33.1 Hz), 128.5 (q, J = 3.8 Hz), 125.9 (q, J = 3.7 Hz), 123.5 (q, J = 272.2 Hz), 94.5, 74.4, 38.6;

^{19}F NMR (376 MHz, $CDCl_3$) δ -62.62;

IR (neat) 3005, 2959, 1760, 1614, 1486, 1427, 1373, 1335, 1279, 1170, 1131, 1084 cm^{-1} ;

HRMS (+p APCI) calcd for $C_{11}H_8Cl_4F_3O_2$ (M+H)⁺ 368.9225 found 368.9219;



2,2,2-Trichloroethyl 2-(2-chloro-5-(trifluoromethyl)phenyl)-2-diazoacetate (240)

A flame-dried 500 mL round bottom flask with magnetic stir bar was charged with 2,2,2-trichloroethyl 2-(2-chloro-5-(trifluoromethyl)phenyl)acetate (8.2 g, 22.2 mmol, 1.00 equiv), *o*-NBSA (7.6 g, 33.2 mmol, 1.50 equiv). After the flask was flushed with argon gas (3 times), 200 mL of dry acetonitrile was added, and the reaction mixture was cooled to 0 °C via ice bath. DBU (7.3 mL, 48.8 mmol, 2.2 equiv) was then added into the reaction mixture dropwise at 0 °C. The reaction mixture was stirred at 0 °C for 1 hour, and then quenched by pouring into a separation funnel with saturated aqueous NH₄Cl (~150 mL). The mixture was extracted with Et₂O (3 X 100 mL), and the combined organic layer was washed by brine. The organic layer was collected and purified by flash column chromatography (hexane/diethyl ether = 50/1) to afford the yellow oil in 93% yield.

Rf = 0.54 (5% ethyl acetate/hexane);

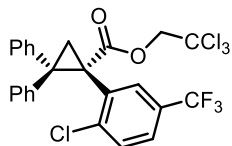
¹H NMR (600 MHz, CDCl₃) δ 7.90 (dd, *J* = 1.5, 0.7 Hz, 1H), 7.61 – 7.52 (m, 2H), 4.90 (s, 2H);

¹³C NMR (151 MHz, CDCl₃) δ 163.3, 137.0, 130.8, 130.0 (q, *J* = 33.5 Hz), 129.3, 126.5 (q, *J* = 3.6 Hz), 124.3, 123.3 (q, *J* = 272.6 Hz), 94.8, 74.3 (The resonance resulting from the diazo carbon was not observed);

¹⁹F NMR (376 MHz, CDCl₃) δ -62.71;

IR (neat) 2957, 2109, 1710, 1420, 1344, 1306, 1241, 1172, 1131, 1080, 828, 775, 719 cm⁻¹;

HRMS (+p NSI) calcd for C₁₁H₅Cl₄F₃N₂O₂Na (M+Na)⁺ 416.8949 found 416.8943.



2,2,2-Trichloroethyl (S)-1-(2-chloro-5-(trifluoromethyl)phenyl)-2,2-diphenylcyclopropane-1-carboxylate (241)

It was obtained as white solid in 87% yield following *G.P. F* using 1,1-diphenylethylene (8.2 mL) and 2,2,2-trichloroethyl 2-(2-chloro-5-(trifluoromethyl)phenyl)-2-diazoacetate (7.92 g) as starting materials, and $\text{Rh}_2(\text{S-PTAD})_4$ (155.9 mg) as catalyst. The enantiopure product was obtained by recrystallization using pentane as solvent at 4 °C (66% yield after recrystallization).

mp: 112-114 °C; **Rf** = 0.60 (10% EtOAc in hexane); **$[\alpha]^{20}_{\text{D}}$** : -268.6° (*c* = 1.00, CHCl_3 , 99.9% ee);

$^1\text{H NMR}$ (600 MHz, CDCl_3) δ 7.60 (d, *J* = 7.5 Hz, 2H), 7.51 – 7.28 (m, 6H), 7.07 (dd, *J* = 5.2, 2.0 Hz, 3H), 6.97 – 6.86 (m, 2H), 4.58 (d, *J* = 11.9 Hz, 1H), 4.31 (d, *J* = 11.9 Hz, 1H), 2.96 (d, *J* = 6.2 Hz, 1H), 2.66 (d, *J* = 6.2 Hz, 1H);

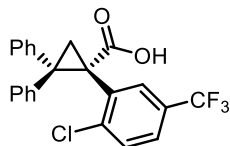
$^{13}\text{C NMR}$ (151 MHz, CDCl_3) δ 168.1, 140.5, 140.4, 137.9, 134.6, 131.9, 130.4, 130.0, 128.6, 128.2, 127.7, 127.5, 126.9, 125.3, 123.4 (q, *J* = 272.2 Hz), 94.2, 75.1, 46.3, 41.4, 26.2;

$^{19}\text{F NMR}$ (376 MHz, CDCl_3) δ -62.76;

IR (neat) 3061, 3027, 2949, 1744, 1612, 1451, 1340, 1324, 1201, 1170, 1131, 1080, 704 cm^{-1} ;

HRMS (+p NSI) calcd for $\text{C}_{25}\text{H}_{18}\text{Cl}_4\text{F}_3\text{O}_2$ ($\text{M}+\text{H}$)⁺ 547.0008 found 547.0004;

HPLC (R,R-Whelk column, 0% *i*-propanol in hexane, 1 mL min^{-1} , 1 mg mL^{-1} , 30 min, UV 230 nm) retention times of 8.13 min (minor) and 10.03 min (major) 94% ee with $\text{Rh}_2(\text{S-PTAD})_4$.



(S)-1-(2-Chloro-5-(trifluoromethyl)phenyl)-2,2-diphenylcyclopropane-1-carboxylic acid

(242)

A 250 mL round bottom flask with magnetic stir bar was charged with 2,2,2-trichloroethyl (S)-1-(2-chloro-5-(trifluoromethyl)phenyl)-2,2-diphenylcyclopropane-1-carboxylate (4.39 g, 8.0 mmol, 1.0 equiv), zinc dust (2.62 g, 40.0 mmol, 5.0 equiv) and 100 mL of glacial acetic acid. The resulted suspension was stirred for 36 h at room temperature (23 °C). After the allowed time passed, the mixture was diluted with DI H₂O and filtered thru Celite[®] (washed with ethyl acetate). The filtrate was washed by DI H₂O (100 mL X 10 times). The organic layer was concentrated and purified thru a short path of silica (5.5 cm diameter with 6 cm height, hexane/ethyl acetate = 3/2) to afford the white solid in 98% yield

mp: 71-73 °C; **Rf** = 0.10 (10% ethyl acetate/hexane); **[α]²⁰_D:** -322.7° (c = 1.00, CHCl₃, 99.9% ee);

¹H NMR (600 MHz, CDCl₃) δ 7.52 (d, *J* = 7.4 Hz, 2H), 7.42 – 7.28 (m, 6H), 7.07 – 6.98 (m, 3H), 6.90 – 6.83 (m, 2H), 2.75 (s, 1H), 2.56 (d, *J* = 6.0 Hz, 1H);

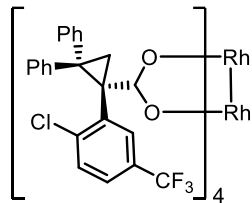
¹³C NMR (151 MHz, CDCl₃) δ 175.8, 140.5, 138.0, 135.0, 130.2, 130.0, 128.5, 128.2, 127.7, 127.3, 126.8, 125.3, 123.39 (q, *J* = 272.3 Hz), 46.6, 41.2, 26.2;

¹⁹F NMR (376 MHz, CDCl₃) δ -62.73;

IR (neat) 3061, 3026, 1694, 1417, 1343, 1324, 1262, 1128, 757, 704 cm⁻¹;

HRMS (+p NSI) calcd for C₂₃H₁₆ClF₃O₂Na (M+Na)⁺ 439.0683 found 439.0679;

HPLC (ADH column, 5% *i*-propanol in hexane, 1 mL min⁻¹, 1 mg mL⁻¹, 30 min, UV 230 nm) retention times of 6.60 min (major) and 9.36 min (minor) >99% ee.



Dirhodium tetrakis((*S*)-1-(5- trifluoromethyl -2-chlorophenyl)-2,2-diphenylcyclopropane-carboxylate) (243)

A 100 mL round-bottom flask was charged with carboxylic acid from previous step (1.67 g, 4.0 mmol, 8.0 equiv) and $\text{Rh}_2(\text{OAc})_4$ (221 mg, 0.5 mmol, 1.0 equiv). Then, approximately 70 mL dry toluene was added into the flask. A Soxhlet extractor with suitable amount of K_2CO_3 in it was added on the top of that flask, as well as a condenser (with slow flow of water). The solution was heated to reflux for 3 days (monitored by the color of the solution & TLC). The reacted mixture was concentrated under reduced pressure, and the residue was purified by flash column chromatography (gradient elution with hexane/ethyl acetate = 10/0 to 9/1) to afford the green solid in 85% yield.

mp: >200 °C (decomp.); **Rf** = 0.60 (20% EtOAc in hexane);

^1H NMR (600 MHz, CDCl_3) δ 7.47 – 7.41 (m, 2H), 7.40 (d, J = 2.2 Hz, 1H), 7.22 – 7.14 (m, 4H), 7.09 – 7.04 (m, 3H), 6.97 – 6.91 (m, 3H), 2.80 (d, J = 5.1 Hz, 1H), 2.35 (d, J = 5.0 Hz, 1H);

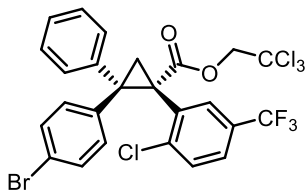
^{13}C NMR (151 MHz, CDCl_3) δ 187.4, 142.1, 140.4, 138.3, 136.8, 131.3, 129.6, 128.4 (q, J = 14.9 Hz), 128.2, 127.7 (q, J = 3.6 Hz), 127.3, 127.3, 126.4, 125.7, 124.8 (q, J = 3.8 Hz), 123.8 (q, J = 272.2 Hz), 45.7, 42.0, 25.3;

^{19}F NMR (376 MHz, CDCl_3) δ -62.57;

IR (neat) 3606, 3531, 3058, 3025, 1585, 1124, 1309, 1168, 1124, 1079, 907, 827, 732, 694 cm^{-1} ;

HRMS (+p ESI) calcd for $\text{C}_{92}\text{H}_{60}\text{Cl}_4\text{F}_{12}\text{O}_8\text{Rh}$ (M)⁺ 1866.0961 found 1866.0978.

Synthesis for Rh₂(S-2-Cl-5-CF₃TPCP)₃(ethynyl@B)



2,2,2-Trichloroethyl (1S,2S)-2-(4-bromophenyl)-1-(2-chloro-5-(trifluoromethyl)phenyl)-2-phenylcyclopropane-1-carboxylate (244)

It was obtained as white solid in 45% yield following *G.P. F* using 1-bromo-4-(1-phenylvinyl)benzene (11.9 g) and 2,2,2-trichloroethyl 2-(2-chloro-5-(trifluoromethyl)phenyl)-2-diazoacetate (7.92 g) as starting materials, and Rh₂(S-PTAD)₄ (155.9 mg) as catalyst.

mp: 54-56 °C; **Rf** = 0.26 (5% diethyl ether/hexane); **[α]²⁰_D:** -224.8° (c = 1.00, CHCl₃, 99.9% ee);

¹H NMR (600 MHz, CDCl₃) δ 7.55 (d, *J* = 7.7 Hz, 2H), 7.45 – 7.30 (m, 6H), 7.16 (d, *J* = 8.4 Hz, 2H), 6.74 (d, *J* = 8.8 Hz, 2H), 4.56 (d, *J* = 11.9 Hz, 1H), 4.28 (d, *J* = 11.9 Hz, 1H), 2.91 (s, 1H), 2.57 (d, *J* = 6.2 Hz, 1H);

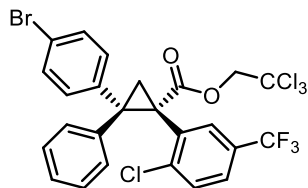
¹³C NMR (151 MHz, CDCl₃) δ 167.9, 140.6, 139.9, 137.2, 134.3, 130.7, 130.3, 130.3, 129.9, 128.8, 128.1, 127.8, 125.7, 123.4 (d, *J* = 272.4 Hz), 121.1, 94.1, 75.1, 45.7, 41.5, 26.3;

¹⁹F NMR (376 MHz, CDCl₃) δ -62.76;

IR (neat) 3027, 2950, 1744, 1492, 1448, 1341, 1320, 1200, 1171, 1132, 1080, 756 cm⁻¹;

HRMS (+p NSI) calcd for C₂₅H₁₇BrCl₄F₃O₂ (M+H)⁺ 624.9113 found 624.9109;

HPLC (R,R-Whelk column, 0% *i*-propanol in hexane, 1.00 mL min⁻¹, 1 mg mL⁻¹, 30 min, UV 230 nm) retention times of 13.76 min (minor) and 17.93 min (major) 94% ee with Rh₂(S-PTAD)₄.



2,2,2-Trichloroethyl (1*S*,2*R*)-2-(4-bromophenyl)-1-(2-chloro-5-(trifluoromethyl)phenyl)-2-phenylcyclopropane-1-carboxylate

It was obtained as white solid in 42% yield following *G.P. F* using 1-bromo-4-(1-phenylvinyl)benzene (11.9 g) and 2,2,2-trichloroethyl 2-(2-chloro-5-(trifluoromethyl)phenyl)-2-diazoacetate (7.92 g) as starting materials, and Rh₂(*S*-PTAD)₄ (155.9 mg) as catalyst. (the other diastereomer of **204**)

mp: 54-56 °C; **R_f** = 0.34 (5% diethyl ether /hexane); **[α]²⁰_D:** -231.4° (c = 1.00, CHCl₃, 93% ee);

¹H NMR (600 MHz, CDCl₃) δ 7.53 (d, *J* = 8.5 Hz, 2H), 7.49 – 7.29 (m, 5H), 7.11 – 6.99 (m, 3H), 6.86 (d, *J* = 8.3 Hz, 2H), 4.56 (d, *J* = 11.9 Hz, 1H), 4.38 (d, *J* = 11.9 Hz, 1H), 2.85 (s, 1H), 2.64 (d, *J* = 6.2 Hz, 1H);

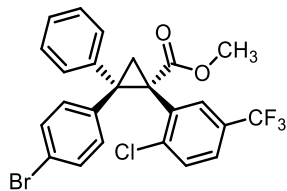
¹³C NMR (151 MHz, CDCl₃) δ 168.0, 140.5, 139.5, 137.3, 134.3, 132.1, 131.8, 130.1, 128.5 (d, *J* = 33.2 Hz), 128.1, 127.8, 127.1, 125.5, 123.36 (d, *J* = 272.3 Hz), 121.6, 94.1, 75.1, 45.6, 41.4, 26.2;

¹⁹F NMR (376 MHz, CDCl₃) δ -62.77;

IR (neat) 3026, 2951, 1744, 1341, 1325, 1201, 1171, 1132, 1080, 760, 740 cm⁻¹;

HRMS (+p NSI) calcd for C₂₅H₁₇BrCl₄F₃O₂ (M+H)⁺ 624.9113 found 624.9109; .

HPLC (R,R-Whelk column, 0% *i*-propanol in hexane, 1.00 mL min⁻¹, 1 mg mL⁻¹, 30 min, UV 230 nm) retention times of 14.41 min (minor) and 19.08 min (major) 92% ee with Rh₂(*S*-PTAD)₄.



Methyl (1*S*,2*S*)-2-(4-bromophenyl)-1-(2-chloro-5-(trifluoromethyl)phenyl)-2-phenylcyclopropane-1-carboxylate (247)

In a 500 mL round bottom flask with magnetic stir bar, the 2,2,2-trichloroethyl (1*S*,2*S*)-2-(4-bromophenyl)-1-(2-chloro-5-(trifluoromethyl)phenyl)-2-phenylcyclopropane-1-carboxylate (95% ee, 15.1 g) was dissolved in 200 mL glacial acetic acid. Then, zinc dust (7.85 g, 120.0 mmol, 5.0 equiv) was added to the solution in one portion, and the resulted slurry was stirred under room temperature (23 °C) for 24 h (checked by TLC for the full consumption of ester starting material). After the allowed time, the slurry was diluted with 300 mL of DI H₂O and filtered thru a plug of Celite[®] 545 in a sintered glass funnel and washed with ethyl acetate (300 mL). The mixture was washed with 100 mL of DI H₂O for 10 times (remove excess acetic acid), as well as 100 mL of brine solution. The organic layer was collected, concentrated and dried for next step.

The carboxylic acid from last step was transferred into a 1000 mL round bottom flask in 400 mL of acetone. After the reaction vessel was flushed with argon, K₂CO₃ (3.32 g, 24 .0 mmol, 1.0 equiv) and dimethyl sulfate (3.33 g, 26.4 mmol, 1.1 equiv) was added to the reaction mixture. The mixture was stirred overnight (15 h) at room temperature (23 °C), and then heated to 40 °C for 5 h. The completion of the reaction was monitored by TLC. The resulted mixture was quenched by 100 mL of 1 M HCl aqueous solution, followed by extraction with ethyl acetate (3 times) and washing with saturated NaHCO₃ aqueous solution (100 mL) and brine (100 mL). The organic layer was concentrated and purified by flash column chromatography (hexane/ethyl acetate = 50/1 to 20/1)

to the desired (1*S*,2*S*) methyl ester product as white solid in 94% yield (91% ee). The enantiopure product was obtained by recrystallization from pentane solution at 4 °C.

mp: 52-54 °C; **R_f** = 0.35 (10% ethyl acetate/hexane); **[α]²⁰_D**: -282.2° (c = 1.00, CHCl₃, 99.9% ee);

¹H NMR (600 MHz, CDCl₃) δ 7.49 (dd, *J* = 8.0, 1.2 Hz, 2H), 7.41 – 7.36 (m, 4H), 7.35 – 7.29 (m, 2H), 7.12 (d, *J* = 8.7 Hz, 2H), 6.70 (d, *J* = 8.8 Hz, 2H), 3.41 (s, 3H), 2.81 (d, *J* = 6.1 Hz, 1H), 2.44 (d, *J* = 6.1 Hz, 1H);

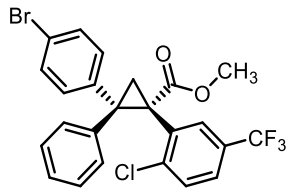
¹³C NMR (151 MHz, CDCl₃) δ 169.8, 140.6, 140.5, 137.7, 135.2, 131.8 (q, *J* = 61.1 Hz), 131.1, 130.6, 130.3, 130.2, 129.9, 128.5, 127.5, 125.4 (q, *J* = 3.9 Hz), 123.4 (q, *J* = 272.3 Hz), 120.9, 52.5, 44.8, 41.7, 25.8;

¹⁹F NMR (376 MHz, CDCl₃) δ -61.68;

IR (neat) 3084, 3060, 3027, 2951, 1732, 1611, 1492, 1434, 1340, 1319, 1213, 1170, 1128, 1078, 1007, 908, 830, 756, 732 cm⁻¹;

HRMS (+p APCI) calcd for C₂₄H₁₈BrClF₃O₂ (M+H)⁺ 509.0125 found 509.0118;

HPLC (R,R-Whelk column, 0.5% *i*-propanol in hexane, 1.0 mL min⁻¹, 1 mg mL⁻¹, 40 min, UV 230 nm) retention times of 18.90 min (major) and 31.05 min (minor) 99% ee.



Methyl (1*S*,2*R*)-2-(4-bromophenyl)-1-(2-chloro-5-(trifluoromethyl)phenyl)-2-phenylcyclopropane-1-carboxylate

It was obtained as white solid in 92% yield (93% ee) following the same procedure above using 2,2,2-trichloroethyl (1*S*,2*R*)-2-(4-bromophenyl)-1-(2-chloro-5-(trifluoromethyl)phenyl)-2-phenylcyclopropane-1-carboxylate (xx% ee) as starting material.

mp: 123-125 °C; **R_f** = 0.45 (10% ethyl acetate/hexane); **[α]²⁰_D**: -260.2° (c = 1.00, CHCl₃, 93% ee);

¹H NMR (600 MHz, CDCl₃) δ 7.44 (d, *J* = 8.4 Hz, 2H), 7.33 (d, *J* = 8.3 Hz, 2H), 7.30 – 7.24 (m, 2H), 7.20 (s, 1H), 6.99 – 6.92 (m, 3H), 6.79 – 6.74 (m, 2H), 3.38 (s, 3H), 2.68 (d, *J* = 6.0 Hz, 1H), 2.45 (d, *J* = 6.1 Hz, 1H);

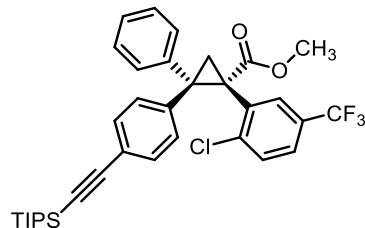
¹³C NMR (151 MHz, CDCl₃) δ 168.0, 138.6, 138.2, 135.8, 133.3, 130.0, 129.6, 129.1, 128.1, 126.5 (q, *J* = 33.1 Hz), 126.2, 125.8, 124.9, 123.3 (q, *J* = 3.8 Hz), 121.5 (q, *J* = 272.5 Hz), 119.3, 50.7, 42.9, 39.6, 23.8;

¹⁹F NMR (376 MHz, CDCl₃) δ -62.67;

IR (neat) 3091, 3061, 3026, 2951, 1728, 1481, 1449, 1434, 1323, 1269, 1253, 1213, 1169, 1126, 1101, 1010, 906, 827, 729, 694, 537 cm⁻¹;

HRMS (+p APCI) calcd for C₂₄H₁₈BrClF₃O₂ (M+H)⁺ 509.0125 found 509.0117;

HPLC (ODH column, 0.5% *i*-propanol in hexane, 1.0 mL min⁻¹, 1 mg mL⁻¹, 30 min, UV 230 nm) retention times of 6.43 min (minor) and 7.12 min (major) 91% ee.



Methyl (1*S*,2*S*)-1-(2-chloro-5-(trifluoromethyl)phenyl)-2-phenyl-2-(4-((triisopropylsilyl)ethynyl)phenyl)-cyclopropane-1-carboxylate (248)

It was obtained in 75% yield following *G.P. G* using enantiopure methyl (1*S*,2*S*)-2-(4-bromophenyl)-1-(2-chloro-5-(trifluoromethyl)phenyl)-2-phenylcyclopropane-1-carboxylate from previous step as starting material.

mp: 154-156 °C; **R_f**= 0.50 (10% ethyl acetate/hexane); **[α]²⁰_D**: -256.0° (c = 1.00, CHCl₃, 99.9% ee);

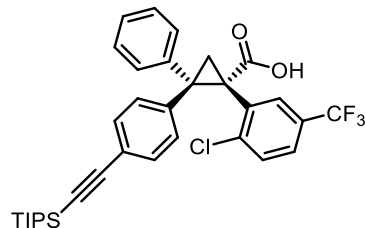
¹H NMR (600 MHz, CDCl₃) δ 7.52 – 7.47 (m, 2H), 7.40 – 7.35 (m, 5H), 7.32 – 7.28 (m, 1H), 7.11 (d, *J* = 8.6 Hz, 2H), 6.77 (d, *J* = 8.6 Hz, 2H), 3.41 (s, 3H), 2.81 (d, *J* = 6.0 Hz, 1H), 2.48 (d, *J* = 6.1 Hz, 1H), 1.07 (s, 21H);

¹³C NMR (151 MHz, CDCl₃) δ 169.9, 140.7, 140.6, 138.8, 135.3, 131.2, 130.3, 130.2, 128.7, 128.5, 128.0, 127.4, 125.5 (q, *J* = 3.8 Hz), 123.5 (d, *J* = 272.3 Hz), 121.8, 106.6, 91.0, 52.5, 45.2, 41.9, 25.9, 18.6, 11.3;

¹⁹F NMR (376 MHz, CDCl₃) δ -62.67;

IR (neat) 3085, 3028, 2944, 2865, 2155, 1733, 1508, 1463, 1435, 1366, 1320, 1212, 1170, 1131, 1079, 883, 823, 732, 704, 676, 619 cm⁻¹;

HRMS (+p NSI) calcd for C₃₅H₃₉ClF₃O₂Si (M+H)⁺ 611.2354 found 611.2350.



(1*S*,2*S*)-1-(2-Chloro-5-(trifluoromethyl)phenyl)-2-phenyl-2-(4-((triisopropylsilyl)ethynyl)phenyl)cyclopropane-1-carboxylic acid (246)

It was obtained in 70% yield following *G.P. H* using methyl (1*S*,2*S*)-1-(2-chloro-5-(trifluoromethyl)phenyl)-2-phenyl-2-(4-((triisopropylsilyl)ethynyl)phenyl)-cyclopropane-1-carboxylate from previous step as starting material.

mp: 108-110 °C; **R_f** = 0.16 (20% ethyl acetate/hexane); **[α]²⁰_D**: -273.7° (c = 1.00, CHCl₃, 99.9% ee);

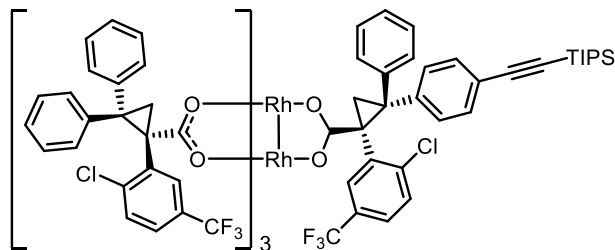
¹H NMR (600 MHz, CDCl₃) δ 7.53 – 7.45 (m, 2H), 7.40 – 7.29 (m, 6H), 7.10 (d, *J* = 8.1 Hz, 2H), 6.77 (d, *J* = 8.6 Hz, 2H), 2.72 (s, 1H), 2.52 (d, *J* = 6.0 Hz, 1H), 1.07 (s, 22H);

¹³C NMR (151 MHz, CDCl₃) δ 175.1, 140.6, 140.2, 138.4, 134.8, 131.2, 130.3, 130.1, 128.7, 128.5, 128.1, 127.4, 125.6, 123.4 (d, *J* = 272.7 Hz), 122.0, 106.5, 91.2, 46.3, 41.4, 26.4, 11.3;

¹⁹F NMR (376 MHz, CDCl₃) δ -62.70;

IR (neat) 3085, 3061, 3028, 2943, 2865, 2626, 2156, 1694, 1508, 1341, 1320, 1264, 1171, 1131, 1104, 908, 882, 825, 736, 703, 682, 617 cm⁻¹;

HRMS (+p APCI) calcd for C₃₄H₃₇ClF₃O₂Si (M+H)⁺ 597.2198 found 597.2190.



Rh₂(S-2-Cl-5-CF₃TPCP)₃(TIPS-ethynyl@B) (249)

It was obtained in 51% yield following *G.P. I* using (1*S*,2*S*)-1-(2-chloro-5-(trifluoromethyl)-phenyl)-2-phenyl-2-(4-((triisopropylsilyl)ethynyl)phenyl)cyclopropane-1-carboxylic acid and Rh₂(S-2-Cl-5-CF₃TPCP)₄ as starting materials. The reaction was refluxed in chlorobenzene at 130 °C for 1 h.

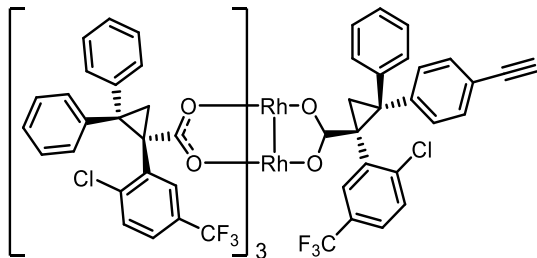
mp: >200 °C (decomp.); **R_f** = 0.78 (30% ethyl acetate/hexane);

¹H NMR (600 MHz, CDCl₃) δ 7.47 – 7.34 (m, 12H), 7.26 – 7.00 (m, 28H), 6.99 – 6.87 (m, 11H), 2.82 – 2.64 (m, 4H), 2.25 (td, *J* = 13.4, 10.7, 4.7 Hz, 4H), 1.09 – 1.03 (m, 21H);

¹³C NMR (151 MHz, CDCl₃) δ 187.9, 187.6, 187.0, 186.7, 141.6, 141.3, 140.4, 140.4, 138.9, 138.9, 138.4, 138.4, 138.3, 136.9, 136.8, 136.7, 131.4, 131.0, 130.9, 129.8, 129.6, 128.5, 128.3, 128.2, 128.2, 128.1, 127.8, 127.5, 127.4, 127.2, 126.4, 126.1, 125.5, 125.2, 125.2, 124.9, 124.7, 122.9, 122.8, 121.4, 121.0, 106.7, 90.8, 60.5, 53.7, 53.5, 45.8, 45.5, 45.5, 42.3, 42.1, 41.9, 31.6, 30.8, 30.7, 29.7, 26.0, 25.8, 25.1, 18.6, 14.1, 11.3;

IR (neat) 2943, 2866, 2154, 1594, 1495, 1381, 1340, 1322, 1266, 1169, 1128, 1080, 1050, 826, 752, 700, 636 cm⁻¹;

HRMS (+p APCI) calcd for C₁₀₃H₈₀Cl₄F₁₂O₂Rh₂Si (M)⁺ 2046.2295 found 2046.2282.



Rh₂(S-2-Cl-5-CF₃TPCP)₃(ethynyl@B) (250)

It was obtained in 82% yield following *G.P. J* using Rh₂(S-2-Cl-5-CF₃TPCP)₃(TIPS-ethynyl@B) from previous step as starting material and was confirmed using mass spectrum.

mp: >200 °C (decomp.); **Rf** = 0.69 (30% ethyl acetate/hexane);

¹H NMR (600 MHz, CDCl₃) δ 7.48 – 7.33 (m, 12H), 7.21 – 7.10 (m, 16H), 7.04 (d, *J* = 8.2 Hz, 12H), 6.97 (d, *J* = 8.3 Hz, 2H), 6.94 – 6.85 (m, 9H), 2.91 (s, 1H), 2.77 – 2.67 (m, 4H), 2.34 – 2.19 (m, 4H);

¹³C NMR (151 MHz, CDCl₃) δ 187.2, 187.1, 186.8, 142.0, 141.5, 140.6, 140.4, 139.8, 138.8, 137.4, 137.1, 131.1, 130.9, 129.8, 129.6, 128.3, 128.3, 128.2, 128.1, 127.7, 127.7, 127.6, 127.5, 127.3, 127.3, 126.6, 126.3, 126.2, 126.0, 124.9, 124.9, 124.8, 124.8, 124.6, 124.6, 124.6, 124.6, 123.0, 123.0, 121.2, 119.9, 83.4, 68.6, 60.5, 45.6, 45.6, 45.2, 42.0, 25.5, 25.4, 24.7, 17.4, 17.3, 14.2, 11.9;

IR (neat) 3623, 3058, 1694, 1589, 1384, 1340, 1321, 1267, 1170, 1130, 1080, 827, 702 cm⁻¹;

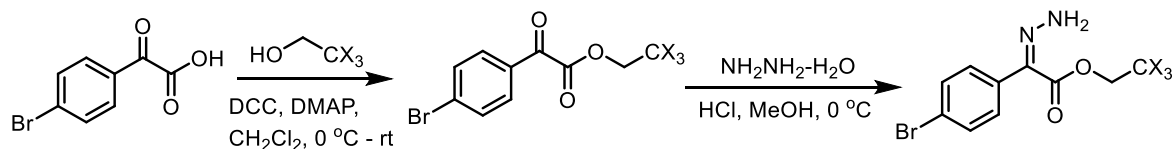
HRMS (+p NSI) calcd for C₉₄H₆₀Cl₄F₁₂O₈Rh (M)⁺ 1890.0961 found 1890.0972.

6.5 Experimental Part for Chapter 5

Synthesis for Starting Materials

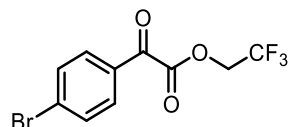
Most of the hydrazones used could be synthesized following literature procedures as noted in session 6.1.

The synthesis for trifluoroethyl and tribromoethyl derivatives were shown as below.



A dry 100 mL round-bottom flask was charged with 2-(4-bromophenyl)-2-oxoacetic acid²¹² (1.15 g, 5 mmol, 1.0 equiv), DMAP (61.1 mg, 0.5 mmol, 0.1 equiv) and 2,2,2-trihaloethanol (6 mmol, 1.2 equiv). After the flask was flushed with argon gas (3 times), 10 mL of dry dichloromethane was added to the mixture. Then, the reaction mixture was cooled to 0 °C via ice bath. The solution of DCC (1.13 g, 5.5 mmol, 1.1 equiv) in 8 mL of dry dichloromethane was then added slowly at 0 °C. The reaction mixture was stirred for 15 hours, at which point it was warmed up to room temperature (23 °C). The reacted mixture was filtered through Celite[®] under reduced pressure and washed with dichloromethane. The filtrate was collected and concentrated under reduced pressure. The crude compound was purified by flash column chromatography (0-6% ethyl acetate in hexane) to afford slightly yellow oil in 55-70% yield. The product was used immediately in the next step. A 250 mL round-bottom flask was charged with hydrazine monohydrate (55% w/w, 1.7 mL, 30 mmol, 10 equiv) and MeOH (45 mL). After flushed with argon, the reaction mixture was cooled to 0 °C via ice bath. To this solution, aqueous HCl (3.0 M, 10.0 mL, 30 mmol, 10 equiv) was added slowly, followed by addition of 2,2,2-trihaloethyl 2-(4-bromophenyl)-2-oxoacetate (3.0 mmol, 1.0 equiv) in MeOH (3 mL) dropwise over about 5 min. The reaction mixture was stirred at 0 °C until full consumption of starting material was observed by TLC control (normally 6-8 h, unnecessary

longer reaction times lead to significantly lower yields). The reaction mixture was quenched by the addition of sat. NaHCO_3 (100 mL), MeOH was evaporated under reduced pressure, the residue was extracted with ethyl acetate (100 mL x 3). The organic layers were washed with brine (100 mL) and concentrated. The residue was purified by flash column chromatography (2-5% ethyl acetate in hexane for *Z*-isomer and 15-25% for *E*-isomer if needed).



2,2,2-Trifluoroethyl 2-(4-bromophenyl)-2-oxoacetate

It was obtained as slightly yellow oil in 58% yield following the general procedure above using 2,2,2-trifluoroethan-1-ol (0.45 mL) as starting material.

Rf = 0.34 (10% ethyl acetate/hexane);

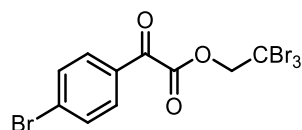
$^1\text{H NMR}$ (600 MHz, CDCl_3) δ 7.89 (d, J = 8.8 Hz, 2H), 7.70 (d, J = 8.7 Hz, 2H), 4.75 (q, J = 8.2 Hz, 2H);

$^{13}\text{C NMR}$ (151 MHz, CDCl_3) δ 183.0, 161.2, 132.6, 131.4, 131.3, 130.8, 122.4 (q, J = 277.3 Hz), 61.2 (q, J = 37.6 Hz);

$^{19}\text{F NMR}$ (282 MHz, CDCl_3) δ -73.40;

IR (neat) 3031, 2971, 1759, 1694, 1586, 1272, 1161, 1072, 1040, 1012, 978 cm^{-1} ;

HRMS (-p NSI) calcd for $\text{C}_{10}\text{H}_6\text{BrF}_3\text{O}_3$ (M^-) 309.9458 found 309.9459.



2,2,2-Tribromoethyl 2-(4-bromophenyl)-2-oxoacetate

It was obtained as white solid in 69% yield following the general procedure above using 2,2,2-tribromoethan-1-ol (1.7 g) as starting material.

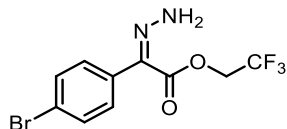
mp: 63-65 °C; **Rf** = 0.60 (20% ethyl acetate/hexane);

¹H NMR (600 MHz, CDCl₃) δ 7.97 (d, *J* = 8.8 Hz, 2H), 7.70 (d, *J* = 8.8 Hz, 2H), 5.22 (s, 2H);

¹³C NMR (151 MHz, CDCl₃) δ 183.5, 161.1, 132.5, 131.6, 131.1, 130.9, 77.5, 33.4;

IR (neat) 3091, 3000, 2949, 1748, 1689, 1586, 1188, 1164, 1070, 1000, 632 cm⁻¹;

HRMS (-p NSI) calcd for C₁₀H₆Br₅O₃ (M+Br)⁻ 568.6239 found 568.6227.



2,2,2-Trifluoroethyl (Z)-2-(4-bromophenyl)-2-hydrazineylideneacetate (257)

It was obtained as white solid in 60% yield following the general procedure above using 2,2,2-trifluoroethyl 2-(4-bromophenyl)-2-oxoacetate (933 mg) as starting material.

mp: 63-65 °C; **Rf** = 0.40 (20% ethyl acetate/hexane);

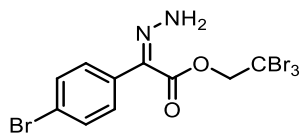
¹H NMR (600 MHz, CDCl₃) δ 8.71 (s, 1H), 7.48 (d, *J* = 8.6 Hz, 1H), 7.38 (d, *J* = 8.6 Hz, 1H), 4.61 (q, *J* = 8.3 Hz, 1H);

¹³C NMR (151 MHz, CDCl₃) δ 160.3, 134.8, 131.1, 129.8, 127.2, 122.8 (d, *J* = 277.4 Hz), 121.9, 60.0 (q, *J* = 36.9 Hz);

¹⁹F NMR (282 MHz, CDCl₃) δ -73.20 – -73.40 (m);

IR (neat) 3466, 3260, 1703, 1568, 1511, 1488, 1287, 1249, 1136, 962, 830, 544 cm⁻¹;

HRMS (+p APCI) calcd for C₁₀H₉BrF₃N₂O₂ (M+H)⁺ 324.9794 found 324.9789.



2,2,2-Tribromoethyl (Z)-2-(4-bromophenyl)-2-hydrazineylideneacetate (258)

It was obtained as white solid in 78% yield following the general procedure above using 2,2,2-tribromoethyl 2-(4-bromophenyl)-2-oxoacetate (1.48 g) as starting material.

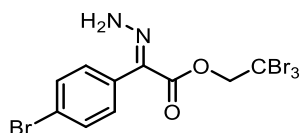
mp: 86-88 °C; **Rf** = 0.42 (20% ethyl acetate/hexane);

¹H NMR (600 MHz, CDCl₃) δ 8.75 (s, 2H), 7.54 (d, *J* = 8.7 Hz, 2H), 7.47 (d, *J* = 8.7 Hz, 2H), 5.09 (s, 2H);

¹³C NMR (151 MHz, CDCl₃) δ 160.2, 134.8, 130.9, 130.3, 127.5, 121.8, 76.9, 34.6;

IR (neat) 3463, 3287, 2943, 1697, 1564, 1508, 1488, 1251, 1136, 1073, 829, 729, 631, 522 cm⁻¹;

HRMS (+p APCI) calcd for C₁₀H₉Br₄N₄O₂ (M+H)⁺ 504.7392 found 504.7388.



2,2,2-Tribromoethyl (*E*)-2-(4-bromophenyl)-2-hydrazineylideneacetate

It was obtained as white solid in 16% yield following the general procedure above using 2,2,2-tribromoethyl 2-(4-bromophenyl)-2-oxoacetate (1.48 g) as starting material.

mp: 129-131 °C; **Rf** = 0.14 (20% ethyl acetate/hexane);

¹H NMR (600 MHz, CDCl₃) δ 7.65 (d, *J* = 8.5 Hz, 2H), 7.25 (d, *J* = 9.1 Hz, 3H), 6.49 (s, 2H), 5.06 (s, 2H);

¹³C NMR (151 MHz, CDCl₃) δ 162.0, 134.5, 132.6, 130.8, 127.8, 123.9, 35.7 (The signal for CBr₃ was buried under the CDCl₃ peaks);

IR (neat) 3409, 3288, 3209, 2940, 1716, 1553, 1484, 1368, 1311, 1126, 1073, 1010, 728, 631, 499 cm⁻¹;

HRMS (+p APCI) calcd for C₁₀H₉Br₄N₄O₂ (M+H)⁺ 504.7392 found 504.7384.

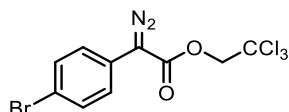
Hydrazone Oxidation

General Procedure K (optimized condition for hydrazone oxidation)

*Unoptimized reactions were following the same procedure with variations as indicated in tables.

*No septum was used in open-air reactions.

A 20 mL scintillation vial equipped with stir bar (bigger size) was charged with Cu(OAc)₂·H₂O (10 mg, 0.05 mmol, 10 mol%), silica powder (100 mg, SiliaFlash® P60, 40-63 μm) and 0.5 mL solution of 0.5% pyridine in dichloromethane. The reaction vessel with a 14/20 septum was flushed with O₂ and the O₂ balloon (double layered) was left on the septum. Another 1.8 mL solution of 0.5% pyridine in dichloromethane was added, and the initial mixture was stirred vigorously (800 rpm) for 5 min. A solution of corresponding hydrazone (0.5 mmol, 1.0 equiv) in 0.5% pyridine /dichloromethane was added in one portion, and the reaction mixture was stirred for 1 h at room temperature (23 °C). After allowed time passed, the resulted mixture was filtered through a short pipet of silica (0.9 cm diameter, 5 cm height) and concentrated for crude ¹H NMR. Further purification was conducted using flash column chromatography (0-3% diethyl ether in hexane).

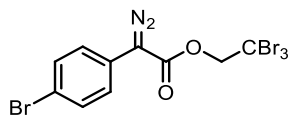


2,2,2-Trichloroethyl 2-(4-bromophenyl)-2-diazoacetate (4b)

It was obtained as yellow solid in 95% yield following *G.P. K* using 2,2,2-trifluoroethyl (*Z*)-2-(4-bromophenyl)-2-hydrazineylideneacetate¹⁷¹ (187 mg) as starting material. The NMR data are consistent with literature values.⁸⁰

¹H NMR (600 MHz, CDCl₃) δ 7.52 (d, *J* = 8.7 Hz, 2H), 7.37 (d, *J* = 8.7 Hz, 2H), 4.91 (s, 2H);

¹³C NMR (151 MHz, CDCl₃) δ 162.9, 132.2, 125.4, 123.8, 119.9, 94.9, 73.9 (The resonance resulting from the diazo carbon was not observed).

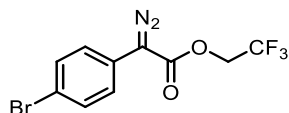


2,2,2-Tribromoethyl 2-(4-bromophenyl)-2-diazoacetate (4c)

It was obtained as yellow solid in 91% yield following *G.P. K* using 2,2,2-tribromoethyl (*Z*)-2-(4-bromophenyl)-2-hydrazineylideneacetate (254 mg) as starting material. The NMR data are consistent with literature values.²⁰⁴

¹H NMR (600 MHz, CDCl₃) δ 7.53 (d, *J* = 8.8 Hz, 1H), 7.40 (d, *J* = 8.8 Hz, 1H), 5.09 (s, 1H);

¹³C NMR (151 MHz, CDCl₃) δ 162.8, 132.2, 125.4, 123.9, 119.9, 78.3, 35.7 (The resonance resulting from the diazo carbon was not observed).

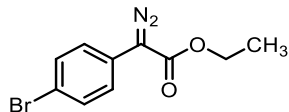


2,2,2-Trifluoroethyl 2-(4-bromophenyl)-2-diazoacetate (4a)

It was obtained as yellow solid in 98% yield following *G.P. K* using 2,2,2-trifluoroethyl (*Z*)-2-(4-bromophenyl)-2-hydrazineylideneacetate (163 mg) as starting material. The NMR data are consistent with literature values.²⁰⁴

¹H NMR (600 MHz, CDCl₃) δ 7.52 (d, *J* = 8.7 Hz, 2H), 7.33 (d, *J* = 8.7 Hz, 2H), 4.65 (q, *J* = 8.3 Hz, 2H);

¹³C NMR (151 MHz, CDCl₃) δ 162.8, 132.2, 125.4, 123.7, 122.9 (q, *J* = 277.5 Hz), 120.0, 60.4 (q, *J* = 37.0 Hz) (The resonance resulting from the diazo carbon was not observed).

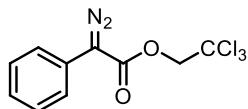


Ethyl 2-(4-bromophenyl)-2-diazoacetate (266)

It was obtained as yellow solid in 95% yield following *G.P. K* using ethyl 2-(4-bromophenyl)-2-hydrazineylideneacetate¹⁹¹ (1:1 *E:Z*, 135.6 mg) as starting material. The NMR data are consistent with literature values.²²²

¹H NMR (600 MHz, CDCl₃) δ 7.49 (d, *J* = 8.9 Hz, 1H), 7.36 (d, *J* = 8.7 Hz, 1H), 4.33 (q, *J* = 7.1 Hz, 1H), 1.34 (t, *J* = 7.1 Hz, 2H);

¹³C NMR (151 MHz, CDCl₃) δ 164.8, 132.0, 132.0, 125.3, 125.3, 124.9, 124.9, 119.3, 119.2, 61.2, 61.2, 14.5, 14.5 (The resonance resulting from the diazo carbon was not observed).

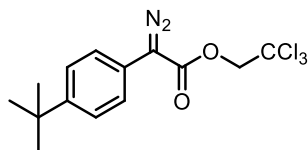


2,2,2-Trichloroethyl 2-diazo-2-phenylacetate (267)

It was obtained as yellow solid in 95% yield following *G.P. K* using 2,2,2-trichloroethyl (*Z*)-2-hydrazineylidene-2-phenylacetate¹⁷¹ (148 mg) as starting material. The NMR data are consistent with literature values.¹⁷⁹

¹H NMR (600 MHz, CDCl₃) δ 7.53 – 7.48 (m, 2H), 7.45 – 7.38 (m, 2H), 7.25 – 7.21 (m, 1H), 4.92 (s, 2H);

¹³C NMR (151 MHz, CDCl₃) δ 163.3, 129.1, 126.3, 124.6, 124.1, 95.0, 73.8 (The resonance resulting from the diazo carbon was not observed).

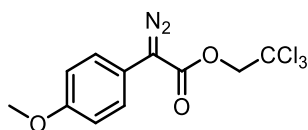


2,2,2-trichloroethyl 2-(4-(*tert*-butyl)phenyl)-2-diazoacetate (268)

It was obtained as yellow solid in 97% yield following *G.P. K* using 2,2,2-trichloroethyl (*Z*)-2-(4-(*tert*-butyl)phenyl)-2-hydrazineylideneacetate¹⁷¹ (176 mg) as starting material. The NMR data are consistent with literature values.²⁰⁴

¹H NMR (600 MHz, CDCl₃) δ 7.47 – 7.40 (m, 4H), 4.92 (s, 2H), 1.33 (s, 9H);

¹³C NMR (151 MHz, CDCl₃) δ 149.6, 126.1, 124.1, 121.3, 95.1, 73.8, 34.5, 31.2 (The resonance resulting from the diazo carbon was not observed).

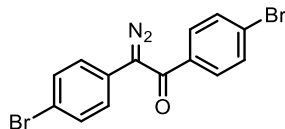


2,2,2-Trichloroethyl 2-diazo-2-(4-methoxyphenyl)acetate (269)

It was obtained as yellow solid in 94% yield following *G.P. K* using 2,2,2-trichloroethyl (*Z*)-2-hydrazineylidene-2-(4-methoxyphenyl)acetate¹⁷¹ (163 mg) as starting material. The NMR data are consistent with literature values.²⁰⁴

¹H NMR (600 MHz, CDCl₃) δ 7.40 (d, *J* = 9.0 Hz, 2H), 6.97 (d, *J* = 8.9 Hz, 2H), 4.90 (s, 2H), 3.82 (s, 3H);

¹³C NMR (151 MHz, CDCl₃) δ 158.4, 126.1, 116.0, 114.7, 95.1, 73.9, 55.4 (The resonance resulting from the diazo carbon was not observed).



1,2-bis(4-bromophenyl)-2-diazoethan-1-one (270)

It was obtained as yellow solid in 92% yield following procedure similar to *G.P. K* using (*Z*)-1,2-bis(4-bromophenyl)-2-hydrazineylideneethan-1-one²¹¹ (191 mg) as starting material, and the variation are: 2% pyridine in dichloromethane was used as solvent and reaction went in dark.

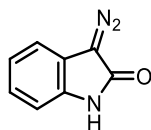
mp: 88-90 °C (decomp.); **Rf** = 0.46 (10% ethyl acetate/hexane);

¹H NMR (600 MHz, CDCl₃) δ 7.57 (d, *J* = 8.6 Hz, 2H), 7.53 (d, *J* = 8.9 Hz, 2H), 7.47 (d, *J* = 8.6 Hz, 2H), 7.33 (d, *J* = 8.7 Hz, 2H);

¹³C NMR (151 MHz, CDCl₃) δ 186.8, 136.3, 132.3, 131.9, 129.3, 127.5, 126.6, 124.9, 121.0 (The resonance resulting from the diazo carbon was not observed);

IR (neat) 3087, 2071, 1621, 1586, 1488, 1337, 1244, 1070, 1010, 856, 822 cm⁻¹;

HRMS (+p APCI) calcd for C₁₄H₈Br₂N₂ONa (M+Na)⁺ 400.8896 found 400.88621.

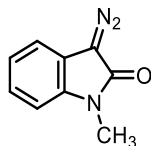


3-diazoindolin-2-one (271)

It was obtained as yellow solid in 99% yield following *G.P. K* using 3-hydrazonoindolin-2-one¹⁹¹ (2:1 *Z:E*, 80.6 mg) as starting material. The NMR data are consistent with literature values.²²³

¹H NMR (600 MHz, CD₃OD) δ 7.32 – 7.25 (m, 1H), 7.13 (td, *J* = 7.7, 1.2 Hz, 1H), 7.06 (td, *J* = 7.6, 1.0 Hz, 1H), 6.97 (dt, *J* = 7.8, 0.8 Hz, 1H);

¹³C NMR (151 MHz, CD₃OD) δ 169.4, 132.3, 125.1, 121.7, 118.3, 117.2, 110.1 (The resonance resulting from the diazo carbon was not observed).



3-diazo-1-methylindolin-2-one (272)

It was obtained as yellow solid in 98% yield following *G.P. K* using 3-hydrazono-1-methylindolin-2-one¹⁹¹ (17:1 *Z:E*, 87.6 mg) as starting material. The NMR data are consistent with literature values.¹⁹¹

¹H NMR (600 MHz, CDCl₃) δ 7.22 – 7.18 (m, 2H), 7.11 – 7.07 (m, 1H), 6.94 – 6.90 (m, 1H), 3.33 (s, 3H);

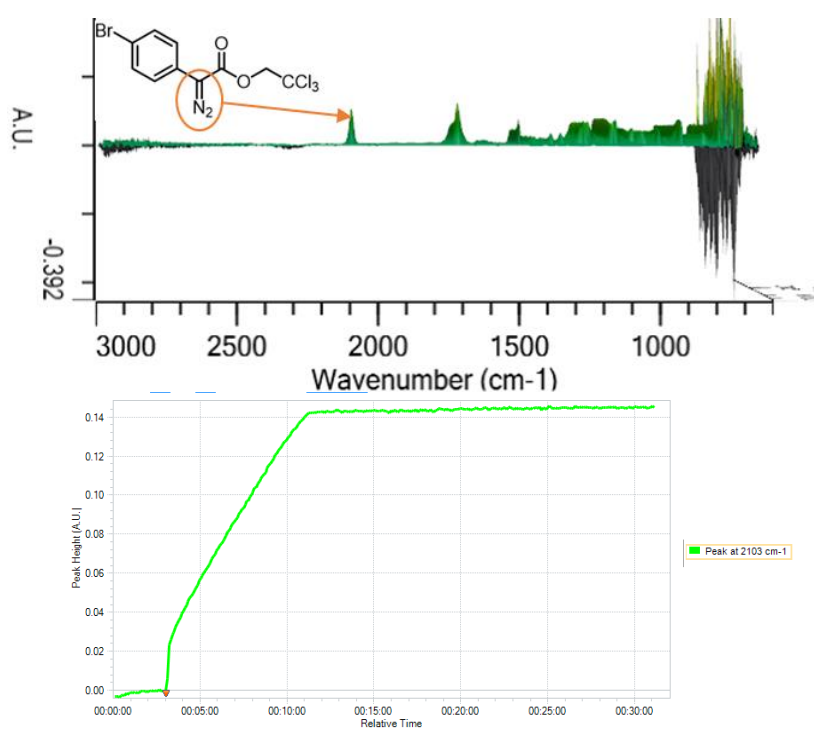
¹³C NMR (151 MHz, CDCl₃) δ 166.8, 134.5, 125.5, 122.1, 118.2, 116.7, 108.6, 26.8 (The resonance resulting from the diazo carbon was not observed).

React-IR Experiment Set-up and Procedure

The React-IR instrument was filled with liquid nitrogen and allowed to equilibrate while the reaction flask was being set-up. An oven-dried 100 mL 3-neck round-bottom flask was fitted with React-IR probe at the center neck (19/25 neck with 24/40 to 19/25 adapter to fit the probe) and the other two necks were fitted with rubber septa (14/20 neck) as shown below.

The flask was cooled to room temperature under vacuum, then backfilled with oxygen (3 times and then left the balloon at the left neck) and placed in a water bath (maintain at room temperature) with stir rate set as 800 rpm. After background and water vapor spectrum were taken for calibration of the instrument, Cu(OAc)₂·H₂O (59.9 mg, 0.3 mmol, 20 mol%) and silica powder (300 mg, SiliaFlash® P60, 40-63 μm) were added. Then, the reaction vessel was purged with oxygen (vacuum/oxygen cycle x 3 and the oxygen balloon was left at the left neck) before the addition of

12 mL of dry and degassed dichloromethane. The data collection was started on the software, and the initial reaction mixture was allowed to stir for 10 minutes. A reference spectrum of the initial reaction mixture was taken, a solution of 2,2,2-trichloroethyl (Z)-2-(4-bromophenyl)-2-hydrazineylideneacetate in 3 mL dry and degassed dichloromethane was added in one portion via syringe from the left neck (noted quickly on the software). The mixture was stirred at room temperature and the increase of C=N₂ stretch frequency (2103 cm⁻¹) was monitored until it reacted the maximum and stay steady for 10 min (or 4 h after the addition, whichever came first).



The data was extracted directly from the software as in text format and pasted into Microsoft Excel. The first time point, where it was noted that the hydrazone was injected, was set as “0” (minutes) and all subsequent time points are set relatively after it. To normalize the absorbance, the absorbance of the maximum value in experiments that went completion (with NEt₃ and pyridine as additive, averaged) was set as “1”, and all subsequent absorbances are divided by the absorbance of that point. In doing so, it is possible to get the relative concentration of diazo and to monitor the time of the diazo generation.

References

1. Gutekunst, W. R. and Baran, P. S., *Chem. Soc. Rev.* **2011**, *40*, 1976.
2. McMurray, L., O'Hara, F. and Gaunt, M., *Chem. Soc. Rev.* **2011**, *40*, 1885.
3. Yamaguchi, J., Yamaguchi, A. D. and Itami, K., *Angew. Chem., Int. Ed.* **2012**, *51*, 8960.
4. Wencel-Delord, J. and Glorius, F., *Nat. Chem.* **2013**, *5*, 369.
5. Hartwig, J. F., *J. Am. Chem. Soc.* **2016**, *138*, 2.
6. Davies, H. M. L. and Morton, D. J., *J. Org. Chem.* **2016**, *81*, 343.
7. Abrams, D. J., Provencher, P. A. and Sorensen, E. J., *Chem. Sci. Rev.* **2018**, *47*, 8925.
8. Harvey, M. E., Musaev, D. G. and Du Bois, J., *J. Am. Chem. Soc.* **2011**, *133*, 17207.
9. Doyle, M. P., Duffy, R., Ratnikov, M. and Zhou, L., *Chem. Rev.* **2010**, *110*, 704.
10. Yang, M., Su, B., Wang, Y., Chen, K., Jiang, X., Zhang, Y. F., Zhang, X. S., Chen, G., Cheng, Y., Cao, Z., Guo, Q. Y., Wang, L. and Shi, Z. J., *Nat. Commun.* **2014**, *5*, 4707.
11. O'Broin, C. Q., Fernández, P., Martínez, C. and Muñoz, K., *Org. Lett.* **2016**, *18*, 436.
12. Wappes, E. A., Fosu, S. C., Chopko, T. C. and Nagib, D. A., *Angew. Chem., Int. Ed.* **2016**, *55*, 9974.
13. Choi, G. J., Zhu, Q., Miller, D. C., Gu, C. J. and Knowles, R. R., *Nature* **2016**, *539*, 268.
14. Becker, P., Duhamel, T., Martínez, C. and Muñoz, K., *Angew. Chem., Int. Ed.* **2018**, *57*, 5166.
15. Bao, X., Wang, Q. and Zhu, J., *Nat. Commun.* **2019**, *10*, 769.
16. Lyons, T. W. and Sanford, M. S., *Chem. Rev.* **2010**, *110*, 1147.
17. Zhang, F. and Spring, D. R., *Chem. Soc. Rev.* **2014**, *43*, 6906.
18. He, J., Wasa, M., Chan, K. S. L., Shao, Q. and Yu, J. Q., *Chem. Rev.* **2017**, *117*, 8754.
19. Saint-Denis, T. G., Zhu, R. Y., Chen, G., Wu, Q. F. and Yu, J. Q., *Science* **2018**, *359*, 759.
20. Shang, M., Feu, K. S., Vantourout, J. C., Barton, L. M., Osswald, H. L., Kato, N., Gagaring, K., McNamara, C. W., Chen, G., Hu, L., Ni, S., Fernández-Canelas, P., Chen, M., Merchant, R. R., Qin, T., Schreiber, S. L., Melillo, B., Yu, J.-Q. and Baran, P. S., *Proc. Natl. Acad. Sci. U.S.A.* **2019**, *116*, 8721.
21. Ravelli, D., Fagnoni, M., Fukuyama, T., Nishikawa, T. and Ryu, I., *ACS Catal.* **2018**, *8*, 701.
22. Quinn, R. K., Könst, Z. A., Michalak, S. E., Schmidt, Y., Szklarski, A. R., Flores, A. R., Nam, S., Horne, D. A., Vanderwal, C. D. and Alexanian, E. J., *J. Am. Chem. Soc.* **2016**, *138*, 696.
23. Thu, H., Tong, G., Huang, J., Chan, S., Deng, Q. and Che, C., *Angew. Chem., Int. Ed.* **2008**, *47*, 9747.
24. Díaz-Requejo, M. M. and Pérez, P. J., *Chem. Rev.* **2008**, *108*, 3379.
25. Roizen, J. L., Zalatan, D. N. and Du Bois, J., *Angew. Chem., Int. Ed.* **2013**, *52*, 11343.
26. Gormisky, P. E. and White, M. C., *J. Am. Chem. Soc.* **2013**, *135*, 14052.
27. Clark, J. R., Feng, K., Sookezian, A. and White, M. C., *Nat. Chem.* **2018**, *10*, 583.
28. Dydio, P., Key, H. M., Hayashi, H., Clark, D. S. and Hartwig, J. F., *J. Am. Chem. Soc.* **2017**, *139*, 1750.
29. Zwick, C. R. and Renata, H., *J. Am. Chem. Soc.* **2018**, *140*, 1165.
30. Zhang, R. K., Chen, K., Huang, X., Wohlschlagler, L., Renata, H. and Arnold, F. H., *Nature* **2019**, *565*, 67.

31. Doyle, M. P., McKervey, M. A. and Ye, T., *Modern catalytic methods for organic synthesis with diazo compounds: From cyclopropanes to ylides*. Wiley, New York: **1998**.
32. Davies, H. M. L. and Beckwith, R. E. J., *Chem. Rev.* **2003**, *103*, 2861.
33. Davies, H. M. L. and Panaro, S. A., *Tetrahedron* **2000**, *56*, 4871.
34. Berry, J. F., *Dalton Trans.* **2012**, *41*, 700.
35. Nakamura, E., Yoshikai, N. and Yamanaka, M., *J. Am. Chem. Soc.* **2002**, *124*, 7181.
36. Kornecki, K. P., Briones, J. F., Boyarskikh, V., Fullilove, F., Autschbach, J., Schrote, K. E., Lancaster, K. M., Davies, H. M. L. and Berry, J. F., *Science* **2013**, *342*, 351.
37. Davies, H. M. L. and Morton, D., *Chem. Sci. Rev.* **2011**, *40*, 1857.
38. Fulton, J. R., Aggarwal, V. K. and de Vicente, J., *Eur. J. Org. Chem.* **2005**, *2005*, 1479.
39. Werlé, C., Goddard, R., Philipps, P., Farès, C. and Fürstner, A., *J. Am. Chem. Soc.* **2016**, *138*, 3797.
40. Soldi, C., Lamb, K. N., Squitieri, R. A., González-López, M., Di Maso, M. J. and Shaw, J. T., *J. Am. Chem. Soc.* **2014**, *136*, 15142.
41. Caballero, A., Díaz-Requejo, M. M., Fructos, M. R., Olmos, A., Urbano, J. and Pérez, P. J., *Dalton Trans.* **2015**, *44*, 20295.
42. Davies, H. M. L., Smith, H. D. and Korkor, O., *Tetrahedron Lett.* **1987**, *28*, 1853.
43. Davies, H. M. L. and Hansen, T., *J. Am. Chem. Soc.* **1997**, *119*, 9075.
44. Davies, H. M. L., Hopper, D. W., Hansen, T., Liu, Q. and Childers, S. R., *Bioorg. Med. Chem. Lett.* **2004**, *14*, 1799.
45. Davies, H. M. L. and Ni, A., *Chem. Commun.* **2006**, 3110.
46. Yamaguchi, A. D., Chepiga, K. M., Yamaguchi, J., Itami, K. and Davies, H. M. L., *J. Am. Chem. Soc.* **2015**, *137*, 644.
47. Lu, P., Mailyan, A., Gu, Z., Guptill, D. M., Wang, H., Davies, H. M. L. and Zakarian, A., *J. Am. Chem. Soc.* **2014**, *136*, 17738.
48. Bedell, T. A., Hone, G. A. B., Valette, D., Yu, J.-Q., Davies, H. M. L. and Sorensen, E. J., *Angew. Chem., Int. Ed.* **2016**, *55*, 8270.
49. Hong, B., Li, C., Wang, Z., Chen, J., Li, H. and Lei, X., *J. Am. Chem. Soc.* **2015**, *137*, 11946.
50. Ren, T., *Coord. Chem. Rev.* **1998**, *175*, 43.
51. Boyar, E. B. and Robinson, S. D., *Coord. Chem. Rev.* **1983**, *50*, 109.
52. Paulissen, R., Reimlinger, H., Hayez, E., Hubert, A. J. and Teysié, P., *Tetrahedron Lett.* **1973**, *14*, 2233.
53. Brunner, H., Kluschanzoff, H. and Wutz, K., *Bull. Soc. Chim. Belg.* **1989**, *98*, 63.
54. Doyle, M. P., *Recl. Trav. Chim. Pays-Bas* **1991**, *110*, 305.
55. Kennedy, M., McKervey, M. A., Maguire, A. R. and Roos, G. H. P., *J. Chem. Soc., Chem. Commun.* **1990**, 361.
56. McKervey, M. A. and Ye, T., *J. Chem. Soc., Chem. Commun.* **1992**, 823.
57. Ye, T., García, C. F. and McKervey, M. A., *J. Chem. Soc., Perkin Trans. 1* **1995**, 1373.
58. Davies, H. M. L., Bruzinski, P. R. and Fall, M. J., *Tetrahedron Lett.* **1996**, *37*, 4133.
59. Davies, H. M. L., *Eur. J. Org. Chem.* **1999**, *1999*, 2459.
60. Davies, H. M. L., Hansen, T. and Churchill, M. R., *J. Am. Chem. Soc.* **2000**, *122*, 3063.
61. Davies, H. M. L., Jin, Q., Ren, P. and Kovalevsky, A. Y., *J. Org. Chem.* **2002**, *67*, 4165.
62. Davies, H. M. L., Antoulinakis, E. G. and Hansen, T., *Org. Lett.* **1999**, *1*, 383.
63. Davies, H. M. L., Beckwith, R. E. J., Antoulinakis, E. G. and Jin, Q., *J. Org. Chem.* **2003**, *68*, 6126.

64. Davies, H. M. L., Venkataramani, C., Hansen, T. and Hopper, D. W., *J. Am. Chem. Soc.* **2003**, *125*, 6462.
65. Davies, H. M. L., Ren, P. and Jin, Q., *Org. Lett.* **2001**, *3*, 3587.
66. Davies, H. M. L. and Kong, N., *Tetrahedron Lett.* **1997**, *38*, 4203.
67. Davies, H. M. L. and Panaro, S. A., *Tetrahedron Lett.* **1999**, *40*, 5287.
68. Hashimoto, S.-i., Watanabe, N., Sato, T., Shiro, M. and Ikegami, S., *Tetrahedron Lett.* **1993**, *34*, 5109.
69. Yamawaki, M., Tsutsui, H., Kitagaki, S., Anada, M. and Hashimoto, S., *Tetrahedron Lett.* **2002**, *43*, 9561.
70. Saito, H., Oishi, H., Kitagaki, S., Nakamura, S., Anada, M. and Hashimoto, S., *Org. Lett.* **2002**, *4*, 3887.
71. Reddy, R. P., Lee, G. H. and Davies, H. M. L., *Org. Lett.* **2006**, *8*, 3437.
72. Reddy, R. P. and Davies, H. M. L., *Org. Lett.* **2006**, *8*, 5013.
73. Denton, J. R., Cheng, K. and L. Davies, H. M., *Chem. Commun.* **2008**, 1238.
74. Denton, J. R., Sukumaran, D. and Davies, H. M. L., *Org. Lett.* **2007**, *9*, 2625.
75. Denton, J. R. and Davies, H. M. L., *Org. Lett.* **2009**, *11*, 787.
76. Liao, K., Pickel, T. C., Boyarskikh, V., Bacsa, J., Musaev, D. G. and Davies, H. M. L., *Nature* **2017**, *551*, 609.
77. Fu, J., Ren, Z., Bacsa, J., Musaev, D. G. and Davies, H. M. L., *Nature* **2018**, *564*, 395.
78. Qin, C., Boyarskikh, V., Hansen, J. H., Hardcastle, K. I., Musaev, D. G. and Davies, H. M. L., *J. Am. Chem. Soc.* **2011**, *133*, 19198.
79. Qin, C. and Davies, H. M. L., *J. Am. Chem. Soc.* **2014**, *136*, 9792.
80. Guptill, D. M. and Davies, H. M. L., *J. Am. Chem. Soc.* **2014**, *136*, 17718.
81. Liao, K., Negretti, S., Musaev, D. G., Bacsa, J. and Davies, H. M. L., *Nature* **2016**, *533*, 230.
82. Liao, K., Yang, Y.-F., Li, Y., Sanders, J. N., Houk, K. N., Musaev, D. G. and Davies, H. M. L., *Nat. Chem.* **2018**, *10*, 1048.
83. Doyle, M. P., *Russ. Chem. Bull.* **1994**, *43*, 1770.
84. Hansen, J. and Davies, H. M. L., *Coord. Chem. Rev.* **2008**, *252*, 545.
85. Davies, H. M. L., Bruzinski, P. R., Lake, D. H., Kong, N. and Fall, M. J., *J. Am. Chem. Soc.* **1996**, *118*, 6897.
86. Ren, Z., Sunderland, T. L., Tortoreto, C., Yang, T., Berry, J. F., Musaev, D. G. and Davies, H. M. L., *ACS Catal.* **2018**, *8*, 10676.
87. Liao, K., Liu, W., Niemeyer, Z. L., Ren, Z., Bacsa, J., Musaev, D. G., Sigman, M. S. and Davies, H. M. L., *ACS Catal.* **2018**, *8*, 678.
88. DeAngelis, A., Dmitrenko, O., Yap, G. P. A. and Fox, J. M., *J. Am. Chem. Soc.* **2009**, *131*, 7230.
89. Lindsay, V. N. G., Lin, W. and Charette, A. B., *J. Am. Chem. Soc.* **2009**, *131*, 16383.
90. Prier, C. K., Zhang, R. K., Buller, A. R., Brinkmann-Chen, S. and Arnold, F. H., *Nat. Chem.* **2017**, *9*, 629.
91. Wang, H., Zhang, D. and Bolm, C., *Angew. Chem., Int. Ed.* **2018**, *57*, 5863.
92. Clark, J. R., Feng, K., Sookezian, A. and White, M. C., *Nat. Chem.* **2018**, *10*, 583.
93. Zhang, W., Chen, P. and Liu, G., *J. Am. Chem. Soc.* **2017**, *139*, 7709.
94. Kerr, J. A., *Chem. Rev.* **1966**, *66*, 465.
95. Ravelli, D., Fagnoni, M., Fukuyama, T., Nishikawa, T. and Ryu, I., *ACS Catal.* **2018**, *8*, 701.

96. Hartwig, J. F. and Larsen, M. A., *ACS Cent. Sci.* **2016**, *2*, 281.
97. Chepiga, K. M., Qin, C., Alford, J. S., Chennamadhavuni, S., Gregg, T. M., Olson, J. P. and Davies, H. M. L., *Tetrahedron* **2013**, *69*, 5765.
98. Minta, E., Boutonnet, C., Boutard, N., Martinez, J. and Rolland, V., *Tetrahedron Lett.* **2005**, *46*, 1795.
99. Doyle, M. P., Westrum, L. J., Wolthuis, W. N. E., See, M. M., Boone, W. P., Bagheri, V. and Pearson, M. M., *J. Am. Chem. Soc.* **1993**, *115*, 958.
100. Fraile, J. M., López-Ram-de-Viu, P., Mayoral, J. A., Roldán, M. and Santafé-Valero, J., *Org. Biomol. Chem.* **2011**, *9*, 6075.
101. Wang, Y. Expanding the scope of donor/acceptor carbenoid chemistry. *Emory University*, **2015**.
102. Davies, H. M. L., Yang, J. and Nikolai, J., *J. Organomet. Chem.* **2005**, *690*, 6111.
103. Nadeau, E., Li, Z., Morton, D. and Davies, H. M. L., *Synlett* **2009**, *2009*, 151.
104. Hansen, J., Autschbach, J. and Davies, H. M. L., *J. Org. Chem.* **2009**, *74*, 6555.
105. Negretti, S., Cohen, C. M., Chang, J. J., Guptill, D. M. and Davies, H. M. L., *Tetrahedron* **2015**, *71*, 7415.
106. Kurland, R. J., Rubin, M. B. and Wise, W. B., *J. Chem. Phys.* **1964**, *40*, 2426.
107. Kost, D., Carlson, E. H. and Raban, M., *J. Chem. Soc. D* **1971**, 656.
108. Fu, L., Wang, H. and Davies, H. M. L., *Org. Lett.* **2014**, *16*, 3036.
109. Shuklov, I. A., Dubrovina, N. V. and Börner, A., *Synthesis* **2007**, *2007*, 2925.
110. Wencel-Delord, J. and Colobert, F., *Org. Chem. Front.* **2016**, *3*, 394.
111. Colomer, I., Chamberlain, A. E. R., Haughey, M. B. and Donohoe, T. J., *Nat. Rev. Chem.* **2017**, *1*, 0088.
112. Doyle, M. P., Hu, W. and Timmons, D. J., *Org. Lett.* **2001**, *3*, 933.
113. Liu, W., Ren, Z., Bosse, A. T., Liao, K., Goldstein, E. L., Bacsá, J., Musaev, D. G., Stoltz, B. M. and Davies, H. M. L., *J. Am. Chem. Soc.* **2018**, *140*, 12247.
114. Vitaku, E., Smith, D. T. and Njardarson, J. T., *J. Med. Chem.* **2014**, *57*, 10257.
115. Taylor, R. D., MacCoss, M. and Lawson, A. D. G., *J. Med. Chem.* **2014**, *57*, 5845.
116. Goel, P., Alam, O., Naim, M. J., Nawaz, F., Iqbal, M. and Alam, M. I., *Eur. J. Med. Chem.* **2018**, *157*, 480.
117. Prashad, M., *Adv. Synth. Catal.* **2001**, *343*, 379.
118. Eicher, T., Hauptmann, S. and Speicher, A., *The chemistry of heterocycles: Structure, reactions, synthesis, and applications*. Wiley: Weinheim, Germany, **2003**.
119. Wolfe, J. P., *Synthesis of heterocycles via metal-catalyzed reactions that generate one or more carbon-heteroatom bonds*. Springer: Berlin, Heidelberg, **2013**.
120. Vo, C.-V. T. and Bode, J. W., *J. Org. Chem.* **2014**, *79*, 2809.
121. Shaw, M. H., Shurtleff, V. W., Terrett, J. A., Cuthbertson, J. D. and MacMillan, D. W. C., *Science* **2016**, *352*, 1304.
122. Jain, P., Verma, P., Xia, G. and Yu, J.-Q., *Nat. Chem.* **2016**, *9*, 140.
123. Coldham, I. and Leonori, D., *Org. Lett.* **2008**, *10*, 3923.
124. Campos, K. R., *Chem. Sci. Rev.* **2007**, *36*, 1069.
125. Peschiulli, A., Smout, V., Storr, T. E., Mitchell, E. A., Eliáš, Z., Herrebout, W., Berthelot, D., Meerpoel, L. and Maes, B. U. W., *Chem. – Eur. J.* **2013**, *19*, 10378.
126. McNally, A., Prier, C. K. and MacMillan, D. W. C., *Science* **2011**, *334*, 1114.
127. Le, C., Liang, Y., Evans, R. W., Li, X. and MacMillan, D. W. C., *Nature* **2017**, *547*, 79.

128. Payne, P. R., Garcia, P., Eisenberger, P., Yim, J. C. H. and Schafer, L. L., *Org. Lett.* **2013**, *15*, 2182.
129. Chen, W., Ma, L., Paul, A. and Seidel, D., *Nat. Chem.* **2017**, *10*, 165.
130. Paul, A. and Seidel, D., *J. Am. Chem. Soc.* **2019**, *141*, 8778.
131. Millet, A., Larini, P., Clot, E. and Baudoin, O., *Chem. Sci.* **2013**, *4*, 2241.
132. Zhang, J., Park, S. and Chang, S., *J. Am. Chem. Soc.* **2018**, *140*, 13209.
133. Gandhamsetty, N., Park, S. and Chang, S., *J. Am. Chem. Soc.* **2015**, *137*, 15176.
134. Park, S. and Chang, S., *Angew. Chem., Int. Ed.* **2017**, *56*, 7720.
135. Topczewski, J. J., Cabrera, P. J., Saper, N. I. and Sanford, M. S., *Nature* **2016**, *531*, 220.
136. Davies, H. M. L., Hansen, T., Hopper, D. W. and Panaro, S. A., *J. Am. Chem. Soc.* **1999**, *121*, 6509.
137. Babl, T. Synthesis of azepanes via heck-coupling driven ring-opening of cyclopropanated piperidines and the synthesis of ritalinTM-analogs via rhodium catalyzed cyclopropanation and c-h insertion chemistry. *Regensburg University*, **2018**.
138. Pils, L. K. A., Ertl, T. and Reiser, O., *Org. Lett.* **2017**, *19*, 2754.
139. Britton, J. and Jamison, T. F., *Nat. Protoc.* **2017**, *12*, 2423.
140. Baumann, M. and Baxendale, I. R., *Beilstein J. Org. Chem.* **2015**, *11*, 1194.
141. Britton, J. and Raston, C. L., *Chem. Sci. Rev.* **2017**, *46*, 1250.
142. Gérardy, R., Emmanuel, N., Toupy, T., Kassin, V.-E., Tshibalonza, N. N., Schmitz, M. and Monbaliu, J.-C. M., *Eur. J. Org. Chem.* **2018**, *2018*, 2301.
143. Gutmann, B., Cantillo, D. and Kappe, C. O., *Angew. Chem., Int. Ed.* **2015**, *54*, 6688.
144. Movsisyan, M., Delbeke, E. I. P., Berton, J. K. E. T., Battilocchio, C., Ley, S. V. and Stevens, C. V., *Chem. Sci. Rev.* **2016**, *45*, 4892.
145. Webb, D. and Jamison, T. F., *Chem. Sci.* **2010**, *1*, 675.
146. Hartman, R. L., McMullen, J. P. and Jensen, K. F., *Angew. Chem., Int. Ed.* **2011**, *50*, 7502.
147. Newman, S. G. and Jensen, K. F., *Green Chem.* **2013**, *15*, 1456.
148. Wörz, O., Jäckel, K.-P., Richter, T. and Wolf, A., *Chem. Eng. Technol.* **2001**, *24*, 138.
149. De Vos, D. E., Vankelecom, I. F. J. and Jacobs, P. A., *Chiral catalyst immobilization and recycling*. Wiley: Weinheim, Germany, **2000**.
150. Zhao, X. S., Bao, X. Y., Guo, W. and Lee, F. Y., *Mater. Today* **2006**, *9*, 32.
151. Sabater, S., Mata, J. A. and Peris, E., *ACS Catal.* **2014**, *4*, 2038.
152. Tornøe, C. W., Christensen, C. and Meldal, M., *J. Org. Chem.* **2002**, *67*, 3057.
153. Schätz, A., Long, T. R., Grass, R. N., Stark, W. J., Hanson, P. R. and Reiser, O., *Adv. Funct. Mater.* **2010**, *20*, 4323.
154. Fredriksen, K. A., Kristensen, T. E. and Hansen, T., *Beilstein J. Org. Chem.* **2012**, *8*, 1126.
155. Takeda, K., Oohara, T., Anada, M., Nambu, H. and Hashimoto, S., *Angew. Chem., Int. Ed.* **2010**, *49*, 6979.
156. Davies, H. M. L. and Liao, K., *Nat. Rev. Chem.* **2019**, *3*, 347.
157. Watanabe, Y., Washio, T., Shimada, N., Anada, M. and Hashimoto, S., *Chem. Commun.* **2010**, 7294.
158. Timmons, D. J. and Doyle, M. P., Chiral dirhodium(ii) catalysts and their applications. In *Multiple bonds between metal atoms*, Cotton, F. A., Murillo, C. A. and Walton, R. A., Eds. Springer US: Boston, MA, 2005; pp 591.
159. Bergbreiter, D. E., Morvant, M. and Chen, B., *Tetrahedron Lett.* **1991**, *32*, 2731.

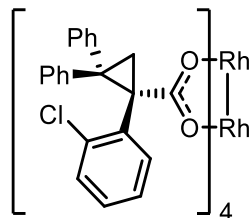
160. Doyle, M. P., Eismont, M. Y., Bergbreiter, D. E. and Gray, H. N., *J. Org. Chem.* **1992**, *57*, 6103.
161. Doyle, M. P., Timmons, D. J., Tumonis, J. S., Gau, H.-M. and Blossey, E. C., *Organometallics* **2002**, *21*, 1747.
162. Doyle, M. P., Yan, M., Gau, H.-M. and Blossey, E. C., *Org. Lett.* **2003**, *5*, 561.
163. Nagashima, T. and Davies, H. M. L., *Org. Lett.* **2002**, *4*, 1989.
164. Davies, H. M. L., Walji, A. M. and Nagashima, T., *J. Am. Chem. Soc.* **2004**, *126*, 4271.
165. Davies, H. M. L., *J. Mol. Catal. A: Chem.* **2002**, *189*, 125.
166. Davies, H. M. L. and Walji, A. M., *Org. Lett.* **2005**, *7*, 2941.
167. Takeda, K., Oohara, T., Shimada, N., Nambu, H. and Hashimoto, S., *Chem. – Eur. J.* **2011**, *17*, 13992.
168. Chepiga, K. M., Feng, Y., Brunelli, N. A., Jones, C. W. and Davies, H. M. L., *Org. Lett.* **2013**, *15*, 6136.
169. Moschetta, E. G., Negretti, S., Chepiga, K. M., Brunelli, N. A., Labreche, Y., Feng, Y., Rezaei, F., Lively, R. P., Koros, W. J., Davies, H. M. L. and Jones, C. W., *Angew. Chem., Int. Ed.* **2015**, *54*, 6470.
170. Yoo, C.-J., Rackl, D., Liu, W., Hoyt, C. B., Pimentel, B., Lively, R. P., Davies, H. M. L. and Jones, C. W., *Angew. Chem., Int. Ed.* **2018**, *57*, 10923.
171. Rackl, D., Yoo, C.-J., Jones, C. W. and Davies, H. M. L., *Org. Lett.* **2017**, *19*, 3055.
172. Rackl, D. *Overview (research summary)*; 2016.
173. Davies, H. M. L., Nagashima, T. and Klino, J. L., *Org. Lett.* **2000**, *2*, 823.
174. Hansch, C., Leo, A. and Taft, R. W., *Chem. Rev.* **1991**, *91*, 165.
175. Eliel, E. L., Wilen, S. H. and Mander, L. N., *Stereochemistry of organic compounds*. Wiley: New York, **1994**.
176. Ford, A., Miel, H., Ring, A., Slattery, C. N., Maguire, A. R. and McKervey, M. A., *Chem. Rev.* **2015**, *115*, 9981.
177. Bamford, W. R. and Stevens, T. S., *J. Chem. Soc.* **1952**, 4735.
178. Peng, C., Cheng, J. and Wang, J., *J. Am. Chem. Soc.* **2007**, *129*, 8708.
179. Fu, L., Mighion, J. D., Voight, E. A. and Davies, H. M. L., *Chem. – Eur. J.* **2017**, *23*, 3272.
180. Staudinger, H. and Gaule, A., *Chem. Ber.* **1916**, 1987.
181. Day, A. C., Raymond, P., Southam, R. M. and Whiting, M. C., *J. Chem. Soc. C* **1966**, 467.
182. Schroeder, W. and Katz, L., *J. Org. Chem.* **1954**, *19*, 718.
183. Morrison, H., Danishefsky, S. and Yates, P., *J. Org. Chem.* **1961**, *26*, 2617.
184. Doyle, M. P. and Yan, M., *J. Org. Chem.* **2002**, *67*, 602.
185. Nakagawa, K., Onoue, H. and Minami, K., *Chem. Commun.* **1966**, 730.
186. Tran, D. N., Battilocchio, C., Lou, S.-B., Hawkins, J. M. and Ley, S. V., *Chem. Sci.* **2015**, *6*, 1120.
187. Rullière, P., Benoit, G., Allouche, E. M. D. and Charette, A. B., *Angew. Chem., Int. Ed.* **2018**, *57*, 5777.
188. Holton, T. L. and Schechter, H., *J. Org. Chem.* **1995**, *60*, 4725.
189. Mitsuhiro, O. and Yukio, T., *Bull. Chem. Soc. Jpn.* **2002**, *75*, 2059.
190. Nicolaou, K. C., Mathison, C. J. N. and Montagnon, T., *J. Am. Chem. Soc.* **2004**, *126*, 5192.
191. Nicolle, S. M. and Moody, C. J., *Chem. – Eur. J.* **2014**, *20*, 4420.

192. Nicolle, S. M., Hayes, C. J. and Moody, C. J., *Chem. – Eur. J.* **2015**, *21*, 4576.
193. Javed, M. I. and Brewer, M., *Org. Lett.* **2007**, *9*, 1789.
194. Tsuji, J., Takahashi, H. and Kajimoto, T., *Tetrahedron Lett.* **1973**, *14*, 4573.
195. Ibata, T. and Singh, G. S., *Tetrahedron Lett.* **1994**, *35*, 2581.
196. Akira, N., Shigekazu, Y. and Teruo, M., *Chem. Lett.* **1986**, *15*, 505.
197. Davies, H. M. L., Cantrell, W. R. J., Romines, K. R. and Baum, J. S., *Org. Synth.* **1992**, *70*, 93.
198. Brodsky, B. H. and Du Bois, J., *Org. Lett.* **2004**, *6*, 2619.
199. Kitagaki, S., Yanamoto, Y., Tsutsui, H., Anada, M., Nakajima, M. and Hashimoto, S., *Tetrahedron Lett.* **2001**, *42*, 6361.
200. Alford, J. S. Expanding the scope of donor/acceptor carbenes and the synthesis of novel therapeutic agents for cocaine abuse. *Emory University*, **2014**.
201. Qu, Z., Shi, W. and Wang, J., *J. Org. Chem.* **2001**, *66*, 8139.
202. Wang, H., Li, G., Engle, K. M., Yu, J.-Q. and Davies, H. M. L., *J. Am. Chem. Soc.* **2013**, *135*, 6774.
203. Chan, W.-W., Yeung, S.-H., Zhou, Z., Chan, A. S. C. and Yu, W.-Y., *Org. Lett.* **2010**, *12*, 604.
204. Bess, E. N., Guptill, D. M., Davies, H. M. L. and Sigman, M. S., *Chem. Sci.* **2015**, *6*, 3057.
205. Mao, H., Lin, A., Shi, Y., Mao, Z., Zhu, X., Li, W., Hu, H., Cheng, Y. and Zhu, C., *Angew. Chem., Int. Ed.* **2013**, *52*, 6288.
206. Goosen, A. and McClelland, C. W., *J. Chem. Soc., Perkin Trans. 1* **1981**, 977.
207. Hale, K. J. and Wang, L., *Org. Lett.* **2014**, *16*, 2154.
208. Takasu, N., Oisaki, K. and Kanai, M., *Org. Lett.* **2013**, *15*, 1918.
209. Du, F.-T. and Ji, J.-X., *Chem. Sci.* **2012**, *3*, 460.
210. Pour, M., Špulák, M., Balšánek, V., Kuneš, J., Kubanová, P. and Buchta, V. r., *Bioorg. Med. Chem.* **2003**, *11*, 2843.
211. Alonazy, H. S., Al-Hazimi, H. M. A. and Korraa, M. M. S., *Arabian J. Chem.* **2009**, *2*, 101.
212. Meng, M., Wang, G., Yang, L., Cheng, K. and Qi, C., *Adv. Synth. Catal.* **2018**, *360*, 1218.
213. Gerard, B., Sangji, S., O'Leary, D. J. and Porco, J. A., *J. Am. Chem. Soc.* **2006**, *128*, 7754.
214. Álvarez-Calero, J. M., Jorge, Z. D. and Massanet, G. M., *Org. Lett.* **2016**, *18*, 6344.
215. Cahiez, G., Chaboche, C., Duplais, C. and Moyeux, A., *Org. Lett.* **2009**, *11*, 277.
216. Campo, B. J., Bevk, D., Kesters, J., Gilot, J., Bolink, H. J., Zhao, J., Bolsée, J.-C., Oosterbaan, W. D., Bertho, S., D'Haen, J., Manca, J., Lutsen, L., Van Assche, G., Maes, W., Janssen, R. A. J. and Vanderzande, D., *Org. Electron.* **2013**, *14*, 523.
217. Sheberla, D., Patra, S., Wijsboom, Y. H., Sharma, S., Sheynin, Y., Haj-Yahia, A.-E., Barak, A. H., Gidron, O. and Bendikov, M., *Chem. Sci.* **2015**, *6*, 360.
218. Davies, H. M. L. and Venkataramani, C., *Org. Lett.* **2003**, *5*, 1403.
219. Zhang, W. and Luo, M., *Chem. Commun.* **2016**, *52*, 2980.
220. Kweon, D.-H., Kim, H.-K., Kim, J.-J., Chung, H. A., Yoon, Y.-J., Lee, W. S. and Kim, S.-K., *J. Heterocycl. Chem.* **2002**, *39*, 203.
221. Zhou, G., Ting, P., Aslanian, R. and Piwinski, J. J., *Org. Lett.* **2008**, *10*, 2517.
222. Hahn, N. D., Nieger, M. and Dötz, K. H., *J. Organomet. Chem.* **2004**, *689*, 2662.

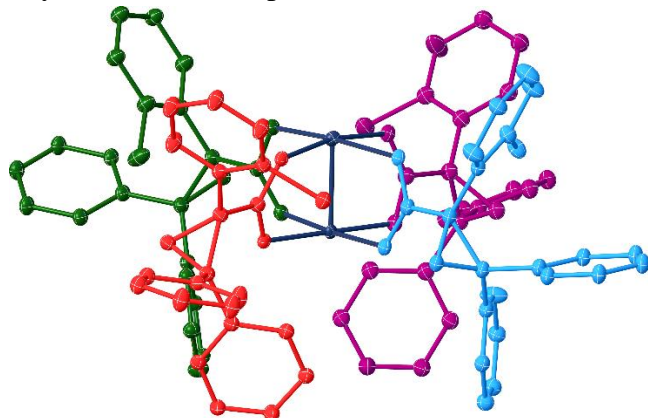
223. Marti, C. and Carreira, E. M., *J. Am. Chem. Soc.* **2005**, *127*, 11505.

Appendix: X-Ray Crystallographic Data

$\text{Rh}_2(\text{S-}o\text{-CITPCP})_4$ (27)



Crystal Data and Experimental



Experimental. Single blue prism-shaped crystals of (WL-NI-ROCT) were chosen from the sample as supplied. A suitable crystal ($0.32 \times 0.21 \times 0.09 \text{ mm}^3$) was selected and mounted on an Bruker D8 APEXII diffractometer. The crystal was cooled to $T = 100(2) \text{ K}$ during data collection. The structure was solved with the XT (Sheldrick, 2015) structure solution program using the Intrinsic Phasing solution method and by using Olex2 (Dolomanov et al., 2009) as the graphical interface. The model was refined with version 2017/1 of ShelXL (Sheldrick, 2015) using Least Squares minimisation.

Crystal Data. $\text{C}_{92}\text{H}_{76}\text{Cl}_4\text{O}_{10}\text{Rh}_2$, $M_r = 1689.14$, orthorhombic, $\text{P}2_12_12_1$ (No. 19), $a = 15.5416(5) \text{ \AA}$, $b = 22.2438(9) \text{ \AA}$, $c = 23.4880(12) \text{ \AA}$, $\alpha = \beta = \gamma = 90^\circ$, $V = 8119.9(6) \text{ \AA}^3$, $T = 100(2) \text{ K}$, $Z = 4$, $Z' = 1$, $(\text{MoK}\alpha) = 0.597 \text{ mm}^{-1}$, 43599 reflections measured, 16445 unique ($R_{int} = 0.0733$) which were used in all calculations. The final wR_2 was 0.2137 (all data) and R_1 was 0.1076 ($I > 2\sigma(I)$).

Compound	WL-NI-ROCT
Formula	C ₉₂ H ₇₆ Cl ₄ O ₁₀ Rh
	2
<i>D</i> _{calc.} / g cm ⁻³	1.382
/mm ⁻¹	0.597
Formula Weight	1689.14
Colour	blue
Shape	prism
Size/mm ³	0.32×0.21×0.09
<i>T</i> /K	100(2)
Crystal System	orthorhombic
Flack Parameter	-0.01(2)
Hooft Parameter	-0.000(13)
Space Group	P2 ₁ 2 ₁ 2 ₁
<i>a</i> /Å	15.5416(5)
<i>b</i> /Å	22.2438(9)
<i>c</i> /Å	23.4880(12)
<i>∠</i>	90
<i>∠</i>	90
<i>∠</i>	90
<i>V</i> /Å ³	8119.9(6)
<i>Z</i>	4
<i>Z</i> '	1
Wavelength/Å	0.710730
Radiation type	MoK
<i>min</i> / <i>∠</i>	1.571
<i>max</i> / <i>∠</i>	26.372
Measured Refl.	43599
Independent Refl.	16445
Reflections with <i>I</i> > 2(<i>I</i>)	13307
<i>R</i> _{int}	0.0733
Parameters	1345
Restraints	3774
Largest Peak	1.295
Deepest Hole	-1.219
GooF	1.142
<i>wR</i> ₂ (all data)	0.2137
<i>wR</i> ₂	0.2028
<i>R</i> ₁ (all data)	0.1316
<i>R</i> ₁	0.1076

Structure Quality Indicators

Reflections:	d min (Mo)	0.80	I/σ	12.3	Rint	7.33%	complete at $2\theta=53^\circ$	99%	
Refinement:	Shift	-0.006	Max Peak	1.3	Min Peak	-1.2	Goof	1.142	-0.01(2)

A blue prism-shaped crystal with dimensions $0.32 \times 0.21 \times 0.09 \text{ mm}^3$ was mounted on a loop with paratone oil. Data were collected using an Bruker D8 APEXII diffractometer equipped with an Oxford Cryosystems low-temperature device, operating at $T = 100(2) \text{ K}$.

Data were measured using ω and ϕ scans of 0.5° per frame for 60.0 s using MoK α radiation (fine-focus sealed X-ray tube, 45 kV, 35 mA). The total number of runs and images was based on the strategy calculation from the program **APEX2** (Bruker). The maximum resolution that was achieved was $d_{\text{min}} = 26.372^\circ$.

The diffraction patterns were indexed using CrysAlisPro (Agilent) and the unit cells were refined using CrysAlisPro (Agilent) on 18181 reflections, 42% of the observed reflections. Data reduction, scaling and absorption corrections were performed using CrysAlisPro (Agilent) and CrysAlisPro 1.171.39.28e (Rigaku Oxford Diffraction, 2015). An empirical absorption correction using spherical harmonics, implemented by the SCALE3 ABSPACK scaling algorithm was applied. The final completeness is 99.7% out to 26.372° in θ . The absorption coefficient μ of this material is 0.597 mm^{-1} at this wavelength ($\lambda = 0.71073 \text{ \AA}$) and the minimum and maximum transmissions are 0.42170 and 1.00000.

The structure was solved and the space group $P2_12_12_1$ (# 19) determined by the XT (Sheldrick, 2015) structure solution program using Intrinsic Phasing and refined by Least Squares using version 2017/1 of **ShelXL** (Sheldrick, 2015). All non-hydrogen atoms were refined anisotropically. Hydrogen atom positions were calculated geometrically and refined using the riding model.

There is a single molecule in the asymmetric unit, which is represented by the reported sum formula. In other words: Z is 4 and Z' is 1. **The molecule shows whole molecule disorder.**

The Flack parameter was refined to -0.01(2). Determination of absolute structure using Bayesian statistics on Bijvoet differences using the Olex2 results in -0.000(13). Note: The Flack parameter is used to determine chirality of the crystal studied, the value should be near 0, a value of 1 means that the stereochemistry is wrong and the model should be inverted. A value of 0.5 means that the crystal consists of a racemic mixture of the two enantiomers.

Images of the Crystal on the Diffractometer



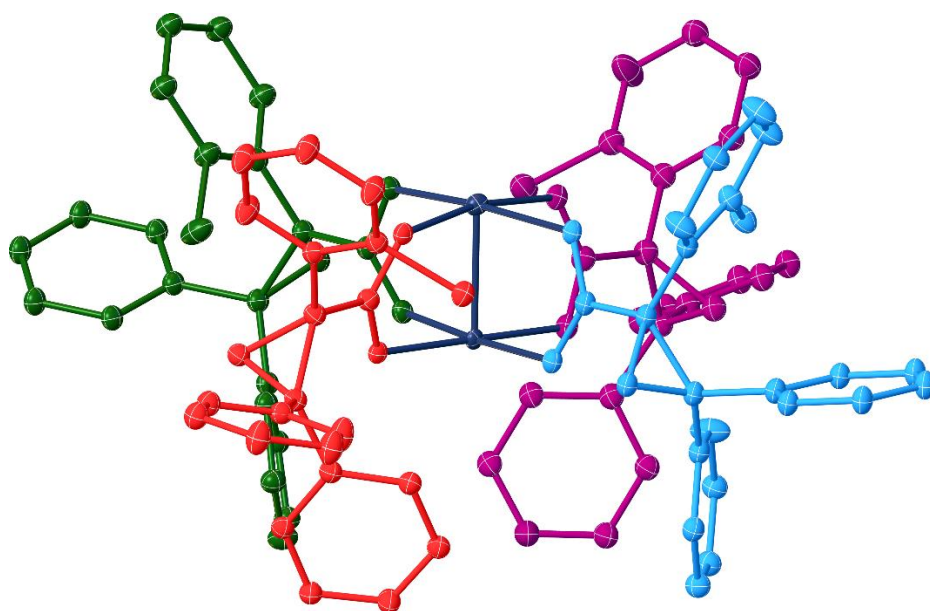
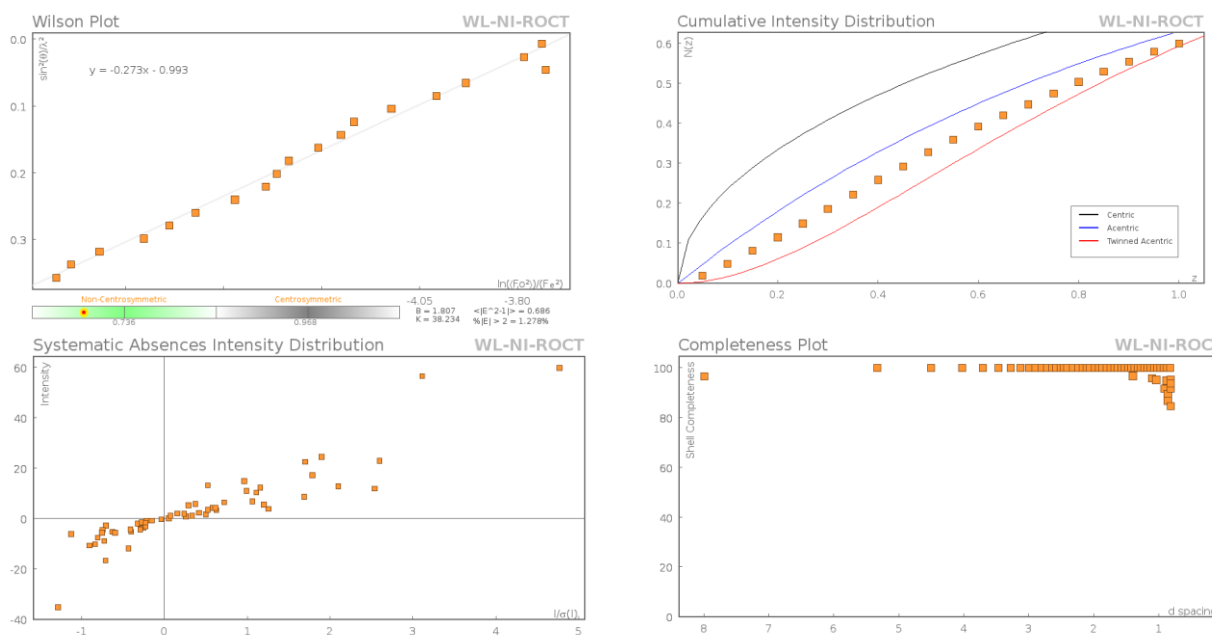
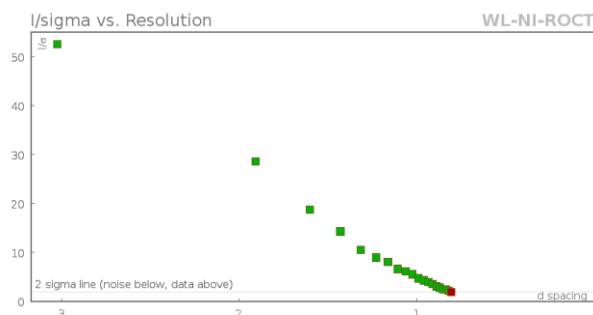


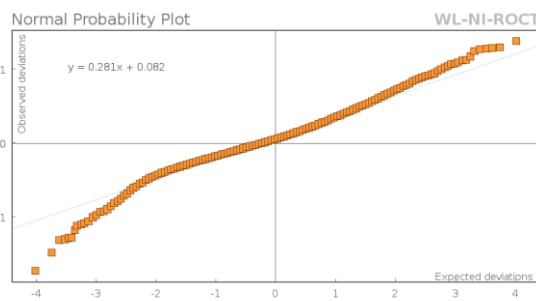
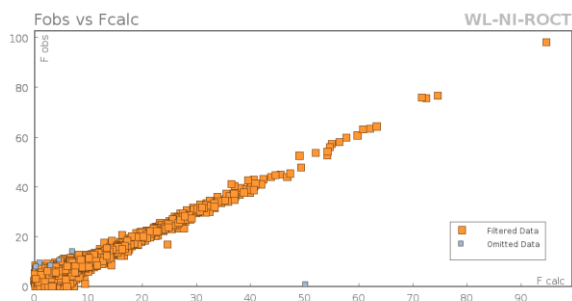
Figure 1: Plot of one of the disorder component with the axial ligands removed for clarity.

Data Plots: Diffraction Data





Data Plots: Refinement and Data



Reflection Statistics

Total reflections (after filtering)	43689	Unique reflections	16445
Completeness	0.991	Mean I/	12.27
hkl _{max} collected	(19, 27, 29)	hkl _{min} collected	(-18, -27, -29)
hkl _{max} used	(19, 27, 29)	hkl _{min} used	(-18, 0, 0)
Lim d _{max} collected	100.0	Lim d _{min} collected	0.36
d _{max} used	12.96	d _{min} used	0.8
Friedel pairs	11019	Friedel pairs merged	0
Inconsistent equivalents	81	R _{int}	0.0733
R _{sigma}	0.0967	Intensity transformed	0
Omitted reflections	0	Omitted by user (OMIT hkl)	22
Multiplicity	(28383, 7524, 86)	Maximum multiplicity	8
Removed systematic absences	68	Filtered off (Shel/OMIT)	0

Images of the Crystal on the Diffractometer



Table 1: Fractional Atomic Coordinates ($\times 10^4$) and Equivalent Isotropic Displacement Parameters ($\text{\AA}^2 \times 10^3$) for **WL-NI-ROCT**. U_{eq} is defined as 1/3 of the trace of the orthogonalised U_{ij} .

Atom	x	y	z	U_{eq}
Rh1	8961.7(7)	3929.0(6)	619.5(5)	23.9(3)
Rh2	8800.3(7)	4415.7(5)	1516.8(5)	20.6(2)
O1W	8607(8)	4837(6)	2419(5)	44(3)
Cl1_3	6516(7)	2643(5)	1446(5)	44(2)
O1_3	8610(40)	3156(11)	1061(8)	27(3)
O2_3	8690(40)	3612(7)	1917(9)	29.4(16)
C1_3	8540(30)	3163(9)	1604(9)	31.4(11)
C2_3	8360(14)	2591(7)	1916(6)	32.5(8)
C3_3	8017(12)	2635(7)	2548(7)	32.2(8)
C4_3	8924(12)	2477(12)	2442(9)	32.2(8)
C5_3	8040(10)	2048(6)	1601(4)	33.5(9)
C6_3	7217(9)	2031(6)	1374(3)	34.6(17)
C7_3	6916(14)	1521(8)	1079(6)	64(6)
C8_3	7441(15)	1035(9)	1014(7)	38.9(18)
C9_3	8270(15)	1045(8)	1239(6)	39.0(16)
C10_3	8569(12)	1551(7)	1533(5)	35.5(18)
C11_3	7792(9)	3219(7)	2838(7)	32.5(10)
C12_3	8137(9)	3340(8)	3365(7)	35(2)
C13_3	7961(11)	3863(10)	3653(9)	40(3)
C14_3	7425(14)	4283(10)	3413(12)	51(5)
C15_3	7071(17)	4179(11)	2890(12)	32(3)
C16_3	7250(15)	3648(10)	2598(10)	31(3)
C17_3	7392(13)	2138(8)	2740(7)	33.5(10)
C18_3	7679(15)	1550(9)	2831(6)	34.4(11)
C19_3	7124(17)	1103(9)	3031(6)	34.4(11)
C20_3	6271(17)	1241(11)	3143(7)	35.0(13)
C21_3	5967(14)	1816(12)	3058(8)	35.2(14)
C22_3	6537(14)	2260(10)	2856(8)	33.8(12)
Cl1_6	10780(8)	2598(9)	1449(6)	38.0(11)
O1_6	10189(16)	3765(16)	789(11)	25.3(19)
O2_6	10127(16)	4371(16)	1560(12)	26.5(17)
C1_6	10506(12)	4002(16)	1240(12)	27.8(9)
C2_6	11458(10)	3895(9)	1315(7)	28.4(7)
C3_6	11871(10)	3996(8)	1916(6)	28.5(7)
C4_6	11961(15)	4462(8)	1467(9)	28.4(8)

Atom	x	y	z	U_{eq}
C5_6	11840(8)	3425(7)	930(5)	28.5(8)
C6_6	11571(6)	2829(7)	962(4)	33(2)
C7_6	11916(10)	2377(9)	606(7)	45(2)
C8_6	12531(12)	2521(10)	218(8)	47(2)
C9_6	12812(12)	3114(10)	177(8)	34.3(16)
C10_6	12469(10)	3561(9)	530(7)	31.5(16)
C11_6	11368(8)	4107(7)	2455(6)	28.8(8)
C12_6	11446(8)	4639(7)	2746(6)	29.8(11)
C13_6	10999(10)	4756(9)	3239(7)	32.8(13)
C14_6	10450(11)	4330(10)	3455(8)	33.0(14)
C15_6	10352(14)	3794(10)	3179(9)	33.0(14)
C16_6	10808(12)	3680(9)	2681(8)	31(3)
C17_6	12713(11)	3660(9)	2058(10)	29.2(8)
C18_6	13472(12)	3994(10)	2136(15)	29.8(11)
C19_6	14239(13)	3718(11)	2306(15)	32.6(16)
C20_6	14264(13)	3097(11)	2340(16)	32.9(16)
C21_6	13519(14)	2760(10)	2308(16)	32.8(17)
C22_6	12747(14)	3048(9)	2144(15)	29.8(12)
C11_2	11345(7)	5249(5)	320(4)	29.6(9)
O1_2	9350(30)	4718(6)	247(10)	24(2)
O2_2	8950(30)	5203(6)	1046(9)	23.8(17)
C1_2	9250(30)	5195(7)	550(10)	27.4(11)
C2_2	9515(12)	5758(5)	249(7)	28.0(9)
C3_2	9701(11)	6348(6)	600(6)	28.6(9)
C4_2	8882(11)	6283(9)	289(9)	28.3(9)
C5_2	10003(9)	5695(4)	-303(6)	27.4(16)
C6_2	10836(8)	5468(3)	-311(6)	29(6)
C7_2	11300(12)	5406(6)	-824(7)	41(3)
C8_2	10937(14)	5569(8)	-1328(8)	41(3)
C9_2	10102(14)	5797(8)	-1331(8)	41(3)
C10_2	9644(12)	5858(6)	-821(7)	41(3)
C11_2	9695(15)	6391(9)	1242(6)	27(3)
C12_2	9253(19)	6854(11)	1499(8)	27.2(17)
C13_2	9170(20)	6901(12)	2080(9)	35(7)
C14_2	9520(20)	6463(13)	2421(9)	30(3)
C15_2	10000(20)	6009(14)	2184(8)	32(7)
C16_2	10060(20)	5956(12)	1595(8)	29(3)
C17_2	10422(9)	6746(4)	352(5)	29(4)
C18_2	10299(12)	7087(7)	-142(7)	32.1(17)

Atom	x	y	z	<i>U</i>_{eq}
C19_2	10946(13)	7450(9)	-373(9)	34.1(17)
C20_2	11736(13)	7474(9)	-104(10)	43(3)
C21_2	11885(13)	7145(10)	384(10)	43(3)
C22_2	11222(11)	6783(8)	608(9)	30(6)
Cl1_4	6527(4)	2856(3)	1120(3)	34.5(14)
O1_4	8490(20)	3142(7)	982(6)	27(3)
O2_4	8680(20)	3574(5)	1842(6)	29.4(16)
C1_4	8454(19)	3145(7)	1527(7)	31.4(11)
C2_4	8197(11)	2557(6)	1792(5)	32.4(9)
C3_4	7874(9)	2542(6)	2424(6)	32.2(8)
C4_4	8774(10)	2382(9)	2296(7)	32.2(8)
C5_4	7846(9)	2082(6)	1400(5)	33.5(9)
C6_4	7069(6)	2165(5)	1114(3)	34.6(17)
C7_4	6671(11)	1698(7)	802(6)	38.3(18)
C8_4	7051(12)	1148(8)	777(7)	39.6(19)
C9_4	7828(11)	1046(8)	1057(6)	39.0(16)
C10_4	8212(11)	1514(7)	1364(7)	35.5(18)
C11_4	7620(7)	3080(5)	2776(6)	32.5(10)
C12_4	7945(8)	3142(6)	3318(6)	35(2)
C13_4	7735(9)	3623(7)	3657(7)	40(3)
C14_4	7189(10)	4059(7)	3458(8)	39(5)
C15_4	6851(11)	4015(8)	2921(8)	32(3)
C16_4	7066(10)	3526(7)	2579(7)	31(3)
C17_4	7287(10)	2015(6)	2603(5)	33.5(10)
C18_4	7621(11)	1558(6)	2949(5)	34.4(11)
C19_4	7092(12)	1101(7)	3159(6)	34.4(11)
C20_4	6227(12)	1101(8)	3022(7)	35.0(13)
C21_4	5880(11)	1544(8)	2682(7)	35.2(14)
C22_4	6420(10)	2004(7)	2473(7)	33.8(12)
Cl1_1	11298(7)	5199(5)	453(4)	29.6(9)
O1_1	9370(30)	4756(6)	336(10)	24(2)
O2_1	8890(20)	5247(6)	1114(9)	23.8(17)
C1_1	9230(20)	5235(7)	630(10)	27.4(11)
C2_1	9538(12)	5816(6)	377(7)	28.0(9)
C3_1	9732(11)	6366(7)	775(6)	28.6(9)
C4_1	8925(11)	6350(9)	446(9)	28.3(9)
C5_1	10037(10)	5758(6)	-169(6)	27.4(10)
C6_1	10864(9)	5518(3)	-168(6)	27.4(12)
C7_1	11373(11)	5523(7)	-664(7)	41(3)

Atom	x	y	z	<i>U</i>_{eq}
C8_1	11068(14)	5765(8)	-1158(8)	41(3)
C9_1	10241(13)	6008(8)	-1166(8)	41(3)
C10_1	9735(12)	6002(8)	-674(7)	41(3)
C11_1	9688(15)	6357(9)	1419(6)	28.6(11)
C12_1	9171(18)	6767(11)	1694(8)	27.2(17)
C13_1	9070(20)	6767(12)	2278(9)	30(4)
C14_1	9460(20)	6326(14)	2596(9)	35(4)
C15_1	9980(20)	5915(14)	2338(9)	28.3(14)
C16_1	10110(20)	5935(13)	1753(8)	28.3(14)
C17_1	10466(11)	6783(6)	579(5)	29.0(11)
C18_1	10327(12)	7265(6)	208(5)	32.1(17)
C19_1	11000(13)	7641(7)	33(6)	34.1(17)
C20_1	11824(13)	7532(9)	234(8)	43(3)
C21_1	11986(12)	7062(10)	601(10)	43(3)
C22_1	11299(12)	6691(9)	770(9)	43(5)
C11_5	10880(7)	2583(9)	1443(5)	38.0(11)
O1_5	10227(15)	3737(14)	891(10)	25.3(19)
O2_5	10104(15)	4351(15)	1658(11)	26.5(17)
C1_5	10524(11)	4016(15)	1326(11)	27.8(9)
C2_5	11469(10)	3924(8)	1432(7)	28.4(7)
C3_5	11850(10)	3988(8)	2046(5)	28.5(7)
C4_5	11920(15)	4494(8)	1646(8)	28.4(8)
C5_5	11930(10)	3491(7)	1046(6)	28.5(8)
C6_5	11697(6)	2889(7)	1015(4)	33(2)
C7_5	12111(12)	2491(9)	635(8)	45(2)
C8_5	12751(13)	2697(10)	290(9)	47(2)
C9_5	12997(12)	3299(10)	313(8)	34.3(16)
C10_5	12584(11)	3691(9)	690(8)	41(4)
C11_5	11337(8)	3992(6)	2592(6)	28.8(8)
C12_5	11529(9)	4406(6)	3006(6)	29.8(11)
C13_5	11090(10)	4436(7)	3514(7)	32.8(13)
C14_5	10432(12)	4038(9)	3616(8)	33.0(14)
C15_5	10219(14)	3617(10)	3215(9)	33.0(14)
C16_5	10668(12)	3592(9)	2703(8)	50(4)
C17_5	12683(10)	3633(7)	2182(4)	29.2(8)
C18_5	13503(11)	3869(8)	2083(5)	29.8(11)
C19_5	14249(12)	3541(9)	2209(6)	32.6(16)
C20_5	14175(12)	2969(9)	2436(7)	32.9(16)
C21_5	13379(13)	2721(9)	2539(9)	32.8(17)

Atom	x	y	z	<i>U</i>_{eq}
C22_5	12639(12)	3060(8)	2409(8)	29.8(12)
Cl1_7	7023(6)	5530(5)	1(4)	46.7(15)
O1_7	7707(13)	4104(12)	457(8)	28.6(12)
O2_7	7504(10)	4414(9)	1370(6)	27.5(14)
C1_7	7272(11)	4355(17)	858(7)	28.6(10)
C2_7	6344(9)	4470(9)	712(6)	29.1(7)
C3_7	5781(10)	4892(8)	1098(6)	29.0(7)
C4_7	5705(14)	4234(8)	1154(9)	29.0(7)
C5_7	6127(10)	4469(7)	89(6)	29.2(9)
C6_7	6404(6)	4932(6)	-261(6)	36.1(13)
C7_7	6199(7)	4940(7)	-844(6)	36.1(13)
C8_7	5720(7)	4487(7)	-1073(7)	36.1(13)
C9_7	5433(9)	4016(8)	-730(8)	36.1(13)
C10_7	5641(11)	4012(8)	-151(7)	36.1(13)
C11_7	6173(12)	5277(10)	1561(7)	29.3(9)
C12_7	5806(17)	5300(15)	2090(8)	30.7(15)
C13_7	6138(17)	5637(13)	2531(8)	33(2)
C14_7	6844(18)	5993(14)	2431(9)	37(4)
C15_7	7232(16)	5983(13)	1910(10)	32(2)
C16_7	6913(15)	5623(14)	1471(9)	30.3(19)
C17_7	5041(9)	5221(8)	792(4)	29.3(8)
C18_7	4330(10)	4901(9)	583(5)	30.2(13)
C19_7	3651(10)	5191(9)	304(6)	33.3(15)
C20_7	3682(11)	5808(9)	232(7)	33.5(15)
C21_7	4373(12)	6135(9)	433(8)	33.1(15)
C22_7	5055(11)	5838(8)	715(7)	29.9(11)
Cl1_8	7028(8)	5289(6)	-116(5)	46.7(15)
O1_8	7699(16)	4211(15)	460(8)	28.6(12)
O2_8	7491	4450.8	1388.5	27.5(14)
C1_8	7223(12)	4330(20)	897(7)	28.6(10)
C2_8	6292(10)	4419(10)	757(6)	29.1(7)
C3_8	5731(12)	4879(9)	1099(7)	29.0(7)
C4_8	5633(16)	4226(10)	1204(9)	29.0(7)
C5_8	6048(15)	4302(9)	146(6)	28.9(9)
C6_8	6310(20)	4704(13)	-272(7)	40(3)
C7_8	6060(20)	4625(13)	-843(8)	36.1(13)
C8_8	5510(20)	4176(14)	-982(9)	36.1(13)
C9_8	5240(20)	3766(13)	-570(10)	36.1(13)
C10_8	5510(20)	3832(12)	-5(9)	32.0(16)

Atom	x	y	z	U_{eq}
C11_8	6026(14)	5258(12)	1598(8)	29.3(9)
C12_8	5590(20)	5203(17)	2103(10)	30.7(15)
C13_8	5790(20)	5534(16)	2577(9)	33(2)
C14_8	6500(20)	5903(16)	2568(11)	35(4)
C15_8	6987(19)	5944(16)	2083(11)	32(2)
C16_8	6728(19)	5646(16)	1589(10)	30.3(19)
C17_8	5052(10)	5218(8)	745(5)	29.3(8)
C18_8	4242(11)	4978(8)	618(5)	30.2(13)
C19_8	3633(12)	5295(10)	296(6)	33.3(15)
C20_8	3831(14)	5863(10)	94(8)	33.5(15)
C21_8	4623(15)	6114(10)	211(10)	33.1(15)
C22_8	5227(13)	5788(9)	536(8)	29.9(11)
O3_9	9180(20)	3543(13)	-308(7)	77(4)
C24_9	8560(30)	4407(19)	-862(19)	77(4)
C25_9	9300(20)	3990(17)	-737(17)	77(4)
C26_9	9942(19)	3191(14)	-260(20)	77(4)
C27_9	9690(30)	2551(13)	-100(20)	77(4)
O3_10	9070(30)	3518(11)	-307(7)	77(4)
C24_10	7970(20)	4050(20)	-914(19)	77(4)
C25_10	8890(20)	3846(15)	-815(7)	77(4)
C26_10	9420(30)	2949(13)	-447(11)	77(4)
C27_10	9940(30)	2716(19)	57(17)	77(4)

Table 2 Anisotropic Displacement Parameters ($\times 10^4$) **WL-NI-ROCT**. The anisotropic displacement factor exponent takes the form: $-2^2 [h^2 a^{*2} \times U_{11} + \dots + 2hka^* \times b^* \times U_{12}]$

Atom	U_{11}	U_{22}	U_{33}	U_{23}	U_{13}	U_{12}
Rh1	16.0(5)	31.2(6)	24.7(6)	0.3(5)	0.3(5)	-3.8(5)
Rh2	14.8(5)	23.2(5)	23.8(6)	0.2(5)	-4.4(5)	0.8(4)
O1W	59(9)	47(6)	26(4)	-12(5)	-8(6)	-7(6)
Cl1_3	39(2)	41(2)	53(5)	-8(3)	-9(3)	2.7(19)
O1_3	18(8)	32.6(18)	30.3(17)	3.9(12)	2.1(18)	1(3)
O2_3	26(4)	32.3(12)	29.5(18)	4.8(14)	2(2)	1.1(16)
C1_3	31(3)	33.2(12)	30.3(17)	4.0(11)	3.3(16)	-0.8(13)
C2_3	33.2(17)	33.2(11)	31.0(15)	4.2(10)	3.5(13)	-1.3(11)
C3_3	33.0(16)	32.4(13)	31.2(15)	4.5(11)	3.9(13)	-1.3(12)
C4_3	32.9(16)	32.7(17)	31.0(16)	4.6(12)	3.7(13)	-1.4(12)
C5_3	35.2(15)	33.7(12)	31.5(18)	3.8(12)	3.3(14)	-2.1(10)
C6_3	35.7(16)	35.5(14)	33(4)	3.0(17)	2.4(19)	-2.2(12)
C7_3	47(3)	48(3)	97(13)	-26(6)	-24(5)	9(3)

Atom	U_{11}	U_{22}	U_{33}	U_{23}	U_{13}	U_{12}
C8_3	38.9(18)	37.3(16)	41(3)	-0.7(18)	-0.9(18)	-0.6(12)
C9_3	39.1(18)	36.2(14)	42(3)	-1.3(15)	-1.3(18)	-0.1(13)
C10_3	37.0(17)	34.5(13)	35(4)	1.8(18)	2(2)	-1.0(12)
C11_3	34(2)	32.3(14)	31.0(16)	4.8(12)	4.5(15)	-1.2(13)
C12_3	40(5)	33(2)	32(2)	3.8(19)	2(3)	1(3)
C13_3	50(6)	35(3)	34(2)	2(2)	-2(3)	5(3)
C14_3	72(9)	42(3)	40(4)	-5(3)	-13(5)	18(5)
C15_3	36(6)	32(2)	29(3)	6(2)	7(3)	-1(3)
C16_3	32(5)	32(2)	29(2)	5.7(19)	7(3)	-2(3)
C17_3	33.3(17)	32.3(14)	35(3)	5.1(13)	5.1(17)	-1.1(13)
C18_3	33.6(18)	32.6(14)	37(3)	6.0(15)	5.3(18)	-0.9(13)
C19_3	33.6(18)	32.6(14)	37(3)	6.0(15)	5.3(18)	-0.9(13)
C20_3	33.5(18)	32.9(17)	39(3)	6.5(18)	5.5(19)	-0.8(13)
C21_3	33.2(17)	33.0(17)	39(4)	6.7(19)	5.4(18)	-0.9(13)
C22_3	33.3(17)	32.5(17)	36(3)	5.2(17)	5.2(17)	-1.1(13)
C11_6	38(2)	28.6(15)	48(2)	1.7(14)	11.7(17)	0.2(16)
O1_6	25.8(15)	24(4)	27(2)	7(3)	-1.2(15)	-0.7(16)
O2_6	26.3(15)	26(3)	28(3)	6(3)	-1.8(13)	0.2(15)
C1_6	26.4(12)	28.0(15)	29.0(16)	4.2(14)	-2.4(11)	0.9(10)
C2_6	26.5(12)	28.9(12)	29.8(13)	3.7(11)	-2.6(10)	1.1(9)
C3_6	26.7(12)	29.0(12)	29.8(13)	3.7(10)	-2.8(10)	1.5(10)
C4_6	26.3(13)	28.9(11)	30.0(14)	3.7(10)	-2.9(12)	1.3(10)
C5_6	26.3(14)	29.2(11)	30.0(14)	3.5(10)	-2.8(11)	1.2(10)
C6_6	31(3)	29.6(11)	38(3)	1.5(13)	4(3)	-0.2(13)
C7_6	46(4)	31.8(12)	56(4)	-4.8(15)	20(3)	-5.8(15)
C8_6	50(4)	33.0(13)	58(4)	-7.1(17)	23(3)	-8.2(16)
C9_6	33(2)	31.7(14)	38(2)	-1.7(15)	5(2)	-3.4(14)
C10_6	31(2)	30.5(13)	33(2)	0.7(13)	1(2)	-1.7(13)
C11_6	27.5(14)	29.0(15)	30.0(13)	3.6(11)	-2.5(11)	1.5(11)
C12_6	30(2)	29.4(16)	30.1(14)	3.3(13)	-2.0(14)	0.6(14)
C13_6	35(3)	31(2)	32.3(15)	1.3(15)	1.4(17)	-2.3(17)
C14_6	35(3)	31(2)	33.2(17)	1.1(15)	2.1(18)	-2.2(19)
C15_6	34(2)	31(2)	33.6(18)	0.6(15)	2.5(18)	-2(2)
C16_6	32(6)	30(2)	32(3)	2(2)	1(4)	-1(3)
C17_6	26.8(12)	30.0(14)	30.9(17)	4.7(14)	-2.7(11)	1.7(10)
C18_6	26.7(12)	30.3(15)	32(3)	5.3(16)	-3.0(12)	1.6(11)
C19_6	26.8(12)	31.2(18)	40(4)	8(2)	-3.8(14)	1.4(12)
C20_6	26.7(13)	31.3(18)	41(4)	8(2)	-3.4(16)	1.6(12)
C21_6	26.7(14)	31.1(17)	41(5)	8(2)	-3.3(17)	1.6(11)

Atom	U_{11}	U_{22}	U_{33}	U_{23}	U_{13}	U_{12}
C22_6	26.6(13)	30.1(14)	33(3)	5.2(15)	-2.5(14)	1.8(11)
Cl1_2	23.4(17)	36(2)	29.7(14)	4.3(15)	2.1(11)	0.8(16)
O1_2	20(5)	27.4(13)	25(3)	0.2(14)	-3(3)	2.0(14)
O2_2	18(4)	27.5(17)	25.5(16)	0.2(13)	-4(2)	3(2)
C1_2	27.1(17)	27.7(12)	27.4(15)	-0.4(9)	0.2(11)	1.1(9)
C2_2	28.3(13)	27.6(12)	27.9(11)	-0.4(8)	0.5(8)	0.8(8)
C3_2	29.9(13)	27.8(13)	28.1(12)	-0.6(8)	0.2(9)	0.7(9)
C4_2	29.5(13)	27.6(14)	27.7(14)	-0.6(11)	0.6(9)	1.2(9)
C5_2	27(2)	27(2)	27.7(17)	0.2(13)	0.2(11)	0.2(14)
C6_2	27(4)	31(15)	30(3)	4(6)	2(3)	1(7)
C7_2	32.3(18)	59(7)	30.3(12)	9(2)	3.6(12)	13(3)
C8_2	32.3(18)	59(7)	30.3(12)	9(2)	3.6(12)	13(3)
C9_2	32.3(18)	59(7)	30.3(12)	9(2)	3.6(12)	13(3)
C10_2	32.3(18)	59(7)	30.3(12)	9(2)	3.6(12)	13(3)
C11_2	25(8)	26(5)	29(2)	-1(2)	0(3)	-3(5)
C12_2	27(3)	27(2)	27.8(13)	-1.2(12)	-0.7(15)	-1(2)
C13_2	45(17)	31(9)	28(3)	-2(4)	0(4)	5(10)
C14_2	30(4)	30(4)	29(3)	0(2)	0(3)	-1(3)
C15_2	36(14)	32(9)	29(3)	0(4)	1(5)	2(10)
C16_2	29(3)	29(3)	29(3)	0.0(14)	0.0(14)	-0.1(14)
C17_2	30(4)	28(7)	31(6)	0(5)	1(4)	1(5)
C18_2	31.4(15)	32(2)	33(3)	3(2)	-0.9(15)	-1.5(13)
C19_2	31.8(15)	34(2)	36(3)	5(2)	-1.5(15)	-2.4(14)
C20_2	32.5(15)	44(4)	51(7)	17(5)	-5(2)	-5.2(16)
C21_2	32.5(15)	44(4)	51(7)	17(5)	-5(2)	-5.2(16)
C22_2	31(4)	23(11)	36(9)	1(8)	-1(5)	1(6)
Cl1_4	32(2)	34.9(16)	37(4)	0.9(18)	-2(2)	-4.1(16)
O1_4	18(8)	32.6(18)	30.3(17)	3.9(12)	2.1(18)	1(3)
O2_4	26(4)	32.3(12)	29.5(18)	4.8(14)	2(2)	1.1(16)
C1_4	31(3)	33.2(12)	30.3(17)	4.0(11)	3.3(16)	-0.8(13)
C2_4	33.0(19)	33.2(12)	31.0(15)	4.1(11)	3.6(13)	-1.2(12)
C3_4	33.0(16)	32.4(13)	31.2(15)	4.5(11)	3.9(13)	-1.3(12)
C4_4	32.9(16)	32.7(17)	31.0(16)	4.6(12)	3.7(13)	-1.4(12)
C5_4	35.2(15)	33.7(12)	31.5(18)	3.8(12)	3.3(14)	-2.1(10)
C6_4	35.7(16)	35.5(14)	33(4)	3.0(17)	2.4(19)	-2.2(12)
C7_4	38(2)	36.8(16)	40(3)	-0.4(16)	-1(2)	-0.9(13)
C8_4	40(2)	37.3(16)	42(3)	-1.1(17)	-2(2)	-0.2(14)
C9_4	39.1(18)	36.2(14)	42(3)	-1.3(15)	-1.3(18)	-0.1(13)
C10_4	37.0(17)	34.5(13)	35(4)	1.8(18)	2(2)	-1.0(12)

Atom	U_{11}	U_{22}	U_{33}	U_{23}	U_{13}	U_{12}
C11_4	34(2)	32.3(14)	31.0(16)	4.8(12)	4.5(15)	-1.2(13)
C12_4	40(5)	33(2)	32(2)	3.8(19)	2(3)	1(3)
C13_4	50(6)	35(3)	34(2)	2(2)	-2(3)	5(3)
C14_4	49(9)	35(4)	32(3)	3(3)	1(4)	5(6)
C15_4	36(6)	32(2)	29(3)	6(2)	7(3)	-1(3)
C16_4	32(5)	32(2)	29(2)	5.7(19)	7(3)	-2(3)
C17_4	33.3(17)	32.3(14)	35(3)	5.1(13)	5.1(17)	-1.1(13)
C18_4	33.6(18)	32.6(14)	37(3)	6.0(15)	5.3(18)	-0.9(13)
C19_4	33.6(18)	32.6(14)	37(3)	6.0(15)	5.3(18)	-0.9(13)
C20_4	33.5(18)	32.9(17)	39(3)	6.5(18)	5.5(19)	-0.8(13)
C21_4	33.2(17)	33.0(17)	39(4)	6.7(19)	5.4(18)	-0.9(13)
C22_4	33.3(17)	32.5(17)	36(3)	5.2(17)	5.2(17)	-1.1(13)
Cl1_1	23.4(17)	36(2)	29.7(14)	4.3(15)	2.1(11)	0.8(16)
O1_1	20(5)	27.4(13)	25(3)	0.2(14)	-3(3)	2.0(14)
O2_1	18(4)	27.5(17)	25.5(16)	0.2(13)	-4(2)	3(2)
C1_1	27.1(17)	27.7(12)	27.4(15)	-0.4(9)	0.2(11)	1.1(9)
C2_1	28.3(13)	27.6(12)	27.9(11)	-0.4(8)	0.5(8)	0.8(8)
C3_1	29.9(13)	27.8(13)	28.1(12)	-0.6(8)	0.2(9)	0.7(9)
C4_1	29.5(13)	27.6(14)	27.7(14)	-0.6(11)	0.6(9)	1.2(9)
C5_1	27.0(12)	27.7(14)	27.6(11)	-0.4(8)	-0.2(8)	0.4(9)
C6_1	27.0(12)	27.2(19)	27.9(12)	-0.3(10)	0.0(8)	0.2(10)
C7_1	32.3(18)	59(7)	30.3(12)	9(2)	3.6(12)	13(3)
C8_1	32.3(18)	59(7)	30.3(12)	9(2)	3.6(12)	13(3)
C9_1	32.3(18)	59(7)	30.3(12)	9(2)	3.6(12)	13(3)
C10_1	32.3(18)	59(7)	30.3(12)	9(2)	3.6(12)	13(3)
C11_1	29.5(18)	28.3(16)	28.1(12)	-0.5(9)	0.2(9)	0.5(14)
C12_1	27(3)	27(2)	27.8(13)	-1.2(12)	-0.7(15)	-1(2)
C13_1	31(8)	30(4)	27.9(13)	-0.7(14)	-0.2(18)	2(6)
C14_1	41(7)	36(4)	28.5(15)	1.2(15)	2.0(19)	10(5)
C15_1	28(2)	28.4(18)	28.3(13)	-0.2(9)	0.2(9)	-0.1(12)
C16_1	28.4(19)	28.1(17)	28.3(13)	-0.2(9)	0.2(9)	-0.2(12)
C17_1	30.9(14)	28.7(16)	27(2)	-1.3(13)	0.3(12)	-0.5(11)
C18_1	31.4(15)	32(2)	33(3)	3(2)	-0.9(15)	-1.5(13)
C19_1	31.8(15)	34(2)	36(3)	5(2)	-1.5(15)	-2.4(14)
C20_1	32.5(15)	44(4)	51(7)	17(5)	-5(2)	-5.2(16)
C21_1	32.5(15)	44(4)	51(7)	17(5)	-5(2)	-5.2(16)
C22_1	32.1(15)	44(6)	53(10)	19(8)	-5(3)	-5(2)
Cl1_5	38(2)	28.6(15)	48(2)	1.7(14)	11.7(17)	0.2(16)
O1_5	25.8(15)	24(4)	27(2)	7(3)	-1.2(15)	-0.7(16)

Atom	U_{11}	U_{22}	U_{33}	U_{23}	U_{13}	U_{12}
O2_5	26.3(15)	26(3)	28(3)	6(3)	-1.8(13)	0.2(15)
C1_5	26.4(12)	28.0(15)	29.0(16)	4.2(14)	-2.4(11)	0.9(10)
C2_5	26.5(12)	28.9(12)	29.8(13)	3.7(11)	-2.6(10)	1.1(9)
C3_5	26.7(12)	29.0(12)	29.8(13)	3.7(10)	-2.8(10)	1.5(10)
C4_5	26.3(13)	28.9(11)	30.0(14)	3.7(10)	-2.9(12)	1.3(10)
C5_5	26.3(14)	29.2(11)	30.0(14)	3.5(10)	-2.8(11)	1.2(10)
C6_5	31(3)	29.6(11)	38(3)	1.5(13)	4(3)	-0.2(13)
C7_5	46(4)	31.8(12)	56(4)	-4.8(15)	20(3)	-5.8(15)
C8_5	50(4)	33.0(13)	58(4)	-7.1(17)	23(3)	-8.2(16)
C9_5	33(2)	31.7(14)	38(2)	-1.7(15)	5(2)	-3.4(14)
C10_5	44(5)	31.9(14)	48(5)	-4(2)	15(5)	-6.0(19)
C11_5	27.5(14)	29.0(15)	30.0(13)	3.6(11)	-2.5(11)	1.5(11)
C12_5	30(2)	29.4(16)	30.1(14)	3.3(13)	-2.0(14)	0.6(14)
C13_5	35(3)	31(2)	32.3(15)	1.3(15)	1.4(17)	-2.3(17)
C14_5	35(3)	31(2)	33.2(17)	1.1(15)	2.1(18)	-2.2(19)
C15_5	34(2)	31(2)	33.6(18)	0.6(15)	2.5(18)	-2(2)
C16_5	54(5)	55(5)	42(2)	-13(3)	15(3)	-25(5)
C17_5	26.8(12)	30.0(14)	30.9(17)	4.7(14)	-2.7(11)	1.7(10)
C18_5	26.7(12)	30.3(15)	32(3)	5.3(16)	-3.0(12)	1.6(11)
C19_5	26.8(12)	31.2(18)	40(4)	8(2)	-3.8(14)	1.4(12)
C20_5	26.7(13)	31.3(18)	41(4)	8(2)	-3.4(16)	1.6(12)
C21_5	26.7(14)	31.1(17)	41(5)	8(2)	-3.3(17)	1.6(11)
C22_5	26.6(13)	30.1(14)	33(3)	5.2(15)	-2.5(14)	1.8(11)
C11_7	59(3)	48(2)	33.2(16)	3.9(15)	-9.9(17)	-19(2)
O1_7	23.4(16)	31(3)	30.9(13)	-1.5(16)	-1.1(11)	4.3(16)
O2_7	22.9(16)	29(4)	30.7(13)	-0.8(16)	-0.6(11)	3.2(18)
C1_7	23.4(13)	31(3)	31.0(12)	-1.6(13)	-1(1)	4.3(12)
C2_7	23.4(13)	32.3(14)	31.5(11)	-1.9(10)	-1.2(9)	4.5(11)
C3_7	23.4(13)	32.1(13)	31.3(11)	-1.9(10)	-1.3(9)	4.4(11)
C4_7	23.3(14)	32.1(13)	31.5(12)	-2(1)	-1.3(10)	4.3(11)
C5_7	23.0(17)	33.3(16)	31.4(11)	-1.9(10)	-1(1)	4.3(13)
C6_7	38(2)	38.7(18)	32.1(11)	0.2(10)	-4.4(11)	-4.5(17)
C7_7	38(2)	38.7(18)	32.1(11)	0.2(10)	-4.4(11)	-4.5(17)
C8_7	38(2)	38.7(18)	32.1(11)	0.2(10)	-4.4(11)	-4.5(17)
C9_7	38(2)	38.7(18)	32.1(11)	0.2(10)	-4.4(11)	-4.5(17)
C10_7	38(2)	38.7(18)	32.1(11)	0.2(10)	-4.4(11)	-4.5(17)
C11_7	24.8(15)	31.9(15)	31.2(12)	-1.6(11)	-1.3(10)	3.9(12)
C12_7	27(2)	33(2)	31.8(12)	-2.6(13)	-0.2(13)	1.9(18)
C13_7	30(3)	36(4)	32.1(13)	-3.6(18)	0.8(16)	-1(3)

Atom	U_{11}	U_{22}	U_{33}	U_{23}	U_{13}	U_{12}
C14_7	35(4)	44(6)	32.7(18)	-6(3)	2(2)	-7(5)
C15_7	29(3)	37(4)	31.1(16)	-2(2)	-0.8(16)	-1(3)
C16_7	26(2)	34(3)	31.0(15)	-1.6(18)	-1.4(15)	2(3)
C17_7	23.2(14)	33.2(14)	31.4(15)	-1.1(12)	-0.8(11)	4.6(11)
C18_7	23.9(15)	33.9(15)	33(3)	0.3(15)	-2.0(15)	3.8(13)
C19_7	24.5(15)	35.9(18)	39(3)	4(2)	-4.1(18)	2.6(14)
C20_7	23.6(17)	35.9(18)	41(3)	4(2)	-3.6(18)	2.9(14)
C21_7	23.1(18)	35.3(17)	41(4)	3.4(19)	-3.0(19)	3.5(13)
C22_7	22.4(16)	33.3(14)	34(2)	-0.3(14)	-0.7(14)	4.8(11)
Cl1_8	59(3)	48(2)	33.2(16)	3.9(15)	-9.9(17)	-19(2)
O1_8	23.4(16)	31(3)	30.9(13)	-1.5(16)	-1.1(11)	4.3(16)
O2_8	22.9(16)	29(4)	30.7(13)	-0.8(16)	-0.6(11)	3.2(18)
C1_8	23.4(13)	31(3)	31.0(12)	-1.6(13)	-1(1)	4.3(12)
C2_8	23.4(13)	32.3(14)	31.5(11)	-1.9(10)	-1.2(9)	4.5(11)
C3_8	23.4(14)	32.1(13)	31.3(11)	-1.9(10)	-1.3(10)	4.4(11)
C4_8	23.3(14)	32.1(13)	31.5(12)	-2(1)	-1.3(10)	4.3(11)
C5_8	24.4(16)	30.8(16)	31.5(11)	-1.9(10)	-1.6(10)	5.6(13)
C6_8	47(7)	41(4)	32.5(11)	1.2(14)	-6.2(16)	-10(5)
C7_8	38(2)	38.7(18)	32.1(11)	0.2(10)	-4.4(11)	-4.5(17)
C8_8	38(2)	38.7(18)	32.1(11)	0.2(10)	-4.4(11)	-4.5(17)
C9_8	38(2)	38.7(18)	32.1(11)	0.2(10)	-4.4(11)	-4.5(17)
C10_8	30(3)	34(2)	31.8(11)	-1.1(11)	-2.7(12)	1(2)
C11_8	24.8(15)	31.9(15)	31.2(12)	-1.6(11)	-1.3(10)	3.9(12)
C12_8	27(2)	33(2)	31.8(12)	-2.6(13)	-0.2(13)	1.9(18)
C13_8	30(3)	36(4)	32.1(13)	-3.6(18)	0.8(16)	-1(3)
C14_8	32(4)	39(6)	32.1(18)	-4(3)	1(2)	-4(5)
C15_8	29(3)	37(4)	31.1(16)	-2(2)	-0.8(16)	-1(3)
C16_8	26(2)	34(3)	31.0(15)	-1.6(18)	-1.4(15)	2(3)
C17_8	23.2(14)	33.2(14)	31.4(15)	-1.1(12)	-0.8(11)	4.6(11)
C18_8	23.9(15)	33.9(15)	33(3)	0.3(15)	-2.0(15)	3.8(13)
C19_8	24.5(15)	35.9(18)	39(3)	4(2)	-4.1(18)	2.6(14)
C20_8	23.6(17)	35.9(18)	41(3)	4(2)	-3.6(18)	2.9(14)
C21_8	23.1(18)	35.3(17)	41(4)	3.4(19)	-3.0(19)	3.5(13)
C22_8	22.4(16)	33.3(14)	34(2)	-0.3(14)	-0.7(14)	4.8(11)
O3_9	79(5)	77(5)	74(4)	-3(3)	-1(3)	0(3)
C24_9	79(5)	77(5)	74(4)	-3(3)	-1(3)	0(3)
C25_9	79(5)	77(5)	74(4)	-3(3)	-1(3)	0(3)
C26_9	79(5)	77(5)	74(4)	-3(3)	-1(3)	0(3)
C27_9	79(5)	77(5)	74(4)	-3(3)	-1(3)	0(3)

Atom	U_{11}	U_{22}	U_{33}	U_{23}	U_{13}	U_{12}
O3_10	79(5)	77(5)	74(4)	-3(3)	-1(3)	0(3)
C24_10	79(5)	77(5)	74(4)	-3(3)	-1(3)	0(3)
C25_10	79(5)	77(5)	74(4)	-3(3)	-1(3)	0(3)
C26_10	79(5)	77(5)	74(4)	-3(3)	-1(3)	0(3)
C27_10	79(5)	77(5)	74(4)	-3(3)	-1(3)	0(3)

Table 3 Bond Lengths in Å for **WL-NI-ROCT**.

Atom	Atom	Length/Å	Atom	Atom	Length/Å
Rh1	Rh2	2.3827(17)	C5_3	C10_3	1.387(15)
Rh1	O1_3	2.082(11)	C6_3	C7_3	1.410(15)
Rh1	O1_6	1.98(2)	C7_3	C8_3	1.363(17)
Rh1	O1_2	2.053(10)	C8_3	C9_3	1.394(18)
Rh1	O1_4	2.079(10)	C9_3	C10_3	1.399(16)
Rh1	O1_1	2.055(10)	C11_3	C12_3	1.375(14)
Rh1	O1_5	2.11(2)	C11_3	C16_3	1.392(15)
Rh1	O1_7	2.03(2)	C12_3	C13_3	1.373(15)
Rh1	O1_8	2.09(2)	C13_3	C14_3	1.372(17)
Rh1	O3_9	2.366(15)	C14_3	C15_3	1.366(17)
Rh1	O3_10	2.366(15)	C15_3	C16_3	1.393(16)
Rh2	O1W	2.337(11)	C17_3	C18_3	1.400(14)
Rh2	O2_3	2.028(10)	C17_3	C22_3	1.383(15)
Rh2	O2_6	2.07(2)	C18_3	C19_3	1.398(14)
Rh2	O2_2	2.083(10)	C19_3	C20_3	1.385(16)
Rh2	O2_4	2.030(10)	C20_3	C21_3	1.379(17)
Rh2	O2_1	2.081(10)	C21_3	C22_3	1.409(16)
Rh2	O2_5	2.06(2)	C11_6	C6_6	1.756(10)
Rh2	O2_7	2.045(15)	O1_6	C1_6	1.283(13)
Rh2	O2_8	2.0586(11)	O2_6	C1_6	1.259(13)
C11_3	C6_3	1.752(11)	C1_6	C2_6	1.509(13)
O1_3	C1_3	1.280(14)	C2_6	C3_6	1.565(13)
O2_3	C1_3	1.263(13)	C2_6	C4_6	1.526(14)
C1_3	C2_3	1.494(13)	C2_6	C5_6	1.504(14)
C2_3	C3_3	1.581(13)	C3_6	C4_6	1.485(14)
C2_3	C4_3	1.536(15)	C3_6	C11_6	1.509(14)
C2_3	C5_3	1.500(14)	C3_6	C17_6	1.544(12)
C3_3	C4_3	1.474(14)	C5_6	C6_6	1.392(13)
C3_3	C11_3	1.509(14)	C5_6	C10_6	1.390(15)
C3_3	C17_3	1.538(13)	C6_6	C7_6	1.413(14)
C5_3	C6_3	1.387(13)	C7_6	C8_6	1.359(16)

Atom	Atom	Length/Å	Atom	Atom	Length/Å
C8_6	C9_6	1.393(17)	C19_2	C20_2	1.383(16)
C9_6	C10_6	1.400(16)	C20_2	C21_2	1.379(17)
C11_6	C12_6	1.371(14)	C21_2	C22_2	1.408(15)
C11_6	C16_6	1.393(15)	C11_4	C6_4	1.751(11)
C12_6	C13_6	1.374(15)	O1_4	C1_4	1.280(13)
C13_6	C14_6	1.372(17)	O2_4	C1_4	1.258(13)
C14_6	C15_6	1.367(17)	C1_4	C2_4	1.503(13)
C15_6	C16_6	1.391(16)	C2_4	C3_4	1.568(13)
C17_6	C18_6	1.405(13)	C2_4	C4_4	1.536(14)
C17_6	C22_6	1.378(15)	C2_4	C5_4	1.503(14)
C18_6	C19_6	1.399(14)	C3_4	C4_4	1.474(14)
C19_6	C20_6	1.384(16)	C3_4	C11_4	1.507(14)
C20_6	C21_6	1.381(16)	C3_4	C17_4	1.545(12)
C21_6	C22_6	1.414(16)	C5_4	C6_4	1.395(13)
C11_2	C6_2	1.750(11)	C5_4	C10_4	1.388(15)
O1_2	C1_2	1.287(13)	C6_4	C7_4	1.414(14)
O2_2	C1_2	1.260(13)	C7_4	C8_4	1.359(16)
C1_2	C2_2	1.494(13)	C8_4	C9_4	1.394(17)
C2_2	C3_2	1.577(13)	C9_4	C10_4	1.399(16)
C2_2	C4_2	1.530(14)	C11_4	C12_4	1.377(14)
C2_2	C5_2	1.509(14)	C11_4	C16_4	1.392(14)
C3_2	C4_2	1.475(14)	C12_4	C13_4	1.375(15)
C3_2	C11_2	1.510(14)	C13_4	C14_4	1.371(16)
C3_2	C17_2	1.542(12)	C14_4	C15_4	1.369(16)
C5_2	C6_2	1.390(13)	C15_4	C16_4	1.392(15)
C5_2	C10_2	1.387(15)	C17_4	C18_4	1.400(13)
C6_2	C7_2	1.410(14)	C17_4	C22_4	1.382(15)
C7_2	C8_2	1.360(16)	C18_4	C19_4	1.398(13)
C8_2	C9_2	1.393(17)	C19_4	C20_4	1.381(15)
C9_2	C10_2	1.399(16)	C20_4	C21_4	1.379(16)
C11_2	C12_2	1.377(14)	C21_4	C22_4	1.411(15)
C11_2	C16_2	1.392(15)	C11_1	C6_1	1.755(11)
C12_2	C13_2	1.375(16)	O1_1	C1_1	1.287(13)
C13_2	C14_2	1.373(17)	O2_1	C1_1	1.258(13)
C14_2	C15_2	1.369(16)	C1_1	C2_1	1.500(13)
C15_2	C16_2	1.392(16)	C2_1	C3_1	1.570(13)
C17_2	C18_2	1.400(13)	C2_1	C4_1	1.531(14)
C17_2	C22_2	1.384(15)	C2_1	C5_1	1.505(14)
C18_2	C19_2	1.400(14)	C3_1	C4_1	1.474(14)

Atom	Atom	Length/Å	Atom	Atom	Length/Å
C3_1	C11_1	1.513(14)	C13_5	C14_5	1.375(17)
C3_1	C17_1	1.541(13)	C14_5	C15_5	1.368(17)
C5_1	C6_1	1.392(13)	C15_5	C16_5	1.392(16)
C5_1	C10_1	1.385(15)	C17_5	C18_5	1.398(13)
C6_1	C7_1	1.409(14)	C17_5	C22_5	1.383(15)
C7_1	C8_1	1.362(16)	C18_5	C19_5	1.401(14)
C8_1	C9_1	1.396(17)	C19_5	C20_5	1.385(16)
C9_1	C10_1	1.398(16)	C20_5	C21_5	1.376(16)
C11_1	C12_1	1.377(14)	C21_5	C22_5	1.409(15)
C11_1	C16_1	1.391(15)	C11_7	C6_7	1.754(11)
C12_1	C13_1	1.379(16)	O1_7	C1_7	1.289(13)
C13_1	C14_1	1.372(17)	O2_7	C1_7	1.260(13)
C14_1	C15_1	1.368(16)	C1_7	C2_7	1.504(13)
C15_1	C16_1	1.392(16)	C2_7	C3_7	1.572(13)
C17_1	C18_1	1.399(13)	C2_7	C4_7	1.530(14)
C17_1	C22_1	1.384(15)	C2_7	C5_7	1.500(14)
C18_1	C19_1	1.401(14)	C3_7	C4_7	1.475(14)
C19_1	C20_1	1.386(16)	C3_7	C11_7	1.512(14)
C20_1	C21_1	1.378(17)	C3_7	C17_7	1.541(12)
C21_1	C22_1	1.405(15)	C5_7	C6_7	1.388(14)
C11_5	C6_5	1.756(10)	C5_7	C10_7	1.386(15)
O1_5	C1_5	1.282(13)	C6_7	C7_7	1.406(14)
O2_5	C1_5	1.260(13)	C7_7	C8_7	1.364(15)
C1_5	C2_5	1.504(13)	C8_7	C9_7	1.395(17)
C2_5	C3_5	1.566(13)	C9_7	C10_7	1.400(16)
C2_5	C4_5	1.533(14)	C11_7	C12_7	1.369(14)
C2_5	C5_5	1.504(14)	C11_7	C16_7	1.399(15)
C3_5	C4_5	1.469(14)	C12_7	C13_7	1.379(15)
C3_5	C11_5	1.511(14)	C13_7	C14_7	1.374(17)
C3_5	C17_5	1.549(12)	C14_7	C15_7	1.366(17)
C5_5	C6_5	1.389(13)	C15_7	C16_7	1.395(16)
C5_5	C10_5	1.389(15)	C17_7	C18_7	1.403(13)
C6_5	C7_5	1.413(14)	C17_7	C22_7	1.384(15)
C7_5	C8_5	1.362(16)	C18_7	C19_7	1.399(13)
C8_5	C9_5	1.393(17)	C19_7	C20_7	1.384(15)
C9_5	C10_5	1.399(16)	C20_7	C21_7	1.381(16)
C11_5	C12_5	1.373(14)	C21_7	C22_7	1.413(15)
C11_5	C16_5	1.393(15)	C11_8	C6_8	1.751(12)
C12_5	C13_5	1.375(15)	O1_8	C1_8	1.290(14)

Atom	Atom	Length/Å
O2_8	C1_8	1.258(13)
C1_8	C2_8	1.499(13)
C2_8	C3_8	1.565(13)
C2_8	C4_8	1.530(14)
C2_8	C5_8	1.507(14)
C3_8	C4_8	1.481(14)
C3_8	C11_8	1.515(14)
C3_8	C17_8	1.540(13)
C5_8	C6_8	1.389(14)
C5_8	C10_8	1.384(15)
C6_8	C7_8	1.408(15)
C7_8	C8_8	1.359(17)
C8_8	C9_8	1.394(18)
C9_8	C10_8	1.402(16)
C11_8	C12_8	1.374(14)
C11_8	C16_8	1.392(15)
C12_8	C13_8	1.373(16)
C13_8	C14_8	1.375(17)
C14_8	C15_8	1.368(17)
C15_8	C16_8	1.397(16)
C17_8	C18_8	1.400(13)
C17_8	C22_8	1.388(15)
C18_8	C19_8	1.402(14)
C19_8	C20_8	1.383(15)
C20_8	C21_8	1.379(16)
C21_8	C22_8	1.410(16)
O3_9	C25_9	1.428(8)
O3_9	C26_9	1.419(8)
C24_9	C25_9	1.514(8)
C26_9	C27_9	1.520(7)
O3_10	C25_10	1.427(7)
O3_10	C26_10	1.419(7)
C24_10	C25_10	1.515(7)
C26_10	C27_10	1.520(8)

Table 4 Bond Angles in ° for **WL-NI-ROCT**.

Atom	Atom	Atom	Angle/°	Atom	Atom	Atom	Angle/°
O1_3	Rh1	Rh2	84.7(7)	O2_6	Rh2	O1W	95.9(7)
O1_3	Rh1	O1_5	85.9(19)	O2_6	Rh2	O2_2	87.6(16)
O1_3	Rh1	O3_9	101.4(11)	O2_2	Rh2	Rh1	84.3(6)
O1_6	Rh1	Rh2	90.4(7)	O2_2	Rh2	O1W	99.1(6)
O1_6	Rh1	O1_2	87.5(17)	O2_4	Rh2	Rh1	85.6(5)
O1_6	Rh1	O1_4	95.8(14)	O2_4	Rh2	O1W	91.0(6)
O1_6	Rh1	O1_8	173.1(13)	O2_4	Rh2	O2_6	91.7(15)
O1_6	Rh1	O3_10	92.6(11)	O2_4	Rh2	O2_2	169.9(8)
O1_2	Rh1	Rh2	91.1(5)	O2_4	Rh2	O2_8	89.9(11)
O1_2	Rh1	O1_4	176.7(16)	O2_1	Rh2	Rh1	89.7(6)
O1_2	Rh1	O1_8	86.9(16)	O2_1	Rh2	O1W	93.7(6)
O1_2	Rh1	O3_10	85.2(9)	O2_5	Rh2	Rh1	90.4(6)
O1_4	Rh1	Rh2	89.0(5)	O2_5	Rh2	O1W	90.5(6)
O1_4	Rh1	O1_8	89.7(13)	O2_5	Rh2	O2_1	94.1(15)
O1_4	Rh1	O3_10	94.4(9)	O2_7	Rh2	Rh1	87.3(4)
O1_1	Rh1	Rh2	85.0(5)	O2_7	Rh2	O1W	91.6(5)
O1_1	Rh1	O1_3	169.0(10)	O2_7	Rh2	O2_1	89.4(12)
O1_1	Rh1	O1_5	89.6(16)	O2_7	Rh2	O2_5	175.8(11)
O1_1	Rh1	O3_9	88.9(9)	O2_8	Rh2	Rh1	89.53(5)
O1_5	Rh1	Rh2	85.6(6)	O2_8	Rh2	O1W	89.5(3)
O1_5	Rh1	O3_9	93.9(9)	O2_8	Rh2	O2_6	174.4(7)
O1_7	Rh1	Rh2	88.8(5)	O2_8	Rh2	O2_2	89.9(12)
O1_7	Rh1	O1_3	89.9(19)	C1_3	O1_3	Rh1	120.6(12)
O1_7	Rh1	O1_1	93.6(15)	C1_3	O2_3	Rh2	116.3(13)
O1_7	Rh1	O1_5	173.3(9)	O1_3	C1_3	C2_3	119.6(14)
O1_7	Rh1	O3_9	92.1(9)	O2_3	C1_3	O1_3	125.0(15)
O1_8	Rh1	Rh2	85.6(5)	O2_3	C1_3	C2_3	115.0(13)
O1_8	Rh1	O3_10	91.1(10)	C1_3	C2_3	C3_3	118.0(13)
O3_9	Rh1	Rh2	173.9(8)	C1_3	C2_3	C4_3	115.5(14)
O3_10	Rh1	Rh2	175.2(5)	C1_3	C2_3	C5_3	120.3(10)
O1W	Rh2	Rh1	176.4(3)	C4_3	C2_3	C3_3	56.4(7)
O2_3	Rh2	Rh1	91.1(8)	C5_3	C2_3	C3_3	113.6(8)
O2_3	Rh2	O1W	85.5(9)	C5_3	C2_3	C4_3	117.0(12)
O2_3	Rh2	O2_1	179(2)	C4_3	C3_3	C2_3	60.2(7)
O2_3	Rh2	O2_5	87(2)	C4_3	C3_3	C11_3	120.2(12)
O2_3	Rh2	O2_7	90(2)	C4_3	C3_3	C17_3	118.8(14)
O2_6	Rh2	Rh1	85.2(6)	C11_3	C3_3	C2_3	123.7(11)

Atom	Atom	Atom	Angle/°
C11_3	C3_3	C17_3	109.9(9)
C17_3	C3_3	C2_3	116.4(11)
C3_3	C4_3	C2_3	63.3(7)
C6_3	C5_3	C2_3	121.1(12)
C6_3	C5_3	C10_3	118.7(12)
C10_3	C5_3	C2_3	120.2(13)
C5_3	C6_3	C11_3	121.1(10)
C5_3	C6_3	C7_3	121.1(12)
C7_3	C6_3	C11_3	117.8(11)
C8_3	C7_3	C6_3	119.7(15)
C7_3	C8_3	C9_3	119.9(16)
C8_3	C9_3	C10_3	120.5(15)
C5_3	C10_3	C9_3	120.1(14)
C12_3	C11_3	C3_3	119.0(13)
C12_3	C11_3	C16_3	117.7(13)
C16_3	C11_3	C3_3	123.3(14)
C13_3	C12_3	C11_3	122.1(13)
C14_3	C13_3	C12_3	119.6(15)
C15_3	C14_3	C13_3	119.9(16)
C14_3	C15_3	C16_3	120.4(16)
C11_3	C16_3	C15_3	120.2(15)
C18_3	C17_3	C3_3	121.0(13)
C22_3	C17_3	C3_3	121.6(13)
C22_3	C17_3	C18_3	117.3(13)
C19_3	C18_3	C17_3	121.3(14)
C20_3	C19_3	C18_3	119.8(15)
C21_3	C20_3	C19_3	120.4(15)
C20_3	C21_3	C22_3	118.9(16)
C17_3	C22_3	C21_3	122.3(15)
C1_6	O1_6	Rh1	117.4(16)
C1_6	O2_6	Rh2	117.9(18)
O1_6	C1_6	C2_6	114.1(14)
O2_6	C1_6	O1_6	125.6(15)
O2_6	C1_6	C2_6	119.4(14)
C1_6	C2_6	C3_6	119.0(12)
C1_6	C2_6	C4_6	113.6(13)
C4_6	C2_6	C3_6	57.4(6)
C5_6	C2_6	C1_6	115.2(10)
C5_6	C2_6	C3_6	118.7(9)

Atom	Atom	Atom	Angle/°
C5_6	C2_6	C4_6	120.8(12)
C4_6	C3_6	C2_6	60.0(6)
C4_6	C3_6	C11_6	122.1(12)
C4_6	C3_6	C17_6	114.3(12)
C11_6	C3_6	C2_6	124.6(9)
C11_6	C3_6	C17_6	109.6(10)
C17_6	C3_6	C2_6	118.3(11)
C3_6	C4_6	C2_6	62.6(7)
C6_6	C5_6	C2_6	120.8(11)
C10_6	C5_6	C2_6	122.2(13)
C10_6	C5_6	C6_6	117.0(11)
C5_6	C6_6	C11_6	121.6(10)
C5_6	C6_6	C7_6	122.2(11)
C7_6	C6_6	C11_6	116.2(11)
C8_6	C7_6	C6_6	119.7(14)
C7_6	C8_6	C9_6	119.3(15)
C8_6	C9_6	C10_6	120.8(15)
C5_6	C10_6	C9_6	120.9(14)
C12_6	C11_6	C3_6	121.0(12)
C12_6	C11_6	C16_6	116.9(12)
C16_6	C11_6	C3_6	122.1(13)
C11_6	C12_6	C13_6	122.7(13)
C14_6	C13_6	C12_6	119.6(14)
C15_6	C14_6	C13_6	119.8(15)
C14_6	C15_6	C16_6	120.0(15)
C15_6	C16_6	C11_6	121.0(14)
C18_6	C17_6	C3_6	119.0(13)
C22_6	C17_6	C3_6	122.8(13)
C22_6	C17_6	C18_6	118.1(12)
C19_6	C18_6	C17_6	121.4(14)
C20_6	C19_6	C18_6	118.5(14)
C21_6	C20_6	C19_6	121.1(14)
C20_6	C21_6	C22_6	118.7(15)
C17_6	C22_6	C21_6	121.4(14)
C1_2	O1_2	Rh1	115.6(10)
C1_2	O2_2	Rh2	121.3(11)
O1_2	C1_2	C2_2	113.4(11)
O2_2	C1_2	O1_2	124.8(13)
O2_2	C1_2	C2_2	121.8(12)

Atom	Atom	Atom	Angle/°
C1_2	C2_2	C3_2	120.1(12)
C1_2	C2_2	C4_2	115.8(14)
C1_2	C2_2	C5_2	117.7(9)
C4_2	C2_2	C3_2	56.7(6)
C5_2	C2_2	C3_2	115.8(8)
C5_2	C2_2	C4_2	116.5(12)
C4_2	C3_2	C2_2	60.1(7)
C4_2	C3_2	C11_2	119.7(12)
C4_2	C3_2	C17_2	119.7(12)
C11_2	C3_2	C2_2	125.0(11)
C11_2	C3_2	C17_2	110.2(10)
C17_2	C3_2	C2_2	114.4(8)
C3_2	C4_2	C2_2	63.3(7)
C6_2	C5_2	C2_2	120.9(12)
C10_2	C5_2	C2_2	121.9(12)
C10_2	C5_2	C6_2	117.2(12)
C5_2	C6_2	C11_2	120.7(10)
C5_2	C6_2	C7_2	121.6(11)
C7_2	C6_2	C11_2	117.8(10)
C8_2	C7_2	C6_2	120.4(14)
C7_2	C8_2	C9_2	119.1(15)
C8_2	C9_2	C10_2	120.4(15)
C5_2	C10_2	C9_2	121.4(14)
C12_2	C11_2	C3_2	119.1(13)
C12_2	C11_2	C16_2	117.4(13)
C16_2	C11_2	C3_2	123.2(13)
C13_2	C12_2	C11_2	122.4(14)
C14_2	C13_2	C12_2	119.3(15)
C15_2	C14_2	C13_2	120.0(15)
C14_2	C15_2	C16_2	120.1(15)
C15_2	C16_2	C11_2	120.5(14)
C18_2	C17_2	C3_2	121.6(11)
C22_2	C17_2	C3_2	121.6(11)
C22_2	C17_2	C18_2	116.7(12)
C19_2	C18_2	C17_2	122.5(14)
C20_2	C19_2	C18_2	118.8(14)
C21_2	C20_2	C19_2	120.6(14)
C20_2	C21_2	C22_2	119.4(15)
C17_2	C22_2	C21_2	122.0(14)

Atom	Atom	Atom	Angle/°
C1_4	O1_4	Rh1	114.9(9)
C1_4	O2_4	Rh2	120.3(11)
O1_4	C1_4	C2_4	115.0(11)
O2_4	C1_4	O1_4	125.3(12)
O2_4	C1_4	C2_4	119.4(12)
C1_4	C2_4	C3_4	119.7(11)
C1_4	C2_4	C4_4	112.6(12)
C4_4	C2_4	C3_4	56.7(6)
C5_4	C2_4	C1_4	117.0(10)
C5_4	C2_4	C3_4	116.7(10)
C5_4	C2_4	C4_4	120.4(12)
C4_4	C3_4	C2_4	60.6(7)
C4_4	C3_4	C11_4	123.4(10)
C4_4	C3_4	C17_4	115.6(11)
C11_4	C3_4	C2_4	125.9(9)
C11_4	C3_4	C17_4	107.4(7)
C17_4	C3_4	C2_4	117.6(10)
C3_4	C4_4	C2_4	62.7(7)
C6_4	C5_4	C2_4	121.1(11)
C10_4	C5_4	C2_4	121.9(12)
C10_4	C5_4	C6_4	116.5(11)
C5_4	C6_4	C11_4	122.0(9)
C5_4	C6_4	C7_4	122.0(11)
C7_4	C6_4	C11_4	116.0(9)
C8_4	C7_4	C6_4	119.7(14)
C7_4	C8_4	C9_4	120.1(14)
C8_4	C9_4	C10_4	119.4(14)
C5_4	C10_4	C9_4	122.3(14)
C12_4	C11_4	C3_4	119.4(11)
C12_4	C11_4	C16_4	117.6(12)
C16_4	C11_4	C3_4	123.1(12)
C13_4	C12_4	C11_4	121.8(12)
C14_4	C13_4	C12_4	120.0(13)
C15_4	C14_4	C13_4	120.1(14)
C14_4	C15_4	C16_4	119.7(14)
C11_4	C16_4	C15_4	120.9(13)
C18_4	C17_4	C3_4	119.4(11)
C22_4	C17_4	C3_4	121.9(11)
C22_4	C17_4	C18_4	118.5(11)

Atom	Atom	Atom	Angle/°
C19_4	C18_4	C17_4	121.0(12)
C20_4	C19_4	C18_4	119.3(13)
C21_4	C20_4	C19_4	121.0(13)
C20_4	C21_4	C22_4	119.1(14)
C17_4	C22_4	C21_4	121.1(13)
C1_1	O1_1	Rh1	121.1(11)
C1_1	O2_1	Rh2	114.8(11)
O1_1	C1_1	C2_1	116.6(11)
O2_1	C1_1	O1_1	125.0(13)
O2_1	C1_1	C2_1	118.3(12)
C1_1	C2_1	C3_1	119.8(12)
C1_1	C2_1	C4_1	115.4(13)
C1_1	C2_1	C5_1	115.4(10)
C4_1	C2_1	C3_1	56.7(7)
C5_1	C2_1	C3_1	118.3(10)
C5_1	C2_1	C4_1	118.4(12)
C4_1	C3_1	C2_1	60.3(7)
C4_1	C3_1	C11_1	119.1(12)
C4_1	C3_1	C17_1	119.2(12)
C11_1	C3_1	C2_1	125.2(12)
C11_1	C3_1	C17_1	109.8(10)
C17_1	C3_1	C2_1	115.7(8)
C3_1	C4_1	C2_1	63.0(7)
C6_1	C5_1	C2_1	120.4(12)
C10_1	C5_1	C2_1	121.5(12)
C10_1	C5_1	C6_1	117.8(11)
C5_1	C6_1	C11_1	120.8(10)
C5_1	C6_1	C7_1	120.8(11)
C7_1	C6_1	C11_1	118.4(10)
C8_1	C7_1	C6_1	120.8(13)
C7_1	C8_1	C9_1	119.1(14)
C8_1	C9_1	C10_1	120.1(15)
C5_1	C10_1	C9_1	121.4(14)
C12_1	C11_1	C3_1	119.1(13)
C12_1	C11_1	C16_1	117.4(13)
C16_1	C11_1	C3_1	123.4(13)
C11_1	C12_1	C13_1	122.2(14)
C14_1	C13_1	C12_1	119.5(15)
C15_1	C14_1	C13_1	119.8(15)

Atom	Atom	Atom	Angle/°
C14_1	C15_1	C16_1	120.4(15)
C11_1	C16_1	C15_1	120.5(14)
C18_1	C17_1	C3_1	122.2(12)
C22_1	C17_1	C3_1	120.4(12)
C22_1	C17_1	C18_1	117.3(12)
C17_1	C18_1	C19_1	121.7(13)
C20_1	C19_1	C18_1	119.0(13)
C21_1	C20_1	C19_1	121.0(14)
C20_1	C21_1	C22_1	118.8(15)
C17_1	C22_1	C21_1	122.2(14)
C1_5	O1_5	Rh1	118.5(15)
C1_5	O2_5	Rh2	116.8(15)
O1_5	C1_5	C2_5	114.6(13)
O2_5	C1_5	O1_5	126.5(14)
O2_5	C1_5	C2_5	118.9(13)
C1_5	C2_5	C3_5	120.6(12)
C1_5	C2_5	C4_5	112.8(13)
C4_5	C2_5	C3_5	56.6(6)
C5_5	C2_5	C1_5	116.9(11)
C5_5	C2_5	C3_5	115.7(10)
C5_5	C2_5	C4_5	120.6(12)
C4_5	C3_5	C2_5	60.6(7)
C4_5	C3_5	C11_5	125.3(11)
C4_5	C3_5	C17_5	117.4(12)
C11_5	C3_5	C2_5	125.7(10)
C11_5	C3_5	C17_5	105.6(6)
C17_5	C3_5	C2_5	117.3(8)
C3_5	C4_5	C2_5	62.8(7)
C6_5	C5_5	C2_5	121.6(11)
C10_5	C5_5	C2_5	120.5(12)
C10_5	C5_5	C6_5	117.9(11)
C5_5	C6_5	C11_5	122.2(10)
C5_5	C6_5	C7_5	121.2(11)
C7_5	C6_5	C11_5	116.6(11)
C8_5	C7_5	C6_5	119.9(14)
C7_5	C8_5	C9_5	120.0(15)
C8_5	C9_5	C10_5	119.8(14)
C5_5	C10_5	C9_5	121.2(14)
C12_5	C11_5	C3_5	119.4(12)

Atom	Atom	Atom	Angle/°
C12_5	C11_5	C16_5	117.3(12)
C16_5	C11_5	C3_5	123.3(12)
C11_5	C12_5	C13_5	122.6(12)
C14_5	C13_5	C12_5	119.3(14)
C15_5	C14_5	C13_5	120.0(15)
C14_5	C15_5	C16_5	120.1(15)
C15_5	C16_5	C11_5	120.7(14)
C18_5	C17_5	C3_5	122.4(12)
C22_5	C17_5	C3_5	120.6(12)
C22_5	C17_5	C18_5	117.0(12)
C17_5	C18_5	C19_5	121.7(13)
C20_5	C19_5	C18_5	119.4(14)
C21_5	C20_5	C19_5	120.7(14)
C20_5	C21_5	C22_5	118.8(14)
C17_5	C22_5	C21_5	122.5(14)
C1_7	O1_7	Rh1	116.8(13)
C1_7	O2_7	Rh2	116.3(12)
O1_7	C1_7	C2_7	114.1(13)
O2_7	C1_7	O1_7	126.3(15)
O2_7	C1_7	C2_7	118.4(13)
C1_7	C2_7	C3_7	120.2(11)
C1_7	C2_7	C4_7	114.1(13)
C4_7	C2_7	C3_7	56.8(6)
C5_7	C2_7	C1_7	116.0(10)
C5_7	C2_7	C3_7	116.0(10)
C5_7	C2_7	C4_7	121.0(12)
C4_7	C3_7	C2_7	60.2(7)
C4_7	C3_7	C11_7	122.1(12)
C4_7	C3_7	C17_7	116.9(12)
C11_7	C3_7	C2_7	122.0(11)
C11_7	C3_7	C17_7	111.5(10)
C17_7	C3_7	C2_7	115.4(8)
C3_7	C4_7	C2_7	63.1(7)
C6_7	C5_7	C2_7	120.5(12)
C10_7	C5_7	C2_7	121.3(12)
C10_7	C5_7	C6_7	118.2(12)
C5_7	C6_7	C11_7	121.6(10)
C5_7	C6_7	C7_7	121.1(11)
C7_7	C6_7	C11_7	117.3(10)

Atom	Atom	Atom	Angle/°
C8_7	C7_7	C6_7	119.9(13)
C7_7	C8_7	C9_7	120.1(14)
C8_7	C9_7	C10_7	119.5(14)
C5_7	C10_7	C9_7	121.1(14)
C12_7	C11_7	C3_7	120.4(12)
C12_7	C11_7	C16_7	117.4(12)
C16_7	C11_7	C3_7	122.3(13)
C11_7	C12_7	C13_7	123.1(14)
C14_7	C13_7	C12_7	119.0(14)
C15_7	C14_7	C13_7	119.8(15)
C14_7	C15_7	C16_7	121.0(15)
C15_7	C16_7	C11_7	119.7(14)
C18_7	C17_7	C3_7	120.7(12)
C22_7	C17_7	C3_7	121.4(12)
C22_7	C17_7	C18_7	117.9(12)
C19_7	C18_7	C17_7	121.7(13)
C20_7	C19_7	C18_7	119.1(13)
C21_7	C20_7	C19_7	120.6(14)
C20_7	C21_7	C22_7	119.7(14)
C17_7	C22_7	C21_7	121.0(14)
C1_8	O1_8	Rh1	117.1(15)
C1_8	O2_8	Rh2	117.0(8)
O1_8	C1_8	C2_8	114.0(14)
O2_8	C1_8	O1_8	125.7(16)
O2_8	C1_8	C2_8	119.4(12)
C1_8	C2_8	C3_8	121.0(13)
C1_8	C2_8	C4_8	117.1(14)
C1_8	C2_8	C5_8	115.4(12)
C4_8	C2_8	C3_8	57.1(7)
C5_8	C2_8	C3_8	117.5(12)
C5_8	C2_8	C4_8	115.9(12)
C4_8	C3_8	C2_8	60.2(7)
C4_8	C3_8	C11_8	116.6(12)
C4_8	C3_8	C17_8	120.0(13)
C11_8	C3_8	C2_8	126.3(12)
C11_8	C3_8	C17_8	110.6(11)
C17_8	C3_8	C2_8	115.2(8)
C3_8	C4_8	C2_8	62.6(7)
C6_8	C5_8	C2_8	119.1(12)

Atom	Atom	Atom	Angle/°	Atom	Atom	Atom	Angle/°
C10_8	C5_8	C2_8	121.7(13)	C22_8	C17_8	C18_8	116.7(12)
C10_8	C5_8	C6_8	118.9(12)	C17_8	C18_8	C19_8	122.1(13)
C5_8	C6_8	C11_8	121.2(11)	C20_8	C19_8	C18_8	119.6(14)
C5_8	C6_8	C7_8	120.7(12)	C21_8	C20_8	C19_8	120.0(14)
C7_8	C6_8	C11_8	118.0(12)	C20_8	C21_8	C22_8	119.6(15)
C8_8	C7_8	C6_8	119.8(15)	C17_8	C22_8	C21_8	122.1(14)
C7_8	C8_8	C9_8	120.3(15)	C25_9	O3_9	Rh1	115(2)
C8_8	C9_8	C10_8	119.9(15)	C26_9	O3_9	Rh1	104(2)
C5_8	C10_8	C9_8	120.3(15)	C26_9	O3_9	C25_9	109.8(11)
C12_8	C11_8	C3_8	118.0(13)	O3_9	C25_9	C24_9	118(2)
C12_8	C11_8	C16_8	117.2(13)	O3_9	C26_9	C27_9	109.0(18)
C16_8	C11_8	C3_8	124.9(14)	C25_1	O3_10	Rh1	123.9(9)
C13_8	C12_8	C11_8	122.5(15)	0			
C12_8	C13_8	C14_8	119.6(15)	C26_1	O3_10	Rh1	125.9(8)
C15_8	C14_8	C13_8	119.6(15)	0			
C14_8	C15_8	C16_8	120.1(16)	C26_1	O3_10	C25_10	109.7(11)
C11_8	C16_8	C15_8	120.6(15)	0			
C18_8	C17_8	C3_8	123.0(12)	O3_10	C25_10	C24_10	118(2)
C22_8	C17_8	C3_8	120.3(13)	O3_10	C26_10	C27_10	109.0(18)

Table 5 Torsion Angles in ° for **WL-NI-ROCT**.

Atom	Atom	Atom	Atom	Angle/°
Rh1	O1_3	C1_3	O2_3	-2(8)
Rh1	O1_3	C1_3	C2_3	-174(3)
Rh1	O1_6	C1_6	O2_6	-6(6)
Rh1	O1_6	C1_6	C2_6	-176(2)
Rh1	O1_2	C1_2	O2_2	1(6)
Rh1	O1_2	C1_2	C2_2	-178(2)
Rh1	O1_4	C1_4	O2_4	0(5)
Rh1	O1_4	C1_4	C2_4	-174.2(18)
Rh1	O1_1	C1_1	O2_1	3(6)
Rh1	O1_1	C1_1	C2_1	-179(2)
Rh1	O1_5	C1_5	O2_5	9(6)
Rh1	O1_5	C1_5	C2_5	-171(2)
Rh1	O1_7	C1_7	O2_7	-12(5)
Rh1	O1_7	C1_7	C2_7	-179.7(18)

Atom	Atom	Atom	Atom	Angle/°
Rh1	O1_8	C1_8	O2_8	22(6)
Rh1	O1_8	C1_8	C2_8	-170(2)
Rh1	O3_9	C25_9	C24_9	-64(5)
Rh1	O3_9	C26_9	C27_9	90(4)
Rh1	O3_10	C25_10	C24_10	-66(5)
Rh1	O3_10	C26_10	C27_10	-15(5)
Rh2	O2_3	C1_3	O1_3	14(8)
Rh2	O2_3	C1_3	C2_3	-173(3)
Rh2	O2_6	C1_6	O1_6	20(6)
Rh2	O2_6	C1_6	C2_6	-172(2)
Rh2	O2_2	C1_2	O1_2	13(7)
Rh2	O2_2	C1_2	C2_2	-168(2)
Rh2	O2_4	C1_4	O1_4	19(5)
Rh2	O2_4	C1_4	C2_4	-168(2)
Rh2	O2_1	C1_1	O1_1	14(6)
Rh2	O2_1	C1_1	C2_1	-164(2)
Rh2	O2_5	C1_5	O1_5	4(6)
Rh2	O2_5	C1_5	C2_5	-176(2)
Rh2	O2_7	C1_7	O1_7	25(5)
Rh2	O2_7	C1_7	C2_7	-168.3(19)
Rh2	O2_8	C1_8	O1_8	-4(5)
Rh2	O2_8	C1_8	C2_8	-172(2)
Cl1_3	C6_3	C7_3	C8_3	180.00(8)
O1_3	C1_3	C2_3	C3_3	-163(4)
O1_3	C1_3	C2_3	C4_3	133(4)
O1_3	C1_3	C2_3	C5_3	-16(5)
O2_3	C1_3	C2_3	C3_3	24(5)
O2_3	C1_3	C2_3	C4_3	-40(5)
O2_3	C1_3	C2_3	C5_3	171(4)
C1_3	C2_3	C3_3	C4_3	-103(2)
C1_3	C2_3	C3_3	C11_3	5(3)
C1_3	C2_3	C3_3	C17_3	147(2)
C1_3	C2_3	C4_3	C3_3	107.9(18)
C1_3	C2_3	C5_3	C6_3	-70(2)
C1_3	C2_3	C5_3	C10_3	110(2)
C2_3	C3_3	C11_3	C12_3	-128.9(16)
C2_3	C3_3	C11_3	C16_3	51.1(16)
C2_3	C3_3	C17_3	C18_3	70.9(18)
C2_3	C3_3	C17_3	C22_3	-112.3(14)

Atom	Atom	Atom	Atom	Angle/°
C2_3	C5_3	C6_3	C11_3	0.02(8)
C2_3	C5_3	C6_3	C7_3	-179.98(10)
C2_3	C5_3	C10_3	C9_3	179.98(8)
C3_3	C2_3	C5_3	C6_3	78.5(13)
C3_3	C2_3	C5_3	C10_3	-101.5(13)
C3_3	C11_3	C12_3	C13_3	180.00(8)
C3_3	C11_3	C16_3	C15_3	180.00(15)
C3_3	C17_3	C18_3	C19_3	176.9(15)
C3_3	C17_3	C22_3	C21_3	-176.9(15)
C4_3	C2_3	C3_3	C11_3	108.3(17)
C4_3	C2_3	C3_3	C17_3	-109.7(17)
C4_3	C2_3	C5_3	C6_3	141.5(13)
C4_3	C2_3	C5_3	C10_3	-38.5(13)
C4_3	C3_3	C11_3	C12_3	-56.5(17)
C4_3	C3_3	C11_3	C16_3	123.5(17)
C4_3	C3_3	C17_3	C18_3	2(2)
C4_3	C3_3	C17_3	C22_3	178.8(13)
C5_3	C2_3	C3_3	C4_3	107.7(16)
C5_3	C2_3	C3_3	C11_3	-144.0(14)
C5_3	C2_3	C3_3	C17_3	-2(2)
C5_3	C2_3	C4_3	C3_3	-101.7(12)
C5_3	C6_3	C7_3	C8_3	0.00(12)
C6_3	C5_3	C10_3	C9_3	0.00(5)
C6_3	C7_3	C8_3	C9_3	0.00(15)
C7_3	C8_3	C9_3	C10_3	0.01(13)
C8_3	C9_3	C10_3	C5_3	-0.01(6)
C10_3	C5_3	C6_3	C11_3	180.00(4)
C10_3	C5_3	C6_3	C7_3	0.00(8)
C11_3	C3_3	C4_3	C2_3	-114.0(14)
C11_3	C3_3	C17_3	C18_3	-142.1(12)
C11_3	C3_3	C17_3	C22_3	34.7(17)
C11_3	C12_3	C13_3	C14_3	0.00(9)
C12_3	C11_3	C16_3	C15_3	0.00(19)
C12_3	C13_3	C14_3	C15_3	0.0(2)
C13_3	C14_3	C15_3	C16_3	0.0(3)
C14_3	C15_3	C16_3	C11_3	0.0(3)
C16_3	C11_3	C12_3	C13_3	0.00(9)
C17_3	C3_3	C4_3	C2_3	105.6(14)
C17_3	C3_3	C11_3	C12_3	87.0(14)

Atom	Atom	Atom	Atom	Angle/°
C17_3	C3_3	C11_3	C16_3	-93.0(14)
C17_3	C18_3	C19_3	C20_3	0.00(6)
C18_3	C17_3	C22_3	C21_3	0.00(12)
C18_3	C19_3	C20_3	C21_3	0.00(8)
C19_3	C20_3	C21_3	C22_3	0.00(9)
C20_3	C21_3	C22_3	C17_3	0.00(10)
C22_3	C17_3	C18_3	C19_3	0.00(9)
Cl1_6	C6_6	C7_6	C8_6	-179.99(10)
O1_6	C1_6	C2_6	C3_6	-163(3)
O1_6	C1_6	C2_6	C4_6	133(3)
O1_6	C1_6	C2_6	C5_6	-13(4)
O2_6	C1_6	C2_6	C3_6	27(4)
O2_6	C1_6	C2_6	C4_6	-37(4)
O2_6	C1_6	C2_6	C5_6	177(3)
C1_6	C2_6	C3_6	C4_6	-100.9(18)
C1_6	C2_6	C3_6	C11_6	9(2)
C1_6	C2_6	C3_6	C17_6	155.9(19)
C1_6	C2_6	C4_6	C3_6	110.4(16)
C1_6	C2_6	C5_6	C6_6	-62.8(18)
C1_6	C2_6	C5_6	C10_6	117.2(18)
C2_6	C3_6	C11_6	C12_6	-116.7(15)
C2_6	C3_6	C11_6	C16_6	63.3(15)
C2_6	C3_6	C17_6	C18_6	114(3)
C2_6	C3_6	C17_6	C22_6	-70(3)
C2_6	C5_6	C6_6	Cl1_6	0.00(6)
C2_6	C5_6	C6_6	C7_6	179.99(9)
C2_6	C5_6	C10_6	C9_6	-179.99(11)
C3_6	C2_6	C5_6	C6_6	87.4(13)
C3_6	C2_6	C5_6	C10_6	-92.6(13)
C3_6	C11_6	C12_6	C13_6	-179.99(8)
C3_6	C11_6	C16_6	C15_6	179.98(15)
C3_6	C17_6	C18_6	C19_6	175(3)
C3_6	C17_6	C22_6	C21_6	-176(3)
C4_6	C2_6	C3_6	C11_6	110.3(16)
C4_6	C2_6	C3_6	C17_6	-103.2(15)
C4_6	C2_6	C5_6	C6_6	154.6(13)
C4_6	C2_6	C5_6	C10_6	-25.4(13)
C4_6	C3_6	C11_6	C12_6	-43.3(15)
C4_6	C3_6	C11_6	C16_6	136.7(15)

Atom	Atom	Atom	Atom	Angle/°
C4_6	C3_6	C17_6	C18_6	46(3)
C4_6	C3_6	C17_6	C22_6	-138(3)
C5_6	C2_6	C3_6	C4_6	110.1(15)
C5_6	C2_6	C3_6	C11_6	-139.6(14)
C5_6	C2_6	C3_6	C17_6	7(2)
C5_6	C2_6	C4_6	C3_6	-106.4(12)
C5_6	C6_6	C7_6	C8_6	0.01(15)
C6_6	C5_6	C10_6	C9_6	0.01(15)
C6_6	C7_6	C8_6	C9_6	0.0(2)
C7_6	C8_6	C9_6	C10_6	0.0(2)
C8_6	C9_6	C10_6	C5_6	0.0(2)
C10_6	C5_6	C6_6	C11_6	180.00(7)
C10_6	C5_6	C6_6	C7_6	0.00(9)
C11_6	C3_6	C4_6	C2_6	-114.3(13)
C11_6	C3_6	C17_6	C18_6	-95(2)
C11_6	C3_6	C17_6	C22_6	81(3)
C11_6	C12_6	C13_6	C14_6	0.01(9)
C12_6	C11_6	C16_6	C15_6	-0.02(19)
C12_6	C13_6	C14_6	C15_6	0.0(2)
C13_6	C14_6	C15_6	C16_6	0.0(3)
C14_6	C15_6	C16_6	C11_6	0.0(3)
C16_6	C11_6	C12_6	C13_6	0.01(9)
C17_6	C3_6	C4_6	C2_6	109.8(13)
C17_6	C3_6	C11_6	C12_6	94.4(12)
C17_6	C3_6	C11_6	C16_6	-85.6(12)
C17_6	C18_6	C19_6	C20_6	7(5)
C18_6	C17_6	C22_6	C21_6	0(5)
C18_6	C19_6	C20_6	C21_6	-11(6)
C19_6	C20_6	C21_6	C22_6	11(6)
C20_6	C21_6	C22_6	C17_6	-5(5)
C22_6	C17_6	C18_6	C19_6	-1(5)
C11_2	C6_2	C7_2	C8_2	180.00(10)
O1_2	C1_2	C2_2	C3_2	-162(3)
O1_2	C1_2	C2_2	C4_2	134(3)
O1_2	C1_2	C2_2	C5_2	-11(4)
O2_2	C1_2	C2_2	C3_2	20(5)
O2_2	C1_2	C2_2	C4_2	-45(4)
O2_2	C1_2	C2_2	C5_2	170(4)
C1_2	C2_2	C3_2	C4_2	-102.8(18)

Atom	Atom	Atom	Atom	Angle/°
C1_2	C2_2	C3_2	C11_2	4(2)
C1_2	C2_2	C3_2	C17_2	145.7(19)
C1_2	C2_2	C4_2	C3_2	110.4(16)
C1_2	C2_2	C5_2	C6_2	-68.3(19)
C1_2	C2_2	C5_2	C10_2	111.7(19)
C2_2	C3_2	C11_2	C12_2	-132(2)
C2_2	C3_2	C11_2	C16_2	42(3)
C2_2	C3_2	C17_2	C18_2	73.2(13)
C2_2	C3_2	C17_2	C22_2	-106.8(13)
C2_2	C5_2	C6_2	C11_2	0.01(6)
C2_2	C5_2	C6_2	C7_2	-179.98(9)
C2_2	C5_2	C10_2	C9_2	179.99(11)
C3_2	C2_2	C5_2	C6_2	83.7(12)
C3_2	C2_2	C5_2	C10_2	-96.3(12)
C3_2	C11_2	C12_2	C13_2	176(3)
C3_2	C11_2	C16_2	C15_2	-177(3)
C3_2	C17_2	C18_2	C19_2	180.00(8)
C3_2	C17_2	C22_2	C21_2	179.99(11)
C4_2	C2_2	C3_2	C11_2	107.2(16)
C4_2	C2_2	C3_2	C17_2	-111.6(14)
C4_2	C2_2	C5_2	C6_2	147.5(12)
C4_2	C2_2	C5_2	C10_2	-32.5(12)
C4_2	C3_2	C11_2	C12_2	-60(3)
C4_2	C3_2	C11_2	C16_2	115(3)
C4_2	C3_2	C17_2	C18_2	5.0(13)
C4_2	C3_2	C17_2	C22_2	-175.0(13)
C5_2	C2_2	C3_2	C4_2	106.0(15)
C5_2	C2_2	C3_2	C11_2	-146.8(14)
C5_2	C2_2	C3_2	C17_2	-5.6(18)
C5_2	C2_2	C4_2	C3_2	-104.7(11)
C5_2	C6_2	C7_2	C8_2	-0.01(15)
C6_2	C5_2	C10_2	C9_2	-0.01(15)
C6_2	C7_2	C8_2	C9_2	0.0(2)
C7_2	C8_2	C9_2	C10_2	0.0(2)
C8_2	C9_2	C10_2	C5_2	0.0(2)
C10_2	C5_2	C6_2	C11_2	-179.99(7)
C10_2	C5_2	C6_2	C7_2	0.01(9)
C11_2	C3_2	C4_2	C2_2	-115.7(13)
C11_2	C3_2	C17_2	C18_2	-139.9(12)

Atom	Atom	Atom	Atom	Angle/°
C11_2	C3_2	C17_2	C22_2	40.1(12)
C11_2	C12_2	C13_2	C14_2	-2(5)
C12_2	C11_2	C16_2	C15_2	-3(5)
C12_2	C13_2	C14_2	C15_2	5(6)
C13_2	C14_2	C15_2	C16_2	-6(6)
C14_2	C15_2	C16_2	C11_2	5(6)
C16_2	C11_2	C12_2	C13_2	1(5)
C17_2	C3_2	C4_2	C2_2	102.7(10)
C17_2	C3_2	C11_2	C12_2	85(2)
C17_2	C3_2	C11_2	C16_2	-100(3)
C17_2	C18_2	C19_2	C20_2	0.01(17)
C18_2	C17_2	C22_2	C21_2	-0.01(17)
C18_2	C19_2	C20_2	C21_2	0.0(2)
C19_2	C20_2	C21_2	C22_2	0.0(2)
C20_2	C21_2	C22_2	C17_2	0.0(2)
C22_2	C17_2	C18_2	C19_2	0.01(11)
Cl1_4	C6_4	C7_4	C8_4	180.00(10)
O1_4	C1_4	C2_4	C3_4	-163(2)
O1_4	C1_4	C2_4	C4_4	134(2)
O1_4	C1_4	C2_4	C5_4	-12(3)
O2_4	C1_4	C2_4	C3_4	23(4)
O2_4	C1_4	C2_4	C4_4	-40(3)
O2_4	C1_4	C2_4	C5_4	174(3)
C1_4	C2_4	C3_4	C4_4	-99.0(16)
C1_4	C2_4	C3_4	C11_4	13(2)
C1_4	C2_4	C3_4	C17_4	155.7(16)
C1_4	C2_4	C4_4	C3_4	111.6(14)
C1_4	C2_4	C5_4	C6_4	-65.2(19)
C1_4	C2_4	C5_4	C10_4	123.5(15)
C2_4	C3_4	C11_4	C12_4	-131.6(13)
C2_4	C3_4	C11_4	C16_4	48.4(13)
C2_4	C3_4	C17_4	C18_4	106.4(13)
C2_4	C3_4	C17_4	C22_4	-79.2(14)
C2_4	C5_4	C6_4	Cl1_4	8.3(12)
C2_4	C5_4	C6_4	C7_4	-171.7(12)
C2_4	C5_4	C10_4	C9_4	171.7(12)
C3_4	C2_4	C5_4	C6_4	86.2(14)
C3_4	C2_4	C5_4	C10_4	-85.1(13)
C3_4	C11_4	C12_4	C13_4	-179.99(8)

Atom	Atom	Atom	Atom	Angle/°
C3_4	C11_4	C16_4	C15_4	179.98(15)
C3_4	C17_4	C18_4	C19_4	174.6(11)
C3_4	C17_4	C22_4	C21_4	-174.4(12)
C4_4	C2_4	C3_4	C11_4	111.9(14)
C4_4	C2_4	C3_4	C17_4	-105.4(14)
C4_4	C2_4	C5_4	C6_4	151.6(11)
C4_4	C2_4	C5_4	C10_4	-19.7(15)
C4_4	C3_4	C11_4	C12_4	-56.0(13)
C4_4	C3_4	C11_4	C16_4	124.0(13)
C4_4	C3_4	C17_4	C18_4	37.8(15)
C4_4	C3_4	C17_4	C22_4	-147.8(11)
C5_4	C2_4	C3_4	C4_4	110.4(14)
C5_4	C2_4	C3_4	C11_4	-137.7(12)
C5_4	C2_4	C3_4	C17_4	5.0(18)
C5_4	C2_4	C4_4	C3_4	-103.7(13)
C5_4	C6_4	C7_4	C8_4	0.00(15)
C6_4	C5_4	C10_4	C9_4	-0.02(15)
C6_4	C7_4	C8_4	C9_4	0.0(2)
C7_4	C8_4	C9_4	C10_4	0.0(2)
C8_4	C9_4	C10_4	C5_4	0.0(2)
C10_4	C5_4	C6_4	C11_4	-179.99(7)
C10_4	C5_4	C6_4	C7_4	0.01(9)
C11_4	C3_4	C4_4	C2_4	-115.8(12)
C11_4	C3_4	C17_4	C18_4	-104.5(12)
C11_4	C3_4	C17_4	C22_4	69.9(13)
C11_4	C12_4	C13_4	C14_4	0.00(9)
C12_4	C11_4	C16_4	C15_4	-0.01(19)
C12_4	C13_4	C14_4	C15_4	0.0(2)
C13_4	C14_4	C15_4	C16_4	0.0(3)
C14_4	C15_4	C16_4	C11_4	0.0(3)
C16_4	C11_4	C12_4	C13_4	0.00(8)
C17_4	C3_4	C4_4	C2_4	108.6(12)
C17_4	C3_4	C11_4	C12_4	82.6(10)
C17_4	C3_4	C11_4	C16_4	-97.4(10)
C17_4	C18_4	C19_4	C20_4	0.00(8)
C18_4	C17_4	C22_4	C21_4	-0.01(19)
C18_4	C19_4	C20_4	C21_4	-0.01(19)
C19_4	C20_4	C21_4	C22_4	0.0(2)
C20_4	C21_4	C22_4	C17_4	0.0(2)

Atom	Atom	Atom	Atom	Angle/°
C22_4	C17_4	C18_4	C19_4	0.01(8)
Cl1_1	C6_1	C7_1	C8_1	180.00(11)
O1_1	C1_1	C2_1	C3_1	-156(3)
O1_1	C1_1	C2_1	C4_1	139(3)
O1_1	C1_1	C2_1	C5_1	-5(4)
O2_1	C1_1	C2_1	C3_1	22(4)
O2_1	C1_1	C2_1	C4_1	-43(4)
O2_1	C1_1	C2_1	C5_1	173(3)
C1_1	C2_1	C3_1	C4_1	-102.5(18)
C1_1	C2_1	C3_1	C11_1	4(2)
C1_1	C2_1	C3_1	C17_1	147.2(19)
C1_1	C2_1	C4_1	C3_1	110.3(16)
C1_1	C2_1	C5_1	C6_1	-71(2)
C1_1	C2_1	C5_1	C10_1	116.6(18)
C2_1	C3_1	C11_1	C12_1	-124(2)
C2_1	C3_1	C11_1	C16_1	52(3)
C2_1	C3_1	C17_1	C18_1	87.3(14)
C2_1	C3_1	C17_1	C22_1	-92.7(14)
C2_1	C5_1	C6_1	C11_1	7.1(12)
C2_1	C5_1	C6_1	C7_1	-172.9(12)
C2_1	C5_1	C10_1	C9_1	172.8(12)
C3_1	C2_1	C5_1	C6_1	81.0(15)
C3_1	C2_1	C5_1	C10_1	-91.6(14)
C3_1	C11_1	C12_1	C13_1	177(3)
C3_1	C11_1	C16_1	C15_1	-174(3)
C3_1	C17_1	C18_1	C19_1	180.00(8)
C3_1	C17_1	C22_1	C21_1	179.99(14)
C4_1	C2_1	C3_1	C11_1	106.4(16)
C4_1	C2_1	C3_1	C17_1	-110.4(15)
C4_1	C2_1	C5_1	C6_1	146.3(13)
C4_1	C2_1	C5_1	C10_1	-26.3(15)
C4_1	C3_1	C11_1	C12_1	-52(3)
C4_1	C3_1	C11_1	C16_1	125(3)
C4_1	C3_1	C17_1	C18_1	18.4(13)
C4_1	C3_1	C17_1	C22_1	-161.6(13)
C5_1	C2_1	C3_1	C4_1	107.0(15)
C5_1	C2_1	C3_1	C11_1	-146.6(14)
C5_1	C2_1	C3_1	C17_1	-3.4(19)
C5_1	C2_1	C4_1	C3_1	-106.9(13)

Atom	Atom	Atom	Atom	Angle/°
C5_1	C6_1	C7_1	C8_1	0.00(9)
C6_1	C5_1	C10_1	C9_1	-0.01(19)
C6_1	C7_1	C8_1	C9_1	0.00(19)
C7_1	C8_1	C9_1	C10_1	0.0(2)
C8_1	C9_1	C10_1	C5_1	0.0(3)
C10_1	C5_1	C6_1	C11_1	-179.99(10)
C10_1	C5_1	C6_1	C7_1	0.00(8)
C11_1	C3_1	C4_1	C2_1	-116.2(14)
C11_1	C3_1	C17_1	C18_1	-124.1(12)
C11_1	C3_1	C17_1	C22_1	55.9(12)
C11_1	C12_1	C13_1	C14_1	-4(5)
C12_1	C11_1	C16_1	C15_1	3(5)
C12_1	C13_1	C14_1	C15_1	4(6)
C13_1	C14_1	C15_1	C16_1	-1(6)
C14_1	C15_1	C16_1	C11_1	-3(6)
C16_1	C11_1	C12_1	C13_1	0(5)
C17_1	C3_1	C4_1	C2_1	104.7(11)
C17_1	C3_1	C11_1	C12_1	91(2)
C17_1	C3_1	C11_1	C16_1	-93(3)
C17_1	C18_1	C19_1	C20_1	0.00(8)
C18_1	C17_1	C22_1	C21_1	0.00(19)
C18_1	C19_1	C20_1	C21_1	0.00(19)
C19_1	C20_1	C21_1	C22_1	0.0(3)
C20_1	C21_1	C22_1	C17_1	0.0(3)
C22_1	C17_1	C18_1	C19_1	0.00(8)
C11_5	C6_5	C7_5	C8_5	-179.99(10)
O1_5	C1_5	C2_5	C3_5	-154(3)
O1_5	C1_5	C2_5	C4_5	143(3)
O1_5	C1_5	C2_5	C5_5	-4(4)
O2_5	C1_5	C2_5	C3_5	26(4)
O2_5	C1_5	C2_5	C4_5	-37(4)
O2_5	C1_5	C2_5	C5_5	176(3)
C1_5	C2_5	C3_5	C4_5	-98.6(18)
C1_5	C2_5	C3_5	C11_5	16(2)
C1_5	C2_5	C3_5	C17_5	153.7(18)
C1_5	C2_5	C4_5	C3_5	112.6(16)
C1_5	C2_5	C5_5	C6_5	-61(2)
C1_5	C2_5	C5_5	C10_5	116.5(18)
C2_5	C3_5	C11_5	C12_5	-136.0(14)

Atom	Atom	Atom	Atom	Angle/°
C2_5	C3_5	C11_5	C16_5	44.0(14)
C2_5	C3_5	C17_5	C18_5	88.5(13)
C2_5	C3_5	C17_5	C22_5	-91.5(13)
C2_5	C5_5	C6_5	C11_5	-2.5(15)
C2_5	C5_5	C6_5	C7_5	177.5(15)
C2_5	C5_5	C10_5	C9_5	-177.5(14)
C3_5	C2_5	C5_5	C6_5	90.5(16)
C3_5	C2_5	C5_5	C10_5	-92.1(14)
C3_5	C11_5	C12_5	C13_5	-179.98(8)
C3_5	C11_5	C16_5	C15_5	179.96(15)
C3_5	C17_5	C18_5	C19_5	179.99(8)
C3_5	C17_5	C22_5	C21_5	-179.99(14)
C4_5	C2_5	C3_5	C11_5	114.3(15)
C4_5	C2_5	C3_5	C17_5	-107.7(14)
C4_5	C2_5	C5_5	C6_5	155.3(13)
C4_5	C2_5	C5_5	C10_5	-27.3(16)
C4_5	C3_5	C11_5	C12_5	-59.5(15)
C4_5	C3_5	C11_5	C16_5	120.5(15)
C4_5	C3_5	C17_5	C18_5	19.3(12)
C4_5	C3_5	C17_5	C22_5	-160.7(12)
C5_5	C2_5	C3_5	C4_5	111.1(15)
C5_5	C2_5	C3_5	C11_5	-134.6(13)
C5_5	C2_5	C3_5	C17_5	3.4(18)
C5_5	C2_5	C4_5	C3_5	-102.3(14)
C5_5	C6_5	C7_5	C8_5	0.01(15)
C6_5	C5_5	C10_5	C9_5	0.00(15)
C6_5	C7_5	C8_5	C9_5	0.0(2)
C7_5	C8_5	C9_5	C10_5	0.0(2)
C8_5	C9_5	C10_5	C5_5	0.0(2)
C10_5	C5_5	C6_5	C11_5	180.00(7)
C10_5	C5_5	C6_5	C7_5	-0.01(9)
C11_5	C3_5	C4_5	C2_5	-114.9(14)
C11_5	C3_5	C17_5	C18_5	-125.8(11)
C11_5	C3_5	C17_5	C22_5	54.2(11)
C11_5	C12_5	C13_5	C14_5	0.01(9)
C12_5	C11_5	C16_5	C15_5	-0.02(19)
C12_5	C13_5	C14_5	C15_5	0.0(2)
C13_5	C14_5	C15_5	C16_5	0.0(3)
C14_5	C15_5	C16_5	C11_5	0.0(3)

Atom	Atom	Atom	Atom	Angle/°
C16_5	C11_5	C12_5	C13_5	0.00(9)
C17_5	C3_5	C4_5	C2_5	107.5(10)
C17_5	C3_5	C11_5	C12_5	82.0(10)
C17_5	C3_5	C11_5	C16_5	-98.0(11)
C17_5	C18_5	C19_5	C20_5	0.00(8)
C18_5	C17_5	C22_5	C21_5	0.00(19)
C18_5	C19_5	C20_5	C21_5	0.00(19)
C19_5	C20_5	C21_5	C22_5	0.0(2)
C20_5	C21_5	C22_5	C17_5	0.0(3)
C22_5	C17_5	C18_5	C19_5	0.00(8)
Cl1_7	C6_7	C7_7	C8_7	179.99(9)
O1_7	C1_7	C2_7	C3_7	-167(3)
O1_7	C1_7	C2_7	C4_7	129(3)
O1_7	C1_7	C2_7	C5_7	-19(4)
O2_7	C1_7	C2_7	C3_7	25(4)
O2_7	C1_7	C2_7	C4_7	-40(4)
O2_7	C1_7	C2_7	C5_7	173(3)
C1_7	C2_7	C3_7	C4_7	-100.6(17)
C1_7	C2_7	C3_7	C11_7	11(2)
C1_7	C2_7	C3_7	C17_7	151.7(18)
C1_7	C2_7	C4_7	C3_7	111.4(15)
C1_7	C2_7	C5_7	C6_7	-71(2)
C1_7	C2_7	C5_7	C10_7	110.0(17)
C2_7	C3_7	C11_7	C12_7	-134(3)
C2_7	C3_7	C11_7	C16_7	46(3)
C2_7	C3_7	C17_7	C18_7	68.4(13)
C2_7	C3_7	C17_7	C22_7	-111.6(13)
C2_7	C5_7	C6_7	Cl1_7	0.6(12)
C2_7	C5_7	C6_7	C7_7	-179.4(12)
C2_7	C5_7	C10_7	C9_7	179.4(12)
C3_7	C2_7	C5_7	C6_7	78.8(15)
C3_7	C2_7	C5_7	C10_7	-100.6(13)
C3_7	C11_7	C12_7	C13_7	179(3)
C3_7	C11_7	C16_7	C15_7	178(3)
C3_7	C17_7	C18_7	C19_7	-179.99(8)
C3_7	C17_7	C22_7	C21_7	179.99(14)
C4_7	C2_7	C3_7	C11_7	111.4(15)
C4_7	C2_7	C3_7	C17_7	-107.7(14)
C4_7	C2_7	C5_7	C6_7	144.1(13)

Atom	Atom	Atom	Atom	Angle/°
C4_7	C2_7	C5_7	C10_7	-35.4(15)
C4_7	C3_7	C11_7	C12_7	-62(3)
C4_7	C3_7	C11_7	C16_7	118(3)
C4_7	C3_7	C17_7	C18_7	0.5(12)
C4_7	C3_7	C17_7	C22_7	-179.5(12)
C5_7	C2_7	C3_7	C4_7	111.4(15)
C5_7	C2_7	C3_7	C11_7	-137.3(14)
C5_7	C2_7	C3_7	C17_7	3.7(18)
C5_7	C2_7	C4_7	C3_7	-102.6(14)
C5_7	C6_7	C7_7	C8_7	-0.01(19)
C6_7	C5_7	C10_7	C9_7	0.0(3)
C6_7	C7_7	C8_7	C9_7	0.00(8)
C7_7	C8_7	C9_7	C10_7	0.00(8)
C8_7	C9_7	C10_7	C5_7	0.02(19)
C10_7	C5_7	C6_7	C11_7	-179.98(15)
C10_7	C5_7	C6_7	C7_7	0.0(3)
C11_7	C3_7	C4_7	C2_7	-111.1(14)
C11_7	C3_7	C17_7	C18_7	-146.7(11)
C11_7	C3_7	C17_7	C22_7	33.3(11)
C11_7	C12_7	C13_7	C14_7	4(5)
C12_7	C11_7	C16_7	C15_7	-2(5)
C12_7	C13_7	C14_7	C15_7	-4(5)
C13_7	C14_7	C15_7	C16_7	1(5)
C14_7	C15_7	C16_7	C11_7	1(5)
C16_7	C11_7	C12_7	C13_7	-1(5)
C17_7	C3_7	C4_7	C2_7	105.3(10)
C17_7	C3_7	C11_7	C12_7	84(3)
C17_7	C3_7	C11_7	C16_7	-96(3)
C17_7	C18_7	C19_7	C20_7	0.01(8)
C18_7	C17_7	C22_7	C21_7	-0.01(18)
C18_7	C19_7	C20_7	C21_7	-0.01(19)
C19_7	C20_7	C21_7	C22_7	0.0(3)
C20_7	C21_7	C22_7	C17_7	0.0(3)
C22_7	C17_7	C18_7	C19_7	0.00(8)
C11_8	C6_8	C7_8	C8_8	-180(3)
O1_8	C1_8	C2_8	C3_8	-146(3)
O1_8	C1_8	C2_8	C4_8	148(3)
O1_8	C1_8	C2_8	C5_8	6(4)
O2_8	C1_8	C2_8	C3_8	24(4)

Atom	Atom	Atom	Atom	Angle/°
O2_8	C1_8	C2_8	C4_8	-43(4)
O2_8	C1_8	C2_8	C5_8	175(3)
C1_8	C2_8	C3_8	C4_8	-104.2(19)
C1_8	C2_8	C3_8	C11_8	-1(3)
C1_8	C2_8	C3_8	C17_8	144(2)
C1_8	C2_8	C4_8	C3_8	111.0(18)
C1_8	C2_8	C5_8	C6_8	-72(3)
C1_8	C2_8	C5_8	C10_8	114(3)
C2_8	C3_8	C11_8	C12_8	-123(3)
C2_8	C3_8	C11_8	C16_8	55(4)
C2_8	C3_8	C17_8	C18_8	83.3(15)
C2_8	C3_8	C17_8	C22_8	-96.7(15)
C2_8	C5_8	C6_8	C11_8	8(4)
C2_8	C5_8	C6_8	C7_8	-177(3)
C2_8	C5_8	C10_8	C9_8	174(3)
C3_8	C2_8	C5_8	C6_8	81(3)
C3_8	C2_8	C5_8	C10_8	-93(3)
C3_8	C11_8	C12_8	C13_8	-179(3)
C3_8	C11_8	C16_8	C15_8	-175(3)
C3_8	C17_8	C18_8	C19_8	-179.99(8)
C3_8	C17_8	C22_8	C21_8	179.99(14)
C4_8	C2_8	C3_8	C11_8	102.7(17)
C4_8	C2_8	C3_8	C17_8	-111.6(16)
C4_8	C2_8	C5_8	C6_8	146(3)
C4_8	C2_8	C5_8	C10_8	-29(3)
C4_8	C3_8	C11_8	C12_8	-51(3)
C4_8	C3_8	C11_8	C16_8	126(3)
C4_8	C3_8	C17_8	C18_8	14.5(14)
C4_8	C3_8	C17_8	C22_8	-165.5(14)
C5_8	C2_8	C3_8	C4_8	104.5(16)
C5_8	C2_8	C3_8	C11_8	-152.8(15)
C5_8	C2_8	C3_8	C17_8	-7(2)
C5_8	C2_8	C4_8	C3_8	-107.3(15)
C5_8	C6_8	C7_8	C8_8	5(6)
C6_8	C5_8	C10_8	C9_8	0(5)
C6_8	C7_8	C8_8	C9_8	-5(6)
C7_8	C8_8	C9_8	C10_8	3(6)
C8_8	C9_8	C10_8	C5_8	0(5)
C10_8	C5_8	C6_8	C11_8	-177(3)

Atom	Atom	Atom	Atom	Angle/°
C10_8	C5_8	C6_8	C7_8	-2(5)
C11_8	C3_8	C4_8	C2_8	-118.4(14)
C11_8	C3_8	C17_8	C18_8	-125.7(13)
C11_8	C3_8	C17_8	C22_8	54.3(13)
C11_8	C12_8	C13_8	C14_8	-5(7)
C12_8	C11_8	C16_8	C15_8	3(6)
C12_8	C13_8	C14_8	C15_8	1(6)
C13_8	C14_8	C15_8	C16_8	4(6)
C14_8	C15_8	C16_8	C11_8	-6(6)
C16_8	C11_8	C12_8	C13_8	3(6)
C17_8	C3_8	C4_8	C2_8	103.6(11)
C17_8	C3_8	C11_8	C12_8	90(3)
C17_8	C3_8	C11_8	C16_8	-92(3)
C17_8	C18_8	C19_8	C20_8	0.01(8)
C18_8	C17_8	C22_8	C21_8	0.00(19)
C18_8	C19_8	C20_8	C21_8	-0.02(19)
C19_8	C20_8	C21_8	C22_8	0.0(3)
C20_8	C21_8	C22_8	C17_8	0.0(3)
C22_8	C17_8	C18_8	C19_8	0.00(8)
C25_9	O3_9	C26_9	C27_9	-147(4)
C26_9	O3_9	C25_9	C24_9	179(4)
C25_10	O3_10	C26_10	C27_10	157(4)
C26_10	O3_10	C25_10	C24_10	121(4)

Table 6 Hydrogen Fractional Atomic Coordinates ($\times 10^4$) and Equivalent Isotropic Displacement Parameters ($\text{\AA}^2 \times 10^3$) for **WL-NI-ROCT**. U_{eq} is defined as 1/3 of the trace of the orthogonalised U_{ij} .

Atom	x	y	z	U_{eq}
H1WA	8960.22	5086.51	2605.88	66
H1WB	8159.83	4785.71	2654.78	66
H4A_3	9098.05	2065.76	2517.44	39
H4B_3	9355.77	2776.58	2534.13	39
H7_3	6362.44	1516.6	929.17	77
H8_3	7245.68	697.2	819.15	47
H9_3	8627.67	712.66	1194.46	47
H10_3	9123.48	1553.69	1681.84	43
H12_3	8500.66	3058.5	3531.08	42
H13_3	8203.61	3931.69	4009.17	48
H14_3	7303.65	4637.61	3606.72	62
H15_3	6707.9	4463.9	2728.38	39
H16_3	7006.47	3580.65	2242.45	37
H18_3	8250.8	1453.81	2756.91	41
H19_3	7325.84	714.02	3089.37	41
H20_3	5901.87	943.54	3276.5	42
H21_3	5394.61	1909.88	3133.19	42
H22_3	6331.99	2648.04	2799.02	41
H4A_6	12524.33	4512.4	1295	34
H4B_6	11637.96	4831.44	1513.43	34
H7_6	11722.95	1983.02	637.9	54
H8_6	12761.88	2226.23	-17.42	56
H9_6	13232.81	3213.99	-87.96	41
H10_6	12665.39	3954.71	496.04	38
H12_6	11815.38	4931.58	2604.99	36
H13_6	11068.38	5122.08	3424.78	39
H14_6	10146.09	4406.66	3788.36	40
H15_6	9980.92	3504.09	3324.7	40
H16_6	10737.51	3314.14	2495.87	38
H18_6	13463.63	4406.45	2073.71	36
H19_6	14722.05	3946.86	2393.71	39
H20_6	14789.76	2903.95	2385.55	39
H21_6	13525.22	2351.75	2393.74	39
H22_6	12252.32	2819.36	2091.53	36
H4A_2	8802.07	6527.63	-48.48	34

Atom	x	y	z	U_{eq}
H4B_2	8364.39	6222.5	512.94	34
H7_2	11856.56	5253.69	-817.45	49
H8_2	11242.51	5528.69	-1666.58	49
H9_2	9848.4	5909.87	-1672.93	49
H10_2	9087.53	6010.91	-830.29	49
H12_2	8998.17	7145.11	1270.3	33
H13_2	8887.1	7226.15	2240.58	42
H14_2	9439.59	6475.35	2812.65	36
H15_2	10281.62	5734.79	2417.35	38
H16_2	10339.23	5627.99	1436.08	35
H18_2	9767.29	7070.94	-323.35	38
H19_2	10845.39	7671.88	-702.28	41
H20_2	12171.37	7713.39	-253.1	51
H21_2	12417.44	7162.07	564.08	51
H22_2	11326.37	6562.32	936.88	36
H4A_4	8935.94	1962.65	2332.18	39
H4B_4	9216.84	2664.98	2409.43	39
H7_4	6152.64	1766.61	615.74	46
H8_4	6791.32	839.37	572.2	48
H9_4	8089	670.34	1040.45	47
H10_4	8730.65	1442.16	1549	43
H12_4	8316.57	2849.47	3458.13	42
H13_4	7964.14	3653.66	4021.81	48
H14_4	7046.85	4384.62	3687.63	46
H15_4	6480.21	4309.87	2785.32	39
H16_4	6836.15	3496.86	2214.41	37
H18_4	8203.06	1559.07	3039.76	41
H19_4	7319.5	799.24	3387.91	41
H20_4	5874	796.97	3161.05	42
H21_4	5296.73	1540.76	2592.7	42
H22_4	6188.22	2303.83	2243.95	41
H4A_1	8872.63	6625.23	127.78	34
H4B_1	8395.45	6282.38	654.69	34
H7_1	11923.88	5360.44	-654.76	49
H8_1	11407.07	5767.5	-1483.92	49
H9_1	10025.01	6174.3	-1500.38	49
H10_1	9184.7	6165.94	-685.31	49
H12_1	8879.66	7053.55	1479.76	33
H13_1	8742.75	7063.91	2453.55	36

Atom	x	y	z	U_{eq}
H14_1	9361.87	6307.52	2987.06	42
H15_1	10248.64	5619.11	2554.76	34
H16_1	10492.81	5664.98	1583.11	34
H18_1	9774.25	7337.26	72.98	38
H19_1	10896.22	7959.06	-214.85	41
H20_1	12274.01	7779.36	119.98	51
H21_1	12539.81	6990.73	734.64	51
H22_1	11407.11	6374.06	1017.25	52
H4A_5	12485.04	4583.11	1492.6	34
H4B_5	11564.67	4844.02	1718.22	34
H7_5	11946.56	2089.34	620.47	54
H8_5	13024.25	2434.99	39.9	56
H9_5	13433.81	3439.29	77.38	41
H10_5	12751.4	4091.75	702.93	50
H12_5	11973.67	4677.47	2940.78	36
H13_5	11237.63	4722.89	3785.14	39
H14_5	10131.32	4054.29	3958.3	40
H15_5	9773.51	3347.94	3285.07	40
H16_5	10520.18	3305.11	2432.59	60
H18_5	13554.43	4252.64	1930.68	36
H19_5	14788.91	3706.11	2140.21	39
H20_5	14668.98	2749.79	2520.43	39
H21_5	13330.33	2336.82	2692.17	39
H22_5	12101.29	2892.42	2478.96	36
H4A_7	5181.46	4048.07	1013.44	35
H4B_7	5939.08	4050.26	1494.46	35
H7_7	6389.81	5253.73	-1073.69	43
H8_7	5583.83	4491.73	-1459.06	43
H9_7	5106.18	3706.49	-885.72	43
H10_7	5449.31	3697.85	77.76	43
H12_7	5309.28	5076.99	2155.52	37
H13_7	5888	5622.96	2890.84	39
H14_7	7056.85	6240.28	2717.79	45
H15_7	7716.72	6218.56	1846.02	39
H16_7	7191.06	5613.43	1120.76	36
H18_7	4309.83	4486.7	631.31	36
H19_7	3184.77	4970.87	168.26	40
H20_7	3233.58	6003.58	47.33	40
H21_7	4389.54	6549.73	383.81	40

Atom	x	y	z	U_{eq}
H22_7	5519.07	6059.52	849.36	36
H4A_8	5109.45	4034.99	1070.43	35
H4B_8	5850.9	4069.11	1561.61	35
H7_8	6274.41	4878.51	-1124.38	43
H8_8	5305.33	4141.94	-1353.57	43
H9_8	4876.12	3449.65	-669.93	43
H10_8	5331.87	3558.12	269.96	38
H12_8	5135.46	4930.06	2125.03	37
H13_8	5453.04	5509.73	2902.23	39
H14_8	6653.94	6122.1	2890.32	41
H15_8	7489.73	6171.16	2083	39
H16_8	7027.19	5707.62	1250.86	36
H18_8	4102.99	4596.88	751.68	36
H19_8	3099.75	5124.79	217.71	40
H20_8	3430.09	6075.54	-119.96	40
H21_8	4757.86	6495.74	76.43	40
H22_8	5759.3	5961.54	612.79	36
H24A_9	8325.97	4318.15	-1232.05	115
H24B_9	8751.06	4816.29	-852.83	115
H24C_9	8115.19	4351.13	-580.1	115
H25A_9	9453.09	3786.46	-1088.59	92
H25B_9	9791.62	4235.54	-629.45	92
H26A_9	10312.45	3358.51	35.69	92
H26B_9	10254.73	3192.9	-614.03	92
H27A_9	9678.28	2308.66	-438.39	115
H27B_9	9134.04	2551.74	74.24	115
H27C_9	10106.99	2389.84	160.86	115
H24A_10	7755.19	3864.3	-1257.25	115
H24B_10	7951.13	4474.99	-950.36	115
H24C_10	7619.12	3923.04	-598.26	115
H25A_10	9061.77	3599.24	-1136.24	92
H25B_10	9250.91	4201.05	-817.79	92
H26A_10	9794.06	2985.71	-777.48	92
H26B_10	8965.09	2668.85	-538.21	92
H27A_10	10509.98	2616.56	-64.64	115
H27B_10	9663.79	2364.28	209.02	115
H27C_10	9965.03	3021.14	346.03	115

Table 7 Atomic Occupancies for all atoms that are not fully occupied in **WL-NI-ROCT**.

Atom	Occupancy	Atom	Occupancy	Atom	Occupancy
C11_3	0.361(8)	C21_3	0.361(8)	C19_6	0.479(12)
O1_3	0.361(8)	H21_3	0.361(8)	H19_6	0.479(12)
O2_3	0.361(8)	C22_3	0.361(8)	C20_6	0.479(12)
C1_3	0.361(8)	H22_3	0.361(8)	H20_6	0.479(12)
C2_3	0.361(8)	C11_6	0.479(12)	C21_6	0.479(12)
C3_3	0.361(8)	O1_6	0.479(12)	H21_6	0.479(12)
C4_3	0.361(8)	O2_6	0.479(12)	C22_6	0.479(12)
H4A_3	0.361(8)	C1_6	0.479(12)	H22_6	0.479(12)
H4B_3	0.361(8)	C2_6	0.479(12)	C11_2	0.489(12)
C5_3	0.361(8)	C3_6	0.479(12)	O1_2	0.489(12)
C6_3	0.361(8)	C4_6	0.479(12)	O2_2	0.489(12)
C7_3	0.361(8)	H4A_6	0.479(12)	C1_2	0.489(12)
H7_3	0.361(8)	H4B_6	0.479(12)	C2_2	0.489(12)
C8_3	0.361(8)	C5_6	0.479(12)	C3_2	0.489(12)
H8_3	0.361(8)	C6_6	0.479(12)	C4_2	0.489(12)
C9_3	0.361(8)	C7_6	0.479(12)	H4A_2	0.489(12)
H9_3	0.361(8)	H7_6	0.479(12)	H4B_2	0.489(12)
C10_3	0.361(8)	C8_6	0.479(12)	C5_2	0.489(12)
H10_3	0.361(8)	H8_6	0.479(12)	C6_2	0.489(12)
C11_3	0.361(8)	C9_6	0.479(12)	C7_2	0.489(12)
C12_3	0.361(8)	H9_6	0.479(12)	H7_2	0.489(12)
H12_3	0.361(8)	C10_6	0.479(12)	C8_2	0.489(12)
C13_3	0.361(8)	H10_6	0.479(12)	H8_2	0.489(12)
H13_3	0.361(8)	C11_6	0.479(12)	C9_2	0.489(12)
C14_3	0.361(8)	C12_6	0.479(12)	H9_2	0.489(12)
H14_3	0.361(8)	H12_6	0.479(12)	C10_2	0.489(12)
C15_3	0.361(8)	C13_6	0.479(12)	H10_2	0.489(12)
H15_3	0.361(8)	H13_6	0.479(12)	C11_2	0.489(12)
C16_3	0.361(8)	C14_6	0.479(12)	C12_2	0.489(12)
H16_3	0.361(8)	H14_6	0.479(12)	H12_2	0.489(12)
C17_3	0.361(8)	C15_6	0.479(12)	C13_2	0.489(12)
C18_3	0.361(8)	H15_6	0.479(12)	H13_2	0.489(12)
H18_3	0.361(8)	C16_6	0.479(12)	C14_2	0.489(12)
C19_3	0.361(8)	H16_6	0.479(12)	H14_2	0.489(12)
H19_3	0.361(8)	C17_6	0.479(12)	C15_2	0.489(12)
C20_3	0.361(8)	C18_6	0.479(12)	H15_2	0.489(12)
H20_3	0.361(8)	H18_6	0.479(12)	C16_2	0.489(12)

Atom	Occupancy	Atom	Occupancy	Atom	Occupancy
H16_2	0.489(12)	H15_4	0.639(8)	H14_1	0.511(12)
C17_2	0.489(12)	C16_4	0.639(8)	C15_1	0.511(12)
C18_2	0.489(12)	H16_4	0.639(8)	H15_1	0.511(12)
H18_2	0.489(12)	C17_4	0.639(8)	C16_1	0.511(12)
C19_2	0.489(12)	C18_4	0.639(8)	H16_1	0.511(12)
H19_2	0.489(12)	H18_4	0.639(8)	C17_1	0.511(12)
C20_2	0.489(12)	C19_4	0.639(8)	C18_1	0.511(12)
H20_2	0.489(12)	H19_4	0.639(8)	H18_1	0.511(12)
C21_2	0.489(12)	C20_4	0.639(8)	C19_1	0.511(12)
H21_2	0.489(12)	H20_4	0.639(8)	H19_1	0.511(12)
C22_2	0.489(12)	C21_4	0.639(8)	C20_1	0.511(12)
H22_2	0.489(12)	H21_4	0.639(8)	H20_1	0.511(12)
Cl1_4	0.639(8)	C22_4	0.639(8)	C21_1	0.511(12)
O1_4	0.639(8)	H22_4	0.639(8)	H21_1	0.511(12)
O2_4	0.639(8)	Cl1_1	0.511(12)	C22_1	0.511(12)
C1_4	0.639(8)	O1_1	0.511(12)	H22_1	0.511(12)
C2_4	0.639(8)	O2_1	0.511(12)	Cl1_5	0.521(12)
C3_4	0.639(8)	C1_1	0.511(12)	O1_5	0.521(12)
C4_4	0.639(8)	C2_1	0.511(12)	O2_5	0.521(12)
H4A_4	0.639(8)	C3_1	0.511(12)	C1_5	0.521(12)
H4B_4	0.639(8)	C4_1	0.511(12)	C2_5	0.521(12)
C5_4	0.639(8)	H4A_1	0.511(12)	C3_5	0.521(12)
C6_4	0.639(8)	H4B_1	0.511(12)	C4_5	0.521(12)
C7_4	0.639(8)	C5_1	0.511(12)	H4A_5	0.521(12)
H7_4	0.639(8)	C6_1	0.511(12)	H4B_5	0.521(12)
C8_4	0.639(8)	C7_1	0.511(12)	C5_5	0.521(12)
H8_4	0.639(8)	H7_1	0.511(12)	C6_5	0.521(12)
C9_4	0.639(8)	C8_1	0.511(12)	C7_5	0.521(12)
H9_4	0.639(8)	H8_1	0.511(12)	H7_5	0.521(12)
C10_4	0.639(8)	C9_1	0.511(12)	C8_5	0.521(12)
H10_4	0.639(8)	H9_1	0.511(12)	H8_5	0.521(12)
C11_4	0.639(8)	C10_1	0.511(12)	C9_5	0.521(12)
C12_4	0.639(8)	H10_1	0.511(12)	H9_5	0.521(12)
H12_4	0.639(8)	C11_1	0.511(12)	C10_5	0.521(12)
C13_4	0.639(8)	C12_1	0.511(12)	H10_5	0.521(12)
H13_4	0.639(8)	H12_1	0.511(12)	C11_5	0.521(12)
C14_4	0.639(8)	C13_1	0.511(12)	C12_5	0.521(12)
H14_4	0.639(8)	H13_1	0.511(12)	H12_5	0.521(12)
C15_4	0.639(8)	C14_1	0.511(12)	C13_5	0.521(12)

Atom	Occupancy	Atom	Occupancy	Atom	Occupancy
H13_5	0.521(12)	H12_7	0.548(11)	C11_8	0.452(11)
C14_5	0.521(12)	C13_7	0.548(11)	C12_8	0.452(11)
H14_5	0.521(12)	H13_7	0.548(11)	H12_8	0.452(11)
C15_5	0.521(12)	C14_7	0.548(11)	C13_8	0.452(11)
H15_5	0.521(12)	H14_7	0.548(11)	H13_8	0.452(11)
C16_5	0.521(12)	C15_7	0.548(11)	C14_8	0.452(11)
H16_5	0.521(12)	H15_7	0.548(11)	H14_8	0.452(11)
C17_5	0.521(12)	C16_7	0.548(11)	C15_8	0.452(11)
C18_5	0.521(12)	H16_7	0.548(11)	H15_8	0.452(11)
H18_5	0.521(12)	C17_7	0.548(11)	C16_8	0.452(11)
C19_5	0.521(12)	C18_7	0.548(11)	H16_8	0.452(11)
H19_5	0.521(12)	H18_7	0.548(11)	C17_8	0.452(11)
C20_5	0.521(12)	C19_7	0.548(11)	C18_8	0.452(11)
H20_5	0.521(12)	H19_7	0.548(11)	H18_8	0.452(11)
C21_5	0.521(12)	C20_7	0.548(11)	C19_8	0.452(11)
H21_5	0.521(12)	H20_7	0.548(11)	H19_8	0.452(11)
C22_5	0.521(12)	C21_7	0.548(11)	C20_8	0.452(11)
H22_5	0.521(12)	H21_7	0.548(11)	H20_8	0.452(11)
C11_7	0.548(11)	C22_7	0.548(11)	C21_8	0.452(11)
O1_7	0.548(11)	H22_7	0.548(11)	H21_8	0.452(11)
O2_7	0.548(11)	C11_8	0.452(11)	C22_8	0.452(11)
C1_7	0.548(11)	O1_8	0.452(11)	H22_8	0.452(11)
C2_7	0.548(11)	O2_8	0.452(11)	O3_9	0.50(2)
C3_7	0.548(11)	C1_8	0.452(11)	C24_9	0.50(2)
C4_7	0.548(11)	C2_8	0.452(11)	H24A_9	0.50(2)
H4A_7	0.548(11)	C3_8	0.452(11)	H24B_9	0.50(2)
H4B_7	0.548(11)	C4_8	0.452(11)	H24C_9	0.50(2)
C5_7	0.548(11)	H4A_8	0.452(11)	C25_9	0.50(2)
C6_7	0.548(11)	H4B_8	0.452(11)	H25A_9	0.50(2)
C7_7	0.548(11)	C5_8	0.452(11)	H25B_9	0.50(2)
H7_7	0.548(11)	C6_8	0.452(11)	C26_9	0.50(2)
C8_7	0.548(11)	C7_8	0.452(11)	H26A_9	0.50(2)
H8_7	0.548(11)	H7_8	0.452(11)	H26B_9	0.50(2)
C9_7	0.548(11)	C8_8	0.452(11)	C27_9	0.50(2)
H9_7	0.548(11)	H8_8	0.452(11)	H27A_9	0.50(2)
C10_7	0.548(11)	C9_8	0.452(11)	H27B_9	0.50(2)
H10_7	0.548(11)	H9_8	0.452(11)	H27C_9	0.50(2)
C11_7	0.548(11)	C10_8	0.452(11)	O3_10	0.50(2)
C12_7	0.548(11)	H10_8	0.452(11)	C24_10	0.50(2)

Atom	Occupancy
H24A_10	0.50(2)
H24B_10	0.50(2)
H24C_10	0.50(2)
C25_10	0.50(2)
H25A_10	0.50(2)

Atom	Occupancy
H25B_10	0.50(2)
C26_10	0.50(2)
H26A_10	0.50(2)
H26B_10	0.50(2)
C27_10	0.50(2)

Atom	Occupancy
H27A_10	0.50(2)
H27B_10	0.50(2)
H27C_10	0.50(2)

Compound **WL-N2-137-
27**

Formula	C ₈₈ H ₆₄ Br ₄ Cl ₄ O ₁₀ Rh ₂
$D_{calc.}/\text{g cm}^{-3}$ /mm ⁻¹	1.607 2.586
Formula Weight	1948.61
Colour	bluish green
Shape	needle
Size/mm ³	0.59×0.07×0. 03
T/K	100(2)
Crystal System	tetragonal
Flack Parameter	0.015(11)
Hoof Parameter	0.021(8)
Space Group	$P4_21_2$
$a/\text{Å}$	20.4695(6)
$b/\text{Å}$	20.4695(6)
$c/\text{Å}$	19.2209(8)
$^\circ$	90
$^\circ$	90
$^\circ$	90
$V/\text{Å}^3$	8053.5(6)
Z	4
Z'	0.5
Wavelength/Å	0.710730
Radiation type	MoK
min°	1.761
max°	24.712
Measured Refl.	40044
Independent Refl.	6882
Reflections with $I > 2\sigma(I)$	4969
R_{int}	0.1306
Parameters	481
Restraints	478
Largest Peak	1.526
Deepest Hole	-0.531
Goof	1.027
wR_2 (all data)	0.1273
wR_2	0.1166
R_1 (all data)	0.0938
R_1	0.0611

Structure Quality Indicators

Reflections:	d min (Mo)	0.85	I/σ	11.1	Rint	13.06%	complete 100% (IUCr)	100%
Refinement:	Shift	0.001	Max Peak	1.5	Min Peak	-0.5	Goof	1.027
							Flack	0.015(11)

A bluish green needle-shaped crystal with dimensions $0.59 \times 0.07 \times 0.03 \text{ mm}^3$ was mounted on a mylar loop with paratone oil. Data were collected using an Bruker D8 diffractometer with APEX2 detector equipped with an Oxford Cryosystems low-temperature device operating at $T = 100(2) \text{ K}$.

Data were measured using scans of 0.5° per frame for 120.0 s using MoK α radiation. The total number of runs and images was based on the strategy calculation from the program APEX2 (Bruker, V2 v2014.1-1). The maximum resolution that was achieved was $\lambda = 24.712^\circ$.

The diffraction pattern was indexed using APEX2 (Bruker, V2 v2014.1-1) and the unit cell was refined using **CrysAlisPro** (Rigaku, V1.171.39.43c, 2018) on 14776 reflections, 37% of the observed reflections.

Data reduction, scaling and absorption corrections were performed using **CrysAlisPro** (Rigaku, V1.171.39.43c, 2018). The final completeness is 99.90 % out to 24.712° in θ . A multi-scan absorption correction was performed using CrysAlisPro 1.171.39.43c (Rigaku Oxford Diffraction, 2018). A spherical absorption correction using equivalent radius of 0.11 mm and absorption coefficient 2.586 mm^{-1} was used. An empirical absorption correction using spherical harmonics, implemented in SCALE3 ABSPACK scaling algorithm. The absorption coefficient of this material is 2.586 mm^{-1} at this wavelength ($\lambda = 0.71073 \text{ \AA}$) and the minimum and maximum transmissions are 0.65 and 0.66.

The structure was solved and the space group $P4_21_2$ (# 90) determined by the **ShelXT** (Sheldrick, 2015) structure solution program using Intrinsic Phasing and refined by Least Squares using version 2018/3 of **ShelXL** (Sheldrick, 2015). All non-hydrogen atoms were refined anisotropically. Hydrogen atom positions were calculated geometrically and refined using the riding model. Hydrogen atom positions were calculated geometrically and refined using the riding model.

Images of the Crystal on the Diffractometer



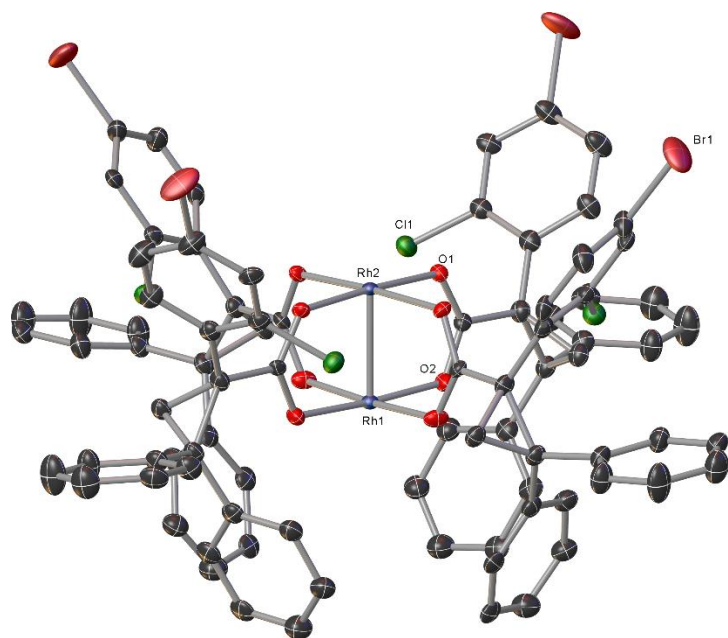


Figure 1:

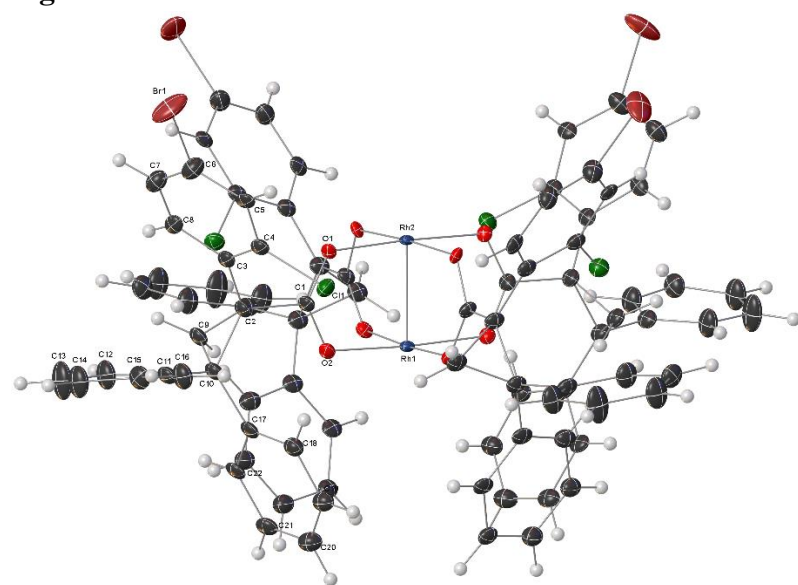
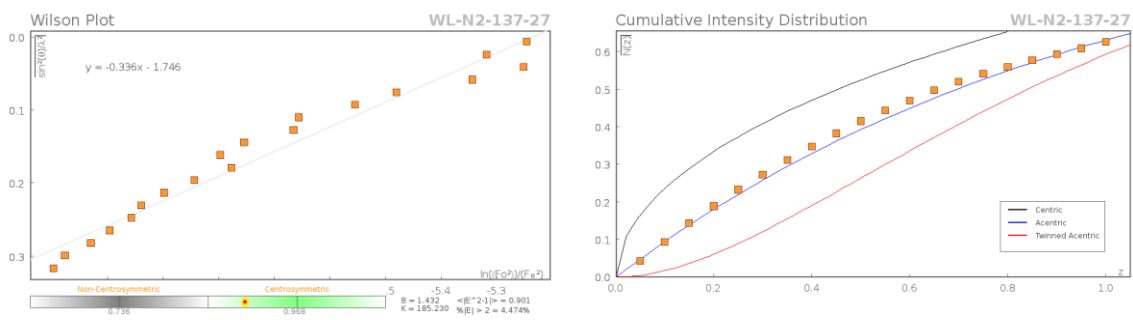
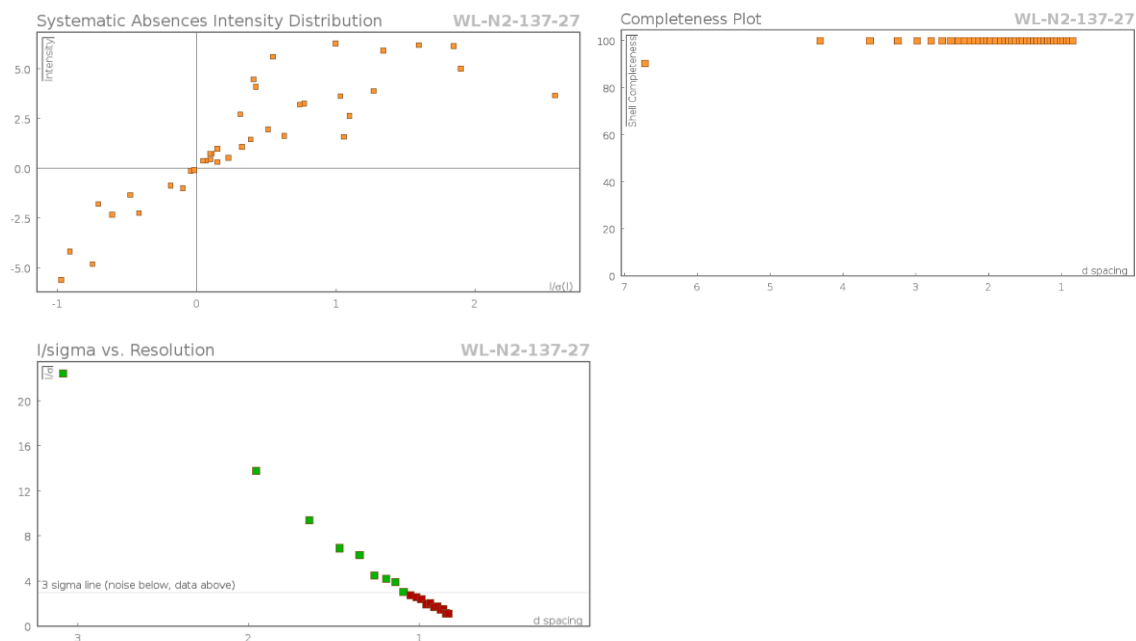


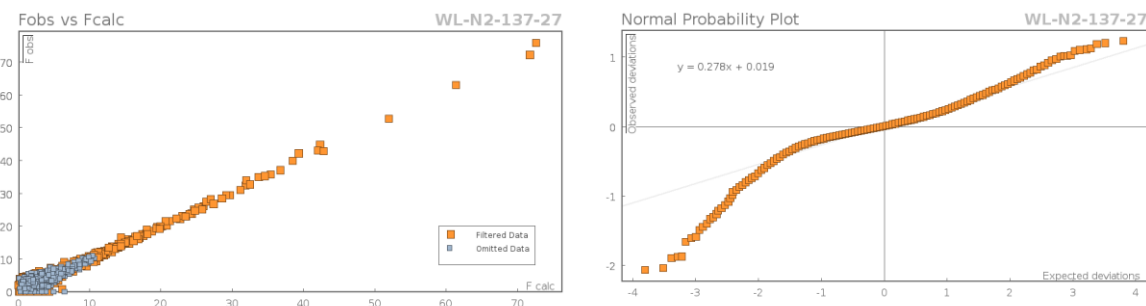
Figure 2:

Data Plots: Diffraction Data





Data Plots: Refinement and Data



Reflection Statistics

Total reflections (after filtering)	40088	Unique reflections	6882
Completeness	1.0	Mean I/	11.75
hkl_{max} collected	(24, 23, 23)	hkl_{min} collected	(-24, -22, -23)
hkl_{max} used	(17, 24, 22)	hkl_{min} used	(-16, 0, 0)
Lim d_{max} collected	20.0	Lim d_{min} collected	0.85
d_{max} used	11.56	d_{min} used	0.85
Friedel pairs	14791	Friedel pairs merged	0
Inconsistent equivalents	1	R_{int}	0.1306
R_{sigma}	0.0899	Intensity transformed	0
Omitted reflections	0	Omitted by user (OMIT hkl)	5
Multiplicity	(37582, 2497, 59)	Maximum multiplicity	15
Removed systematic	39	Filtered off (Shel/OMIT)	2665

absences

Table 1: Fractional Atomic Coordinates ($\times 10^4$) and Equivalent Isotropic Displacement Parameters ($\text{\AA}^2 \times 10^3$) for **WL-N2-137-27**. U_{eq} is defined as 1/3 of the trace of the 364rthogonalized U_{ij} .

Atom	x	y	z	U_{eq}
Rh1	5000	10000	859.6(8)	10.3(4)
Rh2	5000	10000	2096.3(8)	9.3(4)
Rh3	10000	5000	2974.9(9)	10.7(4)
Rh4	10000	5000	4205.3(9)	11.6(4)
Br1_1	6535.6(7)	6761.6(8)	4102.1(8)	46.4(4)
Cl1_1	6672.9(13)	8491.4(13)	1925.3(13)	19.0(6)
O1_1	5229(3)	9030(3)	2067(3)	11.7(14)
O2_1	5151(3)	9031(3)	894(3)	14.4(15)
C1_1	5262(5)	8760(4)	1480(4)	15.0(13)
C2_1	5309(4)	8019(4)	1476(4)	17.4(9)
C3_1	5585(4)	7735(4)	2119(4)	16.5(11)
C4_1	6207(4)	7903(5)	2357(4)	16.9(19)
C5_1	6492(5)	7640(5)	2961(5)	16.4(18)
C6_1	6142(5)	7163(5)	3307(5)	25(2)
C7_1	5556(4)	6949(5)	3073(5)	23(2)
C8_1	5277(5)	7243(4)	2502(5)	17.6(19)
C9_1	4766(4)	7697(4)	1080(4)	18.8(10)
C10_1	5428(4)	7645(4)	792(4)	18.6(9)
C11_1	5777(4)	6986(4)	850(4)	19.6(12)
C12_1	5416(5)	6413(4)	829(7)	29(3)
C13_1	5717(5)	5805(5)	854(8)	41(4)
C14_1	6377(5)	5763(5)	955(7)	34(3)
C15_1	6748(5)	6335(4)	1030(6)	25(2)
C16_1	6439(4)	6931(4)	956(6)	27(3)
C17_1	5610(5)	7985(4)	120(4)	18.4(12)
C18_1	6201(5)	8281(5)	5(5)	21(2)
C19_1	6363(5)	8561(5)	-623(4)	22(2)
C20_1	5922(5)	8561(5)	-1163(5)	25(2)
C21_1	5315(4)	8279(5)	-1072(5)	21(2)
C22_1	5161(4)	7978(5)	-431(4)	18.9(19)
Br1_2	6603.6(8)	3735.8(9)	951.5(8)	67.3(6)
Cl1_2	7673.9(16)	5274.2(14)	3006.1(17)	34.8(8)
O1_2	9092(3)	4554(3)	3026(3)	13.1(14)

Atom	x	y	z	U_{eq}
O2_2	9223(3)	4385(3)	4179(3)	11.2(14)
C1_2	8920(4)	4318(5)	3603(4)	17.1(15)
C2_2	8251(4)	4003(4)	3635(4)	19.3(9)
C3_2	7910(4)	3962(4)	2956(4)	20.8(11)
C4_2	7582(5)	4490(4)	2663(5)	22(2)
C5_2	7188(6)	4442(5)	2065(6)	37(3)
C6_2	7138(6)	3832(5)	1761(5)	32(3)
C7_2	7468(5)	3307(5)	2008(5)	30(2)
C8_2	7841(5)	3371(5)	2597(5)	28(2)
C9_2	8192(4)	3436(4)	4129(4)	19.4(10)
C10_2	7837(4)	4038(4)	4302(4)	19.1(9)
C11_2	7099(4)	4090(4)	4193(5)	18.9(12)
C12_2	6730(4)	3549(5)	4013(7)	30(3)
C13_2	6063(5)	3599(5)	3891(9)	50(4)
C14_2	5751(5)	4185(5)	3974(8)	42(3)
C15_2	6108(5)	4737(5)	4180(8)	42(4)
C16_2	6768(4)	4667(5)	4306(6)	26(2)
C17_2	8036(4)	4406(5)	4953(4)	19.0(12)
C18_2	8202(5)	5054(5)	4972(5)	21(2)
C19_2	8369(6)	5366(5)	5581(5)	24(2)
C20_2	8387(6)	5028(5)	6198(4)	28(2)
C21_2	8224(5)	4373(5)	6209(4)	22(2)
C22_2	8054(5)	4056(5)	5582(4)	17(2)

Table 2: Anisotropic Displacement Parameters ($\times 10^4$) **WL-N2-137-27**. The anisotropic displacement factor exponent takes the form: $-2 \ [h^2 a^{*2} \times U_{11} + \dots + 2hka^* \times b^* \times U_{12}]$

Atom	U_{11}	U_{22}	U_{33}	U_{23}	U_{13}	U_{12}
Rh1	12.2(6)	12.2(6)	6.4(9)	0	0	0
Rh2	11.3(6)	11.3(6)	5.1(8)	0	0	0
Rh3	11.2(6)	11.2(6)	9.8(9)	0	0	0
Rh4	12.8(6)	12.8(6)	9.1(9)	0	0	0
Br1_1	38.0(9)	61.3(10)	39.8(9)	35.4(8)	0.7(7)	11.0(8)
Cl1_1	20.7(14)	18.5(14)	17.7(13)	3.3(12)	1.2(12)	-2.5(12)
O1_1	10(4)	11(2)	13.7(18)	-2.4(16)	3(2)	2(2)
O2_1	16(4)	13(2)	14.1(18)	-2.5(15)	3(2)	1(2)
C1_1	19(4)	12.4(16)	13.9(18)	-3.0(12)	3.4(19)	3.0(14)
C2_1	24(2)	12.2(16)	15.8(15)	-3.8(12)	1.5(15)	2.8(13)
C3_1	22.1(19)	12(2)	15.5(16)	-3.4(16)	3.4(16)	4.3(16)
C4_1	22(2)	14(3)	15(3)	-3(3)	3.6(18)	4(2)

Atom	U_{11}	U_{22}	U_{33}	U_{23}	U_{13}	U_{12}
C5_1	21(2)	15(3)	14(2)	-3(3)	6(2)	7(2)
C6_1	23(2)	25(4)	26(3)	8(3)	3(2)	3(3)
C7_1	22(3)	22(4)	26(3)	6(3)	4(2)	4(3)
C8_1	20(2)	12(3)	20(3)	-1(3)	6(2)	7(2)
C9_1	24.8(18)	14(2)	18(2)	-5.9(18)	0.8(14)	3.2(14)
C10_1	25.1(19)	14.2(16)	16.5(15)	-5.2(13)	0.7(15)	4.0(14)
C11_1	27(2)	14.9(16)	17(3)	-4.2(16)	3(2)	5.3(15)
C12_1	28(2)	14.5(17)	45(8)	-1(2)	-3(3)	5.2(16)
C13_1	31(3)	15.1(17)	78(11)	-2(3)	-7(4)	6.4(18)
C14_1	30(3)	17(2)	54(9)	-1(3)	-3(4)	6.8(19)
C15_1	28(3)	17(2)	31(7)	-2(3)	3(3)	6.7(18)
C16_1	27(2)	16(2)	36(7)	-3(3)	0(2)	5.7(16)
C17_1	27(2)	13(3)	15.8(16)	-6.2(18)	1.0(15)	4.5(18)
C18_1	27(2)	18(5)	18(2)	-2(3)	-0.2(19)	3(3)
C19_1	26(3)	20(5)	19(2)	0(3)	0.8(19)	6(3)
C20_1	27(3)	27(5)	19(3)	1(3)	0(2)	5(3)
C21_1	26(3)	19(5)	16.8(19)	-4(3)	2(2)	8(3)
C22_1	26(3)	15(5)	15.5(18)	-7(2)	1.2(19)	6(3)
Br1_2	66.0(12)	103.3(15)	32.5(9)	17.7(9)	-30.5(9)	-54.7(11)
Cl1_2	43(2)	27.2(17)	33.9(18)	9.6(14)	-9.4(17)	-3.7(13)
O1_2	13(3)	13(3)	13.1(19)	-2(2)	1.8(17)	-2(2)
O2_2	10(3)	11(4)	12.9(18)	-2(2)	3.9(17)	3(2)
C1_2	15.7(18)	22(4)	14.1(19)	1.0(19)	1.3(14)	-5(2)
C2_2	15.9(16)	26(2)	16.3(14)	3.7(14)	0.6(13)	-6.6(14)
C3_2	16(2)	30(2)	16.2(15)	5.1(15)	0.4(17)	-9.5(15)
C4_2	14(4)	32(2)	21(3)	8.4(17)	-1(3)	-10.3(17)
C5_2	40(5)	36(3)	34(3)	7(2)	-20(4)	-11(2)
C6_2	35(5)	36(3)	25(3)	10(2)	-7(4)	-17(2)
C7_2	37(5)	35(3)	17(3)	6(2)	-5(3)	-16(2)
C8_2	36(5)	32(2)	17(3)	3.3(19)	-4(3)	-11(2)
C9_2	16(2)	25.3(19)	16.5(19)	3.7(15)	1.1(17)	-6.3(15)
C10_2	15.3(17)	26(2)	16.3(15)	4.2(15)	0.5(13)	-5.9(14)
C11_2	15.3(17)	27(2)	15(3)	8(2)	0.1(15)	-6.7(14)
C12_2	16(2)	28(2)	46(8)	2(3)	-5(3)	-6.0(17)
C13_2	18(2)	33(3)	98(11)	-9(5)	-15(3)	-4.3(18)
C14_2	16(2)	32(3)	79(10)	-4(5)	-12(3)	-5.1(19)
C15_2	16(2)	32(3)	79(10)	-5(4)	-11(3)	-4.8(19)
C16_2	14(2)	28(2)	36(7)	3(3)	-3(3)	-6.2(17)
C17_2	14(3)	26(2)	16.6(15)	3.5(15)	0.0(16)	-4(2)

Atom	U_{11}	U_{22}	U_{33}	U_{23}	U_{13}	U_{12}
C18_2	18(6)	26(2)	18(2)	2.8(17)	0(2)	-5(2)
C19_2	26(7)	28(3)	19(2)	2.4(18)	-2(3)	-6(3)
C20_2	35(6)	30(3)	19(2)	3(2)	-2(3)	-6(3)
C21_2	19(6)	29(3)	16.9(16)	3(2)	0(2)	-2(3)
C22_2	9(5)	27(2)	16.2(16)	3.7(18)	2(2)	-1(3)

Table 3: Bond Lengths in Å for **WL-N2-137-27**.

Atom	Atom	Length/Å	Atom	Atom	Length/Å
Rh1	Rh2	2.377(2)	C7_1	C8_1	1.374(11)
Rh1	O2_1 ¹	2.008(6)	C9_1	C10_1	1.468(11)
Rh1	O2_1	2.008(6)	C10_1	C11_1	1.531(10)
Rh1	O2_1 ²	2.008(6)	C10_1	C17_1	1.513(11)
Rh1	O2_1 ³	2.008(6)	C11_1	C12_1	1.387(11)
Rh2	O1_1	2.041(6)	C11_1	C16_1	1.374(11)
Rh2	O1_1 ³	2.041(6)	C12_1	C13_1	1.389(11)
Rh2	O1_1 ²	2.041(6)	C13_1	C14_1	1.368(12)
Rh2	O1_1 ¹	2.041(6)	C14_1	C15_1	1.403(11)
Rh3	Rh4	2.365(2)	C15_1	C16_1	1.382(11)
Rh3	O1_2 ⁴	2.072(6)	C17_1	C18_1	1.372(12)
Rh3	O1_2 ⁵	2.072(6)	C17_1	C22_1	1.403(10)
Rh3	O1_2 ⁶	2.072(6)	C18_1	C19_1	1.377(11)
Rh3	O1_2	2.072(6)	C19_1	C20_1	1.375(11)
Rh4	O2_2 ⁵	2.029(6)	C20_1	C21_1	1.382(11)
Rh4	O2_2	2.029(6)	C21_1	C22_1	1.413(11)
Rh4	O2_2 ⁶	2.029(6)	Br1_2	C6_2	1.912(8)
Rh4	O2_2 ⁴	2.029(6)	Cl1_2	C4_2	1.745(8)
Br1_1	C6_1	1.912(8)	O1_2	C1_2	1.260(8)
Cl1_1	C4_1	1.746(8)	O2_2	C1_2	1.276(8)
O1_1	C1_1	1.258(8)	C1_2	C2_2	1.515(10)
O2_1	C1_1	1.276(8)	C2_2	C3_2	1.483(11)
C1_1	C2_1	1.520(10)	C2_2	C9_2	1.504(10)
C2_1	C3_1	1.479(11)	C2_2	C10_2	1.538(10)
C2_1	C9_1	1.501(10)	C3_2	C4_2	1.392(11)
C2_1	C10_1	1.540(10)	C3_2	C8_2	1.400(11)
C3_1	C4_1	1.395(11)	C4_2	C5_2	1.407(11)
C3_1	C8_1	1.399(11)	C5_2	C6_2	1.382(12)
C4_1	C5_1	1.407(11)	C6_2	C7_2	1.356(12)
C5_1	C6_1	1.382(12)	C7_2	C8_2	1.373(11)
C6_1	C7_1	1.355(12)	C9_2	C10_2	1.468(11)

Atom	Atom	Length/Å
C10_2	C11_2	1.529(10)
C10_2	C17_2	1.516(11)
C11_2	C12_2	1.385(11)
C11_2	C16_2	1.378(11)
C12_2	C13_2	1.389(11)
C13_2	C14_2	1.368(12)
C14_2	C15_2	1.403(11)
C15_2	C16_2	1.381(11)

Atom	Atom	Length/Å
C17_2	C18_2	1.370(12)
C17_2	C22_2	1.405(10)
C18_2	C19_2	1.377(11)
C19_2	C20_2	1.374(11)
C20_2	C21_2	1.382(11)
C21_2	C22_2	1.412(11)

¹-1/2+y,3/2-x,+z; ²3/2-y,1/2+x,+z; ³1-x,2-y,+z;
⁴3/2-y,-1/2+x,+z; ⁵2-x,1-y,+z; ⁶1/2+y,3/2-x,+z

Table 4: Bond Angles in ° for WL-N2-137-27.

Atom	Atom	Atom	Angle/°
O2_1	Rh1	Rh2	88.13(17)
O2_1 ¹	Rh1	Rh2	88.13(17)
O2_1 ²	Rh1	Rh2	88.13(17)
O2_1 ³	Rh1	Rh2	88.13(17)
O2_1 ²	Rh1	O2_1 ³	89.939(12)
O2_1	Rh1	O2_1 ³	176.3(3)
O2_1	Rh1	O2_1 ¹	89.940(12)
O2_1 ¹	Rh1	O2_1 ³	89.939(12)
O2_1	Rh1	O2_1 ²	89.938(12)
O2_1 ²	Rh1	O2_1 ¹	176.3(3)
O1_1 ¹	Rh2	Rh1	88.43(17)
O1_1 ³	Rh2	Rh1	88.43(17)
O1_1	Rh2	Rh1	88.42(17)
O1_1 ²	Rh2	Rh1	88.43(17)
O1_1 ²	Rh2	O1_1 ³	89.957(10)
O1_1	Rh2	O1_1 ³	176.8(3)
O1_1 ¹	Rh2	O1_1 ²	176.9(3)
O1_1	Rh2	O1_1 ¹	89.955(10)
O1_1	Rh2	O1_1 ²	89.959(11)
O1_1 ¹	Rh2	O1_1 ³	89.957(10)
O1_2 ⁴	Rh3	Rh4	87.30(17)
O1_2 ⁵	Rh3	Rh4	87.30(17)
O1_2	Rh3	Rh4	87.30(17)
O1_2 ⁶	Rh3	Rh4	87.30(17)
O1_2 ⁵	Rh3	O1_2 ⁶	89.873(17)
O1_2 ⁵	Rh3	O1_2 ⁴	89.873(16)
O1_2 ⁴	Rh3	O1_2 ⁶	174.6(3)

Atom	Atom	Atom	Angle/°
O1_2 ⁵	Rh3	O1_2	174.6(3)
O1_2 ⁶	Rh3	O1_2	89.872(17)
O1_2 ⁴	Rh3	O1_2	89.874(17)
O2_2 ⁵	Rh4	Rh3	88.56(16)
O2_2 ⁶	Rh4	Rh3	88.56(16)
O2_2 ⁴	Rh4	Rh3	88.56(16)
O2_2	Rh4	Rh3	88.56(16)
O2_2 ⁴	Rh4	O2_2	89.966(9)
O2_2 ⁴	Rh4	O2_2 ⁶	177.1(3)
O2_2 ⁵	Rh4	O2_2	177.1(3)
O2_2 ⁶	Rh4	O2_2	89.962(9)
O2_2 ⁵	Rh4	O2_2 ⁴	89.964(9)
O2_2 ⁵	Rh4	O2_2 ⁶	89.964(9)
C1_1	O1_1	Rh2	117.6(5)
C1_1	O2_1	Rh1	119.0(5)
O1_1	C1_1	O2_1	126.3(7)
O1_1	C1_1	C2_1	116.5(7)
O2_1	C1_1	C2_1	116.1(7)
C1_1	C2_1	C10_1	120.7(7)
C3_1	C2_1	C1_1	114.4(7)
C3_1	C2_1	C9_1	122.3(7)
C3_1	C2_1	C10_1	117.2(7)
C9_1	C2_1	C1_1	113.3(7)
C9_1	C2_1	C10_1	57.7(5)
C4_1	C3_1	C2_1	121.7(7)
C4_1	C3_1	C8_1	114.6(7)
C8_1	C3_1	C2_1	123.5(7)

Atom	Atom	Atom	Angle/°
C3_1	C4_1	Cl1_1	120.8(6)
C3_1	C4_1	C5_1	123.7(8)
C5_1	C4_1	Cl1_1	115.4(7)
C6_1	C5_1	C4_1	116.9(8)
C5_1	C6_1	Br1_1	118.0(7)
C7_1	C6_1	Br1_1	120.0(7)
C7_1	C6_1	C5_1	121.8(8)
C6_1	C7_1	C8_1	119.5(8)
C7_1	C8_1	C3_1	123.2(8)
C10_1	C9_1	C2_1	62.5(5)
C9_1	C10_1	C2_1	59.8(5)
C9_1	C10_1	C11_1	117.8(7)
C9_1	C10_1	C17_1	121.0(7)
C11_1	C10_1	C2_1	116.7(6)
C17_1	C10_1	C2_1	122.6(7)
C17_1	C10_1	C11_1	110.6(6)
C12_1	C11_1	C10_1	119.6(8)
C16_1	C11_1	C10_1	122.9(7)
C16_1	C11_1	C12_1	117.5(7)
C11_1	C12_1	C13_1	121.3(8)
C14_1	C13_1	C12_1	120.0(9)
C13_1	C14_1	C15_1	119.7(9)
C16_1	C15_1	C14_1	118.6(9)
C11_1	C16_1	C15_1	122.6(8)
C18_1	C17_1	C10_1	124.0(7)
C18_1	C17_1	C22_1	117.4(8)
C22_1	C17_1	C10_1	118.6(8)
C17_1	C18_1	C19_1	122.5(8)
C20_1	C19_1	C18_1	120.3(8)
C19_1	C20_1	C21_1	119.6(8)
C20_1	C21_1	C22_1	119.6(8)
C17_1	C22_1	C21_1	120.5(8)
C1_2	O1_2	Rh3	117.4(5)
C1_2	O2_2	Rh4	118.0(5)
O1_2	C1_2	O2_2	125.9(7)
O1_2	C1_2	C2_2	116.9(7)
O2_2	C1_2	C2_2	116.6(7)
C1_2	C2_2	C10_2	120.9(7)
C3_2	C2_2	C1_2	114.4(7)

Atom	Atom	Atom	Angle/°
C3_2	C2_2	C9_2	118.3(7)
C3_2	C2_2	C10_2	118.5(6)
C9_2	C2_2	C1_2	115.3(7)
C9_2	C2_2	C10_2	57.7(5)
C4_2	C3_2	C2_2	122.6(7)
C4_2	C3_2	C8_2	115.0(7)
C8_2	C3_2	C2_2	122.1(7)
C3_2	C4_2	Cl1_2	120.6(6)
C3_2	C4_2	C5_2	123.5(8)
C5_2	C4_2	Cl1_2	115.8(7)
C6_2	C5_2	C4_2	116.8(8)
C5_2	C6_2	Br1_2	118.7(7)
C7_2	C6_2	Br1_2	119.2(7)
C7_2	C6_2	C5_2	122.1(8)
C6_2	C7_2	C8_2	119.4(8)
C7_2	C8_2	C3_2	123.1(8)
C10_2	C9_2	C2_2	62.3(5)
C9_2	C10_2	C2_2	60.0(5)
C9_2	C10_2	C11_2	121.1(7)
C9_2	C10_2	C17_2	118.1(7)
C11_2	C10_2	C2_2	115.7(6)
C17_2	C10_2	C2_2	124.2(7)
C17_2	C10_2	C11_2	110.1(6)
C12_2	C11_2	C10_2	121.1(8)
C16_2	C11_2	C10_2	121.6(7)
C16_2	C11_2	C12_2	117.2(7)
C11_2	C12_2	C13_2	121.3(8)
C14_2	C13_2	C12_2	120.3(9)
C13_2	C14_2	C15_2	119.7(9)
C16_2	C15_2	C14_2	118.4(9)
C11_2	C16_2	C15_2	122.9(8)
C18_2	C17_2	C10_2	124.8(7)
C18_2	C17_2	C22_2	117.6(7)
C22_2	C17_2	C10_2	117.7(8)
C17_2	C18_2	C19_2	122.3(8)
C20_2	C19_2	C18_2	120.5(8)
C19_2	C20_2	C21_2	119.7(8)
C20_2	C21_2	C22_2	119.4(7)
C17_2	C22_2	C21_2	120.5(8)

Table 5: Torsion Angles in ° for **WL-N2-137-27**.

Atom	Atom	Atom	Atom	Angle/°
Rh1	O2_1	C1_1	O1_1	7.1(13)
Rh1	O2_1	C1_1	C2_1	174.5(5)
Rh2	O1_1	C1_1	O2_1	-1.8(13)
Rh2	O1_1	C1_1	C2_1	-169.1(6)
Rh3	O1_2	C1_2	O2_2	7.7(13)
Rh3	O1_2	C1_2	C2_2	179.1(6)
Rh4	O2_2	C1_2	O1_2	6.7(13)
Rh4	O2_2	C1_2	C2_2	-164.7(6)
Br1_1	C6_1	C7_1	C8_1	179.8(8)
Cl1_1	C4_1	C5_1	C6_1	-178.7(8)
O1_1	C1_1	C2_1	C3_1	-24.7(11)
O1_1	C1_1	C2_1	C9_1	121.7(9)
O1_1	C1_1	C2_1	C10_1	-173.2(8)
O2_1	C1_1	C2_1	C3_1	166.6(8)
O2_1	C1_1	C2_1	C9_1	-47.0(10)
O2_1	C1_1	C2_1	C10_1	18.1(11)
C1_1	C2_1	C3_1	C4_1	-58.3(11)
C1_1	C2_1	C3_1	C8_1	127.2(9)
C1_1	C2_1	C9_1	C10_1	112.7(8)
C1_1	C2_1	C10_1	C9_1	-99.7(8)
C1_1	C2_1	C10_1	C11_1	152.2(7)
C1_1	C2_1	C10_1	C17_1	10.0(12)
C2_1	C3_1	C4_1	C11_1	3.3(13)
C2_1	C3_1	C4_1	C5_1	-179.3(9)
C2_1	C3_1	C8_1	C7_1	175.4(9)
C2_1	C9_1	C10_1	C11_1	106.3(8)
C2_1	C9_1	C10_1	C17_1	-112.1(8)
C2_1	C10_1	C11_1	C12_1	100.4(11)
C2_1	C10_1	C11_1	C16_1	-76.6(12)
C2_1	C10_1	C17_1	C18_1	69.7(12)
C2_1	C10_1	C17_1	C22_1	-112.9(9)
C3_1	C2_1	C9_1	C10_1	-103.9(8)
C3_1	C2_1	C10_1	C9_1	112.7(8)
C3_1	C2_1	C10_1	C11_1	4.5(11)
C3_1	C2_1	C10_1	C17_1	-137.7(8)
C3_1	C4_1	C5_1	C6_1	3.7(16)
C4_1	C3_1	C8_1	C7_1	0.7(15)

Atom	Atom	Atom	Atom	Angle/°
C4_1	C5_1	C6_1	Br1_1	176.8(8)
C4_1	C5_1	C6_1	C7_1	0.9(17)
C5_1	C6_1	C7_1	C8_1	-4.5(18)
C6_1	C7_1	C8_1	C3_1	3.7(17)
C8_1	C3_1	C4_1	Cl1_1	178.2(7)
C8_1	C3_1	C4_1	C5_1	-4.4(15)
C9_1	C2_1	C3_1	C4_1	158.6(9)
C9_1	C2_1	C3_1	C8_1	-15.8(13)
C9_1	C2_1	C10_1	C11_1	-108.2(8)
C9_1	C2_1	C10_1	C17_1	109.6(9)
C9_1	C10_1	C11_1	C12_1	32.1(12)
C9_1	C10_1	C11_1	C16_1	-144.8(10)
C9_1	C10_1	C17_1	C18_1	141.5(10)
C9_1	C10_1	C17_1	C22_1	-41.1(11)
C10_1	C2_1	C3_1	C4_1	91.3(10)
C10_1	C2_1	C3_1	C8_1	-83.1(11)
C10_1	C11_1	C12_1	C13_1	177.6(11)
C10_1	C11_1	C16_1	C15_1	177.9(10)
C10_1	C17_1	C18_1	C19_1	177.1(9)
C10_1	C17_1	C22_1	C21_1	-178.8(9)
C11_1	C10_1	C17_1	C18_1	-74.5(11)
C11_1	C10_1	C17_1	C22_1	102.9(9)
C11_1	C12_1	C13_1	C14_1	5(2)
C12_1	C11_1	C16_1	C15_1	0.9(18)
C12_1	C13_1	C14_1	C15_1	0(2)
C13_1	C14_1	C15_1	C16_1	-4(2)
C14_1	C15_1	C16_1	C11_1	3.7(19)
C16_1	C11_1	C12_1	C13_1	-5.3(19)
C17_1	C10_1	C11_1	C12_1	-113.1(10)
C17_1	C10_1	C11_1	C16_1	69.9(11)
C17_1	C18_1	C19_1	C20_1	1.0(17)
C18_1	C17_1	C22_1	C21_1	-1.2(15)
C18_1	C19_1	C20_1	C21_1	0.1(17)
C19_1	C20_1	C21_1	C22_1	-1.7(17)
C20_1	C21_1	C22_1	C17_1	2.3(16)
C22_1	C17_1	C18_1	C19_1	-0.4(15)
Br1_2	C6_2	C7_2	C8_2	-178.6(9)
Cl1_2	C4_2	C5_2	C6_2	176.4(10)
O1_2	C1_2	C2_2	C3_2	5.4(11)

Atom	Atom	Atom	Atom	Angle/°
O1_2	C1_2	C2_2	C9_2	147.5(8)
O1_2	C1_2	C2_2	C10_2	-146.4(9)
O2_2	C1_2	C2_2	C3_2	177.6(8)
O2_2	C1_2	C2_2	C9_2	-40.3(11)
O2_2	C1_2	C2_2	C10_2	25.8(12)
C1_2	C2_2	C3_2	C4_2	-80.0(11)
C1_2	C2_2	C3_2	C8_2	106.6(10)
C1_2	C2_2	C9_2	C10_2	111.9(8)
C1_2	C2_2	C10_2	C9_2	-102.2(8)
C1_2	C2_2	C10_2	C11_2	145.2(8)
C1_2	C2_2	C10_2	C17_2	3.1(12)
C2_2	C3_2	C4_2	C11_2	11.5(13)
C2_2	C3_2	C4_2	C5_2	-171.8(10)
C2_2	C3_2	C8_2	C7_2	172.7(10)
C2_2	C9_2	C10_2	C11_2	103.7(8)
C2_2	C9_2	C10_2	C17_2	-115.3(8)
C2_2	C10_2	C11_2	C12_2	77.4(11)
C2_2	C10_2	C11_2	C16_2	-106.2(11)
C2_2	C10_2	C17_2	C18_2	55.0(13)
C2_2	C10_2	C17_2	C22_2	-124.8(10)
C3_2	C2_2	C9_2	C10_2	-107.5(8)
C3_2	C2_2	C10_2	C9_2	107.1(8)
C3_2	C2_2	C10_2	C11_2	-5.5(11)
C3_2	C2_2	C10_2	C17_2	-147.5(8)
C3_2	C4_2	C5_2	C6_2	-0.4(19)
C4_2	C3_2	C8_2	C7_2	-1.2(16)
C4_2	C5_2	C6_2	Br1_2	179.5(9)
C4_2	C5_2	C6_2	C7_2	-2(2)
C5_2	C6_2	C7_2	C8_2	3(2)
C6_2	C7_2	C8_2	C3_2	-1.4(19)
C8_2	C3_2	C4_2	C11_2	-174.6(8)
C8_2	C3_2	C4_2	C5_2	2.1(16)
C9_2	C2_2	C3_2	C4_2	139.0(9)
C9_2	C2_2	C3_2	C8_2	-34.4(12)
C9_2	C2_2	C10_2	C11_2	-112.6(8)
C9_2	C2_2	C10_2	C17_2	105.3(9)
C9_2	C10_2	C11_2	C12_2	8.3(13)
C9_2	C10_2	C11_2	C16_2	-175.2(9)
C9_2	C10_2	C17_2	C18_2	126.1(10)

Atom	Atom	Atom	Atom	Angle/°
C9_2	C10_2	C17_2	C22_2	-53.7(11)
C10_2	C2_2	C3_2	C4_2	72.5(11)
C10_2	C2_2	C3_2	C8_2	-100.9(11)
C10_2	C11_2	C12_2	C13_2	-177.8(12)
C10_2	C11_2	C16_2	C15_2	176.8(11)
C10_2	C17_2	C18_2	C19_2	178.8(10)
C10_2	C17_2	C22_2	C21_2	-178.9(9)
C11_2	C10_2	C17_2	C18_2	-88.9(11)
C11_2	C10_2	C17_2	C22_2	91.3(10)
C11_2	C12_2	C13_2	C14_2	-3(2)
C12_2	C11_2	C16_2	C15_2	-6.6(18)
C12_2	C13_2	C14_2	C15_2	0(3)
C13_2	C14_2	C15_2	C16_2	-1(2)
C14_2	C15_2	C16_2	C11_2	4(2)
C16_2	C11_2	C12_2	C13_2	5.6(18)
C17_2	C10_2	C11_2	C12_2	-135.5(10)
C17_2	C10_2	C11_2	C16_2	41.0(12)
C17_2	C18_2	C19_2	C20_2	1.3(18)
C18_2	C17_2	C22_2	C21_2	1.3(15)
C18_2	C19_2	C20_2	C21_2	-1.2(18)
C19_2	C20_2	C21_2	C22_2	1.2(18)
C20_2	C21_2	C22_2	C17_2	-1.3(17)
C22_2	C17_2	C18_2	C19_2	-1.3(15)

Table 6: Hydrogen Fractional Atomic Coordinates ($\times 10^4$) and Equivalent Isotropic Displacement Parameters ($\text{\AA}^2 \times 10^3$) for **WL-N2-137-27**. U_{eq} is defined as 1/3 of the trace of the 373rthogonalized U_{ij} .

Atom	x	y	z	Atom	x	y	z
H15_1	7202.26	6312.58	1129.43	H15_1	7202.26	6312.58	1129.43
H16_1	6693.91	7318.23	979.22	H16_1	6693.91	7318.23	979.22
H18_1	6511.52	8293.8	372.23	H18_1	6511.52	8293.8	372.23
H19_1	6780.32	8755.55	-684.1	H19_1	6780.32	8755.55	-684.1
H20_1	6034.62	8753.46	-1596.79	H20_1	6034.62	8753.46	-1596.79
H22_1	4749.7	7770.07	-372.72	H22_1	4749.7	7770.07	-372.72
H5_2	6967.47	4811.27	1879.36	H5_2	6967.47	4811.27	1879.36
H7_2	7441.75	2898.82	1774.28	H7_2	7441.75	2898.82	1774.28
H8_2	8062.15	2996.52	2769.8	H8_2	8062.15	2996.52	2769.8
H9A_2	7931.41	3055.25	3974.19	H9A_2	7931.41	3055.25	3974.19
H9B_2	8578.65	3325.27	4414.41	H9B_2	8578.65	3325.27	4414.41
H12_2	6937.29	3135.25	3971.91	H12_2	6937.29	3135.25	3971.91
H13_2	5822.65	3224.91	3748.75	H13_2	5822.65	3224.91	3748.75

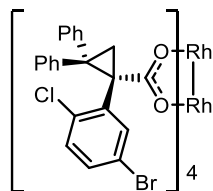
Atom	x	y	z	U_{eq}
H14_2	5294.14	4217.55	3892.66	51
H15_2	5900.18	5149.35	4232.1	51
H16_2	7005.09	5032.09	4477.17	32
H18_2	8202.68	5296.11	4550.2	25
H19_2	8472.13	5818.4	5574.59	29
H20_2	8510.07	5243.36	6615.77	34
H21_2	8227.19	4136.73	6634.61	26
H22_2	7950.72	3604.07	5584.88	21

Table 7: Hydrogen Bond information for **WL-N2-137-27**.

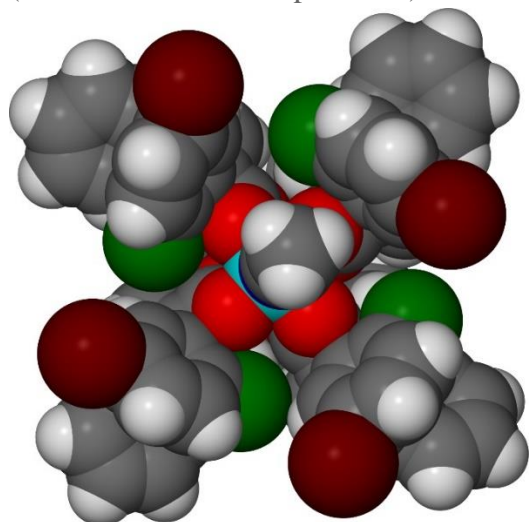
D	H	A	d(D-H)/Å	d(H-A)/Å	d(D-A)/Å	D-H-A/deg
C46	H46	O3 ¹	0.95	2.71	3.223(14)	114.4

Table 8: Solvent masking (Olex2) information for **WL-N2-137-27**.

No	x	y	z	V	e	Content
1	-0.951	-0.966	-0.862	2648.4	0.0	?
2	0.135	0.865	0.000	1.1	0.0	?
3	0.140	0.700	0.896	0.2	0.0	?
4	0.200	0.360	0.896	0.2	0.0	?
5	0.300	0.860	0.104	0.2	0.0	?
6	0.365	0.365	0.000	1.1	0.0	?
7	0.360	0.200	0.104	0.2	0.0	?
8	0.635	0.635	0.000	1.1	0.0	?
9	0.640	0.800	0.104	0.2	0.0	?
10	0.700	0.140	0.104	0.2	0.0	?
11	0.800	0.640	0.896	0.2	0.0	?
12	0.865	0.135	0.000	1.1	0.0	?
13	0.860	0.300	0.896	0.2	0.0	?

Rh₂(S-2-Cl-5-BrTPCP)₄ (57b)

Crystal Data and Experimental
(with CH₃CN at axial positions)



Experimental. Single green needle-shaped crystals of **WL-2ClBr** were chosen from the sample as supplied. A suitable crystal 0.34×0.11×0.08 mm³ was selected and mounted on a loop with paratone oil on an XtaLAB Synergy, Dualflex, HyPix diffractometer. The crystal was kept at a steady $T = 100.3(5)$ K during the data collection. The structure was solved with the **ShelXT** (Sheldrick, 2015) structure solution program using the Intrinsic Phasing solution method and by using **Olex2** (Dolomanov et al., 2009) as the graphical interface. The model was refined with version 2018/3 of **ShelXL** (Sheldrick, 2015) using Least Squares minimisation.

Crystal Data. C₁₈₂H₁₃₁Br₈Cl₈N₃O₁₇Rh₄, $M_r = 3966.41$, monoclinic, $P2_1$ (No. 4), $a = 21.4690(3)$ Å, $b = 17.1974(3)$ Å, $c = 29.1637(4)$ Å, $\beta = 106.965(2)^\circ$, $\alpha = \gamma = 90^\circ$, $V = 10299.0(3)$ Å³, $T = 100.3(5)$ K, $Z = 2$, $Z' = 1$, $(\text{CuK}\alpha) = 5.741$ mm⁻¹, 121262 reflections measured, 36989 unique ($R_{int} = 0.0704$) which were used in all calculations. The final wR_2 was 0.2353 (all data) and R_1 was 0.0813 ($I > 2\sigma(I)$).

Compound	WL-2ClBr
Formula	C ₁₈₂ H ₁₃₁ Br ₈ Cl ₈ N ₃ O ₁₇ Rh ₄
$D_{calc.}/\text{g cm}^{-3}$ /mm ⁻¹	1.279 5.741
Formula Weight	3966.41
Colour	green
Shape	needle
Size/mm ³	0.34×0.11×0.08
T/K	100.3(5)
Crystal System	monoclinic
Flack Parameter	0.066(12)
Hooft Parameter	0.047(3)
Space Group	$P2_1$
$a/\text{Å}$	21.4690(3)
$b/\text{Å}$	17.1974(3)
$c/\text{Å}$	29.1637(4)
$\beta/^\circ$	90
$\alpha/^\circ$	106.965(2)
$\gamma/^\circ$	90
$V/\text{Å}^3$	10299.0(3)
Z	2
Z'	1
Wavelength/Å	1.54184
Radiation type	CuK
$\text{min}/^\circ$	2.152
$\text{max}/^\circ$	68.249
Measured Refl.	121262
Independent Refl.	36989
Reflections with $I > 2\sigma(I)$	30571
R_{int}	0.0704
Parameters	2131
Restraints	4101
Largest Peak	2.315
Deepest Hole	-2.101
GooF	1.079
wR_2 (all data)	0.2353
wR_2	0.2229
R_1 (all data)	0.0935
R_1	0.0813

Structure Quality Indicators

Reflections:	d min (Cu) 0.83	I/σ 15.6	Rint 7.04%	complete 99% (IUCr) 98%
Refinement:	Shift 0.010	Max Peak 2.3	Min Peak -2.1	Goof 1.079

A green needle-shaped crystal with dimensions $0.34 \times 0.11 \times 0.08 \text{ mm}^3$ was mounted on a loop with paratone oil. Data were collected using an XtaLAB Synergy, Dualflex, HyPix diffractometer equipped with an Oxford Cryosystems low-temperature device operating at $T = 100.3(5) \text{ K}$.

Data were measured using scans of 0.5° per frame for 3.0/7.2 s using CuK radiation. The total number of runs and images was based on the strategy calculation from the program

CrysAlisPro (Rigaku, V1.171.39.33a, 2017). The maximum resolution that was achieved was $= 68.249^\circ$.

The diffraction pattern was indexed using **CrysAlisPro** (Rigaku, V1.171.39.33a, 2017) and the unit cell was refined using **CrysAlisPro** (Rigaku, V1.171.39.33a, 2017) on 49303 reflections, 41% of the observed reflections.

Data reduction, scaling and absorption corrections were performed using **CrysAlisPro** (Rigaku, V1.171.39.33a, 2017). The final completeness is 99.60 % out to 68.249° in . A numerical absorption correction based on Gaussian integration over a multifaceted crystal model was performed using CrysAlisPro 1.171.39.33a (Rigaku Oxford Diffraction, 2017). An empirical absorption correction using spherical harmonics as implemented by SCALE3 ABSPACK was also performed. The absorption coefficient of this material is 5.741 mm^{-1} at this wavelength ($\lambda = 1.54184 \text{ \AA}$) and the minimum and maximum transmissions are 0.028 and 0.486.

The structure was solved and the space group $P2_1$ (# 4) determined by the **ShelXT** (Sheldrick, 2015) structure solution program using Intrinsic Phasing and refined by Least Squares using version 2018/3 of **ShelXL** (Sheldrick, 2015). All non-hydrogen atoms were refined anisotropically. Hydrogen atom positions were calculated geometrically and refined using the riding model. Hydrogen atom positions were calculated geometrically and refined using the riding model.

_refine_special_details: Refined as a 2-component inversion twin.

The Flack parameter was refined to 0.066(12). Determination of absolute structure using Bayesian statistics on Bijvoet differences using the Olex2 results in 0.047(3). Note: The Flack parameter is used to determine chirality of the crystal studied, the value should be near 0, a value of 1 means that the stereochemistry is wrong and the model should be inverted. A value of 0.5 means that the crystal consists of a racemic mixture of the two enantiomers.

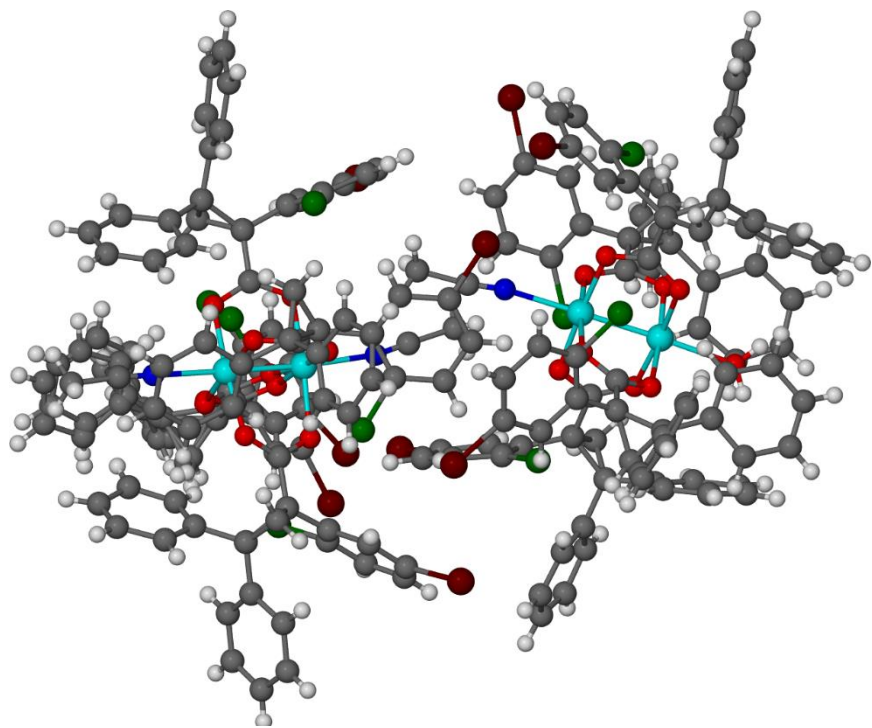


Figure 2:

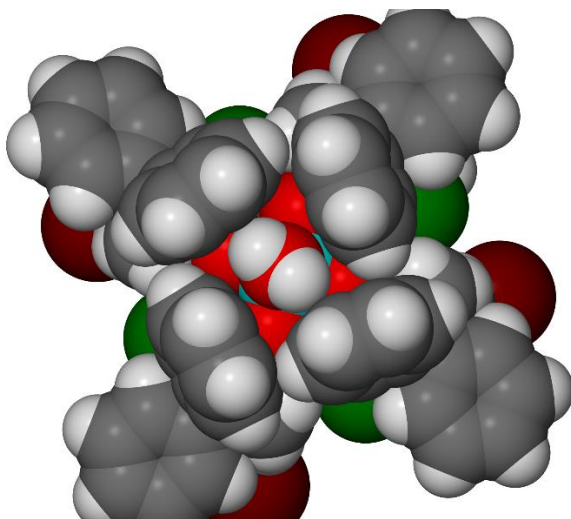


Figure 3:

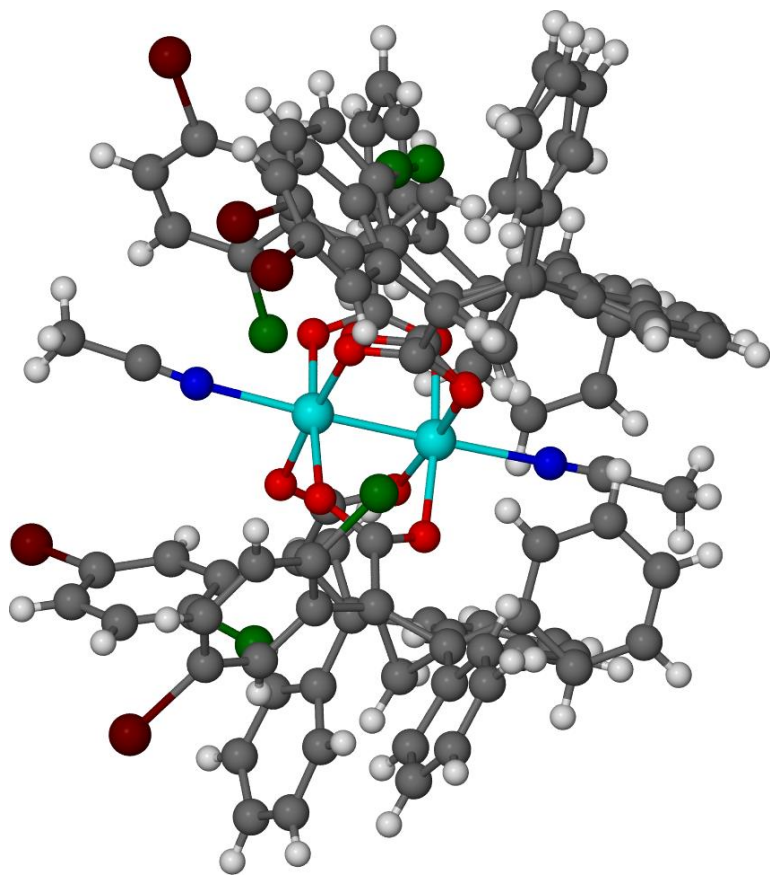


Figure 3:

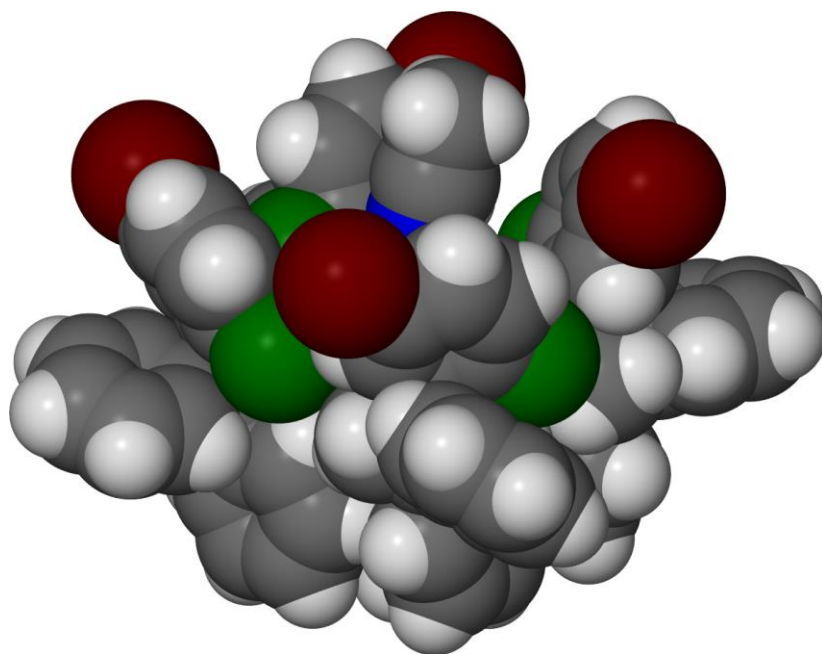


Figure 4:

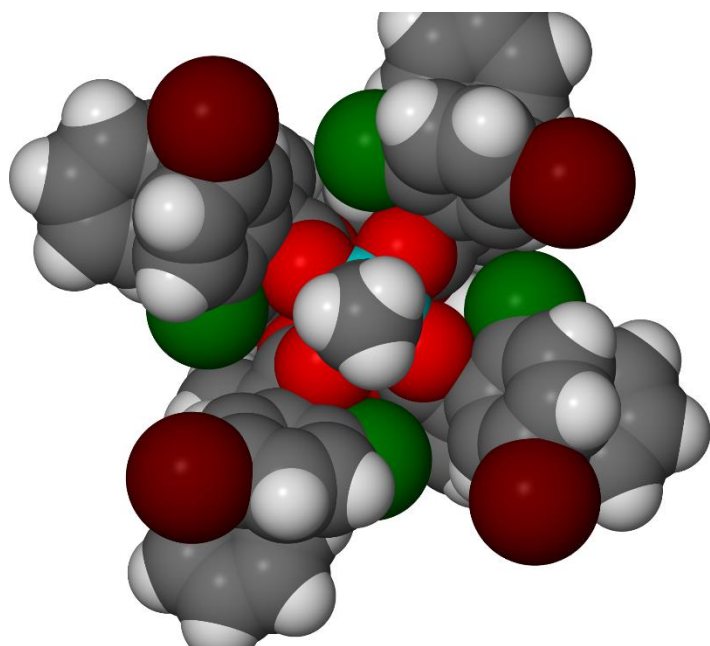


Figure 5:

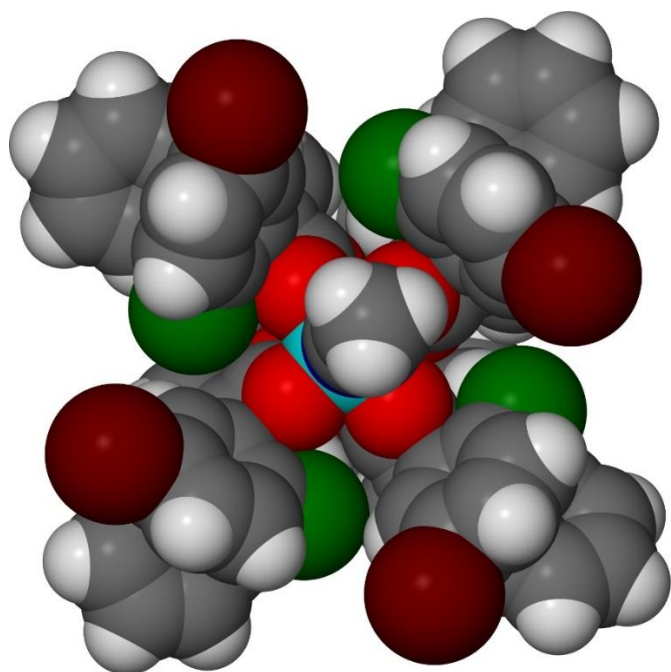
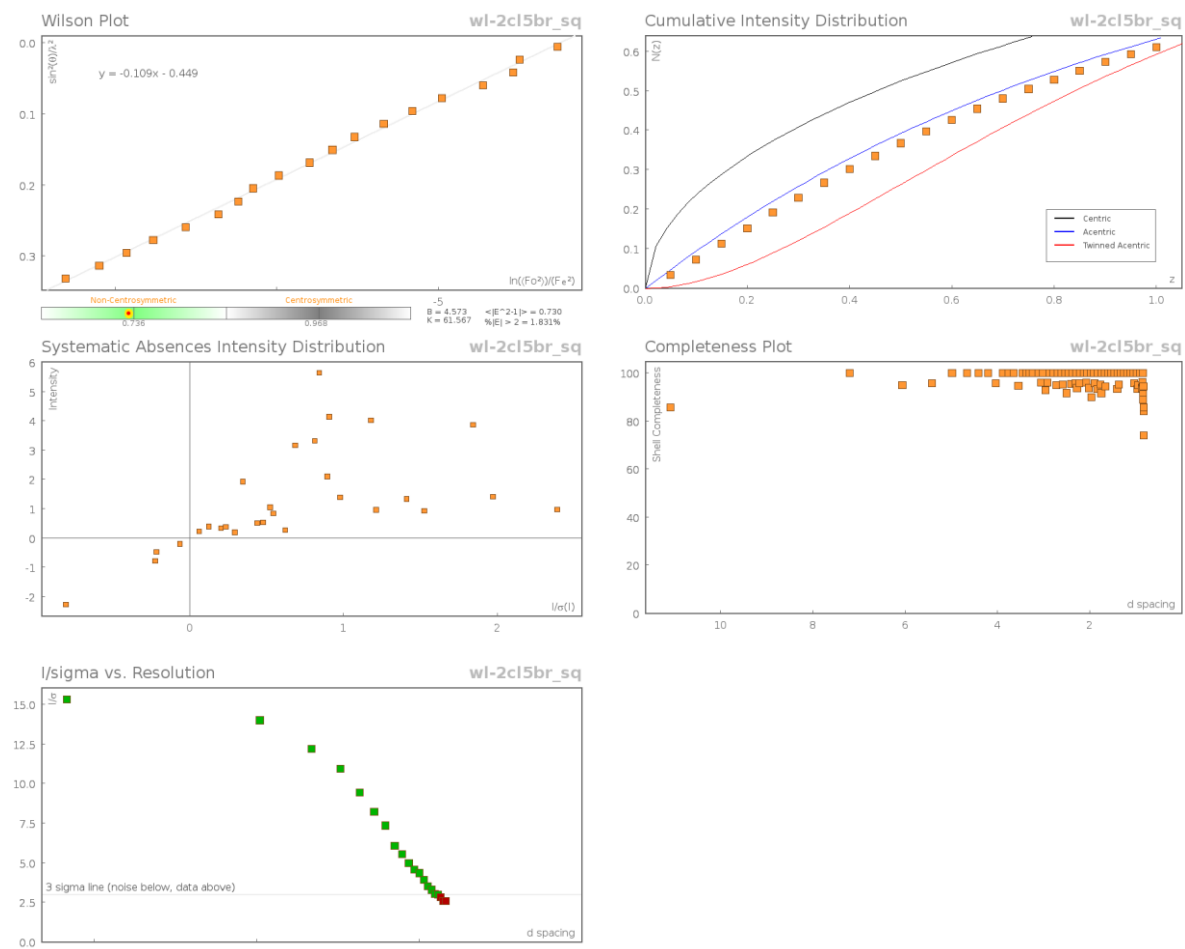
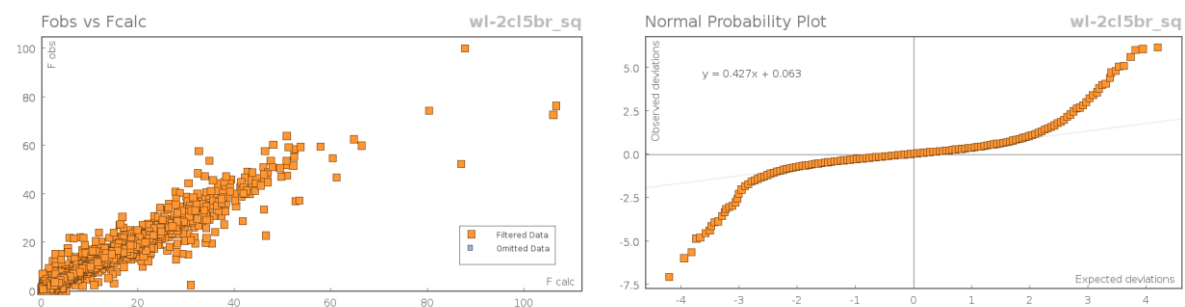


Figure 6:

Data Plots: Diffraction Data



Data Plots: Refinement and Data



Reflection Statistics

Total reflections (after filtering) 121291

Completeness 0.98

hkl_{\max} collected (25, 20, 35)

hkl_{\max} used (24, 20, 35)

Unique reflections 36989

Mean I/ 10.9

hkl_{\min} collected (-24, -20, -34)

hkl_{\min} used (-25, -20, 0)

Lim d_{\max} collected	100.0	Lim d_{\min} collected	0.77
d_{\max} used	20.53	d_{\min} used	0.83
Friedel pairs	17130	Friedel pairs merged	0
Inconsistent equivalents	81	R_{int}	0.0704
R_{sigma}	0.064	Intensity transformed	0
Omitted reflections	0	Omitted by user (OMIT 0 hkl)	
Multiplicity	(19710, 16351, 9388, 4202, 1923, 1046, 607, 307, 120, 22, 1)	Maximum multiplicity	11
Removed systematic absences	29	Filtered off (Shel/OMIT)	0

Images of the Crystal on the Diffractometer

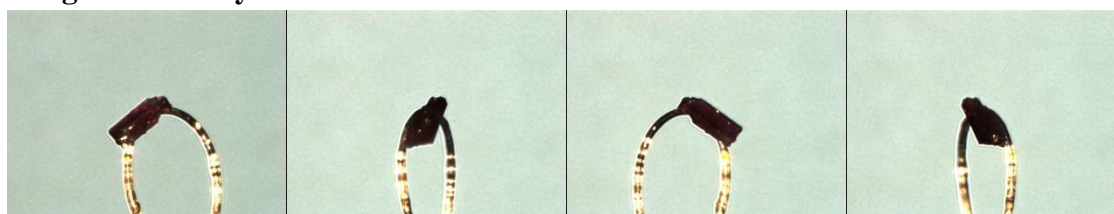


Table 9: Fractional Atomic Coordinates ($\times 10^4$) and Equivalent Isotropic Displacement Parameters ($\text{\AA}^2 \times 10^3$) for **WL-2ClBr**. U_{eq} is defined as 1/3 of the trace of the orthogonalised U_{ij} .

Atom	x	y	z	U_{eq}
Rh3	3819.6(5)	5342.6(9)	6409.1(3)	48.0(2)
Rh4	2877.8(5)	6113.9(9)	6064.4(4)	51.4(2)
O4	1997(6)	6889(8)	5752(5)	86(4)
Rh1	7456.2(5)	5161.4(10)	8208.2(3)	56.6(3)
Rh2	8218.9(5)	4500.0(10)	8843.4(3)	58.5(3)
N1_9	8939(6)	3871(10)	9432(5)	84(4)
C23_9	9296(8)	3563(13)	9715(6)	102(7)
C24_9	9743(10)	3193(17)	10128(8)	123(10)
N1_10	6743(6)	5711(8)	7573(4)	66(3)
C23_10	6427(9)	5916(11)	7232(6)	86(4)
C24_10	5974(13)	6139(15)	6777(7)	125(9)
Br1_3	4923.9(9)	7484(2)	9084.7(8)	110.4(9)
Cl1_3	7939.8(13)	7437(2)	9214.5(15)	76.1(10)
O1_3	7781(4)	4999(4)	9299(2)	57(2)
O2_3	7237(4)	5846(5)	8727.7(17)	58(2)
C1_3	7456(3)	5613(4)	9159(2)	56(2)
C2_3	7232(3)	6064(3)	9527(2)	63(2)

Atom	x	y	z	U_{eq}
C3_3	7626(3)	6083(4)	10066(2)	65(2)
C4_3	6839(3)	6770(3)	9319(3)	69(3)
C5_3	7117(3)	7426(4)	9188(5)	68(3)
C6_3	6757(4)	8115(5)	9023(6)	85(4)
C7_3	6117(4)	8138(5)	9007(6)	87(4)
C8_3	5830(3)	7496(5)	9140(5)	79(3)
C9_3	6181(3)	6818(5)	9299(5)	71(3)
C10_3	7049(3)	5577(4)	9891(2)	65(3)
C11_3	8301(3)	5709(5)	10246(2)	67(3)
C12_3	8433(5)	5297(9)	10680(4)	84(4)
C13_3	9050(5)	4959(9)	10865(4)	91(4)
C14_3	9513(4)	5052(9)	10635(4)	88(4)
C15_3	9362(5)	5408(11)	10200(5)	109(7)
C16_3	8771(4)	5784(8)	10017(4)	72(4)
C17_3	7587(3)	6811(4)	10342(3)	63(3)
C18_3	8073(5)	7358(7)	10444(6)	90(5)
C19_3	8044(6)	8031(7)	10698(6)	89(5)
C20_3	7505(6)	8171(8)	10843(7)	105(7)
C21_3	6987(6)	7690(8)	10716(7)	109(7)
C22_3	7019(5)	7010(7)	10465(6)	85(5)
Br1_5	6881.4(8)	7903.3(14)	7678.3(8)	84.2(5)
Cl1_5	4129.3(13)	6613(2)	7749.8(12)	63.0(8)
O1_5	3426(3)	7065(4)	6340(3)	57(2)
O2_5	4256(3)	6307(3)	6764(3)	55(2)
C1_5	3945(3)	6945(3)	6676(2)	55(2)
C2_5	4303(3)	7655(3)	6930(2)	58(2)
C3_5	3942(3)	8423(3)	6970(2)	65(2)
C4_5	4896(3)	7450(4)	7331(2)	55(2)
C5_5	4871(3)	6960(6)	7702(3)	61(3)
C6_5	5440(3)	6680(6)	8046(3)	63(3)
C7_5	6028(3)	6977(7)	8046(4)	72(3)
C8_5	6065(3)	7489(8)	7693(4)	73(4)
C9_5	5512(3)	7719(7)	7333(3)	67(3)
C10_5	4299(3)	8333(4)	6610(2)	67(3)
C11_5	3197(3)	8462(4)	6804(3)	70(3)
C12_5	2914(4)	8965(9)	6421(5)	86(4)
C13_5	2234(4)	9030(12)	6264(7)	117(8)
C14_5	1859(4)	8603(10)	6474(6)	110(6)
C15_5	2140(4)	8093(11)	6831(7)	106(6)

Atom	x	y	z	U_{eq}
C16_5	2810(4)	8030(10)	7007(6)	92(5)
C17_5	4220(4)	8929(4)	7402(3)	74(3)
C18_5	4235(8)	8697(6)	7855(3)	84(4)
C19_5	4507(9)	9150(7)	8257(3)	101(5)
C20_5	4741(10)	9871(8)	8201(4)	122(7)
C21_5	4682(12)	10159(7)	7760(4)	128(8)
C22_5	4432(11)	9693(6)	7359(4)	113(7)
Br1_6	4165.1(8)	4290.3(16)	9056.8(5)	85.0(6)
Cl1_6	2390.4(16)	3674(2)	6919.4(9)	62.6(8)
O1_6	2657(4)	6036(4)	6688(2)	53(2)
O2_6	3405(3)	5083(5)	6950(3)	51.4(19)
C1_6	2918(3)	5489(4)	6969(2)	52(3)
C2_6	2640(3)	5309(3)	7377.8(19)	55(2)
C3_6	1923(3)	5486(4)	7354(2)	61(2)
C4_6	2965(3)	4625(3)	7671.1(19)	50(2)
C5_6	2864(5)	3869(3)	7504(2)	54(2)
C6_6	3139(6)	3218(4)	7792(3)	63(3)
C7_6	3512(6)	3343(4)	8252(3)	67(3)
C8_6	3617(5)	4088(4)	8427(2)	61(3)
C9_6	3327(4)	4725(4)	8151(2)	53(2)
C10_6	2457(3)	6003(4)	7618(2)	62(2)
C11_6	1435(3)	5788(5)	6894(2)	64(3)
C12_6	1025(7)	6395(9)	6950(3)	93(6)
C13_6	561(8)	6682(10)	6541(4)	119(8)
C14_6	479(8)	6338(11)	6107(4)	116(8)
C15_6	881(7)	5752(10)	6059(3)	95(6)
C16_6	1361(5)	5470(7)	6451(2)	66(3)
C17_6	1599(3)	4950(5)	7622(2)	61(3)
C18_6	1188(6)	4366(7)	7395(3)	72(3)
C19_6	907(7)	3848(7)	7640(4)	82(4)
C20_6	1008(6)	3944(7)	8121(4)	76(4)
C21_6	1422(5)	4492(7)	8366(3)	72(3)
C22_6	1734(5)	4984(7)	8124(3)	65(3)
Br1_7	3271.6(13)	1027.9(14)	6392.8(12)	129.9(11)
Cl1_7	3331(3)	3856(2)	4995.1(17)	105.6(17)
O1_7	2389(3)	5089(3)	5844(3)	57(2)
O2_7	3340(3)	4423(4)	6031(3)	55.1(19)
C1_7	2724(3)	4478(4)	5862(3)	52(2)
C2_7	2377(3)	3762(3)	5611(2)	70(2)

Atom	x	y	z	U_{eq}
C3_7	1748(3)	3810(4)	5183(2)	90(3)
C4_7	2833(3)	3093(3)	5628(2)	73(3)
C5_7	3272(6)	3077(5)	5363(4)	86(4)
C6_7	3680(6)	2428(5)	5363(5)	99(4)
C7_7	3659(7)	1812(5)	5653(5)	102(5)
C8_7	3272(7)	1847(6)	5954(5)	98(5)
C9_7	2863(6)	2478(5)	5948(4)	78(3)
C10_7	1719(3)	3620(4)	5670(3)	75(3)
C11_7	1473(3)	4590(4)	4962(3)	86(3)
C12_7	805(4)	4711(7)	4894(8)	109(6)
C13_7	531(5)	5422(7)	4700(7)	109(6)
C14_7	912(6)	5989(7)	4599(7)	116(6)
C15_7	1551(6)	5850(7)	4647(7)	113(6)
C16_7	1842(4)	5158(5)	4839(5)	92(4)
C17_7	1643(4)	3187(4)	4805(3)	96(3)
C18_7	1814(10)	3295(7)	4392(4)	122(3)
C19_7	1755(10)	2713(8)	4053(5)	121(3)
C20_7	1459(11)	2031(8)	4107(5)	131(5)
C21_7	1307(12)	1878(7)	4515(5)	133(5)
C22_7	1421(9)	2438(5)	4875(4)	111(4)
Br1_8	5826(2)	4561.9(18)	4562.8(15)	178.7(13)
Cl1_8	4949.9(18)	7183(2)	5790.6(13)	76.4(10)
O1_8	3160(3)	6147(6)	5453(2)	58(2)
O2_8	4153(3)	5657(5)	5842(2)	54(2)
C1_8	3741(3)	5964(5)	5483(2)	55(3)
C2_8	3982(3)	6139(3)	5056(2)	62(2)
C3_8	3665(3)	6772(4)	4681(2)	60(2)
C4_8	4697(3)	5985(4)	5153(2)	79(2)
C5_8	5167(3)	6454(7)	5450(5)	83(2)
C6_8	5844(3)	6329(8)	5529(5)	87(3)
C7_8	6036(3)	5767(8)	5269(5)	91(3)
C8_8	5578(3)	5308(7)	4959(5)	90(3)
C9_8	4914(3)	5419(7)	4890(5)	85(2)
C10_8	3518(3)	5940(4)	4580(2)	65(3)
C11_8	3128(3)	7305(4)	4749(3)	64(3)
C12_8	2560(4)	7356(8)	4360(4)	79(4)
C13_8	2062(5)	7857(9)	4398(5)	96(5)
C14_8	2133(5)	8286(8)	4802(5)	88(4)
C15_8	2697(5)	8252(8)	5167(5)	86(4)

Atom	x	y	z	U_{eq}
C16_8	3189(5)	7744(7)	5152(3)	68(3)
C17_8	4102(4)	7199(4)	4446(2)	54(2)
C18_8	4370(5)	7907(5)	4611(3)	57(3)
C19_8	4777(6)	8305(6)	4401(4)	68(3)
C20_8	4897(6)	8005(7)	4002(4)	69(3)
C21_8	4650(6)	7310(7)	3825(4)	72(3)
C22_8	4238(6)	6911(6)	4034(3)	65(3)
Br1_12	8344(4)	9472(3)	7955(3)	143.5(16)
Cl1_12	9279(5)	6059(4)	7617(3)	89.4(19)
O1_12	8811(10)	5469(10)	8898(6)	61.1(12)
O2_12	8136(6)	5989(10)	8221(5)	56(3)
C1_12	8649(4)	5985(5)	8576(4)	61.4(11)
C2_12	9133(4)	6629(4)	8587(3)	63.1(8)
C3_12	9874(4)	6533(4)	8832(3)	62.6(8)
C4_12	8918(4)	7161(4)	8161(3)	64.2(10)
C5_12	8990(12)	6972(6)	7718(4)	69(3)
C6_12	8848(18)	7503(8)	7329(5)	87(3)
C7_12	8653(16)	8237(7)	7399(4)	78(3)
C8_12	8600(14)	8448(6)	7841(4)	82(6)
C9_12	8695(11)	7911(6)	8212(4)	68(4)
C10_12	9457(5)	6956(5)	9072(3)	62.4(9)
C11_12	10168(5)	5753(4)	9042(3)	62.3(9)
C12_12	10583(12)	5772(6)	9514(5)	60(5)
C13_12	10856(12)	5070(7)	9726(6)	65(6)
C14_12	10675(13)	4384(6)	9493(6)	68(5)
C15_12	10248(12)	4375(5)	9045(6)	63(3)
C16_12	10020(11)	5059(5)	8805(5)	58(4)
C17_12	10332(4)	6971(5)	8622(5)	62.3(11)
C18_12	10848(7)	6614(7)	8520(8)	63.4(14)
C19_12	11241(10)	6995(8)	8292(10)	75(3)
C20_12	11164(12)	7776(9)	8211(12)	93(4)
C21_12	10686(9)	8168(7)	8325(9)	69(2)
C22_12	10270(9)	7776(6)	8533(9)	63.4(18)
Br1_1	7881.2(12)	5147.3(16)	5873.2(8)	103.0(7)
Cl1_1	7126.6(16)	2748(3)	7286.8(13)	79.9(12)
O1_1	8600(4)	4046(6)	8330.8(17)	68(3)
O2_1	7709(3)	4452(6)	7749(2)	61(2)
C1_1	8245(3)	4086(5)	7901(2)	66(4)
C2_1	8451(3)	3617(3)	7530.7(19)	54(3)

Atom	x	y	z	U_{eq}
C3_1	8851(3)	2856(4)	7659(2)	60(3)
C4_1	7988(3)	3701(4)	7035(2)	54(3)
C5_1	7380(4)	3357(6)	6897(3)	55(3)
C6_1	6925(4)	3488(6)	6442(3)	56(3)
C7_1	7073(4)	4017(7)	6142(3)	70(4)
C8_1	7655(4)	4410(7)	6285(3)	69(4)
C9_1	8124(4)	4234(6)	6715(3)	60(3)
C10_1	9168(3)	3596(4)	7599(2)	66(4)
C11_1	9009(3)	2498(5)	8161(2)	80(6)
C12_1	9665(4)	2309(9)	8381(3)	72(4)
C13_1	9831(5)	1961(11)	8836(4)	90(6)
C14_1	9366(6)	1821(14)	9057(5)	118(10)
C15_1	8742(6)	2058(13)	8853(4)	119(10)
C16_1	8562(5)	2418(11)	8410(4)	88(6)
C17_1	8739(4)	2235(4)	7280(3)	65(4)
C18_1	8372(7)	1586(6)	7293(4)	74(5)
C19_1	8270(8)	1006(7)	6951(5)	91(6)
C20_1	8588(8)	1039(6)	6609(4)	88(6)
C21_1	8964(10)	1655(8)	6582(6)	123(10)
C22_1	9042(7)	2258(6)	6912(4)	77(5)
Br1_4	8222(3)	9019(3)	7503(2)	143.5(16)
Cl1_4	9498(5)	5644(3)	7692(2)	89.4(19)
O1_4	8822(9)	5462(10)	8918(4)	61.1(12)
O2_4	8224(5)	5823(9)	8174(4)	56(3)
C1_4	8729(4)	5849(5)	8535(3)	61.4(11)
C2_4	9200(3)	6503(4)	8534(2)	63.1(8)
C3_4	9920(3)	6488(4)	8851(3)	62.6(8)
C4_4	9049(4)	6910(4)	8059(2)	64.5(10)
C5_4	9166(11)	6575(6)	7661(3)	69(3)
C6_4	9062(14)	6978(8)	7221(4)	87(3)
C7_4	8803(13)	7708(8)	7181(4)	87(3)
C8_4	8616(11)	8019(7)	7555(4)	78(3)
C9_4	8749(10)	7640(7)	7995(3)	64(4)
C10_4	9424(4)	6950(4)	8991(3)	62.4(9)
C11_4	10211(4)	5771(4)	9147(3)	62.3(9)
C12_4	10625(11)	5911(6)	9611(4)	66(5)
C13_4	10966(10)	5281(7)	9872(5)	64(5)
C14_4	10855(9)	4546(7)	9695(5)	59(4)
C15_4	10458(10)	4422(6)	9244(5)	63(3)

Atom	x	y	z	<i>U</i>_{eq}
C16_4	10107(8)	5026(4)	8976(5)	54(3)
C17_4	10416(4)	6890(5)	8661(4)	62.3(11)
C18_4	10807(7)	6483(6)	8448(7)	63.4(14)
C19_4	11245(10)	6845(8)	8251(9)	82(3)
C20_4	11244(9)	7637(8)	8219(9)	70(3)
C21_4	10821(9)	8065(7)	8376(8)	69(2)
C22_4	10429(8)	7705(5)	8619(7)	63.4(18)
Br1_2	4316.8(7)	2706.9(14)	7064.4(6)	78.6(5)
Cl1_2	5909.2(14)	4638(2)	8897.4(9)	57.6(8)
O1_2	7557(2)	3594(5)	8744(3)	65(3)
O2_2	6781(3)	4360(4)	8260(3)	59(2)
C1_2	6977(3)	3748(4)	8503(3)	61(4)
C2_2	6455(3)	3173(3)	8528(2)	60(4)
C3_2	6533(3)	2626(4)	8965(2)	66(4)
C4_2	5782(3)	3444(4)	8261(2)	64(4)
C5_2	5511(4)	4113(5)	8384(3)	54(3)
C6_2	4909(3)	4419(5)	8097(3)	48(3)
C7_2	4564(4)	4009(5)	7705(3)	56(3)
C8_2	4807(4)	3321(6)	7589(4)	66(4)
C9_2	5404(4)	3028(6)	7866(4)	70(5)
C10_2	6636(3)	2338(4)	8515(2)	67(4)
C11_2	7120(3)	2689(4)	9412(2)	65(4)
C12_2	7435(5)	1989(5)	9591(4)	85(6)
C13_2	7924(7)	2003(7)	10032(4)	95(7)
C14_2	8111(7)	2687(7)	10265(4)	103(8)
C15_2	7815(7)	3363(6)	10079(5)	89(6)
C16_2	7312(6)	3371(5)	9656(4)	81(5)
C17_2	5926(3)	2410(5)	9094(3)	89(4)
C18_2	5738(5)	2807(7)	9440(4)	87(4)
C19_2	5184(5)	2613(9)	9566(5)	90(4)
C20_2	4774(6)	2058(10)	9309(5)	107(5)
C21_2	4882(5)	1739(10)	8916(5)	104(4)
C22_2	5470(6)	1878(11)	8818(6)	145(8)
N1_11	4754(6)	4696(8)	6715(4)	67(3)
C23_11	5242(7)	4476(10)	6880(7)	87(4)
C24_11	5860(8)	4089(14)	7090(7)	102(6)

Table 10: Anisotropic Displacement Parameters ($\times 10^4$) **WL-2ClBr**. The anisotropic displacement factor exponent takes the form: $-2^2[h^2a^{*2} \times U_{11} + \dots + 2hka^* \times b^* \times U_{12}]$

Atom	U_{11}	U_{22}	U_{33}	U_{23}	U_{13}	U_{12}
Rh3	57.0(5)	46.7(5)	43.7(5)	9.8(4)	19.9(4)	12.9(4)
Rh4	57.1(6)	48.6(5)	49.3(5)	11.1(4)	16.7(4)	12.3(4)
O4	63(7)	77(8)	115(10)	22(8)	19(7)	25(6)
Rh1	43.9(5)	85.3(8)	36.4(4)	-1.8(4)	5.1(4)	11.7(5)
Rh2	39.9(5)	90.6(8)	40.0(5)	3.7(5)	4.0(4)	7.3(5)
N1_9	62(7)	124(12)	59(7)	17(7)	9(5)	10(7)
C23_9	62(8)	148(18)	86(11)	46(12)	6(7)	3(10)
C24_9	83(12)	170(20)	101(13)	60(15)	5(10)	20(14)
N1_10	62(6)	71(7)	69(5)	-8(5)	25(4)	2(5)
C23_10	88(5)	85(5)	80(5)	2(3)	18(3)	1(3)
C24_10	161(18)	92(15)	91(9)	9(11)	-13(11)	-9(15)
Br1_3	64.4(11)	184(3)	87.4(13)	-23.9(15)	28.4(10)	28.2(13)
Cl1_3	67(2)	88(3)	75(2)	-3(2)	23.4(18)	-6(2)
O1_3	44(4)	84(5)	39(4)	1(3)	7(3)	-3(3)
O2_3	57(5)	69(6)	41(3)	-5(3)	5(3)	1(4)
C1_3	39(5)	82(6)	42(3)	-2(3)	3(3)	-6(4)
C2_3	56(5)	82(5)	52(3)	-7(4)	16(3)	-8(4)
C3_3	61(4)	88(6)	49(4)	-3(4)	19(3)	-18(4)
C4_3	64(5)	89(6)	55(6)	-6(5)	16(5)	0(4)
C5_3	71(6)	82(6)	53(7)	-11(5)	21(6)	2(4)
C6_3	89(7)	82(7)	85(11)	-9(7)	24(7)	9(6)
C7_3	91(7)	83(8)	88(12)	-20(7)	28(8)	13(6)
C8_3	80(7)	93(8)	64(8)	-17(6)	19(7)	13(5)
C9_3	66(5)	92(7)	58(8)	-11(6)	22(5)	4(5)
C10_3	57(5)	82(6)	56(6)	-8(4)	18(5)	-12(5)
C11_3	60(4)	90(8)	45(5)	-13(5)	7(3)	-20(4)
C12_3	85(7)	107(11)	48(6)	-3(6)	1(5)	-24(7)
C13_3	89(7)	102(13)	63(8)	-5(7)	-8(5)	-22(7)
C14_3	84(7)	75(11)	88(8)	-4(7)	-2(6)	-18(7)
C15_3	54(6)	151(18)	116(11)	41(11)	15(7)	-3(8)
C16_3	54(5)	105(11)	50(6)	-11(6)	6(5)	-14(5)
C17_3	62(6)	86(6)	43(5)	0(4)	19(5)	-20(4)
C18_3	74(7)	102(8)	103(13)	-32(8)	42(8)	-34(7)
C19_3	72(7)	104(9)	93(12)	-31(9)	28(8)	-28(7)
C20_3	78(8)	132(13)	112(15)	-63(12)	38(9)	-41(8)
C21_3	78(8)	136(11)	123(16)	-74(12)	43(9)	-42(8)

Atom	U_{11}	U_{22}	U_{33}	U_{23}	U_{13}	U_{12}
C22_3	72(6)	116(10)	76(10)	-41(8)	33(7)	-35(6)
Br1_5	67.6(10)	85.3(13)	98.5(14)	-9.5(10)	22.5(9)	-13.4(9)
Cl1_5	63.9(19)	72(2)	56.8(18)	2.4(16)	23.9(15)	6.4(17)
O1_5	60(4)	50(5)	60(4)	15(4)	20(3)	13(3)
O2_5	61(5)	53(4)	51(5)	5(3)	16(4)	14(3)
C1_5	59(4)	54(4)	55(5)	8(3)	21(3)	13(3)
C2_5	62(4)	54(4)	63(5)	5(3)	29(3)	9(3)
C3_5	66(4)	53(4)	82(5)	3(4)	30(4)	8(4)
C4_5	65(4)	46(6)	58(5)	-4(4)	24(3)	4(4)
C5_5	72(5)	59(7)	56(6)	-1(5)	24(4)	4(5)
C6_5	75(5)	61(8)	57(6)	-1(5)	24(5)	11(5)
C7_5	76(5)	72(8)	68(7)	-8(6)	22(5)	2(6)
C8_5	67(5)	76(9)	79(7)	-1(6)	25(5)	1(6)
C9_5	67(4)	70(9)	67(7)	-6(6)	26(4)	-3(5)
C10_5	73(7)	56(5)	80(6)	14(5)	32(6)	14(5)
C11_5	66(4)	51(7)	98(8)	-5(5)	29(4)	13(4)
C12_5	82(6)	63(9)	104(10)	1(7)	14(7)	13(7)
C13_5	82(6)	120(16)	139(17)	26(13)	17(8)	24(9)
C14_5	85(8)	93(13)	151(15)	8(11)	35(9)	30(9)
C15_5	65(5)	90(13)	164(16)	16(11)	33(8)	11(7)
C16_5	65(5)	81(11)	131(13)	11(9)	31(7)	3(6)
C17_5	71(8)	63(6)	96(5)	-11(5)	35(5)	-4(6)
C18_5	87(10)	83(9)	89(6)	-16(5)	37(6)	10(7)
C19_5	102(13)	103(10)	101(7)	-31(7)	35(8)	7(9)
C20_5	115(15)	107(10)	154(12)	-48(10)	53(12)	-9(10)
C21_5	143(19)	81(10)	171(13)	-39(8)	62(12)	-37(11)
C22_5	134(17)	71(7)	149(12)	-21(6)	63(12)	-29(8)
Br1_6	63.2(9)	142.3(18)	49.7(8)	19.9(10)	16.9(7)	19.9(10)
Cl1_6	59.1(18)	62(2)	64(2)	2.9(16)	15.0(15)	-0.6(16)
O1_6	52(5)	59(5)	49(4)	8(3)	16(4)	11(4)
O2_6	50(4)	57(5)	49(4)	9(4)	18(3)	11(3)
C1_6	47(5)	61(6)	48(5)	8(4)	13(4)	12(4)
C2_6	49(4)	69(5)	47(4)	8(4)	15(3)	12(4)
C3_6	53(4)	74(6)	60(4)	8(4)	22(3)	20(3)
C4_6	37(4)	70(4)	49(4)	10(3)	21(3)	9(4)
C5_6	41(5)	68(4)	58(5)	10(3)	25(4)	10(4)
C6_6	48(6)	72(5)	73(6)	19(4)	24(5)	9(5)
C7_6	52(6)	82(5)	71(5)	23(5)	23(4)	19(5)
C8_6	50(6)	85(6)	56(5)	22(4)	24(4)	14(5)

Atom	U_{11}	U_{22}	U_{33}	U_{23}	U_{13}	U_{12}
C9_6	42(5)	78(6)	46(4)	14(4)	24(3)	11(4)
C10_6	54(5)	75(5)	61(6)	8(5)	23(4)	19(4)
C11_6	56(5)	70(7)	68(4)	15(4)	19(4)	20(5)
C12_6	71(9)	100(11)	99(8)	0(8)	11(7)	43(8)
C13_6	88(12)	152(18)	109(8)	19(9)	15(8)	71(12)
C14_6	93(13)	141(16)	101(8)	25(10)	10(9)	56(11)
C15_6	72(9)	124(13)	77(6)	16(7)	5(6)	31(9)
C16_6	49(6)	82(9)	66(4)	12(5)	17(4)	9(6)
C17_6	40(5)	82(6)	63(5)	16(4)	16(4)	23(4)
C18_6	55(6)	97(7)	64(6)	14(5)	17(5)	7(5)
C19_6	60(8)	102(9)	86(6)	23(6)	25(6)	6(6)
C20_6	53(7)	96(9)	87(6)	29(6)	31(6)	10(6)
C21_6	47(6)	94(8)	81(6)	25(5)	30(5)	19(5)
C22_6	49(6)	85(8)	64(4)	12(5)	20(4)	10(5)
Br1_7	107.5(17)	57.3(12)	188(3)	17.7(15)	-14.3(17)	7.2(11)
Cl1_7	133(4)	121(4)	78(3)	-18(3)	54(3)	-6(3)
O1_7	62(5)	58(4)	51(5)	11(4)	17(4)	12(4)
O2_7	67(3)	55(5)	47(4)	4(4)	23(3)	14(3)
C1_7	67(4)	53(4)	43(5)	16(3)	25(3)	12(3)
C2_7	74(4)	62(4)	73(6)	3(4)	22(3)	7(3)
C3_7	72(6)	96(3)	94(3)	15(3)	11(3)	2(4)
C4_7	73(6)	64(5)	74(8)	-17(4)	9(5)	5(5)
C5_7	86(9)	88(8)	81(9)	-38(6)	21(7)	-1(6)
C6_7	86(10)	86(8)	119(13)	-49(7)	21(8)	-2(7)
C7_7	70(10)	87(9)	135(13)	-38(8)	9(8)	-1(7)
C8_7	78(10)	72(8)	128(13)	-13(7)	8(8)	19(7)
C9_7	74(9)	58(6)	90(9)	-12(5)	6(6)	7(5)
C10_7	70(5)	50(7)	102(5)	17(5)	20(6)	8(4)
C11_7	93(7)	94(5)	57(7)	5(5)	1(6)	4(5)
C12_7	99(7)	114(11)	104(15)	36(11)	15(9)	20(7)
C13_7	115(10)	117(12)	84(12)	34(10)	14(10)	27(7)
C14_7	128(10)	133(13)	74(12)	52(12)	9(10)	20(9)
C15_7	124(9)	122(10)	80(13)	41(10)	7(10)	9(9)
C16_7	100(8)	106(8)	48(8)	15(7)	-13(7)	-7(6)
C17_7	59(6)	109(3)	105(2)	3(2)	1(3)	12(3)
C18_7	123(3)	121(3)	122(3)	-2.4(11)	34.1(14)	-0.2(12)
C19_7	121(3)	120(3)	120(3)	-1.2(12)	34.6(15)	0.4(12)
C20_7	140(11)	124(3)	131(4)	-6(3)	45(5)	-8(5)
C21_7	151(12)	119(4)	133(4)	-12(3)	48(6)	-20(6)

Atom	U_{11}	U_{22}	U_{33}	U_{23}	U_{13}	U_{12}
C22_7	94(10)	111(3)	123(4)	-3(2)	22(5)	2(5)
Br1_8	266(3)	108.4(17)	240(2)	69.1(16)	196(2)	91.3(17)
Cl1_8	71.4(18)	90(2)	65.9(18)	13.0(16)	17.4(15)	-0.8(17)
O1_8	68(4)	55(5)	49(5)	13(4)	14(3)	10(4)
O2_8	65(4)	57(5)	44(4)	10(3)	23(3)	17(4)
C1_8	72(4)	45(7)	48(4)	11(4)	16(3)	12(4)
C2_8	81(3)	58(6)	47(4)	12(4)	18(3)	5(3)
C3_8	75(5)	57(4)	46(5)	10(3)	14(4)	1(3)
C4_8	79(2)	79(3)	78(3)	2.6(14)	23.3(14)	1.4(13)
C5_8	83(3)	83(3)	82(3)	1.0(14)	24.3(14)	-0.1(13)
C6_8	86(3)	88(3)	87(3)	1.5(14)	25.4(15)	0.2(14)
C7_8	91(3)	91(3)	91(3)	0.7(14)	27.6(15)	1.3(13)
C8_8	90(3)	90(3)	91(3)	0.6(14)	27.7(15)	1.8(14)
C9_8	86(3)	84(3)	84(3)	-0.4(14)	26.2(15)	1.6(14)
C10_8	90(6)	57(4)	46(4)	13(4)	18(4)	-2(5)
C11_8	66(5)	58(6)	68(5)	18(4)	18(4)	0(4)
C12_8	74(6)	72(9)	81(6)	24(6)	8(5)	3(6)
C13_8	73(7)	87(10)	120(10)	32(8)	17(7)	11(7)
C14_8	70(7)	78(10)	121(9)	39(7)	33(7)	18(7)
C15_8	73(7)	78(9)	113(9)	15(7)	34(6)	20(6)
C16_8	63(6)	69(7)	75(6)	12(5)	22(5)	11(5)
C17_8	60(6)	56(5)	40(5)	11(3)	4(4)	4(4)
C18_8	57(6)	57(5)	49(6)	7(4)	6(5)	4(4)
C19_8	62(7)	77(7)	60(6)	6(5)	9(5)	-9(6)
C20_8	59(8)	85(7)	60(6)	9(5)	12(5)	-4(6)
C21_8	72(8)	86(8)	58(7)	6(5)	18(6)	-5(6)
C22_8	70(7)	72(7)	50(5)	1(5)	14(5)	-3(6)
Br1_12	148(3)	139(3)	146(3)	26(2)	47(3)	12(2)
Cl1_12	98(4)	96(4)	68(3)	9.3(18)	15(3)	2(3)
O1_12	55(2)	70(2)	56(2)	9.0(18)	13.5(15)	3.8(18)
O2_12	51(2)	65(4)	53(3)	5(3)	17(2)	8(3)
C1_12	54.7(17)	70.6(18)	56.9(19)	9.7(14)	13.3(14)	3.5(16)
C2_12	55.7(15)	71.9(16)	58.8(14)	10.9(11)	12.2(12)	2.3(12)
C3_12	55.5(15)	70.8(15)	58.7(15)	10.4(12)	12.4(11)	2.4(12)
C4_12	56(2)	73.0(18)	58.9(14)	11.5(13)	10.5(14)	0.2(15)
C5_12	73(8)	73(2)	60.5(16)	12.5(15)	16(3)	2(3)
C6_12	119(8)	79(2)	65.2(17)	17.8(16)	29(3)	17(3)
C7_12	93(7)	77(2)	60.2(19)	14.5(17)	18(3)	10(3)
C8_12	107(17)	77(2)	61(2)	16(2)	21(5)	13(5)

Atom	U_{11}	U_{22}	U_{33}	U_{23}	U_{13}	U_{12}
C9_12	66(12)	75(2)	58(2)	12.5(19)	10(4)	5(4)
C10_12	55.0(17)	70.7(16)	58.7(14)	11.1(13)	12.3(12)	2.5(13)
C11_12	55.8(19)	70.8(15)	57.6(17)	9.9(12)	12.5(13)	2.6(13)
C12_12	50(10)	71(2)	57(3)	9.9(17)	15(4)	2(3)
C13_12	61(10)	72(2)	58(4)	8.8(18)	10(5)	4(3)
C14_12	66(10)	72(2)	59(4)	8.7(18)	8(5)	5(3)
C15_12	58(5)	71.0(15)	57(3)	9.4(16)	12(3)	3.3(17)
C16_12	48(9)	70.9(15)	57(3)	10.0(15)	15(4)	2.0(18)
C17_12	56.0(16)	69.7(16)	59(2)	9.3(16)	13.0(15)	2.4(13)
C18_12	58(2)	69.7(17)	61(3)	9.5(19)	15(2)	2.7(16)
C19_12	73(5)	71(2)	89(8)	16(3)	36(6)	8(3)
C20_12	94(5)	73(2)	133(10)	24(3)	66(7)	13(3)
C21_12	66(3)	69.8(18)	75(5)	12(2)	26(3)	4.6(17)
C22_12	57(3)	69.8(16)	61(5)	9.6(17)	15(3)	2.7(14)
Br1_1	115.0(16)	97.3(16)	88.0(13)	39.5(12)	16.2(11)	-18.1(13)
Cl1_1	49.3(18)	115(3)	73(2)	34(2)	14.8(17)	0(2)
O1_1	44(5)	113(9)	42(5)	18(5)	7(4)	22(5)
O2_1	45(5)	92(7)	40(4)	1(5)	5(4)	19(5)
C1_1	47(7)	88(11)	63(9)	-2(8)	16(7)	12(7)
C2_1	50(7)	59(8)	61(8)	11(6)	28(6)	11(6)
C3_1	45(7)	68(9)	72(9)	0(7)	25(6)	2(6)
C4_1	49(7)	60(8)	56(7)	0(6)	21(6)	8(6)
C5_1	61(8)	52(8)	52(7)	5(6)	18(6)	7(6)
C6_1	63(8)	57(8)	49(7)	-3(6)	18(6)	-6(6)
C7_1	84(11)	65(10)	57(8)	-7(7)	13(8)	11(8)
C8_1	78(10)	57(9)	67(9)	12(7)	12(8)	2(8)
C9_1	70(9)	48(8)	59(8)	8(6)	14(7)	-1(7)
C10_1	64(9)	90(12)	51(8)	4(7)	26(7)	9(8)
C11_1	40(7)	139(17)	61(9)	32(10)	16(6)	15(9)
C12_1	60(9)	68(10)	83(11)	13(9)	16(8)	16(8)
C13_1	65(10)	114(16)	81(12)	19(11)	4(9)	48(11)
C14_1	98(14)	190(30)	73(12)	51(14)	40(11)	88(17)
C15_1	123(17)	170(20)	82(13)	62(15)	50(13)	92(18)
C16_1	81(11)	122(16)	72(11)	34(11)	38(9)	40(11)
C17_1	71(9)	63(9)	68(9)	10(7)	30(8)	27(8)
C18_1	61(9)	111(14)	58(9)	-6(9)	28(7)	-29(9)
C19_1	83(12)	75(12)	115(16)	10(11)	29(11)	-26(10)
C20_1	121(16)	58(10)	70(11)	1(8)	3(10)	-3(10)
C21_1	240(30)	72(13)	77(13)	-20(10)	85(17)	-11(16)

Atom	U_{11}	U_{22}	U_{33}	U_{23}	U_{13}	U_{12}
C22_1	97(12)	71(11)	63(9)	-6(8)	22(9)	2(9)
Br1_4	148(3)	139(3)	146(3)	26(2)	47(3)	12(2)
Cl1_4	98(4)	96(4)	68(3)	9.3(18)	15(3)	2(3)
O1_4	55(2)	70(2)	56(2)	9.0(18)	13.5(15)	3.8(18)
O2_4	51(2)	65(4)	53(3)	5(3)	17(2)	8(3)
C1_4	54.7(17)	70.6(18)	56.9(19)	9.7(14)	13.3(14)	3.5(16)
C2_4	55.7(15)	71.9(16)	58.8(14)	10.9(11)	12.2(12)	2.3(12)
C3_4	55.5(15)	70.8(15)	58.7(15)	10.4(12)	12.4(11)	2.4(12)
C4_4	58(2)	72.4(19)	58.8(14)	11.1(13)	10.5(13)	-0.9(16)
C5_4	73(8)	73(2)	60.5(16)	12.5(15)	16(3)	2(3)
C6_4	119(8)	79(2)	65.2(17)	17.8(16)	29(3)	17(3)
C7_4	119(8)	79(2)	65.2(17)	17.8(16)	29(3)	17(3)
C8_4	93(7)	77(2)	60.2(19)	14.5(17)	18(3)	10(3)
C9_4	58(9)	73(3)	58(2)	11(2)	9(3)	-1(5)
C10_4	55.0(17)	70.7(16)	58.7(14)	11.1(13)	12.3(12)	2.5(13)
C11_4	55.8(19)	70.8(15)	57.6(17)	9.9(12)	12.5(13)	2.6(13)
C12_4	62(9)	71.6(19)	59(3)	8.8(17)	9(4)	4(3)
C13_4	59(8)	71(2)	58(3)	9.0(19)	11(5)	4(3)
C14_4	51(7)	71(2)	56(3)	9.7(19)	15(4)	2(3)
C15_4	58(5)	71.0(15)	57(3)	9.4(16)	12(3)	3.3(17)
C16_4	43(6)	70.5(15)	53(3)	11.1(14)	20(3)	0.5(16)
C17_4	56.0(16)	69.7(16)	59(2)	9.3(16)	13.0(15)	2.4(13)
C18_4	58(2)	69.7(17)	61(3)	9.5(19)	15(2)	2.7(16)
C19_4	83(5)	69.7(18)	107(8)	12(3)	49(6)	5(2)
C20_4	66(5)	69.6(18)	78(8)	11(3)	27(6)	4(2)
C21_4	66(3)	69.8(18)	75(5)	12(2)	26(3)	4.6(17)
C22_4	57(3)	69.8(16)	61(5)	9.6(17)	15(3)	2.7(14)
Br1_2	46.2(8)	118.9(15)	63.3(9)	-28.9(10)	4.4(7)	0.3(8)
Cl1_2	54.8(17)	72(2)	45.0(15)	-5.2(14)	13.1(13)	3.6(15)
O1_2	46(5)	93(8)	53(5)	-2(5)	10(4)	17(5)
O2_2	48(5)	78(7)	44(4)	-16(5)	2(4)	16(5)
C1_2	32(6)	87(11)	58(8)	-23(8)	5(5)	20(7)
C2_2	38(6)	80(10)	57(8)	-9(7)	6(6)	20(6)
C3_2	67(9)	61(9)	72(10)	-7(7)	21(8)	8(7)
C4_2	39(7)	86(11)	58(8)	-19(8)	0(6)	16(7)
C5_2	54(7)	69(9)	47(7)	-8(6)	27(6)	9(6)
C6_2	30(5)	76(9)	39(6)	2(6)	9(4)	1(6)
C7_2	37(6)	89(11)	44(7)	1(7)	15(5)	7(6)
C8_2	41(7)	93(12)	69(9)	-23(8)	22(6)	4(7)

Atom	U_{11}	U_{22}	U_{33}	U_{23}	U_{13}	U_{12}
C9_2	46(7)	88(12)	61(9)	-28(8)	-8(6)	22(7)
C10_2	37(6)	84(11)	73(10)	-17(8)	3(6)	8(7)
C11_2	24(5)	98(12)	67(9)	16(8)	4(5)	8(7)
C12_2	45(8)	104(14)	109(14)	38(12)	29(9)	18(9)
C13_2	66(11)	123(18)	96(14)	65(14)	21(10)	16(11)
C14_2	57(10)	150(20)	85(13)	58(15)	3(9)	-21(12)
C15_2	73(11)	92(13)	69(10)	9(9)	-31(9)	-19(10)
C16_2	66(10)	80(12)	83(12)	2(10)	0(9)	-1(9)
C17_2	87(4)	79(7)	102(7)	9(6)	31(4)	16(4)
C18_2	75(5)	88(6)	98(7)	10(6)	24(5)	22(5)
C19_2	74(5)	97(7)	96(5)	10(5)	21(5)	19(5)
C20_2	92(6)	120(9)	109(6)	-5(7)	31(5)	-1(6)
C21_2	100(4)	107(5)	108(4)	-1(3)	34(3)	-3(3)
C22_2	126(6)	170(14)	159(10)	-60(11)	71(7)	-42(8)
N1_11	80(4)	67(7)	61(6)	5(5)	33(3)	-8(3)
C23_11	85(4)	90(5)	88(5)	1(3)	26(3)	2(3)
C24_11	99(6)	126(15)	75(10)	-18(10)	17(6)	25(8)

Table 11: Bond Lengths in Å for **WL-2CIBr**.

Atom	Atom	Length/Å	Atom	Atom	Length/Å
Rh3	Rh4	2.3816(13)	Rh2	O1_3	2.028(5)
Rh3	O2_5	2.032(6)	Rh2	O1_12	2.073(6)
Rh3	O2_6	2.075(5)	Rh2	O1_1	2.056(6)
Rh3	O2_7	2.029(6)	Rh2	O1_4	2.073(6)
Rh3	O2_8	2.055(6)	Rh2	O1_2	2.071(7)
Rh3	N1_11	2.239(12)	N1_9	C23_9	1.086(12)
Rh4	O4	2.276(11)	C23_9	C24_9	1.450(16)
Rh4	O1_5	2.038(6)	N1_10	C23_10	1.086(12)
Rh4	O1_6	2.013(5)	C23_10	C24_10	1.450(16)
Rh4	O1_7	2.057(6)	Br1_3	C8_3	1.904(6)
Rh4	O1_8	2.043(6)	C11_3	C5_3	1.745(6)
Rh1	Rh2	2.3740(14)	O1_3	C1_3	1.266(6)
Rh1	N1_10	2.240(12)	O2_3	C1_3	1.271(6)
Rh1	O2_3	2.078(6)	C1_3	C2_3	1.514(6)
Rh1	O2_12	2.032(7)	C2_3	C3_3	1.552(6)
Rh1	O2_1	2.000(6)	C2_3	C4_3	1.501(7)
Rh1	O2_4	2.030(7)	C2_3	C10_3	1.492(7)
Rh1	O2_2	2.037(6)	C3_3	C10_3	1.478(7)
Rh2	N1_9	2.227(12)	C3_3	C11_3	1.530(7)

Atom	Atom	Length/Å	Atom	Atom	Length/Å
C3_3	C17_3	1.505(7)	C13_5	C14_5	1.360(10)
C4_3	C5_3	1.383(7)	C14_5	C15_5	1.360(10)
C4_3	C9_3	1.398(7)	C15_5	C16_5	1.383(8)
C5_3	C6_3	1.419(7)	C17_5	C18_5	1.372(8)
C6_3	C7_3	1.363(8)	C17_5	C22_5	1.409(8)
C7_3	C8_3	1.374(9)	C18_5	C19_5	1.385(8)
C8_3	C9_3	1.393(8)	C19_5	C20_5	1.365(9)
C11_3	C12_3	1.405(8)	C20_5	C21_5	1.349(9)
C11_3	C16_3	1.370(8)	C21_5	C22_5	1.392(9)
C12_3	C13_3	1.402(9)	Br1_6	C8_6	1.903(6)
C13_3	C14_3	1.361(10)	C11_6	C5_6	1.745(6)
C14_3	C15_3	1.360(10)	O1_6	C1_6	1.265(6)
C15_3	C16_3	1.383(8)	O2_6	C1_6	1.271(6)
C17_3	C18_3	1.372(8)	C1_6	C2_6	1.513(6)
C17_3	C22_3	1.408(8)	C2_6	C3_6	1.552(6)
C18_3	C19_3	1.385(8)	C2_6	C4_6	1.502(7)
C19_3	C20_3	1.365(9)	C2_6	C10_6	1.493(7)
C20_3	C21_3	1.349(9)	C3_6	C10_6	1.478(7)
C21_3	C22_3	1.392(9)	C3_6	C11_6	1.531(7)
Br1_5	C8_5	1.904(6)	C3_6	C17_6	1.505(7)
C11_5	C5_5	1.745(6)	C4_6	C5_6	1.382(7)
O1_5	C1_5	1.267(6)	C4_6	C9_6	1.398(7)
O2_5	C1_5	1.271(6)	C5_6	C6_6	1.419(7)
C1_5	C2_5	1.516(7)	C6_6	C7_6	1.363(8)
C2_5	C3_5	1.553(6)	C7_6	C8_6	1.374(9)
C2_5	C4_5	1.500(7)	C8_6	C9_6	1.393(8)
C2_5	C10_5	1.492(7)	C11_6	C12_6	1.405(8)
C3_5	C10_5	1.478(7)	C11_6	C16_6	1.370(8)
C3_5	C11_5	1.530(7)	C12_6	C13_6	1.402(9)
C3_5	C17_5	1.505(7)	C13_6	C14_6	1.361(10)
C4_5	C5_5	1.383(7)	C14_6	C15_6	1.360(10)
C4_5	C9_5	1.399(7)	C15_6	C16_6	1.383(8)
C5_5	C6_5	1.419(7)	C17_6	C18_6	1.372(8)
C6_5	C7_5	1.363(8)	C17_6	C22_6	1.408(8)
C7_5	C8_5	1.374(9)	C18_6	C19_6	1.385(8)
C8_5	C9_5	1.393(8)	C19_6	C20_6	1.365(9)
C11_5	C12_5	1.404(8)	C20_6	C21_6	1.349(9)
C11_5	C16_5	1.370(8)	C21_6	C22_6	1.392(9)
C12_5	C13_5	1.402(9)	Br1_7	C8_7	1.903(6)

Atom	Atom	Length/Å
C11_7	C5_7	1.744(6)
O1_7	C1_7	1.266(6)
O2_7	C1_7	1.272(6)
C1_7	C2_7	1.513(7)
C2_7	C3_7	1.551(6)
C2_7	C4_7	1.501(7)
C2_7	C10_7	1.493(7)
C3_7	C10_7	1.478(7)
C3_7	C11_7	1.531(7)
C3_7	C17_7	1.505(7)
C4_7	C5_7	1.382(7)
C4_7	C9_7	1.399(7)
C5_7	C6_7	1.419(7)
C6_7	C7_7	1.363(8)
C7_7	C8_7	1.374(9)
C8_7	C9_7	1.393(8)
C11_7	C12_7	1.405(8)
C11_7	C16_7	1.369(8)
C12_7	C13_7	1.402(9)
C13_7	C14_7	1.361(10)
C14_7	C15_7	1.360(10)
C15_7	C16_7	1.383(8)
C17_7	C18_7	1.373(8)
C17_7	C22_7	1.408(8)
C18_7	C19_7	1.385(8)
C19_7	C20_7	1.365(9)
C20_7	C21_7	1.349(9)
C21_7	C22_7	1.393(9)
Br1_8	C8_8	1.904(6)
C11_8	C5_8	1.745(6)
O1_8	C1_8	1.265(6)
O2_8	C1_8	1.271(6)
C1_8	C2_8	1.513(6)
C2_8	C3_8	1.552(6)
C2_8	C4_8	1.502(7)
C2_8	C10_8	1.492(7)
C3_8	C10_8	1.477(7)
C3_8	C11_8	1.531(7)
C3_8	C17_8	1.505(7)

Atom	Atom	Length/Å
C4_8	C5_8	1.383(7)
C4_8	C9_8	1.399(7)
C5_8	C6_8	1.419(7)
C6_8	C7_8	1.363(8)
C7_8	C8_8	1.374(9)
C8_8	C9_8	1.393(8)
C11_8	C12_8	1.405(8)
C11_8	C16_8	1.369(8)
C12_8	C13_8	1.402(9)
C13_8	C14_8	1.360(10)
C14_8	C15_8	1.360(10)
C15_8	C16_8	1.383(8)
C17_8	C18_8	1.372(8)
C17_8	C22_8	1.408(8)
C18_8	C19_8	1.384(8)
C19_8	C20_8	1.365(9)
C20_8	C21_8	1.349(9)
C21_8	C22_8	1.392(9)
Br1_12	C8_12	1.904(6)
C11_12	C5_12	1.745(6)
O1_12	C1_12	1.266(6)
O2_12	C1_12	1.271(6)
C1_12	C2_12	1.513(7)
C2_12	C3_12	1.551(6)
C2_12	C4_12	1.502(7)
C2_12	C10_12	1.493(7)
C3_12	C10_12	1.478(7)
C3_12	C11_12	1.531(7)
C3_12	C17_12	1.505(7)
C4_12	C5_12	1.382(7)
C4_12	C9_12	1.399(7)
C5_12	C6_12	1.419(7)
C6_12	C7_12	1.363(8)
C7_12	C8_12	1.374(9)
C8_12	C9_12	1.393(8)
C11_12	C12_12	1.405(8)
C11_12	C16_12	1.370(8)
C12_12	C13_12	1.402(9)
C13_12	C14_12	1.361(10)

Atom	Atom	Length/Å
C14_12	C15_12	1.360(10)
C15_12	C16_12	1.383(8)
C17_12	C18_12	1.372(8)
C17_12	C22_12	1.408(8)
C18_12	C19_12	1.385(9)
C19_12	C20_12	1.365(9)
C20_12	C21_12	1.349(9)
C21_12	C22_12	1.392(9)
Br1_1	C8_1	1.904(6)
Cl1_1	C5_1	1.745(6)
O1_1	C1_1	1.266(6)
O2_1	C1_1	1.271(6)
C1_1	C2_1	1.514(7)
C2_1	C3_1	1.551(6)
C2_1	C4_1	1.502(7)
C2_1	C10_1	1.494(7)
C3_1	C10_1	1.478(7)
C3_1	C11_1	1.531(7)
C3_1	C17_1	1.505(7)
C4_1	C5_1	1.382(7)
C4_1	C9_1	1.400(7)
C5_1	C6_1	1.419(7)
C6_1	C7_1	1.363(8)
C7_1	C8_1	1.374(9)
C8_1	C9_1	1.393(8)
C11_1	C12_1	1.405(8)
C11_1	C16_1	1.370(8)
C12_1	C13_1	1.403(9)
C13_1	C14_1	1.361(10)
C14_1	C15_1	1.360(10)
C15_1	C16_1	1.383(8)
C17_1	C18_1	1.372(8)
C17_1	C22_1	1.408(8)
C18_1	C19_1	1.385(8)
C19_1	C20_1	1.365(9)
C20_1	C21_1	1.349(9)
C21_1	C22_1	1.392(9)
Br1_4	C8_4	1.904(6)
Cl1_4	C5_4	1.745(6)

Atom	Atom	Length/Å
O1_4	C1_4	1.266(6)
O2_4	C1_4	1.272(6)
C1_4	C2_4	1.514(7)
C2_4	C3_4	1.552(6)
C2_4	C4_4	1.501(7)
C2_4	C10_4	1.492(7)
C3_4	C10_4	1.478(7)
C3_4	C11_4	1.530(7)
C3_4	C17_4	1.506(7)
C4_4	C5_4	1.383(7)
C4_4	C9_4	1.398(7)
C5_4	C6_4	1.419(7)
C6_4	C7_4	1.363(8)
C7_4	C8_4	1.374(9)
C8_4	C9_4	1.393(8)
C11_4	C12_4	1.405(8)
C11_4	C16_4	1.370(8)
C12_4	C13_4	1.403(9)
C13_4	C14_4	1.361(10)
C14_4	C15_4	1.360(10)
C15_4	C16_4	1.383(8)
C17_4	C18_4	1.373(8)
C17_4	C22_4	1.409(8)
C18_4	C19_4	1.385(8)
C19_4	C20_4	1.365(9)
C20_4	C21_4	1.349(9)
C21_4	C22_4	1.392(9)
Br1_2	C8_2	1.904(6)
Cl1_2	C5_2	1.745(6)
O1_2	C1_2	1.266(6)
O2_2	C1_2	1.271(6)
C1_2	C2_2	1.514(7)
C2_2	C3_2	1.552(6)
C2_2	C4_2	1.501(7)
C2_2	C10_2	1.493(7)
C3_2	C10_2	1.477(7)
C3_2	C11_2	1.531(7)
C3_2	C17_2	1.505(7)
C4_2	C5_2	1.382(7)

Atom	Atom	Length/Å
C4_2	C9_2	1.399(7)
C5_2	C6_2	1.419(7)
C6_2	C7_2	1.363(8)
C7_2	C8_2	1.374(9)
C8_2	C9_2	1.393(8)
C11_2	C12_2	1.405(8)
C11_2	C16_2	1.370(8)
C12_2	C13_2	1.402(9)
C13_2	C14_2	1.360(10)
C14_2	C15_2	1.360(10)

Atom	Atom	Length/Å
C15_2	C16_2	1.383(8)
C17_2	C18_2	1.373(8)
C17_2	C22_2	1.409(8)
C18_2	C19_2	1.385(8)
C19_2	C20_2	1.365(9)
C20_2	C21_2	1.349(9)
C21_2	C22_2	1.393(9)
N1_11	C23_11	1.086(12)
C23_11	C24_11	1.450(16)

Table 12: Bond Angles in ° for WL-2ClBr.

Atom	Atom	Atom	Angle/°
O2_5	Rh3	Rh4	88.21(16)
O2_5	Rh3	O2_6	91.4(4)
O2_5	Rh3	O2_8	88.7(4)
O2_5	Rh3	N1_11	88.7(4)
O2_6	Rh3	Rh4	86.62(15)
O2_6	Rh3	N1_11	97.1(3)
O2_7	Rh3	Rh4	88.33(17)
O2_7	Rh3	O2_5	176.5(3)
O2_7	Rh3	O2_6	89.0(4)
O2_7	Rh3	O2_8	90.5(4)
O2_7	Rh3	N1_11	94.8(4)
O2_8	Rh3	Rh4	88.04(16)
O2_8	Rh3	O2_6	174.7(2)
O2_8	Rh3	N1_11	88.2(3)
N1_11	Rh3	Rh4	175.2(3)
O4	Rh4	Rh3	177.9(4)
O1_5	Rh4	Rh3	87.67(17)
O1_5	Rh4	O4	90.3(4)
O1_5	Rh4	O1_7	174.0(3)
O1_5	Rh4	O1_8	92.2(4)
O1_6	Rh4	Rh3	88.63(16)
O1_6	Rh4	O4	90.8(4)
O1_6	Rh4	O1_5	87.6(4)
O1_6	Rh4	O1_7	89.6(4)
O1_6	Rh4	O1_8	175.9(3)
O1_7	Rh4	Rh3	87.00(17)

Atom	Atom	Atom	Angle/°
O1_7	Rh4	O4	95.0(4)
O1_8	Rh4	Rh3	87.28(17)
O1_8	Rh4	O4	93.3(4)
O1_8	Rh4	O1_7	90.3(4)
N1_10	Rh1	Rh2	175.7(3)
O2_3	Rh1	Rh2	87.35(16)
O2_3	Rh1	N1_10	96.8(4)
O2_12	Rh1	Rh2	89.6(3)
O2_12	Rh1	N1_10	91.9(4)
O2_12	Rh1	O2_3	84.5(7)
O2_12	Rh1	O2_2	174.6(6)
O2_1	Rh1	Rh2	88.28(18)
O2_1	Rh1	N1_10	87.5(4)
O2_1	Rh1	O2_3	175.6(3)
O2_1	Rh1	O2_12	96.1(8)
O2_1	Rh1	O2_4	85.7(6)
O2_1	Rh1	O2_2	88.6(4)
O2_4	Rh1	Rh2	85.5(3)
O2_4	Rh1	N1_10	95.2(4)
O2_4	Rh1	O2_3	94.5(6)
O2_4	Rh1	O2_2	171.4(5)
O2_2	Rh1	Rh2	87.83(17)
O2_2	Rh1	N1_10	91.0(4)
O2_2	Rh1	O2_3	90.7(4)
N1_9	Rh2	Rh1	179.2(4)
O1_3	Rh2	Rh1	87.85(17)

Atom	Atom	Atom	Angle/°	Atom	Atom	Atom	Angle/°
O1_3	Rh2	N1_9	92.9(4)	C5_3	C4_3	C2_3	122.3(5)
O1_3	Rh2	O1_12	90.1(9)	C5_3	C4_3	C9_3	116.9(5)
O1_3	Rh2	O1_1	174.7(3)	C9_3	C4_3	C2_3	120.4(5)
O1_3	Rh2	O1_4	89.3(8)	C4_3	C5_3	C11_3	120.7(4)
O1_3	Rh2	O1_2	88.8(4)	C4_3	C5_3	C6_3	122.6(5)
O1_12	Rh2	Rh1	86.7(3)	C6_3	C5_3	C11_3	116.8(4)
O1_12	Rh2	N1_9	93.4(6)	C7_3	C6_3	C5_3	118.7(6)
O1_1	Rh2	Rh1	86.84(17)	C6_3	C7_3	C8_3	119.9(5)
O1_1	Rh2	N1_9	92.4(4)	C7_3	C8_3	Br1_3	121.1(4)
O1_1	Rh2	O1_12	89.8(9)	C7_3	C8_3	C9_3	121.5(6)
O1_1	Rh2	O1_4	90.6(8)	C9_3	C8_3	Br1_3	117.4(5)
O1_1	Rh2	O1_2	90.8(4)	C8_3	C9_3	C4_3	120.4(6)
O1_4	Rh2	Rh1	88.1(4)	C3_3	C10_3	C2_3	63.0(3)
O1_4	Rh2	N1_9	92.0(6)	C12_3	C11_3	C3_3	116.4(5)
O1_2	Rh2	Rh1	87.82(17)	C16_3	C11_3	C3_3	123.5(5)
O1_2	Rh2	N1_9	92.1(5)	C16_3	C11_3	C12_3	120.1(5)
O1_2	Rh2	O1_12	174.5(5)	C13_3	C12_3	C11_3	118.5(6)
O1_2	Rh2	O1_4	175.6(6)	C14_3	C13_3	C12_3	120.3(6)
C23_9	N1_9	Rh2	178.9(15)	C15_3	C14_3	C13_3	120.1(6)
N1_9	C23_9	C24_9	174(2)	C14_3	C15_3	C16_3	120.9(7)
C23_10	N1_10	Rh1	171.2(15)	C11_3	C16_3	C15_3	119.4(6)
N1_10	C23_10	C24_10	176(2)	C18_3	C17_3	C3_3	121.8(5)
C1_3	O1_3	Rh2	117.2(4)	C18_3	C17_3	C22_3	116.0(5)
C1_3	O2_3	Rh1	116.4(4)	C22_3	C17_3	C3_3	121.8(5)
O1_3	C1_3	O2_3	126.3(5)	C17_3	C18_3	C19_3	122.5(6)
O1_3	C1_3	C2_3	117.2(4)	C20_3	C19_3	C18_3	119.3(6)
O2_3	C1_3	C2_3	116.0(4)	C21_3	C20_3	C19_3	120.7(6)
C1_3	C2_3	C3_3	122.4(4)	C20_3	C21_3	C22_3	119.8(6)
C4_3	C2_3	C1_3	112.7(4)	C21_3	C22_3	C17_3	121.2(6)
C4_3	C2_3	C3_3	117.9(4)	C1_5	O1_5	Rh4	116.7(4)
C10_3	C2_3	C1_3	115.0(4)	C1_5	O2_5	Rh3	117.7(4)
C10_3	C2_3	C3_3	58.0(3)	O1_5	C1_5	O2_5	126.1(5)
C10_3	C2_3	C4_3	120.6(4)	O1_5	C1_5	C2_5	116.9(4)
C10_3	C3_3	C2_3	58.9(3)	O2_5	C1_5	C2_5	115.8(4)
C10_3	C3_3	C11_3	119.0(5)	C1_5	C2_5	C3_5	121.9(4)
C10_3	C3_3	C17_3	120.1(5)	C4_5	C2_5	C1_5	112.7(4)
C11_3	C3_3	C2_3	121.4(4)	C4_5	C2_5	C3_5	118.1(4)
C17_3	C3_3	C2_3	117.4(4)	C10_5	C2_5	C1_5	114.5(4)
C17_3	C3_3	C11_3	111.2(4)	C10_5	C2_5	C3_5	58.0(3)

Atom	Atom	Atom	Angle/°
C10_5	C2_5	C4_5	121.4(4)
C10_5	C3_5	C2_5	58.9(3)
C10_5	C3_5	C11_5	119.5(5)
C10_5	C3_5	C17_5	119.6(5)
C11_5	C3_5	C2_5	120.8(4)
C17_5	C3_5	C2_5	118.0(4)
C17_5	C3_5	C11_5	111.2(4)
C5_5	C4_5	C2_5	122.4(5)
C5_5	C4_5	C9_5	116.7(5)
C9_5	C4_5	C2_5	120.8(5)
C4_5	C5_5	C11_5	121.0(4)
C4_5	C5_5	C6_5	122.5(5)
C6_5	C5_5	C11_5	116.4(4)
C7_5	C6_5	C5_5	118.6(6)
C6_5	C7_5	C8_5	119.7(5)
C7_5	C8_5	Br1_5	120.7(4)
C7_5	C8_5	C9_5	121.5(6)
C9_5	C8_5	Br1_5	117.7(5)
C8_5	C9_5	C4_5	120.5(6)
C3_5	C10_5	C2_5	63.1(3)
C12_5	C11_5	C3_5	116.6(5)
C16_5	C11_5	C3_5	123.3(5)
C16_5	C11_5	C12_5	120.1(5)
C13_5	C12_5	C11_5	118.4(6)
C14_5	C13_5	C12_5	120.4(6)
C15_5	C14_5	C13_5	120.3(6)
C14_5	C15_5	C16_5	121.0(7)
C11_5	C16_5	C15_5	119.6(6)
C18_5	C17_5	C3_5	122.1(5)
C18_5	C17_5	C22_5	116.1(5)
C22_5	C17_5	C3_5	121.6(5)
C17_5	C18_5	C19_5	122.5(6)
C20_5	C19_5	C18_5	119.3(6)
C21_5	C20_5	C19_5	120.8(6)
C20_5	C21_5	C22_5	119.8(6)
C21_5	C22_5	C17_5	121.1(6)
C1_6	O1_6	Rh4	117.3(4)
C1_6	O2_6	Rh3	117.0(4)
O1_6	C1_6	O2_6	126.5(5)

Atom	Atom	Atom	Angle/°
O1_6	C1_6	C2_6	117.4(4)
O2_6	C1_6	C2_6	116.0(4)
C1_6	C2_6	C3_6	122.6(4)
C4_6	C2_6	C1_6	112.6(4)
C4_6	C2_6	C3_6	118.0(4)
C10_6	C2_6	C1_6	115.1(4)
C10_6	C2_6	C3_6	58.0(3)
C10_6	C2_6	C4_6	120.1(4)
C10_6	C3_6	C2_6	59.0(3)
C10_6	C3_6	C11_6	118.8(5)
C10_6	C3_6	C17_6	120.3(5)
C11_6	C3_6	C2_6	121.6(4)
C17_6	C3_6	C2_6	117.4(4)
C17_6	C3_6	C11_6	111.1(4)
C5_6	C4_6	C2_6	122.5(5)
C5_6	C4_6	C9_6	116.9(5)
C9_6	C4_6	C2_6	120.2(5)
C4_6	C5_6	C11_6	120.8(4)
C4_6	C5_6	C6_6	122.5(5)
C6_6	C5_6	C11_6	116.7(4)
C7_6	C6_6	C5_6	118.7(6)
C6_6	C7_6	C8_6	119.8(5)
C7_6	C8_6	Br1_6	121.1(4)
C7_6	C8_6	C9_6	121.4(6)
C9_6	C8_6	Br1_6	117.4(5)
C8_6	C9_6	C4_6	120.3(6)
C3_6	C10_6	C2_6	63.0(3)
C12_6	C11_6	C3_6	116.3(5)
C16_6	C11_6	C3_6	123.5(5)
C16_6	C11_6	C12_6	120.1(5)
C13_6	C12_6	C11_6	118.4(6)
C14_6	C13_6	C12_6	120.3(6)
C15_6	C14_6	C13_6	120.3(6)
C14_6	C15_6	C16_6	121.1(7)
C11_6	C16_6	C15_6	119.6(6)
C18_6	C17_6	C3_6	121.8(5)
C18_6	C17_6	C22_6	116.1(5)
C22_6	C17_6	C3_6	121.9(5)
C17_6	C18_6	C19_6	122.5(6)

Atom	Atom	Atom	Angle/°
C20_6	C19_6	C18_6	119.3(6)
C21_6	C20_6	C19_6	120.7(6)
C20_6	C21_6	C22_6	119.8(6)
C21_6	C22_6	C17_6	121.2(6)
C1_7	O1_7	Rh4	117.7(4)
C1_7	O2_7	Rh3	117.3(4)
O1_7	C1_7	O2_7	126.3(5)
O1_7	C1_7	C2_7	117.5(4)
O2_7	C1_7	C2_7	115.8(4)
C1_7	C2_7	C3_7	122.4(4)
C4_7	C2_7	C1_7	112.6(4)
C4_7	C2_7	C3_7	118.2(4)
C10_7	C2_7	C1_7	115.2(4)
C10_7	C2_7	C3_7	58.0(3)
C10_7	C2_7	C4_7	120.0(4)
C10_7	C3_7	C2_7	59.0(3)
C10_7	C3_7	C11_7	118.6(5)
C10_7	C3_7	C17_7	120.5(5)
C11_7	C3_7	C2_7	121.6(4)
C17_7	C3_7	C2_7	117.4(4)
C17_7	C3_7	C11_7	111.1(4)
C5_7	C4_7	C2_7	122.7(5)
C5_7	C4_7	C9_7	116.8(5)
C9_7	C4_7	C2_7	120.3(5)
C4_7	C5_7	C11_7	120.9(4)
C4_7	C5_7	C6_7	122.5(5)
C6_7	C5_7	C11_7	116.6(4)
C7_7	C6_7	C5_7	118.6(6)
C6_7	C7_7	C8_7	119.8(6)
C7_7	C8_7	Br1_7	121.1(4)
C7_7	C8_7	C9_7	121.5(6)
C9_7	C8_7	Br1_7	117.5(5)
C8_7	C9_7	C4_7	120.2(6)
C3_7	C10_7	C2_7	63.0(3)
C12_7	C11_7	C3_7	116.2(5)
C16_7	C11_7	C3_7	123.6(5)
C16_7	C11_7	C12_7	120.2(5)
C13_7	C12_7	C11_7	118.5(6)
C14_7	C13_7	C12_7	120.3(6)

Atom	Atom	Atom	Angle/°
C15_7	C14_7	C13_7	120.3(6)
C14_7	C15_7	C16_7	121.0(7)
C11_7	C16_7	C15_7	119.5(6)
C18_7	C17_7	C3_7	121.7(5)
C18_7	C17_7	C22_7	116.0(5)
C22_7	C17_7	C3_7	122.0(5)
C17_7	C18_7	C19_7	122.5(6)
C20_7	C19_7	C18_7	119.2(6)
C21_7	C20_7	C19_7	120.6(6)
C20_7	C21_7	C22_7	119.7(6)
C21_7	C22_7	C17_7	121.1(6)
C1_8	O1_8	Rh4	118.0(4)
C1_8	O2_8	Rh3	116.8(4)
O1_8	C1_8	O2_8	126.5(5)
O1_8	C1_8	C2_8	117.4(4)
O2_8	C1_8	C2_8	116.1(4)
C1_8	C2_8	C3_8	122.3(4)
C4_8	C2_8	C1_8	112.7(4)
C4_8	C2_8	C3_8	118.1(4)
C10_8	C2_8	C1_8	115.2(4)
C10_8	C2_8	C3_8	58.0(3)
C10_8	C2_8	C4_8	120.2(4)
C10_8	C3_8	C2_8	59.0(3)
C10_8	C3_8	C11_8	118.7(5)
C10_8	C3_8	C17_8	120.5(5)
C11_8	C3_8	C2_8	121.5(4)
C17_8	C3_8	C2_8	117.4(4)
C17_8	C3_8	C11_8	111.1(4)
C5_8	C4_8	C2_8	122.3(5)
C5_8	C4_8	C9_8	116.8(5)
C9_8	C4_8	C2_8	120.3(5)
C4_8	C5_8	C11_8	120.6(4)
C4_8	C5_8	C6_8	122.5(5)
C6_8	C5_8	C11_8	116.7(4)
C7_8	C6_8	C5_8	118.7(6)
C6_8	C7_8	C8_8	119.8(5)
C7_8	C8_8	Br1_8	120.9(4)
C7_8	C8_8	C9_8	121.4(6)
C9_8	C8_8	Br1_8	117.4(5)

Atom	Atom	Atom	Angle/°
C8_8	C9_8	C4_8	120.4(6)
C3_8	C10_8	C2_8	63.0(3)
C12_8	C11_8	C3_8	116.3(5)
C16_8	C11_8	C3_8	123.5(5)
C16_8	C11_8	C12_8	120.1(5)
C13_8	C12_8	C11_8	118.5(6)
C14_8	C13_8	C12_8	120.4(6)
C15_8	C14_8	C13_8	120.3(6)
C14_8	C15_8	C16_8	121.1(7)
C11_8	C16_8	C15_8	119.5(6)
C18_8	C17_8	C3_8	121.8(5)
C18_8	C17_8	C22_8	116.1(5)
C22_8	C17_8	C3_8	122.0(5)
C17_8	C18_8	C19_8	122.6(6)
C20_8	C19_8	C18_8	119.3(6)
C21_8	C20_8	C19_8	120.8(6)
C20_8	C21_8	C22_8	119.8(6)
C21_8	C22_8	C17_8	121.2(6)
C1_12	O1_12	Rh2	118.5(5)
C1_12	O2_12	Rh1	117.2(5)
O1_12	C1_12	O2_12	126.4(5)
O1_12	C1_12	C2_12	117.4(4)
O2_12	C1_12	C2_12	116.0(4)
C1_12	C2_12	C3_12	122.5(4)
C4_12	C2_12	C1_12	112.6(4)
C4_12	C2_12	C3_12	118.3(4)
C10_12	C2_12	C1_12	115.0(4)
C10_12	C2_12	C3_12	58.1(3)
C10_12	C2_12	C4_12	120.0(4)
C10_12	C3_12	C2_12	59.0(3)
C10_12	C3_12	C11_12	118.5(5)
C10_12	C3_12	C17_12	120.2(5)
C11_12	C3_12	C2_12	121.7(4)
C17_12	C3_12	C2_12	117.5(4)
C17_12	C3_12	C11_12	111.1(4)
C5_12	C4_12	C2_12	122.5(5)
C5_12	C4_12	C9_12	116.8(5)
C9_12	C4_12	C2_12	120.3(5)
C4_12	C5_12	C11_12	120.8(4)

Atom	Atom	Atom	Angle/°
C4_12	C5_12	C6_12	122.6(5)
C6_12	C5_12	C11_12	116.6(4)
C7_12	C6_12	C5_12	118.7(6)
C6_12	C7_12	C8_12	119.8(5)
C7_12	C8_12	Br1_12	121.0(4)
C7_12	C8_12	C9_12	121.4(6)
C9_12	C8_12	Br1_12	117.5(5)
C8_12	C9_12	C4_12	120.3(6)
C3_12	C10_12	C2_12	62.9(3)
C12_12	C11_12	C3_12	116.2(5)
C16_12	C11_12	C3_12	123.6(5)
C16_12	C11_12	C12_12	120.0(5)
C13_12	C12_12	C11_12	118.4(6)
C14_12	C13_12	C12_12	120.3(6)
C15_12	C14_12	C13_12	120.2(6)
C14_12	C15_12	C16_12	121.0(7)
C11_12	C16_12	C15_12	119.4(6)
C18_12	C17_12	C3_12	121.9(5)
C18_12	C17_12	C22_12	116.1(5)
C22_12	C17_12	C3_12	122.0(5)
C17_12	C18_12	C19_12	122.4(6)
C20_12	C19_12	C18_12	119.3(6)
C21_12	C20_12	C19_12	120.8(6)
C20_12	C21_12	C22_12	119.8(6)
C21_12	C22_12	C17_12	121.2(6)
C1_1	O1_1	Rh2	116.5(4)
C1_1	O2_1	Rh1	117.6(4)
O1_1	C1_1	O2_1	126.5(5)
O1_1	C1_1	C2_1	117.4(4)
O2_1	C1_1	C2_1	116.0(4)
C1_1	C2_1	C3_1	122.4(4)
C4_1	C2_1	C1_1	112.7(4)
C4_1	C2_1	C3_1	118.6(4)
C10_1	C2_1	C1_1	114.9(4)
C10_1	C2_1	C3_1	58.0(3)
C10_1	C2_1	C4_1	119.8(4)
C10_1	C3_1	C2_1	59.1(3)
C10_1	C3_1	C11_1	118.6(5)
C10_1	C3_1	C17_1	120.4(5)

Atom	Atom	Atom	Angle/°
C11_1	C3_1	C2_1	121.5(4)
C17_1	C3_1	C2_1	117.6(4)
C17_1	C3_1	C11_1	111.1(4)
C5_1	C4_1	C2_1	122.8(5)
C5_1	C4_1	C9_1	116.7(5)
C9_1	C4_1	C2_1	119.9(5)
C4_1	C5_1	C11_1	121.0(4)
C4_1	C5_1	C6_1	122.6(5)
C6_1	C5_1	C11_1	116.4(4)
C7_1	C6_1	C5_1	118.7(6)
C6_1	C7_1	C8_1	119.7(5)
C7_1	C8_1	Br1_1	120.9(4)
C7_1	C8_1	C9_1	121.4(6)
C9_1	C8_1	Br1_1	117.5(5)
C8_1	C9_1	C4_1	120.5(6)
C3_1	C10_1	C2_1	62.9(3)
C12_1	C11_1	C3_1	116.3(5)
C16_1	C11_1	C3_1	123.5(5)
C16_1	C11_1	C12_1	120.0(5)
C13_1	C12_1	C11_1	118.4(6)
C14_1	C13_1	C12_1	120.3(6)
C15_1	C14_1	C13_1	120.3(6)
C14_1	C15_1	C16_1	121.0(7)
C11_1	C16_1	C15_1	119.4(6)
C18_1	C17_1	C3_1	121.7(5)
C18_1	C17_1	C22_1	116.1(5)
C22_1	C17_1	C3_1	122.0(5)
C17_1	C18_1	C19_1	122.5(6)
C20_1	C19_1	C18_1	119.3(6)
C21_1	C20_1	C19_1	120.8(6)
C20_1	C21_1	C22_1	119.8(6)
C21_1	C22_1	C17_1	121.2(6)
C1_4	O1_4	Rh2	113.1(5)
C1_4	O2_4	Rh1	119.1(5)
O1_4	C1_4	O2_4	126.2(5)
O1_4	C1_4	C2_4	117.2(4)
O2_4	C1_4	C2_4	115.6(4)
C1_4	C2_4	C3_4	122.5(4)
C4_4	C2_4	C1_4	112.6(4)

Atom	Atom	Atom	Angle/°
C4_4	C2_4	C3_4	117.9(4)
C10_4	C2_4	C1_4	115.0(4)
C10_4	C2_4	C3_4	58.0(3)
C10_4	C2_4	C4_4	120.7(4)
C10_4	C3_4	C2_4	58.9(3)
C10_4	C3_4	C11_4	119.1(5)
C10_4	C3_4	C17_4	120.0(5)
C11_4	C3_4	C2_4	121.4(4)
C17_4	C3_4	C2_4	117.4(4)
C17_4	C3_4	C11_4	111.2(4)
C5_4	C4_4	C2_4	122.4(5)
C5_4	C4_4	C9_4	116.9(5)
C9_4	C4_4	C2_4	120.6(5)
C4_4	C5_4	C11_4	120.7(4)
C4_4	C5_4	C6_4	122.4(5)
C6_4	C5_4	C11_4	116.7(4)
C7_4	C6_4	C5_4	118.6(6)
C6_4	C7_4	C8_4	119.8(6)
C7_4	C8_4	Br1_4	121.0(4)
C7_4	C8_4	C9_4	121.4(6)
C9_4	C8_4	Br1_4	117.5(5)
C8_4	C9_4	C4_4	120.3(6)
C3_4	C10_4	C2_4	63.0(3)
C12_4	C11_4	C3_4	116.4(5)
C16_4	C11_4	C3_4	123.5(5)
C16_4	C11_4	C12_4	120.1(5)
C13_4	C12_4	C11_4	118.4(6)
C14_4	C13_4	C12_4	120.3(6)
C15_4	C14_4	C13_4	120.2(6)
C14_4	C15_4	C16_4	121.0(7)
C11_4	C16_4	C15_4	119.5(6)
C18_4	C17_4	C3_4	121.7(5)
C18_4	C17_4	C22_4	115.9(5)
C22_4	C17_4	C3_4	121.6(5)
C17_4	C18_4	C19_4	122.5(6)
C20_4	C19_4	C18_4	119.3(6)
C21_4	C20_4	C19_4	120.7(6)
C20_4	C21_4	C22_4	119.7(6)
C21_4	C22_4	C17_4	121.2(6)

Atom	Atom	Atom	Angle/°	Atom	Atom	Atom	Angle/°
C1_2	O1_2	Rh2	116.4(4)	C6_2	C7_2	C8_2	119.9(5)
C1_2	O2_2	Rh1	118.3(4)	C7_2	C8_2	Br1_2	120.9(4)
O1_2	C1_2	O2_2	126.5(5)	C7_2	C8_2	C9_2	121.3(6)
O1_2	C1_2	C2_2	117.3(4)	C9_2	C8_2	Br1_2	117.6(5)
O2_2	C1_2	C2_2	116.0(4)	C8_2	C9_2	C4_2	120.4(6)
C1_2	C2_2	C3_2	122.1(4)	C3_2	C10_2	C2_2	63.0(3)
C4_2	C2_2	C1_2	112.7(4)	C12_2	C11_2	C3_2	116.3(5)
C4_2	C2_2	C3_2	118.2(4)	C16_2	C11_2	C3_2	123.5(5)
C10_2	C2_2	C1_2	115.1(4)	C16_2	C11_2	C12_2	120.1(5)
C10_2	C2_2	C3_2	58.0(3)	C13_2	C12_2	C11_2	118.5(6)
C10_2	C2_2	C4_2	120.3(4)	C14_2	C13_2	C12_2	120.4(6)
C10_2	C3_2	C2_2	59.0(3)	C15_2	C14_2	C13_2	120.3(6)
C10_2	C3_2	C11_2	118.8(5)	C14_2	C15_2	C16_2	121.1(7)
C10_2	C3_2	C17_2	120.3(5)	C11_2	C16_2	C15_2	119.6(6)
C11_2	C3_2	C2_2	121.4(4)	C18_2	C17_2	C3_2	121.6(5)
C17_2	C3_2	C2_2	117.4(4)	C18_2	C17_2	C22_2	115.9(5)
C17_2	C3_2	C11_2	111.1(4)	C22_2	C17_2	C3_2	121.7(5)
C5_2	C4_2	C2_2	122.6(5)	C17_2	C18_2	C19_2	122.4(6)
C5_2	C4_2	C9_2	116.9(5)	C20_2	C19_2	C18_2	119.2(6)
C9_2	C4_2	C2_2	120.5(5)	C21_2	C20_2	C19_2	120.6(6)
C4_2	C5_2	C11_2	120.9(4)	C20_2	C21_2	C22_2	119.6(6)
C4_2	C5_2	C6_2	122.4(5)	C21_2	C22_2	C17_2	121.0(6)
C6_2	C5_2	C11_2	116.7(4)	C23_11	N1_11	Rh3	170.6(14)
C7_2	C6_2	C5_2	118.7(6)	N1_11	C23_11	C24_11	173.1(18)

Table 13: Torsion Angles in ° for WL-2ClBr.

Atom	Atom	Atom	Atom	Angle/°
Rh3	O2_5	C1_5	O1_5	-10.4(12)
Rh3	O2_5	C1_5	C2_5	-177.1(5)
Rh3	O2_6	C1_6	O1_6	0.3(13)
Rh3	O2_6	C1_6	C2_6	-177.8(5)
Rh3	O2_7	C1_7	O1_7	11.0(12)
Rh3	O2_7	C1_7	C2_7	-176.0(5)
Rh3	O2_8	C1_8	O1_8	5.6(14)
Rh3	O2_8	C1_8	C2_8	-175.7(5)
Rh4	O1_5	C1_5	O2_5	21.9(12)
Rh4	O1_5	C1_5	C2_5	-171.5(5)

Atom	Atom	Atom	Atom	Angle/°
Rh4	O1_6	C1_6	O2_6	15.9(14)
Rh4	O1_6	C1_6	C2_6	-166.0(5)
Rh4	O1_7	C1_7	O2_7	4.6(12)
Rh4	O1_7	C1_7	C2_7	-168.2(5)
Rh4	O1_8	C1_8	O2_8	10.3(14)
Rh4	O1_8	C1_8	C2_8	-168.4(5)
Rh1	O2_3	C1_3	O1_3	-1.7(13)
Rh1	O2_3	C1_3	C2_3	-173.4(5)
Rh1	O2_12	C1_12	O1_12	8(3)
Rh1	O2_12	C1_12	C2_12	-177.4(9)
Rh1	O2_1	C1_1	O1_1	9.6(16)
Rh1	O2_1	C1_1	C2_1	-174.3(5)
Rh1	O2_4	C1_4	O1_4	4(2)
Rh1	O2_4	C1_4	C2_4	-164.6(8)
Rh1	O2_2	C1_2	O1_2	4.1(13)
Rh1	O2_2	C1_2	C2_2	-180.0(5)
Rh2	O1_3	C1_3	O2_3	19.1(12)
Rh2	O1_3	C1_3	C2_3	-169.3(5)
Rh2	O1_12	C1_12	O2_12	3(3)
Rh2	O1_12	C1_12	C2_12	-171.9(11)
Rh2	O1_1	C1_1	O2_1	8.3(16)
Rh2	O1_1	C1_1	C2_1	-167.8(5)
Rh2	O1_4	C1_4	O2_4	19(2)
Rh2	O1_4	C1_4	C2_4	-172.5(9)
Rh2	O1_2	C1_2	O2_2	11.0(13)
Rh2	O1_2	C1_2	C2_2	-164.9(5)
Br1_3	C8_3	C9_3	C4_3	175.9(9)
Cl1_3	C5_3	C6_3	C7_3	-178.5(14)
O1_3	C1_3	C2_3	C3_3	31.4(9)
O1_3	C1_3	C2_3	C4_3	-178.6(7)
O1_3	C1_3	C2_3	C10_3	-35.3(8)
O2_3	C1_3	C2_3	C3_3	-156.2(7)
O2_3	C1_3	C2_3	C4_3	-6.2(9)
O2_3	C1_3	C2_3	C10_3	137.2(7)
C1_3	C2_3	C3_3	C10_3	-101.1(5)
C1_3	C2_3	C3_3	C11_3	6.0(7)
C1_3	C2_3	C3_3	C17_3	148.6(5)
C1_3	C2_3	C4_3	C5_3	-72.3(9)
C1_3	C2_3	C4_3	C9_3	114.7(9)

Atom	Atom	Atom	Atom	Angle/°
C1_3	C2_3	C10_3	C3_3	114.0(5)
C2_3	C3_3	C11_3	C12_3	-138.9(10)
C2_3	C3_3	C11_3	C16_3	43.6(11)
C2_3	C3_3	C17_3	C18_3	-101.2(12)
C2_3	C3_3	C17_3	C22_3	71.7(11)
C2_3	C4_3	C5_3	Cl1_3	5.1(14)
C2_3	C4_3	C5_3	C6_3	-175.4(12)
C2_3	C4_3	C9_3	C8_3	175.0(10)
C3_3	C2_3	C4_3	C5_3	79.2(9)
C3_3	C2_3	C4_3	C9_3	-93.8(9)
C3_3	C11_3	C12_3	C13_3	-178.5(12)
C3_3	C11_3	C16_3	C15_3	-178.3(12)
C3_3	C17_3	C18_3	C19_3	180.0(14)
C3_3	C17_3	C22_3	C21_3	-179.2(15)
C4_3	C2_3	C3_3	C10_3	110.3(5)
C4_3	C2_3	C3_3	C11_3	-142.5(5)
C4_3	C2_3	C3_3	C17_3	0.0(7)
C4_3	C2_3	C10_3	C3_3	-105.8(5)
C4_3	C5_3	C6_3	C7_3	2(2)
C5_3	C4_3	C9_3	C8_3	1.6(18)
C5_3	C6_3	C7_3	C8_3	-1(3)
C6_3	C7_3	C8_3	Br1_3	-176.0(14)
C6_3	C7_3	C8_3	C9_3	1(3)
C7_3	C8_3	C9_3	C4_3	-1(2)
C9_3	C4_3	C5_3	Cl1_3	178.4(10)
C9_3	C4_3	C5_3	C6_3	-2.2(19)
C10_3	C2_3	C3_3	C11_3	107.2(6)
C10_3	C2_3	C3_3	C17_3	-110.3(5)
C10_3	C2_3	C4_3	C5_3	146.6(9)
C10_3	C2_3	C4_3	C9_3	-26.4(10)
C10_3	C3_3	C11_3	C12_3	-69.6(10)
C10_3	C3_3	C11_3	C16_3	112.9(10)
C10_3	C3_3	C17_3	C18_3	-169.5(11)
C10_3	C3_3	C17_3	C22_3	3.4(11)
C11_3	C3_3	C10_3	C2_3	-111.2(5)
C11_3	C3_3	C17_3	C18_3	44.9(12)
C11_3	C3_3	C17_3	C22_3	-142.2(10)
C11_3	C12_3	C13_3	C14_3	2(2)
C12_3	C11_3	C16_3	C15_3	4.2(19)

Atom	Atom	Atom	Atom	Angle/°
C12_3	C13_3	C14_3	C15_3	-6(2)
C13_3	C14_3	C15_3	C16_3	10(2)
C14_3	C15_3	C16_3	C11_3	-9(2)
C16_3	C11_3	C12_3	C13_3	-1(2)
C17_3	C3_3	C10_3	C2_3	105.8(5)
C17_3	C3_3	C11_3	C12_3	76.5(10)
C17_3	C3_3	C11_3	C16_3	-101.0(10)
C17_3	C18_3	C19_3	C20_3	-2(3)
C18_3	C17_3	C22_3	C21_3	-6(2)
C18_3	C19_3	C20_3	C21_3	-4(3)
C19_3	C20_3	C21_3	C22_3	5(3)
C20_3	C21_3	C22_3	C17_3	0(3)
C22_3	C17_3	C18_3	C19_3	7(2)
Br1_5	C8_5	C9_5	C4_5	-178.4(10)
Cl1_5	C5_5	C6_5	C7_5	-175.2(11)
O1_5	C1_5	C2_5	C3_5	28.4(8)
O1_5	C1_5	C2_5	C4_5	177.9(7)
O1_5	C1_5	C2_5	C10_5	-37.9(8)
O2_5	C1_5	C2_5	C3_5	-163.6(7)
O2_5	C1_5	C2_5	C4_5	-14.1(8)
O2_5	C1_5	C2_5	C10_5	130.1(7)
C1_5	C2_5	C3_5	C10_5	-100.8(5)
C1_5	C2_5	C3_5	C11_5	7.2(7)
C1_5	C2_5	C3_5	C17_5	149.8(5)
C1_5	C2_5	C4_5	C5_5	-55.2(9)
C1_5	C2_5	C4_5	C9_5	121.5(9)
C1_5	C2_5	C10_5	C3_5	113.6(5)
C2_5	C3_5	C11_5	C12_5	-116.6(10)
C2_5	C3_5	C11_5	C16_5	62.4(13)
C2_5	C3_5	C17_5	C18_5	-66.7(11)
C2_5	C3_5	C17_5	C22_5	118.5(13)
C2_5	C4_5	C5_5	C11_5	-5.4(13)
C2_5	C4_5	C5_5	C6_5	171.2(10)
C2_5	C4_5	C9_5	C8_5	-176.2(11)
C3_5	C2_5	C4_5	C5_5	95.6(9)
C3_5	C2_5	C4_5	C9_5	-87.7(10)
C3_5	C11_5	C12_5	C13_5	-178.8(16)
C3_5	C11_5	C16_5	C15_5	-179.2(15)
C3_5	C17_5	C18_5	C19_5	178.1(13)

Atom	Atom	Atom	Atom	Angle/°
C3_5	C17_5	C22_5	C21_5	179.2(17)
C4_5	C2_5	C3_5	C10_5	111.2(5)
C4_5	C2_5	C3_5	C11_5	-140.7(5)
C4_5	C2_5	C3_5	C17_5	1.8(7)
C4_5	C2_5	C10_5	C3_5	-105.6(5)
C4_5	C5_5	C6_5	C7_5	8.1(19)
C5_5	C4_5	C9_5	C8_5	0.7(18)
C5_5	C6_5	C7_5	C8_5	-5(2)
C6_5	C7_5	C8_5	Br1_5	-179.2(11)
C6_5	C7_5	C8_5	C9_5	1(2)
C7_5	C8_5	C9_5	C4_5	2(2)
C9_5	C4_5	C5_5	C11_5	177.8(10)
C9_5	C4_5	C5_5	C6_5	-5.7(16)
C10_5	C2_5	C3_5	C11_5	108.0(6)
C10_5	C2_5	C3_5	C17_5	-109.4(5)
C10_5	C2_5	C4_5	C5_5	163.4(8)
C10_5	C2_5	C4_5	C9_5	-19.8(10)
C10_5	C3_5	C11_5	C12_5	-47.2(11)
C10_5	C3_5	C11_5	C16_5	131.7(12)
C10_5	C3_5	C17_5	C18_5	-134.9(10)
C10_5	C3_5	C17_5	C22_5	50.2(13)
C11_5	C3_5	C10_5	C2_5	-110.3(5)
C11_5	C3_5	C17_5	C18_5	79.3(11)
C11_5	C3_5	C17_5	C22_5	-95.5(13)
C11_5	C12_5	C13_5	C14_5	-1(3)
C12_5	C11_5	C16_5	C15_5	0(3)
C12_5	C13_5	C14_5	C15_5	-2(4)
C13_5	C14_5	C15_5	C16_5	4(3)
C14_5	C15_5	C16_5	C11_5	-3(3)
C16_5	C11_5	C12_5	C13_5	2(2)
C17_5	C3_5	C10_5	C2_5	106.8(5)
C17_5	C3_5	C11_5	C12_5	98.6(10)
C17_5	C3_5	C11_5	C16_5	-82.4(13)
C17_5	C18_5	C19_5	C20_5	3(3)
C18_5	C17_5	C22_5	C21_5	4(3)
C18_5	C19_5	C20_5	C21_5	3(3)
C19_5	C20_5	C21_5	C22_5	-6(4)
C20_5	C21_5	C22_5	C17_5	2(4)
C22_5	C17_5	C18_5	C19_5	-7(2)

Atom	Atom	Atom	Atom	Angle/°
Br1_6	C8_6	C9_6	C4_6	174.4(7)
Cl1_6	C5_6	C6_6	C7_6	-179.9(10)
O1_6	C1_6	C2_6	C3_6	26.6(10)
O1_6	C1_6	C2_6	C4_6	177.0(7)
O1_6	C1_6	C2_6	C10_6	-40.2(9)
O2_6	C1_6	C2_6	C3_6	-155.2(8)
O2_6	C1_6	C2_6	C4_6	-4.7(9)
O2_6	C1_6	C2_6	C10_6	138.0(8)
C1_6	C2_6	C3_6	C10_6	-101.2(5)
C1_6	C2_6	C3_6	C11_6	5.6(8)
C1_6	C2_6	C3_6	C17_6	148.2(5)
C1_6	C2_6	C4_6	C5_6	-72.5(8)
C1_6	C2_6	C4_6	C9_6	115.0(7)
C1_6	C2_6	C10_6	C3_6	114.1(5)
C2_6	C3_6	C11_6	C12_6	-136.7(11)
C2_6	C3_6	C11_6	C16_6	47.1(11)
C2_6	C3_6	C17_6	C18_6	-99.6(10)
C2_6	C3_6	C17_6	C22_6	75.9(9)
C2_6	C4_6	C5_6	C11_6	4.6(12)
C2_6	C4_6	C5_6	C6_6	-176.0(9)
C2_6	C4_6	C9_6	C8_6	178.5(8)
C3_6	C2_6	C4_6	C5_6	79.5(8)
C3_6	C2_6	C4_6	C9_6	-93.0(8)
C3_6	C11_6	C12_6	C13_6	-178.8(15)
C3_6	C11_6	C16_6	C15_6	176.2(13)
C3_6	C17_6	C18_6	C19_6	177.4(11)
C3_6	C17_6	C22_6	C21_6	178.8(10)
C4_6	C2_6	C3_6	C10_6	109.8(5)
C4_6	C2_6	C3_6	C11_6	-143.4(5)
C4_6	C2_6	C3_6	C17_6	-0.8(7)
C4_6	C2_6	C10_6	C3_6	-106.1(5)
C4_6	C5_6	C6_6	C7_6	0.7(19)
C5_6	C4_6	C9_6	C8_6	5.6(14)
C5_6	C6_6	C7_6	C8_6	0(2)
C6_6	C7_6	C8_6	Br1_6	-177.2(10)
C6_6	C7_6	C8_6	C9_6	3(2)
C7_6	C8_6	C9_6	C4_6	-5.5(17)
C9_6	C4_6	C5_6	C11_6	177.3(7)
C9_6	C4_6	C5_6	C6_6	-3.3(15)

Atom	Atom	Atom	Atom	Angle/°
C10_6	C2_6	C3_6	C11_6	106.8(6)
C10_6	C2_6	C3_6	C17_6	-110.5(5)
C10_6	C2_6	C4_6	C5_6	146.8(8)
C10_6	C2_6	C4_6	C9_6	-25.6(8)
C10_6	C3_6	C11_6	C12_6	-67.3(12)
C10_6	C3_6	C11_6	C16_6	116.4(10)
C10_6	C3_6	C17_6	C18_6	-167.9(9)
C10_6	C3_6	C17_6	C22_6	7.6(10)
C11_6	C3_6	C10_6	C2_6	-111.5(5)
C11_6	C3_6	C17_6	C18_6	46.8(10)
C11_6	C3_6	C17_6	C22_6	-137.7(8)
C11_6	C12_6	C13_6	C14_6	5(3)
C12_6	C11_6	C16_6	C15_6	0(2)
C12_6	C13_6	C14_6	C15_6	-5(3)
C13_6	C14_6	C15_6	C16_6	3(3)
C14_6	C15_6	C16_6	C11_6	0(3)
C16_6	C11_6	C12_6	C13_6	-2(2)
C17_6	C3_6	C10_6	C2_6	105.7(5)
C17_6	C3_6	C11_6	C12_6	78.6(12)
C17_6	C3_6	C11_6	C16_6	-97.6(10)
C17_6	C18_6	C19_6	C20_6	4(2)
C18_6	C17_6	C22_6	C21_6	-5.4(17)
C18_6	C19_6	C20_6	C21_6	-6(2)
C19_6	C20_6	C21_6	C22_6	2(2)
C20_6	C21_6	C22_6	C17_6	4(2)
C22_6	C17_6	C18_6	C19_6	1.6(18)
Br1_7	C8_7	C9_7	C4_7	-178.9(10)
Cl1_7	C5_7	C6_7	C7_7	178.6(13)
O1_7	C1_7	C2_7	C3_7	25.5(9)
O1_7	C1_7	C2_7	C4_7	176.1(7)
O1_7	C1_7	C2_7	C10_7	-41.3(9)
O2_7	C1_7	C2_7	C3_7	-148.1(7)
O2_7	C1_7	C2_7	C4_7	2.5(8)
O2_7	C1_7	C2_7	C10_7	145.1(7)
C1_7	C2_7	C3_7	C10_7	-101.4(5)
C1_7	C2_7	C3_7	C11_7	5.2(7)
C1_7	C2_7	C3_7	C17_7	147.8(5)
C1_7	C2_7	C4_7	C5_7	-71.9(10)
C1_7	C2_7	C4_7	C9_7	102.9(9)

Atom	Atom	Atom	Atom	Angle/°
C1_7	C2_7	C10_7	C3_7	113.9(5)
C2_7	C3_7	C11_7	C12_7	-131.2(13)
C2_7	C3_7	C11_7	C16_7	47.8(12)
C2_7	C3_7	C17_7	C18_7	-96.0(13)
C2_7	C3_7	C17_7	C22_7	78.0(12)
C2_7	C4_7	C5_7	Cl1_7	1.1(15)
C2_7	C4_7	C5_7	C6_7	-177.0(11)
C2_7	C4_7	C9_7	C8_7	178.2(11)
C3_7	C2_7	C4_7	C5_7	80.1(10)
C3_7	C2_7	C4_7	C9_7	-105.1(9)
C3_7	C11_7	C12_7	C13_7	179.0(16)
C3_7	C11_7	C16_7	C15_7	-179.2(13)
C3_7	C17_7	C18_7	C19_7	176.3(15)
C3_7	C17_7	C22_7	C21_7	178.0(15)
C4_7	C2_7	C3_7	C10_7	109.5(5)
C4_7	C2_7	C3_7	C11_7	-143.9(5)
C4_7	C2_7	C3_7	C17_7	-1.3(7)
C4_7	C2_7	C10_7	C3_7	-106.5(5)
C4_7	C5_7	C6_7	C7_7	-3(2)
C5_7	C4_7	C9_7	C8_7	-6.6(18)
C5_7	C6_7	C7_7	C8_7	-3(2)
C6_7	C7_7	C8_7	Br1_7	-176.1(14)
C6_7	C7_7	C8_7	C9_7	4(3)
C7_7	C8_7	C9_7	C4_7	1(2)
C9_7	C4_7	C5_7	Cl1_7	-173.9(10)
C9_7	C4_7	C5_7	C6_7	8.0(18)
C10_7	C2_7	C3_7	C11_7	106.6(6)
C10_7	C2_7	C3_7	C17_7	-110.8(5)
C10_7	C2_7	C4_7	C5_7	147.5(9)
C10_7	C2_7	C4_7	C9_7	-37.7(10)
C10_7	C3_7	C11_7	C12_7	-61.9(13)
C10_7	C3_7	C11_7	C16_7	117.1(11)
C10_7	C3_7	C17_7	C18_7	-164.4(12)
C10_7	C3_7	C17_7	C22_7	9.6(12)
C11_7	C3_7	C10_7	C2_7	-111.6(5)
C11_7	C3_7	C17_7	C18_7	50.3(13)
C11_7	C3_7	C17_7	C22_7	-135.7(11)
C11_7	C12_7	C13_7	C14_7	-3(3)
C12_7	C11_7	C16_7	C15_7	0(2)

Atom	Atom	Atom	Atom	Angle/°
C12_7	C13_7	C14_7	C15_7	5(3)
C13_7	C14_7	C15_7	C16_7	-6(3)
C14_7	C15_7	C16_7	C11_7	3(3)
C16_7	C11_7	C12_7	C13_7	0(3)
C17_7	C3_7	C10_7	C2_7	105.6(5)
C17_7	C3_7	C11_7	C12_7	84.2(13)
C17_7	C3_7	C11_7	C16_7	-96.8(11)
C17_7	C18_7	C19_7	C20_7	7(3)
C18_7	C17_7	C22_7	C21_7	-8(2)
C18_7	C19_7	C20_7	C21_7	-9(3)
C19_7	C20_7	C21_7	C22_7	4(3)
C20_7	C21_7	C22_7	C17_7	5(3)
C22_7	C17_7	C18_7	C19_7	2(3)
Br1_8	C8_8	C9_8	C4_8	-176.9(11)
Cl1_8	C5_8	C6_8	C7_8	-179.6(14)
O1_8	C1_8	C2_8	C3_8	23.0(10)
O1_8	C1_8	C2_8	C4_8	173.2(8)
O1_8	C1_8	C2_8	C10_8	-43.7(9)
O2_8	C1_8	C2_8	C3_8	-155.8(8)
O2_8	C1_8	C2_8	C4_8	-5.6(9)
O2_8	C1_8	C2_8	C10_8	137.4(8)
C1_8	C2_8	C3_8	C10_8	-101.5(5)
C1_8	C2_8	C3_8	C11_8	5.4(7)
C1_8	C2_8	C3_8	C17_8	147.8(5)
C1_8	C2_8	C4_8	C5_8	-71.6(10)
C1_8	C2_8	C4_8	C9_8	117.4(10)
C1_8	C2_8	C10_8	C3_8	113.8(5)
C2_8	C3_8	C11_8	C12_8	-128.8(10)
C2_8	C3_8	C11_8	C16_8	54.0(11)
C2_8	C3_8	C17_8	C18_8	-96.2(9)
C2_8	C3_8	C17_8	C22_8	86.4(9)
C2_8	C4_8	C5_8	Cl1_8	8.3(15)
C2_8	C4_8	C5_8	C6_8	-177.5(12)
C2_8	C4_8	C9_8	C8_8	176.1(12)
C3_8	C2_8	C4_8	C5_8	80.0(10)
C3_8	C2_8	C4_8	C9_8	-91.0(10)
C3_8	C11_8	C12_8	C13_8	-177.8(12)
C3_8	C11_8	C16_8	C15_8	175.3(11)
C3_8	C17_8	C18_8	C19_8	179.5(10)

Atom	Atom	Atom	Atom	Angle/°
C3_8	C17_8	C22_8	C21_8	-179.3(11)
C4_8	C2_8	C3_8	C10_8	109.8(5)
C4_8	C2_8	C3_8	C11_8	-143.3(5)
C4_8	C2_8	C3_8	C17_8	-0.9(7)
C4_8	C2_8	C10_8	C3_8	-106.2(5)
C4_8	C5_8	C6_8	C7_8	6(2)
C5_8	C4_8	C9_8	C8_8	4.7(19)
C5_8	C6_8	C7_8	C8_8	-4(3)
C6_8	C7_8	C8_8	Br1_8	176.2(14)
C6_8	C7_8	C8_8	C9_8	2(3)
C7_8	C8_8	C9_8	C4_8	-3(2)
C9_8	C4_8	C5_8	C11_8	179.5(11)
C9_8	C4_8	C5_8	C6_8	-6.3(19)
C10_8	C2_8	C3_8	C11_8	106.8(6)
C10_8	C2_8	C3_8	C17_8	-110.8(5)
C10_8	C2_8	C4_8	C5_8	147.4(9)
C10_8	C2_8	C4_8	C9_8	-23.5(11)
C10_8	C3_8	C11_8	C12_8	-59.5(10)
C10_8	C3_8	C11_8	C16_8	123.3(10)
C10_8	C3_8	C17_8	C18_8	-164.6(8)
C10_8	C3_8	C17_8	C22_8	18.1(10)
C11_8	C3_8	C10_8	C2_8	-111.4(5)
C11_8	C3_8	C17_8	C18_8	49.9(9)
C11_8	C3_8	C17_8	C22_8	-127.5(9)
C11_8	C12_8	C13_8	C14_8	0(3)
C12_8	C11_8	C16_8	C15_8	-1.8(19)
C12_8	C13_8	C14_8	C15_8	2(3)
C13_8	C14_8	C15_8	C16_8	-5(3)
C14_8	C15_8	C16_8	C11_8	5(2)
C16_8	C11_8	C12_8	C13_8	0(2)
C17_8	C3_8	C10_8	C2_8	105.6(5)
C17_8	C3_8	C11_8	C12_8	86.8(10)
C17_8	C3_8	C11_8	C16_8	-90.5(10)
C17_8	C18_8	C19_8	C20_8	3(2)
C18_8	C17_8	C22_8	C21_8	3.2(17)
C18_8	C19_8	C20_8	C21_8	-3(2)
C19_8	C20_8	C21_8	C22_8	4(2)
C20_8	C21_8	C22_8	C17_8	-4(2)
C22_8	C17_8	C18_8	C19_8	-3.0(17)

Atom	Atom	Atom	Atom	Angle ^o
Br1_12	C8_12	C9_12	C4_12	-176.5(17)
Cl1_12	C5_12	C6_12	C7_12	-177(3)
O1_12	C1_12	C2_12	C3_12	23.5(19)
O1_12	C1_12	C2_12	C4_12	174.3(18)
O1_12	C1_12	C2_12	C10_12	-43.3(19)
O2_12	C1_12	C2_12	C3_12	-151.9(15)
O2_12	C1_12	C2_12	C4_12	-1.1(15)
O2_12	C1_12	C2_12	C10_12	141.4(15)
C1_12	C2_12	C3_12	C10_12	-101.2(5)
C1_12	C2_12	C3_12	C11_12	5.3(8)
C1_12	C2_12	C3_12	C17_12	148.3(5)
C1_12	C2_12	C4_12	C5_12	-80.0(15)
C1_12	C2_12	C4_12	C9_12	106.7(12)
C1_12	C2_12	C10_12	C3_12	114.0(5)
C2_12	C3_12	C11_12	C12_12	-130.0(16)
C2_12	C3_12	C11_12	C16_12	46.7(16)
C2_12	C3_12	C17_12	C18_12	-130.4(14)
C2_12	C3_12	C17_12	C22_12	51.9(16)
C2_12	C4_12	C5_12	C11_12	5(2)
C2_12	C4_12	C5_12	C6_12	-174(2)
C2_12	C4_12	C9_12	C8_12	169.2(17)
C3_12	C2_12	C4_12	C5_12	72.2(15)
C3_12	C2_12	C4_12	C9_12	-101.1(13)
C3_12	C11_12	C12_12	C13_12	179.0(19)
C3_12	C11_12	C16_12	C15_12	-172.2(16)
C3_12	C17_12	C18_12	C19_12	174.7(17)
C3_12	C17_12	C22_12	C21_12	-178.1(19)
C4_12	C2_12	C3_12	C10_12	109.5(5)
C4_12	C2_12	C3_12	C11_12	-144.0(5)
C4_12	C2_12	C3_12	C17_12	-0.9(7)
C4_12	C2_12	C10_12	C3_12	-106.5(5)
C4_12	C5_12	C6_12	C7_12	2(5)
C5_12	C4_12	C9_12	C8_12	-5(3)
C5_12	C6_12	C7_12	C8_12	0(5)
C6_12	C7_12	C8_12	Br1_12	179(3)
C6_12	C7_12	C8_12	C9_12	-5(4)
C7_12	C8_12	C9_12	C4_12	7(3)
C9_12	C4_12	C5_12	C11_12	178.8(17)
C9_12	C4_12	C5_12	C6_12	0(3)

Atom	Atom	Atom	Atom	Angle/°
C10_12	C2_12	C3_12	C11_12	106.5(6)
C10_12	C2_12	C3_12	C17_12	-110.4(5)
C10_12	C2_12	C4_12	C5_12	139.7(15)
C10_12	C2_12	C4_12	C9_12	-33.7(13)
C10_12	C3_12	C11_12	C12_12	-60.6(17)
C10_12	C3_12	C11_12	C16_12	116.1(15)
C10_12	C3_12	C17_12	C18_12	161.3(14)
C10_12	C3_12	C17_12	C22_12	-16.5(16)
C11_12	C3_12	C10_12	C2_12	-111.8(5)
C11_12	C3_12	C17_12	C18_12	16.4(15)
C11_12	C3_12	C17_12	C22_12	-161.4(15)
C11_12	C12_12	C13_12	C14_12	-6(4)
C12_12	C11_12	C16_12	C15_12	4(3)
C12_12	C13_12	C14_12	C15_12	3(4)
C13_12	C14_12	C15_12	C16_12	4(4)
C14_12	C15_12	C16_12	C11_12	-8(3)
C16_12	C11_12	C12_12	C13_12	2(3)
C17_12	C3_12	C10_12	C2_12	105.9(5)
C17_12	C3_12	C11_12	C12_12	84.9(16)
C17_12	C3_12	C11_12	C16_12	-98.4(15)
C17_12	C18_12	C19_12	C20_12	8(3)
C18_12	C17_12	C22_12	C21_12	4(3)
C18_12	C19_12	C20_12	C21_12	-4(4)
C19_12	C20_12	C21_12	C22_12	1(5)
C20_12	C21_12	C22_12	C17_12	-1(4)
C22_12	C17_12	C18_12	C19_12	-7(3)
Br1_1	C8_1	C9_1	C4_1	179.5(9)
Cl1_1	C5_1	C6_1	C7_1	173.8(11)
O1_1	C1_1	C2_1	C3_1	27.8(10)
O1_1	C1_1	C2_1	C4_1	179.2(8)
O1_1	C1_1	C2_1	C10_1	-38.8(10)
O2_1	C1_1	C2_1	C3_1	-148.7(8)
O2_1	C1_1	C2_1	C4_1	2.8(10)
O2_1	C1_1	C2_1	C10_1	144.7(8)
C1_1	C2_1	C3_1	C10_1	-101.1(5)
C1_1	C2_1	C3_1	C11_1	5.6(7)
C1_1	C2_1	C3_1	C17_1	148.3(5)
C1_1	C2_1	C4_1	C5_1	-73.5(9)
C1_1	C2_1	C4_1	C9_1	96.9(8)

Atom	Atom	Atom	Atom	Angle/°
C1_1	C2_1	C10_1	C3_1	113.9(5)
C2_1	C3_1	C11_1	C12_1	-129.4(10)
C2_1	C3_1	C11_1	C16_1	45.0(13)
C2_1	C3_1	C17_1	C18_1	-102.8(10)
C2_1	C3_1	C17_1	C22_1	81.9(10)
C2_1	C4_1	C5_1	Cl1_1	-3.8(13)
C2_1	C4_1	C5_1	C6_1	174.9(9)
C2_1	C4_1	C9_1	C8_1	-169.7(10)
C3_1	C2_1	C4_1	C5_1	79.1(9)
C3_1	C2_1	C4_1	C9_1	-110.5(8)
C3_1	C11_1	C12_1	C13_1	-178.4(13)
C3_1	C11_1	C16_1	C15_1	177.3(15)
C3_1	C17_1	C18_1	C19_1	-179.3(12)
C3_1	C17_1	C22_1	C21_1	176.0(15)
C4_1	C2_1	C3_1	C10_1	109.1(5)
C4_1	C2_1	C3_1	C11_1	-144.3(5)
C4_1	C2_1	C3_1	C17_1	-1.5(7)
C4_1	C2_1	C10_1	C3_1	-107.0(5)
C4_1	C5_1	C6_1	C7_1	-4.9(19)
C5_1	C4_1	C9_1	C8_1	1.3(16)
C5_1	C6_1	C7_1	C8_1	0(2)
C6_1	C7_1	C8_1	Br1_1	179.6(11)
C6_1	C7_1	C8_1	C9_1	6(2)
C7_1	C8_1	C9_1	C4_1	-6(2)
C9_1	C4_1	C5_1	Cl1_1	-174.5(9)
C9_1	C4_1	C5_1	C6_1	4.1(15)
C10_1	C2_1	C3_1	C11_1	106.6(6)
C10_1	C2_1	C3_1	C17_1	-110.6(5)
C10_1	C2_1	C4_1	C5_1	146.6(8)
C10_1	C2_1	C4_1	C9_1	-43.0(9)
C10_1	C3_1	C11_1	C12_1	-60.1(10)
C10_1	C3_1	C11_1	C16_1	114.4(12)
C10_1	C3_1	C17_1	C18_1	-171.3(10)
C10_1	C3_1	C17_1	C22_1	13.4(11)
C11_1	C3_1	C10_1	C2_1	-111.5(5)
C11_1	C3_1	C17_1	C18_1	43.6(11)
C11_1	C3_1	C17_1	C22_1	-131.7(10)
C11_1	C12_1	C13_1	C14_1	-1(3)
C12_1	C11_1	C16_1	C15_1	-8(2)

Atom	Atom	Atom	Atom	Angle/°
C12_1	C13_1	C14_1	C15_1	-4(3)
C13_1	C14_1	C15_1	C16_1	2(4)
C14_1	C15_1	C16_1	C11_1	4(3)
C16_1	C11_1	C12_1	C13_1	7(2)
C17_1	C3_1	C10_1	C2_1	105.9(5)
C17_1	C3_1	C11_1	C12_1	85.7(10)
C17_1	C3_1	C11_1	C16_1	-99.9(12)
C17_1	C18_1	C19_1	C20_1	6(2)
C18_1	C17_1	C22_1	C21_1	0(2)
C18_1	C19_1	C20_1	C21_1	-5(3)
C19_1	C20_1	C21_1	C22_1	1(3)
C20_1	C21_1	C22_1	C17_1	1(3)
C22_1	C17_1	C18_1	C19_1	-4(2)
Br1_4	C8_4	C9_4	C4_4	-178.8(15)
Cl1_4	C5_4	C6_4	C7_4	180(2)
O1_4	C1_4	C2_4	C3_4	29.2(15)
O1_4	C1_4	C2_4	C4_4	179.0(14)
O1_4	C1_4	C2_4	C10_4	-37.5(15)
O2_4	C1_4	C2_4	C3_4	-161.2(12)
O2_4	C1_4	C2_4	C4_4	-11.3(12)
O2_4	C1_4	C2_4	C10_4	132.1(12)
C1_4	C2_4	C3_4	C10_4	-101.1(5)
C1_4	C2_4	C3_4	C11_4	6.1(8)
C1_4	C2_4	C3_4	C17_4	148.7(5)
C1_4	C2_4	C4_4	C5_4	-73.0(13)
C1_4	C2_4	C4_4	C9_4	103.8(13)
C1_4	C2_4	C10_4	C3_4	114.0(5)
C2_4	C3_4	C11_4	C12_4	-139.3(14)
C2_4	C3_4	C11_4	C16_4	43.4(14)
C2_4	C3_4	C17_4	C18_4	-99.9(12)
C2_4	C3_4	C17_4	C22_4	69.3(12)
C2_4	C4_4	C5_4	Cl1_4	0(2)
C2_4	C4_4	C5_4	C6_4	-176.0(18)
C2_4	C4_4	C9_4	C8_4	179.3(16)
C3_4	C2_4	C4_4	C5_4	78.4(13)
C3_4	C2_4	C4_4	C9_4	-104.9(13)
C3_4	C11_4	C12_4	C13_4	-172.1(17)
C3_4	C11_4	C16_4	C15_4	171.3(14)
C3_4	C17_4	C18_4	C19_4	176.9(16)

Atom	Atom	Atom	Atom	Angle/°
C3_4	C17_4	C22_4	C21_4	-170.0(14)
C4_4	C2_4	C3_4	C10_4	110.5(5)
C4_4	C2_4	C3_4	C11_4	-142.2(5)
C4_4	C2_4	C3_4	C17_4	0.3(7)
C4_4	C2_4	C10_4	C3_4	-105.7(5)
C4_4	C5_4	C6_4	C7_4	-4(4)
C5_4	C4_4	C9_4	C8_4	-4(3)
C5_4	C6_4	C7_4	C8_4	-4(4)
C6_4	C7_4	C8_4	Br1_4	-178(2)
C6_4	C7_4	C8_4	C9_4	7(4)
C7_4	C8_4	C9_4	C4_4	-3(3)
C9_4	C4_4	C5_4	C11_4	-176.5(16)
C9_4	C4_4	C5_4	C6_4	7(3)
C10_4	C2_4	C3_4	C11_4	107.3(6)
C10_4	C2_4	C3_4	C17_4	-110.2(5)
C10_4	C2_4	C4_4	C5_4	145.9(13)
C10_4	C2_4	C4_4	C9_4	-37.3(14)
C10_4	C3_4	C11_4	C12_4	-69.9(15)
C10_4	C3_4	C11_4	C16_4	112.7(13)
C10_4	C3_4	C17_4	C18_4	-168.1(11)
C10_4	C3_4	C17_4	C22_4	1.2(12)
C11_4	C3_4	C10_4	C2_4	-111.2(5)
C11_4	C3_4	C17_4	C18_4	46.2(12)
C11_4	C3_4	C17_4	C22_4	-144.5(11)
C11_4	C12_4	C13_4	C14_4	-5(3)
C12_4	C11_4	C16_4	C15_4	-6(2)
C12_4	C13_4	C14_4	C15_4	6(3)
C13_4	C14_4	C15_4	C16_4	-7(3)
C14_4	C15_4	C16_4	C11_4	7(3)
C16_4	C11_4	C12_4	C13_4	5(3)
C17_4	C3_4	C10_4	C2_4	105.8(5)
C17_4	C3_4	C11_4	C12_4	76.1(15)
C17_4	C3_4	C11_4	C16_4	-101.2(13)
C17_4	C18_4	C19_4	C20_4	-7(3)
C18_4	C17_4	C22_4	C21_4	0(2)
C18_4	C19_4	C20_4	C21_4	0(4)
C19_4	C20_4	C21_4	C22_4	7(3)
C20_4	C21_4	C22_4	C17_4	-7(3)
C22_4	C17_4	C18_4	C19_4	7(2)

Atom	Atom	Atom	Atom	Angle/°
Br1_2	C8_2	C9_2	C4_2	-178.8(10)
Cl1_2	C5_2	C6_2	C7_2	-176.8(9)
O1_2	C1_2	C2_2	C3_2	25.3(9)
O1_2	C1_2	C2_2	C4_2	175.4(8)
O1_2	C1_2	C2_2	C10_2	-41.4(9)
O2_2	C1_2	C2_2	C3_2	-151.0(7)
O2_2	C1_2	C2_2	C4_2	-0.9(9)
O2_2	C1_2	C2_2	C10_2	142.3(7)
C1_2	C2_2	C3_2	C10_2	-101.4(5)
C1_2	C2_2	C3_2	C11_2	5.5(7)
C1_2	C2_2	C3_2	C17_2	148.0(5)
C1_2	C2_2	C4_2	C5_2	-62.0(9)
C1_2	C2_2	C4_2	C9_2	116.7(10)
C1_2	C2_2	C10_2	C3_2	113.6(5)
C2_2	C3_2	C11_2	C12_2	-132.6(9)
C2_2	C3_2	C11_2	C16_2	52.1(12)
C2_2	C3_2	C17_2	C18_2	-95.6(10)
C2_2	C3_2	C17_2	C22_2	74.0(13)
C2_2	C4_2	C5_2	C11_2	-6.3(13)
C2_2	C4_2	C5_2	C6_2	172.1(9)
C2_2	C4_2	C9_2	C8_2	-173.5(11)
C3_2	C2_2	C4_2	C5_2	89.4(9)
C3_2	C2_2	C4_2	C9_2	-91.8(10)
C3_2	C11_2	C12_2	C13_2	-172.4(11)
C3_2	C11_2	C16_2	C15_2	174.8(14)
C3_2	C17_2	C18_2	C19_2	-179.5(11)
C3_2	C17_2	C22_2	C21_2	-174.0(15)
C4_2	C2_2	C3_2	C10_2	109.9(5)
C4_2	C2_2	C3_2	C11_2	-143.1(5)
C4_2	C2_2	C3_2	C17_2	-0.7(7)
C4_2	C2_2	C10_2	C3_2	-106.2(5)
C4_2	C5_2	C6_2	C7_2	4.8(17)
C5_2	C4_2	C9_2	C8_2	5.4(19)
C5_2	C6_2	C7_2	C8_2	-1.3(18)
C6_2	C7_2	C8_2	Br1_2	176.6(10)
C6_2	C7_2	C8_2	C9_2	0(2)
C7_2	C8_2	C9_2	C4_2	-2(2)
C9_2	C4_2	C5_2	C11_2	174.9(10)
C9_2	C4_2	C5_2	C6_2	-6.7(16)

Atom	Atom	Atom	Atom	Angle/°
C10_2	C2_2	C3_2	C11_2	106.9(6)
C10_2	C2_2	C3_2	C17_2	-110.6(5)
C10_2	C2_2	C4_2	C5_2	156.9(8)
C10_2	C2_2	C4_2	C9_2	-24.3(11)
C10_2	C3_2	C11_2	C12_2	-63.3(10)
C10_2	C3_2	C11_2	C16_2	121.4(11)
C10_2	C3_2	C17_2	C18_2	-163.9(9)
C10_2	C3_2	C17_2	C22_2	5.6(13)
C11_2	C3_2	C10_2	C2_2	-111.3(5)
C11_2	C3_2	C17_2	C18_2	50.5(10)
C11_2	C3_2	C17_2	C22_2	-139.9(13)
C11_2	C12_2	C13_2	C14_2	-4(2)
C12_2	C11_2	C16_2	C15_2	0(2)
C12_2	C13_2	C14_2	C15_2	1(3)
C13_2	C14_2	C15_2	C16_2	1(3)
C14_2	C15_2	C16_2	C11_2	-2(3)
C16_2	C11_2	C12_2	C13_2	3.1(19)
C17_2	C3_2	C10_2	C2_2	105.7(5)
C17_2	C3_2	C11_2	C12_2	82.8(9)
C17_2	C3_2	C11_2	C16_2	-92.5(11)
C17_2	C18_2	C19_2	C20_2	-7(2)
C18_2	C17_2	C22_2	C21_2	-4(2)
C18_2	C19_2	C20_2	C21_2	-4(3)
C19_2	C20_2	C21_2	C22_2	11(2)
C20_2	C21_2	C22_2	C17_2	-6(3)
C22_2	C17_2	C18_2	C19_2	10.3(19)

Table 14: Hydrogen Fractional Atomic Coordinates ($\times 10^4$) and Equivalent Isotropic Displacement Parameters ($\text{\AA}^2 \times 10^3$) for **WL-2CIBr**. U_{eq} is defined as 1/3 of the trace of the orthogonalised U_{ij} .

Atom	x	y	z	U_{eq}
H4A	2007.75	7396.24	5699.83	130
H4B	1585.34	6730.96	5662.1	130
H24A_9	10014.35	2833.01	10023.06	185
H24B_9	9500	2919.29	10306.53	185
H24C_9	10009.78	3581.55	10328.84	185
H24A_10	6152.6	6003.51	6521.46	188
H24B_10	5901.23	6689.85	6773.77	188
H24C_10	5568.82	5870.92	6733.52	188

Atom	x	y	z	U_{eq}
H6_3	6954.75	8541.6	8927.86	103
H7_3	5874.38	8587.28	8906.3	104
H9_3	5977.05	6394.5	9391.54	85
H10A_3	6659.66	5720.99	9975.41	78
H10B_3	7123.78	5021.16	9885.32	78
H12_3	8118.83	5249.7	10840.08	101
H13_3	9143.21	4670.64	11146.66	109
H14_3	9934.04	4871.6	10776.1	106
H15_3	9658.44	5397.68	10023.13	131
H16_3	8695.02	6084.53	9741.3	86
H18_3	8436.54	7274.01	10338.2	107
H19_3	8387.04	8383.35	10767.86	106
H20_3	7495.34	8603.67	11032.71	126
H21_3	6609.37	7812.26	10795.66	131
H22_3	6659.97	6681.45	10376.85	102
H6_5	5411.55	6301.39	8266.54	76
H7_5	6403.64	6834.02	8283.91	87
H9_5	5551.87	8053.85	7093.22	80
H10A_5	4701.95	8621.3	6661.53	81
H10B_5	4043.5	8287	6276.6	81
H12_5	3172.14	9247.83	6273.91	103
H13_5	2036.85	9366.21	6013.66	140
H14_5	1408.97	8660.49	6374.29	132
H15_5	1878.05	7782.22	6959.12	128
H16_5	2996.79	7695.34	7260.12	110
H18_5	4055.86	8218.4	7894.51	101
H19_5	4530.9	8963.97	8560.66	121
H20_5	4942.9	10166.67	8470.4	147
H21_5	4807.52	10667.84	7725.17	154
H22_5	4405.18	9888.79	7056.24	136
H6_6	3066.03	2716.75	7668.68	76
H7_6	3694.83	2924.22	8446.2	81
H9_6	3375.36	5219.06	8285.99	63
H10A_6	2571.85	5998.3	7964.89	75
H10B_6	2489.31	6508.82	7479.05	75
H12_6	1060.56	6601.48	7251.53	112
H13_6	308.07	7109.9	6566.01	143
H14_6	146.8	6503.43	5842.62	139
H15_6	832.4	5537.11	5758.23	114

Atom	x	y	z	U_{eq}
H16_6	1631	5068.1	6413.35	79
H18_6	1095.65	4315.05	7064.66	86
H19_6	651.32	3440	7478.13	98
H20_6	789.09	3627.04	8281.2	92
H21_6	1497.59	4542.38	8694.85	86
H22_6	2038.15	5340.75	8296.91	78
H6_7	3955.64	2421.86	5169.77	119
H7_7	3906.05	1370.3	5647.62	123
H9_7	2608.88	2490.85	6157.15	93
H10A_7	1610.19	3090.19	5730.45	90
H10B_7	1545.47	4013.39	5837.75	90
H12_7	550.18	4328.64	4976.72	130
H13_7	86.09	5505.64	4640.44	131
H14_7	734.39	6474.24	4495.64	140
H15_7	1797.24	6224.9	4549.15	136
H16_7	2284.19	5079.68	4885.28	110
H18_7	1975.77	3776.42	4336.46	146
H19_7	1915.71	2786.39	3792.45	145
H20_7	1360.16	1668.75	3859.36	157
H21_7	1127.94	1400.25	4556.3	159
H22_7	1349.01	2315.97	5165.9	133
H6_8	6149.64	6623.37	5752.63	104
H7_8	6476.01	5695.58	5301.23	109
H9_8	4613.32	5115.99	4668.1	101
H10A_8	3695.5	5692.36	4346.46	78
H10B_8	3088.34	5758.8	4574.95	78
H12_8	2514.89	7063.36	4084.02	94
H13_8	1681.23	7897.37	4144.83	115
H14_8	1794.61	8603.35	4828.49	106
H15_8	2751.64	8576.59	5430.9	104
H16_8	3559.66	7700.41	5412.82	82
H18_8	4275.11	8128.35	4873.68	68
H19_8	4967.01	8772.49	4531.34	82
H20_8	5151.38	8283.96	3850.47	83
H21_8	4754.2	7097.53	3563.21	86
H22_8	4049.8	6446.55	3898.93	77
H6_12	8886.76	7353.34	7032.44	104
H7_12	8556.74	8593.6	7148.46	94
H9_12	8610.35	8051.48	8495.92	81

Atom	x	y	z	U_{eq}
H10A_12	9506.55	7516.6	9098.97	75
H10B_12	9367.75	6707.08	9344.33	75
H12_12	10674.78	6237.5	9682.29	71
H13_12	11162.57	5074.72	10026.12	78
H14_12	10843.65	3919.29	9640.97	81
H15_12	10106	3900.89	8897.5	76
H16_12	9769.97	5048.1	8485.87	70
H18_12	10936.58	6096.96	8608.39	76
H19_12	11554.77	6722.68	8194.17	90
H20_12	11444.12	8040.73	8074.61	111
H21_12	10635.32	8699.15	8265.53	83
H22_12	9944.45	8051.34	8614.71	76
H6_1	6532.14	3218.57	6349.95	67
H7_1	6781.8	4111.09	5841.39	85
H9_1	8530.34	4472.21	6788.86	72
H10A_1	9314.27	3652.89	7316.33	79
H10B_1	9447.93	3839.67	7885.56	79
H12_1	9981.75	2411.79	8229.06	86
H13_1	10261.89	1824.9	8986.37	108
H14_1	9474.85	1561.46	9349.73	141
H15_1	8432.02	1976.09	9013.62	143
H16_1	8140.01	2605.37	8281.75	106
H18_1	8185.69	1534.96	7542.23	89
H19_1	7986.45	597.45	6953.17	109
H20_1	8545.37	631.33	6391.95	106
H21_1	9170.91	1677.33	6342.68	148
H22_1	9298.23	2683.6	6889.47	92
H6_4	9167.56	6749.48	6964.15	104
H7_4	8752.01	7993.67	6901.88	104
H9_4	8637.39	7874	8247.77	77
H10A_4	9446.6	7510.98	8968.21	75
H10B_4	9286.61	6764.67	9260.56	75
H12_4	10670.88	6408.44	9740.7	79
H13_4	11269.99	5366.14	10168.76	77
H14_4	11051.99	4125.75	9883	71
H15_4	10422.09	3924.9	9113.42	76
H16_4	9802.89	4926.69	8681.34	65
H18_4	10777.01	5943.34	8435.57	76
H19_4	11536.79	6551.88	8141.26	98

Atom	x	y	z	U_{eq}
H20_4	11537.24	7883.49	8087.36	84
H21_4	10790.36	8598.62	8321.71	83
H22_4	10172.5	8008.35	8755.83	76
H6_2	4753.12	4890.57	8174.45	58
H7_2	4164.88	4194.73	7515.73	67
H9_2	5551.15	2552.4	7786.75	84
H10A_2	6310.75	1989.35	8319.24	81
H10B_2	7079.76	2221.69	8518.39	81
H12_2	7322.72	1527.77	9420.64	102
H13_2	8121.85	1541.14	10164.75	114
H14_2	8442.02	2692.21	10553.97	123
H15_2	7953.76	3828.32	10239.08	107
H16_2	7105	3834.99	9537.78	97
H18_2	5991.08	3221.4	9594.75	105
H19_2	5092.08	2857.19	9823.73	107
H20_2	4416.96	1898.75	9404.1	128
H21_2	4566.67	1427.2	8712.31	125
H22_2	5561.69	1616.83	8566.42	174
H24A_11	6191	4331.77	6977.93	153
H24B_11	5823.24	3550.89	6998.24	153
H24C_11	5975.26	4127.95	7433.02	153

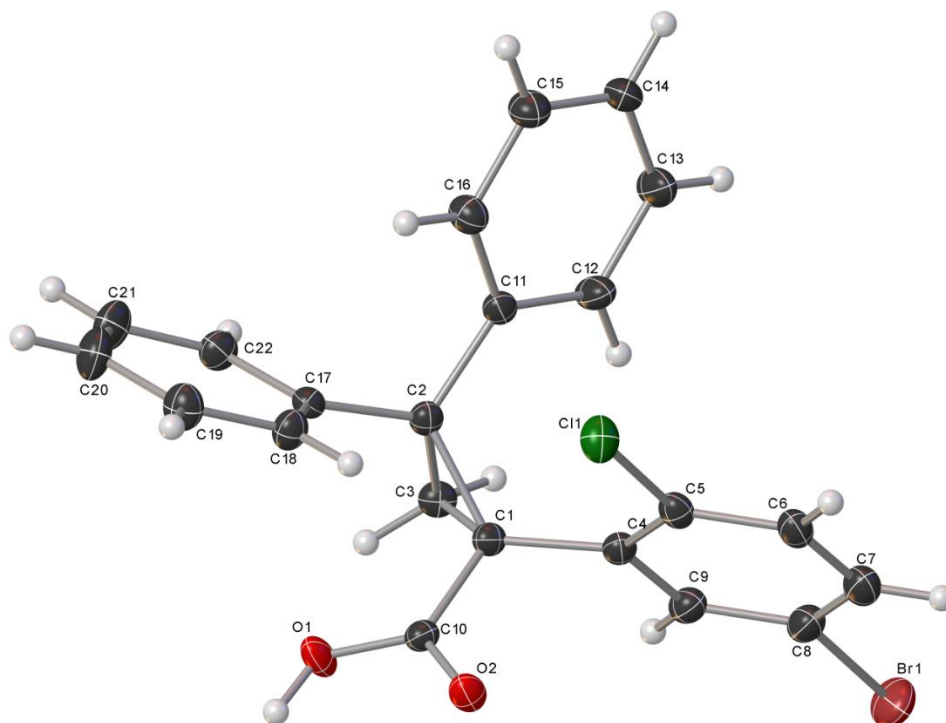
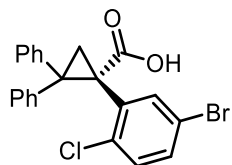
Table 15: Atomic Occupancies for all atoms that are not fully occupied in **WL-2ClBr**.

Atom	Occupancy	Atom	Occupancy	Atom	Occupancy
Br1_12	0.460(4)	H9_12	0.460(4)	C17_12	0.460(4)
Cl1_12	0.460(4)	C10_12	0.460(4)	C18_12	0.460(4)
O1_12	0.460(4)	H10A_12	0.460(4)	H18_12	0.460(4)
O2_12	0.460(4)	H10B_12	0.460(4)	C19_12	0.460(4)
C1_12	0.460(4)	C11_12	0.460(4)	H19_12	0.460(4)
C2_12	0.460(4)	C12_12	0.460(4)	C20_12	0.460(4)
C3_12	0.460(4)	H12_12	0.460(4)	H20_12	0.460(4)
C4_12	0.460(4)	C13_12	0.460(4)	C21_12	0.460(4)
C5_12	0.460(4)	H13_12	0.460(4)	H21_12	0.460(4)
C6_12	0.460(4)	C14_12	0.460(4)	C22_12	0.460(4)
H6_12	0.460(4)	H14_12	0.460(4)	H22_12	0.460(4)
C7_12	0.460(4)	C15_12	0.460(4)	Br1_4	0.540(4)
H7_12	0.460(4)	H15_12	0.460(4)	Cl1_4	0.540(4)
C8_12	0.460(4)	C16_12	0.460(4)	O1_4	0.540(4)
C9_12	0.460(4)	H16_12	0.460(4)	O2_4	0.540(4)

Atom	Occupancy	Atom	Occupancy	Atom	Occupancy
C1_4	0.540(4)	H10A_4	0.540(4)	C17_4	0.540(4)
C2_4	0.540(4)	H10B_4	0.540(4)	C18_4	0.540(4)
C3_4	0.540(4)	C11_4	0.540(4)	H18_4	0.540(4)
C4_4	0.540(4)	C12_4	0.540(4)	C19_4	0.540(4)
C5_4	0.540(4)	H12_4	0.540(4)	H19_4	0.540(4)
C6_4	0.540(4)	C13_4	0.540(4)	C20_4	0.540(4)
H6_4	0.540(4)	H13_4	0.540(4)	H20_4	0.540(4)
C7_4	0.540(4)	C14_4	0.540(4)	C21_4	0.540(4)
H7_4	0.540(4)	H14_4	0.540(4)	H21_4	0.540(4)
C8_4	0.540(4)	C15_4	0.540(4)	C22_4	0.540(4)
C9_4	0.540(4)	H15_4	0.540(4)	H22_4	0.540(4)
H9_4	0.540(4)	C16_4	0.540(4)		
C10_4	0.540(4)	H16_4	0.540(4)		

Table 16: Solvent masking (PLATON/SQUEEZE) information for **WL-2ClBr**.

No	x	y	z	V	e	Content
1	0.426	0.021	-0.073	3377	586	
2	0.520	0.082	0.136	6	0	
3	0.571	0.485	0.605	11	1	
4	0.480	0.582	0.864	7	0	
5	0.429	0.985	0.395	11	1	

(S)-1-(5-Bromo-2-chlorophenyl)-2,2-diphenylcyclopropane-1-carboxylic acid (56b)**Table 1 Crystal data and structure refinement for WL-S2Cl5Br-ligand.**

Identification code	WL-S2Cl5Br-ligand
Empirical formula	C ₂₂ H ₁₆ BrClO ₂
Formula weight	427.71
Temperature/K	100(2)
Crystal system	orthorhombic
Space group	P2 ₁ 2 ₁ 2 ₁
a/Å	8.91980(10)
b/Å	14.41860(10)
c/Å	29.7333(2)
α/°	90
β/°	90
γ/°	90
Volume/Å ³	3824.03(6)
Z	8
ρ _{calc} /cm ³	1.486

μ/mm^{-1}	4.317
F(000)	1728.0
Crystal size/ mm^3	$0.21 \times 0.168 \times 0.094$
Radiation	$\text{CuK}\alpha$ ($\lambda = 1.54184$)
2Θ range for data collection/ $^\circ$	6.814 to 155.826
Index ranges	$-8 \leq h \leq 11, -17 \leq k \leq 16, -35 \leq l \leq 37$
Reflections collected	23741
Independent reflections	7890 [$R_{\text{int}} = 0.0333, R_{\text{sigma}} = 0.0319$]
Data/restraints/parameters	7890/308/528
Goodness-of-fit on F^2	1.057
Final R indexes [$I \geq 2\sigma(I)$]	$R_1 = 0.0242, wR_2 = 0.0618$
Final R indexes [all data]	$R_1 = 0.0253, wR_2 = 0.0621$
Largest diff. peak/hole / $e \text{ \AA}^{-3}$	0.47/-0.39
Flack parameter	-0.010(5)

Table 2 Fractional Atomic Coordinates ($\times 10^4$) and Equivalent Isotropic Displacement Parameters ($\text{\AA}^2 \times 10^3$) for WL-S2Cl5Br-ligand. U_{eq} is defined as 1/3 of the trace of the orthogonalised U_{ij} tensor.

Atom	x	y	z	U(eq)
C11	3547(3)	5496.6(16)	7003.4(8)	17.0(4)
C1	5253(2)	4585.3(16)	6423.6(8)	16.0(4)
C16	2915(3)	5305.3(17)	7422.7(9)	21.5(5)
C2	3707(3)	4723.8(16)	6661.5(8)	16.2(4)
C15	2664(3)	6007.2(18)	7735.5(9)	24.0(5)
C3	3913(3)	4996.6(17)	6176.8(8)	18.2(5)
C14	3048(3)	6912.9(19)	7635.1(10)	25.1(5)
C13	3703(3)	7108.3(19)	7224.3(11)	29.7(6)
C12	3946(3)	6408.1(18)	6910.1(10)	24.4(5)
C10	5648(3)	3620.4(16)	6280.5(8)	16.1(4)
C17	2796(3)	3878.4(16)	6774.6(8)	16.3(4)
C18	3404(3)	3129.3(17)	7009.2(9)	20.6(5)
C19	2517(3)	2385.5(18)	7138.1(10)	25.7(5)
C20	997(3)	2389(2)	7041.5(11)	29.1(6)
C21	374(3)	3133(2)	6812.6(10)	28.4(6)
C22	1274(3)	3869.5(18)	6676.5(9)	21.4(5)

O1	4665(2)	3187.9(11)	6043.1(7)	23.8(4)
O2	6888(2)	3284.4(11)	6383.8(7)	20.9(4)
C1'	6977(3)	175.5(16)	5815.8(8)	17.0(4)
C2'	7088(3)	71.1(16)	5290.3(8)	17.3(4)
C3'	5828(3)	-360.7(16)	5550.2(9)	19.7(5)
C10'	6529(3)	1134.6(16)	5961.5(8)	16.6(5)
C17'	6741(3)	901.0(17)	4998.2(8)	19.5(5)
C18'	7633(3)	1694.7(18)	5007.1(9)	23.9(5)
C19'	7331(4)	2429.2(19)	4716.3(10)	31.6(6)
C20'	6155(4)	2369(2)	4415.0(11)	35.3(7)
C21'	5261(4)	1590(2)	4406.2(10)	34.5(7)
C22'	5556(3)	855.6(19)	4697.3(9)	25.7(5)
O1'	5258.5(19)	1442.6(8)	5884.6(7)	22.8(4)
O2'	7577(2)	1600.7(12)	6161.5(6)	22.2(4)
Br1_1	9360.8(4)	6964.9(2)	5835.5(2)	36.85(10)
Cl1_1	6634.0(7)	4428.1(4)	7390.4(2)	23.08(13)
C4_1	6605(2)	5159.1(15)	6544.4(7)	16.8(4)
C5_1	7331(2)	5116.1(15)	6958.8(7)	18.1(4)
C6_1	8642(3)	5604.3(16)	7045.0(8)	22.2(4)
C7_1	9268(3)	6163.9(17)	6713.6(8)	25.0(4)
C8_1	8553(3)	6212.3(16)	6301.2(8)	23.8(4)
C9_1	7246(3)	5726.5(16)	6215.8(8)	20.5(4)
Br1_2	12597.1(5)	146.7(10)	6382.7(2)	37.2(2)
Cl1_2	5892.7(16)	-1347.8(19)	6506.2(7)	34.8(3)
C4_2	8084(3)	-276(3)	6128.0(16)	17.7(5)
C5_2	7722(3)	-949(3)	6446.7(15)	21.4(5)
C6_2	8779(3)	-1314(4)	6740.8(15)	26.1(5)
C7_2	10252(3)	-1000(3)	6729.7(14)	27.3(5)
C8_2	10614(3)	-320(2)	6420.6(10)	23.3(6)
C9_2	9564(3)	42(2)	6126.7(11)	18.9(8)
Br1_3	12597(4)	-240(5)	6369.7(13)	37.2(2)
Cl1_3	5701(9)	-1381(14)	6441(6)	34.8(3)
C4_3	8037(9)	-365(19)	6109(10)	17.7(5)
C5_3	7556(12)	-1010(20)	6425(9)	21.4(5)
C6_3	8509(12)	-1360(20)	6754(9)	26.1(5)
C7_3	10025(10)	-1130(20)	6749(8)	27.3(5)
C8_3	10540(7)	-569(16)	6406(6)	23.3(6)

C9_3	9565(9)	-150(20)	6104(8)	18.9(8)
C11_4	8325(8)	-514(7)	5096(7)	19.5(6)
C12_4	8028(8)	-1413(7)	4943(4)	20.1(9)
C13_4	9157(10)	-1964(5)	4762(3)	23.2(9)
C14_4	10622(9)	-1639(6)	4762(3)	22.6(8)
C15_4	10936(7)	-748(7)	4902(3)	21.9(8)
C16_4	9790(8)	-175(6)	5058(4)	20.1(8)
C11_5	8222(6)	-592(5)	5098(5)	19.5(6)
C12_5	7720(6)	-1403(5)	4888(3)	20.1(9)
C13_5	8716(8)	-2022(4)	4689(2)	23.2(9)
C14_5	10240(8)	-1830(4)	4696(2)	22.6(8)
C15_5	10762(6)	-1027(5)	4894(2)	21.9(8)
C16_5	9762(6)	-400(4)	5088(3)	20.1(8)

Table 3 Anisotropic Displacement Parameters ($\text{\AA}^2 \times 10^3$) for WL-S2Cl5Br-ligand.

The Anisotropic displacement factor exponent takes the form: -

$2\pi^2[h^2a^*U_{11}+2hka^*b^*U_{12}+\dots]$.

Atom	U ₁₁	U ₂₂	U ₃₃	U ₂₃	U ₁₃	U ₁₂
C11	14.2(10)	16.9(10)	19.7(12)	-1.5(9)	-0.4(9)	1.8(9)
C1	14.5(10)	18.2(11)	15.3(10)	-0.9(8)	-1.4(8)	0.5(8)
C16	27.0(13)	17.6(11)	19.9(12)	0.8(9)	0.9(10)	-0.4(9)
C2	14.7(10)	15.8(10)	18.0(11)	0.3(9)	-0.7(8)	1.2(8)
C15	27.0(13)	25.5(12)	19.5(12)	-1.3(10)	3.4(10)	-1.1(11)
C3	18.4(10)	18.9(11)	17.4(11)	1.7(9)	-1.6(9)	2.9(9)
C14	23.8(12)	23.1(12)	28.5(13)	-9.9(11)	6.0(10)	-1.7(10)
C13	32.6(14)	17.7(11)	38.7(16)	-5.6(11)	12.2(12)	-5.3(11)
C12	26.7(13)	19.7(11)	26.8(14)	-1.7(10)	11.1(11)	-2.1(10)
C10	14.1(10)	18.5(10)	15.7(10)	-0.5(8)	1.4(9)	0.5(9)
C17	16.8(11)	16.6(10)	15.7(10)	-3.1(8)	0.6(9)	-0.6(9)
C18	16.2(11)	20.3(11)	25.1(12)	1.8(10)	-1.8(10)	-0.3(9)
C19	26.9(13)	20.0(11)	30.2(14)	4.0(10)	-1.9(12)	-1.3(10)
C20	23.8(14)	29.0(13)	34.5(15)	5.0(11)	-1.7(11)	-9.6(11)
C21	17.2(12)	34.6(14)	33.3(15)	1.7(12)	-4.8(11)	-4.5(11)
C22	17.9(12)	23.2(12)	23.2(13)	-0.2(10)	-2.5(10)	1.5(10)
O1	20.8(9)	22.4(9)	28.2(10)	-10.6(7)	-7.0(7)	1.1(7)
O2	17.1(8)	19.3(8)	26.4(9)	-3.9(7)	-3.3(7)	3.3(6)
C1'	17.0(10)	16.9(10)	17.0(11)	-0.7(9)	1.9(9)	-1.4(8)

C2'	17.5(11)	17.8(10)	16.5(11)	-2.5(9)	-1.5(9)	0.1(9)
C3'	18.8(11)	18.5(11)	21.8(12)	-2.1(9)	1.8(10)	-2.0(9)
C10'	18.2(11)	17.9(11)	13.7(10)	0.6(8)	2.7(9)	-2.6(9)
C17'	21.1(12)	22.1(11)	15.4(11)	-3.7(9)	2.1(10)	3.3(9)
C18'	25.2(13)	25.3(12)	21.3(12)	0.5(10)	4.5(11)	-1.8(10)
C19'	41.8(17)	23.3(13)	29.8(14)	3.1(11)	12.5(13)	2.2(12)
C20'	45.8(18)	33.6(15)	26.7(15)	8.3(12)	10.8(13)	20.0(13)
C21'	35.0(16)	43.4(16)	25.1(14)	0.2(12)	-3.5(12)	16.8(13)
C22'	24.1(12)	29.8(13)	23.1(13)	-4.2(10)	-1.3(11)	5.4(11)
O1'	18.1(8)	21.8(8)	28.7(10)	-4.3(7)	1.4(7)	2.9(7)
O2'	22.9(9)	17.7(8)	25.9(9)	-4.1(7)	-3.3(8)	0.0(7)
Br1_1	38.92(17)	34.89(16)	36.75(17)	3.10(13)	14.12(14)	-14.05(13)
Cl1_1	25.5(3)	24.0(3)	19.7(3)	5.3(2)	-5.9(2)	-3.3(2)
C4_1	14.8(8)	16.3(9)	19.3(8)	-1.4(6)	0.9(6)	1.1(7)
C5_1	19.3(8)	14.3(8)	20.8(8)	-1.3(7)	-1.9(6)	1.7(7)
C6_1	19.9(8)	19.1(9)	27.5(10)	-5.4(7)	-1.4(7)	-0.2(7)
C7_1	23.2(10)	20.0(10)	31.7(9)	-4.5(7)	1.9(7)	-1.2(8)
C8_1	20.2(8)	22.1(10)	29.2(9)	-1.9(8)	5.5(7)	-1.8(7)
C9_1	20.2(8)	18.8(9)	22.4(9)	0.3(7)	3.6(7)	-0.2(7)
Br1_2	19.10(14)	56.6(6)	35.83(18)	-4.0(2)	-4.60(12)	-1.8(2)
Cl1_2	27.4(5)	41.5(4)	35.4(9)	16.7(6)	1.5(4)	-9.5(5)
C4_2	19.3(6)	16.3(10)	17.5(9)	-2.9(8)	1.4(5)	1.7(6)
C5_2	23.6(7)	19.0(9)	21.7(8)	0.5(7)	2.8(6)	1.2(6)
C6_2	27.9(8)	25.9(12)	24.5(10)	1.3(8)	0.6(9)	5.8(9)
C7_2	27.6(8)	30.3(14)	24.1(10)	-0.4(9)	-0.2(8)	5.4(9)
C8_2	22.8(8)	26.3(15)	20.7(9)	-4.3(10)	-0.7(7)	5.9(7)
C9_2	19.3(6)	17.9(17)	19.4(11)	-4.1(12)	1.0(6)	1.3(7)
Br1_3	19.10(14)	56.6(6)	35.83(18)	-4.0(2)	-4.60(12)	-1.8(2)
Cl1_3	27.4(5)	41.5(4)	35.4(9)	16.7(6)	1.5(4)	-9.5(5)
C4_3	19.3(6)	16.3(10)	17.5(9)	-2.9(8)	1.4(5)	1.7(6)
C5_3	23.6(7)	19.0(9)	21.7(8)	0.5(7)	2.8(6)	1.2(6)
C6_3	27.9(8)	25.9(12)	24.5(10)	1.3(8)	0.6(9)	5.8(9)
C7_3	27.6(8)	30.3(14)	24.1(10)	-0.4(9)	-0.2(8)	5.4(9)
C8_3	22.8(8)	26.3(15)	20.7(9)	-4.3(10)	-0.7(7)	5.9(7)
C9_3	19.3(6)	17.9(17)	19.4(11)	-4.1(12)	1.0(6)	1.3(7)
C11_4	21.5(8)	19.6(9)	17.4(9)	2.0(8)	0.7(7)	1.2(8)
C12_4	21.8(12)	18.5(8)	20(2)	2.7(11)	-3.2(15)	2.9(11)

C13_4	22.4(15)	18.7(10)	29(2)	-0.3(11)	-0.7(16)	1.6(13)
C14_4	22.4(14)	20.6(15)	24.8(18)	2.2(11)	-1.4(15)	1.3(12)
C15_4	21.4(11)	21.7(18)	22.6(13)	1.6(16)	2.2(11)	-0.2(12)
C16_4	21.6(8)	21.7(16)	17.0(16)	2.4(18)	0.5(7)	0.6(10)
C11_5	21.5(8)	19.6(9)	17.4(9)	2.0(8)	0.7(7)	1.2(8)
C12_5	21.8(12)	18.5(8)	20(2)	2.7(11)	-3.2(15)	2.9(11)
C13_5	22.4(15)	18.7(10)	29(2)	-0.3(11)	-0.7(16)	1.6(13)
C14_5	22.4(14)	20.6(15)	24.8(18)	2.2(11)	-1.4(15)	1.3(12)
C15_5	21.4(11)	21.7(18)	22.6(13)	1.6(16)	2.2(11)	-0.2(12)
C16_5	21.6(8)	21.7(16)	17.0(16)	2.4(18)	0.5(7)	0.6(10)

Table 4 Bond Lengths for WL-S2Cl5Br-ligand.

Atom	Atom	Length/Å	Atom	Atom	Length/Å
C11	C16	1.396(4)	C21'	C22'	1.393(4)
C11	C2	1.515(3)	Br1_1	C8_1	1.901(2)
C11	C12	1.390(3)	Cl1_1	C5_1	1.737(2)
C1	C2	1.563(3)	C4_1	C5_1	1.393(3)
C1	C3	1.523(3)	C4_1	C9_1	1.397(3)
C1	C10	1.497(3)	C5_1	C6_1	1.388(3)
C1	C4_1	1.506(3)	C6_1	C7_1	1.390(3)
C16	C15	1.393(4)	C7_1	C8_1	1.384(3)
C2	C3	1.505(3)	C8_1	C9_1	1.383(3)
C2	C17	1.503(3)	Br1_2	C8_2	1.895(2)
C15	C14	1.383(4)	Cl1_2	C5_2	1.739(2)
C14	C13	1.383(4)	C4_2	C5_2	1.394(3)
C13	C12	1.392(4)	C4_2	C9_2	1.397(3)
C10	O1	1.287(3)	C5_2	C6_2	1.390(3)
C10	O2	1.247(3)	C6_2	C7_2	1.390(3)
C17	C18	1.396(3)	C7_2	C8_2	1.382(3)
C17	C22	1.389(4)	C8_2	C9_2	1.384(3)
C18	C19	1.387(4)	Br1_3	C8_3	1.898(3)
C19	C20	1.386(4)	Cl1_3	C5_3	1.738(3)
C20	C21	1.387(4)	C4_3	C5_3	1.394(3)
C21	C22	1.390(4)	C4_3	C9_3	1.397(3)
C1'	C2'	1.573(3)	C5_3	C6_3	1.390(3)
C1'	C3'	1.507(3)	C6_3	C7_3	1.391(4)
C1'	C10'	1.504(3)	C7_3	C8_3	1.383(4)

C1'	C4_2	1.503(3)	C8_3	C9_3	1.385(3)
C1'	C4_3	1.503(3)	C11_4	C12_4	1.398(4)
C2'	C3'	1.499(3)	C11_4	C16_4	1.400(4)
C2'	C17'	1.511(3)	C12_4	C13_4	1.392(5)
C2'	C11_4	1.505(4)	C13_4	C14_4	1.388(6)
C2'	C11_5	1.505(3)	C14_4	C15_4	1.380(6)
C10'	O1'	1.238(3)	C15_4	C16_4	1.393(5)
C10'	O2'	1.296(3)	C11_5	C12_5	1.399(4)
C17'	C18'	1.394(4)	C11_5	C16_5	1.401(4)
C17'	C22'	1.387(4)	C12_5	C13_5	1.391(4)
C18'	C19'	1.394(4)	C13_5	C14_5	1.387(6)
C19'	C20'	1.382(5)	C14_5	C15_5	1.380(6)
C20'	C21'	1.378(5)	C15_5	C16_5	1.394(5)

Table 5 Bond Angles for WL-S2Cl5Br-ligand.

Atom	Atom	Atom	Angle/°	Atom	Atom	Atom	Angle/°
C16	C11	C2	119.5(2)	C19'	C18'	C17'	120.1(3)
C12	C11	C16	117.9(2)	C20'	C19'	C18'	120.0(3)
C12	C11	C2	122.5(2)	C21'	C20'	C19'	120.2(3)
C3	C1	C2	58.37(15)	C20'	C21'	C22'	119.9(3)
C10	C1	C2	117.0(2)	C17'	C22'	C21'	120.6(3)
C10	C1	C4_1	112.99(19)	C5_1	C4_1	C1	123.97(19)
C4_1	C1	C2	121.91(19)	C5_1	C4_1	C9_1	117.01(19)
C4_1	C1	C3	122.0(2)	C9_1	C4_1	C1	118.87(19)
C15	C16	C11	121.2(2)	C4_1	C5_1	C11_1	120.80(16)
C11	C2	C1	118.7(2)	C6_1	C5_1	C11_1	117.05(16)
C3	C2	C11	117.5(2)	C6_1	C5_1	C4_1	122.15(19)
C3	C2	C1	59.49(15)	C5_1	C6_1	C7_1	120.1(2)
C17	C2	C11	113.3(2)	C8_1	C7_1	C6_1	118.2(2)
C17	C2	C1	118.34(19)	C7_1	C8_1	Br1_1	119.97(17)
C17	C2	C3	119.5(2)	C9_1	C8_1	Br1_1	118.35(18)
C14	C15	C16	120.2(2)	C9_1	C8_1	C7_1	121.7(2)
C2	C3	C1	62.14(16)	C8_1	C9_1	C4_1	120.9(2)
C15	C14	C13	119.2(2)	C5_2	C4_2	C1'	124.6(2)
C14	C13	C12	120.7(3)	C5_2	C4_2	C9_2	116.7(2)
C11	C12	C13	120.8(3)	C9_2	C4_2	C1'	118.5(2)
				C4_2	C5_2	C11_2	121.13(18)

O1	C10	C1	116.5(2)	C6_2	C5_2	C11_2	116.56(18)
O2	C10	C1	120.0(2)	C6_2	C5_2	C4_2	122.3(2)
O2	C10	O1	123.5(2)	C7_2	C6_2	C5_2	120.2(2)
C18	C17	C2	122.0(2)	C8_2	C7_2	C6_2	117.9(2)
C22	C17	C2	119.3(2)	C7_2	C8_2	Br1_2	120.64(18)
C22	C17	C18	118.5(2)	C7_2	C8_2	C9_2	121.9(2)
C19	C18	C17	121.0(2)	C9_2	C8_2	Br1_2	117.43(19)
C20	C19	C18	119.9(3)	C8_2	C9_2	C4_2	121.0(2)
C19	C20	C21	119.7(3)	C5_3	C4_3	C1'	123.0(7)
C20	C21	C22	120.2(3)	C5_3	C4_3	C9_3	116.9(3)
C17	C22	C21	120.7(2)	C9_3	C4_3	C1'	119.7(5)
C3'	C1'	C2'	58.21(16)	C4_3	C5_3	C11_3	121.0(3)
C10'	C1'	C2'	113.0(2)	C6_3	C5_3	C11_3	117.0(3)
C10'	C1'	C3'	116.2(2)	C6_3	C5_3	C4_3	121.9(4)
C10'	C1'	C4_2	113.2(3)	C5_3	C6_3	C7_3	120.1(4)
C4_2	C1'	C2'	122.1(3)	C8_3	C7_3	C6_3	118.0(3)
C4_2	C1'	C3'	123.3(2)	C7_3	C8_3	Br1_3	120.6(3)
C4_3	C1'	C2'	119.1(15)	C7_3	C8_3	C9_3	121.5(4)
C4_3	C1'	C3'	117.8(11)	C9_3	C8_3	Br1_3	117.6(3)
C4_3	C1'	C10'	118.5(15)	C8_3	C9_3	C4_3	120.9(3)
C3'	C2'	C1'	58.72(15)	C12_4	C11_4	C2'	120.4(5)
C3'	C2'	C17'	118.2(2)	C12_4	C11_4	C16_4	118.3(3)
C3'	C2'	C11_4	121.0(6)	C16_4	C11_4	C2'	121.3(5)
C3'	C2'	C11_5	115.9(4)	C13_4	C12_4	C11_4	121.2(4)
C17'	C2'	C1'	118.9(2)	C14_4	C13_4	C12_4	119.2(4)
C11_4	C2'	C1'	118.8(8)	C15_4	C14_4	C13_4	120.4(4)
C11_4	C2'	C17'	111.9(8)	C14_4	C15_4	C16_4	120.2(4)
C11_5	C2'	C1'	118.7(6)	C15_4	C16_4	C11_4	120.4(4)
C11_5	C2'	C17'	115.0(6)	C12_5	C11_5	C2'	119.0(4)
C2'	C3'	C1'	63.07(16)	C12_5	C11_5	C16_5	118.0(3)
O1'	C10'	C1'	121.3(2)	C16_5	C11_5	C2'	122.8(4)
O1'	C10'	O2'	124.0(2)	C13_5	C12_5	C11_5	121.4(3)
O2'	C10'	C1'	114.7(2)	C14_5	C13_5	C12_5	119.5(4)
C18'	C17'	C2'	121.5(2)	C15_5	C14_5	C13_5	120.3(3)
C22'	C17'	C2'	119.3(2)	C14_5	C15_5	C16_5	120.3(4)
C22'	C17'	C18'	119.1(3)	C15_5	C16_5	C11_5	120.5(3)

Table 6 Hydrogen Atom Coordinates ($\text{\AA}\times 10^4$) and Isotropic Displacement Parameters ($\text{\AA}^2\times 10^3$) for WL-S2Cl5Br-ligand.

Atom	x	y	z	U(eq)
H16	2656.53	4698.17	7494.43	26
H15	2236.63	5866.44	8012.5	29
H3A	3960(40)	5668(11)	6098(11)	21(4)
H3B	3460(30)	4586(18)	5944(8)	21(4)
H1	4917.2	2548.6	5994.8	32
H14	2869.02	7384.93	7841.35	30
H13	3984.5	7713.73	7157.18	36
H12	4380.31	6552.33	6634.47	29
H18	4419.2	3129.03	7080.33	25
H19	2941.62	1885.3	7288.97	31
H20	397.29	1893.78	7129.77	35
H21	-647.02	3140.27	6750.06	34
H22	851.33	4360.8	6518.33	26
H3'A	5870(40)	-1040(11)	5611(11)	21(4)
H3'B	4800(20)	-90(20)	5528(11)	21(4)
H18'	8430.53	1734.11	5207.57	29
H19'	7921.44	2960.5	4724.88	38
H20'	5967.55	2855.13	4217.59	42
H21'	4461.03	1554.88	4206.17	41
H22'	4952.17	329.85	4689.78	31
H2'	7223.53	2211.63	6226.42	27
H6_1	9102.13	5556.9	7324.7	27
H7_1	10142.49	6496.52	6767.68	30
H9_1	6788.21	5778.38	5935.95	25
H6_2	8500.81	-1770.43	6945.59	31
H7_2	10971	-1239.86	6924.16	33
H9_2	9846.73	503	5925.24	23
H6_3	8133.58	-1744.12	6978.71	31
H7_3	10672.72	-1354.92	6968.79	33
H9_3	9933.25	269.12	5895.55	23
H12_4	7058.07	-1646.5	4963.05	24
H13_4	8933.64	-2543.8	4642.02	28
H14_4	11395.58	-2023.54	4666.45	27
H15_4	11916.56	-528.81	4893.46	26

H16_49998.76	435.31	5136.53	24
H12_56698.54	-1531.14	4881.68	24
H13_58362.87	-2559.82	4553.35	28
H14_510911.83	-2244.17	4566.16	27
H15_511784.8	-902.73	4897.52	26
H16_510119.72	149.32	5211.14	24

Table 7 Atomic Occupancy for WL-S2Cl5Br-ligand.

Atom	Occupancy	Atom	Occupancy	Atom	Occupancy
Br1_2	0.867(4)	C11_2	0.867(4)	C4_2	0.867(4)
C5_2	0.867(4)	C6_2	0.867(4)	H6_2	0.867(4)
C7_2	0.867(4)	H7_2	0.867(4)	C8_2	0.867(4)
C9_2	0.867(4)	H9_2	0.867(4)	Br1_3	0.133(4)
C11_3	0.133(4)	C4_3	0.133(4)	C5_3	0.133(4)
C6_3	0.133(4)	H6_3	0.133(4)	C7_3	0.133(4)
H7_3	0.133(4)	C8_3	0.133(4)	C9_3	0.133(4)
H9_3	0.133(4)	C11_4	0.410(11)	C12_4	0.410(11)
H12_4	0.410(11)	C13_4	0.410(11)	H13_4	0.410(11)
C14_4	0.410(11)	H14_4	0.410(11)	C15_4	0.410(11)
H15_4	0.410(11)	C16_4	0.410(11)	H16_4	0.410(11)
C11_5	0.590(11)	C12_5	0.590(11)	H12_5	0.590(11)
C13_5	0.590(11)	H13_5	0.590(11)	C14_5	0.590(11)
H14_5	0.590(11)	C15_5	0.590(11)	H15_5	0.590(11)
C16_5	0.590(11)	H16_5	0.590(11)		

Experimental

Single crystals of C₂₂H₁₆BrClO₂ [WL-S2Cl5Br-ligand] were [slow evaporation of 2% EtOAc in hexane]. A suitable crystal was selected and [The crystal was mounted on a loop with paratone oil] on a XtaLAB Synergy, Dualflex, HyPix diffractometer. The crystal was kept at 100(2) K during data collection. Using Olex2 [1], the structure was solved with the ShelXT [2] structure solution program using Intrinsic Phasing and refined with the ShelXL [3] refinement package using Least Squares minimisation.

1. Dolomanov, O.V., Bourhis, L.J., Gildea, R.J., Howard, J.A.K. & Puschmann, H. (2009), *J. Appl. Cryst.* 42, 339-341.
2. Sheldrick, G.M. (2015). *Acta Cryst.* A71, 3-8.
3. Sheldrick, G.M. (2015). *Acta Cryst.* C71, 3-8.

Crystal structure determination of [WL-S2Cl5Br-ligand]

Crystal Data for C₂₂H₁₆BrClO₂ (*M* = 427.71 g/mol): orthorhombic, space group P2₁2₁2₁ (no. 19), *a* = 8.91980(10) Å, *b* = 14.41860(10) Å, *c* = 29.7333(2) Å, *V* = 3824.03(6) Å³, *Z* = 8, *T* = 100(2) K, μ (CuK α) = 4.317 mm⁻¹, *D*_{calc} = 1.486 g/cm³, 23741 reflections measured (6.814° ≤ 2 θ ≤ 155.826°), 7890 unique (*R*_{int} = 0.0333, *R*_{sigma} = 0.0319) which were used in all calculations. The final *R*₁ was 0.0242 (*I* > 2 σ (*I*)) and *wR*₂ was 0.0621 (all data).

Refinement model description

Number of restraints - 308, number of constraints - unknown.

Details:

1. Fixed Uiso

At 1.2 times of:

All C(H) groups, All O(H) groups

At 1.5 times of:

All H(H) groups

2. Restrained distances

O1-H1

0.955 with sigma of 0.002

H1-O1'

1.655 with sigma of 0.001

C3'-H3'B \approx C3'-H3'A

with sigma of 0.002

C3-H3A \approx C3'-H3'B

with sigma of 0.002

C4_2-C1' \approx C4_3-C1'

with sigma of 0.001

C3-H3A \approx C3-H3B

with sigma of 0.001

C2'-C11_5 \approx C2'-C11_4

with sigma of 0.001

3. Uiso/Uanis restraints and constraints

Uanis(C4_3) \approx Ueq: with sigma of 0.001 and sigma for terminal atoms of 0.002

Uanis(C5_3) \approx Ueq: with sigma of 0.001 and sigma for terminal atoms of 0.002

Uanis(C11_4) \approx Ueq: with sigma of 0.001 and sigma for terminal atoms of 0.002

Uiso(H3'B) = Uiso(H3'A)

Uanis(C11_4) = Uanis(C11_5)

Uanis(C16_4) = Uanis(C16_5)

Uanis(C15_4) = Uanis(C15_5)

Uanis(C14_4) = Uanis(C14_5)

Uanis(C13_4) = Uanis(C13_5)

Uanis(C12_4) = Uanis(C12_5)

Uanis(C5_2) = Uanis(C5_3)

Uanis(C4_2) = Uanis(C4_3)

Uanis(C9_2) = Uanis(C9_3)

Uanis(C8_2) = Uanis(C8_3)

Uanis(C7_2) = Uanis(C7_3)

Uanis(C6_2) = Uanis(C6_3)

Uiso(H3A) = Uiso(H3B)

Uiso(H3B) = Uiso(H3'B)

Uanis(Br1_2) = Uanis(Br1_3)

Uanis(C11_3) = Uanis(C11_2)

4. Rigid body (RIGU) restraints

Br1_1, C11_1, C4_1, C5_1, C6_1, C7_1, C8_1, C9_1

Br1_2, C11_2, C4_2, C5_2, C6_2, C7_2, C8_2, C9_2

Br1_3, C11_3, C4_3, C5_3, C6_3, C7_3, C8_3, C9_3

with sigma for 1-2 distances of 0.0002 and sigma for 1-3 distances of 0.0004

C11_4, C12_4, C13_4, C14_4, C15_4, C16_4

C11_5, C12_5, C13_5, C14_5, C15_5, C16_5

with sigma for 1-2 distances of 0.0002 and sigma for 1-3 distances of 0.0004

5. Same fragment restraints

{Br1_2, C11_2, C4_2, C5_2, C6_2, C7_2, C8_2, C9_2}

{Br1_3, C11_3, C4_3, C5_3, C6_3, C7_3, C8_3, C9_3}

as

{Br1_1, C11_1, C4_1, C5_1, C6_1, C7_1, C8_1, C9_1} sigma for 1-2: 0.002 1-3: 0.004

{C11_5, C12_5, C13_5, C14_5, C15_5, C16_5}

as

{C11_4, C12_4, C13_4, C14_4, C15_4, C16_4} sigma for 1-2: 0.002 1-3: 0.004

6. Others

Sof(Br1)=Sof(C11)=Sof(C4)=Sof(C5)=Sof(C6)=Sof(H6)=Sof(C7)=Sof(H7)=Sof(C8)=
Sof(C9)=Sof(H9)=1-FVAR(1)

Sof(Br1)=Sof(C11)=Sof(C4)=Sof(C5)=Sof(C6)=Sof(H6)=Sof(C7)=Sof(H7)=Sof(C8)=
Sof(C9)=Sof(H9)=FVAR(1)

Sof(C11)=Sof(C12)=Sof(H12)=Sof(C13)=Sof(H13)=Sof(C14)=Sof(H14)=Sof(C15)=
Sof(H15)=Sof(C16)=Sof(H16)=1-FVAR(2)

Sof(C11)=Sof(C12)=Sof(H12)=Sof(C13)=Sof(H13)=Sof(C14)=Sof(H14)=Sof(C15)=
Sof(H15)=Sof(C16)=Sof(H16)=FVAR(2)

Fixed X: H1(0.49172)

Fixed Y: H1(0.25486)

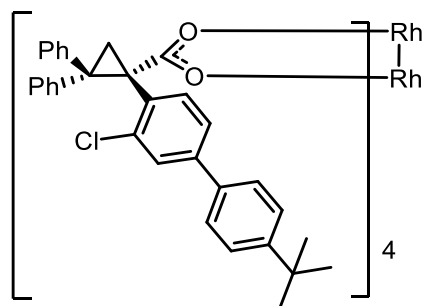
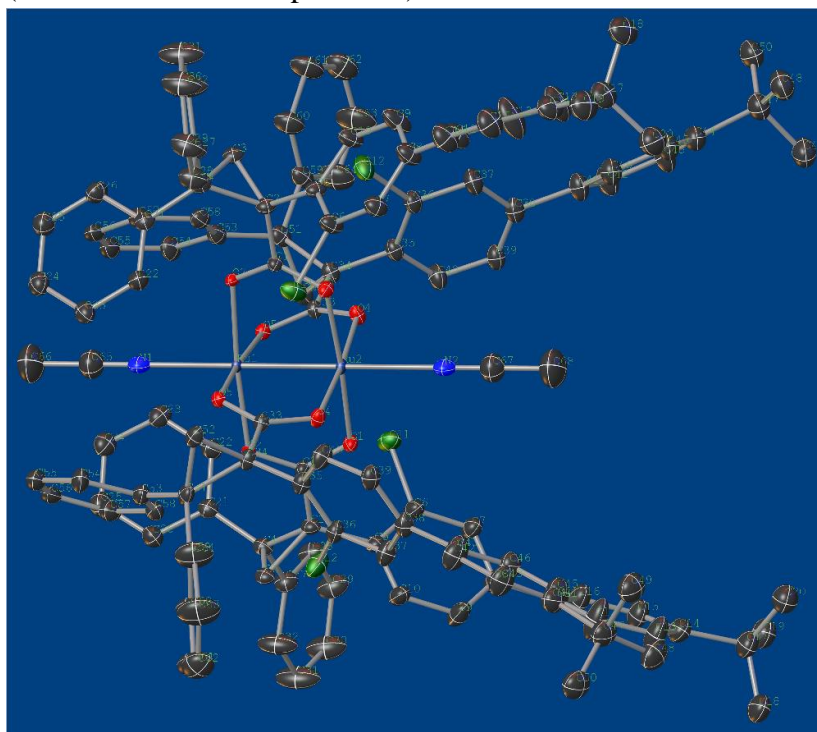
Fixed Z: H1(0.59948)

7.a Aromatic/amide H refined with riding coordinates:

C16(H16), C15(H15), C14(H14), C13(H13), C12(H12), C18(H18), C19(H19),
C20(H20), C21(H21), C22(H22), C18'(H18'), C19'(H19'), C20'(H20'), C21'(H21'),
C22'(H22'), C6(H6), C7(H7), C9(H9), C6(H6), C7(H7), C9(H9), C6(H6), C7(H7),
C9(H9), C12(H12), C13(H13), C14(H14), C15(H15), C16(H16), C12(H12), C13(H13),
C14(H14), C15(H15), C16(H16)

7.b Idealised tetrahedral OH refined as rotating group:

O2'(H2')

Rh₂[S-2-Cl-4-(*p*-^tBuC₆H₄)TPCP]₄ (128)(with CH₃CN at axial positions)**Table 1 Crystal data and structure refinement for twin4_sq.**

Identification code	twin4_sq
Empirical formula	C ₅₂₈ H ₄₇₂ Cl ₁₆ N ₈ O ₃₂ Ru ₈
Formula weight	8816.90
Temperature/K	100(2)
Crystal system	tetragonal
Space group	P4
a/Å	29.685(3)
b/Å	29.685(3)
c/Å	14.3753(14)
α/°	90
β/°	90

$\gamma/^\circ$	90
Volume/ \AA^3	12668(3)
Z	1
$\rho_{\text{calc}}/\text{g/cm}^3$	1.156
μ/mm^{-1}	0.375
F(000)	4576.0
Crystal size/ mm^3	$0.514 \times 0.26 \times 0.216$
Radiation	MoK α ($\lambda = 0.71073$)
2Θ range for data collection/ $^\circ$	2.744 to 61.01
Index ranges	$? \leq h \leq ?, ? \leq k \leq ?, ? \leq l \leq ?$
Reflections collected	37362
Independent reflections	37362 [$R_{\text{int}} = ?, R_{\text{sigma}} = 0.0955$]
Data/restraints/parameters	37362/1424/1333
Goodness-of-fit on F^2	1.048
Final R indexes [$I \geq 2\sigma(I)$]	$R_1 = 0.0926, wR_2 = 0.2325$
Final R indexes [all data]	$R_1 = 0.1246, wR_2 = 0.2508$
Largest diff. peak/hole / $e \text{\AA}^{-3}$	7.46/-4.52
Flack parameter	0.021(12)

Table 2 Fractional Atomic Coordinates ($\times 10^4$) and Equivalent Isotropic Displacement Parameters ($\text{\AA}^2 \times 10^3$) for twin4_sq. U_{eq} is defined as 1/3 of the trace of the orthogonalised U_{IJ} tensor.

Atom	x	y	z	U(eq)
Ru1	5000	0	5803.1(11)	8.13(16)
Ru2	5000	0	4137.8(11)	9.34(16)
Cl1	6243.6(7)	888.9(7)	4137.0(19)	27.7(4)
Cl2	4024.9(8)	1282.2(7)	4149.1(19)	31.3(5)
O1	5226.3(17)	649.0(17)	4186(4)	14.5(9)
O2	5095.1(17)	683.3(16)	5746(4)	11.6(8)
O4	4355.0(17)	234.5(17)	4196(4)	15.8(9)
O5	4316.9(16)	89.3(16)	5740(4)	11.7(8)
N1	5000	0	7360(7)	24.6(8)
N2	5000	0	2486(7)	24.6(8)
C1	5223(2)	845(2)	4973(6)	14.2(11)
C2	5384(3)	1329(2)	4981(6)	18.1(10)

C3	5121(3)	1649(3)	5608(6)	17.7(11)
C4	5593(3)	1543(3)	5878(6)	18.4(10)
C5	5558(3)	1502(3)	4073(6)	19.6(12)
C6	5947(3)	1336(3)	3636(6)	25.2(16)
C7	6108(3)	1515(3)	2820(6)	25.4(16)
C8	5885(3)	1864(3)	2374(7)	29.7(16)
C9	5492(3)	2021(4)	2757(7)	37(2)
C10	5330(3)	1843(3)	3597(6)	27.8(17)
C11	6069(3)	2052(3)	1500(7)	34.7(18)
C12	5804(4)	2128(5)	750(8)	56(3)
C13	5984(4)	2286(4)	-92(8)	47(3)
C14	6424(3)	2366(3)	-223(7)	34.1(16)
C15	6713(4)	2316(4)	588(7)	38(2)
C16	6538(3)	2157(3)	1412(8)	38(2)
C17	6607(4)	2514(4)	-1189(8)	38.1(15)
C18	6395(4)	2955(4)	-1441(8)	44(2)
C19	7133(4)	2565(4)	-1163(8)	43(2)
C20	6516(4)	2141(4)	-1886(8)	43(2)
C21	5674(3)	1274(3)	6767(6)	19.0(12)
C22	5909(3)	877(3)	6790(6)	24.7(16)
C23	5983(3)	647(3)	7629(6)	25.4(15)
C24	5809(3)	821(3)	8435(7)	28.4(16)
C25	5588(3)	1225(3)	8426(7)	31.0(17)
C26	5521(3)	1454(3)	7594(6)	26.2(16)
C27	5951(3)	1903(3)	5744(6)	23.1(13)
C28	6399(3)	1794(3)	5554(7)	29.7(18)
C29	6717(3)	2127(3)	5435(8)	36(2)
C30	6609(4)	2572(4)	5530(10)	48(3)
C31	6165(3)	2692(4)	5760(11)	55(3)
C32	5838(3)	2353(3)	5871(10)	46(3)
C33	4160(2)	225(2)	4987(6)	13.5(11)
C34	3673(2)	386(3)	4969(6)	17.7(10)
C35	3504(3)	522(3)	4029(6)	20.5(12)
C36	3636(3)	926(3)	3614(6)	21.9(14)
C37	3479(3)	1046(3)	2722(6)	27.0(16)
C38	3187(3)	756(3)	2249(6)	24.1(13)
C39	3054(3)	358(3)	2669(6)	24.5(15)

C40	3219(3)	246(3)	3524(6)	26.4(16)
C41	2999(3)	892(3)	1313(7)	30.3(16)
C42	2544(3)	823(4)	1111(7)	35(2)
C43	2365(3)	969(4)	282(7)	38(2)
C44	2624(3)	1179(3)	-372(7)	32.1(15)
C45	3085(3)	1227(3)	-196(6)	33.6(18)
C46	3258(3)	1076(3)	639(6)	30.7(17)
C47	2393(4)	1371(4)	-1284(7)	38.3(15)
C48	2740(4)	1624(4)	-1874(8)	44(2)
C49	2213(4)	973(4)	-1868(8)	44(2)
C50	2018(4)	1677(4)	-1007(8)	41.9(19)
C51	3454(3)	606(3)	5855(6)	20.9(10)
C52	3355(3)	135(3)	5615(6)	20.1(12)
C53	3726(3)	683(3)	6727(6)	22.2(13)
C54	3536(3)	526(3)	7581(6)	28.5(17)
C55	3774(3)	586(3)	8418(6)	29.4(16)
C56	4178(3)	802(3)	8419(6)	27.6(15)
C57	4362(3)	969(3)	7594(6)	27.9(16)
C58	4128(3)	904(3)	6751(6)	22.2(14)
C59	3116(3)	977(3)	5656(6)	27.6(14)
C60	3228(3)	1421(3)	5753(8)	37(2)
C61	2927(4)	1774(4)	5587(9)	45(2)
C62	2500(4)	1675(4)	5278(9)	47(2)
C63	2383(4)	1233(4)	5154(12)	60(3)
C64	2682(4)	873(4)	5349(10)	49(3)
C65	5000	0	8123(8)	40.9(10)
C66	5000	0	9088(10)	70(3)
C67	5000	0	1723(7)	40.9(10)
C68	5000	0	759(10)	70(3)
Ru3	5000	5000	8251.1(13)	21.5(3)
Ru4	5000	5000	6591.1(14)	24.7(3)
Cl3	3886.3(8)	3916.9(8)	6709(2)	35.2(5)
O6	4880(2)	4324.4(19)	6639(5)	24.1(11)
O7	4969(2)	4321(2)	8189(5)	26.7(12)
N3	5000	5000	5141(6)	24.6(8)
N4	5000	5000	9795(8)	24.6(8)
C0AA	4687(4)	2506(3)	8394(9)	41(2)

C69	4896(3)	4131(3)	7407(7)	25.0(13)
C70	4830(3)	3630(3)	7386(7)	27.9(12)
C71	4678(3)	3443(3)	6487(7)	28.3(14)
C72	4248(3)	3540(3)	6117(7)	30.5(16)
C73	4096(3)	3370(3)	5268(7)	35.5(19)
C74	4382(3)	3098(3)	4750(7)	35.0(17)
C75	4802(3)	3005(3)	5049(7)	33.6(17)
C76	4951(3)	3196(3)	5918(7)	31.3(17)
C77	4207(4)	2907(3)	3836(8)	39.2(18)
C78	4475(4)	2914(3)	3042(8)	40.0(19)
C79	4324(4)	2771(4)	2220(9)	48(2)
C80	3878(4)	2600(4)	2100(8)	44.1(18)
C81	3622(4)	2574(4)	2925(8)	44(2)
C82	3778(4)	2731(4)	3757(8)	41(2)
C83	3715(4)	2435(4)	1157(8)	48.7(17)
C84	4021(4)	2066(4)	779(9)	52(2)
C85	3239(4)	2262(4)	1179(8)	48(2)
C86	3745(5)	2836(4)	485(9)	54(2)
C87	4719(3)	3360(3)	8291(7)	29.9(12)
C88	5197(3)	3375(3)	7926(7)	29.5(14)
C89	4623(4)	3589(3)	9176(8)	36.0(15)
C90	4854(4)	3508(4)	9985(8)	41.3(19)
C91	4737(4)	3713(4)	10837(9)	51(2)
C92	4357(4)	3977(4)	10885(10)	53(2)
C93	4104(4)	4051(4)	10105(9)	52(2)
C94	4222(4)	3861(3)	9266(8)	40(2)
C95	4467(3)	2916(3)	8177(7)	29.5(14)
C96	4015(3)	2892(3)	7921(7)	32.7(18)
C97	3793(4)	2489(4)	7849(9)	41(2)
C98	4011(3)	2082(3)	8028(8)	40(2)
C99	4471(4)	2096(3)	8333(8)	41(2)
C100	5000	5000	4378(8)	40.9(10)
C102	5000	5000	10558(8)	40.9(10)
Ru4B	0	0	5552.0(11)	6.0(2)
Ru3B	0	0	7217.5(11)	6.5(2)
Cl3B	1188.1(9)	-1136.4(7)	5548.3(18)	32.6(5)
O7B	685.3(15)	-10.7(17)	7165(4)	11.1(9)

O6B	667.3(16)	-159.6(16)	5604(3)	10.3(8)
N4B	0	0	8791(8)	24.6(8)
N3B	0	0	4054(8)	24.6(8)
C70B	1368(2)	-190(2)	6388(5)	10.9(9)
C69B	865(2)	-125(2)	6386(5)	6.9(9)
C71B	1570(2)	-308(2)	5461(5)	11.8(10)
C72B	1518(3)	-722(2)	5038(6)	19.4(13)
C73B	1718(3)	-818(3)	4179(6)	29.0(18)
C74B	1952(3)	-478(3)	3708(6)	24.2(14)
C75B	1980(3)	-54(3)	4088(6)	25.0(15)
C76B	1792(3)	28(3)	4955(6)	20.2(14)
C77B	2173(3)	-580(3)	2780(6)	25.5(14)
C78B	2084(3)	-309(4)	2017(6)	31.4(18)
C79B	2313(3)	-382(4)	1170(6)	34.4(19)
C80B	2613(3)	-720(4)	1048(7)	34.6(17)
C81B	2688(5)	-989(5)	1818(8)	57(4)
C82B	2480(4)	-925(5)	2674(8)	53(3)
C83B	2849(4)	-799(4)	122(7)	45.5(17)
C84B	2903(4)	-355(4)	-441(8)	55(2)
C86B	2549(4)	-1121(5)	-449(9)	57(2)
C85B	3309(4)	-1019(4)	249(8)	50(2)
C87B	1610(2)	-366(2)	7276(5)	12.1(9)
C88B	1633(3)	119(3)	7031(5)	14.9(11)
C89B	1353(2)	-507(3)	8144(5)	13.9(11)
C90B	1487(3)	-326(3)	9009(5)	23.8(16)
C91B	1272(3)	-450(3)	9821(6)	29.8(19)
C92B	923(3)	-757(3)	9790(6)	28.2(18)
C93B	788(3)	-934(3)	8956(6)	22.4(15)
C94B	1003(3)	-815(3)	8124(6)	19.3(14)
C95B	2031(2)	-665(3)	7131(6)	18.0(12)
C1A	2444(3)	-479(3)	6992(8)	36(2)
C99B	2821(3)	-762(4)	6890(8)	41(3)
C98B	2781(3)	-1216(4)	6920(7)	38(2)
C97B	2370(3)	-1404(4)	7038(9)	42(2)
C96B	1988(3)	-1129(3)	7137(7)	27.9(16)
C1B	0	0	9554(8)	40.9(10)
C103	0	0	10571(9)	40.9(10)

C1C	0	0	3292(8)	40.9(10)
C101	0	0	2276(9)	40.9(10)
C1D	5000	5000	3354(10)	139(14)
C1E	5000	5000	11582(11)	139(14)

Table 3 Anisotropic Displacement Parameters ($\text{\AA}^2 \times 10^3$) for twin4_sq. The Anisotropic displacement factor exponent takes the form: - $2\pi^2[h^2a^{*2}U_{11}+2hka^*b^*U_{12}+\dots]$.

Atom	U_{11}	U_{22}	U_{33}	U_{23}	U_{13}	U_{12}
Ru1	8.9(3)	9.9(3)	5.7(3)	0	0	-0.8(3)
Ru2	9.0(3)	13.0(4)	6.0(3)	0	0	-2.4(3)
Cl1	25.4(10)	23.5(9)	34.2(11)	5.9(8)	6.8(8)	5.6(8)
Cl2	39.5(12)	29(1)	25.4(10)	7.1(8)	-7.5(9)	-11.1(9)
O1	17(2)	13.5(16)	12.9(15)	0.7(12)	2.4(14)	-3.8(15)
O2	15(2)	8.3(15)	11.2(15)	-0.8(12)	0.8(14)	-1.1(14)
O4	12.3(16)	21(2)	13.7(16)	3.5(15)	0.8(12)	1.4(15)
O5	8.9(15)	14(2)	12.1(15)	-0.2(14)	1.7(12)	-1.1(14)
N1	32(2)	14(2)	28.4(8)	0	0	-0.9(19)
N2	32(2)	14(2)	28.4(8)	0	0	-0.9(19)
C1	17(3)	13.5(16)	12.4(16)	1.1(12)	0.9(16)	-3.0(15)
C2	19(2)	13.1(16)	22.2(16)	0.2(13)	1.9(15)	-3.1(14)
C3	16(2)	13(2)	24(2)	-0.7(18)	2.1(16)	-4.0(16)
C4	16(2)	16(2)	23.8(18)	-2.5(14)	2.0(15)	-2.4(15)
C5	22(2)	14(2)	23.4(18)	1.8(16)	3.9(16)	-2.2(17)
C6	27(2)	22(3)	27(2)	6(2)	7(2)	5(2)
C7	26(3)	24(3)	27(2)	6(2)	5(2)	1(2)
C8	30(3)	29(3)	31(2)	10(2)	6(2)	4(2)
C9	35(3)	40(4)	37(3)	19(3)	12(3)	13(3)
C10	31(3)	22(3)	30(3)	8(2)	7(2)	6(3)
C11	35(3)	36(4)	33(2)	14(2)	7.9(19)	2(2)
C12	35(3)	92(9)	40(3)	31(4)	3(2)	-8(3)
C13	39(3)	66(7)	36(3)	23(3)	3(2)	-6(3)
C14	39(3)	30(4)	33(2)	6(2)	7.4(19)	-2(2)
C15	36(3)	46(5)	32(3)	10(3)	8(2)	-3(3)
C16	35(3)	44(5)	34(3)	12(3)	8(2)	1(3)
C17	43(3)	38(3)	33(3)	7(2)	8(2)	-5(2)
C18	51(4)	42(3)	37(4)	10(3)	13(3)	0(3)

C19	45(3)	45(5)	38(4)	6(4)	9(2)	-4(3)
C20	49(5)	43(4)	38(3)	3(3)	4(3)	-2(3)
C21	15(3)	18(2)	23.9(18)	-1.1(15)	0.8(16)	-4(2)
C22	29(4)	22(2)	23(2)	-1.5(18)	-1(2)	4(3)
C23	27(4)	24(3)	25(2)	1.3(19)	-6(2)	-5(3)
C24	30(4)	29(3)	26(3)	-1(2)	-5(2)	-5(3)
C25	36(4)	31(3)	26(2)	0(2)	0(2)	-2(3)
C26	28(4)	26(3)	24(2)	-3.1(18)	3(2)	2(3)
C27	18(2)	20(2)	31(3)	2(2)	-0.5(19)	-5.3(16)
C28	19(2)	25(3)	45(5)	5(3)	3(2)	-3.1(18)
C29	22(3)	29(3)	57(6)	9(3)	1(3)	-7(2)
C30	26(3)	29(3)	89(8)	6(3)	-2(4)	-6(2)
C31	27(3)	24(3)	113(10)	0(3)	3(4)	-8(2)
C32	25(3)	21(2)	91(8)	-5(2)	3(3)	-4.4(19)
C33	10.4(15)	17(3)	13.3(16)	1.4(16)	0.5(12)	-2.8(15)
C34	11.6(16)	24(2)	17.4(16)	3.5(15)	1.2(12)	-1.3(15)
C35	16(2)	28(2)	18.5(17)	4.1(15)	-0.6(16)	0.0(18)
C36	20(3)	27(2)	18(2)	3.4(17)	0.7(19)	-1(2)
C37	25(3)	36(3)	20(2)	6.4(19)	-2(2)	-3(3)
C38	17(3)	35(3)	20.5(19)	1.6(18)	0.6(18)	2(2)
C39	19(3)	35(3)	19(2)	1.5(19)	-2(2)	0(2)
C40	24(3)	33(3)	22(2)	4.8(19)	-6(2)	-6(2)
C41	25(2)	42(4)	24(2)	4(2)	-5.1(17)	0(2)
C42	26(3)	47(5)	31(3)	8(3)	-7.9(19)	-3(3)
C43	31(3)	51(5)	32(3)	10(3)	-9(2)	-1(3)
C44	35(3)	33(4)	28(2)	0(2)	-4.7(18)	1(2)
C45	36(3)	39(4)	26(3)	1(3)	-4.3(19)	0(2)
C46	29(3)	37(4)	25(2)	1(2)	-2.3(19)	-1(2)
C47	44(3)	40(3)	31(3)	4(2)	-9(2)	1(2)
C48	50(4)	47(4)	34(4)	7(3)	-8(3)	-4(3)
C49	54(5)	45(4)	34(4)	2(3)	-9(3)	-3(3)
C50	46(3)	45(4)	36(4)	4(3)	-10(3)	3(3)
C51	20(2)	25(2)	17.9(17)	5.3(15)	6.2(15)	0.4(16)
C52	12(2)	26(2)	22(2)	6.3(17)	3.4(18)	1.5(17)
C53	24(2)	24(3)	18.7(18)	3.1(17)	3.3(16)	4(2)
C54	34(3)	33(4)	19(2)	4(2)	5.8(19)	2(3)
C55	41(3)	26(4)	21(2)	1(2)	1(2)	7(3)

C56	40(3)	19(3)	24(2)	-2(2)	1(2)	9(3)
C57	36(3)	23(4)	25(2)	-1(2)	-2(2)	5(3)
C58	25(2)	22(3)	20(2)	0(2)	4.2(18)	5(2)
C59	27(2)	30(2)	25(3)	6.4(19)	6(2)	7.2(18)
C60	30(3)	30(2)	51(6)	6(2)	-1(3)	7(2)
C61	38(3)	35(3)	62(7)	9(3)	0(4)	14(2)
C62	35(3)	46(3)	58(6)	8(3)	2(3)	13(2)
C63	37(3)	47(3)	96(9)	7(4)	-10(4)	12(2)
C64	30(3)	40(3)	76(8)	3(3)	-10(3)	7(2)
C65	44.9(14)	44.6(14)	33.2(9)	0	0	-0.2(10)
C66	93(6)	82(6)	36.2(17)	0	0	6(5)
C67	44.9(14)	44.6(14)	33.2(9)	0	0	-0.2(10)
C68	93(6)	82(6)	36.2(17)	0	0	6(5)
Ru3	17.2(4)	17.2(4)	30.0(7)	0	0	0
Ru4	15.9(4)	15.9(4)	42.3(9)	0	0	0
Cl3	28.4(11)	34.8(12)	42.3(12)	-2.5(10)	-3.1(10)	3(1)
O6	20(3)	17.6(18)	35(2)	-1.9(14)	-0.6(18)	0.3(17)
O7	23(3)	20.6(19)	37(2)	-3.8(14)	-3.9(18)	-0.6(17)
N3	32(2)	14(2)	28.4(8)	0	0	-0.9(19)
N4	32(2)	14(2)	28.4(8)	0	0	-0.9(19)
C0AA	29(3)	27(2)	67(6)	2(2)	-1(3)	-1(2)
C69	19(3)	20.3(17)	35(2)	-1.4(13)	-3.2(18)	1.9(16)
C70	28(3)	22.4(18)	33.8(19)	-0.9(14)	-1.7(17)	0.3(16)
C71	29(2)	22(3)	34(2)	-0.2(18)	-2.5(17)	0.7(19)
C72	29(2)	25(3)	38(3)	1(2)	-3.9(18)	0(2)
C73	36(3)	31(4)	39(3)	-2(3)	-8(2)	4(3)
C74	38(3)	29(4)	38(2)	0(2)	-5.4(19)	3(2)
C75	36(3)	28(4)	36(3)	-2(3)	-4(2)	5(2)
C76	34(3)	26(4)	35(3)	0(2)	-3(2)	4(2)
C77	43(3)	35(4)	39(2)	0(2)	-6.4(19)	-1(3)
C78	45(3)	33(5)	42(3)	0(2)	-3(2)	-3(3)
C79	57(3)	45(6)	41(3)	0(3)	-2(2)	-16(3)
C80	56(3)	39(4)	36(2)	2(2)	-5(2)	-14(3)
C81	52(4)	44(5)	35(3)	4(3)	-8(2)	-12(3)
C82	44(3)	45(5)	34(3)	0(3)	-6(2)	-5(3)
C83	62(4)	45(4)	39(3)	0(2)	-8(2)	-13(3)
C84	63(4)	50(4)	42(4)	-6(3)	-10(3)	-11(3)

C85	62(4)	41(5)	39(5)	0(3)	-10(3)	-12(3)
C86	71(6)	50(4)	42(4)	3(3)	-9(3)	-14(4)
C87	31(2)	25(2)	34(2)	-0.1(15)	-1.2(17)	-0.1(17)
C88	30(2)	25(3)	34(3)	0(2)	-2.5(18)	1.3(18)
C89	42(3)	28(3)	37(2)	-5(2)	3(2)	-5(2)
C90	43(4)	42(4)	38(2)	-1(2)	1(2)	-10(3)
C91	57(4)	54(5)	41(3)	-8(3)	5(3)	-12(4)
C92	58(4)	53(5)	49(3)	-7(3)	8(3)	-11(4)
C93	59(4)	50(5)	48(3)	-14(3)	9(3)	0(4)
C94	44(3)	34(4)	43(3)	-5(3)	6(2)	-1(3)
C95	29(2)	25(2)	34(4)	-3.4(19)	3(2)	0.2(17)
C96	29(3)	29(3)	41(5)	-3(3)	2(2)	0.5(19)
C97	33(3)	31(3)	59(6)	-5(3)	2(3)	-2(2)
C98	31(3)	30(3)	59(6)	-2(3)	6(3)	-3(2)
C99	32(3)	29(3)	62(6)	-1(3)	5(3)	-2(2)
C100	44.9(14)	44.6(14)	33.2(9)	0	0	-0.2(10)
C102	44.9(14)	44.6(14)	33.2(9)	0	0	-0.2(10)
Ru4B	6.8(3)	6.8(3)	4.4(4)	0	0	0
Ru3B	8.8(3)	8.8(3)	1.9(4)	0	0	0
Cl3B	50.6(14)	20.4(10)	26.8(10)	-3.3(8)	13.1(9)	-12.6(9)
O7B	6.5(15)	21(2)	5.8(14)	-2.8(15)	-0.9(12)	0.4(14)
O6B	9.1(14)	16.4(19)	5.4(13)	-1.3(12)	0.6(11)	2.1(13)
N4B	32(2)	14(2)	28.4(8)	0	0	-0.9(19)
N3B	32(2)	14(2)	28.4(8)	0	0	-0.9(19)
C70B	8.5(15)	15(2)	9.7(14)	2.0(14)	1.4(11)	0.5(13)
C69B	8.5(14)	7(2)	5.4(14)	1.8(14)	1.5(11)	-0.2(13)
C71B	9(2)	15.2(19)	11.5(16)	0.5(13)	2.5(15)	0.4(16)
C72B	27(3)	16.8(19)	15(2)	-2.1(15)	5(2)	-1.9(18)
C73B	37(4)	29(3)	20(2)	-7.6(18)	12(3)	-6(2)
C74B	23(3)	32(2)	18(2)	-2.6(16)	4(2)	-4(2)
C75B	27(4)	32(2)	16(2)	-0.7(18)	8(2)	-6(2)
C76B	24(3)	22(2)	14(2)	0.8(17)	6(2)	-7(2)
C77B	19(3)	40(3)	18.3(19)	-5.2(18)	3.7(18)	-5(2)
C78B	26(4)	47(4)	21(2)	-1(2)	6(2)	1(3)
C79B	27(4)	56(4)	21(2)	-2(2)	7(2)	2(3)
C80B	23(3)	55(4)	26(2)	-5(2)	5(2)	0(3)
C81B	62(6)	78(5)	30(3)	5(3)	20(3)	33(5)

C82B	60(6)	68(5)	30(3)	5(3)	18(3)	29(5)
C83B	39(3)	69(4)	29(3)	-6(2)	13(2)	5(3)
C84B	54(5)	71(4)	38(4)	-1(3)	20(4)	7(3)
C86B	51(4)	80(5)	39(4)	-12(3)	10(3)	-1(4)
C85B	40(3)	67(5)	42(4)	-5(4)	14(3)	3(3)
C87B	9.0(17)	15.8(19)	11.4(16)	0.5(14)	-0.4(13)	1.5(14)
C88B	13(2)	15.9(19)	16(2)	0.0(15)	-2.8(17)	0.3(16)
C89B	11(2)	19(2)	12.2(17)	2.6(15)	1.4(14)	4.1(18)
C90B	22(3)	36(4)	13.2(19)	-1.5(18)	2.5(17)	-7(3)
C91B	31(3)	44(4)	15(2)	1(2)	5.9(19)	-9(3)
C92B	26(3)	40(4)	18(2)	3(2)	6(2)	-5(3)
C93B	21(3)	28(3)	18(2)	5(2)	3.7(19)	1(2)
C94B	18(2)	23(3)	18(2)	3.1(19)	2.1(18)	-1(2)
C95B	13.3(18)	22(2)	19(3)	5.8(19)	4.8(17)	6.6(15)
C1A	14(2)	28(3)	66(7)	17(3)	9(2)	5.6(18)
C99B	19(3)	35(3)	68(7)	22(3)	14(3)	12(2)
C98B	26(3)	34(3)	54(6)	21(3)	14(3)	13(2)
C97B	28(3)	28(3)	69(7)	15(3)	19(3)	14(2)
C96B	21(3)	23(2)	40(4)	6(2)	9(3)	6.1(17)
C1B	44.9(14)	44.6(14)	33.2(9)	0	0	-0.2(10)
C103	44.9(14)	44.6(14)	33.2(9)	0	0	-0.2(10)
C1C	44.9(14)	44.6(14)	33.2(9)	0	0	-0.2(10)
C101	44.9(14)	44.6(14)	33.2(9)	0	0	-0.2(10)
C1D	190(20)	190(20)	33(2)	0	0	0
C1E	190(20)	190(20)	33(2)	0	0	0

Table 4 Bond Lengths for twin4_sq.

Atom	Atom	Length/Å	Atom	Atom	Length/Å
Ru1	Ru2	2.3940(10)	Ru4	O6 ³	2.038(6)
Ru1	O2	2.049(5)	Ru4	O6	2.038(6)
Ru1	O2 ¹	2.049(5)	Ru4	N3	2.085(9)
Ru1	O5 ¹	2.047(5)	Cl3	C72	1.768(10)
Ru1	O5	2.047(5)	O6	C69	1.245(11)
Ru1	N1	2.239(10)	O7	C69	1.276(11)
Ru2	O1	2.042(5)	N3	C100	1.097(8)
Ru2	O1 ¹	2.042(5)	N4	C102	1.097(8)
Ru2	O4 ¹	2.039(5)	C0AA	C95	1.417(13)

Ru2	O4	2.039(5)	C0AAC99	1.380(14)
Ru2	N2	2.375(10)	C69 C70	1.501(12)
Cl1	C6	1.748(9)	C70 C71	1.479(14)
Cl2	C36	1.744(9)	C70 C87	1.564(14)
O1	C1	1.272(9)	C70 C88	1.536(13)
O2	C1	1.268(9)	C71 C72	1.411(13)
O4	C33	1.276(9)	C71 C76	1.363(13)
O5	C33	1.245(9)	C72 C73	1.397(14)
N1	C65	1.097(8)	C73 C74	1.388(14)
N2	C67	1.096(8)	C74 C75	1.348(13)
C1	C2	1.514(10)	C74 C77	1.524(14)
C2	C3	1.524(11)	C75 C76	1.442(14)
C2	C4	1.566(12)	C77 C78	1.391(16)
C2	C5	1.496(12)	C77 C82	1.379(15)
C3	C4	1.488(11)	C78 C79	1.334(16)
C4	C21	1.524(12)	C79 C80	1.429(16)
C4	C27	1.519(11)	C80 C81	1.411(17)
C5	C6	1.405(11)	C80 C83	1.521(16)
C5	C10	1.397(11)	C81 C82	1.364(15)
C6	C7	1.373(12)	C83 C84	1.524(18)
C7	C8	1.388(12)	C83 C85	1.502(17)
C8	C9	1.370(13)	C83 C86	1.537(16)
C8	C11	1.480(13)	C87 C88	1.514(14)
C9	C10	1.402(12)	C87 C89	1.469(14)
C11	C12	1.352(15)	C87 C95	1.526(13)
C11	C16	1.430(14)	C89 C90	1.372(15)
C12	C13	1.405(15)	C89 C94	1.446(15)
C13	C14	1.339(14)	C90 C91	1.413(16)
C14	C15	1.456(14)	C91 C92	1.375(17)
C14	C17	1.554(14)	C92 C93	1.367(18)
C15	C16	1.379(13)	C93 C94	1.377(16)
C17	C18	1.498(15)	C95 C96	1.392(13)
C17	C19	1.570(15)	C96 C97	1.369(14)
C17	C20	1.518(15)	C97 C98	1.396(15)
C21	C22	1.371(12)	C98 C99	1.434(15)
C21	C26	1.380(12)	C100 C1D	1.472(12)
C22	C23	1.403(12)	C102 C1E	1.473(12)

C23	C24	1.371(13)	Ru4B Ru3B	2.3941(13)
C24	C25	1.367(13)	Ru4B O6B ⁵	2.038(5)
C25	C26	1.389(13)	Ru4B O6B ⁶	2.038(5)
C27	C28	1.397(12)	Ru4B O6B	2.038(5)
C27	C32	1.389(13)	Ru4B O6B ⁷	2.038(5)
C28	C29	1.378(13)	Ru4B N3B	2.154(12)
C29	C30	1.365(15)	Ru3B O7B	2.036(4)
C30	C31	1.405(15)	Ru3B O7B ⁶	2.036(4)
C31	C32	1.406(14)	Ru3B O7B ⁵	2.036(4)
C33	C34	1.523(10)	Ru3B O7B ⁷	2.036(4)
C34	C35	1.497(11)	Ru3B N4B	2.263(12)
C34	C51	1.571(12)	Cl3B C72B	1.735(8)
C34	C52	1.520(11)	O7B C69B	1.287(8)
C35	C36	1.397(11)	O6B C69B	1.272(8)
C35	C40	1.383(12)	N4B C1B	1.097(8)
C36	C37	1.410(11)	N3B C1C	1.095(8)
C37	C38	1.398(12)	C70B C69B	1.504(9)
C38	C39	1.383(12)	C70B C71B	1.502(10)
C38	C41	1.512(12)	C70B C87B	1.556(10)
C39	C40	1.365(12)	C70B C88B	1.520(10)
C41	C42	1.397(13)	C71B C72B	1.381(10)
C41	C46	1.352(13)	C71B C76B	1.399(10)
C42	C43	1.375(13)	C72B C73B	1.399(11)
C43	C44	1.365(14)	C73B C74B	1.398(12)
C44	C45	1.398(14)	C74B C75B	1.375(12)
C44	C47	1.585(14)	C74B C77B	1.516(11)
C45	C46	1.380(13)	C75B C76B	1.387(11)
C47	C48	1.532(15)	C77B C78B	1.386(13)
C47	C49	1.544(15)	C77B C82B	1.380(14)
C47	C50	1.491(15)	C78B C79B	1.411(12)
C51	C52	1.470(12)	C79B C80B	1.354(14)
C51	C53	1.510(12)	C80B C81B	1.382(16)
C51	C59	1.518(12)	C80B C83B	1.522(13)
C53	C54	1.429(12)	C81B C82B	1.389(14)
C53	C58	1.361(12)	C83B C84B	1.555(17)
C54	C55	1.409(13)	C83B C86B	1.544(17)
C55	C56	1.359(14)	C83B C85B	1.524(15)

C56	C57	1.396(13)	C87B	C88B	1.482(10)
C57	C58	1.410(12)	C87B	C89B	1.523(10)
C59	C60	1.367(14)	C87B	C95B	1.545(10)
C59	C64	1.394(14)	C89B	C90B	1.411(11)
C60	C61	1.398(14)	C89B	C94B	1.385(11)
C61	C62	1.375(16)	C90B	C91B	1.381(11)
C62	C63	1.368(17)	C91B	C92B	1.383(13)
C63	C64	1.417(15)	C92B	C93B	1.369(12)
C65	C66	1.386(15)	C93B	C94B	1.401(11)
C67	C68	1.386(15)	C95B	C1A	1.358(12)
Ru3	Ru4	2.386(2)	C95B	C96B	1.385(11)
Ru3	O7 ²	2.021(6)	C1A	C99B	1.407(13)
Ru3	O7 ³	2.021(6)	C99B	C98B	1.352(15)
Ru3	O7 ⁴	2.021(6)	C98B	C97B	1.352(14)
Ru3	O7	2.021(6)	C97B	C96B	1.405(12)
Ru3	N4	2.219(12)	C1B	C103	1.461(9)
Ru4	O6 ⁴	2.038(6)	C1C	C101	1.460(9)
Ru4	O6 ²	2.038(6)			

¹1-X,-Y,+Z; ²+Y,1-X,+Z; ³1-X,1-Y,+Z; ⁴1-Y,+X,+Z; ⁵-X,-Y,+Z; ⁶-Y,+X,+Z; ⁷+Y,-X,+Z

Table 5 Bond Angles for twin4_sq.

Atom	Atom	Atom	Angle/°	Atom	Atom	Atom	Angle/°
O2	Ru1	Ru2	87.71(14)	O6 ³	Ru4	Ru3	88.07(19)
O2 ¹	Ru1	Ru2	87.71(14)	O6 ²	Ru4	Ru3	88.07(19)
O2 ¹	Ru1	O2	175.4(3)	O6 ³	Ru4	O6 ⁴	89.935(14)
O2	Ru1	N1	92.29(14)	O6	Ru4	O6 ²	89.936(14)
O2 ¹	Ru1	N1	92.29(14)	O6	Ru4	O6 ³	176.1(4)
O5 ¹	Ru1	Ru2	87.47(14)	O6 ²	Ru4	O6 ⁴	176.1(4)
O5	Ru1	Ru2	87.47(14)	O6	Ru4	O6 ⁴	89.934(15)
O5 ¹	Ru1	O2	89.43(18)	O6 ³	Ru4	O6 ²	89.935(15)
O5	Ru1	O2 ¹	89.43(18)	O6 ²	Ru4	N3	91.93(19)
O5	Ru1	O2	90.37(18)	O6	Ru4	N3	91.93(19)
O5 ¹	Ru1	O2 ¹	90.37(18)	O6 ⁴	Ru4	N3	91.93(19)
O5	Ru1	O5 ¹	174.9(3)	O6 ³	Ru4	N3	91.93(19)
O5	Ru1	N1	92.53(14)	N3	Ru4	Ru3	180.0
O5 ¹	Ru1	N1	92.53(14)	C69	O6	Ru4	118.4(6)
N1	Ru1	Ru2	180.0	C69	O7	Ru3	119.1(6)

O1 ¹	Ru2	Ru1	88.06(15)	C100	N3	Ru4	180.0
O1	Ru2	Ru1	88.06(15)	C102	N4	Ru3	180.0
O1	Ru2	O1 ¹	176.1(3)	C99	C0AA	C95	122.0(10)
O1	Ru2	N2	91.94(15)	O6	C69	O7	125.8(8)
O1 ¹	Ru2	N2	91.94(15)	O6	C69	C70	115.7(8)
O4	Ru2	Ru1	87.63(15)	O7	C69	C70	118.5(8)
O4 ¹	Ru2	Ru1	87.63(15)	C69	C70	C87	121.2(8)
O4	Ru2	O1 ¹	90.68(19)	C69	C70	C88	112.7(7)
O4 ¹	Ru2	O1	90.68(19)	C71	C70	C69	115.5(8)
O4 ¹	Ru2	O1 ¹	89.16(19)	C71	C70	C87	118.0(8)
O4	Ru2	O1	89.16(19)	C71	C70	C88	118.3(8)
O4 ¹	Ru2	O4	175.3(3)	C88	C70	C87	58.5(6)
O4 ¹	Ru2	N2	92.37(15)	C72	C71	C70	121.9(8)
O4	Ru2	N2	92.37(15)	C76	C71	C70	122.9(9)
N2	Ru2	Ru1	180.0	C76	C71	C72	114.9(9)
C1	O1	Ru2	117.3(4)	C71	C72	Cl3	119.9(7)
C1	O2	Ru1	116.8(4)	C73	C72	Cl3	116.9(7)
C33	O4	Ru2	117.1(4)	C73	C72	C71	123.1(9)
C33	O5	Ru1	116.8(4)	C74	C73	C72	118.8(9)
C65	N1	Ru1	180.0	C73	C74	C77	118.1(9)
C67	N2	Ru2	180.0	C75	C74	C73	120.9(9)
O1	C1	C2	115.9(6)	C75	C74	C77	121.0(9)
O2	C1	O1	127.6(6)	C74	C75	C76	118.6(9)
O2	C1	C2	116.5(7)	C71	C76	C75	123.3(9)
C1	C2	C3	115.7(6)	C78	C77	C74	120.4(9)
C1	C2	C4	121.1(7)	C82	C77	C74	121.8(10)
C3	C2	C4	57.6(5)	C82	C77	C78	117.8(10)
C5	C2	C1	115.4(7)	C79	C78	C77	122.0(11)
C5	C2	C3	118.6(6)	C78	C79	C80	122.1(12)
C5	C2	C4	116.3(6)	C79	C80	C83	121.2(11)
C4	C3	C2	62.6(5)	C81	C80	C79	114.6(10)
C3	C4	C2	59.8(5)	C81	C80	C83	124.0(10)
C3	C4	C21	118.4(7)	C82	C81	C80	122.4(11)
C3	C4	C27	118.4(7)	C81	C82	C77	120.9(11)
C21	C4	C2	122.7(6)	C80	C83	C84	111.0(10)
C27	C4	C2	117.3(7)	C80	C83	C86	106.9(9)
C27	C4	C21	111.5(7)	C84	C83	C86	107.4(10)

C6	C5	C2	123.6(7)	C85	C83	C80	113.0(10)
C10	C5	C2	120.7(7)	C85	C83	C84	108.8(10)
C10	C5	C6	115.7(8)	C85	C83	C86	109.5(10)
C5	C6	C11	119.8(6)	C88	C87	C70	59.8(6)
C7	C6	C11	118.1(7)	C88	C87	C95	116.6(8)
C7	C6	C5	122.1(8)	C89	C87	C70	121.6(8)
C6	C7	C8	121.2(9)	C89	C87	C88	117.9(9)
C7	C8	C11	119.8(8)	C89	C87	C95	113.5(8)
C9	C8	C7	118.3(8)	C95	C87	C70	117.2(8)
C9	C8	C11	121.9(8)	C87	C88	C70	61.7(6)
C8	C9	C10	120.7(9)	C90	C89	C87	123.7(9)
C5	C10	C9	121.9(8)	C90	C89	C94	115.8(10)
C12	C11	C8	121.6(9)	C94	C89	C87	119.7(10)
C12	C11	C16	117.3(9)	C89	C90	C91	122.4(11)
C16	C11	C8	121.1(9)	C92	C91	C90	119.5(12)
C11	C12	C13	121.4(10)	C93	C92	C91	120.2(12)
C14	C13	C12	123.4(11)	C92	C93	C94	120.8(12)
C13	C14	C15	116.4(9)	C93	C94	C89	121.2(11)
C13	C14	C17	121.1(10)	C0AAC95	C87	C87	119.5(9)
C15	C14	C17	122.5(9)	C96	C95	C0AA	117.4(9)
C16	C15	C14	120.0(9)	C96	C95	C87	123.0(8)
C15	C16	C11	121.2(10)	C97	C96	C95	121.8(10)
C14	C17	C19	110.8(9)	C96	C97	C98	121.3(10)
C18	C17	C14	108.5(9)	C97	C98	C99	118.2(9)
C18	C17	C19	109.8(9)	C0AAC99	C98	C98	119.2(10)
C18	C17	C20	113.8(10)	N3	C100	C1D	180.0
C20	C17	C14	108.7(8)	N4	C102	C1E	180.000(10)
C20	C17	C19	105.2(9)	O6B	Ru4B	Ru3B	87.88(13)
C22	C21	C4	123.4(8)	O6B ⁵	Ru4B	Ru3B	87.88(13)
C22	C21	C26	118.6(8)	O6B ⁶	Ru4B	Ru3B	87.88(13)
C26	C21	C4	117.9(7)	O6B ⁷	Ru4B	Ru3B	87.88(13)
C21	C22	C23	121.3(8)	O6B ⁵	Ru4B	O6B	175.8(3)
C24	C23	C22	119.0(8)	O6B ⁷	Ru4B	O6B ⁵	89.922(10)
C25	C24	C23	120.2(9)	O6B ⁷	Ru4B	O6B	89.919(10)
C24	C25	C26	120.4(9)	O6B ⁶	Ru4B	O6B	89.925(10)
C21	C26	C25	120.4(8)	O6B ⁶	Ru4B	O6B ⁵	89.922(10)
C28	C27	C4	121.8(8)	O6B ⁷	Ru4B	O6B ⁶	175.8(3)

C32	C27	C4	119.5(8)	O6B	Ru4B	N3B	92.12(13)
C32	C27	C28	118.5(8)	O6B ⁶	Ru4B	N3B	92.12(13)
C29	C28	C27	120.7(9)	O6B ⁷	Ru4B	N3B	92.12(13)
C30	C29	C28	121.4(9)	O6B ⁵	Ru4B	N3B	92.12(13)
C29	C30	C31	119.3(10)	N3B	Ru4B	Ru3B	180.0
C30	C31	C32	119.5(10)	O7B ⁷	Ru3B	Ru4B	87.90(14)
C27	C32	C31	120.5(10)	O7B	Ru3B	Ru4B	87.90(14)
O4	C33	C34	114.1(6)	O7B ⁶	Ru3B	Ru4B	87.90(14)
O5	C33	O4	127.8(6)	O7B ⁵	Ru3B	Ru4B	87.90(14)
O5	C33	C34	118.1(6)	O7B ⁵	Ru3B	O7B	175.8(3)
C33	C34	C51	120.6(7)	O7B ⁶	Ru3B	O7B ⁵	89.923(11)
C35	C34	C33	114.8(7)	O7B ⁶	Ru3B	O7B ⁷	175.8(3)
C35	C34	C51	118.7(6)	O7B ⁵	Ru3B	O7B ⁷	89.923(11)
C35	C34	C52	118.3(6)	O7B ⁷	Ru3B	O7B	89.922(11)
C52	C34	C33	115.2(6)	O7B ⁶	Ru3B	O7B	89.923(11)
C52	C34	C51	56.8(5)	O7B ⁵	Ru3B	N4B	92.10(14)
C36	C35	C34	121.5(7)	O7B	Ru3B	N4B	92.10(14)
C40	C35	C34	121.3(7)	O7B ⁶	Ru3B	N4B	92.10(14)
C40	C35	C36	117.1(8)	O7B ⁷	Ru3B	N4B	92.10(14)
C35	C36	Cl2	121.2(6)	N4B	Ru3B	Ru4B	180.0
C35	C36	C37	120.9(8)	C69B	O7B	Ru3B	116.8(4)
C37	C36	Cl2	117.8(7)	C69B	O6B	Ru4B	117.6(4)
C38	C37	C36	119.4(8)	C1B	N4B	Ru3B	180.0
C37	C38	C41	119.7(8)	C1C	N3B	Ru4B	180.0
C39	C38	C37	119.4(8)	C69B	C70B	C87B	120.3(6)
C39	C38	C41	120.7(8)	C69B	C70B	C88B	115.9(6)
C40	C39	C38	119.9(8)	C71B	C70B	C69B	115.1(6)
C39	C40	C35	123.2(8)	C71B	C70B	C87B	117.7(5)
C42	C41	C38	120.2(8)	C71B	C70B	C88B	118.2(6)
C46	C41	C38	122.4(8)	C88B	C70B	C87B	57.6(5)
C46	C41	C42	117.4(9)	O7B	C69B	C70B	116.3(6)
C43	C42	C41	120.5(9)	O6B	C69B	O7B	126.8(6)
C44	C43	C42	121.5(9)	O6B	C69B	C70B	116.7(6)
C43	C44	C45	118.2(9)	C72B	C71B	C70B	123.6(6)
C43	C44	C47	119.3(9)	C72B	C71B	C76B	117.3(7)
C45	C44	C47	122.4(9)	C76B	C71B	C70B	118.9(6)
C46	C45	C44	119.3(9)	C71B	C72B	Cl3B	120.5(6)

C41	C46	C45	122.8(9)	C71B	C72B	C73B	121.5(7)
C48	C47	C44	110.0(8)	C73B	C72B	C13B	117.9(6)
C48	C47	C49	108.0(9)	C74B	C73B	C72B	119.4(8)
C49	C47	C44	108.9(8)	C73B	C74B	C77B	119.8(8)
C50	C47	C44	108.7(9)	C75B	C74B	C73B	119.8(8)
C50	C47	C48	110.5(9)	C75B	C74B	C77B	120.3(8)
C50	C47	C49	110.7(9)	C74B	C75B	C76B	119.6(8)
C52	C51	C34	59.9(5)	C75B	C76B	C71B	122.1(7)
C52	C51	C53	116.5(7)	C78B	C77B	C74B	119.9(8)
C52	C51	C59	120.9(8)	C82B	C77B	C74B	122.0(9)
C53	C51	C34	120.9(7)	C82B	C77B	C78B	118.0(8)
C53	C51	C59	113.6(7)	C77B	C78B	C79B	120.0(9)
C59	C51	C34	115.1(7)	C80B	C79B	C78B	123.0(10)
C51	C52	C34	63.4(5)	C79B	C80B	C81B	115.4(9)
C54	C53	C51	116.8(7)	C79B	C80B	C83B	122.1(10)
C58	C53	C51	124.3(8)	C81B	C80B	C83B	122.5(10)
C58	C53	C54	118.9(8)	C80B	C81B	C82B	124.0(11)
C55	C54	C53	119.5(9)	C77B	C82B	C81B	119.5(11)
C56	C55	C54	120.3(9)	C80B	C83B	C84B	111.9(10)
C55	C56	C57	120.8(9)	C80B	C83B	C86B	107.1(9)
C56	C57	C58	119.3(9)	C80B	C83B	C85B	112.0(9)
C53	C58	C57	121.2(8)	C86B	C83B	C84B	107.9(10)
C60	C59	C51	121.3(8)	C85B	C83B	C84B	109.5(9)
C60	C59	C64	118.0(9)	C85B	C83B	C86B	108.4(10)
C64	C59	C51	120.7(9)	C88B	C87B	C70B	60.0(5)
C59	C60	C61	123.4(10)	C88B	C87B	C89B	119.0(6)
C62	C61	C60	118.9(11)	C88B	C87B	C95B	119.3(6)
C63	C62	C61	118.7(10)	C89B	C87B	C70B	122.3(6)
C62	C63	C64	122.6(11)	C89B	C87B	C95B	110.9(6)
C59	C64	C63	118.3(11)	C95B	C87B	C70B	117.1(6)
N1	C65	C66	180.0	C87B	C88B	C70B	62.4(5)
N2	C67	C68	180.0	C90B	C89B	C87B	118.4(7)
O7 ²	Ru3	Ru4	87.48(19)	C94B	C89B	C87B	122.7(6)
O7 ³	Ru3	Ru4	87.48(19)	C94B	C89B	C90B	118.8(7)
O7 ⁴	Ru3	Ru4	87.48(19)	C91B	C90B	C89B	120.9(8)
O7	Ru3	Ru4	87.48(19)	C90B	C91B	C92B	119.7(8)
O7 ³	Ru3	O7 ²	89.889(19)	C93B	C92B	C91B	120.0(8)

O7	Ru3	O7 ³	175.0(4)	C92B	C93B	C94B	121.2(8)
O7	Ru3	O7 ²	89.889(18)	C89B	C94B	C93B	119.4(7)
O7 ⁴	Ru3	O7 ²	175.0(4)	C1A	C95B	C87B	121.1(7)
O7 ⁴	Ru3	O7 ³	89.889(18)	C1A	C95B	C96B	119.2(8)
O7	Ru3	O7 ⁴	89.889(19)	C96B	C95B	C87B	119.7(7)
O7 ²	Ru3	N4	92.52(19)	C95B	C1A	C99B	119.4(9)
O7 ³	Ru3	N4	92.52(19)	C98B	C99B	C1A	121.5(10)
O7	Ru3	N4	92.52(19)	C99B	C98B	C97B	119.5(9)
O7 ⁴	Ru3	N4	92.52(19)	C98B	C97B	C96B	120.2(10)
N4	Ru3	Ru4	180.0	C95B	C96B	C97B	120.1(8)
O6 ⁴	Ru4	Ru3	88.07(19)	N4B	C1B	C103	180.0
O6	Ru4	Ru3	88.07(19)	N3B	C1C	C101	180.0

¹1-X,-Y,+Z; ²1-Y,+X,+Z; ³1-X,1-Y,+Z; ⁴+Y,1-X,+Z; ⁵-X,-Y,+Z; ⁶+Y,-X,+Z; ⁷-Y,+X,+Z

Table 6 Torsion Angles for twin4_sq.

A	B	C	D	Angle/°	A	B	C	D	Angle/°
Ru1	O2	C1	O1	13.1(10)	Ru3	O7	C69	O6	6.8(12)
Ru1	O2	C1	C2	-167.9(5)	Ru3	O7	C69	C70	-174.3(5)
Ru1	O5	C33	O4	14.7(10)	Ru4	O6	C69	O7	2.2(11)
Ru1	O5	C33	C34	-167.7(5)	Ru4	O6	C69	C70	-176.6(5)
Ru2	O1	C1	O2	0.2(10)	Cl3	C72	C73	C74	175.7(8)
Ru2	O1	C1	C2	-178.8(5)	O6	C69	C70	C71	-10.2(11)
Ru2	O4	C33	O5	0.2(10)	O6	C69	C70	C87	-164.1(8)
Ru2	O4	C33	C34	-177.5(4)	O6	C69	C70	C88	130.0(8)
Cl1	C6	C7	C8	178.7(7)	O7	C69	C70	C71	170.8(8)
Cl2	C36	C37	C38	176.2(7)	O7	C69	C70	C87	16.9(12)
O1	C1	C2	C3	140.5(7)	O7	C69	C70	C88	-48.9(11)
O1	C1	C2	C4	-153.4(7)	C0AA	C95	C96	C97	-2.3(16)
O1	C1	C2	C5	-4.2(10)	C69	C70	C71	C72	-66.4(12)
O2	C1	C2	C3	-38.7(10)	C69	C70	C71	C76	107.9(10)
O2	C1	C2	C4	27.4(10)	C69	C70	C87	C88	-99.1(9)
O2	C1	C2	C5	176.6(7)	C69	C70	C87	C89	7.0(13)
O4	C33	C34	C35	0.8(9)	C69	C70	C87	C95	154.4(8)
O4	C33	C34	C51	-151.8(7)	C69	C70	C88	C87	113.7(9)
O4	C33	C34	C52	143.4(7)	C70	C71	C72	Cl3	2.9(13)
O5	C33	C34	C35	-177.1(7)	C70	C71	C72	C73	179.6(9)
O5	C33	C34	C51	30.3(10)	C70	C71	C76	C75	178.7(9)

O5 C33C34C52	-34.5(10)	C70 C87 C89 C90	-124.3(11)
C1 C2 C3 C4	111.9(8)	C70 C87 C89 C94	66.4(13)
C1 C2 C4 C3	-102.5(8)	C70 C87 C95 C0AA	112.9(11)
C1 C2 C4 C21	3.8(11)	C70 C87 C95 C96	-71.4(12)
C1 C2 C4 C27	148.8(7)	C71 C70 C87 C88	107.6(9)
C1 C2 C5 C6	-65.3(11)	C71 C70 C87 C89	-146.2(9)
C1 C2 C5 C10	113.7(9)	C71 C70 C87 C95	1.2(12)
C2 C3 C4 C21	-113.3(7)	C71 C70 C88 C87	-107.2(9)
C2 C3 C4 C27	106.7(8)	C71 C72 C73 C74	-1.1(15)
C2 C4 C21C22	53.0(11)	C72 C71 C76 C75	-6.7(14)
C2 C4 C21C26	-130.5(8)	C72 C73 C74 C75	-1.3(15)
C2 C4 C27C28	-81.0(11)	C72 C73 C74 C77	178.6(9)
C2 C4 C27C32	103.2(11)	C73 C74 C75 C76	-0.3(15)
C2 C5 C6 C11	2.3(12)	C73 C74 C77 C78	135.4(11)
C2 C5 C6 C7	-177.3(8)	C73 C74 C77 C82	-43.2(15)
C2 C5 C10C9	178.2(9)	C74 C75 C76 C71	4.7(15)
C3 C2 C4 C21	106.3(8)	C74 C77 C78 C79	-176.5(10)
C3 C2 C4 C27	-108.6(8)	C74 C77 C82 C81	178.0(10)
C3 C2 C5 C6	151.0(8)	C75 C74 C77 C78	-44.6(15)
C3 C2 C5 C10	-30.0(11)	C75 C74 C77 C82	136.8(11)
C3 C4 C21C22	123.6(9)	C76 C71 C72 C13	-171.8(7)
C3 C4 C21C26	-60.0(10)	C76 C71 C72 C73	4.9(14)
C3 C4 C27C28	-149.6(8)	C77 C74 C75 C76	179.7(9)
C3 C4 C27C32	34.6(13)	C77 C78 C79 C80	-0.2(18)
C4 C2 C5 C6	85.3(10)	C78 C77 C82 C81	-0.6(17)
C4 C2 C5 C10	-95.6(9)	C78 C79 C80 C81	-3.1(17)
C4 C21C22C23	178.5(8)	C78 C79 C80 C83	-179.4(11)
C4 C21C26C25	-179.5(8)	C79 C80 C81 C82	4.7(17)
C4 C27C28C29	-180.0(9)	C79 C80 C83 C84	56.5(15)
C4 C27C32C31	179.2(11)	C79 C80 C83 C85	179.1(11)
C5 C2 C3 C4	-104.5(7)	C79 C80 C83 C86	-60.3(15)
C5 C2 C4 C3	108.6(7)	C80 C81 C82 C77	-3.0(18)
C5 C2 C4 C21	-145.1(7)	C81 C80 C83 C84	-119.4(13)
C5 C2 C4 C27	-0.1(10)	C81 C80 C83 C85	3.2(17)
C5 C6 C7 C8	-1.7(15)	C81 C80 C83 C86	123.7(13)
C6 C5 C10C9	-2.7(14)	C82 C77 C78 C79	2.2(17)
C6 C7 C8 C9	-1.4(15)	C83 C80 C81 C82	-179.1(11)

C6 C7 C8 C11	179.4(9)	C87 C70 C71 C72	88.4(11)
C7 C8 C9 C10	2.3(16)	C87 C70 C71 C76	-97.4(11)
C7 C8 C11 C12	133.5(12)	C87 C89 C90 C91	-176.1(10)
C7 C8 C11 C16	-45.6(15)	C87 C89 C94 C93	174.8(10)
C8 C9 C10 C5	-0.2(16)	C87 C95 C96 C97	-178.1(10)
C8 C11 C12 C13	-176.9(12)	C88 C70 C71 C72	155.6(9)
C8 C11 C16 C15	177.5(10)	C88 C70 C71 C76	-30.1(14)
C9 C8 C11 C12	-45.6(17)	C88 C70 C87 C89	106.1(10)
C9 C8 C11 C16	135.2(11)	C88 C70 C87 C95	-106.5(9)
C10 C5 C6 C11	-176.7(7)	C88 C87 C89 C90	-54.3(13)
C10 C5 C6 C7	3.7(13)	C88 C87 C89 C94	136.4(10)
C11 C8 C9 C10	-178.5(10)	C88 C87 C95 C0AA	44.9(13)
C11 C12 C13 C14	1(2)	C88 C87 C95 C96	-139.4(10)
C12 C11 C16 C15	-1.7(17)	C89 C87 C88 C70	-112.3(9)
C12 C13 C14 C15	-4.9(18)	C89 C87 C95 C0AA	-97.1(11)
C12 C13 C14 C17	176.3(12)	C89 C87 C95 C96	78.6(12)
C13 C14 C15 C16	5.3(16)	C89 C90 C91 C92	5.4(18)
C13 C14 C17 C18	61.9(13)	C90 C89 C94 C93	4.7(15)
C13 C14 C17 C19	-177.5(10)	C90 C91 C92 C93	-2.2(19)
C13 C14 C17 C20	-62.4(14)	C91 C92 C93 C94	0.6(19)
C14 C15 C16 C11	-2.1(16)	C92 C93 C94 C89	-1.9(18)
C15 C14 C17 C18	-116.8(11)	C94 C89 C90 C91	-6.4(16)
C15 C14 C17 C19	3.8(14)	C95 C0AA C99 C98	0.9(18)
C15 C14 C17 C20	118.9(11)	C95 C87 C88 C70	107.4(9)
C16 C11 C12 C13	2.2(19)	C95 C87 C89 C90	87.2(12)
C17 C14 C15 C16	-175.9(10)	C95 C87 C89 C94	-82.1(11)
C21 C4 C27 C28	67.8(11)	C95 C96 C97 C98	-0.1(17)
C21 C4 C27 C32	-108.0(11)	C96 C97 C98 C99	2.8(17)
C21 C22 C23 C24	1.1(14)	C97 C98 C99 C0AA	-3.2(17)
C22 C21 C26 C25	-2.9(14)	C99 C0AA C95 C87	177.8(10)
C22 C23 C24 C25	-3.5(14)	C99 C0AA C95 C96	1.8(17)
C23 C24 C25 C26	2.7(14)	Ru4B O6B C69B O7B	2.2(9)
C24 C25 C26 C21	0.6(15)	Ru4B O6B C69B C70B	-172.9(4)
C26 C21 C22 C23	2.1(13)	Ru3B O7B C69B O6B	12.5(9)
C27 C4 C21 C22	-93.8(10)	Ru3B O7B C69B C70B	-172.3(4)
C27 C4 C21 C26	82.7(9)	Cl3B C72B C73B C74B	174.2(7)
C27 C28 C29 C30	2.4(17)	C70B C71B C72B Cl3B	2.4(11)

C28C27C32C31 3.3(18)	C70B C71B C72B C73B -179.1(8)
C28C29C30C31 0(2)	C70B C71B C76B C75B -179.0(7)
C29C30C31 C32 -1(2)	C70B C87B C89B C90B -129.1(8)
C30C31 C32 C27 -1(2)	C70B C87B C89B C94B 52.6(10)
C32C27C28 C29 -4.2(15)	C70B C87B C95B C1A 84.4(10)
C33C34C35 C36 -74.5(10)	C70B C87B C95B C96B -95.2(9)
C33C34C35 C40 103.8(9)	C69B C70B C71B C72B -72.0(9)
C33C34C51 C52 -101.7(8)	C69B C70B C71B C76B 102.3(8)
C33C34C51 C53 2.9(11)	C69B C70B C87B C88B -103.2(7)
C33C34C51 C59 145.7(7)	C69B C70B C87B C89B 4.1(10)
C33C34C52 C51 111.4(8)	C69B C70B C87B C95B 147.0(6)
C34C35 C36 C12 3.0(11)	C69B C70B C88B C87B 110.8(7)
C34C35 C36 C37 179.0(8)	C71B C70B C69B O7B -178.0(6)
C34C35 C40 C39 179.4(8)	C71B C70B C69B O6B -2.4(9)
C34C51 C53 C54 -129.9(8)	C71B C70B C87B C88B 107.4(7)
C34C51 C53 C58 52.5(12)	C71B C70B C87B C89B -145.3(7)
C34C51 C59 C60 -102.1(10)	C71B C70B C87B C95B -2.4(9)
C34C51 C59 C64 76.4(11)	C71B C70B C88B C87B -106.5(7)
C35C34C51 C52 106.7(8)	C71B C72B C73B C74B -4.3(13)
C35C34C51 C53 -148.6(8)	C72B C71B C76B C75B -4.3(12)
C35C34C51 C59 -5.9(10)	C72B C73B C74B C75B -0.4(14)
C35C34C52 C51 -107.4(8)	C72B C73B C74B C77B 179.7(8)
C35C36 C37 C38 0.1(13)	C73B C74B C75B C76B 2.5(13)
C36C35 C40 C39 -2.2(13)	C73B C74B C77B C78B 127.6(10)
C36C37 C38 C39 0.8(13)	C73B C74B C77B C82B -55.5(13)
C36C37 C38 C41 176.9(8)	C74B C75B C76B C71B -0.1(13)
C37C38 C39 C40 -2.3(13)	C74B C77B C78B C79B 175.5(9)
C37C38 C41 C42 -136.1(10)	C74B C77B C82B C81B -176.9(12)
C37C38 C41 C46 45.1(13)	C75B C74B C77B C78B -52.4(12)
C38C39 C40 C35 3.1(14)	C75B C74B C77B C82B 124.6(12)
C38C41 C42 C43 176.4(10)	C76B C71B C72B C13B -172.0(6)
C38C41 C46 C45 -175.9(9)	C76B C71B C72B C73B 6.6(12)
C39C38 C41 C42 40.0(14)	C77B C74B C75B C76B -177.5(8)
C39C38 C41 C46 -138.8(10)	C77B C78B C79B C80B 2.1(16)
C40C35 C36 C12 -175.4(7)	C78B C77B C82B C81B 0.0(19)
C40C35 C36 C37 0.6(12)	C78B C79B C80B C81B -1.0(17)
C41 C38 C39 C40 -178.4(8)	C78B C79B C80B C83B 178.8(10)

C41 C42 C43 C44 0.9(17)	C79B C80B C81B C82B -1(2)
C42 C41 C46 C45 5.3(15)	C79B C80B C83B C84B 28.5(15)
C42 C43 C44 C45 2.5(16)	C79B C80B C83B C86B -89.5(13)
C42 C43 C44 C47 -175.7(10)	C79B C80B C83B C85B 151.8(11)
C43 C44 C45 C46 -2.0(15)	C80B C81B C82B C77B 1(2)
C43 C44 C47 C48 175.3(10)	C81B C80B C83B C84B -151.8(12)
C43 C44 C47 C49 -66.5(12)	C81B C80B C83B C86B 90.2(14)
C43 C44 C47 C50 54.2(13)	C81B C80B C83B C85B -28.4(16)
C44 C45 C46 C41 -2.0(15)	C82B C77B C78B C79B -1.6(15)
C45 C44 C47 C48 -2.7(13)	C83B C80B C81B C82B 179.6(14)
C45 C44 C47 C49 115.5(11)	C87B C70B C69B O7B 31.8(9)
C45 C44 C47 C50 -123.8(10)	C87B C70B C69B O6B -152.5(6)
C46 C41 C42 C43 -4.7(16)	C87B C70B C71B C72B 78.9(9)
C47 C44 C45 C46 176.1(9)	C87B C70B C71B C76B -106.8(8)
C51 C34 C35 C36 78.7(10)	C87B C89B C90B C91B -178.5(8)
C51 C34 C35 C40 -103.0(10)	C87B C89B C94B C93B 178.9(7)
C51 C53 C54 C55 179.7(8)	C87B C95B C1A C99B 178.2(9)
C51 C53 C58 C57 179.1(8)	C87B C95B C96B C97B -177.8(9)
C51 C59 C60 C61 -179.4(10)	C88B C70B C69B O7B -34.2(8)
C51 C59 C64 C63 -178.5(11)	C88B C70B C69B O6B 141.5(6)
C52 C34 C35 C36 144.2(8)	C88B C70B C71B C72B 145.0(7)
C52 C34 C35 C40 -37.5(11)	C88B C70B C71B C76B -40.7(9)
C52 C34 C51 C53 104.7(8)	C88B C70B C87B C89B 107.3(8)
C52 C34 C51 C59 -112.6(8)	C88B C70B C87B C95B -109.8(7)
C52 C51 C53 C54 -60.8(10)	C88B C87B C89B C90B -58.2(9)
C52 C51 C53 C58 121.7(9)	C88B C87B C89B C94B 123.5(8)
C52 C51 C59 C60 -170.6(9)	C88B C87B C95B C1A 15.3(12)
C52 C51 C59 C64 7.9(13)	C88B C87B C95B C96B -164.3(8)
C53 C51 C52 C34 -112.0(7)	C89B C87B C88B C70B -112.6(7)
C53 C51 C59 C60 43.4(11)	C89B C87B C95B C1A -128.8(9)
C53 C51 C59 C64 -138.1(10)	C89B C87B C95B C96B 51.7(10)
C53 C54 C55 C56 1.7(14)	C89B C90B C91B C92B 0.1(14)
C54 C53 C58 C57 1.7(13)	C90B C89B C94B C93B 0.6(12)
C54 C55 C56 C57 0.2(14)	C90B C91B C92B C93B -0.5(15)
C55 C56 C57 C58 -1.2(13)	C91B C92B C93B C94B 1.0(14)
C56 C57 C58 C53 0.2(13)	C92B C93B C94B C89B -1.1(13)
C58 C53 C54 C55 -2.6(13)	C94B C89B C90B C91B -0.2(13)

C59C51C52C34 102.9(8)	C95B C87B C88B C70B 106.3(7)
C59C51C53C54 86.8(9)	C95B C87B C89B C90B 86.0(9)
C59C51C53C58 -90.7(10)	C95B C87B C89B C94B -92.3(8)
C59C60C61C62 -2.4(18)	C95B C1A C99B C98B 0.5(17)
C60C59C64C63 0.0(17)	C1A C95B C96B C97B 2.6(15)
C60C61C62C63 0.7(19)	C1A C99B C98B C97B 0.9(17)
C61C62C63C64 1(2)	C99B C98B C97B C96B -0.6(17)
C62C63C64C59 -2(2)	C98B C97B C96B C95B -1.2(17)
C64C59C60C61 2.0(16)	C96B C95B C1A C99B -2.2(15)

Table 7 Hydrogen Atom Coordinates ($\text{\AA} \times 10^4$) and Isotropic Displacement Parameters ($\text{\AA}^2 \times 10^3$) for twin4_sq.

Atom	x	y	z	U(eq)
H3A	5060	1949	5373	21
H3B	4882	1521	5985	21
H7	6372	1400	2563	31
H9	5331	2247	2457	45
H10	5063	1956	3844	33
H12	5497	2073	793	67
H13	5788	2338	-585	57
H15	7017	2391	550	45
H16	6727	2116	1920	45
H18A	6113	2902	-1748	65
H18B	6592	3118	-1850	65
H18C	6345	3129	-887	65
H19A	7220	2726	-613	64
H19B	7232	2728	-1703	64
H19C	7270	2272	-1159	64
H20A	6603	1857	-1622	65
H20B	6687	2195	-2442	65
H20C	6201	2135	-2034	65
H22	6022	757	6239	30
H23	6148	380	7638	30
H24	5841	664	8991	34
H25	5482	1348	8979	37
H26	5373	1730	7595	31
H28	6484	1493	5507	36

H29	7011	2047	5286	43
H30	6827	2793	5444	58
H31	6088	2993	5839	66
H32	5545	2431	6030	55
H37	3568	1316	2451	32
H39	2852	168	2369	29
H40	3136	-30	3780	32
H42	2360	678	1541	42
H43	2060	924	164	46
H45	3272	1360	-635	40
H46	3566	1101	741	37
H48A	3019	1459	-1878	66
H48B	2790	1918	-1613	66
H48C	2630	1654	-2499	66
H49A	2047	1087	-2391	67
H49B	2018	791	-1491	67
H49C	2461	794	-2085	67
H50A	2131	1902	-586	63
H50B	1786	1506	-707	63
H50C	1898	1822	-1551	63
H52A	3055	68	5383	24
H52B	3483	-97	6009	24
H54	3256	385	7583	34
H55	3655	477	8973	35
H56	4333	839	8975	33
H57	4636	1121	7601	34
H58	4251	1014	6201	27
H60	3519	1492	5939	44
H61	3014	2072	5683	54
H62	2294	1904	5155	56
H63	2097	1166	4933	72
H64	2592	576	5274	59
H66A	5305	9	9310	106
H66B	4855	-268	9310	106
H66C	4840	260	9310	106
H68A	4850	-266	536	106
H68B	5305	3	536	106

H68C 4845	262	536	106
H0AA4987	2514	8584	49
H73 3809	3438	5052	43
H75 4992	2821	4702	40
H76 5248	3150	6100	38
H78 4768	3022	3087	48
H79 4515	2783	1708	58
H81 3337	2445	2901	52
H82 3593	2720	4278	49
H84D 4318	2185	682	78
H84E 3903	1957	200	78
H84F 4035	1822	1219	78
H85D 3225	1998	1564	71
H85E 3145	2187	559	71
H85F 3044	2490	1427	71
H86D 3519	3055	644	81
H86E 3698	2734	-140	81
H86F 4038	2972	533	81
H88C 5317	3103	7648	35
H88D 5415	3553	8271	35
H90 5097	3310	9972	50
H91 4915	3671	11362	61
H92 4271	4105	11448	64
H93 3848	4232	10142	63
H94 4040	3909	8748	48
H96 3860	3157	7796	39
H97 3491	2487	7677	49
H98 3862	1809	7951	48
H99 4621	1831	8489	49
H73B 1696	-1105	3924	35
H75B 2125	176	3767	30
H76B 1813	316	5207	24
H78B 1873	-78	2063	38
H79B 2255	-190	674	41
H81B 2889	-1227	1760	68
H82B 2547	-1113	3172	63
H84A 2610	-242	-607	82

H84B 3073	-414	-996	82
H84C 3058	-136	-70	82
H86A 2257	-989	-533	86
H86B 2519	-1402	-124	86
H86C 2685	-1174	-1046	86
H85A 3441	-1076	-349	75
H85B 3275	-1298	579	75
H85C 3501	-821	598	75
H88A 1918	234	6805	18
H88B 1463	327	7414	18
H90B 1722	-119	9031	29
H91B 1363	-328	10387	36
H92B 779	-844	10337	34
H93B 549	-1137	8941	27
H94B 912	-942	7563	23
H1A 2477	-168	6964	43
H99B 3103	-634	6799	49
H98B 3035	-1397	6860	46
H97B 2341	-1715	7054	50
H96B 1705	-1260	7207	33
H10A -295	76	10793	61
H10B 213	218	10793	61
H10C 82	-294	10793	61
H10D -286	106	2053	61
H10E 52	-301	2053	61
H10F 234	195	2053	61
H1DA 5140	4729	3131	208
H1DB 5165	5257	3131	208
H1DC 4695	5014	3131	208
H1EA 4839	5259	11805	208
H1EB 5305	5011	11805	208
H1EC 4857	4731	11805	208

Table 8 Atomic Occupancy for twin4_sq.

<i>Atom Occupancy</i>	<i>Atom Occupancy</i>	<i>Atom Occupancy</i>
H66A 0.5	H66B 0.5	H66C 0.5
H68A 0.5	H68B 0.5	H68C 0.5

H10A 0.25	H10B 0.25	H10C 0.25
H10D 0.25	H10E 0.25	H10F 0.25
H1DA 0.25	H1DB 0.25	H1DC 0.25
H1EA 0.25	H1EB 0.25	H1EC 0.25

Experimental

Single crystals of $C_{528}H_{472}Cl_{16}N_8O_{32}Ru_8$ [twin4_sq] were [slow evaporation in 50% dichloromethane in acetonitrile]. A suitable crystal was selected and [The crystal was mounted on a] on a 'Bruker APEX-II CCD' diffractometer. The crystal was kept at 100(2) K during data collection. Using Olex2 [1], the structure was solved with the XT [2] structure solution program using Intrinsic Phasing and refined with the XL [3] refinement package using Least Squares minimisation.

1. Dolomanov, O.V., Bourhis, L.J., Gildea, R.J., Howard, J.A.K. & Puschmann, H. (2009), *J. Appl. Cryst.* 42, 339-341.
2. Sheldrick, G.M. (2015). *Acta Cryst.* A71, 3-8.
3. Sheldrick, G.M. (2008). *Acta Cryst.* A64, 112-122.

Crystal structure determination of [twin4_sq]

Crystal Data for $C_{528}H_{472}Cl_{16}N_8O_{32}Ru_8$ ($M = 8816.90$ g/mol): tetragonal, space group P4 (no. 75), $a = 29.685(3)$ Å, $c = 14.3753(14)$ Å, $V = 12668(3)$ Å³, $Z = 1$, $T = 100(2)$ K, $\mu(\text{MoK}\alpha) = 0.375$ mm⁻¹, $D_{\text{calc}} = 1.156$ g/cm³, 37362 reflections measured ($2.744^\circ \leq 2\theta \leq 61.01^\circ$), 37362 unique ($R_{\text{int}} = ?$, $R_{\text{sigma}} = 0.0955$) which were used in all calculations. The final R_1 was 0.0926 ($I > 2\sigma(I)$) and wR_2 was 0.2508 (all data).

Refinement model description

Number of restraints - 1424, number of constraints - unknown.

Details:

1. Fixed Uiso

At 1.2 times of:

All C(H) groups, All C(H,H) groups

At 1.5 times of:

All C(H,H,H) groups

2. Restrained distances

Ru4-N3

2.2 with sigma of 0.01

C100-C1D

1.44 with sigma of 0.01

C101-C1C = C103-C1B

1.47 with sigma of 0.01

N3B-C1C \approx N4B-C1B

with sigma of 0.002

C67-C68 \approx C66-C65

with sigma of 0.002

C103-C1B \approx C101-C1C

with sigma of 0.002

N1-C65 \approx N2-C67 \approx N4-C102 \approx N3-C100 \approx N4B-C1B

with sigma of 0.002

C1E-C102 \approx C100-C1D

with sigma of 0.002

N1-C65 \approx N2-C67 \approx N4-C102 \approx N3-C100 \approx N3B-C1C \approx N4B-C1B

with sigma of 0.002

3. Uiso/Uanis restraints and constraints

: within 2A with sigma of 0.04 and sigma for terminal atoms of 0.08

Uanis(Ru3B) \approx Ueq, Uanis(C1C) \approx Ueq, Uanis(C1B) \approx Ueq: with sigma of 0.001 and sigma for terminal atoms of 0.001

Uanis(C66) \approx Ueq: with sigma of 0.002 and sigma for terminal atoms of 0.004

Uanis(O6B) \approx Ueq: with sigma of 0.002 and sigma for terminal atoms of 0.004

Uanis(N1) = Uanis(N2) = Uanis(N3) = Uanis(N4) = Uanis(N4B) = Uanis(N3B)

Uanis(C103) = Uanis(C101)

Uanis(C1C) = Uanis(C101) = Uanis(C1B)

Uanis(C68) = Uanis(C66)

Uanis(C1E) = Uanis(C1D)

Uanis(C100) = Uanis(C102) = Uanis(C1B) = Uanis(C101) = Uanis(C67) = Uanis(C65)

4. Rigid body (RIGU) restrains

Ru1, Ru2, C11, C12, O1, O2, O4, O5, N1, N2, C1, C2, C3, C4, C5, C6, C7, C8, C9, C10, C11, C12, C13, C14, C15, C16, C17, C18, C19, C20, C21, C22, C23, C24, C25, C26, C27, C28, C29, C30, C31, C32, C33, C34, C35, C36, C37, C38, C39, C40, C41, C42, C43, C44, C45, C46, C47, C48, C49, C50, C51, C52, C53, C54, C55, C56, C57, C58, C59, C60, C61, C62, C63, C64, C65, C66, C67, C68

with sigma for 1-2 distances of 0.001 and sigma for 1-3 distances of 0.001

Ru3, Ru4, C13, O6, O7, N3, N4, C0AA, C69, C70, C71, C72, C73, C74, C75, C76, C77, C78, C79, C80, C81, C82, C83, C84, C85, C86, C87, C88, C89, C90, C91, C92, C93, C94, C95, C96, C97, C98, C99, C100, C102, C1D, C1E

with sigma for 1-2 distances of 0.001 and sigma for 1-3 distances of 0.001

Ru4B, Ru3B, C13B, O7B, O6B, N4B, N3B, C70B, C69B, C71B, C72B, C73B, C74B, C75B, C76B, C77B, C78B, C79B, C80B, C81B, C82B, C83B, C84B, C86B, C85B, C87B, C88B, C89B, C90B, C91B, C92B, C93B, C94B, C95B, C1A, C99B, C98B, C97B, C96B, C1B, C103, C1C, C101

with sigma for 1-2 distances of 0.001 and sigma for 1-3 distances of 0.001

5. Others

Fixed Sof: H66A(0.5) H66B(0.5) H66C(0.5) H68A(0.5) H68B(0.5) H68C(0.5)

H10A(0.25) H10B(0.25) H10C(0.25) H10D(0.25) H10E(0.25) H10F(0.25) H1DA(0.25)

H1DB(0.25) H1DC(0.25) H1EA(0.25) H1EB(0.25) H1EC(0.25)

6.a Secondary CH2 refined with riding coordinates:

C3(H3A,H3B), C52(H52A,H52B), C88(H88C,H88D), C88B(H88A,H88B)

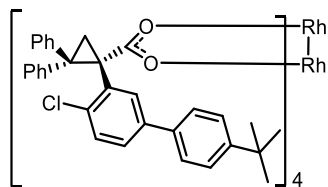
6.b Aromatic/amide H refined with riding coordinates:

C7(H7), C9(H9), C10(H10), C12(H12), C13(H13), C15(H15), C16(H16), C22(H22),
C23(H23), C24(H24), C25(H25), C26(H26), C28(H28), C29(H29), C30(H30), C31(H31),
C32(H32), C37(H37), C39(H39), C40(H40), C42(H42), C43(H43), C45(H45),
C46(H46), C54(H54), C55(H55), C56(H56), C57(H57), C58(H58), C60(H60), C61(H61),
C62(H62), C63(H63), C64(H64), C0AA(H0AA), C73(H73), C75(H75), C76(H76),
C78(H78), C79(H79), C81(H81), C82(H82), C90(H90), C91(H91), C92(H92), C93(H93),
C94(H94), C96(H96), C97(H97), C98(H98), C99(H99), C73B(H73B), C75B(H75B),
C76B(H76B), C78B(H78B), C79B(H79B), C81B(H81B), C82B(H82B), C90B(H90B),
C91B(H91B), C92B(H92B), C93B(H93B), C94B(H94B), C1A(H1A), C99B(H99B),
C98B(H98B), C97B(H97B), C96B(H96B)

6.c Idealised Me refined as rotating group:

C18(H18A,H18B,H18C), C19(H19A,H19B,H19C), C20(H20A,H20B,H20C),
C48(H48A,H48B,
H48C), C49(H49A,H49B,H49C), C50(H50A,H50B,H50C), C66(H66A,H66B,H66C),
C68(H68A,
H68B,H68C), C84(H84D,H84E,H84F), C85(H85D,H85E,H85F), C86(H86D,H86E,H86F),
C84B(H84A,H84B,H84C), C86B(H86A,H86B,H86C), C85B(H85A,H85B,H85C),
C103(H10A,
H10B,H10C), C101(H10D,H10E,H10F), C1D(H1DA,H1DB,H1DC), C1E(H1EA,H1EB,H1EC)

Rh₂[S-2-Cl-5-(p-^tBuC₆H₄)TPCP]₄ (135)



(with H₂O at axial positions)

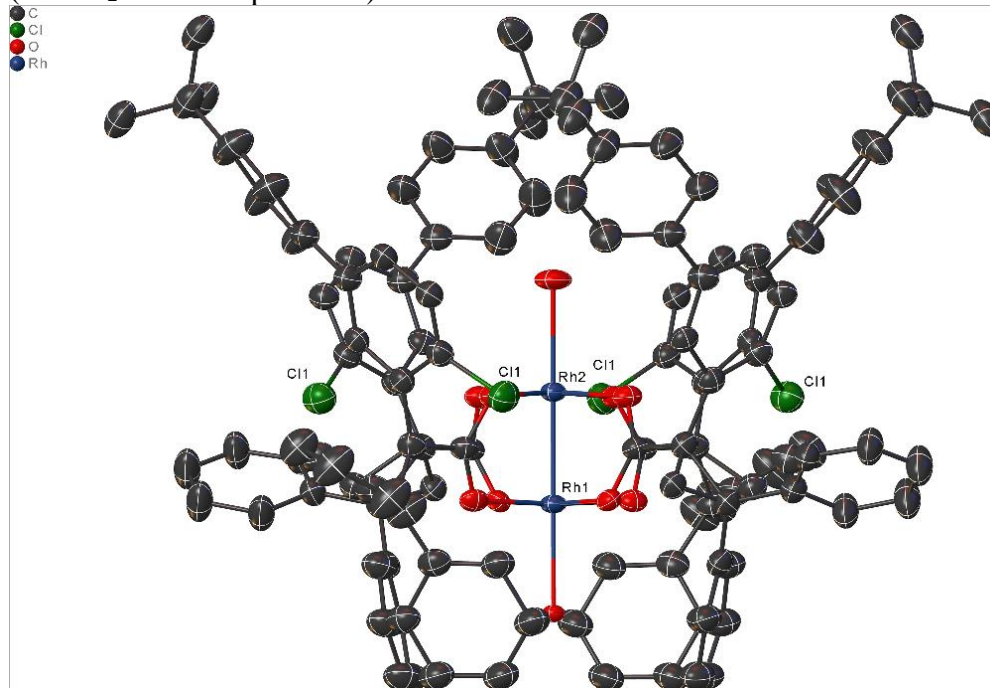


Table 1 Crystal data and structure refinement for Rh-2Cl5tBuPh.

Identification code	Rh-2Cl5tBuPh
Empirical formula	C ₁₂₈ H ₁₁₈ Cl ₄ O ₁₀ Rh ₂
Formula weight	2163.84
Temperature/K	100(2)
Crystal system	tetragonal
Space group	P4
a/Å	32.0493(5)
b/Å	32.0493(5)
c/Å	11.9878(3)
α/°	90
β/°	90
γ/°	90
Volume/Å ³	12313.3(5)
Z	4

$\rho_{\text{calc}}/\text{cm}^3$	1.167
μ/mm^{-1}	3.384
F(000)	4496.0
Crystal size/ mm^3	$0.55 \times 0.067 \times 0.031$
Radiation	CuK α ($\lambda = 1.54184$)
2 Θ range for data collection/ $^\circ$	6.166 to 130.158
Index ranges	$-37 \leq h \leq 37, -36 \leq k \leq 33, -13 \leq l \leq 12$
Reflections collected	69630
Independent reflections	19495 [$R_{\text{int}} = 0.0730, R_{\text{sigma}} = 0.0671$]
Data/restraints/parameters	19495/1226/1318
Goodness-of-fit on F^2	1.034
Final R indexes [$I \geq 2\sigma(I)$]	$R_1 = 0.0766, wR_2 = 0.1911$
Final R indexes [all data]	$R_1 = 0.0931, wR_2 = 0.2019$
Largest diff. peak/hole / $e \text{ \AA}^{-3}$	1.71/-2.02
Flack parameter	0.070(6)

Table 2 Fractional Atomic Coordinates ($\times 10^4$) and Equivalent Isotropic Displacement Parameters ($\text{\AA}^2 \times 10^3$) for Rh-2Cl5tBuPh. U_{eq} is defined as 1/3 of of the trace of the orthogonalised U_{IJ} tensor.

Atom	x	y	z	$U(\text{eq})$
C1	974(4)	4176(3)	4487(12)	34.8(18)
C2	1237(4)	4063(4)	3414(11)	38(3)
C3	891(4)	3774(4)	3810(11)	38(3)
C4	620(3)	4482(3)	4409(10)	27.9(15)
C5	1174(4)	4140(4)	5617(12)	35.8(19)
C6	1483(4)	4408(4)	5985(12)	42(2)
C7	1651(4)	4365(4)	7029(12)	45(2)
C8	1509(4)	4073(4)	7749(12)	46(2)
C9	1172(4)	3802(4)	7459(11)	39(2)
C10	1017(4)	3848(3)	6389(11)	33.1(18)
C11	1683(4)	3922(4)	3532(13)	46(3)
C12	1989(5)	4093(5)	2914(15)	57(4)
C13	2401(4)	3970(6)	3010(16)	64(5)
C14	2522(5)	3677(6)	3736(19)	81(6)
C15	2210(5)	3498(6)	4390(20)	83(6)

C16	1807(4)	3622(4)	4347(15)	56(4)
C17	1156(4)	4313(4)	2362(11)	35(3)
C18	1072(4)	4102(5)	1377(12)	46(3)
C19	1024(5)	4325(5)	417(14)	60(4)
C20	1055(5)	4759(5)	420(13)	59(4)
C21	1137(5)	4959(4)	1370(14)	59(4)
C22	1198(4)	4736(4)	2373(11)	39(3)
C23	980(4)	3528(3)	8268(11)	33.7(19)
C24	555(4)	3483(4)	8332(11)	37(3)
C25	364(4)	3247(4)	9158(11)	41(3)
C26	606(4)	3024(3)	9943(10)	38(3)
C27	1034(4)	3053(4)	9857(9)	38(3)
C28	1228(5)	3310(4)	9055(12)	46(3)
C29	413(5)	2746(4)	10866(11)	42(3)
C30	-49(5)	2727(4)	10798(12)	57(4)
C31	577(4)	2316(4)	10794(13)	50(4)
C32	517(5)	2952(4)	12001(13)	52(4)
Cl1	1660.3(11)	4811.2(10)	5140(3)	50.7(8)
O1	541(2)	4667(2)	5329(7)	35.7(15)
O2	418(3)	4521(3)	3533(7)	35.6(15)
O3	0	10000	3097(18)	54(6)
O4	0	10000	-2778(13)	24(3)
O9	0	5000	7365(13)	57(5)
O10	0	5000	1479(12)	38(3)
O13	5000	5000	-3325(15)	31(4)
O14	5000	5000	2480(20)	47(5)
Rh1	0	10000	-846.8(18)	28.1(4)
Rh2	0	10000	1129.1(19)	28.0(4)
Rh3	0	5000	3455.2	28.0(3)
Rh4	0	5000	5431.2(12)	28.7(3)
Rh5	5000	5000	626(2)	24.3(4)
Rh6	5000	5000	-1347(2)	28.1(4)
Cl1_2	3949.1(12)	3808.6(12)	441(4)	65.4(10)
O1_2	4405(3)	4764(3)	538(8)	45.7(15)
O2_2	4364(3)	4936(3)	-1282(8)	45.3(15)
C1_2	3759(4)	4710(4)	-314(11)	55.7(9)
C2_2	3515(4)	4541(4)	-1362(12)	59.5(9)

C3_2 3472(5)	4979(4)	-999(13)	56.8(9)
C4_2 4220(4)	4806(4)	-393(12)	50.8(17)
C5_2 3622(4)	4568(4)	829(11)	55.2(10)
C6_2 3696(4)	4170(4)	1274(12)	56(2)
C7_2 3591(4)	4066(5)	2325(12)	58(3)
C8_2 3397(4)	4355(4)	2990(13)	55(2)
C9_2 3355(4)	4767(4)	2660(11)	52.6(16)
C10_2 3455(3)	4861(4)	1570(10)	44.9(17)
C11_2 3160(4)	4247(5)	-1185(13)	61.7(14)
C12_2 3156(6)	3860(5)	-1730(20)	91(4)
C13_2 2833(5)	3576(5)	-1690(15)	68.1(16)
C14_2 2529(6)	3644(6)	-847(18)	91(4)
C15_2 2515(6)	4008(6)	-350(20)	100(5)
C16_2 2835(5)	4311(5)	-491(19)	81(4)
C17_2 3759(4)	4457(5)	-2431(12)	59.9(11)
C18_2 3642(5)	4655(6)	-3395(13)	71(3)
C19_2 3848(6)	4605(7)	-4398(16)	95(4)
C20_2 4173(6)	4330(6)	-4437(16)	90(4)
C21_2 4310(6)	4121(6)	-3496(14)	81(4)
C22_2 4081(5)	4187(5)	-2489(13)	64(3)
C23_2 3181(4)	5093(4)	3419(12)	50.7(15)
C24_2 3357(5)	5481(4)	3474(15)	62(3)
C25_2 3246(5)	5786(5)	4235(14)	65(3)
C26_2 2930(5)	5685(5)	5032(14)	69.6(17)
C27_2 2749(4)	5300(5)	4956(13)	58(2)
C28_2 2863(5)	5005(5)	4198(13)	63(3)
C29_2 2790(5)	6014(5)	5896(14)	70.7(16)
C30_2 3061(5)	6408(5)	5922(16)	72.3(19)
C31_2 2342(4)	6118(6)	5687(16)	71.0(18)
C32_2 2834(5)	5818(6)	7078(14)	72.3(19)
C11_3 114.1(10)	6573.8(10)	5018(3)	41.7(7)
O1_3 332(2)	5550(2)	5325(7)	34.5(14)
O2_3 482(2)	5408(2)	3531(7)	34.7(15)
C1_3 831(3)	5964(3)	4442(10)	36.1(8)
C2_3 951(4)	6207(3)	3346(10)	36.1(8)
C3_3 1224(4)	5870(4)	3802(10)	36.0(9)
C4_3 516(3)	5613(3)	4421(10)	32.0(14)

C5_3 852(3)	6198(3)	5526(10)	37.5(12)
C6_3 537(4)	6478(4)	5885(9)	36.8(19)
C7_3 562(4)	6671(4)	6889(11)	45(2)
C8_3 876(4)	6578(4)	7613(11)	46(2)
C9_3 1189(4)	6291(4)	7343(10)	45.3(19)
C10_3 1169(4)	6114(4)	6299(10)	42(2)
C11_3 1100(3)	6644(3)	3412(10)	35.8(11)
C12_3 845(4)	6967(3)	3038(12)	45(3)
C13_3 978(4)	7373(4)	3010(12)	44(3)
C14_3 1379(4)	7473(4)	3382(13)	49(3)
C15_3 1622(5)	7166(4)	3744(15)	59(4)
C16_3 1488(4)	6756(4)	3743(16)	63(4)
C17_3 709(3)	6114(4)	2268(9)	36.3(10)
C18_3 931(4)	6072(4)	1296(10)	38(2)
C19_3 738(4)	6000(4)	276(11)	47(3)
C20_3 307(4)	5983(4)	221(11)	42(2)
C21_3 79(4)	6052(4)	1175(11)	46(3)
C22_3 286(3)	6115(3)	2204(10)	34.8(18)
C23_3 1517(4)	6151(4)	8170(10)	44.0(17)
C24_3 1636(4)	5742(4)	8257(12)	53(2)
C25_3 1885(5)	5599(5)	9120(13)	59.7(17)
C26_3 2043(5)	5887(5)	9922(12)	62.1(19)
C27_3 1937(5)	6292(5)	9794(11)	56(3)
C28_3 1669(5)	6432(5)	8954(12)	57(3)
C29_3 2320(5)	5711(5)	10887(13)	68.6(19)
C30_3 2340(5)	5229(5)	10975(15)	68(2)
C31_3 2752(4)	5865(6)	10693(16)	71(2)
C32_3 2163(5)	5910(6)	11980(14)	73(2)
C11_4 1324.9(11)	9142.5(11)	1028(3)	51.0(8)
O1_4 310(3)	9448(2)	1037(7)	34.9(16)
O2_4 153(2)	9379(2)	-785(6)	32.6(14)
C1_4 471(3)	8817(3)	175(10)	37.1(10)
C2_4 697(3)	8608(4)	-841(9)	39.2(10)
C3_4 268(3)	8491(3)	-535(11)	38.3(10)
C4_4 295(3)	9253(3)	123(10)	32.7(16)
C5_4 616(3)	8691(3)	1323(9)	35.4(11)
C6_4 997(4)	8817(4)	1800(10)	39(2)

C7_4	1119(4)	8696(4)	2832(10)	41(2)
C8_4	846(4)	8479(4)	3501(11)	39(2)
C9_4	443(4)	8377(4)	3130(10)	40.8(19)
C10_4	343(4)	8478(4)	2035(9)	37(2)
C11_4	1055(3)	8318(4)	-608(12)	44.6(19)
C12_4	1456(4)	8412(5)	-982(13)	58(4)
C13_4	1796(4)	8165(5)	-768(15)	65(4)
C14_4	1737(4)	7783(5)	-204(14)	65(4)
C15_4	1351(4)	7683(5)	138(15)	59(4)
C16_4	1011(4)	7955(4)	-37(11)	47(3)
C17_4	747(4)	8871(4)	-1890(10)	42.6(13)
C18_4	582(4)	8715(4)	-2880(10)	46(2)
C19_4	608(5)	8936(4)	-3878(12)	54(3)
C20_4	810(5)	9319(4)	-3881(12)	58(3)
C21_4	987(5)	9468(5)	-2932(11)	56(3)
C22_4	946(4)	9242(4)	-1923(11)	50(3)
C23_4	130(4)	8196(4)	3892(10)	43(2)
C24_4	-277(4)	8309(5)	3864(13)	56(3)
C25_4	-579(4)	8169(5)	4583(15)	63(4)
C26_4	-455(4)	7881(4)	5435(12)	53.4(19)
C27_4	-49(4)	7768(5)	5473(13)	57(3)
C28_4	248(4)	7908(5)	4726(11)	54(3)
C29_4	-784(4)	7723(4)	6267(13)	56.6(18)
C30_4	-1193(4)	7984(4)	6280(14)	59(2)
C31_4	-887(5)	7279(4)	5951(14)	59(2)
C32_4	-602(5)	7728(5)	7457(12)	59(2)

Table 3 Anisotropic Displacement Parameters ($\text{\AA}^2 \times 10^3$) for Rh-2Cl5tBuPh. The Anisotropic displacement factor exponent takes the form: - $2\pi^2[h^2a^{*2}U_{11}+2hka^*b^*U_{12}+\dots]$.

Atom	U ₁₁	U ₂₂	U ₃₃	U ₂₃	U ₁₃	U ₁₂
C1	41(3)	37(4)	27(3)	-5(3)	-3(3)	-2(3)
C2	54(8)	38(7)	23(7)	1(5)	7(5)	-8(6)
C3	42(7)	30(6)	43(8)	6(5)	0(5)	-3(5)
C4	33(3)	27(3)	24(2)	1(2)	1.8(19)	-11(2)
C5	38(3)	29(3)	41(2)	1.5(19)	-4(2)	-4(3)
C6	46(4)	38(3)	42(2)	4(2)	-7(2)	-13(3)

C7	50(4)	43(4)	43(2)	7(2)	-9(2)	-17(3)
C8	49(4)	45(4)	44(2)	8(2)	-10(2)	-17(3)
C9	41(3)	35(3)	42(2)	4(2)	-6(2)	-9(3)
C10	33(3)	26(3)	40(2)	0(2)	-3(2)	0(3)
C11	35(7)	53(8)	51(9)	-10(7)	-3(6)	4(6)
C12	49(9)	55(9)	68(11)	10(7)	2(7)	-4(7)
C13	27(7)	82(12)	84(13)	7(9)	8(7)	10(7)
C14	43(10)	89(14)	111(18)	3(11)	6(9)	13(9)
C15	37(8)	89(13)	122(18)	42(13)	-7(10)	11(8)
C16	48(8)	54(8)	66(11)	15(8)	-1(7)	2(6)
C17	28(6)	39(7)	38(7)	4(5)	6(5)	-1(5)
C18	55(8)	50(8)	33(8)	-8(6)	3(6)	-2(6)
C19	57(9)	85(11)	39(10)	-9(8)	8(7)	-15(8)
C20	80(11)	62(10)	36(10)	17(7)	3(7)	2(8)
C21	82(11)	30(7)	65(11)	9(6)	24(8)	-14(7)
C22	58(8)	32(7)	27(7)	-4(5)	2(5)	-5(6)
C23	36(4)	26(3)	40(3)	0(2)	-3(2)	-1(3)
C24	32(6)	40(7)	37(7)	-5(5)	-9(5)	9(5)
C25	33(7)	49(8)	41(8)	-6(5)	4(5)	-7(5)
C26	59(9)	12(5)	42(8)	-5(4)	1(5)	-1(5)
C27	57(9)	30(6)	25(7)	8(4)	-2(5)	7(6)
C28	47(8)	42(8)	49(9)	2(6)	-13(6)	-1(6)
C29	71(10)	20(6)	35(8)	0(4)	7(6)	-8(6)
C30	100(13)	30(7)	41(9)	-4(5)	29(8)	-10(7)
C31	49(8)	44(8)	58(10)	6(6)	2(6)	-12(6)
C32	64(9)	46(8)	47(9)	-2(6)	14(7)	6(7)
Cl1	60.2(19)	44.9(16)	46.8(18)	9.9(14)	-9.1(14)	-20.9(14)
O1	45(4)	38(3)	24(2)	-2(2)	-1.9(19)	1(3)
O2	40(3)	42(4)	25(2)	-4(2)	-1(2)	0(2)
O3	66(9)	66(9)	31(13)	0	0	0
O4	28(5)	28(5)	16(9)	0	0	0
O9	67(11)	84(12)	21(10)	0	0	-2(8)
O10	43(8)	33(7)	38(10)	0	0	11(5)
O13	28(6)	28(6)	35(12)	0	0	0
O14	40(7)	40(7)	61(16)	0	0	0
Rh1	34.0(6)	34.0(6)	16.2(11)	0	0	0
Rh2	32.7(6)	32.7(6)	18.7(11)	0	0	0

Rh3	33.3(7)	34.4(7)	16.3(7)	0	0	0.1(5)
Rh4	33.2(6)	36.7(7)	16.2(7)	0	0	-1.8(5)
Rh5	24.5(5)	24.5(5)	23.9(11)	0	0	0
Rh6	30.6(6)	30.6(6)	23.0(12)	0	0	0
C11_2	57(2)	58.7(17)	80(2)	13.3(16)	21.1(19)	1.7(15)
O1_2	45(2)	43(4)	49(2)	-3(2)	-3.7(16)	6(2)
O2_2	49(2)	39(4)	48(2)	-6(2)	-4.8(15)	5(2)
C1_2	47.7(17)	63.7(18)	55.5(15)	4.4(11)	-7.9(11)	0.3(13)
C2_2	51.3(17)	68.0(16)	59.1(15)	1.6(13)	-10.9(12)	0.2(13)
C3_2	48.5(18)	67.0(16)	55.0(17)	4.4(13)	-9.2(15)	0.9(13)
C4_2	47.6(17)	55(4)	50(2)	0(2)	-5.6(12)	3.1(16)
C5_2	45(2)	63.1(17)	57.5(15)	6.1(13)	-6.5(13)	2.7(15)
C6_2	37(6)	64.5(18)	66(2)	10.0(15)	0(3)	4(2)
C7_2	41(6)	66(2)	67(2)	12.3(16)	3(3)	9(3)
C8_2	33(5)	66.8(18)	64(2)	11.1(15)	-3(3)	9(2)
C9_2	36(4)	65.6(17)	56.0(17)	7.6(13)	-10(2)	6.8(18)
C10_2	19(4)	62.5(17)	53.4(16)	4.0(13)	-16.5(19)	-3(2)
C11_2	54(2)	70.3(19)	61(2)	-0.3(18)	-10.1(17)	-2.4(16)
C12_2	81(3)	84(3)	107(7)	-25(4)	23(4)	-21(3)
C13_2	66.7(19)	67.9(18)	70(2)	-0.7(13)	-0.6(13)	-5.8(12)
C14_2	85(4)	91(3)	97(5)	-28(3)	22(5)	-27(3)
C15_2	83(4)	96(3)	120(8)	-38(5)	31(6)	-31(3)
C16_2	67(3)	85(3)	93(6)	-21(4)	10(4)	-17(3)
C17_2	53(2)	68(2)	58.7(15)	-1.3(14)	-11.2(14)	-2.1(18)
C18_2	72(5)	83(6)	58.3(18)	1(3)	-8(2)	16(5)
C19_2	102(6)	119(8)	63(2)	13(3)	4(3)	47(6)
C20_2	97(6)	112(8)	61(3)	10(3)	2(3)	41(6)
C21_2	82(5)	100(8)	62(3)	9(3)	0(3)	27(6)
C22_2	59(4)	75(5)	58(2)	0(3)	-10(2)	5(4)
C23_2	31(3)	67.4(17)	54(2)	6.3(15)	-15(2)	7.8(18)
C24_2	49(4)	72(2)	66(4)	-1(2)	-1(4)	-1(3)
C25_2	53(4)	73(2)	68(4)	-3(2)	0(4)	-2(3)
C26_2	60(3)	76(2)	73(3)	-7(2)	7(2)	-5(2)
C27_2	42(4)	71(2)	61(3)	1(2)	-7(3)	4(2)
C28_2	49(4)	72(2)	69(4)	-3(2)	2(3)	-1(2)
C29_2	62(3)	77(2)	73(3)	-8(2)	5(2)	-4(2)
C30_2	63(4)	78(3)	77(5)	-9(3)	5(3)	-5(2)

C31_2	62(3)	78(3)	73(4)	-8(3)	6(3)	-4(2)
C32_2	63(4)	81(4)	73(3)	-8(3)	6(3)	-2(3)
C11_3	39.5(15)	49.7(18)	35.9(16)	-3.3(12)	-1.8(12)	11.2(13)
O1_3	41(3)	36(3)	26(2)	1.1(18)	3(2)	-1(2)
O2_3	40(4)	37(3)	27(2)	3(2)	5(2)	1(2)
C1_3	40.8(18)	34.7(16)	32.8(15)	3.4(12)	4.9(12)	1.2(13)
C2_3	41.7(17)	34.0(16)	32.5(16)	3.0(13)	5.3(12)	1.7(13)
C3_3	40.7(17)	34.1(17)	33.1(18)	3.5(15)	5.0(13)	1.0(15)
C4_3	37(2)	32(2)	27(2)	4.3(16)	2.4(17)	5(2)
C5_3	43(2)	36(2)	33.3(15)	2.3(17)	7.0(14)	-3.6(17)
C6_3	42(2)	33(4)	35(2)	1(2)	7.3(19)	-6(2)
C7_3	44(3)	51(4)	41(2)	-9(3)	4(2)	-1(3)
C8_3	43(3)	55(5)	39(2)	-7(3)	6(2)	-2(3)
C9_3	43(3)	57(4)	36.5(19)	-6(2)	5.8(19)	-2(3)
C10_3	45(3)	45(4)	34(2)	0(2)	5.3(19)	0(3)
C11_3	42.2(19)	34.0(16)	31(3)	2.6(14)	5.9(18)	1.6(13)
C12_3	46(2)	34.3(17)	53(7)	5(2)	-3(3)	1.0(15)
C13_3	47(3)	34.0(18)	53(7)	4(2)	1(4)	1.1(17)
C14_3	49(3)	35(2)	63(8)	5(3)	-3(4)	-0.3(18)
C15_3	52(3)	35(2)	91(11)	9(3)	-14(5)	-2.2(18)
C16_3	51(2)	35.5(19)	101(11)	11(3)	-19(4)	-2.0(17)
C17_3	43.4(18)	32(2)	33.1(15)	3.4(16)	4.2(13)	1.7(17)
C18_3	45(2)	37(6)	32.5(16)	3(2)	4.0(16)	3(3)
C19_3	47(2)	59(7)	33.9(18)	-1(3)	2.9(19)	4(3)
C20_3	47(2)	45(6)	36(2)	2(3)	2.0(19)	4(3)
C21_3	45(2)	56(7)	36(2)	0(3)	2.0(16)	3(3)
C22_3	43.4(18)	26(5)	34(2)	6(3)	3.4(15)	1.1(18)
C23_3	39(3)	59(2)	34(2)	-2.3(18)	8(2)	-4(2)
C24_3	49(5)	60(2)	51(3)	-0.5(19)	5(3)	0(2)
C25_3	59(2)	62.4(19)	58(2)	1.5(12)	-1.8(13)	1.7(12)
C26_3	57(4)	73(2)	57(2)	-0.4(18)	-2(3)	-2(2)
C27_3	53(5)	71(2)	44(4)	-6(2)	-2(4)	-6(2)
C28_3	58(5)	67(3)	46(4)	-8(2)	-5(4)	-4(2)
C29_3	57(3)	92(4)	57(2)	5(3)	-1(2)	4(3)
C30_3	56(5)	93(4)	54(5)	9(3)	-3(5)	5(3)
C31_3	56(3)	94(5)	63(6)	7(5)	-2(3)	3(3)
C32_3	62(6)	102(5)	56(2)	3(4)	-2(3)	12(5)

C11_4	48.7(17)	57.6(19)	46.5(19)	3.8(14)	2.5(13)	-10.0(15)
O1_4	48(4)	33(2)	23(2)	0.9(18)	3(2)	0(3)
O2_4	32(3)	42(3)	24(2)	-1.9(17)	5(2)	2(2)
C1_4	40(2)	38(2)	33.8(17)	-3.2(13)	3.1(14)	2.8(15)
C2_4	40(2)	43(2)	34.6(18)	-4.3(15)	2.3(16)	6.5(16)
C3_4	40.3(19)	39(2)	36(2)	-5.6(19)	1.1(16)	5.4(17)
C4_4	35(4)	38(2)	25(2)	-2.1(14)	3(2)	1(2)
C5_4	41(2)	31(3)	34.4(17)	-3.7(15)	2.3(14)	2.6(18)
C6_4	42(2)	41(4)	34(2)	-4(3)	2.5(18)	0(3)
C7_4	46(2)	41(5)	35(2)	-3(3)	0.0(18)	-4(3)
C8_4	47(2)	37(5)	33(3)	-6(3)	1.0(17)	-3(3)
C9_4	48(2)	40(5)	34(2)	-2(2)	-0.3(16)	-5(2)
C10_4	43(2)	35(5)	33(2)	-4(2)	1.9(17)	-1(3)
C11_4	43(2)	52(3)	38(4)	1(3)	5(2)	12(2)
C12_4	43(2)	70(5)	60(8)	20(5)	8(3)	15(2)
C13_4	44(3)	74(5)	78(11)	27(6)	8(4)	17(3)
C14_4	46(3)	74(5)	76(11)	27(6)	11(4)	19(3)
C15_4	46(3)	61(4)	71(9)	16(5)	12(4)	18(3)
C16_4	45(3)	53(3)	42(6)	3(3)	7(3)	15(2)
C17_4	45(3)	46(2)	36.7(19)	-1.5(17)	7.7(17)	12(2)
C18_4	54(6)	48(3)	35.6(19)	1(2)	5(2)	10(3)
C19_4	69(7)	55(4)	38(2)	5(3)	5(3)	7(4)
C20_4	77(7)	57(4)	39(3)	7(3)	6(3)	3(4)
C21_4	71(7)	57(4)	40(3)	5(2)	8(3)	4(4)
C22_4	62(6)	51(3)	37(3)	1(2)	7(3)	3(3)
C23_4	49(2)	47(5)	34(3)	-1(3)	0(2)	-7(2)
C24_4	50(2)	63(7)	56(6)	19(5)	5(2)	-3(3)
C25_4	56(3)	63(7)	71(5)	28(5)	15(3)	4(3)
C26_4	61(3)	44(4)	56(4)	11(3)	16(3)	5(3)
C27_4	62(3)	59(7)	51(5)	14(5)	16(3)	10(3)
C28_4	57(3)	63(6)	41(4)	11(4)	9(3)	5(3)
C29_4	65(3)	44(4)	61(4)	13(3)	21(3)	7(3)
C30_4	67(3)	47(4)	62(6)	17(4)	24(3)	10(4)
C31_4	66(5)	45(3)	66(6)	10(3)	24(4)	5(3)
C32_4	70(4)	46(6)	60(4)	16(3)	20(3)	5(4)

Table 4 Bond Lengths for Rh-2Cl5tBuPh.

Atom	Atom	Length/Å	Atom	Atom	Length/Å
C1	C2	1.579(18)	C24_2	C25_2	1.384(18)
C1	C3	1.545(17)	C25_2	H25_2	0.9300
C1	C4	1.503(16)	C25_2	C26_2	1.431(18)
C1	C5	1.503(18)	C26_2	C27_2	1.364(18)
C2	C3	1.521(17)	C26_2	C29_2	1.545(18)
C2	C11	1.506(18)	C27_2	H27_2	0.9300
C2	C17	1.516(18)	C27_2	C28_2	1.362(17)
C3	H3A	0.9700	C28_2	H28_2	0.9300
C3	H3B	0.9700	C29_2	C30_2	1.532(18)
C4	O1	1.277(15)	C29_2	C31_2	1.495(18)
C4	O2	1.240(15)	C29_2	C32_2	1.56(2)
C5	C6	1.384(17)	C30_2	H30A_2	0.9600
C5	C10	1.409(17)	C30_2	H30B_2	0.9600
C6	C7	1.370(19)	C30_2	H30C_2	0.9600
C6	C11	1.737(13)	C31_2	H31A_2	0.9600
C7	H7	0.9300	C31_2	H31B_2	0.9600
C7	C8	1.351(19)	C31_2	H31C_2	0.9600
C8	H8	0.9300	C32_2	H32A_2	0.9600
C8	C9	1.429(17)	C32_2	H32B_2	0.9600
C9	C10	1.384(18)	C32_2	H32C_2	0.9600
C9	C23	1.445(17)	C11_3	C6_3	1.735(12)
C10	H10	0.9300	O1_3	C4_3	1.251(13)
C11	C12	1.35(2)	O2_3	C4_3	1.256(13)
C11	C16	1.43(2)	C1_3	C2_3	1.576(14)
C12	H12	0.9300	C1_3	C3_3	1.507(14)
C12	C13	1.38(2)	C1_3	C4_3	1.511(13)
C13	H13	0.9300	C1_3	C5_3	1.502(15)
C13	C14	1.34(3)	C2_3	C3_3	1.495(14)
C14	H14	0.9300	C2_3	C11_3	1.480(14)
C14	C15	1.39(3)	C2_3	C17_3	1.535(15)
C15	H15	0.9300	C3_3	H3A_3	0.9700
C15	C16	1.35(2)	C3_3	H3B_3	0.9700
C16	H16	0.9300	C5_3	C6_3	1.419(14)
C17	C18	1.387(18)	C5_3	C10_3	1.402(15)
C17	C22	1.363(17)	C6_3	C7_3	1.355(15)

C18	H18	0.9300	C7_3	H7_3	0.9300
C18	C19	1.36(2)	C7_3	C8_3	1.360(16)
C19	H19	0.9300	C8_3	H8_3	0.9300
C19	C20	1.40(2)	C8_3	C9_3	1.401(15)
C20	H20	0.9300	C9_3	C10_3	1.376(15)
C20	C21	1.33(2)	C9_3	C23_3	1.511(15)
C21	H21	0.9300	C10_3	H10_3	0.9300
C21	C22	1.41(2)	C11_3	C12_3	1.394(15)
C22	H22	0.9300	C11_3	C16_3	1.355(16)
C23	C24	1.374(17)	C12_3	H12_3	0.9300
C23	C28	1.417(18)	C12_3	C13_3	1.370(15)
C24	H24	0.9300	C13_3	H13_3	0.9300
C24	C25	1.386(18)	C13_3	C14_3	1.396(16)
C25	H25	0.9300	C14_3	H14_3	0.9300
C25	C26	1.414(18)	C14_3	C15_3	1.328(16)
C26	C27	1.381(19)	C15_3	H15_3	0.9300
C26	C29	1.547(17)	C15_3	C16_3	1.383(16)
C27	H27	0.9300	C16_3	H16_3	0.9300
C27	C28	1.412(19)	C17_3	C18_3	1.372(15)
C28	H28	0.9300	C17_3	C22_3	1.358(14)
C29	C30	1.49(2)	C18_3	H18_3	0.9300
C29	C31	1.479(19)	C18_3	C19_3	1.390(16)
C29	C32	1.548(19)	C19_3	H19_3	0.9300
C30	H30A	0.9600	C19_3	C20_3	1.385(15)
C30	H30B	0.9600	C20_3	H20_3	0.9300
C30	H30C	0.9600	C20_3	C21_3	1.375(16)
C31	H31A	0.9600	C21_3	H21_3	0.9300
C31	H31B	0.9600	C21_3	C22_3	1.415(16)
C31	H31C	0.9600	C22_3	H22_3	0.9300
C32	H32A	0.9600	C23_3	C24_3	1.368(16)
C32	H32B	0.9600	C23_3	C28_3	1.389(16)
C32	H32C	0.9600	C24_3	H24_3	0.9300
O1	Rh4	2.041(8)	C24_3	C25_3	1.387(17)
O2	Rh3	2.041(8)	C25_3	H25_3	0.9300
O3	H3C	0.9252	C25_3	C26_3	1.424(18)
O3	H3D	0.9255	C26_3	C27_3	1.352(18)
O3	Rh2	2.36(2)	C26_3	C29_3	1.562(17)

O4	H4A	1.0657	C27_3 H27_3	0.9300
O4	H4B	1.0657	C27_3 C28_3	1.397(17)
O4	Rh1	2.315(16)	C28_3 H28_3	0.9300
O9	H9A	0.8576	C29_3 C30_3	1.551(18)
O9	H9B	0.8576	C29_3 C31_3	1.489(18)
O9	Rh4	2.318(15)	C29_3 C32_3	1.542(19)
O10	H10A	0.8900	C30_3 H30A_3	0.9600
O10	H10B	0.8900	C30_3 H30B_3	0.9600
O10	Rh3	2.369(14)	C30_3 H30C_3	0.9600
O13	Rh6	2.371(18)	C31_3 H31A_3	0.9600
O14	H14A	1.3649	C31_3 H31B_3	0.9600
O14	H14B	1.3651	C31_3 H31C_3	0.9600
O14	Rh5	2.22(2)	C32_3 H32A_3	0.9600
Rh1	Rh2	2.369(2)	C32_3 H32B_3	0.9600
Rh1	O2_4	2.051(8)	C32_3 H32C_3	0.9600
Rh1	O2_4 ¹	2.051(8)	C11_4 C6_4	1.747(11)
Rh1	O2_4 ²	2.051(8)	O1_4 C4_4	1.263(13)
Rh1	O2_4 ³	2.051(8)	O2_4 C4_4	1.245(13)
Rh2	O1_4 ²	2.032(8)	C1_4 C2_4	1.569(14)
Rh2	O1_4 ¹	2.032(8)	C1_4 C3_4	1.497(14)
Rh2	O1_4 ³	2.032(8)	C1_4 C4_4	1.508(13)
Rh2	O1_4	2.032(8)	C1_4 C5_4	1.508(15)
Rh3	Rh4	2.3688(14)	C2_4 C3_4	1.472(14)
Rh3	O2_3	2.027(8)	C2_4 C11_4	1.502(14)
Rh3	O2_3 ⁴	2.027(8)	C2_4 C17_4	1.522(15)
Rh4	O1_3	2.062(7)	C3_4 H3A_4	0.9700
Rh4	O1_3 ⁴	2.062(7)	C3_4 H3B_4	0.9700
Rh5	Rh6	2.366(2)	C5_4 C6_4	1.406(15)
Rh5	O1_2 ⁵	2.053(9)	C5_4 C10_4	1.400(14)
Rh5	O1_2 ⁶	2.053(9)	C6_4 C7_4	1.356(15)
Rh5	O1_2	2.053(9)	C7_4 H7_4	0.9300
Rh5	O1_2 ⁷	2.053(9)	C7_4 C8_4	1.377(15)
Rh6	O2_2 ⁶	2.050(9)	C8_4 H8_4	0.9300
Rh6	O2_2 ⁷	2.050(9)	C8_4 C9_4	1.405(15)
Rh6	O2_2 ⁵	2.050(9)	C9_4 C10_4	1.389(15)
Rh6	O2_2	2.050(9)	C9_4 C23_4	1.474(15)
C11_2	C6_2	1.731(14)	C10_4 H10_4	0.9300

O1_2	C4_2	1.272(15)	C11_4C12_4	1.395(15)
O2_2	C4_2	1.234(15)	C11_4C16_4	1.356(16)
C1_2	C2_2	1.577(16)	C12_4H12_4	0.9300
C1_2	C3_2	1.506(16)	C12_4C13_4	1.371(16)
C1_2	C4_2	1.511(15)	C13_4H13_4	0.9300
C1_2	C5_2	1.508(16)	C13_4C14_4	1.409(17)
C2_2	C3_2	1.479(17)	C14_4H14_4	0.9300
C2_2	C11_2	1.492(16)	C14_4C15_4	1.341(17)
C2_2	C17_2	1.525(17)	C15_4H15_4	0.9300
C3_2	H3A_2	0.9700	C15_4C16_4	1.412(16)
C3_2	H3B_2	0.9700	C16_4H16_4	0.9300
C5_2	C6_2	1.405(16)	C17_4C18_4	1.391(16)
C5_2	C10_2	1.400(16)	C17_4C22_4	1.350(16)
C6_2	C7_2	1.346(17)	C18_4H18_4	0.9300
C7_2	H7_2	0.9300	C18_4C19_4	1.392(16)
C7_2	C8_2	1.372(17)	C19_4H19_4	0.9300
C8_2	H8_2	0.9300	C19_4C20_4	1.386(17)
C8_2	C9_2	1.383(16)	C20_4H20_4	0.9300
C9_2	C10_2	1.379(16)	C20_4C21_4	1.360(17)
C9_2	C23_2	1.495(16)	C21_4H21_4	0.9300
C10_2	H10_2	0.9300	C21_4C22_4	1.416(16)
C11_2	C12_2	1.401(18)	C22_4H22_4	0.9300
C11_2	C16_2	1.348(18)	C23_4C24_4	1.353(16)
C12_2	H12_2	0.9300	C23_4C28_4	1.411(16)
C12_2	C13_2	1.381(18)	C24_4H24_4	0.9300
C13_2	H13_2	0.9300	C24_4C25_4	1.372(17)
C13_2	C14_2	1.419(19)	C25_4H25_4	0.9300
C14_2	H14_2	0.9300	C25_4C26_4	1.432(17)
C14_2	C15_2	1.312(19)	C26_4C27_4	1.353(16)
C15_2	H15_2	0.9300	C26_4C29_4	1.536(16)
C15_2	C16_2	1.423(18)	C27_4H27_4	0.9300
C16_2	H16_2	0.9300	C27_4C28_4	1.382(16)
C17_2	C18_2	1.371(17)	C28_4H28_4	0.9300
C17_2	C22_2	1.348(17)	C29_4C30_4	1.557(17)
C18_2	H18_2	0.9300	C29_4C31_4	1.510(17)
C18_2	C19_2	1.381(19)	C29_4C32_4	1.540(19)
C19_2	H19_2	0.9300	C30_4H30A_4	0.9600

C19_2C20_2	1.367(19)	C30_4H30B_4	0.9600
C20_2H20_2	0.9300	C30_4H30C_4	0.9600
C20_2C21_2	1.383(19)	C31_4H31A_4	0.9600
C21_2H21_2	0.9300	C31_4H31B_4	0.9600
C21_2C22_2	1.428(19)	C31_4H31C_4	0.9600
C22_2H22_2	0.9300	C32_4H32A_4	0.9600
C23_2C24_2	1.365(17)	C32_4H32B_4	0.9600
C23_2C28_2	1.412(17)	C32_4H32C_4	0.9600
C24_2H24_2	0.9300		

Table 5 Bond Angles for Rh-2Cl5tBuPh.

Atom	Atom	Atom	Angle/°	Atom	Atom	Atom	Angle/°
C3	C1	C2	58.3(8)	C20_2	C19_2	H19_2	121.0
C4	C1	C2	120.1(11)	C19_2	C20_2	H20_2	119.1
C4	C1	C3	112.4(10)	C19_2	C20_2	C21_2	121.7(17)
C4	C1	C5	115.3(11)	C21_2	C20_2	H20_2	119.1
C5	C1	C2	119.3(10)	C20_2	C21_2	H21_2	121.5
C5	C1	C3	118.9(10)	C20_2	C21_2	C22_2	117.1(15)
C3	C2	C1	59.7(8)	C22_2	C21_2	H21_2	121.5
C11	C2	C1	119.9(11)	C17_2	C22_2	C21_2	122.1(14)
C11	C2	C3	118.7(11)	C17_2	C22_2	H22_2	118.9
C11	C2	C17	113.5(11)	C21_2	C22_2	H22_2	118.9
C17	C2	C1	117.7(11)	C24_2	C23_2	C9_2	120.8(12)
C17	C2	C3	117.1(11)	C24_2	C23_2	C28_2	116.6(13)
C1	C3	H3A	117.6	C28_2	C23_2	C9_2	122.2(12)
C1	C3	H3B	117.6	C23_2	C24_2	H24_2	117.6
C2	C3	C1	62.0(8)	C23_2	C24_2	C25_2	124.7(14)
C2	C3	H3A	117.6	C25_2	C24_2	H24_2	117.6
C2	C3	H3B	117.6	C24_2	C25_2	H25_2	121.3
H3A	C3	H3B	114.7	C24_2	C25_2	C26_2	117.4(14)
O1	C4	C1	113.5(10)	C26_2	C25_2	H25_2	121.3
O2	C4	C1	120.8(11)	C25_2	C26_2	C29_2	119.8(13)
O2	C4	O1	125.6(10)	C27_2	C26_2	C25_2	117.5(13)
C6	C5	C1	123.0(11)	C27_2	C26_2	C29_2	122.6(13)
C6	C5	C10	117.3(12)	C26_2	C27_2	H27_2	118.0
C10	C5	C1	119.4(11)	C28_2	C27_2	C26_2	123.9(14)

C5	C6	C11	120.7(10)	C28_2	C27_2	H27_2	118.0
C7	C6	C5	120.6(12)	C23_2	C28_2	H28_2	120.1
C7	C6	C11	118.7(10)	C27_2	C28_2	C23_2	119.7(14)
C6	C7	H7	119.3	C27_2	C28_2	H28_2	120.1
C8	C7	C6	121.5(12)	C26_2	C29_2	C32_2	107.9(13)
C8	C7	H7	119.3	C30_2	C29_2	C26_2	114.4(13)
C7	C8	H8	119.3	C30_2	C29_2	C32_2	105.2(13)
C7	C8	C9	121.3(13)	C31_2	C29_2	C26_2	108.6(13)
C9	C8	H8	119.3	C31_2	C29_2	C30_2	111.3(14)
C8	C9	C23	121.9(12)	C31_2	C29_2	C32_2	109.2(13)
C10	C9	C8	115.6(12)	C29_2	C30_2	H30A_2	109.5
C10	C9	C23	122.2(11)	C29_2	C30_2	H30B_2	109.5
C5	C10	H10	118.3	C29_2	C30_2	H30C_2	109.5
C9	C10	C5	123.5(11)	H30A_2	C30_2	H30B_2	109.5
C9	C10	H10	118.3	H30A_2	C30_2	H30C_2	109.5
C12	C11	C2	121.2(14)	H30B_2	C30_2	H30C_2	109.5
C12	C11	C16	116.6(13)	C29_2	C31_2	H31A_2	109.5
C16	C11	C2	122.1(13)	C29_2	C31_2	H31B_2	109.5
C11	C12	H12	118.9	C29_2	C31_2	H31C_2	109.5
C11	C12	C13	122.2(16)	H31A_2	C31_2	H31B_2	109.5
C13	C12	H12	118.9	H31A_2	C31_2	H31C_2	109.5
C12	C13	H13	119.0	H31B_2	C31_2	H31C_2	109.5
C14	C13	C12	122.1(16)	C29_2	C32_2	H32A_2	109.5
C14	C13	H13	119.0	C29_2	C32_2	H32B_2	109.5
C13	C14	H14	121.8	C29_2	C32_2	H32C_2	109.5
C13	C14	C15	116.5(16)	H32A_2	C32_2	H32B_2	109.5
C15	C14	H14	121.8	H32A_2	C32_2	H32C_2	109.5
C14	C15	H15	118.5	H32B_2	C32_2	H32C_2	109.5
C16	C15	C14	123.1(17)	C4_3	O1_3	Rh4	115.7(7)
C16	C15	H15	118.5	C4_3	O2_3	Rh3	116.1(7)
C11	C16	H16	120.4	C3_3	C1_3	C2_3	58.0(7)
C15	C16	C11	119.2(15)	C3_3	C1_3	C4_3	113.7(9)
C15	C16	H16	120.4	C4_3	C1_3	C2_3	121.2(10)
C18	C17	C2	119.0(12)	C5_3	C1_3	C2_3	117.5(9)
C22	C17	C2	120.0(11)	C5_3	C1_3	C3_3	120.1(10)
C22	C17	C18	120.8(12)	C5_3	C1_3	C4_3	114.7(9)
C17	C18	H18	120.5	C3_3	C2_3	C1_3	58.7(7)

C19	C18	C17	119.0(14)	C3_3	C2_3	C17_3	117.5(10)
C19	C18	H18	120.5	C11_3	C2_3	C1_3	120.2(10)
C18	C19	H19	119.6	C11_3	C2_3	C3_3	118.3(10)
C18	C19	C20	120.9(14)	C11_3	C2_3	C17_3	113.1(9)
C20	C19	H19	119.6	C17_3	C2_3	C1_3	118.8(9)
C19	C20	H20	120.1	C1_3	C3_3	H3A_3	117.4
C21	C20	C19	119.8(14)	C1_3	C3_3	H3B_3	117.4
C21	C20	H20	120.1	C2_3	C3_3	C1_3	63.4(7)
C20	C21	H21	119.7	C2_3	C3_3	H3A_3	117.4
C20	C21	C22	120.7(13)	C2_3	C3_3	H3B_3	117.4
C22	C21	H21	119.7	H3A_3	C3_3	H3B_3	114.5
C17	C22	C21	118.9(12)	O1_3	C4_3	O2_3	127.7(10)
C17	C22	H22	120.6	O1_3	C4_3	C1_3	114.8(10)
C21	C22	H22	120.6	O2_3	C4_3	C1_3	117.4(10)
C24	C23	C9	121.7(11)	C6_3	C5_3	C1_3	123.2(10)
C24	C23	C28	117.8(12)	C10_3	C5_3	C1_3	120.6(10)
C28	C23	C9	120.4(11)	C10_3	C5_3	C6_3	115.9(11)
C23	C24	H24	118.8	C5_3	C6_3	C11_3	119.1(9)
C23	C24	C25	122.4(11)	C7_3	C6_3	C11_3	120.0(9)
C25	C24	H24	118.8	C7_3	C6_3	C5_3	121.0(11)
C24	C25	H25	119.7	C6_3	C7_3	H7_3	119.6
C24	C25	C26	120.6(12)	C6_3	C7_3	C8_3	120.8(12)
C26	C25	H25	119.7	C8_3	C7_3	H7_3	119.6
C25	C26	C29	123.3(12)	C7_3	C8_3	H8_3	119.1
C27	C26	C25	117.5(11)	C7_3	C8_3	C9_3	121.7(12)
C27	C26	C29	119.2(11)	C9_3	C8_3	H8_3	119.1
C26	C27	H27	119.1	C8_3	C9_3	C23_3	122.8(11)
C26	C27	C28	121.9(11)	C10_3	C9_3	C8_3	116.5(11)
C28	C27	H27	119.1	C10_3	C9_3	C23_3	120.5(11)
C23	C28	H28	120.2	C5_3	C10_3	H10_3	118.1
C27	C28	C23	119.6(13)	C9_3	C10_3	C5_3	123.9(11)
C27	C28	H28	120.2	C9_3	C10_3	H10_3	118.1
C26	C29	C32	107.3(10)	C12_3	C11_3	C2_3	119.8(10)
C30	C29	C26	112.4(11)	C16_3	C11_3	C2_3	124.3(10)
C30	C29	C32	106.3(11)	C16_3	C11_3	C12_3	115.8(10)
C31	C29	C26	110.7(11)	C11_3	C12_3	H12_3	119.0
C31	C29	C30	108.2(11)	C13_3	C12_3	C11_3	122.1(12)

C31	C29	C32	111.9(12)	C13_3	C12_3H12_3	119.0
C29	C30	H30A	109.5	C12_3	C13_3H13_3	120.1
C29	C30	H30B	109.5	C12_3	C13_3C14_3	119.8(12)
C29	C30	H30C	109.5	C14_3	C13_3H13_3	120.1
H30A	C30	H30B	109.5	C13_3	C14_3H14_3	120.9
H30A	C30	H30C	109.5	C15_3	C14_3C13_3	118.3(12)
H30B	C30	H30C	109.5	C15_3	C14_3H14_3	120.9
C29	C31	H31A	109.5	C14_3	C15_3H15_3	119.3
C29	C31	H31B	109.5	C14_3	C15_3C16_3	121.4(13)
C29	C31	H31C	109.5	C16_3	C15_3H15_3	119.3
H31A	C31	H31B	109.5	C11_3	C16_3C15_3	122.5(12)
H31A	C31	H31C	109.5	C11_3	C16_3H16_3	118.7
H31B	C31	H31C	109.5	C15_3	C16_3H16_3	118.7
C29	C32	H32A	109.5	C18_3	C17_3C2_3	118.2(10)
C29	C32	H32B	109.5	C22_3	C17_3C2_3	123.4(10)
C29	C32	H32C	109.5	C22_3	C17_3C18_3	118.0(11)
H32A	C32	H32B	109.5	C17_3	C18_3H18_3	118.9
H32A	C32	H32C	109.5	C17_3	C18_3C19_3	122.2(11)
H32B	C32	H32C	109.5	C19_3	C18_3H18_3	118.9
C4	O1	Rh4	117.6(7)	C18_3	C19_3H19_3	120.3
C4	O2	Rh3	117.2(7)	C20_3	C19_3C18_3	119.5(12)
H3C	O3	H3D	105.2	C20_3	C19_3H19_3	120.3
Rh2	O3	H3C	127.4	C19_3	C20_3H20_3	120.5
Rh2	O3	H3D	127.4	C21_3	C20_3C19_3	119.0(12)
H4A	O4	H4B	105.8	C21_3	C20_3H20_3	120.5
Rh1	O4	H4A	127.1	C20_3	C21_3H21_3	120.1
Rh1	O4	H4B	127.1	C20_3	C21_3C22_3	119.9(11)
H9A	O9	H9B	109.5	C22_3	C21_3H21_3	120.1
Rh4	O9	H9A	125.3	C17_3	C22_3C21_3	121.2(11)
Rh4	O9	H9B	125.3	C17_3	C22_3H22_3	119.4
H10A	O10	H10B	109.1	C21_3	C22_3H22_3	119.4
Rh3	O10	H10A	125.5	C24_3	C23_3C9_3	121.9(11)
Rh3	O10	H10B	125.5	C24_3	C23_3C28_3	118.0(12)
H14A	O14	H14B	95.9	C28_3	C23_3C9_3	119.7(12)
Rh5	O14	H14A	132.0	C23_3	C24_3H24_3	118.8
Rh5	O14	H14B	132.0	C23_3	C24_3C25_3	122.4(13)
O4	Rh1	Rh2	180.0	C25_3	C24_3H24_3	118.8

O2_4 ¹	Rh1	O4	92.1(2)	C24_3	C25_3	H25_3	120.2
O2_4	Rh1	O4	92.1(2)	C24_3	C25_3	C26_3	119.5(14)
O2_4 ²	Rh1	O4	92.1(2)	C26_3	C25_3	H25_3	120.2
O2_4 ³	Rh1	O4	92.1(2)	C25_3	C26_3	C29_3	117.9(13)
O2_4 ³	Rh1	Rh2	87.9(2)	C27_3	C26_3	C25_3	117.2(13)
O2_4 ¹	Rh1	Rh2	87.9(2)	C27_3	C26_3	C29_3	124.9(13)
O2_4	Rh1	Rh2	87.9(2)	C26_3	C27_3	H27_3	118.6
O2_4 ²	Rh1	Rh2	87.9(2)	C26_3	C27_3	C28_3	122.9(13)
O2_4	Rh1	O2_4 ³	89.927(19)	C28_3	C27_3	H27_3	118.6
O2_4 ²	Rh1	O2_4 ¹	89.924(18)	C23_3	C28_3	C27_3	119.8(14)
O2_4 ³	Rh1	O2_4 ¹	89.924(18)	C23_3	C28_3	H28_3	120.1
O2_4	Rh1	O2_4 ²	89.92(2)	C27_3	C28_3	H28_3	120.1
O2_4	Rh1	O2_4 ¹	175.8(4)	C30_3	C29_3	C26_3	115.7(13)
O2_4 ²	Rh1	O2_4 ³	175.8(4)	C31_3	C29_3	C26_3	107.1(13)
O3	Rh2	Rh1	180.0	C31_3	C29_3	C30_3	107.5(13)
O1_4	Rh2	O3	93.1(2)	C31_3	C29_3	C32_3	107.4(14)
O1_4 ¹	Rh2	O3	93.1(2)	C32_3	C29_3	C26_3	107.2(12)
O1_4 ³	Rh2	O3	93.1(2)	C32_3	C29_3	C30_3	111.6(13)
O1_4 ²	Rh2	O3	93.1(2)	C29_3	C30_3	H30A_3	109.5
O1_4	Rh2	Rh1	86.9(2)	C29_3	C30_3	H30B_3	109.5
O1_4 ³	Rh2	Rh1	86.9(2)	C29_3	C30_3	H30C_3	109.5
O1_4 ²	Rh2	Rh1	86.9(2)	H30A_3	C30_3	H30B_3	109.5
O1_4 ¹	Rh2	Rh1	86.9(2)	H30A_3	C30_3	H30C_3	109.5
O1_4	Rh2	O1_4 ³	89.83(3)	H30B_3	C30_3	H30C_3	109.5
O1_4 ³	Rh2	O1_4 ¹	89.83(3)	C29_3	C31_3	H31A_3	109.5
O1_4 ³	Rh2	O1_4 ²	173.8(5)	C29_3	C31_3	H31B_3	109.5
O1_4	Rh2	O1_4 ¹	173.8(5)	C29_3	C31_3	H31C_3	109.5
O1_4	Rh2	O1_4 ²	89.83(3)	H31A_3	C31_3	H31B_3	109.5
O1_4 ²	Rh2	O1_4 ¹	89.83(3)	H31A_3	C31_3	H31C_3	109.5
O2	Rh3	O2 ⁴	174.8(5)	H31B_3	C31_3	H31C_3	109.5
O2 ⁴	Rh3	O10	92.6(2)	C29_3	C32_3	H32A_3	109.5
O2	Rh3	O10	92.6(2)	C29_3	C32_3	H32B_3	109.5
O2	Rh3	Rh4	87.4(2)	C29_3	C32_3	H32C_3	109.5
O2 ⁴	Rh3	Rh4	87.4(2)	H32A_3	C32_3	H32B_3	109.5
Rh4	Rh3	O10	180.0	H32A_3	C32_3	H32C_3	109.5
O2_3 ⁴	Rh3	O2 ⁴	89.0(3)	H32B_3	C32_3	H32C_3	109.5
O2_3 ⁴	Rh3	O2	90.8(3)	C4_4	O1_4	Rh2	117.3(7)

O2_3	Rh3	O2	89.0(3)	C4_4	O2_4	Rh1	115.7(7)
O2_3	Rh3	O2 ⁴	90.8(3)	C3_4	C1_4	C2_4	57.3(7)
O2_3	Rh3	O10	92.6(2)	C3_4	C1_4	C4_4	117.3(10)
O2_3 ⁴	Rh3	O10	92.6(2)	C3_4	C1_4	C5_4	117.8(10)
O2_3 ⁴	Rh3	Rh4	87.4(2)	C4_4	C1_4	C2_4	122.5(9)
O2_3	Rh3	Rh4	87.4(2)	C4_4	C1_4	C5_4	113.8(9)
O2_3 ⁴	Rh3	O2_3	174.9(5)	C5_4	C1_4	C2_4	116.8(9)
O1	Rh4	O1 ⁴	173.1(5)	C3_4	C2_4	C1_4	58.9(7)
O1	Rh4	O9	93.4(2)	C3_4	C2_4	C11_4	120.7(10)
O1 ⁴	Rh4	O9	93.4(2)	C3_4	C2_4	C17_4	116.4(10)
O1 ⁴	Rh4	Rh3	86.6(2)	C11_4	C2_4	C1_4	118.2(10)
O1	Rh4	Rh3	86.6(2)	C11_4	C2_4	C17_4	114.6(9)
O1 ⁴	Rh4	O1_3 ⁴	90.3(3)	C17_4	C2_4	C1_4	116.9(9)
O1	Rh4	O1_3	90.3(3)	C1_4	C3_4	H3A_4	117.4
O1	Rh4	O1_3 ⁴	89.3(3)	C1_4	C3_4	H3B_4	117.4
O1 ⁴	Rh4	O1_3	89.3(3)	C2_4	C3_4	C1_4	63.8(7)
O9	Rh4	Rh3	180.0	C2_4	C3_4	H3A_4	117.4
O1_3 ⁴	Rh4	O9	93.5(2)	C2_4	C3_4	H3B_4	117.4
O1_3	Rh4	O9	93.5(2)	H3A_4	C3_4	H3B_4	114.4
O1_3	Rh4	Rh3	86.5(2)	O1_4	C4_4	C1_4	114.0(9)
O1_3 ⁴	Rh4	Rh3	86.5(2)	O2_4	C4_4	O1_4	127.8(10)
O1_3	Rh4	O1_3 ⁴	172.9(5)	O2_4	C4_4	C1_4	118.2(10)
O14	Rh5	Rh6	180.0	C6_4	C5_4	C1_4	124.2(10)
O1_2 ⁵	Rh5	O14	92.9(3)	C10_4	C5_4	C1_4	119.6(10)
O1_2 ⁶	Rh5	O14	92.9(3)	C10_4	C5_4	C6_4	115.7(10)
O1_2 ⁷	Rh5	O14	92.9(3)	C5_4	C6_4	C11_4	118.6(9)
O1_2	Rh5	O14	92.9(3)	C7_4	C6_4	C11_4	118.7(9)
O1_2	Rh5	Rh6	87.1(3)	C7_4	C6_4	C5_4	122.7(11)
O1_2 ⁶	Rh5	Rh6	87.1(3)	C6_4	C7_4	H7_4	120.3
O1_2 ⁵	Rh5	Rh6	87.1(3)	C6_4	C7_4	C8_4	119.4(11)
O1_2 ⁷	Rh5	Rh6	87.1(3)	C8_4	C7_4	H7_4	120.3
O1_2	Rh5	O1_2 ⁵	89.85(3)	C7_4	C8_4	H8_4	119.4
O1_2	Rh5	O1_2 ⁶	89.85(3)	C7_4	C8_4	C9_4	121.3(12)
O1_2 ⁷	Rh5	O1_2 ⁶	89.85(3)	C9_4	C8_4	H8_4	119.4
O1_2	Rh5	O1_2 ⁷	174.1(6)	C8_4	C9_4	C23_4	121.3(11)
O1_2 ⁷	Rh5	O1_2 ⁵	89.85(3)	C10_4	C9_4	C8_4	117.1(11)
O1_2 ⁶	Rh5	O1_2 ⁵	174.1(6)	C10_4	C9_4	C23_4	121.4(10)

Rh5	Rh6	O13	180.0	C5_4	C10_4H10_4	118.4
O2_2 ⁶	Rh6	O13	92.2(3)	C9_4	C10_4C5_4	123.1(11)
O2_2	Rh6	O13	92.2(3)	C9_4	C10_4H10_4	118.4
O2_2 ⁵	Rh6	O13	92.2(3)	C12_4	C11_4C2_4	120.7(11)
O2_2 ⁷	Rh6	O13	92.2(3)	C16_4	C11_4C2_4	123.0(10)
O2_2 ⁶	Rh6	Rh5	87.8(3)	C16_4	C11_4C12_4	116.3(11)
O2_2 ⁷	Rh6	Rh5	87.8(3)	C11_4	C12_4H12_4	118.4
O2_2	Rh6	Rh5	87.8(3)	C13_4	C12_4C11_4	123.2(13)
O2_2 ⁵	Rh6	Rh5	87.8(3)	C13_4	C12_4H12_4	118.4
O2_2 ⁷	Rh6	O2_2 ⁵	89.92(2)	C12_4	C13_4H13_4	120.5
O2_2	Rh6	O2_2 ⁷	175.7(5)	C12_4	C13_4C14_4	118.9(13)
O2_2 ⁷	Rh6	O2_2 ⁶	89.92(2)	C14_4	C13_4H13_4	120.5
O2_2 ⁵	Rh6	O2_2 ⁶	175.7(5)	C13_4	C14_4H14_4	120.7
O2_2	Rh6	O2_2 ⁶	89.92(2)	C15_4	C14_4C13_4	118.6(13)
O2_2	Rh6	O2_2 ⁵	89.91(2)	C15_4	C14_4H14_4	120.7
C4_2	O1_2	Rh5	116.1(8)	C14_4	C15_4H15_4	119.4
C4_2	O2_2	Rh6	116.0(8)	C14_4	C15_4C16_4	121.2(13)
C3_2	C1_2	C2_2	57.3(8)	C16_4	C15_4H15_4	119.4
C3_2	C1_2	C4_2	116.4(12)	C11_4	C16_4C15_4	121.6(12)
C3_2	C1_2	C5_2	119.4(12)	C11_4	C16_4H16_4	119.2
C4_2	C1_2	C2_2	120.3(11)	C15_4	C16_4H16_4	119.2
C5_2	C1_2	C2_2	118.5(11)	C18_4	C17_4C2_4	117.8(11)
C5_2	C1_2	C4_2	113.7(11)	C22_4	C17_4C2_4	124.2(11)
C3_2	C2_2	C1_2	58.9(8)	C22_4	C17_4C18_4	118.1(11)
C3_2	C2_2	C11_2	119.1(12)	C17_4	C18_4H18_4	119.0
C3_2	C2_2	C17_2	117.6(12)	C17_4	C18_4C19_4	121.9(13)
C11_2	C2_2	C1_2	118.8(12)	C19_4	C18_4H18_4	119.0
C11_2	C2_2	C17_2	113.6(12)	C18_4	C19_4H19_4	120.7
C17_2	C2_2	C1_2	118.4(11)	C20_4	C19_4C18_4	118.7(13)
C1_2	C3_2	H3A_2	117.4	C20_4	C19_4H19_4	120.7
C1_2	C3_2	H3B_2	117.4	C19_4	C20_4H20_4	119.8
C2_2	C3_2	C1_2	63.8(8)	C21_4	C20_4C19_4	120.3(13)
C2_2	C3_2	H3A_2	117.4	C21_4	C20_4H20_4	119.8
C2_2	C3_2	H3B_2	117.4	C20_4	C21_4H21_4	120.2
H3A_2	C3_2	H3B_2	114.4	C20_4	C21_4C22_4	119.7(13)
O1_2	C4_2	C1_2	112.4(11)	C22_4	C21_4H21_4	120.2
O2_2	C4_2	O1_2	128.2(11)	C17_4	C22_4C21_4	121.3(13)

O2_2	C4_2	C1_2	119.3(11)	C17_4	C22_4H22_4	119.3
C6_2	C5_2	C1_2	124.8(12)	C21_4	C22_4H22_4	119.3
C10_2	C5_2	C1_2	119.1(12)	C24_4	C23_4C9_4	122.3(11)
C10_2	C5_2	C6_2	115.7(12)	C24_4	C23_4C28_4	116.8(11)
C5_2	C6_2	C11_2	117.9(10)	C28_4	C23_4C9_4	120.9(11)
C7_2	C6_2	C11_2	119.6(11)	C23_4	C24_4H24_4	117.4
C7_2	C6_2	C5_2	122.5(13)	C23_4	C24_4C25_4	125.3(13)
C6_2	C7_2	H7_2	120.3	C25_4	C24_4H24_4	117.4
C6_2	C7_2	C8_2	119.5(13)	C24_4	C25_4H25_4	121.2
C8_2	C7_2	H7_2	120.3	C24_4	C25_4C26_4	117.6(13)
C7_2	C8_2	H8_2	119.3	C26_4	C25_4H25_4	121.2
C7_2	C8_2	C9_2	121.4(14)	C25_4	C26_4C29_4	119.1(11)
C9_2	C8_2	H8_2	119.3	C27_4	C26_4C25_4	117.6(12)
C8_2	C9_2	C23_2	121.9(12)	C27_4	C26_4C29_4	123.4(12)
C10_2	C9_2	C8_2	117.3(13)	C26_4	C27_4H27_4	118.2
C10_2	C9_2	C23_2	120.6(12)	C26_4	C27_4C28_4	123.7(13)
C5_2	C10_2H10_2	118.6	C28_4	C27_4H27_4	118.2	
C9_2	C10_2C5_2	122.8(12)	C23_4	C28_4H28_4	120.4	
C9_2	C10_2H10_2	118.6	C27_4	C28_4C23_4	119.1(13)	
C12_2	C11_2C2_2	119.8(13)	C27_4	C28_4H28_4	120.4	
C16_2	C11_2C2_2	125.6(13)	C26_4	C29_4C30_4	114.0(10)	
C16_2	C11_2C12_2	114.5(13)	C26_4	C29_4C32_4	109.9(12)	
C11_2	C12_2H12_2	117.5	C31_4	C29_4C26_4	107.3(11)	
C13_2	C12_2C11_2	125.1(16)	C31_4	C29_4C30_4	108.9(12)	
C13_2	C12_2H12_2	117.5	C31_4	C29_4C32_4	108.9(12)	
C12_2	C13_2H13_2	122.0	C32_4	C29_4C30_4	107.7(12)	
C12_2	C13_2C14_2	115.9(15)	C29_4	C30_4H30A_4	109.5	
C14_2	C13_2H13_2	122.0	C29_4	C30_4H30B_4	109.5	
C13_2	C14_2H14_2	120.5	C29_4	C30_4H30C_4	109.5	
C15_2	C14_2C13_2	119.0(16)	H30A_4	C30_4H30B_4	109.5	
C15_2	C14_2H14_2	120.5	H30A_4	C30_4H30C_4	109.5	
C14_2	C15_2H15_2	119.1	H30B_4	C30_4H30C_4	109.5	
C14_2	C15_2C16_2	121.8(17)	C29_4	C31_4H31A_4	109.5	
C16_2	C15_2H15_2	119.1	C29_4	C31_4H31B_4	109.5	
C11_2	C16_2C15_2	121.8(15)	C29_4	C31_4H31C_4	109.5	
C11_2	C16_2H16_2	119.1	H31A_4	C31_4H31B_4	109.5	
C15_2	C16_2H16_2	119.1	H31A_4	C31_4H31C_4	109.5	

C18_2 C17_2 C2_2	119.0(13)	H31B_4 C31_4 H31C_4	109.5
C22_2 C17_2 C2_2	123.3(13)	C29_4 C32_4 H32A_4	109.5
C22_2 C17_2 C18_2	117.6(14)	C29_4 C32_4 H32B_4	109.5
C17_2 C18_2 H18_2	118.3	C29_4 C32_4 H32C_4	109.5
C17_2 C18_2 C19_2	123.3(15)	H32A_4 C32_4 H32B_4	109.5
C19_2 C18_2 H18_2	118.3	H32A_4 C32_4 H32C_4	109.5
C18_2 C19_2 H19_2	121.0	H32B_4 C32_4 H32C_4	109.5
C20_2 C19_2 C18_2	118.0(16)		

Table 6 Torsion Angles for Rh-2Cl5tBuPh.

A	B	C	D	Angle/°	A	B	C	D	Angle/°
C1	C2	C11	C12	-130.9(15)	C25_2 C26_2 C29_2 C31_2				115.9(18)
C1	C2	C11	C16	45.0(19)	C25_2 C26_2 C29_2 C32_2				-125.8(17)
C1	C2	C17	C18	-127.9(12)	C26_2 C27_2 C28_2 C23_2				-1(3)
C1	C2	C17	C22	57.2(16)	C27_2 C26_2 C29_2 C30_2				174.3(16)
C1	C4	O1	Rh4	-167.9(7)	C27_2 C26_2 C29_2 C31_2				-61(2)
C1	C4	O2	Rh3	-171.8(7)	C27_2 C26_2 C29_2 C32_2				58(2)
C1	C5	C6	C7	179.2(13)	C28_2 C23_2 C24_2 C25_2				0(2)
C1	C5	C6	C11	0.1(19)	C29_2 C26_2 C27_2 C28_2				179.4(16)
C1	C5	C10	C9	-178.0(12)	C11_3 C6_3 C7_3 C8_3				175.4(11)
C2	C1	C4	O1	-154.3(10)	C1_3 C2_3 C11_3 C12_3				-108.9(13)
C2	C1	C4	O2	29.8(15)	C1_3 C2_3 C11_3 C16_3				76.1(18)
C2	C1	C5	C6	70.3(16)	C1_3 C2_3 C17_3 C18_3				-136.3(11)
C2	C1	C5	C10	-115.9(13)	C1_3 C2_3 C17_3 C22_3				51.1(15)
C2	C11	C12	C13	179.7(15)	C1_3 C5_3 C6_3 C11_3				-2.6(16)
C2	C11	C16	C15	177.9(16)	C1_3 C5_3 C6_3 C7_3				177.5(12)
C2	C17	C18	C19	-176.1(12)	C1_3 C5_3 C10_3 C9_3				-174.4(12)
C2	C17	C22	C21	177.5(12)	C2_3 C1_3 C4_3 O1_3				-154.4(10)
C3	C1	C2	C11	-107.8(13)	C2_3 C1_3 C4_3 O2_3				28.7(15)
C3	C1	C2	C17	106.8(13)	C2_3 C1_3 C5_3 C6_3				79.1(14)
C3	C1	C4	O1	140.4(10)	C2_3 C1_3 C5_3 C10_3				-107.8(13)
C3	C1	C4	O2	-35.5(15)	C2_3 C11_3 C12_3 C13_3				-175.5(12)
C3	C1	C5	C6	138.0(13)	C2_3 C11_3 C16_3 C15_3				176.9(15)
C3	C1	C5	C10	-48.2(17)	C2_3 C17_3 C18_3 C19_3				-177.9(11)
C3	C2	C11	C12	159.5(14)	C2_3 C17_3 C22_3 C21_3				176.1(11)
C3	C2	C11	C16	-25(2)	C3_3 C1_3 C2_3 C11_3				-106.7(12)

C3	C2	C17	C18	-59.7(16)	C3_3	C1_3	C2_3	C17_3	106.4(11)
C3	C2	C17	C22	125.4(13)	C3_3	C1_3	C4_3	O1_3	139.9(10)
C4	C1	C2	C3	-99.2(11)	C3_3	C1_3	C4_3	O2_3	-37.0(14)
C4	C1	C2	C11	153.0(11)	C3_3	C1_3	C5_3	C6_3	146.2(11)
C4	C1	C2	C17	7.6(16)	C3_3	C1_3	C5_3	C10_3	-40.7(16)
C4	C1	C3	C2	112.5(12)	C3_3	C2_3	C11_3	C12_3	-177.2(12)
C4	C1	C5	C6	-84.0(15)	C3_3	C2_3	C11_3	C16_3	8(2)
C4	C1	C5	C10	89.8(13)	C3_3	C2_3	C17_3	C18_3	-68.8(14)
C5	C1	C2	C3	107.7(12)	C3_3	C2_3	C17_3	C22_3	118.6(13)
C5	C1	C2	C11	0.0(16)	C4_3	C1_3	C2_3	C3_3	-100.2(11)
C5	C1	C2	C17	-145.5(11)	C4_3	C1_3	C2_3	C11_3	153.1(10)
C5	C1	C3	C2	-108.4(12)	C4_3	C1_3	C2_3	C17_3	6.3(15)
C5	C1	C4	O1	-0.2(14)	C4_3	C1_3	C3_3	C2_3	113.1(11)
C5	C1	C4	O2	-176.1(10)	C4_3	C1_3	C5_3	C6_3	-72.6(14)
C5	C6	C7	C8	-3(2)	C4_3	C1_3	C5_3	C10_3	100.4(13)
C6	C5	C10	C9	-3.8(19)	C5_3	C1_3	C2_3	C3_3	110.0(11)
C6	C7	C8	C9	-1(2)	C5_3	C1_3	C2_3	C11_3	3.3(15)
C7	C8	C9	C10	2(2)	C5_3	C1_3	C2_3	C17_3	-143.6(10)
C7	C8	C9	C23	-171.4(14)	C5_3	C1_3	C3_3	C2_3	-105.5(11)
C8	C9	C10	C5	0.0(19)	C5_3	C1_3	C4_3	O1_3	-3.7(14)
C8	C9	C23	C24	136.3(14)	C5_3	C1_3	C4_3	O2_3	179.4(10)
C8	C9	C23	C28	-41.0(19)	C5_3	C6_3	C7_3	C8_3	-5(2)
C9	C23	C24	C25	-174.8(12)	C6_3	C5_3	C10_3	C9_3	-0.9(19)
C9	C23	C28	C27	178.4(12)	C6_3	C7_3	C8_3	C9_3	2(2)
C10	C5	C6	C7	5(2)	C7_3	C8_3	C9_3	C10_3	1(2)
C10	C5	C6	C11	-173.8(10)	C7_3	C8_3	C9_3	C23_3	-173.9(13)
C10	C9	C23	C24	-37.2(19)	C8_3	C9_3	C10_3	C5_3	-2(2)
C10	C9	C23	C28	145.5(13)	C8_3	C9_3	C23_3	C24_3	137.4(14)
C11	C2	C3	C1	109.8(13)	C8_3	C9_3	C23_3	C28_3	-35(2)
C11	C2	C17	C18	84.5(15)	C9_3	C23_3	C24_3	C25_3	-169.7(14)
C11	C2	C17	C22	-90.4(14)	C9_3	C23_3	C28_3	C27_3	173.0(13)
C11	C12	C13	C14	-1(3)	C10_3	C5_3	C6_3	C11_3	-175.9(9)
C12	C11	C16	C15	-6(3)	C10_3	C5_3	C6_3	C7_3	4.1(18)
C12	C13	C14	C15	0(3)	C10_3	C9_3	C23_3	C24_3	-38(2)
C13	C14	C15	C16	-3(4)	C10_3	C9_3	C23_3	C28_3	149.8(14)
C14	C15	C16	C11	6(3)	C11_3	C2_3	C3_3	C1_3	109.9(11)
C16	C11	C12	C13	4(2)	C11_3	C2_3	C17_3	C18_3	74.6(14)

C17	C2	C3	C1	-107.9(12)	C11_3C2_3 C17_3C22_3	-98.0(13)
C17	C2	C11	C12	15.9(19)	C11_3C12_3C13_3C14_3	-1(2)
C17	C2	C11	C16	-168.2(13)	C12_3C11_3C16_3C15_3	2(3)
C17	C18	C19	C20	0(2)	C12_3C13_3C14_3C15_3	1(2)
C18	C17	C22	C21	3(2)	C13_3C14_3C15_3C16_3	1(3)
C18	C19	C20	C21	0(2)	C14_3C15_3C16_3C11_3	-2(3)
C19	C20	C21	C22	1(2)	C16_3C11_3C12_3C13_3	0(2)
C20	C21	C22	C17	-3(2)	C17_3C2_3 C3_3 C1_3	-108.6(11)
C22	C17	C18	C19	-1(2)	C17_3C2_3 C11_3C12_3	39.7(16)
C23	C9	C10	C5	173.9(12)	C17_3C2_3 C11_3C16_3	-135.3(15)
C23	C24	C25	C26	-3.4(19)	C17_3C18_3C19_3C20_3	2(2)
C24	C23	C28	C27	1.0(19)	C18_3C17_3C22_3C21_3	3.5(18)
C24	C25	C26	C27	0.4(18)	C18_3C19_3C20_3C21_3	2.3(19)
C24	C25	C26	C29	-178.3(11)	C19_3C20_3C21_3C22_3	-4(2)
C25	C26	C27	C28	3.1(18)	C20_3C21_3C22_3C17_3	0.8(19)
C25	C26	C29	C30	2.5(16)	C22_3C17_3C18_3C19_3	-4.9(18)
C25	C26	C29	C31	123.7(14)	C23_3C9_3 C10_3C5_3	173.7(12)
C25	C26	C29	C32	-113.9(14)	C23_3C24_3C25_3C26_3	-3(2)
C26	C27	C28	C23	-4(2)	C24_3C23_3C28_3C27_3	0(2)
C27	C26	C29	C30	-176.2(11)	C24_3C25_3C26_3C27_3	0(2)
C27	C26	C29	C31	-55.0(15)	C24_3C25_3C26_3C29_3	179.4(14)
C27	C26	C29	C32	67.3(14)	C25_3C26_3C27_3C28_3	3(2)
C28	C23	C24	C25	2.6(18)	C25_3C26_3C29_3C30_3	-9(2)
C29	C26	C27	C28	-178.1(11)	C25_3C26_3C29_3C31_3	110.9(17)
C11	C6	C7	C8	176.1(12)	C25_3C26_3C29_3C32_3	-134.1(16)
O1	C4	O2	Rh3	12.8(14)	C26_3C27_3C28_3C23_3	-3(2)
O2	C4	O1	Rh4	7.7(14)	C27_3C26_3C29_3C30_3	170.4(15)
Rh1	O2_4	C4_4	O1_4	8.9(16)	C27_3C26_3C29_3C31_3	-70(2)
Rh1	O2_4	C4_4	C1_4	-171.3(7)	C27_3C26_3C29_3C32_3	45(2)
Rh2	O1_4	C4_4	O2_4	9.3(16)	C28_3C23_3C24_3C25_3	3(2)
Rh2	O1_4	C4_4	C1_4	-170.6(7)	C29_3C26_3C27_3C28_3	-176.2(15)
Rh3	O2_3	C4_3	O1_3	12.5(15)	C11_4 C6_4 C7_4 C8_4	172.7(10)
Rh3	O2_3	C4_3	C1_3	-171.1(7)	C1_4 C2_4 C11_4C12_4	-116.8(15)
Rh4	O1_3	C4_3	O2_3	9.3(15)	C1_4 C2_4 C11_4C16_4	63.4(18)
Rh4	O1_3	C4_3	C1_3	-167.2(7)	C1_4 C2_4 C17_4C18_4	-123.0(12)
Rh5	O1_2	C4_2	O2_2	7(2)	C1_4 C2_4 C17_4C22_4	58.1(16)
Rh5	O1_2	C4_2	C1_2	-167.7(9)	C1_4 C5_4 C6_4 C11_4	0.3(16)

Rh6	O2_2	C4_2	O1_2	11(2)	C1_4	C5_4	C6_4	C7_4	-179.6(11)
Rh6	O2_2	C4_2	C1_2	-174.1(10)	C1_4	C5_4	C10_4	C9_4	-175.3(11)
C11_2	C6_2	C7_2	C8_2	178.8(12)	C2_4	C1_4	C4_4	O1_4	-147.5(10)
C1_2	C2_2	C11_2	C12_2	-125.3(18)	C2_4	C1_4	C4_4	O2_4	32.7(16)
C1_2	C2_2	C11_2	C16_2	52(2)	C2_4	C1_4	C5_4	C6_4	73.0(15)
C1_2	C2_2	C17_2	C18_2	-123.0(17)	C2_4	C1_4	C5_4	C10_4	-115.2(12)
C1_2	C2_2	C17_2	C22_2	59(2)	C2_4	C11_4	C12_4	C13_4	178.2(15)
C1_2	C5_2	C6_2	C11_2	-2(2)	C2_4	C11_4	C16_4	C15_4	178.0(14)
C1_2	C5_2	C6_2	C7_2	175.7(14)	C2_4	C17_4	C18_4	C19_4	179.2(12)
C1_2	C5_2	C10_2	C9_2	-174.4(12)	C2_4	C17_4	C22_4	C21_4	178.9(12)
C2_2	C1_2	C4_2	O1_2	-151.8(12)	C3_4	C1_4	C2_4	C11_4	-110.6(12)
C2_2	C1_2	C4_2	O2_2	32.7(19)	C3_4	C1_4	C2_4	C17_4	106.0(12)
C2_2	C1_2	C5_2	C6_2	74.0(19)	C3_4	C1_4	C4_4	O1_4	145.6(11)
C2_2	C1_2	C5_2	C10_2	-114.2(15)	C3_4	C1_4	C4_4	O2_4	-34.3(15)
C2_2	C11_2	C12_2	C13_2	-175.3(19)	C3_4	C1_4	C5_4	C6_4	138.4(12)
C2_2	C11_2	C16_2	C15_2	-178(2)	C3_4	C1_4	C5_4	C10_4	-49.9(15)
C2_2	C17_2	C18_2	C19_2	178.7(19)	C3_4	C2_4	C11_4	C12_4	174.5(14)
C2_2	C17_2	C22_2	C21_2	-178.7(16)	C3_4	C2_4	C11_4	C16_4	-5(2)
C3_2	C1_2	C2_2	C11_2	-108.5(15)	C3_4	C2_4	C17_4	C18_4	-56.3(15)
C3_2	C1_2	C2_2	C17_2	106.8(15)	C3_4	C2_4	C17_4	C22_4	124.8(14)
C3_2	C1_2	C4_2	O1_2	142.3(13)	C4_4	C1_4	C2_4	C3_4	-103.8(12)
C3_2	C1_2	C4_2	O2_2	-33.2(19)	C4_4	C1_4	C2_4	C11_4	145.6(11)
C3_2	C1_2	C5_2	C6_2	140.4(15)	C4_4	C1_4	C2_4	C17_4	42.2(16)
C3_2	C1_2	C5_2	C10_2	-47.7(18)	C4_4	C1_4	C3_4	C2_4	112.7(11)
C3_2	C2_2	C11_2	C12_2	166.3(17)	C4_4	C1_4	C5_4	C6_4	-78.6(14)
C3_2	C2_2	C11_2	C16_2	-17(3)	C4_4	C1_4	C5_4	C10_4	93.2(13)
C3_2	C2_2	C17_2	C18_2	-55(2)	C5_4	C1_4	C2_4	C3_4	107.2(11)
C3_2	C2_2	C17_2	C22_2	126.7(17)	C5_4	C1_4	C2_4	C11_4	-3.4(15)
C4_2	C1_2	C2_2	C3_2	-103.7(14)	C5_4	C1_4	C2_4	C17_4	-146.8(10)
C4_2	C1_2	C2_2	C11_2	147.8(13)	C5_4	C1_4	C3_4	C2_4	-105.5(11)
C4_2	C1_2	C2_2	C17_2	3.0(19)	C5_4	C1_4	C4_4	O1_4	2.3(14)
C4_2	C1_2	C3_2	C2_2	110.5(13)	C5_4	C1_4	C4_4	O2_4	-177.5(10)
C4_2	C1_2	C5_2	C6_2	-75.9(18)	C5_4	C6_4	C7_4	C8_4	-7(2)
C4_2	C1_2	C5_2	C10_2	95.9(15)	C6_4	C5_4	C10_4	C9_4	-2.9(18)
C5_2	C1_2	C2_2	C3_2	108.4(14)	C6_4	C7_4	C8_4	C9_4	0.7(19)
C5_2	C1_2	C2_2	C11_2	-0.1(19)	C7_4	C8_4	C9_4	C10_4	44.3(19)
C5_2	C1_2	C2_2	C17_2	-144.8(13)	C7_4	C8_4	C9_4	C23_4	-171.5(12)

C5_2 C1_2 C3_2 C2_2 -106.8(14) C8_4 C9_4 C10_4 C5_4 -3.1(19)
 C5_2 C1_2 C4_2 O1_2 -2.5(17) C8_4 C9_4 C23_4 C24_4 140.1(15)
 C5_2 C1_2 C4_2 O2_2 -178.0(13) C8_4 C9_4 C23_4 C28_4 -37.2(19)
 C5_2 C6_2 C7_2 C8_2 1(2) C9_4 C23_4 C24_4 C25_4 -176.6(16)
 C6_2 C5_2 C10_2 C9_2 -2(2) C9_4 C23_4 C28_4 C27_4 175.6(14)
 C6_2 C7_2 C8_2 C9_2 -9(2) C10_4 C5_4 C6_4 C11_4 -171.8(9)
 C7_2 C8_2 C9_2 C10_2 10(2) C10_4 C5_4 C6_4 C7_4 8.3(18)
 C7_2 C8_2 C9_2 C23_2 -174.1(13) C10_4 C9_4 C23_4 C24_4 -36(2)
 C8_2 C9_2 C10_2 C5_2 -5(2) C10_4 C9_4 C23_4 C28_4 147.1(14)
 C8_2 C9_2 C23_2 C24_2 138.0(15) C11_4 C2_4 C3_4 C1_4 106.5(12)
 C8_2 C9_2 C23_2 C28_2 -35(2) C11_4 C2_4 C17_4 C18_4 92.3(14)
 C9_2 C23_2 C24_2 C25_2 -172.7(15) C11_4 C2_4 C17_4 C22_4 -86.6(15)
 C9_2 C23_2 C28_2 C27_2 172.5(14) C11_4 C12_4 C13_4 C14_4 4(3)
 C10_2 C5_2 C6_2 C11_2 -173.8(10) C12_4 C11_4 C16_4 C15_4 -2(2)
 C10_2 C5_2 C6_2 C7_2 4(2) C12_4 C13_4 C14_4 C15_4 -2(3)
 C10_2 C9_2 C23_2 C24_2 -46.3(19) C13_4 C14_4 C15_4 C16_4 -1(3)
 C10_2 C9_2 C23_2 C28_2 141.2(15) C14_4 C15_4 C16_4 C11_4 4(3)
 C11_2 C2_2 C3_2 C1_2 107.9(14) C16_4 C11_4 C12_4 C13_4 -2(3)
 C11_2 C2_2 C17_2 C18_2 90.5(19) C17_4 C2_4 C3_4 C1_4 -106.9(11)
 C11_2 C2_2 C17_2 C22_2 -87.5(19) C17_4 C2_4 C11_4 C12_4 27.4(19)
 C11_2 C12_2 C13_2 C14_2 -15(3) C17_4 C2_4 C11_4 C16_4 -152.4(14)
 C12_2 C11_2 C16_2 C15_2 -1(3) C17_4 C18_4 C19_4 C20_4 1(2)
 C12_2 C13_2 C14_2 C15_2 16(3) C18_4 C17_4 C22_4 C21_4 0(2)
 C13_2 C14_2 C15_2 C16_2 -11(4) C18_4 C19_4 C20_4 C21_4 2(2)
 C14_2 C15_2 C16_2 C11_2 3(4) C19_4 C20_4 C21_4 C22_4 -4(2)
 C16_2 C11_2 C12_2 C13_2 27(3) C20_4 C21_4 C22_4 C17_4 3(2)
 C17_2 C2_2 C3_2 C1_2 -108.2(13) C22_4 C17_4 C18_4 C19_4 -2(2)
 C17_2 C2_2 C11_2 C12_2 21(2) C23_4 C9_4 C10_4 C5_4 172.7(12)
 C17_2 C2_2 C11_2 C16_2 -161.9(18) C23_4 C24_4 C25_4 C26_4 0(3)
 C17_2 C18_2 C19_2 C20_2 3(4) C24_4 C23_4 C28_4 C27_4 -2(2)
 C18_2 C17_2 C22_2 C21_2 3(3) C24_4 C25_4 C26_4 C27_4 0(3)
 C18_2 C19_2 C20_2 C21_2 -3(4) C24_4 C25_4 C26_4 C29_4 179.0(16)
 C19_2 C20_2 C21_2 C22_2 3(4) C25_4 C26_4 C27_4 C28_4 -1(3)
 C20_2 C21_2 C22_2 C17_2 -3(3) C25_4 C26_4 C29_4 C30_4 -15(2)
 C22_2 C17_2 C18_2 C19_2 -3(3) C25_4 C26_4 C29_4 C31_4 105.5(16)
 C23_2 C9_2 C10_2 C5_2 179.3(12) C25_4 C26_4 C29_4 C32_4 -136.2(15)
 C23_2 C24_2 C25_2 C26_2 1(3) C26_4 C27_4 C28_4 C23_4 2(3)

C24_2C23_2C28_2C27_20(2)	C27_4C26_4C29_4C30_4163.4(15)
C24_2C25_2C26_2C27_2-3(3)	C27_4C26_4C29_4C31_4-75.8(19)
C24_2C25_2C26_2C29_2-179.4(15)	C27_4C26_4C29_4C32_442.4(19)
C25_2C26_2C27_2C28_23(3)	C28_4C23_4C24_4C25_41(3)
C25_2C26_2C29_2C30_2-9(2)	C29_4C26_4C27_4C28_4179.9(15)

Table 7 Hydrogen Atom Coordinates ($\text{\AA}\times 10^4$) and Isotropic Displacement Parameters ($\text{\AA}^2\times 10^3$) for Rh-2Cl5tBuPh.

Atom	<i>x</i>	<i>y</i>	<i>z</i>	U(eq)
H3A	972.48	3510.64	4143.92	46
H3B	637.77	3762.64	3368.62	46
H7	1867.35	4539.83	7247.47	55
H8	1632.82	4048.78	8447.7	55
H10	797.86	3676.91	6167.3	40
H12	1921.45	4301.73	2405.04	69
H13	2600.65	4095.5	2556.46	77
H14	2799.74	3596.56	3801.17	97
H15	2282.15	3283.78	4872.41	99
H16	1613.18	3512.96	4844.35	67
H18	1048.96	3812.69	1370.45	55
H19	968.97	4186.24	-248.04	73
H20	1020.03	4908.62	-238.27	71
H21	1153.23	5249.13	1373.63	71
H22	1265.04	4874.8	3029.87	47
H24	388.48	3614.37	7802.46	44
H25	74.23	3236.45	9195.58	49
H27	1199.97	2897.71	10340.3	45
H28	1517.07	3337.14	9042.78	55
H30A	-160.31	3005.51	10780.81	86
H30B	-156.55	2582.44	11437.09	86
H30C	-129.67	2582.06	10131.35	86
H31A	532.03	2208.55	10056.1	76
H31B	434.89	2142.18	11325.43	76
H31C	870.48	2316.38	10955.16	76
H32A	813.21	2944.52	12120.71	79
H32B	378.85	2803.11	12588.38	79

H32C	423.84	3236.89	11996.12	79
H3C	221.26	9939.92	3565.97	81
H3D	-221.36	10060.18	3565.97	81
H4A	-205.2	10168.1	-3314.11	36
H4B	205.2	9831.9	-3314.11	36
H9A	216.1	4967.8	7777.81	86
H9B	-216.1	5032.2	7777.81	86
H10A	-166.5	5153.1	1047.96	57
H10B	166.5	4846.9	1047.96	57
H14A	5302.43	5092.64	3241.19	70
H14B	4697.48	4907.35	3241.09	70
H3A_2	3208.98	5061.21	-663.57	68
H3B_2	3599.3	5192.1	-1463.43	68
H7_2	3649.21	3801.05	2597.99	70
H8_2	3291.15	4273.11	3678.67	66
H10_2	3408.7	5131.68	1316.33	54
H12_2	3390.01	3789.12	-2146.09	109
H13_2	2814.64	3353.84	-2186.39	82
H14_2	2342.83	3433.77	-652.15	109
H15_2	2289.38	4069.73	112.08	120
H16_2	2819.18	4560.32	-95.45	98
H18_2	3411.29	4830.98	-3372.42	86
H19_2	3768.11	4755.07	-5027.25	114
H20_2	4306.01	4281.5	-5114.59	108
H21_2	4539.97	3944.38	-3518.3	97
H22_2	4156.65	4039.1	-1852.26	77
H24_2	3566.27	5543.73	2964.14	75
H25_2	3372.52	6047.37	4227.43	78
H27_2	2534.67	5236.59	5450.5	70
H28_2	2731.34	4746.22	4194.37	76
H30A_2	3348.33	6331.2	6005.92	108
H30B_2	2977.63	6580.31	6539.21	108
H30C_2	3025.07	6560.17	5238.77	108
H31A_2	2182.96	5864.97	5636.83	106
H31B_2	2318.32	6270.23	5000.2	106
H31C_2	2237.8	6285.29	6289.45	106
H32A_2	2721.57	5540.28	7072.31	108

H32B_2	2684.8	5984.73	7609.54	108
H32C_2	3123.85	5807.26	7282.09	108
H3A_3	1486.92	5954.01	4136.58	43
H3B_3	1236.01	5609.36	3392.77	43
H7_3	363.06	6868.28	7086.17	55
H8_3	881.96	6708.71	8305.7	55
H10_3	1378.69	5928.82	6093.24	50
H12_3	575.52	6905.29	2801.41	53
H13_3	802.7	7581.13	2743.13	53
H14_3	1472.7	7747.4	3376.02	58
H15_3	1887.99	7228.35	4004.37	71
H16_3	1671.57	6549.09	3978.24	75
H18_3	1220.74	6091.74	1321.29	46
H19_3	897.69	5964.14	-365.64	56
H20_3	173.8	5924.87	-450.44	51
H21_3	-210.84	6056.98	1144.33	55
H22_3	130.06	6157.98	2846.87	42
H24_3	1545.58	5554.07	7718.5	64
H25_3	1949.66	5316.59	9175.38	72
H27_3	2047.61	6487.06	10287.13	67
H28_3	1592.82	6711.32	8919.36	69
H30A_3	2063.14	5116.06	10952.61	101
H30B_3	2471.72	5152.11	11665.09	101
H30C_3	2499.6	5119.89	10362.34	101
H31A_3	2854.55	5755.81	10000.15	107
H31B_3	2928.74	5775.05	11291.72	107
H31C_3	2750.21	6164.69	10661.51	107
H32A_3	2187.37	6208.02	11932.6	110
H32B_3	2327.12	5809.72	12593.38	110
H32C_3	1875.53	5836.15	12095.87	110
H3A_4	225.73	8218.06	-206.96	46
H3B_4	45.24	8581.31	-1028.65	46
H7_4	1386.21	8758.68	3086.8	49
H8_4	929.06	8398.89	4212.81	47
H10_4	83.03	8399.98	1761.84	45
H12_4	1495.08	8654.08	-1396.37	69
H13_4	2061.14	8247.17	-991.84	78

H14_4	1960.16	7605	-72.79	78
H15_4	1307.23	7429.77	497.77	71
H16_4	750.38	7884.04	246.76	56
H18_4	450.75	8456.75	-2874.42	55
H19_4	492.94	8828.39	-4529.02	65
H20_4	823.07	9473.92	-4535.47	69
H21_4	1135.51	9717.71	-2945.58	67
H22_4	1058.3	9351.34	-1270.06	60
H24_4	-357.85	8495.77	3311.96	68
H25_4	-854.1	8258.12	4519.73	76
H27_4	35.78	7586.71	6033.99	69
H28_4	522.2	7814.26	4771.07	65
H30A_4	-1128.11	8271.03	6430.18	88
H30B_4	-1375.58	7879.5	6850.62	88
H30C_4	-1328.47	7962.59	5568.07	88
H31A_4	-633.72	7120.65	5883.98	89
H31B_4	-1032.44	7276.35	5251.11	89
H31C_4	-1060.19	7156.88	6517.05	89
H32A_4	-402.74	7506.18	7533.76	88
H32B_4	-823.72	7688.76	7986.7	88
H32C_4	-468.11	7990.45	7592.04	88

Table 8 Atomic Occupancy for Rh-2Cl5tBuPh.

<i>Atom Occupancy</i>	<i>Atom Occupancy</i>	<i>Atom</i>	<i>Occupancy</i>
H3C 0.25	H3D 0.25	H4A	0.25
H4B 0.25	H9A 0.5	H9B	0.5
H10A 0.5	H10B 0.5	H14A	0.25
H14B 0.25			

Table 9 Solvent masks information for Rh-2Cl5tBuPh.

Number	X	Y	Z	Volume	Electron count	Content
1	-0.255	0.242	-0.017	558.5	103.2	?
2	-0.070	0.461	0.758	40.1	11.0	?
3	0.070	0.539	0.758	40.1	9.4	?
4	0.255	0.758	-0.827	558.5	103.6	?
5	0.242	0.255	-0.799	558.5	103.3	?

6	0.461	0.070	0.758	40.1	10.2	?
7	0.425	0.544	0.242	8.1	2.3	?
8	0.456	0.425	0.242	8.1	2.4	?
9	0.539	0.930	0.758	40.1	10.2	?
10	0.544	0.575	0.242	8.1	2.4	?
11	0.575	0.456	0.242	8.1	2.5	?
12	0.758	0.745	-0.584	558.5	103.5	?

Experimental

Single crystals of $C_{128}H_{118}Cl_4O_{10}Rh_2$ [**Rh-2Cl5tBuPh**] were [**The material was recrystallised from --- by as supplied**]. A suitable crystal was selected and [**The crystal was mounted on a loop**] on a **XtaLAB Synergy, Dualflex, HyPix** diffractometer. The crystal was kept at 100(2) K during data collection. Using Olex2 [1], the structure was solved with the ShelXT [2] structure solution program using Intrinsic Phasing and refined with the ShelXL [3] refinement package using Least Squares minimisation.

Crystal structure determination of [**Rh-2Cl5tBuPh**]

Crystal Data for $C_{128}H_{118}Cl_4O_{10}Rh_2$ ($M = 2163.84$ g/mol): tetragonal, space group P4 (no. 75), $a = 32.0493(5)$ Å, $c = 11.9878(3)$ Å, $V = 12313.3(5)$ Å³, $Z = 4$, $T = 100(2)$ K, $\mu(\text{CuK}\alpha) = 3.384$ mm⁻¹, $D_{\text{calc}} = 1.167$ g/cm³, 69630 reflections measured ($6.166^\circ \leq 2\theta \leq 130.158^\circ$), 19495 unique ($R_{\text{int}} = 0.0730$, $R_{\text{sigma}} = 0.0671$) which were used in all calculations. The final R_1 was 0.0766 ($I > 2\sigma(I)$) and wR_2 was 0.2019 (all data).

Refinement model description

Number of restraints - 1226, number of constraints - unknown.

Details:

1. Fixed Uiso

At 1.2 times of:

All C(H) groups, All C(H,H) groups

At 1.5 times of:

All C(H,H,H) groups, All O(H,H) groups

2. Restrained distances

O14-H14A = O14-H14B

0.975 with sigma of 0.002

3. Uiso/Uanis restraints and constraints

Uanis(C25_3) \approx Ueq: with sigma of 0.001 and sigma for terminal atoms of 0.002

Uanis(C13_2) \approx Ueq: with sigma of 0.001 and sigma for terminal atoms of 0.002

4. Rigid body (RIGU) restrains

C11_2, O1_2, O2_2, C1_2, C2_2, C3_2, C4_2, C5_2, C6_2, C7_2, C8_2, C9_2,
C10_2, C11_2, C12_2, C13_2, C14_2, C15_2, C16_2, C17_2, C18_2, C19_2, C20_2,
C21_2, C22_2, C23_2, C24_2, C25_2, C26_2, C27_2, C28_2, C29_2, C30_2, C31_2,
C32_2

C11_3, O1_3, O2_3, C1_3, C2_3, C3_3, C4_3, C5_3, C6_3, C7_3, C8_3, C9_3,
C10_3, C11_3, C12_3, C13_3, C14_3, C15_3, C16_3, C17_3, C18_3, C19_3, C20_3,
C21_3, C22_3, C23_3, C24_3, C25_3, C26_3, C27_3, C28_3, C29_3, C30_3, C31_3,

C32_3

C11_4, O1_4, O2_4, C1_4, C2_4, C3_4, C4_4, C5_4, C6_4, C7_4, C8_4, C9_4,
C10_4, C11_4, C12_4, C13_4, C14_4, C15_4, C16_4, C17_4, C18_4, C19_4, C20_4,
C21_4, C22_4, C23_4, C24_4, C25_4, C26_4, C27_4, C28_4, C29_4, C30_4, C31_4,
C32_4

with sigma for 1-2 distances of 0.0002 and sigma for 1-3 distances of 0.0002

C11_3, O1_3, O2_3, C1_3, C2_3, C3_3, C5_3, C6_3, C10_3

with sigma for 1-2 distances of 0.0002 and sigma for 1-3 distances of 0.0002

C1_3, C2_3, C3_3, C11_3, C17_3

with sigma for 1-2 distances of 0.0001 and sigma for 1-3 distances of 0.0001

C11_3, C2_3, C7_3, C9_3, C11_3, C12_3, C16_3, C17_3

with sigma for 1-2 distances of 0.0001 and sigma for 1-3 distances of 0.0001

C11_2, O1_2, O2_2, C1_2, C2_2, C3_2, C4_2, C5_2, C6_2, C7_2, C8_2, C9_2,
C10_2, C11_2, C12_2, C13_2, C14_2, C15_2, C16_2, C17_2, C18_2, C19_2, C20_2,
C21_2, C22_2, C23_2, C24_2, C25_2, C26_2, C27_2, C28_2, C29_2, C30_2, C31_2,
C32_2

with sigma for 1-2 distances of 0.0001 and sigma for 1-3 distances of 0.0001

C1, C4, O1, O2

with sigma for 1-2 distances of 0.0001 and sigma for 1-3 distances of 0.0001

C5, C6, C7, C8, C9, C10, C23, C11

with sigma for 1-2 distances of 0.0001 and sigma for 1-3 distances of 0.0001

5. Same fragment restrains

{C11_3, O1_3, O2_3, C1_3, C2_3, C3_3, C4_3, C5_3, C6_3, C7_3, C8_3, C9_3,
C10_3, C11_3, C12_3, C13_3, C14_3, C15_3, C16_3, C17_3, C18_3, C19_3, C20_3,
C21_3, C22_3, C23_3, C24_3, C25_3, C26_3, C27_3, C28_3, C29_3, C30_3, C31_3,
C32_3}

{C11_4, O1_4, O2_4, C1_4, C2_4, C3_4, C4_4, C5_4, C6_4, C7_4, C8_4, C9_4,
C10_4, C11_4, C12_4, C13_4, C14_4, C15_4, C16_4, C17_4, C18_4, C19_4, C20_4,
C21_4, C22_4, C23_4, C24_4, C25_4, C26_4, C27_4, C28_4, C29_4, C30_4, C31_4,
C32_4}

as

{C11_2, O1_2, O2_2, C1_2, C2_2, C3_2, C4_2, C5_2, C6_2, C7_2, C8_2, C9_2,
C10_2, C11_2, C12_2, C13_2, C14_2, C15_2, C16_2, C17_2, C18_2, C19_2, C20_2,
C21_2, C22_2, C23_2, C24_2, C25_2, C26_2, C27_2, C28_2, C29_2, C30_2, C31_2,
C32_2} sigma for 1-2: 0.02 1-3: 0.04

6. Others

Fixed Sof: H3C(0.25) H3D(0.25) H4A(0.25) H4B(0.25) H9A(0.5) H9B(0.5)

H10A(0.5) H10B(0.5) H14A(0.25) H14B(0.25)

Fixed X: Rh3(0)

Fixed Y: Rh3(0.5)

Fixed Z: Rh3(0.34552)

7.a Riding coordinates:

O4(H4A,H4B), O9(H9A,H9B), O10(H10A,H10B)

7.b Rotating group:

O3(H3C,H3D), O14(H14A,H14B)

7.c Secondary CH2 refined with riding coordinates:

C3(H3A,H3B), C3(H3A,H3B), C3(H3A,H3B), C3(H3A,H3B)

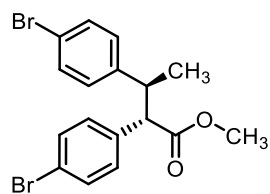
7.d Aromatic/amide H refined with riding coordinates:

C7(H7), C8(H8), C10(H10), C12(H12), C13(H13), C14(H14), C15(H15), C16(H16),
C18(H18), C19(H19), C20(H20), C21(H21), C22(H22), C24(H24), C25(H25), C27(H27),
C28(H28), C7(H7), C8(H8), C10(H10), C12(H12), C13(H13), C14(H14), C15(H15),
C16(H16), C18(H18), C19(H19), C20(H20), C21(H21), C22(H22), C24(H24), C25(H25),
C27(H27), C28(H28), C7(H7), C8(H8), C10(H10), C12(H12), C13(H13), C14(H14),
C15(H15), C16(H16), C18(H18), C19(H19), C20(H20), C21(H21), C22(H22), C24(H24),
C25(H25), C27(H27), C28(H28), C7(H7), C8(H8), C10(H10), C12(H12), C13(H13),
C14(H14), C15(H15), C16(H16), C18(H18), C19(H19), C20(H20), C21(H21), C22(H22),
C24(H24), C25(H25), C27(H27), C28(H28)

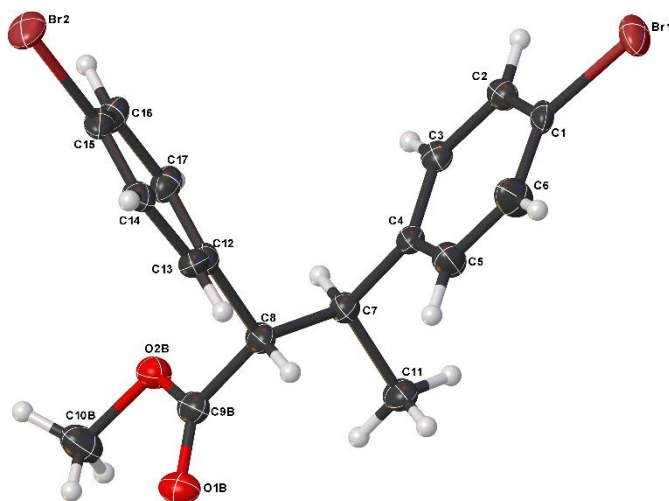
7.e Idealised Me refined as rotating group:

C30(H30A,H30B,H30C), C31(H31A,H31B,H31C), C32(H32A,H32B,H32C),
C30(H30A,H30B,
H30C), C31(H31A,H31B,H31C), C32(H32A,H32B,H32C), C30(H30A,H30B,H30C),
C31(H31A,
H31B,H31C), C32(H32A,H32B,H32C), C30(H30A,H30B,H30C), C31(H31A,H31B,H31C),
C32(H32A,H32B,H32C)

Methyl (2*S*,3*S*)-2,3-bis(4-bromophenyl)butanoate (51)



Crystal Data and Experimental



Experimental. Single colourless needle-shaped crystals of **WL-N3-134** were recrystallised from DCM by slow evaporation. A suitable crystal $0.32 \times 0.11 \times 0.11$ mm³ was selected and mounted on a loop with paratone oil on an XtaLAB Synergy, Dualflex, HyPix diffractometer. The crystal was kept at a steady $T = 99.9(6)$ K during data collection. The structure was solved with the **ShelXT** (Sheldrick, 2015) structure solution program using the Intrinsic Phasing solution method and by using **Olex2** (Dolomanov et al., 2009) as the graphical interface. The model was refined with version 2017/1 of **ShelXL** (Sheldrick, 2015) using Least Squares minimisation.

Crystal Data. C₃₄H₃₂Br₄O₄, $M_r = 824.23$, triclinic, *P*1 (No. 1), $a = 8.7463(2)$ Å, $b = 10.1160(3)$ Å, $c = 10.5040(2)$ Å, $\alpha = 76.378(2)^\circ$, $\beta = 88.4024(19)^\circ$, $\gamma = 64.471(3)^\circ$, $V = 812.16(4)$ Å³, $T = 99.9(6)$ K, $Z = 1$, $Z' = 1$, $m(\text{MoK}\alpha) = 4.992$ mm⁻¹, 29465 reflections measured, 10339 unique ($R_{int} = 0.0365$) which were used in all calculations. The final wR_2 was 0.0940 (all data) and R_1 was 0.0386 ($I > 2\sigma(I)$).

Compound **WL-N3-134**

Formula	C ₃₄ H ₃₂ Br ₄ O ₄
<i>D</i> _{calc.} / g cm ⁻³	1.685
<i>m</i> /mm ⁻¹	4.992
Formula Weight	824.23
Colour	colourless
Shape	needle
Size/mm ³	0.32×0.11×0.11
<i>T</i> /K	99.9(6)
Crystal System	triclinic
Flack Parameter	0.005(5)
Hooft Parameter	0.027(3)
Space Group	<i>P</i> 1
<i>a</i> /Å	8.7463(2)
<i>b</i> /Å	10.1160(3)
<i>c</i> /Å	10.5040(2)
<i>a</i> [°]	76.378(2)
<i>b</i> [°]	88.4024(19)
<i>g</i> [°]	64.471(3)
<i>V</i> /Å ³	812.16(4)
<i>Z</i>	1
<i>Z</i> '	1
Wavelength/Å	0.71073
Radiation type	MoK _α
<i>Q</i> _{min} [°]	2.303
<i>Q</i> _{max} [°]	30.997
Measured Refl.	29465
Independent Refl.	10339
Reflections with <i>I</i> > 2σ(<i>I</i>)	9282
<i>R</i> _{int}	0.0365
Parameters	408
Restraints	198
Largest Peak	1.603
Deepest Hole	-0.703
Goof	1.032
<i>wR</i> ₂ (all data)	0.0940
<i>wR</i> ₂	0.0910
<i>R</i> ₁ (all data)	0.0455
<i>R</i> ₁	0.0386

Structure Quality Indicators

Reflections:	d min (Mo)	0.69	<i>I</i> /σ	18.2	<i>R</i> _{int}	3.65%	complete at 2θ=72°	100%		
Refinement:	Shift	-0.001	Max Peak	1.6	Min Peak	-0.7	Goof	1.032	Flack	.005(5)

A colourless needle-shaped crystal with dimensions 0.32×0.11×0.11 mm³ was mounted on a

loop with paratone oil. Data were collected using an **SYNERGY** diffractometer equipped with an Oxford Cryosystems low-temperature device operating at $T = 99.9(6)$ K.

Data were measured using w scans of $^{\circ}$ per frame for s using MoK_{α} radiation. The total number of runs and images was based on the strategy calculation from the program **CrysAlisPro** (Rigaku, V1.171.39.43c, 2018). The maximum resolution that was achieved was $Q = 30.997^{\circ}$. The diffraction pattern was indexed using **CrysAlisPro** (Rigaku, V1.171.39.43c, 2018) and the unit cell was refined using **CrysAlisPro** (Rigaku, V1.171.39.43c, 2018) on 16866 reflections, 57% of the observed reflections.

Data reduction, scaling and absorption corrections were performed using **CrysAlisPro** (Rigaku, V1.171.39.43c, 2018). The final completeness is 100.00 % out to 30.997° in Q . A Gaussian absorption correction was performed using CrysAlisPro 1.171.39.43c (Rigaku Oxford Diffraction, 2018). This is a numerical absorption correction based on Gaussian integration over a multifaceted crystal model. An empirical absorption correction using spherical harmonics as implemented by SCALE3 ABSPACK algorithm was also applied. The absorption coefficient m of this material is 4.992 mm^{-1} at this wavelength ($\lambda = 0.71073 \text{ \AA}$) and the minimum and maximum transmissions are 0.287 and 1.000.

The structure was solved and the space group $P1$ (# 1) determined by the **ShelXT** (Sheldrick, 2015) structure solution program using Intrinsic Phasing and refined by Least Squares using version 2017/1 of **ShelXL** (Sheldrick, 2015). All non-hydrogen atoms were refined anisotropically. Hydrogen atom positions were calculated geometrically and refined using the riding model.

There are single molecule in the asymmetric unit, which is represented by the reported sum formula. In other words: Z is 1 and Z' is 1.

The Flack parameter was refined to 0.005(5). Determination of absolute structure using Bayesian statistics on Bijvoet differences using the Olex2 results in 0.027(3). Note: The Flack parameter is used to determine chirality of the crystal studied, the value should be near 0, a value of 1 means that the stereochemistry is wrong and the model should be inverted. A value of 0.5 means that the crystal consists of a racemic mixture of the two enantiomers. **Images of the Crystal on the Diffractometer**



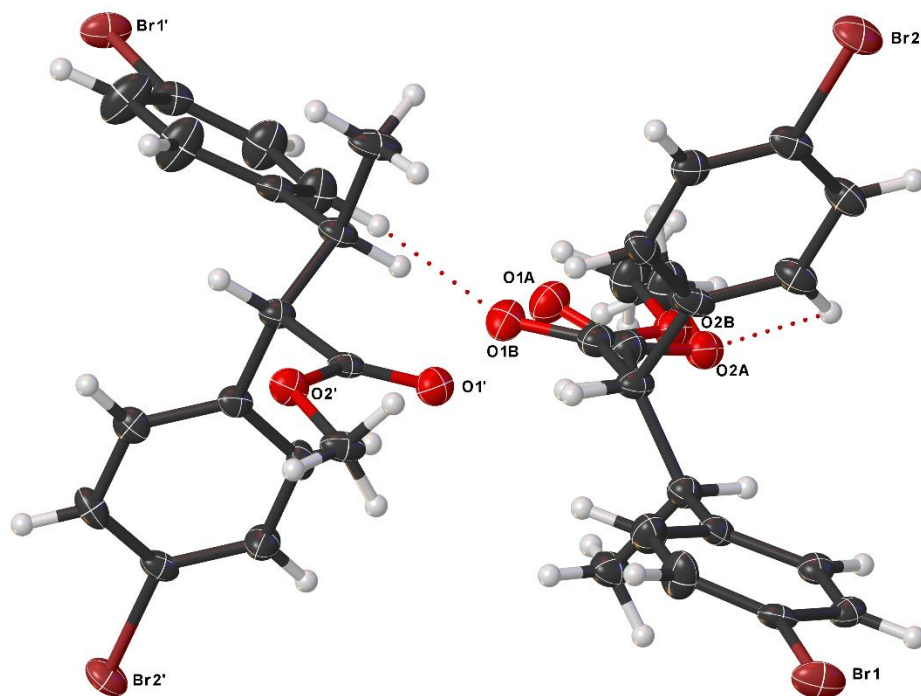


Figure 4:

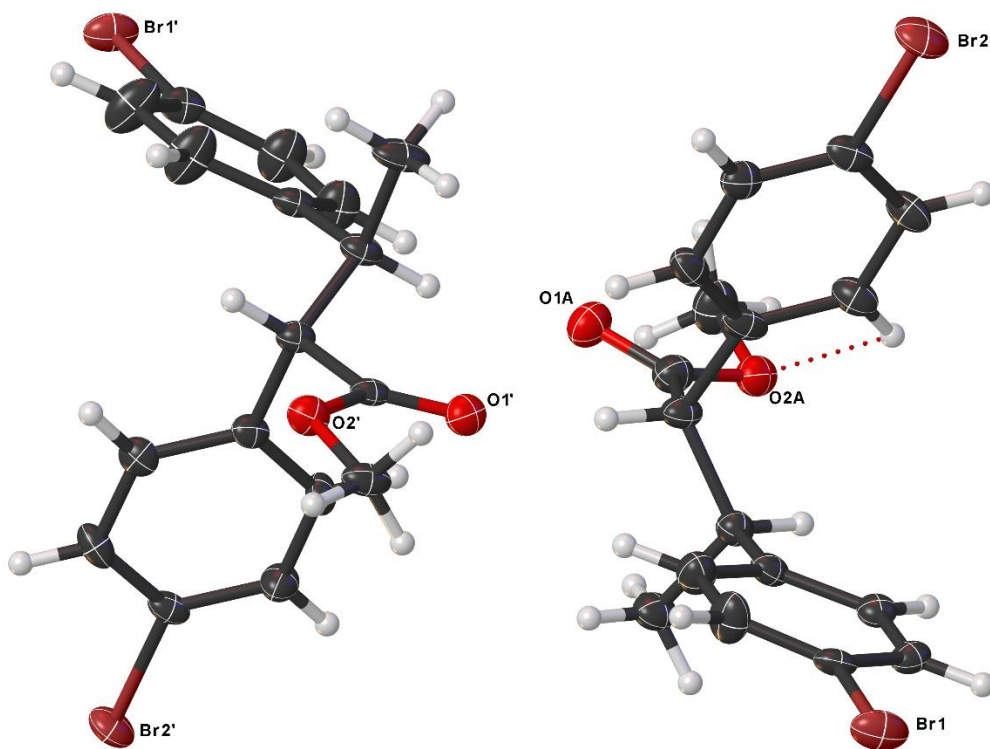
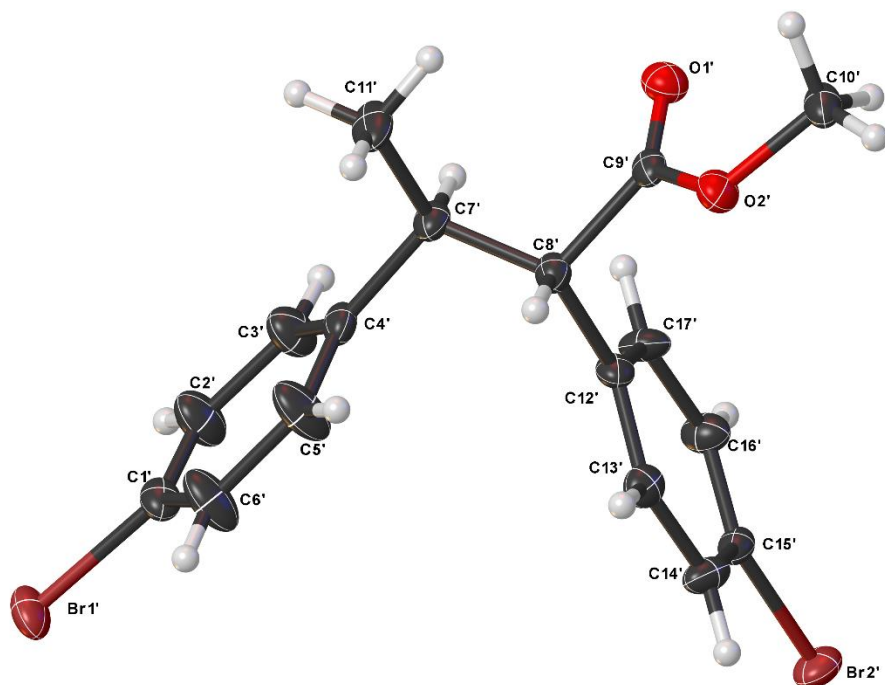
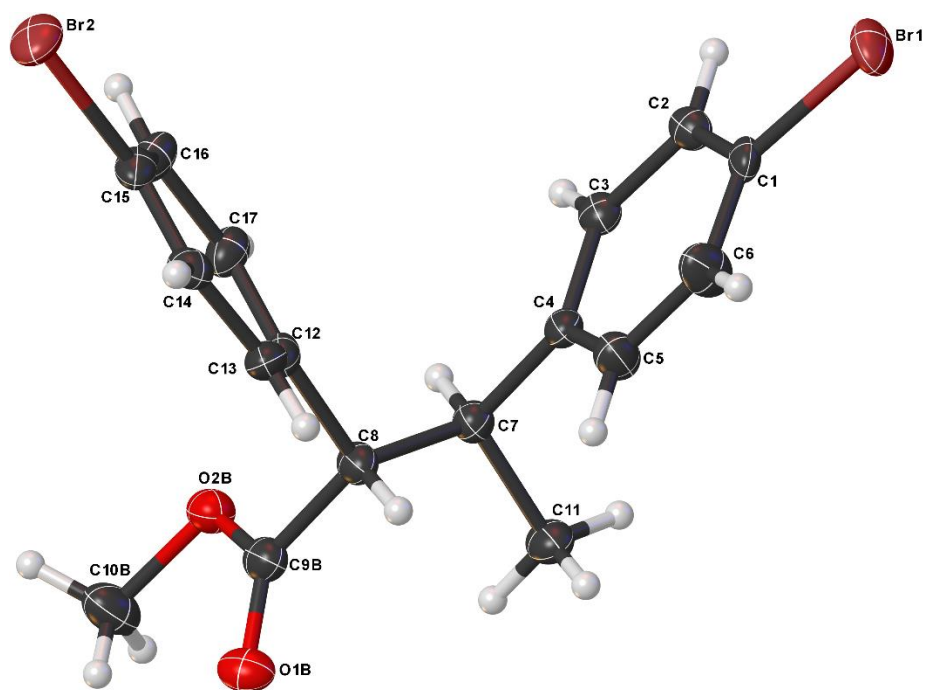


Figure 5:

**Figure 6:****Figure 7:**

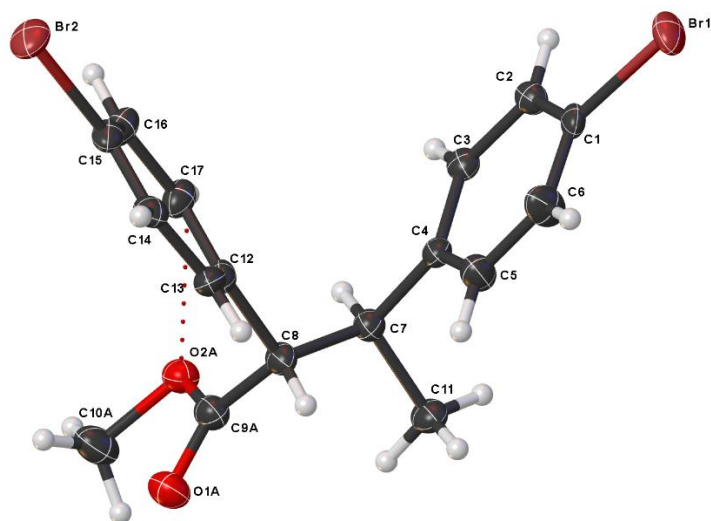
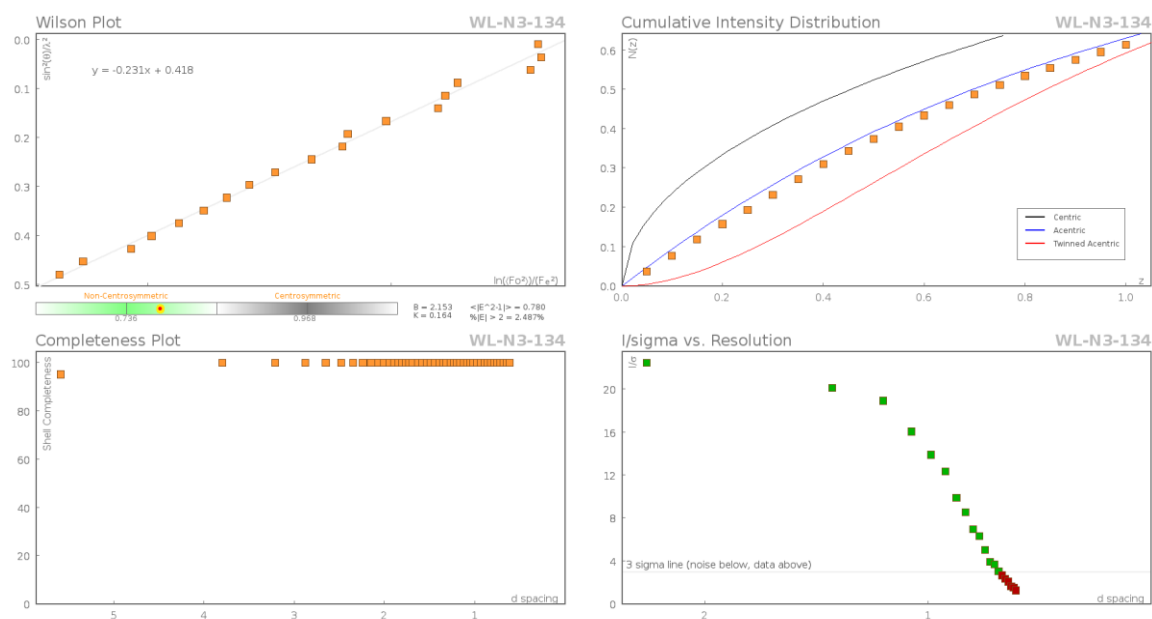
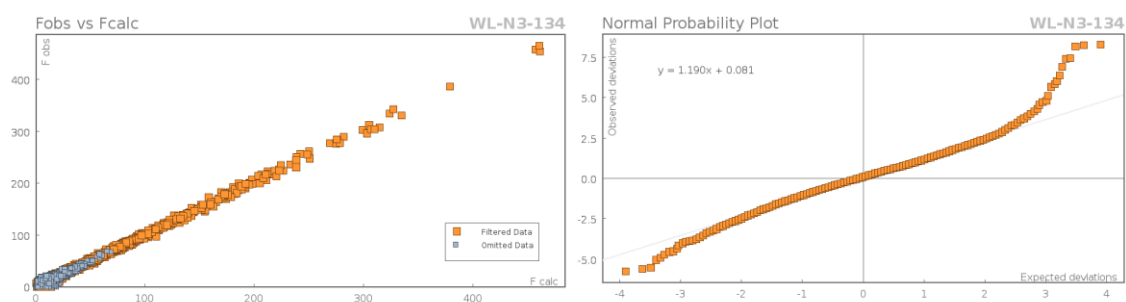


Figure 8:
Data Plots: Diffraction Data



Data Plots: Refinement and Data



Reflection Statistics

Total reflections (after filtering)	29465	Unique reflections	10339
Completeness	0.996	Mean I/s	18.22
hkl _{max} collected	(14, 16, 17)	hkl _{min} collected	(-14, -16, -17)
hkl _{max} used	(12, 14, 15)	hkl _{min} used	(-12, -14, -15)
Lim d _{max} collected	20.0	Lim d _{min} collected	0.69
d _{max} used	8.84	d _{min} used	0.69
Friedel pairs	7733	Friedel pairs merged	0
Inconsistent equivalents	2	R _{int}	0.0365
R _{sigma}	0.0399	Intensity transformed	0
Omitted reflections	0	Omitted by user (OMIT hkl)	0
Multiplicity	(2389, 6425, 4302, 1578, 569, 243, 74, 26, 10, 1, 1)	Maximum multiplicity	11
Removed systematic absences	0	Filtered off (Shel/OMIT)	10132

Table 17: Fractional Atomic Coordinates ($\times 10^4$) and Equivalent Isotropic Displacement Parameters ($\text{\AA}^2 \times 10^3$) for **WL-N3-134**. U_{eq} is defined as 1/3 of the trace of the orthogonalised U_{ij} .

Atom	x	y	z	U_{eq}
Br2'	1718.0(7)	5497.7(6)	-988.4(5)	28.21(12)
Br1'	5882.0(7)	11422.1(6)	356.7(5)	29.86(14)
C14'	443(6)	7536(6)	663(5)	24.1(10)
C16'	2939(7)	5235(6)	1576(5)	24.9(10)
C13'	460(6)	8010(6)	1811(5)	21.7(9)
C8'	1595(6)	7621(5)	4115(5)	19.5(6)
C1'	5005(7)	10252(6)	1564(5)	23.2(8)
C4'	3827(6)	8559(6)	3435(5)	21.4(6)
C2'	6039(8)	8767(7)	2093(6)	34.7(11)
C3'	5435(7)	7913(7)	3017(6)	31.3(10)
C12'	1667(6)	7106(5)	2844(4)	18.7(8)
C10'	-1139(7)	6085(6)	6110(5)	25.3(8)
C7'	3264(6)	7625(6)	4528(4)	21.2(7)
C11'	3080(8)	8206(7)	5785(5)	33.1(11)
C17'	2926(7)	5720(6)	2716(5)	24.3(10)

Atom	x	y	z	U_{eq}
C9'	1173(6)	6527(5)	5182(4)	18.6(7)
C15'	1695(6)	6138(6)	579(4)	20.2(9)
C6'	3354(8)	10930(7)	1889(7)	37.4(13)
C5'	2778(8)	10058(7)	2838(7)	38.1(14)
O1'	2169(5)	5340(4)	5829(4)	25.5(6)
O2'	-527(5)	7091(4)	5226(4)	24.4(6)
Br1	3371.0(7)	-1363.3(7)	9389.7(5)	33.36(14)
Br2	8108.7(7)	4083.6(7)	10991.9(5)	34.27(14)
C1	4661(6)	-542(6)	8290(5)	21.2(8)
C2	6403(6)	-1407(5)	8318(5)	21.5(8)
C3	7342(6)	-818(6)	7475(5)	20.5(8)
C4	6574(6)	602(6)	6612(5)	21.3(8)
C5	4838(7)	1462(7)	6624(6)	28.7(10)
C6	3880(7)	904(7)	7483(6)	32.3(11)
C7	7637(6)	1127(5)	5647(5)	21.3(8)
C8	7423(7)	2714(6)	5665(5)	22.8(9)
C11	7175(7)	1102(6)	4261(5)	27.2(10)
C12	7600(7)	2975(6)	7005(5)	23.6(9)
C13	6301(7)	4184(6)	7359(5)	26.2(10)
C14	6465(7)	4536(6)	8533(5)	25(1)
C15	7921(7)	3633(6)	9364(5)	24.6(10)
C16	9222(6)	2388(7)	9060(5)	26.3(10)
C17	9063(7)	2069(7)	7864(5)	25.8(10)
C9A	8780(11)	2939(13)	4882(11)	26.6(16)
C10A	11271(16)	2828(16)	4287(16)	37.4(17)
O1A	8489(13)	4167(9)	4109(8)	31.5(16)
O2A	10373(9)	1964(9)	5081(9)	26.9(10)
C9B	8357(13)	3368(12)	4713(10)	25.2(16)
C10B	10872(16)	3303(17)	4028(16)	37.4(17)
O1B	7678(12)	4517(8)	3811(7)	27.1(15)
O2B	9984(9)	2527(9)	4955(8)	26.9(10)

Table 18: Anisotropic Displacement Parameters ($\times 10^4$) **WL-N3-134**. The anisotropic displacement factor exponent takes the form: $-2p^2[h^2a^{*2} \times U_{11} + \dots + 2hka^* \times b^* \times U_{12}]$

Atom	U_{11}	U_{22}	U_{33}	U_{23}	U_{13}	U_{12}
Br2'	32.7(3)	40.7(3)	17.0(2)	-12.3(2)	2.03(19)	-18.7(2)
Br1'	39.7(3)	36.3(3)	28.6(3)	-13.9(2)	16.8(2)	-28.2(2)
C14'	19(2)	37(3)	15.8(19)	-5.4(19)	0.1(16)	-12(2)
C16'	32(3)	22(2)	19(2)	-7.7(17)	2.1(19)	-9(2)

Atom	U_{11}	U_{22}	U_{33}	U_{23}	U_{13}	U_{12}
C13'	17(2)	28(2)	22(2)	-7.7(19)	5.3(17)	-10.9(18)
C8'	23.0(13)	22.5(15)	18.3(13)	-8(1)	4.8(10)	-13.3(12)
C1'	28.9(14)	31.2(12)	17.7(17)	-10.5(10)	10.1(11)	-18.9(10)
C4'	26.0(13)	28.9(13)	19.3(12)	-11.2(10)	5.1(11)	-18.8(11)
C2'	29.2(15)	34.3(12)	39(2)	-2.9(12)	12.9(15)	-16.5(11)
C3'	26.4(14)	33.8(14)	32(2)	-2.4(13)	9.1(13)	-15.1(11)
C12'	25(2)	23(2)	12.0(17)	-5.5(16)	5.4(16)	-13.8(18)
C10'	36(2)	34.6(19)	19.1(17)	-12.5(14)	10.0(16)	-25.3(18)
C7'	26.1(15)	29.6(17)	16.4(11)	-10.6(10)	4.9(9)	-17.6(13)
C11'	51(3)	49(3)	21.4(13)	-20.2(16)	12.6(16)	-37(3)
C17'	29(2)	22(2)	14.8(19)	-1.8(17)	-3.3(18)	-6(2)
C9'	26.3(10)	23.2(12)	14.3(13)	-9.6(10)	4.8(9)	-15.7(9)
C15'	25(2)	31(2)	13.2(18)	-8.9(17)	5.4(16)	-18(2)
C6'	36.1(15)	28.8(15)	47(3)	-6.7(14)	23.9(16)	-15.9(11)
C5'	31.6(16)	32.1(14)	45(3)	-2.2(14)	20.6(16)	-13.9(12)
O1'	30.0(12)	27.2(12)	19.9(14)	-5.2(9)	4.5(11)	-13.5(10)
O2'	26.5(10)	29.4(14)	21.1(14)	-5.9(11)	6.4(9)	-16.0(9)
Br1	42.6(3)	46.8(3)	29.5(3)	-15.7(3)	15.9(2)	-34.3(3)
Br2	45.7(3)	49.0(3)	20.3(2)	-17.5(2)	6.9(2)	-27.4(3)
C1	26.5(18)	27.1(19)	20(2)	-10.6(15)	4.1(15)	-18.9(15)
C2	28.8(18)	19.5(18)	19.7(19)	-8.3(15)	5.7(15)	-12.1(15)
C3	24.2(19)	22.4(19)	17.6(18)	-9.9(15)	5.0(15)	-10.6(15)
C4	26.5(18)	26.4(19)	16.2(17)	-5.7(14)	0.6(14)	-16.0(15)
C5	28(2)	27(2)	30(3)	-1.9(18)	-0.7(18)	-14.0(17)
C6	17.9(19)	33(2)	39(3)	-0.7(19)	0.7(18)	-9.5(17)
C7	23(2)	22.9(19)	19.9(17)	-6.0(15)	2.3(15)	-11.7(17)
C8	32(3)	24.0(19)	18.5(18)	-8.2(16)	4.0(18)	-16.4(19)
C11	37(3)	30(3)	19.3(18)	-9.0(18)	3.5(18)	-18(2)
C12	33(2)	33(2)	17.8(18)	-8.3(17)	6.1(18)	-26(2)
C13	33(3)	33(3)	18(2)	-1.6(19)	-2.7(19)	-20(2)
C14	33(3)	26(2)	19(2)	-4.4(18)	5.2(19)	-17(2)
C15	33(3)	37(3)	15.3(19)	-9.5(19)	8.3(19)	-24(2)
C16	20(2)	40(3)	24(2)	-14(2)	3.4(18)	-15(2)
C17	24(2)	37(3)	23(2)	-14(2)	5.7(18)	-17(2)
C9A	32.9(17)	26(2)	24(3)	-5.7(17)	2.3(16)	-15.5(16)
C10A	36(2)	37(5)	36(4)	2(3)	5(3)	-18(3)
O1A	39(3)	26(2)	28(3)	-4(2)	5(3)	-15(2)
O2A	32.6(17)	28(2)	22.1(19)	-5.1(18)	2.6(13)	-15.2(15)
C9B	32.6(17)	25(2)	22(2)	-7.2(17)	1.9(15)	-15.1(16)

Atom	U_{11}	U_{22}	U_{33}	U_{23}	U_{13}	U_{12}
C10B	36(2)	37(5)	36(4)	2(3)	5(3)	-18(3)
O1B	34(3)	25(2)	20(2)	-8.5(18)	8(2)	-9(2)
O2B	32.6(17)	28(2)	22.1(19)	-5.1(18)	2.6(13)	-15.2(15)

Table 19: Bond Lengths in Å for WL-N3-134.

Atom	Atom	Length/Å	Atom	Atom	Length/Å
Br2'	C15'	1.902(5)	C1	C2	1.389(7)
Br1'	C1'	1.902(5)	C1	C6	1.383(7)
C14'	C13'	1.401(7)	C2	C3	1.395(7)
C14'	C15'	1.388(7)	C3	C4	1.388(7)
C16'	C17'	1.394(7)	C4	C5	1.388(8)
C16'	C15'	1.368(7)	C4	C7	1.514(7)
C13'	C12'	1.376(7)	C5	C6	1.401(8)
C8'	C12'	1.534(6)	C7	C8	1.538(7)
C8'	C7'	1.536(7)	C7	C11	1.531(7)
C8'	C9'	1.536(7)	C8	C12	1.516(7)
C1'	C2'	1.359(8)	C8	C9A	1.493(8)
C1'	C6'	1.379(7)	C8	C9B	1.488(8)
C4'	C3'	1.381(7)	C12	C13	1.384(8)
C4'	C7'	1.521(7)	C12	C17	1.398(7)
C4'	C5'	1.385(8)	C13	C14	1.389(7)
C2'	C3'	1.392(7)	C14	C15	1.379(8)
C12'	C17'	1.396(7)	C15	C16	1.384(7)
C10'	O2'	1.478(6)	C16	C17	1.393(7)
C7'	C11'	1.546(7)	C9A	O1A	1.238(10)
C9'	O1'	1.188(6)	C9A	O2A	1.301(11)
C9'	O2'	1.347(6)	C10A	O2A	1.513(9)
C6'	C5'	1.402(8)	C9B	O1B	1.232(10)
Br1	C1	1.892(5)	C9B	O2B	1.300(11)
Br2	C15	1.899(5)	C10B	O2B	1.514(9)

Table 20: Bond Angles in ° for WL-N3-134.

Atom	Atom	Atom	Angle/°	Atom	Atom	Atom	Angle/°
C15'	C14'	C13'	118.4(4)	C7'	C8'	C9'	110.5(4)
C15'	C16'	C17'	119.1(5)	C2'	C1'	Br1'	118.7(4)
C12'	C13'	C14'	121.2(5)	C2'	C1'	C6'	121.8(5)
C12'	C8'	C7'	113.1(4)	C6'	C1'	Br1'	119.5(4)
C12'	C8'	C9'	106.4(4)	C3'	C4'	C7'	119.7(5)

Atom	Atom	Atom	Angle/°	Atom	Atom	Atom	Angle/°
C3'	C4'	C5'	118.1(5)	C4	C5	C6	120.7(5)
C5'	C4'	C7'	122.1(5)	C1	C6	C5	119.5(5)
C1'	C2'	C3'	119.3(5)	C4	C7	C8	112.3(4)
C4'	C3'	C2'	121.2(5)	C4	C7	C11	109.7(4)
C13'	C12'	C8'	119.9(4)	C11	C7	C8	110.2(4)
C13'	C12'	C17'	118.8(4)	C12	C8	C7	116.3(4)
C17'	C12'	C8'	121.2(4)	C9A	C8	C7	105.8(6)
C8'	C7'	C11'	110.3(4)	C9A	C8	C12	108.0(6)
C4'	C7'	C8'	112.0(4)	C9B	C8	C7	116.8(6)
C4'	C7'	C11'	110.5(4)	C9B	C8	C12	110.4(6)
C16'	C17'	C12'	120.8(4)	C13	C12	C8	118.7(5)
O1'	C9'	C8'	125.9(4)	C13	C12	C17	119.4(5)
O1'	C9'	O2'	124.9(4)	C17	C12	C8	121.8(5)
O2'	C9'	C8'	109.2(4)	C12	C13	C14	120.7(5)
C14'	C15'	Br2'	118.9(4)	C15	C14	C13	119.0(5)
C16'	C15'	Br2'	119.4(4)	C14	C15	Br2	118.8(4)
C16'	C15'	C14'	121.6(5)	C14	C15	C16	121.8(5)
C1'	C6'	C5'	118.0(5)	C16	C15	Br2	119.4(4)
C4'	C5'	C6'	121.4(5)	C15	C16	C17	118.7(5)
C9'	O2'	C10'	115.4(4)	C16	C17	C12	120.3(5)
C2	C1	Br1	119.0(4)	O1A	C9A	C8	121.1(9)
C6	C1	Br1	120.4(4)	O1A	C9A	O2A	114.9(8)
C6	C1	C2	120.6(5)	O2A	C9A	C8	123.3(8)
C1	C2	C3	118.9(5)	C9A	O2A	C10A	103.5(8)
C4	C3	C2	121.5(5)	O1B	C9B	C8	124.8(9)
C3	C4	C5	118.6(5)	O1B	C9B	O2B	125.3(8)
C3	C4	C7	119.0(4)	O2B	C9B	C8	109.9(8)
C5	C4	C7	122.3(5)	C9B	O2B	C10B	107.7(8)

Table 21: Hydrogen Fractional Atomic Coordinates ($\times 10^4$) and Equivalent Isotropic Displacement Parameters ($\text{\AA}^2 \times 10^3$) for **WL-N3-134**. U_{eq} is defined as 1/3 of the trace of the orthogonalised U_{ij} .

Atom	x	y	z	U_{eq}
H14'	-387.88	8143.74	-25.95	29
H16'	3780.88	4309.87	1495.67	30
H13'	-358.28	8952	1874.94	26
H8'	674.06	8642.96	3992.57	23
H2'	7137.21	8326.02	1839.74	42

Atom	x	y	z	U_{eq}
H3'	6126.82	6888.82	3358.96	38
H10G	-613.89	5098.75	5941.72	38
H10H	-2351.02	6491.63	5956.23	38
H10I	-849.85	6011.2	7007.54	38
H7'	4149.05	6579.41	4730.55	25
H11D	2199	9222.73	5615.79	50
H11E	4135.88	8188.77	6039.88	50
H11F	2792.52	7568.22	6480.96	50
H17'	3766.38	5111.93	3398.38	29
H6'	2642.86	11935.08	1490.21	45
H5'	1669.08	10495.49	3072.73	46
H2	6934.21	-2362.29	8888.12	26
H3	8510.11	-1389.56	7492.65	25
H5	4306.56	2419.15	6054.98	34
H6	2726.06	1501.68	7509.51	39
H7	8835.56	415.3	5892.97	26
H8A	6310.93	3463.63	5223.99	27
H8B	6224.69	3368.96	5361.39	27
H11A	7369.05	95.34	4251.2	41
H11B	7867.53	1415.11	3654.67	41
H11C	5997.97	1779.86	4007.17	41
H13	5309.43	4766.84	6804.52	31
H14	5605.4	5367.28	8755.95	30
H16	10183.08	1777.95	9641.48	32
H17	9933.88	1248.5	7636.26	31
H10A	10786.92	3213.21	3392.22	56
H10B	12458.38	2164.54	4313.49	56
H10C	11137.78	3653.82	4650.47	56
H10D	11340.57	2756.21	3368.93	56
H10E	11769.88	3326.52	4513.41	56
H10F	10069.61	4317.49	3613.15	56

Table 22: Hydrogen Bond information for **WL-N3-134**.

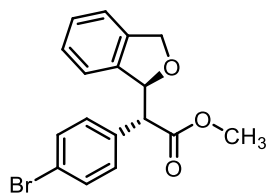
D	H	A	d(D-H)/Å	d(H-A)/Å	d(D-A)/Å	D-H-A/deg
C3'	H3'	O1B	0.93	2.13	3.046(9)	170.3
C7'	H7'	O1'	0.98	2.64	2.910(6)	95.9
C7	H7	O2A	0.98	2.47	2.868(9)	103.8
C7	H7	O2B	0.98	2.71	2.947(9)	94.1
C17	H17	O2A	0.93	2.67	3.118(10)	110.2

D	H	A	d(D-H)/Å	d(H-A)/Å	d(D-A)/Å	D-H-A/deg
C17	H17	O2B	0.93	2.82	3.118(10)	100.1

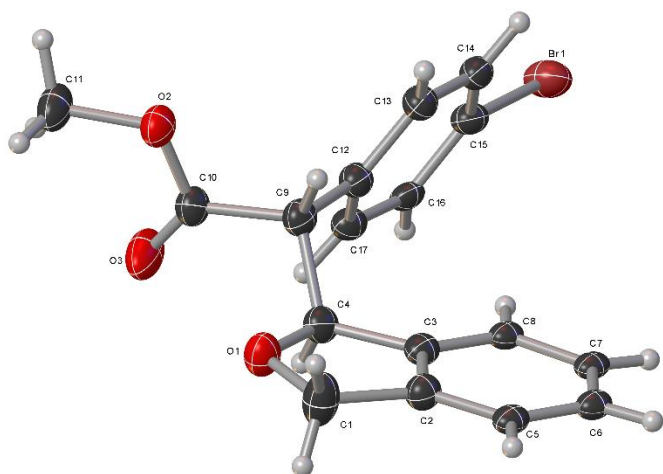
Table 23: Atomic Occupancies for all atoms that are not fully occupied in **WL-N3-134**.

Atom	Occupancy
H8A	0.5
H8B	0.5
C9A	0.5
C10A	0.5
H10A	0.5
H10B	0.5
H10C	0.5
O1A	0.5
O2A	0.5
C9B	0.5
C10B	0.5
H10D	0.5
H10E	0.5
H10F	0.5
O1B	0.5
O2B	0.5

Methyl (*R*)-2-(4-bromophenyl)-2-((*S*)-1,3-dihydroisobenzofuran-1-yl)acetate (83)



Crystal Data and Experimental



Experimental. Single colorless irregular-shaped crystals of (**WL-N5-10**) were grown by slow evaporation of 1:1 DCM/hexane solution. A suitable crystal ($0.33 \times 0.25 \times 0.21 \text{ mm}^3$) was selected and mounted on a loop with paratone oil on a Bruker APEXII diffractometer. The crystal was cooled to $T = 173(2) \text{ K}$ during data collection. The structure was solved with the **XT** (Sheldrick, 2015) structure solution program using the Intrinsic Phasing solution method and by using **Olex2** (Dolomanov et al., 2009) as the graphical interface. The model was refined with version 2014/7 of ShelXL-2014/7 (Sheldrick, 2008) using Least Squares minimisation.

Crystal Data. $\text{C}_{17}\text{H}_{15}\text{BrO}_3$, $M_r = 347.20$, orthorhombic, $P2_12_12_1$ (No. 19), $a = 5.70670(10) \text{ \AA}$, $b = 35.5535(9) \text{ \AA}$, $c = 7.4428(2) \text{ \AA}$, $\alpha = \beta = \gamma = 90^\circ$, $V = 1510.09(6) \text{ \AA}^3$, $T = 173(2) \text{ K}$, $Z = 4$, $Z' = 1$, $(\text{Cu K } \alpha) = 3.775 \text{ mm}^{-1}$, 8626 reflections measured, 2514 unique ($R_{int} = 0.0597$) which were used in all calculations. The final wR_2 was 0.2208 (all data) and R_1 was 0.0957 ($I > 2\sigma(I)$).

Compound	WL-N5-10
Formula	C ₁₇ H ₁₅ BrO ₃
<i>D</i> _{calc.} / g cm ⁻³	1.527
/mm ⁻¹	3.775
Formula Weight	347.20
Colour	colourless
Shape	irregular
Size/mm ³	0.33×0.25×0.21
<i>T</i> /K	173(2)
Crystal System	orthorhombic
Flack Parameter	0.16(12)
Hooft Parameter	0.140(11)
Space Group	P2 ₁ 2 ₁ 2 ₁
<i>a</i> /Å	5.70670(10)
<i>b</i> /Å	35.5535(9)
<i>c</i> /Å	7.4428(2)
<i>∠</i> [°]	90
<i>∠</i> [°]	90
<i>∠</i> [°]	90
<i>V</i> /Å ³	1510.09(6)
<i>Z</i>	4
<i>Z</i> '	1
Wavelength/Å	1.541838
Radiation type	Cu K
<i>min</i> [∠]	4.976
<i>max</i> [∠]	64.993
Measured Refl.	8626
Independent Refl.	2514
Reflections with <i>I</i> > 2σ(<i>I</i>)	2148
<i>R</i> _{int}	0.0597
Parameters	192
Restraints	177
Largest Peak	1.754
Deepest Hole	-1.517
Goof	1.168
<i>wR</i> ₂ (all data)	0.2208
<i>wR</i> ₂	0.1888
<i>R</i> ₁ (all data)	0.1267
<i>R</i> ₁	0.0957

Structure Quality Indicators

Reflections:	d min (Cu)	0.85	<i>I</i> /σ	24.5	<i>R</i> _{int}	5.97%	complete at 2θ=130°	98%
Refinement:	Shift	0.000	Max Peak	1.8	Min Peak	-1.5	Goof	1.168

A colourless irregular-shaped crystal with dimensions 0.33×0.25×0.21 mm³ was mounted on a

loop with paratone oil. Data were collected using a Bruker APEXII detector diffractometer equipped with an Oxford Cryosystems low-temperature device, operating at $T = 173(2)$ K. Data were measured using ω and ϕ scans of 0.5° per frame for 15s and 20.0 s using Cu K radiation (fine-focus sealed X-ray tube, 40 kV, 35 mA). The total number of runs and images was based on the strategy calculation from the program **APEX2** (Bruker). The maximum resolution that was achieved was $d_{\min} = 64.993^\circ$.

The diffraction patterns were indexed using **CrysAlisPro 1.171.39.9g** (Rigaku Oxford Diffraction, 2015) and the unit cells were refined using **CrysAlisPro 1.171.39.9g** (Rigaku Oxford Diffraction, 2015) on 5984 reflections, 69% of the observed reflections. Data reduction, scaling and absorption corrections were performed using **CrysAlisPro 1.171.39.9g** (Rigaku Oxford Diffraction, 2015). A spherical absorption correction using equivalent radius 0.2 mm and an absorption coefficient of 3.775 mm^{-1} was applied. An empirical absorption correction using spherical harmonics, implemented in SCALE3 ABSPACK scaling algorithm was applied. The final completeness is 99.24% out to 64.993° in θ . The absorption coefficient of this material is 3.775 mm^{-1} at this wavelength ($\lambda = 1.54184 \text{ \AA}$) and the minimum and maximum transmissions are 0.33638 and 0.39447.

The structure was solved and the space group $P2_12_12_1$ (# 19) determined by the **XT** (Sheldrick, 2015) structure solution program using Intrinsic Phasing and refined by Least Squares using version 2014/7 of ShelXL-2014/7 (Sheldrick, 2008). All non-hydrogen atoms were refined anisotropically. Hydrogen atom positions were calculated geometrically and refined using the riding model.

_refine_special_details: Refined as a 2-component inversion twin.

There is a single molecule in the asymmetric unit, which is represented by the reported sum formula. In other words: Z is 4 and Z' is 1.

The Flack parameter was refined to 0.16(12). Determination of absolute structure using Bayesian statistics on Bijvoet differences using the Olex2 results in 0.140(11). Note: The Flack parameter is used to determine chirality of the crystal studied, the value should be near 0, a value of 1 means that the stereochemistry is wrong and the model should be inverted. A value of 0.5 means that the crystal consists of a racemic mixture of the two enantiomers.

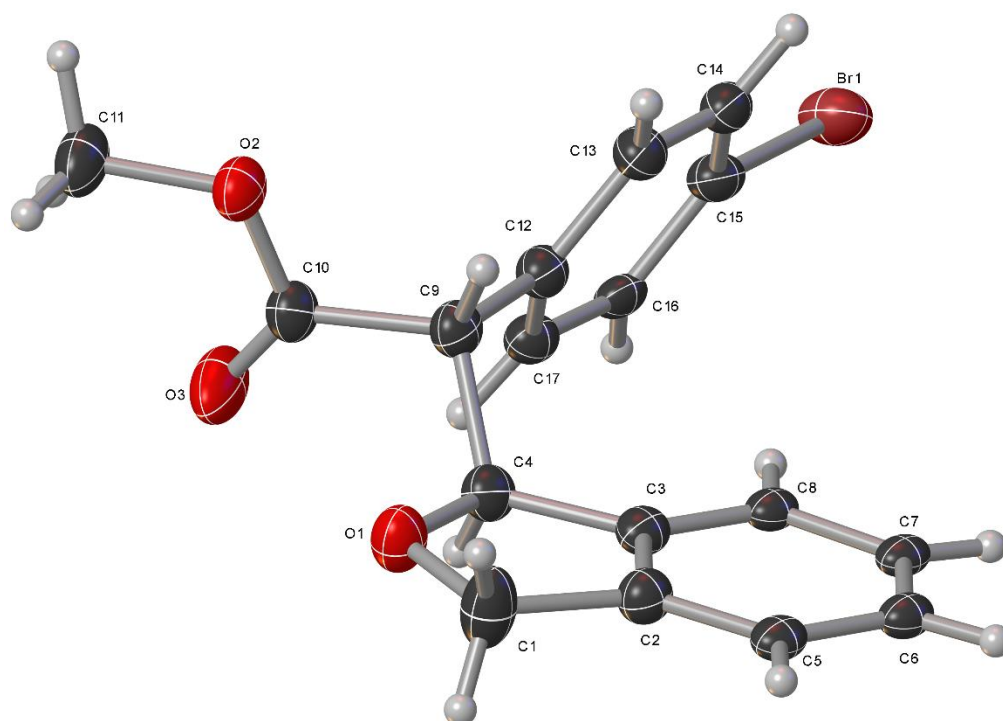
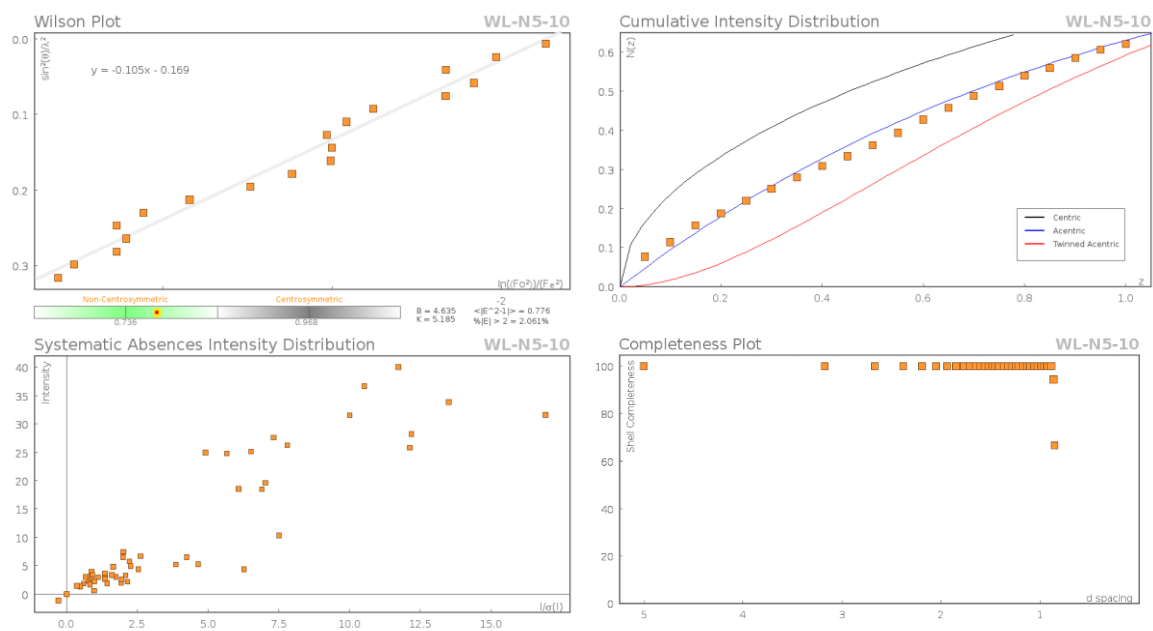
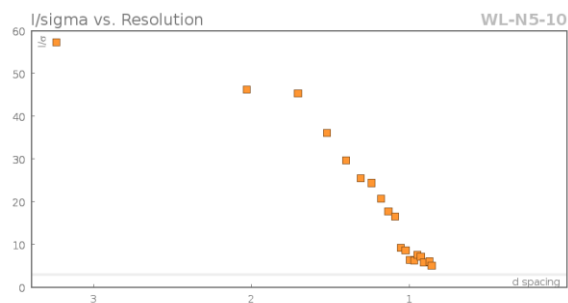


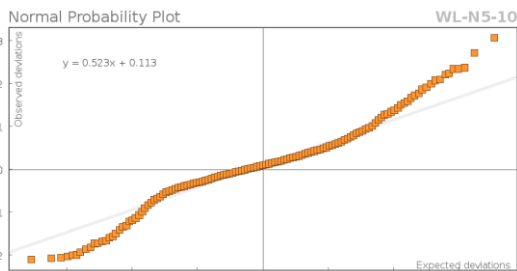
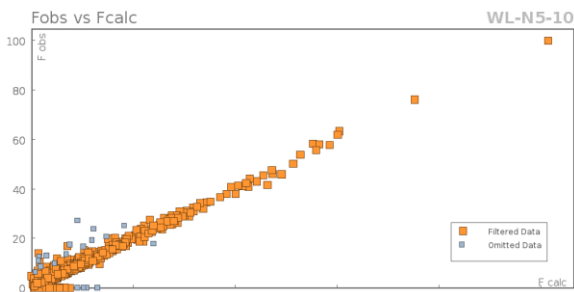
Figure 1:

Data Plots: Diffraction Data





Data Plots: Refinement and Data



Reflection Statistics

Total reflections (after filtering)	8747	Unique reflections	2514
Completeness	0.98	Mean I/	24.52
hkl _{max} collected	(6, 41, 8)	hkl _{min} collected	(-6, -38, -7)
hkl _{max} used	(6, 41, 8)	hkl _{min} used	(-6, 0, 0)
Lim d _{max} collected	100.0	Lim d _{min} collected	0.77
d _{max} used	17.78	d _{min} used	0.85
Friedel pairs	1795	Friedel pairs merged	0
Inconsistent equivalents	246	R _{int}	0.0597
R _{sigma}	0.04	Intensity transformed	0
Omitted reflections	0	Omitted by user (OMIT hkl)	58
Multiplicity	(3749, 1375, 616, 100)	Maximum multiplicity	10
Removed systematic absences	63	Filtered off (Shel/OMIT)	0

Images of the Crystal on the Diffractometer



Table 1: Fractional Atomic Coordinates ($\times 10^4$) and Equivalent Isotropic Displacement Parameters ($\text{\AA}^2 \times 10^3$) for **WL-N5-10**. U_{eq} is defined as 1/3 of the trace of the orthogonalised U_{ij} .

Atom	x	y	z	U_{eq}
Br1	8581(4)	5041.4(6)	4761(3)	67.5(6)
O2	6170(20)	2983(3)	4340(16)	53(3)
O1	4470(20)	3004(3)	9051(17)	58(3)
O3	8880(30)	3053(4)	6430(20)	84(5)
C12	6250(30)	3817(4)	6070(20)	43(2)
C6	110(30)	3980(5)	11560(20)	40(3)
C9	5400(30)	3431(5)	6610(20)	45.1(19)
C3	3630(30)	3640(4)	9620(20)	41(2)
C14	5530(30)	4409(4)	4620(20)	45(3)
C7	1800(30)	4195(5)	10704(19)	38(3)
C5	190(30)	3598(5)	11510(20)	41(3)
C2	1970(30)	3422(5)	10540(20)	46(2)
C17	8380(30)	3955(4)	6680(20)	43(3)
C16	9030(30)	4317(4)	6342(19)	39(3)
C10	7030(30)	3133(5)	5870(20)	48(2)
C8	3550(30)	4026(4)	9691(19)	37(2)
C13	4850(30)	4051(4)	5000(20)	47(3)
C15	7670(30)	4548(5)	5260(20)	46(3)
C4	5230(30)	3382(5)	8670(20)	47(2)
C1	2450(40)	3004(5)	10250(30)	70(6)
C11	7610(30)	2691(6)	3500(30)	65(5)

Table 2: Anisotropic Displacement Parameters ($\times 10^4$) **WL-N5-10**. The anisotropic displacement factor exponent takes the form: $-2^2[h^2a^{*2} \times U_{11} + \dots + 2hka^* \times b^* \times U_{12}]$

Atom	U_{11}	U_{22}	U_{33}	U_{23}	U_{13}	U_{12}
Br1	85.7(14)	65.5(11)	51.3(10)	7.2(9)	-7.0(11)	-7.5(11)
O2	43(5)	59(5)	59(4)	-10(4)	2(4)	8(4)
O1	57(5)	54(3)	62(5)	0(2)	14(4)	6(3)
O3	57(4)	106(9)	88(7)	-40(7)	-19(5)	34(5)
C12	39(3)	48(2)	42(3)	-2.8(18)	-1(2)	4.0(18)
C6	32(4)	57(4)	31(6)	-3(3)	-3(5)	3(3)
C9	38(4)	50(3)	48(3)	-3(2)	2(3)	4(2)
C3	31(4)	53(3)	38(4)	-2(2)	-5(4)	4(2)
C14	45(4)	51(3)	38(7)	-5(3)	-2(4)	8(3)
C7	30(5)	56(4)	28(6)	-3(3)	-6(4)	4(3)
C5	32(4)	58(4)	32(6)	-3(3)	-7(4)	3(3)
C2	41(3)	52(3)	45(3)	-2(2)	2(2)	1.5(19)

Atom	U_{11}	U_{22}	U_{33}	U_{23}	U_{13}	U_{12}
C17	38(3)	53(3)	37(6)	-1(3)	0(4)	3(3)
C16	40(4)	53(3)	26(6)	-4(3)	4(4)	2(3)
C10	40(4)	49(4)	54(4)	-3(3)	5(3)	4(3)
C8	31(4)	53(3)	29(5)	-2(3)	-5(4)	3(3)
C13	44(3)	52(3)	45(5)	-3(3)	-4(3)	6(2)
C15	47(4)	57(3)	35(7)	-1(3)	-2(4)	4(3)
C4	41(4)	54(3)	48(3)	0(2)	2(3)	7(3)
C1	70(7)	53(3)	86(12)	-3(3)	32(9)	2(3)
C11	46(8)	73(9)	75(8)	-25(8)	-3(7)	15(7)

Table 3: Bond Lengths in Å for WL-N5-10.

Atom	Atom	Length/Å
Br1	C15	1.866(17)
O2	C10	1.35(2)
O2	C11	1.46(2)
O1	C4	1.44(2)
O1	C1	1.46(2)
O3	C10	1.16(2)
C12	C9	1.51(2)
C12	C17	1.39(2)
C12	C13	1.40(2)
C6	C7	1.39(2)
C6	C5	1.36(2)
C9	C10	1.52(2)
C9	C4	1.54(2)
C3	C2	1.41(2)
C3	C8	1.373(19)
C3	C4	1.48(2)
C14	C13	1.36(2)
C14	C15	1.40(2)
C7	C8	1.38(2)
C5	C2	1.39(2)
C2	C1	1.53(2)
C17	C16	1.36(2)
C16	C15	1.39(2)

Table 4: Bond Angles in ° for WL-N5-10.

Atom	Atom	Atom	Angle/°	Atom	Atom	Atom	Angle/°
C10	O2	C11	115.9(14)	C17	C12	C13	118.3(15)
C4	O1	C1	111.2(13)	C13	C12	C9	120.5(16)
C17	C12	C9	121.1(15)	C5	C6	C7	120.8(16)

Atom	Atom	Atom	Angle/°	Atom	Atom	Atom	Angle/°
C12	C9	C10	110.0(14)	C17	C16	C15	121.0(16)
C12	C9	C4	112.7(14)	O2	C10	C9	111.0(15)
C10	C9	C4	108.5(14)	O3	C10	O2	122.3(17)
C2	C3	C4	108.0(13)	O3	C10	C9	126.5(17)
C8	C3	C2	120.6(15)	C3	C8	C7	118.7(14)
C8	C3	C4	131.4(15)	C14	C13	C12	120.8(16)
C13	C14	C15	120.4(16)	C14	C15	Br1	120.4(13)
C8	C7	C6	120.9(15)	C16	C15	Br1	121.1(13)
C6	C5	C2	119.1(16)	C16	C15	C14	118.4(16)
C3	C2	C1	110.3(14)	O1	C4	C9	108.7(14)
C5	C2	C3	119.8(15)	O1	C4	C3	107.2(14)
C5	C2	C1	129.8(16)	C3	C4	C9	116.4(14)
C16	C17	C12	120.8(16)	O1	C1	C2	103.2(14)

Table 5: Torsion Angles in ° for **WL-N5-10**.

Atom	Atom	Atom	Atom	Angle/°
C12	C9	C10	O2	-98.4(16)
C12	C9	C10	O3	76(3)
C12	C9	C4	O1	-
				178.6(14)
C12	C9	C4	C3	60(2)
C12	C17	C16	C15	-5(2)
C6	C7	C8	C3	-3(2)
C6	C5	C2	C3	0(2)
C6	C5	C2	C1	-
				179.4(19)
C9	C12	C17	C16	-
				173.3(15)
C9	C12	C13	C14	175.2(16)
C3	C2	C1	O1	-2(2)
C7	C6	C5	C2	-2(2)
C5	C6	C7	C8	4(2)
C5	C2	C1	O1	177.3(16)
C2	C3	C8	C7	1(2)
C2	C3	C4	O1	-0.2(19)
C2	C3	C4	C9	121.7(16)
C17	C12	C9	C10	-64(2)
C17	C12	C9	C4	57(2)
C17	C12	C13	C14	-2(2)

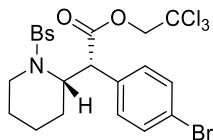
Atom	Atom	Atom	Atom	Angle/°
C17	C16	C15	Br1	- 178.9(12)
C17	C16	C15	C14	4(2)
C10	C9	C4	O1	-56.6(18)
C10	C9	C4	C3	- 177.6(15)
C8	C3	C2	C5	1(2)
C8	C3	C2	C1	- 180.0(16)
C8	C3	C4	O1	- 178.8(16)
C8	C3	C4	C9	-57(2)
C13	C12	C9	C10	118.5(17)
C13	C12	C9	C4	- 120.3(17)
C13	C12	C17	C16	4(2)
C13	C14	C15	Br1	- 179.2(14)
C13	C14	C15	C16	-2(2)
C15	C14	C13	C12	1(3)
C4	O1	C1	C2	2(2)
C4	C9	C10	O2	138.0(15)
C4	C9	C10	O3	-47(3)
C4	C3	C2	C5	- 177.9(15)
C4	C3	C2	C1	1(2)
C4	C3	C8	C7	179.4(16)
C1	O1	C4	C9	- 127.6(16)
C1	O1	C4	C3	-1(2)
C11	O2	C10	O3	5(3)
C11	O2	C10	C9	180.0(15)

Table 6: Hydrogen Fractional Atomic Coordinates ($\times 10^4$) and Equivalent Isotropic Displacement Parameters ($\text{\AA}^2 \times 10^3$) for **WL-N5-10**. U_{eq} is defined as 1/3 of the trace of the orthogonalised U_{ij} .

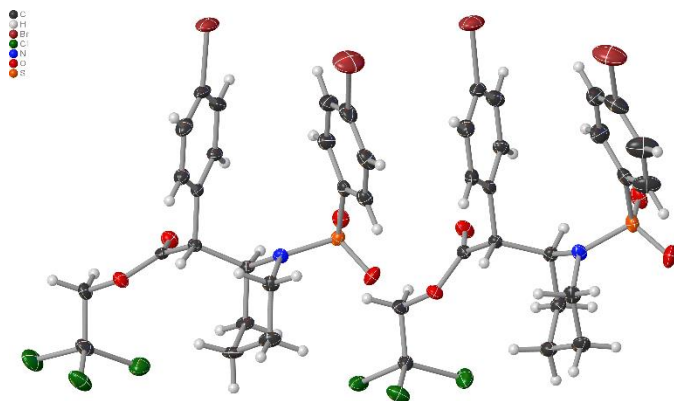
Atom	x	y	z	U_{eq}
H6	-1100	4100	12179	48
H9	3836	3392	6095	54
H14	4564	4563	3928	54

Atom	x	y	z	U_{eq}
H7	1771	4455	10811	45
H5	-933	3456	12115	49
H17	9378	3799	7329	51
H16	10406	4410	6842	47
H8	4636	4171	9071	45
H13	3437	3960	4549	56
H4	6808	3414	9169	57
H1A	2808	2880	11375	84
H1B	1113	2880	9696	84
H11A	7263	2680	2238	97
H11B	7266	2453	4043	97
H11C	9237	2749	3665	97

2,2,2-Trichloroethyl (*R*)-2-((*S*)-1-((4-bromophenyl)sulfonyl)piperidin-2-yl)-2-phenylacetate (146)



Crystal Data and Experimental



Experimental. Single colourless needle-shaped crystals of **WL-ELN09-38R-d1** were recrystallised from DCM by slow evaporation. A suitable crystal $0.49 \times 0.10 \times 0.05$ mm³ was selected and mounted on a loop with paratone oil on an XtaLAB Synergy, Dualflex, HyPix diffractometer. The crystal was kept at a steady $T = 111.4(2)$ K during data collection. The structure was solved with the **ShelXT** (Sheldrick, 2015) structure solution program using the Intrinsic Phasing solution method and by using **Olex2** (Dolomanov et al., 2009) as the graphical interface. The model was refined with version 2018/3 of **ShelXL** (Sheldrick, 2015) using Least Squares minimisation.

Crystal Data. C₂₁H₂₀Br₂Cl₃NO₄S, $M_r = 648.61$, orthorhombic, $P2_12_12_1$ (No. 19), $a = 6.15074(9)$ Å, $b = 26.3980(4)$ Å, $c = 30.1139(5)$ Å, $a = b = g = 90^\circ$, $V = 4889.51(13)$ Å³, $T = 111.4(2)$ K, $Z = 8$, $Z' = 2$, $m(\text{CuK}\alpha) = 8.276$ mm⁻¹, 53908 reflections measured, 9424 unique ($R_{int} = 0.0555$) which were used in all calculations. The final wR_2 was 0.0645 (all data) and R_I was 0.0262 ($I > 2\sigma(I)$).

Compound **WL-ELN09-
38R-d1**

Formula	C ₂₁ H ₂₀ Br ₂ Cl ₃ NO ₄ S
<i>D</i> _{calc.} / g cm ⁻³	1.762
<i>m</i> /mm ⁻¹	8.276
Formula Weight	648.61
Colour	colourless
Shape	needle
Size/mm ³	0.49×0.10×0. 05
<i>T</i> /K	111.4(2)
Crystal System	orthorhombic
Flack Parameter	-0.003(6)
Hooft Parameter	-0.007(6)
Space Group	<i>P</i> 2 ₁ 2 ₁ 2 ₁
<i>a</i> /Å	6.15074(9)
<i>b</i> /Å	26.3980(4)
<i>c</i> /Å	30.1139(5)
<i>a</i> /°	90
<i>b</i> /°	90
<i>g</i> /°	90
<i>V</i> /Å ³	4889.51(13)
<i>Z</i>	8
<i>Z</i> '	2
Wavelength/Å	1.54184
Radiation type	CuK _α
<i>Q</i> _{min} /°	2.935
<i>Q</i> _{max} /°	72.944
Measured Refl.	53908
Independent Refl.	9424
Reflections with <i>I</i> > 2σ(<i>I</i>)	9037
<i>R</i> _{int}	0.0555
Parameters	577
Restraints	84
Largest Peak	0.650
Deepest Hole	-0.502
Goof	1.021
<i>wR</i> ₂ (all data)	0.0645
<i>wR</i> ₂	0.0633
<i>R</i> ₁ (all data)	0.0281
<i>R</i> ₁	0.0262

Structure Quality Indicators

Reflections:	d min (Cu)	0.81	I/σ	29.6	Rint	5.55%	complete 100% (IUCr)	100%		
Refinement:	Shift	0.001	Max Peak	0.7	Min Peak	-0.5	Goof	1.021	Flack	.003(6)

A colourless needle-shaped crystal with dimensions $0.49 \times 0.10 \times 0.05 \text{ mm}^3$ was mounted on a loop with paratone oil. Data were collected using an XtaLAB Synergy, Dualflex, HyPix diffractometer equipped with an Oxford Cryosystems low-temperature device operating at $T = 111.4(2) \text{ K}$.

Data were measured using w scans using $\text{CuK}\alpha$ radiation. The total number of runs and images was based on the strategy calculation from the program **CrysAlisPro** (Rigaku, V1.171.40.37a, 2019). The maximum resolution that was achieved was $Q = 72.944^\circ$ (0.81 \AA).

The diffraction pattern was indexed and the total number of runs and images was based on the strategy calculation from the program **CrysAlisPro** (Rigaku, V1.171.40.37a, 2019) and the unit cell was refined using **CrysAlisPro** (Rigaku, V1.171.40.37a, 2019) on 38372 reflections, 71% of the observed reflections.

Data reduction, scaling and absorption corrections were performed using **CrysAlisPro** (Rigaku, V1.171.40.37a, 2019). The final completeness is 99.90 % out to 72.944° in Q . A numerical absorption correction based on a Gaussian integration over a multifaceted crystal model was performed using **CrysAlisPro** (Rigaku, V1.171.40.37a, 2019). An empirical absorption correction using spherical harmonics as implemented in SCALE3 ABSPACK was also applied. The absorption coefficient m of this material is 8.276 mm^{-1} at this wavelength ($\lambda = 1.542 \text{ \AA}$) and the minimum and maximum transmissions are 0.687 and 1.000.

The structure was solved and the space group $P2_12_12_1$ (# 19) determined by the **ShelXT** (Sheldrick, 2015) structure solution program using Intrinsic Phasing and refined by Least Squares using version 2018/3 of **ShelXL** (Sheldrick, 2015). All non-hydrogen atoms were refined anisotropically. Hydrogen atom positions were calculated geometrically and refined using the riding model.

The value of Z' is 2. This means that there are two independent molecules in the asymmetric unit. The Flack parameter was refined to $-0.003(6)$. Determination of absolute structure using Bayesian statistics on Bijvoet differences using the Olex2 results in $-0.007(6)$. Note: The Flack parameter is used to determine chirality of the crystal studied, the value should be near 0, a value of 1 means that the stereochemistry is wrong and the model should be inverted. A value of 0.5 means that the crystal consists of a racemic mixture of the two enantiomers.

Images of the Crystal on the Diffractometer



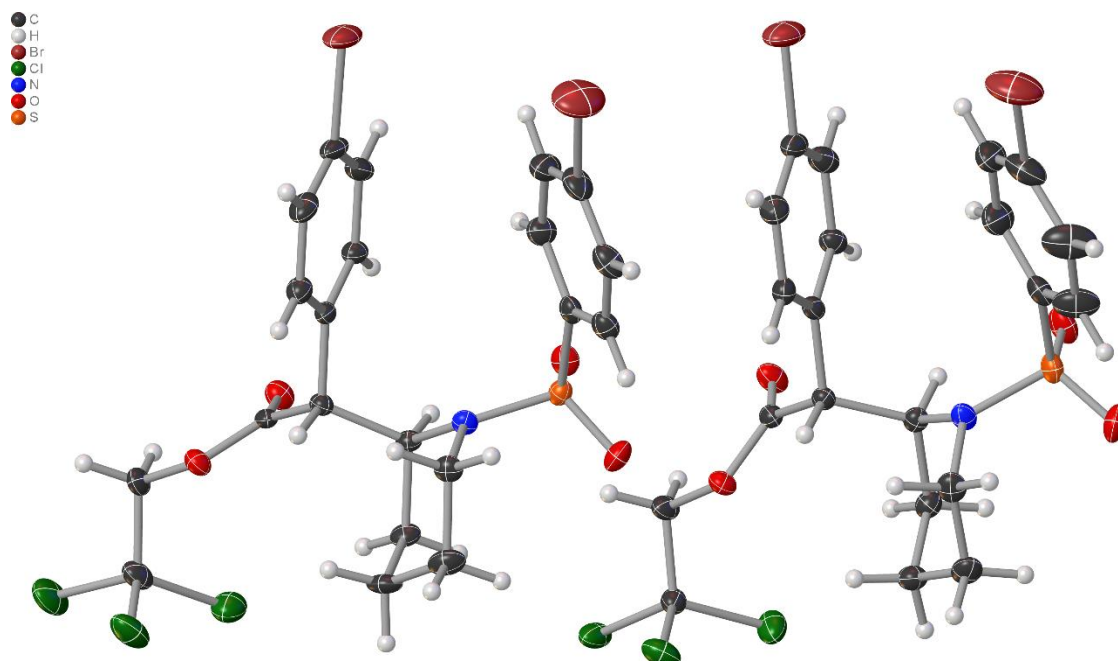


Figure 1: Plot of the asymmetric unit. There are two independent molecules in the asymmetric unit with the same chirality.

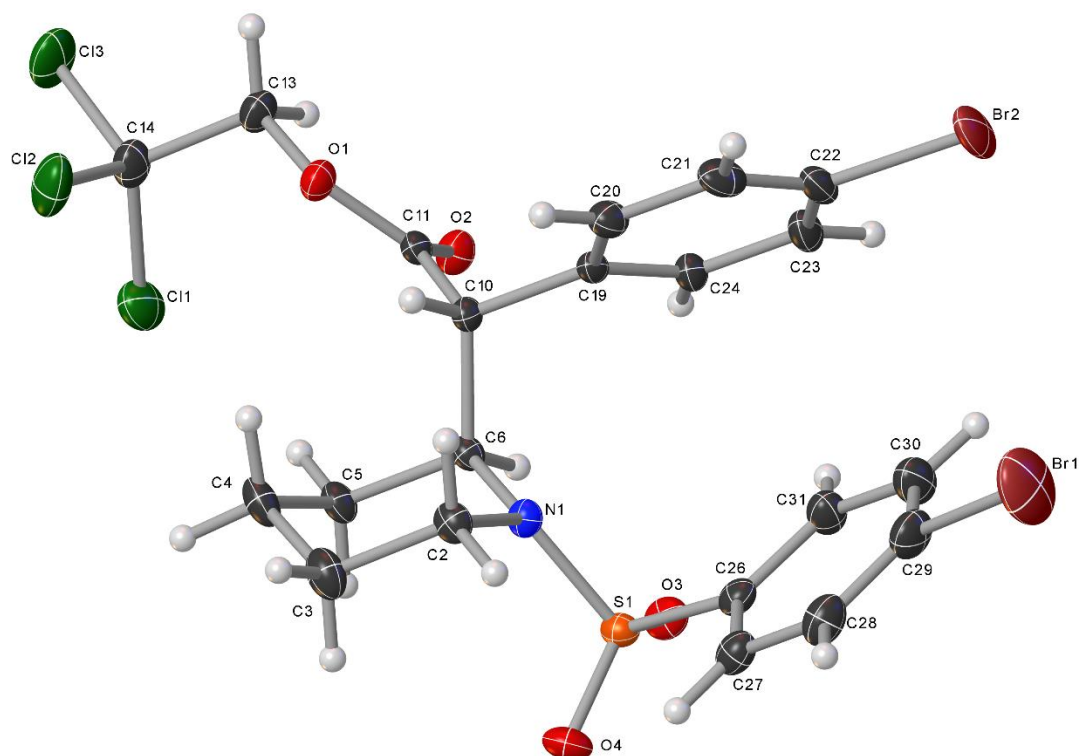
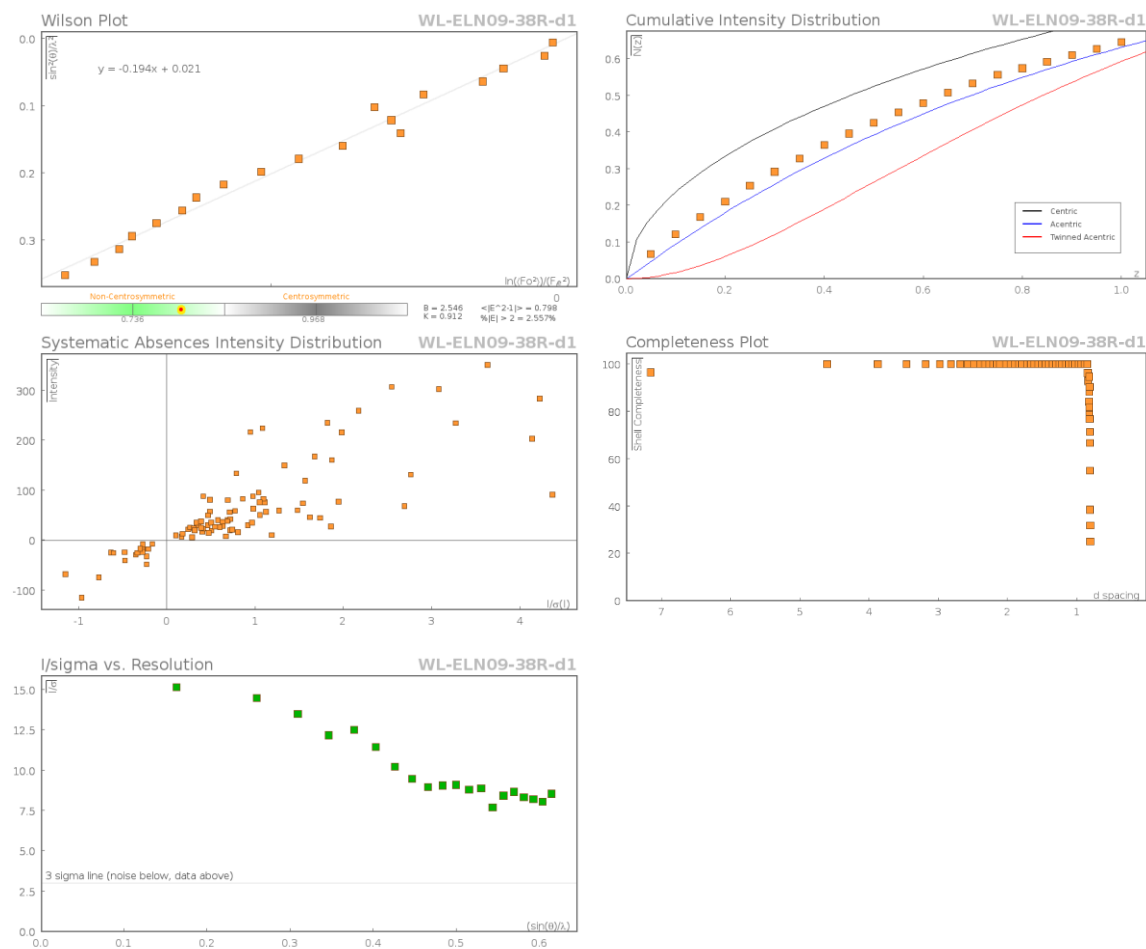
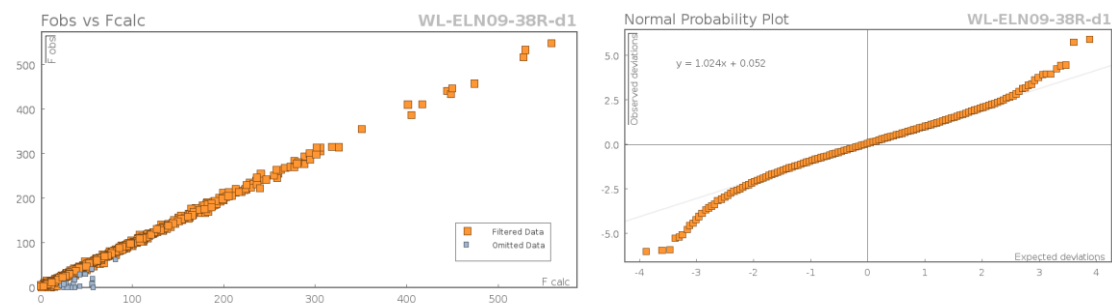


Figure 2: Plot of one of the two independent molecules in the asymmetric unit.

Data Plots: Diffraction Data



Data Plots: Refinement and Data



Reflection Statistics

Total reflections (after filtering) 54043

Completeness 0.963

hkl_{max} collected (7, 32, 33)

hkl_{max} used (7, 32, 37)

Unique reflections 9424

Mean I/s 22.96

hkl_{min} collected (-7, -32, -37)

hkl_{min} used (-7, 0, 0)

Lim d_{\max} collected	100.0	Lim d_{\min} collected	0.77
d_{\max} used	15.06	d_{\min} used	0.81
Friedel pairs	8951	Friedel pairs merged	0
Inconsistent equivalents	25	R_{int}	0.0555
R_{sigma}	0.0338	Intensity transformed	0
Omitted reflections	0	Omitted by user (OMIT hkl)	27
Multiplicity	(12250, 7439, 3904, 1560, 827, 450, 211, 78, 3)	Maximum multiplicity	18
Removed systematic absences	108	Filtered off (Shel/OMIT)	0

Table 1: Fractional Atomic Coordinates ($\times 10^4$) and Equivalent Isotropic Displacement Parameters ($\text{\AA}^2 \times 10^3$) for **WL-ELN09-38R-d1**. U_{eq} is defined as 1/3 of the trace of the orthogonalised U_{ij} .

Atom	x	y	z	U_{eq}
Br1_1	9399.0(11)	6623.9(2)	5923.8(2)	57.82(16)
Br2_1	4129.0(9)	6237.7(2)	7147.5(2)	39.32(12)
Cl1_1	401.7(18)	2394.2(4)	6689.3(3)	34.1(2)
Cl2_1	4311.5(18)	2290.6(4)	7212.2(4)	38.4(2)
Cl3_1	103.5(19)	2097.7(4)	7609.6(4)	40.6(3)
S1_1	4544.3(13)	4550.5(3)	5437.5(2)	17.21(16)
O1_1	2811(4)	3340.6(9)	7132.6(8)	20.7(5)
O2_1	27(4)	3735.4(10)	6789.3(8)	22.9(5)
O3_1	2229(4)	4617.1(10)	5431.8(8)	22.3(5)
O4_1	5601(4)	4342.2(10)	5053.1(7)	24.0(5)
N1_1	5131(4)	4224.0(11)	5879.5(9)	16.4(5)
C2_1	7405(5)	4047.9(14)	5918.7(12)	19.4(7)
C3_1	7617(6)	3498.0(15)	5770.1(14)	26.3(7)
C4_1	6049(6)	3160.0(14)	6025.6(13)	25.0(7)
C5_1	3715(6)	3354.4(13)	5966.8(12)	20.0(6)
C6_1	3485(5)	3910.0(12)	6107.5(10)	15.0(5)
C10_1	3747(6)	3977.3(12)	6617.8(10)	16.1(5)
C11_1	1944(6)	3682.4(13)	6846.4(11)	16.6(5)
C13_1	1339(6)	3026.9(14)	7377.8(12)	23.2(7)
C14_1	1552(7)	2477.7(14)	7225.5(13)	26.8(8)
C19_1	3736(6)	4531.7(12)	6754.1(10)	16.1(6)
C20_1	5603(6)	4726.2(14)	6953.7(11)	21.5(7)
C21_1	5702(7)	5234.4(14)	7075.1(11)	26.7(8)

Atom	x	y	z	U_{eq}
C22_1	3928(7)	5540.5(14)	6994.7(11)	24.4(7)
C23_1	2042(7)	5356.2(14)	6802.3(12)	24.7(7)
C24_1	1961(6)	4845.9(13)	6681.9(11)	19.1(6)
C26_1	5811(6)	5138.4(13)	5545.0(10)	18.8(6)
C27_1	7877(6)	5230.1(14)	5373.7(12)	22.4(7)
C28_1	8925(6)	5681.4(15)	5484.8(13)	27.9(7)
C29_1	7895(7)	6025.1(15)	5758.4(13)	29.9(7)
C30_1	5804(7)	5941.1(15)	5918.8(13)	30.8(8)
C31_1	4773(6)	5492.6(14)	5812.3(12)	25.0(7)
Br1_2	9323.2(10)	7516.7(2)	3726.4(2)	59.28(16)
Br2_2	3339.0(9)	7048.7(2)	4897.6(2)	42.07(13)
Cl1_2	-285.1(18)	3269.3(4)	3886.9(3)	32.9(2)
Cl2_2	3408.3(16)	3118.6(3)	4461.5(3)	31.4(2)
Cl3_2	-895.4(17)	2846.6(3)	4760.9(3)	29.6(2)
S1_2	4047.4(15)	5605.7(3)	2973.3(3)	21.13(18)
O1_2	1707(4)	4153.0(9)	4414.7(8)	19.5(5)
O2_2	-984(4)	4717.8(10)	4300.2(8)	24.8(5)
O3_2	1801(4)	5749.2(11)	2955.3(9)	29.2(6)
O4_2	5151(5)	5457.9(11)	2575.8(8)	29.5(6)
N1_2	4278(5)	5159.9(11)	3342.0(9)	19.2(6)
C2_2	6220(6)	4827.8(14)	3313.8(12)	22.8(7)
C3_2	5676(6)	4327.6(14)	3085.1(12)	25.2(8)
C4_2	3784(6)	4068.9(14)	3319.2(12)	22.7(7)
C5_2	1817(6)	4423.3(14)	3333.5(11)	20.2(7)
C6_2	2330(5)	4936.3(13)	3550.3(11)	17.1(7)
C10_2	2697(5)	4908.7(13)	4061.4(11)	15.2(7)
C11_2	894(6)	4597.2(13)	4270.5(10)	17.4(7)
C13_2	283(6)	3812.3(13)	4640.8(12)	23.0(8)
C14_2	621(6)	3289.5(13)	4443.8(11)	20.6(7)
C19_2	2784(6)	5435.2(13)	4269.0(11)	17.0(7)
C20_2	4696(6)	5591.2(14)	4477.1(11)	20.3(7)
C21_2	4859(7)	6069.0(14)	4668.6(12)	25.6(8)
C22_2	3080(7)	6388.1(14)	4650.0(12)	25.3(8)
C23_2	1162(6)	6244.7(14)	4447.2(12)	25.6(8)
C24_2	1020(6)	5767.0(14)	4256.6(11)	20.8(7)
C26_2	5503(6)	6128.7(14)	3189.2(12)	23.5(7)
C27_2	7523(7)	6241.6(17)	3015.7(17)	37.4(10)
C28_2	8624(7)	6660.9(19)	3173.0(19)	47.9(12)
C29_2	7724(8)	6954.8(16)	3503.2(16)	38.1(10)

Atom	x	y	z	U_{eq}
C30_2	5690(9)	6848.9(15)	3673.2(14)	37.6(10)
C31_2	4585(8)	6429.7(16)	3514.1(13)	36.2(10)

Table 2: Anisotropic Displacement Parameters ($\times 10^4$) **WL-ELN09-38R-d1**. The anisotropic displacement factor exponent takes the form: $-2p^2[h^2a^{*2} \times U_{11} + \dots + 2hka^* \times b^* \times U_{12}]$

Atom	U_{11}	U_{22}	U_{33}	U_{23}	U_{13}	U_{12}
Br1_1	64.3(4)	29.6(2)	79.5(4)	-9.2(2)	7.9(3)	-22.3(3)
Br2_1	62.3(3)	15.68(19)	40.0(2)	-10.61(16)	11.8(2)	-6.9(2)
Cl1_1	44.0(6)	24.1(5)	34.2(5)	-4.5(4)	1.5(4)	-6.9(4)
Cl2_1	34.3(5)	28.5(5)	52.3(6)	13.2(4)	7.0(5)	10.7(4)
Cl3_1	48.8(6)	26.2(5)	46.9(6)	14.7(4)	14.2(5)	-4.6(4)
S1_1	16.0(4)	20.5(4)	15.1(3)	-1.1(3)	-1.0(3)	0.8(3)
O1_1	24.0(10)	16.5(10)	21.7(10)	3.9(8)	-0.1(8)	-0.9(8)
O2_1	22.2(8)	20.5(12)	25.9(12)	3.8(10)	0.3(7)	-0.5(7)
O3_1	16.4(12)	27.2(13)	23.3(12)	2.0(10)	-3.6(10)	1.4(11)
O4_1	23.9(12)	32.2(14)	16.0(11)	-5.9(10)	2.0(10)	-0.3(12)
N1_1	13.0(10)	16.9(12)	19.3(12)	0.7(10)	-0.6(8)	1.2(8)
C2_1	13.7(11)	21.1(13)	23.5(16)	-2.0(11)	-2.1(10)	2.7(9)
C3_1	20.7(14)	22.6(13)	35.6(17)	-6.3(11)	-3.8(13)	4.2(10)
C4_1	22.9(12)	18.5(14)	33.4(17)	-9.7(12)	-2.8(11)	3.6(10)
C5_1	21.0(13)	15.7(11)	23.4(16)	-5.6(10)	-1.6(11)	-0.1(9)
C6_1	13.9(11)	14.7(11)	16.4(10)	-2.6(8)	-0.8(8)	-0.1(9)
C10_1	20.0(11)	12.3(10)	15.9(10)	-0.6(7)	-0.8(8)	0.1(9)
C11_1	22.3(8)	12.2(11)	15.4(11)	-1.6(9)	1.0(7)	-0.3(7)
C13_1	27.8(14)	18.5(12)	23.2(14)	5.3(10)	3.2(12)	-0.4(10)
C14_1	30.9(19)	18.4(12)	31.2(18)	4.6(12)	6.3(15)	0.0(12)
C19_1	22.4(13)	12.4(10)	13.6(13)	-0.3(9)	2.1(11)	-1.0(9)
C20_1	25.3(18)	20.7(17)	18.6(16)	-1.6(13)	-0.8(14)	-2.1(15)
C21_1	35(2)	24.8(19)	20.2(17)	-6.2(14)	-0.4(16)	-10.7(17)
C22_1	35.5(16)	16.6(16)	21.0(15)	-4.1(12)	9.1(12)	-1.9(12)
C23_1	35.0(16)	14.2(11)	24.8(16)	-1.6(10)	7.0(12)	-0.7(10)
C24_1	23.7(13)	14.2(11)	19.5(15)	-0.8(9)	1.0(11)	0.5(9)
C26_1	18.4(12)	20.6(14)	17.3(13)	4.3(11)	-2.3(11)	2.3(11)
C27_1	18.7(13)	23.6(14)	24.9(17)	6.1(12)	-0.4(11)	2.4(11)
C28_1	24.2(16)	25.6(14)	33.8(17)	7.9(12)	-1.3(13)	-2.3(11)
C29_1	36.5(16)	21.6(15)	31.5(18)	7.0(13)	1.0(14)	-5.8(12)
C30_1	40.2(16)	21.5(14)	30.6(18)	0.3(12)	7.4(14)	-3.8(13)
C31_1	27.8(16)	20.9(13)	26.5(16)	1.4(12)	6.3(13)	0.1(11)
Br1_2	56.1(3)	25.8(2)	96.0(4)	-10.3(3)	-12.4(3)	-7.1(3)

Atom	U_{11}	U_{22}	U_{33}	U_{23}	U_{13}	U_{12}
Br2_2	59.3(3)	20.3(2)	46.6(3)	-13.33(19)	9.1(2)	-5.4(2)
Cl1_2	48.9(6)	26.6(5)	23.1(4)	-2.1(3)	-8.6(4)	-9.1(4)
Cl2_2	27.0(4)	20.0(4)	47.3(5)	3.4(4)	-0.4(4)	3.6(4)
Cl3_2	41.8(5)	15.7(4)	31.4(4)	-1.5(3)	13.3(4)	-5.2(4)
S1_2	22.2(4)	24.1(4)	17.2(4)	5.3(3)	-2.4(3)	0.9(4)
O1_2	21.0(12)	13.6(11)	23.9(12)	2.0(9)	0.3(10)	-1.4(10)
O2_2	19.3(13)	22.5(13)	32.6(13)	6.1(10)	4.4(11)	2.6(11)
O3_2	23.9(13)	32.5(15)	31.2(14)	11.5(12)	-5.3(11)	5.4(12)
O4_2	33.3(15)	41.0(16)	14.2(11)	3.0(11)	1.7(11)	-3.9(13)
N1_2	16.6(14)	20.8(14)	20.1(13)	3.7(11)	1.7(12)	4.8(13)
C2_2	15.4(17)	27.4(19)	25.7(17)	1.6(15)	1.0(14)	5.1(15)
C3_2	22.6(17)	27.6(19)	25.5(17)	-2.8(14)	1.3(15)	10.8(16)
C4_2	25.5(19)	18.3(17)	24.3(17)	-3.1(14)	0.0(14)	1.9(15)
C5_2	19.1(17)	22.8(18)	18.7(16)	-2.3(14)	-0.8(13)	-0.7(15)
C6_2	14.6(15)	18.9(17)	17.7(16)	-0.2(13)	0.6(13)	1.9(14)
C10_2	14.2(15)	15.0(16)	16.4(15)	0.7(13)	-0.3(12)	1.2(13)
C11_2	21.8(17)	15.2(16)	15.3(15)	-0.9(12)	-1.8(13)	0.1(15)
C13_2	30(2)	14.6(16)	24.3(17)	1.6(14)	7.8(15)	-1.8(15)
C14_2	26.0(17)	17.0(16)	18.8(15)	0.6(13)	0.8(14)	-3.2(15)
C19_2	20.3(17)	13.9(16)	16.9(15)	2.4(13)	2.1(13)	0.7(14)
C20_2	23.3(18)	21.5(17)	16.1(15)	1.4(13)	0.2(14)	-0.1(15)
C21_2	31(2)	21.8(18)	24.2(18)	-1.4(14)	-3.3(15)	-3.8(16)
C22_2	38(2)	16.0(17)	21.5(17)	-1.5(14)	7.3(16)	-2.8(16)
C23_2	26.6(19)	19.9(18)	30.4(19)	3.1(15)	8.8(15)	3.0(15)
C24_2	19.9(17)	19.2(17)	23.3(16)	0.9(13)	2.7(14)	2.0(15)
C26_2	26.3(18)	19.9(18)	24.2(17)	8.1(14)	-2.7(15)	0.6(16)
C27_2	21.6(19)	30(2)	60(3)	-10(2)	1.1(19)	5.2(18)
C28_2	22(2)	38(3)	83(4)	-12(2)	6(2)	-2(2)
C29_2	40(2)	21(2)	53(3)	5.6(19)	-9(2)	0.4(18)
C30_2	61(3)	23.3(19)	28.8(19)	3.2(16)	9(2)	-5(2)
C31_2	50(3)	27(2)	31(2)	3.5(16)	13(2)	-9(2)

Table 3: Bond Lengths in Å for WL-ELN09-38R-d1.

Atom	Atom	Length/Å	Atom	Atom	Length/Å
Br1_1	C29_1	1.898(4)	S1_1	O3_1	1.435(3)
Br2_1	C22_1	1.901(4)	S1_1	O4_1	1.437(2)
Cl1_1	C14_1	1.777(4)	S1_1	N1_1	1.626(3)
Cl2_1	C14_1	1.768(4)	S1_1	C26_1	1.766(4)
Cl3_1	C14_1	1.771(4)	O1_1	C11_1	1.357(4)

Atom	Atom	Length/Å	Atom	Atom	Length/Å
O1_1	C13_1	1.432(4)	S1_2	O3_2	1.434(3)
O2_1	C11_1	1.200(4)	S1_2	O4_2	1.430(3)
N1_1	C2_1	1.478(4)	S1_2	N1_2	1.624(3)
N1_1	C6_1	1.478(4)	S1_2	C26_2	1.769(4)
C2_1	C3_1	1.525(5)	O1_2	C11_2	1.347(4)
C3_1	C4_1	1.522(6)	O1_2	C13_2	1.428(4)
C4_1	C5_1	1.535(5)	O2_2	C11_2	1.202(5)
C5_1	C6_1	1.533(5)	N1_2	C2_2	1.484(4)
C6_1	C10_1	1.555(4)	N1_2	C6_2	1.475(4)
C10_1	C11_1	1.520(5)	C2_2	C3_2	1.526(5)
C10_1	C19_1	1.520(4)	C3_2	C4_2	1.522(5)
C13_1	C14_1	1.526(5)	C4_2	C5_2	1.530(5)
C19_1	C20_1	1.394(5)	C5_2	C6_2	1.536(5)
C19_1	C24_1	1.388(5)	C6_2	C10_2	1.557(5)
C20_1	C21_1	1.392(5)	C10_2	C11_2	1.517(5)
C21_1	C22_1	1.379(6)	C10_2	C19_2	1.525(5)
C22_1	C23_1	1.385(6)	C13_2	C14_2	1.517(5)
C23_1	C24_1	1.396(5)	C19_2	C20_2	1.395(5)
C26_1	C27_1	1.393(5)	C19_2	C24_2	1.395(5)
C26_1	C31_1	1.389(5)	C20_2	C21_2	1.391(5)
C27_1	C28_1	1.395(5)	C21_2	C22_2	1.382(6)
C28_1	C29_1	1.379(6)	C22_2	C23_2	1.381(6)
C29_1	C30_1	1.392(6)	C23_2	C24_2	1.388(5)
C30_1	C31_1	1.381(6)	C26_2	C27_2	1.380(6)
Br1_2	C29_2	1.903(5)	C26_2	C31_2	1.381(6)
Br2_2	C22_2	1.903(4)	C27_2	C28_2	1.381(7)
Cl1_2	C14_2	1.768(3)	C28_2	C29_2	1.378(7)
Cl2_2	C14_2	1.774(4)	C29_2	C30_2	1.380(7)
Cl3_2	C14_2	1.774(4)	C30_2	C31_2	1.384(6)

Table 4: Bond Angles in ° for **WL-ELN09-38R-d1**.

Atom	Atom	Atom	Angle/°	Atom	Atom	Atom	Angle/°
O3_1	S1_1	O4_1	119.08(15)	C2_1	N1_1	S1_1	116.2(2)
O3_1	S1_1	N1_1	107.16(15)	C6_1	N1_1	S1_1	121.7(2)
O3_1	S1_1	C26_1	109.40(17)	C6_1	N1_1	C2_1	115.8(3)
O4_1	S1_1	N1_1	110.87(15)	N1_1	C2_1	C3_1	110.9(3)
O4_1	S1_1	C26_1	106.53(16)	C4_1	C3_1	C2_1	110.8(3)
N1_1	S1_1	C26_1	102.57(15)	C3_1	C4_1	C5_1	109.8(3)
C11_1	O1_1	C13_1	117.6(3)	C6_1	C5_1	C4_1	112.0(3)

Atom	Atom	Atom	Angle/°
N1_1	C6_1	C5_1	110.2(3)
N1_1	C6_1	C10_1	108.9(3)
C5_1	C6_1	C10_1	111.9(3)
C11_1	C10_1	C6_1	108.3(3)
C11_1	C10_1	C19_1	111.6(3)
C19_1	C10_1	C6_1	112.1(3)
O1_1	C11_1	C10_1	110.0(3)
O2_1	C11_1	O1_1	123.7(3)
O2_1	C11_1	C10_1	126.3(3)
O1_1	C13_1	C14_1	109.9(3)
Cl2_1	C14_1	Cl1_1	109.1(2)
Cl2_1	C14_1	Cl3_1	109.8(2)
Cl3_1	C14_1	Cl1_1	108.8(2)
C13_1	C14_1	Cl1_1	110.9(3)
C13_1	C14_1	Cl2_1	110.8(3)
C13_1	C14_1	Cl3_1	107.4(3)
C20_1	C19_1	C10_1	117.9(3)
C24_1	C19_1	C10_1	122.4(3)
C24_1	C19_1	C20_1	119.7(3)
C21_1	C20_1	C19_1	120.3(4)
C22_1	C21_1	C20_1	118.9(4)
C21_1	C22_1	Br2_1	118.2(3)
C21_1	C22_1	C23_1	122.0(3)
C23_1	C22_1	Br2_1	119.7(3)
C22_1	C23_1	C24_1	118.5(4)
C19_1	C24_1	C23_1	120.5(3)
C27_1	C26_1	S1_1	119.2(3)
C31_1	C26_1	S1_1	119.7(3)
C31_1	C26_1	C27_1	121.1(3)
C26_1	C27_1	C28_1	118.8(4)
C29_1	C28_1	C27_1	119.5(4)
C28_1	C29_1	Br1_1	118.7(3)
C28_1	C29_1	C30_1	121.8(4)
C30_1	C29_1	Br1_1	119.5(3)
C31_1	C30_1	C29_1	118.7(4)
C30_1	C31_1	C26_1	120.1(4)
O3_2	S1_2	N1_2	107.54(16)
O3_2	S1_2	C26_2	107.18(18)
O4_2	S1_2	O3_2	119.85(17)

Atom	Atom	Atom	Angle/°
O4_2	S1_2	N1_2	109.44(16)
O4_2	S1_2	C26_2	106.29(18)
N1_2	S1_2	C26_2	105.67(16)
C11_2	O1_2	C13_2	118.3(3)
C2_2	N1_2	S1_2	117.3(2)
C6_2	N1_2	S1_2	120.6(2)
C6_2	N1_2	C2_2	116.2(3)
N1_2	C2_2	C3_2	111.1(3)
C4_2	C3_2	C2_2	110.3(3)
C3_2	C4_2	C5_2	110.1(3)
C4_2	C5_2	C6_2	112.9(3)
N1_2	C6_2	C5_2	109.8(3)
N1_2	C6_2	C10_2	108.7(3)
C5_2	C6_2	C10_2	114.1(3)
C11_2	C10_2	C6_2	109.3(3)
C11_2	C10_2	C19_2	110.5(3)
C19_2	C10_2	C6_2	111.6(3)
O1_2	C11_2	C10_2	109.6(3)
O2_2	C11_2	O1_2	124.3(3)
O2_2	C11_2	C10_2	126.2(3)
O1_2	C13_2	C14_2	107.6(3)
Cl1_2	C14_2	Cl2_2	109.00(19)
Cl1_2	C14_2	Cl3_2	108.98(19)
Cl2_2	C14_2	Cl3_2	108.92(19)
C13_2	C14_2	Cl1_2	110.8(2)
C13_2	C14_2	Cl2_2	110.6(3)
C13_2	C14_2	Cl3_2	108.5(2)
C20_2	C19_2	C10_2	118.9(3)
C24_2	C19_2	C10_2	122.3(3)
C24_2	C19_2	C20_2	118.9(3)
C21_2	C20_2	C19_2	121.0(3)
C22_2	C21_2	C20_2	118.6(4)
C21_2	C22_2	Br2_2	118.4(3)
C23_2	C22_2	Br2_2	119.7(3)
C23_2	C22_2	C21_2	121.8(3)
C22_2	C23_2	C24_2	119.0(4)
C23_2	C24_2	C19_2	120.7(3)
C27_2	C26_2	S1_2	119.0(3)
C27_2	C26_2	C31_2	120.8(4)

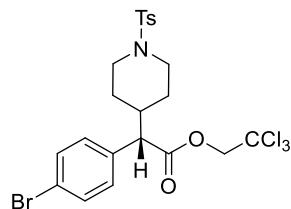
Atom	Atom	Atom	Angle/°	Atom	Atom	Atom	Angle/°
C31_2	C26_2	S1_2	120.1(3)	C28_2	C29_2	C30_2	121.2(4)
C26_2	C27_2	C28_2	119.0(4)	C30_2	C29_2	Br1_2	119.7(4)
C29_2	C28_2	C27_2	120.1(4)	C29_2	C30_2	C31_2	118.6(4)
C28_2	C29_2	Br1_2	119.1(4)	C26_2	C31_2	C30_2	120.3(4)

Table 5: Hydrogen Fractional Atomic Coordinates ($\times 10^4$) and Equivalent Isotropic Displacement Parameters ($\text{\AA}^2 \times 10^3$) for **WL-ELN09-38R-d1**. U_{eq} is defined as 1/3 of the trace of the orthogonalised U_{ij} .

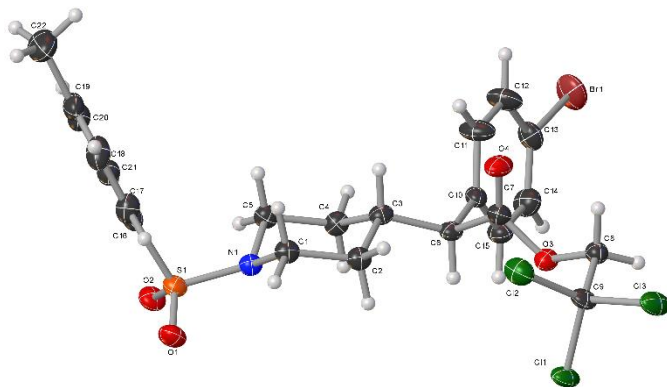
Atom	x	y	z	U_{eq}
H2A_1	7878.12	4078.71	6224.81	23
H2B_1	8337.85	4259.8	5737.18	23
H3A_1	7311.68	3473.79	5454.82	32
H3B_1	9095.49	3382.98	5819.17	32
H4A_1	6429.89	3160.13	6338.15	30
H4B_1	6154.56	2815	5916.72	30
H5A_1	3294.02	3320.28	5657.86	24
H5B_1	2737.01	3147.89	6143.19	24
H6_1	2037.43	4029.66	6021.31	18
H10_1	5143.27	3829.74	6706.03	19
H13A_1	-140.72	3142.74	7331.61	28
H13B_1	1661.75	3050.47	7692.42	28
H20_1	6786.92	4515.45	7005.93	26
H21_1	6944.63	5365.43	7208.35	32
H23_1	855.32	5567.72	6754.52	30
H24_1	708.01	4715.39	6552.3	23
H27_1	8545.69	4994.98	5188.66	27
H28_1	10307.19	5750	5375.22	33
H30_1	5113.99	6182.34	6094.33	37
H31_1	3383.33	5427.67	5919.62	30
H2A_2	6762.05	4760.48	3610.43	27
H2B_2	7355.69	4999.92	3148.97	27
H3A_2	5296.12	4390.63	2777.42	30
H3B_2	6938.15	4107.47	3090.44	30
H4A_2	4207.67	3978.7	3619.28	27
H4B_2	3403.32	3760.28	3162.62	27
H5A_2	654.73	4260.34	3497.75	24
H5B_2	1305.04	4480.6	3033	24
H6_2	1100.42	5163.79	3494.76	20
H10_2	4085.89	4738.38	4117.17	18

Atom	x	y	z	U_{eq}
H13A_2	-1215.64	3917.89	4602.47	28
H13B_2	611.2	3808.61	4955.86	28
H20_2	5879.83	5372.31	4487.91	24
H21_2	6138.87	6171.71	4806.34	31
H23_2	-16.97	6465.06	4438.44	31
H24_2	-264.71	5667.18	4119.16	25
H27_2	8132.66	6038.44	2796.3	45
H28_2	9975.73	6744.83	3055.69	57
H30_2	5075.74	7054.71	3890.13	45
H31_2	3217.68	6350.45	3626.39	43

2,2,2-Trichloroethyl (S)-2-(4-bromophenyl)-2-(1-tosylpiperidin-4-yl)acetate (153)



Crystal Data and Experimental



Experimental. Single colourless prism-shaped crystals of **WL-N9-80-f34** were chosen from the sample as supplied. A suitable crystal $0.35 \times 0.21 \times 0.11 \text{ mm}^3$ was selected and mounted on a loop with paratone oil on an XtaLAB Synergy-S diffractometer. The crystal was kept at a steady $T = 100.01(10) \text{ K}$ during data collection. The structure was solved with the **ShelXT** (Sheldrick, 2015) structure solution program using the Intrinsic Phasing solution method and by using **Olex2** (Dolomanov et al., 2009) as the graphical interface. The model was refined with version 2018/3 of **ShelXL** (Sheldrick, 2015) using Least Squares minimisation.

Crystal Data. $\text{C}_{22}\text{H}_{23}\text{BrCl}_3\text{NO}_4\text{S}$, $M_r = 583.73$, orthorhombic, $P2_12_12_1$ (No. 19), $a = 5.60602(6) \text{ \AA}$, $b = 20.3318(2) \text{ \AA}$, $c = 21.4309(2) \text{ \AA}$, $a = b = c = 90^\circ$, $V = 2442.71(4) \text{ \AA}^3$, $T = 100.01(10) \text{ K}$, $Z = 4$, $Z' = 1$, $m(\text{CuK}\alpha) = 6.365 \text{ mm}^{-1}$, 24631 reflections measured, 4842 unique ($R_{int} = 0.0422$) which were used in all calculations. The final wR_2 was 0.0855 (all data) and R_1 was 0.0326 ($I > 2\sigma(I)$).

Compound	WL-N9-80-f34
Formula	C ₂₂ H ₂₃ BrCl ₃ NO ₄ S
<i>D</i> _{calc.} / g cm ⁻³	1.587
<i>m</i> /mm ⁻¹	6.365
Formula Weight	583.73
Colour	colourless
Shape	prism
Size/mm ³	0.35×0.21×0.11
<i>T</i> /K	100.01(10)
Crystal System	orthorhombic
Flack Parameter	-0.001(8)
Hooft Parameter	-0.007(6)
Space Group	<i>P</i> 2 ₁ 2 ₁ 2 ₁
<i>a</i> /Å	5.60602(6)
<i>b</i> /Å	20.3318(2)
<i>c</i> /Å	21.4309(2)
<i>a</i> /°	90
<i>b</i> /°	90
<i>g</i> /°	90
<i>V</i> /Å ³	2442.71(4)
<i>Z</i>	4
<i>Z</i> '	1
Wavelength/Å	1.54184
Radiation type	CuK _α
<i>Q</i> _{min} /°	2.996
<i>Q</i> _{max} /°	77.056
Measured Refl.	24631
Independent Refl.	4842
Reflections with <i>I</i> > 2σ(<i>I</i>)	4758
<i>R</i> _{int}	0.0422
Parameters	290
Restraints	12
Largest Peak	0.675
Deepest Hole	-0.722
GooF	1.057
<i>wR</i> ₂ (all data)	0.0855
<i>wR</i> ₂	0.0851
<i>R</i> ₁ (all data)	0.0335
<i>R</i> ₁	0.0326

Structure Quality Indicators

Reflections:	d min (Cu)	0.79	l/σ	39.7	Rint	4.22%	complete 100% (IUCr)	100%		
Refinement:	Shift	-0.004	Max Peak	0.7	Min Peak	-0.7	Goof	1.057	Flack	.001(8)

A colourless prism-shaped crystal with dimensions $0.35 \times 0.21 \times 0.11 \text{ mm}^3$ was mounted on a loop with paratone oil. Data were collected using an XtaLAB Synergy, Dualflex, HyPix diffractometer equipped with an Oxford Cryosystems low-temperature device operating at $T = 100.01(10) \text{ K}$.

Data were measured using w scans using CuK_α radiation. The total number of runs and images was based on the strategy calculation from the program **CrysAlisPro** (Rigaku, V1.171.40.37a, 2019). The maximum resolution that was achieved was $Q = 77.056^\circ$ (0.79 \AA).

The diffraction pattern was indexed and then the total number of runs and images was calculated from the program **CrysAlisPro** (Rigaku, V1.171.40.37a, 2019). The unit cell was refined using **CrysAlisPro** (Rigaku, V1.171.40.37a, 2019) on 20665 reflections, 84% of the observed reflections.

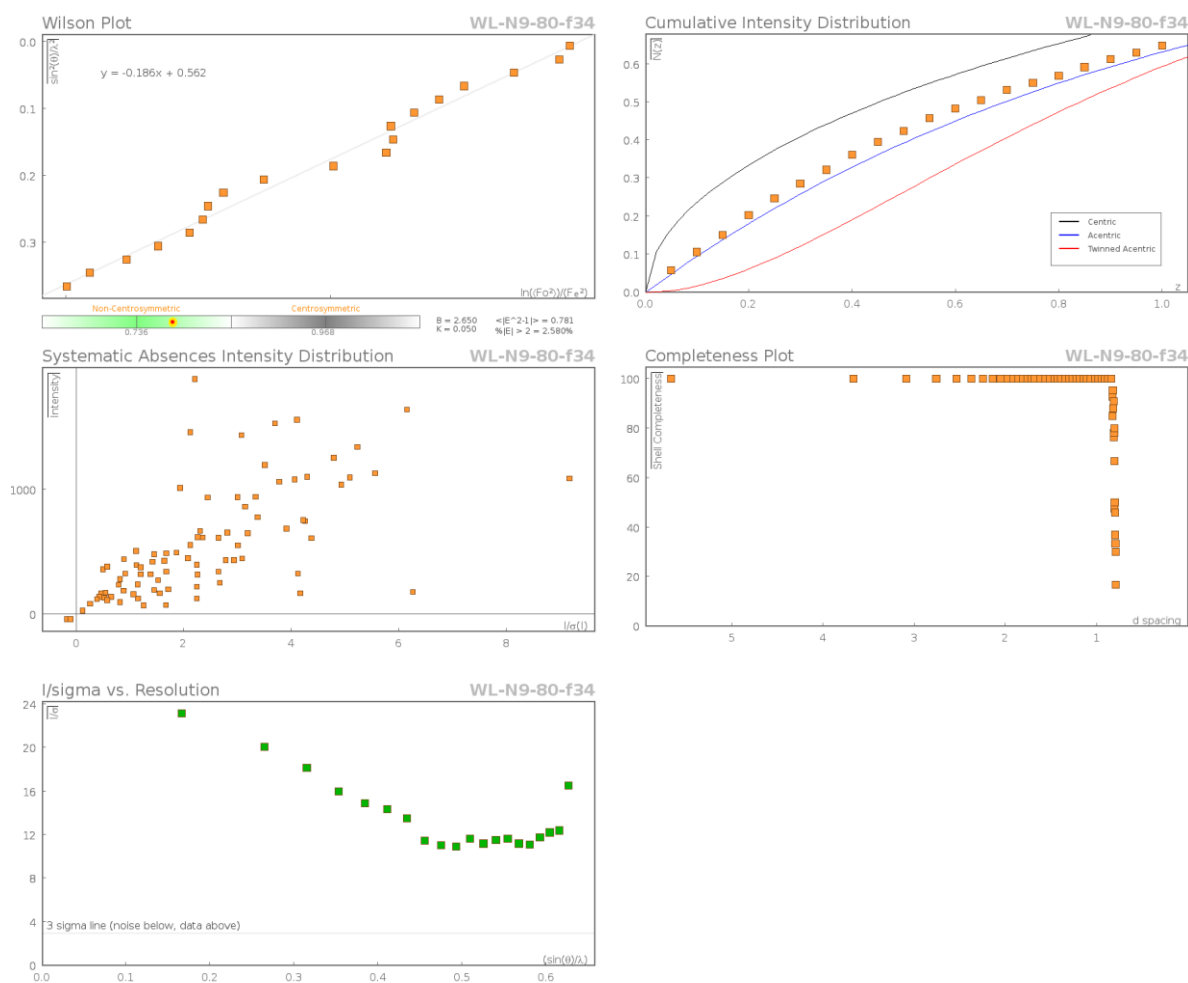
Data reduction, scaling and absorption corrections were performed using **CrysAlisPro** (Rigaku, V1.171.40.37a, 2019). The final completeness is 100.00 % out to 77.056° in Q . A numerical absorption correction based on Gaussian integration over a multifaceted crystal model was performed using (Rigaku Oxford Diffraction, 2019). An empirical absorption correction using spherical harmonics as implemented in SCALE3 ABSPACK was also performed. The absorption coefficient m of this material is 6.365 mm^{-1} at this wavelength ($\lambda = 1.542 \text{ \AA}$) and the minimum and maximum transmissions are 0.158 and 0.975.

The structure was solved and the space group $P2_12_12_1$ (# 19) determined by the **ShelXT** (Sheldrick, 2015) structure solution program using Intrinsic Phasing and refined by Least Squares using version 2018/3 of **ShelXL** (Sheldrick, 2015). All non-hydrogen atoms were refined anisotropically. Hydrogen atom positions were calculated geometrically and refined using the riding model. Hydrogen atom positions were calculated geometrically and refined using the riding model.

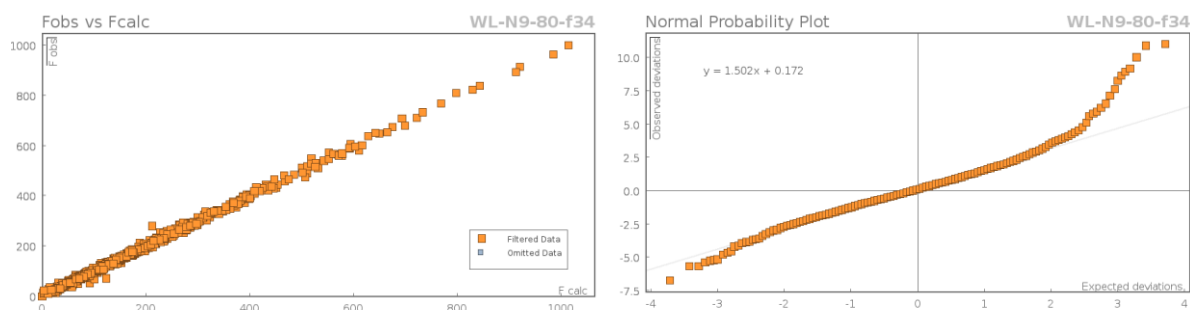
There is a single molecule in the asymmetric unit, which is represented by the reported sum formula. In other words: Z is 4 and Z' is 1.

The Flack parameter was refined to $-0.001(8)$. Determination of absolute structure using Bayesian statistics on Bijvoet differences using the Olex2 results in $-0.007(6)$. Note: The Flack parameter is used to determine chirality of the crystal studied, the value should be near 0, a value of 1 means that the stereochemistry is wrong and the model should be inverted. A value of 0.5 means that the crystal consists of a racemic mixture of the two enantiomers.

Data Plots: Diffraction Data



Data Plots: Refinement and Data



Reflection Statistics

Total reflections (after filtering) 24719

Completeness 0.94

hkl_{max} collected (6, 22, 26)

hkl_{max} used (6, 25, 26)

Unique reflections 4842

Mean I/s 28.61

hkl_{min} collected (-6, -25, -25)

hkl_{min} used (-6, 0, 0)

Lim d_{\max} collected	100.0	Lim d_{\min} collected	0.77
d_{\max} used	14.75	d_{\min} used	0.79
Friedel pairs	2903	Friedel pairs merged	0
Inconsistent equivalents	16	R_{int}	0.0422
R_{sigma}	0.0252	Intensity transformed	0
Omitted reflections	0	Omitted by user (OMIT hkl)	0
Multiplicity	(4573, 3499, 1890, 963, 416, 172, 56, 13, 2)	Maximum multiplicity	16
Removed systematic absences	88	Filtered off (Shel/OMIT)	0

Images of the Crystal on the Diffractometer

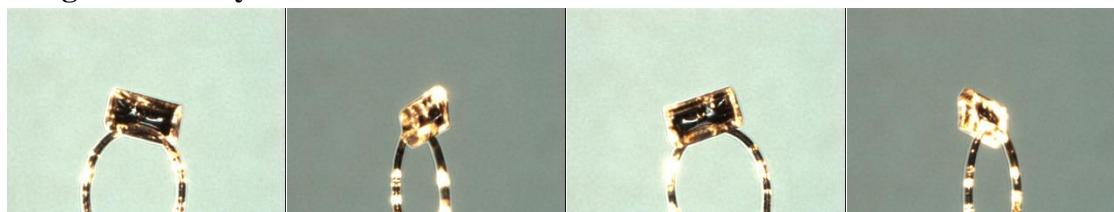


Table 1: Fractional Atomic Coordinates ($\times 10^4$) and Equivalent Isotropic Displacement Parameters ($\text{\AA}^2 \times 10^3$) for **WL-N9-80-f34**. U_{eq} is defined as 1/3 of the trace of the orthogonalised U_{ij} .

Atom	x	y	z	U_{eq}
Br1	2801.8(11)	1784.5(2)	4307.8(3)	49.52(16)
C1	6633(7)	6324.1(18)	4797.0(17)	24.8(7)
C2	6167(7)	5869.2(18)	4242.4(18)	25.2(7)
C3	5315(7)	5184.6(18)	4444.8(16)	22.5(7)
C4	7009(7)	4906.9(17)	4939.5(16)	24.8(8)
C5	7411(7)	5382.3(17)	5473.4(16)	25.3(7)
C6	5239(7)	4718.2(18)	3879.1(17)	22.6(7)
C7	3332(7)	4912.0(18)	3407.4(18)	24.8(8)
C8	2607(7)	4960.3(17)	2306.5(16)	23.9(7)
C9	3411(7)	5610.5(19)	2020.5(18)	25.9(8)
C10	4745(7)	3992.7(19)	4029.2(17)	24.2(7)
C11	2689(8)	3809(2)	4339(2)	38.7(10)
C12	2144(8)	3148(2)	4433(2)	40.3(10)
C13	3686(8)	2680.8(18)	4212(2)	31.1(9)
C14	5814(9)	2844(2)	3932(2)	36.6(10)
C15	6298(7)	3507(2)	3837.6(19)	29.3(8)
C16	7868(7)	6777.2(18)	6246.6(17)	25.3(7)
C17	6642(8)	7360(2)	6117.9(19)	31.8(9)

Atom	x	y	z	U_{eq}
C18	4942(9)	7578(2)	6537(2)	37.0(10)
C19	4397(8)	7229(2)	7076(2)	34.5(9)
C20	5640(8)	6651(2)	7192.3(19)	34.2(10)
C21	7353(8)	6420.8(19)	6782.5(17)	27.7(8)
C22	2503(10)	7463(3)	7523(2)	54.5(14)
Cl1	6532.4(16)	5608.4(5)	1900.9(4)	31.8(2)
Cl3	1966.4(16)	5695.7(6)	1286.8(4)	35.6(2)
Cl2	2634.7(19)	6285.6(4)	2500.5(5)	35.7(2)
N1	8391(6)	6000.3(14)	5214.8(14)	22.0(6)
O1	10817(5)	7001.9(14)	5336.0(14)	32.3(6)
O2	11531(5)	6036.9(14)	6019.9(13)	29.8(6)
O3	4142(5)	4807.2(13)	2820.3(12)	24.3(5)
O4	1346(5)	5097.9(16)	3531.3(14)	33.8(7)
S1	9909.2(16)	6464.1(4)	5693.8(4)	24.63(19)

Table 2: Anisotropic Displacement Parameters ($\times 10^4$) **WL-N9-80-f34**. The anisotropic displacement factor exponent takes the form: $-2p^2[h^2a^{*2} \times U_{11} + \dots + 2hka^* \times b^* \times U_{12}]$

Atom	U_{11}	U_{22}	U_{33}	U_{23}	U_{13}	U_{12}
Br1	59.0(3)	26.0(2)	63.6(3)	-7.0(2)	-3.3(3)	-13.6(2)
C1	24.1(18)	23.4(14)	27.0(14)	4.0(12)	-1.1(13)	3.9(14)
C2	24.0(17)	24.9(12)	26.6(14)	3.6(11)	-0.4(12)	3.3(11)
C3	18.6(16)	23.9(13)	24.9(17)	1.9(12)	2.9(13)	5.4(11)
C4	28(2)	20.6(16)	25.9(17)	3.0(14)	-0.2(15)	3.5(16)
C5	27.2(18)	23.2(12)	25.3(16)	3.3(11)	-0.4(14)	0.4(12)
C6	15.3(16)	27.0(18)	25.6(17)	0.0(14)	1.6(14)	2.7(14)
C7	20.7(18)	26.0(18)	27.8(18)	0.8(15)	1.5(15)	-2.2(15)
C8	21.0(18)	25.0(17)	25.7(17)	-1.1(13)	-0.6(14)	1.2(15)
C9	14.2(16)	31.6(19)	31.8(18)	4.0(16)	-2.6(14)	0.3(15)
C10	17.1(14)	28.3(18)	27.2(16)	-4.6(14)	-0.3(12)	-0.4(13)
C11	25.7(15)	29.0(18)	62(2)	2.2(18)	17.1(17)	3.5(14)
C12	29(2)	30(2)	62(3)	5.3(19)	12(2)	-5.0(18)
C13	34(2)	19.7(17)	39(2)	-0.8(16)	-5.3(18)	-4.4(16)
C14	41(2)	29(2)	40(2)	-7.6(19)	6.0(19)	3.4(19)
C15	25(2)	29.2(19)	34(2)	-4.2(17)	5.6(16)	-0.1(16)
C16	21.4(18)	25.5(17)	28.9(17)	-6.1(14)	-5.1(15)	2.1(16)
C17	39(2)	26.1(19)	30.3(19)	-1.4(15)	-5.1(17)	4.5(17)
C18	38(2)	33(2)	41(2)	-12.6(18)	-11(2)	15(2)
C19	31(2)	40(2)	33(2)	-15.2(18)	-2.3(17)	-1.1(19)
C20	37(2)	39(2)	26.9(19)	-5.7(17)	-1.3(17)	-4.7(19)

Atom	U_{11}	U_{22}	U_{33}	U_{23}	U_{13}	U_{12}
C21	27(2)	28.8(18)	27.2(17)	-3.2(15)	-2.4(15)	2.0(17)
C22	47(3)	63(3)	54(3)	-26(3)	8(3)	4(3)
Cl1	14.4(4)	46.4(5)	34.6(5)	6.4(4)	-1.4(3)	-0.9(4)
Cl3	18.9(4)	54.6(6)	33.2(4)	12.0(4)	-6.5(4)	0.4(4)
Cl2	31.5(5)	24.6(4)	50.9(6)	-3.6(4)	1.8(5)	1.9(4)
N1	20.3(15)	21.5(12)	24.2(14)	1.9(10)	0.4(11)	3.2(11)
O1	26.8(15)	33.1(15)	37.1(15)	2.7(12)	2.7(12)	-7.6(12)
O2	17.6(13)	35.1(14)	36.8(14)	0.4(12)	-4.6(11)	6.2(11)
O3	20.0(12)	26.7(13)	26.3(13)	0.2(10)	-0.1(10)	4.5(11)
O4	18.2(14)	50.2(18)	32.8(15)	0.1(13)	3.8(11)	5.9(13)
S1	18.5(4)	26.3(4)	29.1(4)	0.6(4)	-0.2(4)	0.8(3)

Table 3: Bond Lengths in Å for WL-N9-80-f34.

Atom	Atom	Length/Å	Atom	Atom	Length/Å
Br1	C13	1.900(4)	C10	C11	1.381(6)
C1	C2	1.528(5)	C10	C15	1.379(5)
C1	N1	1.486(5)	C11	C12	1.394(6)
C2	C3	1.534(5)	C12	C13	1.369(6)
C3	C4	1.531(5)	C13	C14	1.376(6)
C3	C6	1.540(5)	C14	C15	1.390(6)
C4	C5	1.515(5)	C16	C17	1.398(5)
C5	N1	1.479(5)	C16	C21	1.388(5)
C6	C7	1.523(5)	C16	S1	1.766(4)
C6	C10	1.535(5)	C17	C18	1.382(6)
C7	O3	1.355(5)	C18	C19	1.391(7)
C7	O4	1.205(5)	C19	C20	1.389(7)
C8	C9	1.525(5)	C19	C22	1.507(6)
C8	O3	1.432(4)	C20	C21	1.383(6)
C9	C11	1.769(4)	N1	S1	1.633(3)
C9	Cl3	1.777(4)	O1	S1	1.429(3)
C9	Cl2	1.770(4)	O2	S1	1.438(3)

Table 4: Bond Angles in ° for WL-N9-80-f34.

Atom	Atom	Atom	Angle/°	Atom	Atom	Atom	Angle/°
N1	C1	C2	108.3(3)	C4	C3	C6	109.6(3)
C1	C2	C3	112.5(3)	C5	C4	C3	112.3(3)
C2	C3	C6	110.2(3)	N1	C5	C4	108.3(3)
C4	C3	C2	109.7(3)	C7	C6	C3	112.5(3)

Atom	Atom	Atom	Angle/°	Atom	Atom	Atom	Angle/°
C7	C6	C10	105.1(3)	C10	C15	C14	121.8(4)
C10	C6	C3	115.6(3)	C17	C16	S1	119.5(3)
O3	C7	C6	109.9(3)	C21	C16	C17	120.2(4)
O4	C7	C6	125.7(4)	C21	C16	S1	120.1(3)
O4	C7	O3	124.3(4)	C18	C17	C16	118.8(4)
O3	C8	C9	108.7(3)	C17	C18	C19	121.9(4)
C8	C9	C11	110.4(3)	C18	C19	C22	121.5(4)
C8	C9	C13	107.8(3)	C20	C19	C18	118.0(4)
C8	C9	C12	111.5(3)	C20	C19	C22	120.4(5)
C11	C9	C13	108.8(2)	C21	C20	C19	121.4(4)
C11	C9	C12	109.2(2)	C20	C21	C16	119.5(4)
C12	C9	C13	109.1(2)	C1	N1	S1	118.0(2)
C11	C10	C6	120.7(3)	C5	N1	C1	110.8(3)
C15	C10	C6	120.8(3)	C5	N1	S1	116.7(2)
C15	C10	C11	118.5(4)	C7	O3	C8	118.6(3)
C10	C11	C12	120.9(4)	N1	S1	C16	107.00(17)
C13	C12	C11	118.8(4)	O1	S1	C16	108.36(18)
C12	C13	Br1	117.6(3)	O1	S1	N1	106.86(17)
C12	C13	C14	122.0(4)	O1	S1	O2	119.84(18)
C14	C13	Br1	120.3(3)	O2	S1	C16	107.54(18)
C13	C14	C15	117.8(4)	O2	S1	N1	106.62(17)

Table 5: Torsion Angles in ° for **WL-N9-80-f34**.

Atom	Atom	Atom	Atom	Angle/°
Br1	C13	C14	C15	175.8(3)
C1	C2	C3	C4	-50.8(4)
C1	C2	C3	C6	-171.5(3)
C1	N1	S1	C16	67.6(3)
C1	N1	S1	O1	-48.3(3)
C1	N1	S1	O2	-177.6(3)
C2	C1	N1	C5	-63.4(4)
C2	C1	N1	S1	158.5(3)
C2	C3	C4	C5	51.7(4)
C2	C3	C6	C7	-67.2(4)
C2	C3	C6	C10	172.0(3)
C3	C4	C5	N1	-58.3(4)
C3	C6	C7	O3	142.4(3)
C3	C6	C7	O4	-41.3(5)
C3	C6	C10	C11	58.2(5)

Atom	Atom	Atom	Atom	Angle/°
C3	C6	C10	C15	-124.3(4)
C4	C3	C6	C7	172.0(3)
C4	C3	C6	C10	51.2(4)
C4	C5	N1	C1	64.4(4)
C4	C5	N1	S1	-156.8(3)
C5	N1	S1	C16	-68.2(3)
C5	N1	S1	O1	175.9(3)
C5	N1	S1	O2	46.6(3)
C6	C3	C4	C5	172.8(3)
C6	C7	O3	C8	-179.9(3)
C6	C10	C11	C12	175.0(4)
C6	C10	C15	C14	-175.8(4)
C7	C6	C10	C11	-66.5(5)
C7	C6	C10	C15	111.0(4)
C9	C8	O3	C7	102.7(4)
C10	C6	C7	O3	-91.0(3)
C10	C6	C7	O4	85.3(5)
C10	C11	C12	C13	-0.1(8)
C11	C10	C15	C14	1.8(6)
C11	C12	C13	Br1	-176.5(4)
C11	C12	C13	C14	3.7(7)
C12	C13	C14	C15	-4.4(7)
C13	C14	C15	C10	1.6(7)
C15	C10	C11	C12	-2.6(7)
C16	C17	C18	C19	-0.9(7)
C17	C16	C21	C20	-0.8(6)
C17	C16	S1	N1	-87.6(3)
C17	C16	S1	O1	27.3(4)
C17	C16	S1	O2	158.1(3)
C17	C18	C19	C20	0.8(7)
C17	C18	C19	C22	-178.6(4)
C18	C19	C20	C21	-0.7(6)
C19	C20	C21	C16	0.7(6)
C21	C16	C17	C18	0.9(6)
C21	C16	S1	N1	87.5(3)
C21	C16	S1	O1	-157.6(3)
C21	C16	S1	O2	-26.7(4)
C22	C19	C20	C21	178.7(4)
N1	C1	C2	C3	56.4(4)

Atom	Atom	Atom	Atom	Angle/°
O3	C8	C9	C11	47.9(3)
O3	C8	C9	C13	166.7(2)
O3	C8	C9	C12	-73.7(3)
O4	C7	O3	C8	3.7(6)
S1	C16	C17	C18	176.0(3)
S1	C16	C21	C20	-175.9(3)

Table 6: Hydrogen Fractional Atomic Coordinates ($\times 10^4$) and Equivalent Isotropic Displacement Parameters ($\text{\AA}^2 \times 10^3$) for **WL-N9-80-f34**. U_{eq} is defined as 1/3 of the trace of the orthogonalised U_{ij} .

Atom	x	y	z	U_{eq}
H1A	7255.43	6742.14	4651.97	30
H1B	5158.82	6405.53	5021.04	30
H2A	7622	5824.44	4001.22	30
H2B	4968.63	6066.72	3974.96	30
H3	3710.53	5220.95	4622.86	27
H4A	6350.34	4500.53	5102.61	30
H4B	8529.19	4805.18	4746.22	30
H5A	5915.99	5469.06	5686.06	30
H5B	8519.72	5194.75	5771.77	30
H6	6789.61	4742.76	3669.28	27
H8A	970.9	4996.29	2449.79	29
H8B	2685.81	4613.49	1996.42	29
H11	1653.94	4131.43	4485.7	46
H12	759.22	3026.49	4642.13	48
H14	6892.78	2521.31	3810.52	44
H15	7708.63	3626.63	3639.39	35
H17	6965.32	7597.88	5756.69	38
H18	4139.21	7968.83	6455.13	44
H20	5312.28	6413.43	7553.11	41
H21	8155.34	6030.09	6865.49	33
H22A	2752.47	7263.5	7924.14	82
H22B	959.11	7340.46	7367.64	82
H22C	2589.51	7932.25	7562.54	82

Citations

CrysAlisPro Software System, Rigaku Oxford Diffraction, (2019).

O.V. Dolomanov and L.J. Bourhis and R.J. Gildea and J.A.K. Howard and H. Puschmann, Olex2: A complete structure solution, refinement and analysis program, *J. Appl. Cryst.*, (2009), **42**, 339-341.

Sheldrick, G.M., Crystal structure refinement with ShelXL, *Acta Cryst.*, (2015), **C27**, 3-8.

Sheldrick, G.M., ShelXT-Integrated space-group and crystal-structure determination, *Acta Cryst.*, (2015), **A71**, 3-8.